Oxidative Medicine and Cellular Longevity

Natural Products: Optimizing Cancer Treatment through Modulation of Redox Balance

Lead Guest Editor: Patrícia Rijo
Guest Editors: Milica Pesic, Ana S. Fernandes, and Cláudia N. Santos

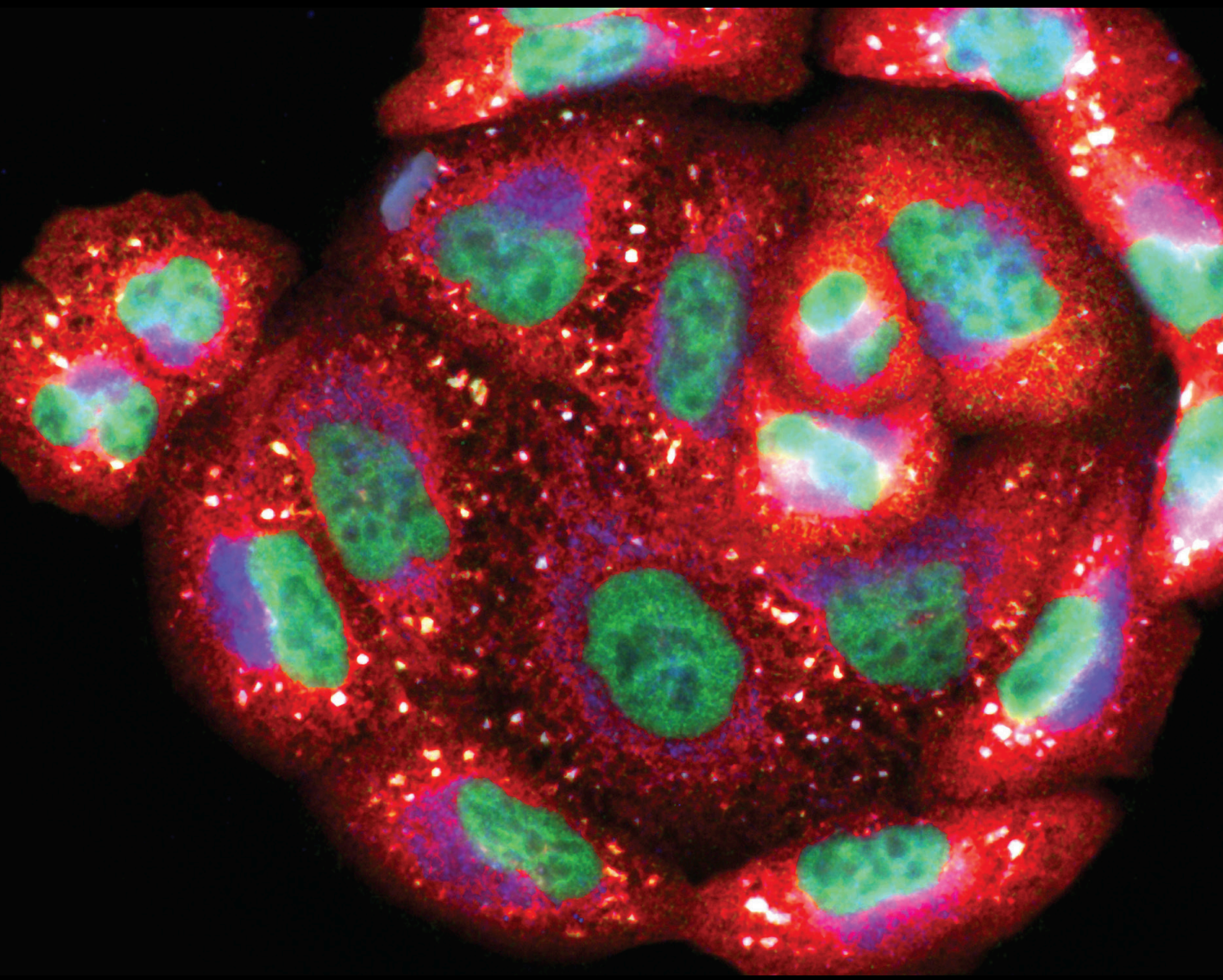

Natural Products: Optimizing Cancer Treatment through Modulation of Redox Balance

Oxidative Medicine and Cellular Longevity

Natural Products: Optimizing Cancer Treatment through Modulation of Redox Balance

Lead Guest Editor: Patrícia Rijo
Guest Editors: Milica Pesic, Ana S. Fernandes, and Cláudia N. Santos

Contents

Hindawi
Oxidative Medicine and Cellular Longevity
Volume 2020, Article ID 2407074, 3 pages
https://doi.org/10.1155/2020/2407074

Editorial

Natural Products: Optimizing Cancer Treatment through Modulation of Redox Balance

Patrícia Rijo,[1,2] **Milica Pešić**,[3] **Ana S. Fernandes**,[1] **and Cláudia N. Santos**[4]

[1]*CBIOS - Universidade Lusófona Research Center for Biosciences & Health Technologies, Lisboa, Portugal*
[2]*IMed.ULisboa-Research Institute for Medicines, Lisboa, Portugal*
[3]*Institute for Biological Research "Siniša Stanković"-National Institute of Republic of Serbia, University of Belgrade, Belgrade, Serbia*
[4]*CEDOC, NOVA Medical School, Faculdade de Ciências Médicas, Universidade NOVA de Lisboa, Lisboa, Portugal*

Correspondence should be addressed to Patrícia Rijo; patricia.rijo@ulusofona.pt

Received 5 December 2019; Accepted 6 December 2019; Published 3 June 2020

Nature is an inexhaustible reservoir of compounds with healing properties, and people used natural products to treat different medical conditions from ancient times. One of the main features of natural products is their ability to modulate directly and indirectly oxidative stress and protect human cells from aging and death [1]. Besides aging, cardiovascular diseases, chronic obstructive pulmonary disease, chronic kidney disease, and neurodegeneration, cancer can be considered as an oxidative stress-related disease [2]. Therefore, natural products are also valuable for treating cancer. Increased generation of reactive oxygen species (ROS) which leads to oxidative stress and provokes inflammation eventually may cause carcinogenesis or stimulate cancer progression and metastatic behavior [3]. Despite still preserved indigenous knowledge about plants and other organisms with medicinal value, clinical development of natural preparations (both compounds and extracts) is difficult and slow. However, some of the most exploited chemotherapeutics have natural origin such as doxorubicin, vincristine, and paclitaxel [4]. Today, we know that natural compounds may also cause unwanted effects particularly due to their interference with redox balance [5].

Therefore, advanced and innovative studies of natural product interactions with human metabolism are warranted. The diversity of natural products should be the advantage in our search for the best anticancer nature-inspired drugs.

This special issue assembles twelve contributions (three reviews and nine original articles) regarding the anticancer effects of different natural products and their derivatives, particularly those with the potential to modulate oxidative-stress in cancer.

A review article by J. T. de Giffoni de Carvalho et al. explores medicinal plants found in the Brazilian Cerrado tropical savanna ecoregion emphasizing the antioxidant properties of their extracts as well as their potential for cell death induction in different malignant cells. Moreover, the authors comprehensively describe other medicinal plants from the same region which showed protective capacity against chemotherapy-induced cell toxicity.

Another review article by P. Aiello et al. comprehensively investigates medicinal plants in the prevention and treatment of colon cancer. Their study revealed that grape, soybean, green tea, garlic, olive, and pomegranate are the most effective plants against colon cancer. Diverse in vitro and in vivo models provided evidence that fruits, seeds, leaves, and roots of these plants are abundant in saponins, polysaccharides, triterpenoids, alkaloids, polyphenol glycosides, including flavonoids, and simple phenols, such as caffeic acid, catechins, quercetin and luteolin, and kaempferol and luteolin glycosides. These natural compounds exert various effects such as induction of superoxide dismutase, reduction of DNA oxidation, cell cycle arrest in S phase, suppression of prosurvival

signaling pathways and cell invasion, reduction of antiapoptotic and increase of proapoptotic factors, and decrease of proliferating cell nuclear antigen (PCNA), cyclin A, cyclin D1, cyclin B1, and cyclin E.

An interesting overview of melatonin protective action against the side effects of chemotherapy is given by Z. Ma et al. Melatonin easily crosses all biological barriers while its concentration within the cells is particularly high in mitochondria. This is important for its ability to resist mitochondrial oxidative-stress damage. In cancer as well as in other aging-related diseases, melatonin can reduce mitochondrial-mediated cell death and thus protect normal cells against the harmful effects of anthracyclines, alkylating agents, platinum compounds, antimetabolites, mitotic inhibitors, and novel targeted therapies.

The remaining original articles are focused on already isolated and identified natural compounds or plant extracts tested for their anticancer effects and protective effects against classic chemotherapy in different cancer models.

D. T. H. Castro et al. investigated antimelanoma effects of ethanolic extract of *Senna velutina* roots shown to contain flavonoid derivatives of the catechin, anthraquinone, and piceatannol groups. B16F10-Nex2 murine cell line was used for the assessment of extract's effects. Results showed that the extract induced apoptotic cell death followed by caspase-3 activation and increased intracellular calcium and ROS levels. Tumor volume and pulmonary metastasis were followed after subcutaneous implantation of B16F10-Nex2 cells in the lumbosacral region of C57Bl/6 mice. Importantly, it was shown that both the primary tumor volume and the number of pulmonary nodules decreased over 50% when this ethanolic extract was applied.

H. P. Vasantha Rupasinghe et al. showed that the application of a bioconversion process using probiotic bacteria *Lactobacillus rhamnosus* can enhance the pharmacological activities of cranberry extracts probably by generating more active metabolites. The proanthocyanidin-rich extract exposed to the bacteria was particularly active against HepG2 cells inducing significantly stronger mitochondria-dependent apoptosis when compared to parental extract which was not exposed to probiotic bacteria.

M. Shen et al. showed both in vitro and in vivo that betulinic acid induces ROS-dependent apoptosis by inhibiting the NF-κB pathway in human multiple myeloma. Betulinic acid exerted its effect mainly through mitochondrial apoptosis induction, cell cycle blockade, mitochondrial membrane potential disruption, intracellular ROS accumulation, and NF-κB signaling inhibition. This comprehensive study above all elucidated the complex regulatory interaction between ROS and the NF-κB pathway in multiple myeloma.

E. Hernández-SanMiguel et al. found that Ocoxin® oral solution affects stem cell properties in certain primary glioblastoma cells by inhibiting their self-renewal capacity. Moreover, systemic treatment of animals bearing heterotopic and orthotopic xenografts with Ocoxin® reduced tumor burden. Importantly, Ocoxin® exerted a direct effect on macrophage polarization in vitro and in vivo, inhibiting the protumoral features of M2 macrophages.

T. Kowalczyk et al. studied protective antioxidant and anti-inflammatory properties of aqueous methanolic extracts derived from the aerial parts and roots of in vitro grown *Menyanthes trifoliata* L. plants on human umbilical vein endothelial cells. The authors found that both extracts demonstrated protective effects against mitochondrial and nuclear DNA damage caused by ROS. Due to the higher content of selected phenolic compounds and betulinic acid in the root extract, it exerted stronger effects than the extract from the aerial part.

G. Isani et al. renewed the interest for the traditional Chinese medicinal plant *Artemisia annua* L. from which famous antimalarial drug artemisinin was isolated. The authors showed that both artemisinin and hydroalcoholic plant extract induced a cytotoxic effect in D-17 canine osteosarcoma cells. Pure artemisinin caused an increase of cells in the S phase, whereas the hydroalcoholic extract induced G2/M arrest. A significant decrease of iron concentration was also observed indicating that ferroptosis as a specific cell death type might contribute to the artemisinin effect. The hydroalcoholic extract was more potent than pure artemisinin demonstrating a possible synergistic effect of its other components with artemisinin.

D. Pang et al. provided the evidence that polyphyllin VII isolated from *Paris polyphylla* var. yunnanensis induces apoptosis and autophagic cell death via ROS-provoked suppression of AKT/mTORC1 signaling cascade. Moreover, polyphyllin VII in combination with temozolomide showed synergistic interaction followed by a decrease of MGMT expression. Therefore, polyphyllin VII can be considered as a valuable drug to attenuate the ability of glioma cells to repair the temozolomide-induced DNA methylation and reduce the resistance to temozolomide.

I. Kumburovic et al. showed that anxiogenic manifestation of widely used chemotherapeutic cisplatin caused by increased oxidative stress and proapoptotic effect in the hippocampus can be attenuated by supplementation with *Satureja hortensis* L. methanolic extract in rats. This work suggests a beneficial role of these natural products in the protection of cisplatin-induced neurotoxicity.

B. Yang et al. demonstrated that tetramethylpyrazine, an alkaloid extracted from the roots of *Ligusticum chuanxiong* Hort, can overcome doxorubicin-induced endothelian toxicity. To that end, the authors used vascular endothelium injury models in mice and human umbilical vein endothelial cells and showed that tetramethylpyrazine protects the vascular endothelium against doxorubicin-induced injury via upregulating 14-3-3γ expression, promoting translocation of Bcl-2 to the mitochondria, closing mitochondria permeability transition pore, maintaining mitochondrial membrane potential, and suppressing oxidative stress.

Overall, the articles presented in this special issue provide experimental evidence and assembled scientific data, which clearly emphasize the medicinal value of natural products to fight cancer and prevent side effects of approved chemotherapeutics by modulating oxidative stress. Our planet has to offer plenty of bioactive molecules of which some are not yet discovered, and this raises the hope that in the future we will be able to sustainably exploit natural resources and find more potent and safer anticancer agents.

Conflicts of Interest

The editors declare that they have no conflicts of interest regarding the publication of this special issue.

Patrícia Rijo
Milica Pešić
Ana S. Fernandes
Cláudia N. Santos

References

[1] C. Ricordi, M. Garcia-Contreras, and S. Farnetti, "Diet and inflammation: possible effects on immunity, chronic diseases, and life span," *Journal of the American College of Nutrition*, vol. 34, no. sup1, pp. 10–13, 2015.

[2] I. Liguori, G. Russo, F. Curcio et al., "Oxidative stress, aging, and diseases," *Clinical Interventions in Aging*, vol. Volume 13, pp. 757–772, 2018.

[3] G. Y. Liou and P. Storz, "Reactive oxygen species in cancer," *Free Radical Research*, vol. 44, no. 5, pp. 479–496, 2010.

[4] A. L. Demain and P. Vaishnav, "Natural products for cancer chemotherapy," *Microbial Biotechnology*, vol. 4, no. 6, pp. 687–699, 2011.

[5] V. Lobo, A. Patil, A. Phatak, and N. Chandra, "Free radicals, antioxidants and functional foods: impact on human health," *Pharmacognosy Reviews*, vol. 4, no. 8, pp. 118–126, 2010.

Hindawi
Oxidative Medicine and Cellular Longevity
Volume 2020, Article ID 6841581, 20 pages
https://doi.org/10.1155/2020/6841581

Review Article

Utilizing Melatonin to Alleviate Side Effects of Chemotherapy: A Potentially Good Partner for Treating Cancer with Ageing

Zhiqiang Ma,[1] **Liqun Xu**,[1,2] **Dong Liu**,[3] **Xiaoyan Zhang**,[1,2] **Shouyin Di**,[1] **Weimiao Li**,[1] **Jiao Zhang**,[1] **Russel J. Reiter**,[4] **Jing Han**,[5] **Xiaofei Li**,[1] **and Xiaolong Yan**[1]

[1]*Department of Thoracic Surgery, Tangdu Hospital, The Fourth Military Medical University, 1 Xinsi Road, Xi'an 710038, China*
[2]*Department of Aerospace Medicine, The Fourth Military Medical University, Xi'an 710032, China*
[3]*State Key Laboratory of Cardiovascular Disease, Fuwai Hospital, National Center for Cardiovascular Diseases, Chinese Academy of Medical Sciences, Peking Union Medical College, 167 Beilishi Road, Beijing 100037, China*
[4]*Department of Cellular and Structural Biology, UT Health Science Center, 7703 Floyd Curl Drive, San Antonio, TX 78229, USA*
[5]*Department of Ophthalmology, Tangdu Hospital, The Fourth Military Medical University, 1 Xinsi Road, Xi'an 710038, China*

Correspondence should be addressed to Jing Han; hanjing_cns@163.com, Xiaofei Li; lxfchest@fmmu.edu.cn, and Xiaolong Yan; yanxiaolong@fmmu.edu.cn

Zhiqiang Ma, Liqun Xu, and Dong Liu contributed equally to this work.

Received 14 February 2019; Revised 14 May 2019; Accepted 27 May 2019; Published 21 May 2020

Guest Editor: Cláudia N. Santos

Persistent senescence seems to exert detrimental effects fostering ageing and age-related disorders, such as cancer. Chemotherapy is one of the most valuable treatments for cancer, but its clinical application is limited due to adverse side effects. Melatonin is a potent antioxidant and antiageing molecule, is nontoxic, and enhances the efficacy and reduces the side effects of chemotherapy. In this review, we first summarize the mitochondrial protective role of melatonin in the context of chemotherapeutic drug-induced toxicity. Thereafter, we tabulate the protective actions of melatonin against ageing and the harmful roles induced by chemotherapy and chemotherapeutic agents, including anthracyclines, alkylating agents, platinum, antimetabolites, mitotic inhibitors, and molecular-targeted agents. Finally, we discuss several novel directions for future research in this area. The information compiled in this review will provide a comprehensive reference for the protective activities of melatonin in the context of chemotherapy drug-induced toxicity and will contribute to the design of future studies and increase the potential of melatonin as a therapeutic agent.

1. Introduction

All organismal functions are affected by senescence, from the disorders of cellular protein production and alterations in the macroscopic characteristics of cells to the decline of organ or system functional efficiency, which may increase the development of age-related diseases such as cancer [1–4]. Chemotherapy is one of the main treatments for cancer patients [5, 6]. Chemotherapeutic agents are divided into several categories according to the factors of their effects, their chemical structures, and their relationships to other drugs [7]. The major categories of chemotherapeutic agents include anthracyclines (e.g., daunorubicin (DNR), doxorubicin (DOX), and epirubicin), alkylating agents (e.g., cyclophosphamide (CP), ifosfamide, melphalan, and busulfan), platinum (e.g., cisplatin and oxaliplatin), antimetabolites (e.g., 5-fluorouracil (5-FU), capecitabine, methotrexate (MTX), and gemcitabine), topoisomerase inhibitors (e.g., topotecan, irinotecan, etoposide, and teniposide), mitotic inhibitors (e.g., paclitaxel, docetaxel, vinblastine, and vincristine), and molecular-targeted agents (e.g., trastuzumab) [8, 9]. Despite advances in the development of effective chemotherapeutic drugs, their toxicity or adverse side effects to multiple organ systems and drug resistance

have remained main barriers to their successful clinical application [7, 10]. For instance, alkylating agents and topoisomerase II inhibitors could increase the risk of secondary cancer (acute leukemia); anthracyclines, such as doxorubicin, can cause cardiotoxicity; and mitotic inhibitors may cause peripheral nerve damage [10].

Melatonin, a widely distributed and functionally diverse molecule, is also known as N-acetyl-5-methoxytryptamine [11–13]. In addition to influencing circadian rhythms, it modulates several molecular pathways related to antitumor effects, antiageing, anti-inflammation, sleep promotion, antivenom, body weight regulation, antidiabetic activity, and vasorelaxant and antifibrotic properties [14–18]. The roles of melatonin in alleviating chemotherapy drug-induced toxicity among the elderly have been widely considered, and a variety of new mechanisms have been confirmed [19–21]. Accumulated evidence suggests that melatonin enhances the efficacy and reduces the side effects of chemotherapy [22–24]. Pineal indoleamine has the double function of inhibiting cancer and protecting normal tissues, having low toxicity, being a highly effective free radical scavenger, and influencing mitochondrial homeostasis and functioning [25–27]. Furthermore, studies have demonstrated that melatonin was superior in preventing free radical destruction compared to other antioxidants, vitamin E, β-carotene, vitamin C, and garlic oil [28, 29]. Accordingly, the results generally showed that melatonin had a favorable therapeutic use in reducing chemotherapy drug-induced toxicity. However, the precise mechanisms of melatonin protection and the key cellular parameters of its influences still need to be clarified [30].

To study the protective actions of melatonin against chemotherapy drug-induced toxicity, herein we evaluated the available published documents regarding recent progress in this field. First, we present the evidence documenting the mitochondrial protective effect of melatonin on the toxicity of chemotherapy drugs. Second, we illustrate and discuss what is known about how melatonin protects against the detrimental roles of chemotherapy drug-induced toxicity while enhancing the efficacy of chemotherapeutic agents against tumor in various organs. Finally, we discuss several novel potential directions for future research in this field. Collectively, the information compiled here will provide a comprehensive reference for the actions of melatonin in protecting against chemotherapy drug-induced toxicity.

2. Correlation between Melatonin and Ageing

Accumulating studies indicate that melatonin is an antiageing agent that may retard the consequences of senescence [31]. Ageing results in circadian rhythm disorders, thus deregulating the melatonin synthesis [1]. The decrease of the melatonin peak in the elderly at night is consistent with the hypothesis that melatonin is related to senescence [32]. Melatonin mediated the important signaling pathways such as SIRT1 that is an ageing inhibitor whose upregulation may be associated with ageing [33]. Furthermore, senescence is an important pathogenic factor, which decreases the efficiency of the respiratory chain, increases electron leakage, generates free radicals, reduces the production of ATP, and finally leads to mitochondrial dysfunction [34], which can be ameliorated by melatonin. Additionally, melatonin may prolong life-span [35]. Chronic nighttime administration of melatonin significantly extended the life-span of mice and increased their immunocompetence [36, 37]. A recent report indicated that the synthesis of melatonin in mitochondria may be a key aspect of indole's role in ageing [14].

3. Senior Patients Are More Susceptible to the Side Effects of Chemotherapy

Senescence gradually restricts the functional reserve of multiple organ systems and affects the pharmacokinetics and pharmacodynamics of chemotherapy drugs, which may affect both the efficacy and the toxicity of chemotherapy [38]. The rate of functional complications of chemotherapy increases with age, including chronic cardiomyopathy, myelosuppression, nephrotoxicity, neutropenic infections, and chronic peripheral neuropathy [38]. Interestingly, there is a considerable overlap in the common biological changes that occur in normal ageing and chemotherapy treatment [39]. As the cause or consequence of mitochondrial dysfunction, oxidative stress is one of the main driving factors. Increasing reactive oxygen species (ROS) and reactive nitrogen species (RNS) levels occur in ageing and age-related diseases, which were also found in chemotherapy treatment [40]. Besides, ageing is related to cellular senescence, DNA damage, inflammation, mitochondrial dysfunction, and telomere length shortening, and chemotherapy is also similarly associated with all of these processes [39]. Pinder et al. demonstrated that there was a statistically significant increase in the risk of congestive heart failure in senior women who received anthracyclines [41]. The accumulation of cisplatin in the kidney of elderly mice was higher than that of young mice, which was highly correlated with the age-dependent sensitivity of cisplatin-induced nephrotoxicity. In addition, the changes in the inflammatory response and antioxidant signals of the elderly kidney led to the age-dependent susceptibility to kidney injury [42]. It was also indicated that senior patients are more susceptible to experience cognitive decline associated with chemotherapy for breast cancer than younger patients [43, 44]. Senescence appears to interact with cognitive reserve and increases the risk of cognitive decline after chemotherapy [43]. The above studies have shown that the biological processes of the ageing body's response to chemotherapy and degenerative changes overlap with each other, thus raising the hypothesis that ageing may increase the side effects of chemotherapy.

4. The Mitochondrial Protective Role of Melatonin in the Context of Chemotherapy Drug-Induced Toxicity in Ageing

Mitochondrial dysfunction has been identified as an important event in chemotherapy-related toxicity in ageing [45, 46]. The mitochondrion is an organelle for ATP production and determines cell fate [30]. An important feature of

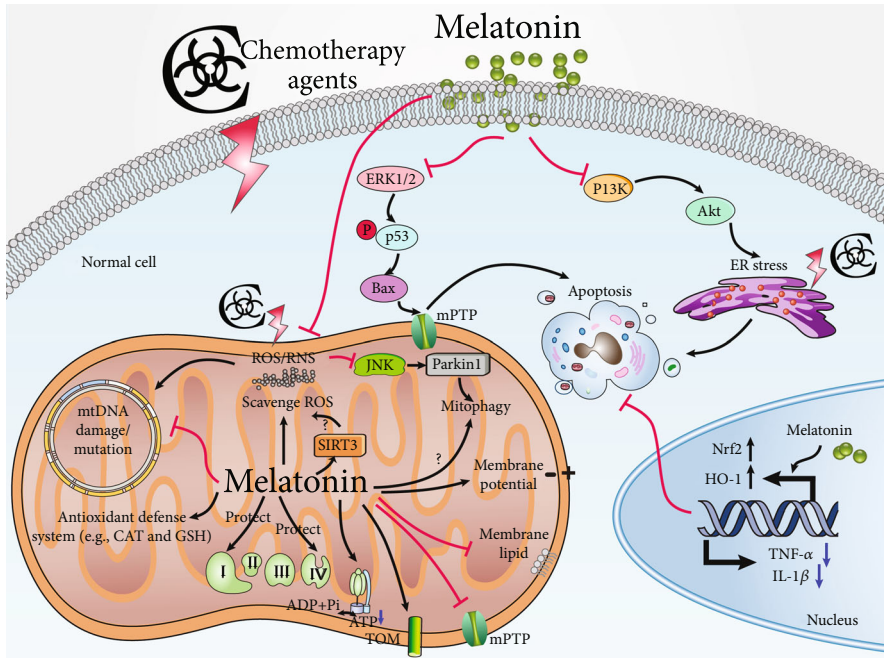

Figure 1: The mechanisms underlying cytoplasmic organellar dysfunction after chemotherapy and melatonin's protective effects under these conditions. Melatonin reverses chemotherapy-induced ER stress, as well as nucleus and mitochondrial dysfunction. In the mitochondrion, chemotherapy drugs lead to electron leakage and excessive free radical production. The ROS directly causes oxidative damage to the mitochondrial respiratory chain, further resulting in elevated electron leakage, free radical production, and ATP depletion. Moreover, ROS injures mitophagy, mtDNA, and the mitochondrial membrane structure (TOM complex reduction and mitochondrial membrane lipid peroxidation increases and elevates mPTP opening), leading to membrane potential loss and proapoptosis factor release. Apart from directly scavenging free radicals, melatonin protects against mtDNA damage/mutation, activates the antioxidant defense system, activates SIRT3 to scavenge ROS, and upregulates the TOM complex, the entry gate for the majority of precursor proteins that are imported into the mitochondria. However, the role of melatonin in mitophagy is less clear. Melatonin inhibits chemotherapy-induced stimulation of ERK1/2, followed via enhanced phosphorylation of p53 by the upregulation of genes such as Bax, thus resulting in mPTP opening. In the nucleus, melatonin upregulates Nrf2 and HO-1 expression and decreases TNF-α and IL-1β levels, thus contributing to cell protection. In the ER, melatonin reverses chemotherapy-induced ER stress via the inhibition of the PI3K/AKT pathway. As a consequence, melatonin protects diverse organs after chemotherapy. Abbreviations: Akt, protein kinase B; ATP, adenosine triphosphate; IL-1β, interleukin-1β; mPTP, mitochondrial permeability transition pore; ER, endoplasmic reticulum; ERK, extracellular regulated protein kinases; HO-1, heme oxygenase-1; JNK, c-Jun-N-terminal kinases; mtDNA, mitochondrial DNA; PI3K, phosphoinositide 3 kinase; ROS, reactive oxygen species; SIRT3, silent information regulator 3; SP, substance P; TOM, translocases in the outer membrane.

mitochondria is that they are closely related to the senescence process, including generation of free radicals, production of ROS and RNS, amplification of damage caused by free radicals, and regulation of the apoptotic pathway due to interference with mitochondrial membrane potential and susceptibility to oxidative/nitrosative stress [1]. Furthermore, chemotherapy drugs often produce free radicals, which are a key cause of cell death [47]. ROS damage mitochondrial DNA (mtDNA), leading to the activation of the extrinsic apoptotic pathway (Figure 1) [48]. In addition, ROS interfere with calcium homeostasis and induce lipid peroxidation, reducing mitochondrial redox potential and opening the mitochondrial permeability transition pore (mPTP), thus resulting in membrane potential loss and cytochrome c release [48]. Excessive free radicals directly cause oxidative damage to the mitochondrial respiratory chain and metabolic enzymes, which further contribute to more electron leakage and free radical production (Figure 1) [49, 50]. Moreover, DOX reduces or inhibits the activity of the cellular antioxidant defense system that further leads to the oxidative stress [46, 51]. This leads to additional molecular damage thereby generating a vicious cycle that eventually leads to cell death [52, 53].

To reduce cell death, it is essential to break the vicious circle between free radical production and mitochondrial injury [14]. Melatonin, an effective free radical scavenger, is highly concentrated in mitochondria, which enhances its ability to resist mitochondrial oxidative damage [54, 55]. However, senescence can lead to the deterioration of circadian rhythmicity; thus, it causes disorders in melatonin synthesis [1, 56]. A certain amount of evidence has been accumulated showing that melatonin supplementation counteracts the exacerbating effects of senescence by inhibiting oxidative stress, mitochondrial dysfunction, and inflammation [1, 57]. Various studies have demonstrated that melatonin protected against mitochondrial dysfunction because of its direct free radical-scavenging activity and its indirect antioxidant properties [30, 58]. Melatonin effectively combats chemotherapy-mediated mitochondrial dysfunction by increasing the expression and activity of the mitochondrial respiration chain complexes (complexes I and IV), thereby increasing ATP production (Figure 1) [59]. When melatonin

inhibits oxidative stress, lipid peroxidation is repressed and the mitochondrial membrane structure is protected [60]. It is also documented that melatonin regulates mitochondrial membrane permeability by modulating the translocases in the outer membrane (TOM) complex and mPTP activity (Figure 1) [61, 62]. In consequence, melatonin protects the mitochondrial membrane potential and inhibits the release of proapoptotic proteins [63, 64].

Compared with other antioxidants, the most attractive property of melatonin is that its metabolites also regulate the mitochondrial redox status by scavenging ROS and RNS and maintaining bioenergetic homeostasis and their antiapoptotic effects [30, 65]. Melatonin and its metabolites form a free radical-scavenging cascade, which makes melatonin highly effective even at low concentrations and can protect the organs against radical-induced damage continuously [66]. Furthermore, cyclic 3-hydroxymelatonin, a major metabolite of melatonin, protects mitochondrial cytochrome c against free radical-induced damage, and therefore it may inhibit apoptosis induced by oxidative cytochrome c release from mitochondria [67].

Additionally, compared with other antioxidants, melatonin has a protective effect on the heart without affecting DOX's antitumor activity, which is a unique characteristic of melatonin [68, 69]. Interestingly, some beneficial effects of melatonin on mitochondrial respiration are independent of its antioxidant activity but are related to its high redox potential [70]. This unique property allows melatonin to interact with the complexes of the electron transport chain, where it donates or accepts electrons thereby increasing electron flow in a way that other antioxidants do not [71]. Melatonin also exerts indirect protective effects through other pathways that do not involve radical scavenging. Melatonin enhances antioxidant defense systems by stimulating gene expression and the activity of antioxidants [59, 72] and improving the de novo synthesis of glutathione (GSH) by promoting the activity of gamma-glutamylcysteine synthetase [73].

Recent studies have revealed that melatonin inhibits the production of nitric oxide synthase (NOS) at the level of NOS gene transcription [74, 75]. Additionally, it was also shown that melatonin could selectively reduce mitochondria-induced NOS levels in the heart, thereby improving mitochondrial function in patients with sepsis [76]. In addition to the above effects, melatonin also maintains a healthy mitochondrial network by regulating mitochondrial biogenesis, dynamics, autophagy and mitophagy, mitochondrial fission and fusion, and its action on mitochondrial sirtuin activity [30, 77].

5. The Role of Melatonin in Anthracycline-Induced Organ Failure

The anthracyclines are the most widely used anticancer drugs in the treatment of human cancers, including their use in acute leukemia, Hodgkin's and non-Hodgkin's lymphoma, and breast cancer [78]. Like all other anticancer agents, anthracyclines are double-edged swords because they may result in the development of tumor cell resistance, and they are toxic to healthy tissues, especially the heart [78]. DOX and DNR are the original anthracyclines isolated from the pigment-producing bacterium *Streptomyces peucetius* in the 1960s. DOX differs from DNR by a single hydroxyl group, which has spurred researchers worldwide to identify five DOX/DNR analogs, one (idarubicin) of which is available in the United States [78]. A number of studies have indicated that DOX-induced cardiotoxicity is based on elevated oxidative stress via increasing ROS and lipid peroxidation, together with reducing the antioxidants and sulfhydryl groups [79, 80]. Compared with other organs, the heart has abundant mitochondria which are sources and targets of ROS, so that it is vulnerable to DOX-induced oxidative damage [45]. Moreover, the heart consumes more oxygen and has limited antioxidant defense systems compared with other tissues [81]. Thus, cardiomyocytes expressed low levels of catalase (CAT) and that antioxidant selenium-dependent glutathione- (GSH-) peroxidase-1 is inactivated when exposed to DOX, thereby reducing cytosolic antioxidant Cu-Zn superoxide dismutase [46, 51].

Although many approaches are designed to prevent or mitigate DOX toxicity, there are limits to the ability of these therapies to protect organs from injury, especially the heart. In contrast, the antioxidant melatonin has been effectively used to reduce cardiomyocyte damage [82, 83]. Melatonin plays a cardioprotective role against DOX-induced damage, including by elevating the ST segment and reducing the R-amplitude, decreasing the serum levels of cardiac injury markers, protecting antioxidant enzyme activity, reducing lipid peroxidation, and altering lipid profiles in the serum in rats (Table 1) [84]. Melatonin ameliorated oxidative stress by controlling iron and binding protein levels in DOX-treated rats [85]. Moreover, melatonin promotes the activity of protective antioxidative enzymes in myocardial cells subjected to the action of DOX. The protective effect is due to increased GSH levels and stimulation of CAT activity by melatonin in cardiomyocytes during DOX exposure (Table 1) [86]. Myocardial zinc accumulation may protect against DOX-induced oxidative stress, and melatonin inhibits the DOX-induced drop in plasma zinc levels, indicating that melatonin may have an action in maintaining plasma zinc levels [87]. Additionally, cardiac function was improved and lipid peroxidation was reduced after melatonin treatment, indicating that melatonin has a protective effect on DOX toxicity by attenuating lipid peroxidation (Figure 2) [88–90]. DOX binds to cardiolipin to form an irreversible complex; thus, it inhibits oxidative phosphorylation and prevents cardiolipin from acting as a cofactor of mitochondrial respiratory enzymes [91, 92]. Melatonin protects the mitochondria via inhibiting cardiolipin oxidation that would facilitate the mPTP, resulting in cell death [93]. Melatonin combined with DOX successfully inhibited DOX-induced apoptosis through AMPK-dependent mechanisms, indicating its potential as a cell death protectant in DOX chemotherapy [94, 95]. Another study reported that the protective effect of melatonin was due in part to inhibiting DOX-induced cardiomyocyte apoptosis by preventing DNA fragmentation (Figure 2) [30, 96, 97]. Furthermore, melatonin not only resists cardiotoxicity induced by DOX therapy, but it also enhances its antitumor

Table 1: Protective effects and mechanisms of melatonin action against the side effect induced by chemotherapy agents.

Chemotherapy agents	Experimental studies	Drugs and doses	Administration route	Outcomes	Underlying mechanisms	References
Anthracyclines	NIH3T3 cells	DOX (2.6 μM for 24 h) + melatonin (1 μM for 24 h)		Countered apoptosis generated by DOX alone	AMPK-Ppar gamma-dependent mechanisms	[94]
	Male Wistar-Albino rats	DOX (18 mg/kg) + melatonin (10 mg/kg/day, 7 days)	Intraperitoneal	Protected the heart against DOX-induced cardiotoxicity	Melatonin treatment prevented the elevation of the ST segment and R amplitude, as well as the elevation of cardiac injury markers and lipid peroxidation, and it prevented the decrease of antioxidant enzyme activity	[84]
	Male Sprague-Dawley rats	DOX (10 mg/kg) + melatonin (15 mg/kg)	Intraperitoneal	Melatonin controlled oxidative stress and modulated iron, ferritin, and transferrin levels	Ameliorated oxidative stress by controlling iron and binding protein levels	[85]
	Buffalo strain rats	DOX (2.5 mg/kg) + melatonin (20 mg/kg)	Intraperitoneal	Melatonin stimulated the activity of protective antioxidative enzymes in myocardial cells of rats	Melatonin increased GSH levels and stimulated CAT activity	[86]
	Sprague-Dawley rats	DOX (15 mg/kg) + melatonin (84 mg/kg)	Intraperitoneal	Melatonin maintained the plasma zinc levels	Zinc accumulation protects against oxidative stress and melatonin inhibited the DOX-induced decrease in plasma zinc levels	[87]
	Male Wistar rats	DOX (7.5 mg/kg) + melatonin (6.0 mg/kg)	Intraperitoneal	Melatonin prevented DOX-induced lipid peroxidation in rat liver	Melatonin-induced gene expression changes	[87]
	Male Wistar rats	Melatonin (90 mg/kg)	Intraperitoneal	Cardiac function was improved and lipid peroxidation was decreased	Melatonin provides protection against DOX toxicity via an attenuation of lipid peroxidation	[88]
	Ehrlich ascite carcinoma-bearing mice	DOX (4 mg/kg/week, 2 weeks) + melatonin (5 mg/kg/day, 15 days)	Intraperitoneal	Melatonin protected against cardiotoxicity and enhanced its antitumor activity to a more significant extent than did vitamin E	The cardiac contents of total protein, GSH, and SOD were increased, while the cardiac content of MDA was decreased	[98]
	Male Wistar rats	Epirubicin (10 mg/kg) + melatonin (200 mg/kg)	Intraperitoneal	Melatonin protected against cardiotoxicity induced by epirubicin	Melatonin was partially attributed to the suppression of epirubicin-induced nitrozative stress	[101]

Table 1: Continued.

Chemotherapy agents	Experimental studies	Drugs and doses	Administration route	Outcomes	Underlying mechanisms	References
Alkylating agents	HBE cells	Yperite or with MEC + melatonin (100 μM)		Melatonin prevented mustard-induced anoikis	Inhibition of caspase-dependent mitochondrial permeability transition	[120]
	NMRI mice	CP (200 mg/kg) + melatonin at different concentrations (2.5, 5, 10, and 20 mg/kg)	Intraperitoneal	Melatonin prevented CP-induced oxidative toxicity in mouse lung tissues	The activities of the antioxidant defense system, ROS scavenging, and free radical quenching were increased	[106]
	Female Wistar rats	CP (75 mg/kg) + melatonin (5 mg/kg)	Intraperitoneal	Melatonin significantly improved bladder symptoms and histological damage due to CP-induced cystitis	Diminishing bladder oxidative stress, blocking iNOS and peroxynitrite production, upregulating HO-1, and downregulating the expression of SP	[107]
	Male Sprague-Dawley rats	CP (150 mg/kg) + melatonin (10 mg/kg)	Intraperitoneal	Melatonin treatment reduced bladder damage and apoptosis	Upregulating Nrf2 and nuclear transcription factor NF-κB expression	[109]
	Male ICR mice	CP (150 mg/kg) + melatonin (10 mg/kg)	Intraperitoneal	Melatonin cotreatment prevented the development of hyperplastic urothelium	Decreasing proliferation and apoptotic indices and causing the higher differentiation state of superficial urothelial cells	[110]
	Male Wistar albino rats	CP (100 mg/kg) + melatonin (10 mg/kg)	Intraperitoneal	Melatonin may reduce CP-induced testicular damage	The antioxidative properties of indoleamine existed in the chemical structure	[111]
	NMRI mice	CP (60 mg/kg) + melatonin (2.5, 5, 10, and 20 mg/kg)	Intraperitoneal	Melatonin has potent antigenotoxic effects and suppression of chromosome aberrations	Scavenging of free radicals and increased antioxidant status	[112]
	Albino Wistar rats	CP (75 mg/kg) + melatonin (40 or 100 mg/kg)	Intraperitoneal	Melatonin resulted in global ANS activity elevation, with a marked sympathetic tone predominance	Melatonin modulates autonomic activity via nonreceptor mechanisms	[114]
	Male Wistar rats	HN2 (0.5 mg/kg) + melatonin (20 mg/kg or 40 mg/kg)	Intraperitoneal	Melatonin reduced mustard-induced toxicity in the lungs	Melatonin restored oxidative and nitrosative stress markers in a dose-dependent manner	[117]
	Male Sprague-Dawley rats	MEC (3.5 mg/kg) + melatonin (100 mg/kg)	MEC via transdermal route and melatonin via intraperitoneal route	Melatonin has anti-inflammatory properties, as well as antioxidant properties	These increases and elevated NOx levels were ameliorated	[196]

Table 1: Continued.

Chemotherapy agents	Experimental studies	Drugs and doses	Administration route	Outcomes	Underlying mechanisms	References
Platinum	Hepatocellular carcinoma HepG2 cells	Melatonin (1 mM) + cisplatin (20 μM)		Melatonin attenuated cisplatin-induced HepG2 cell death	Regulation of mTOR and ERCC1 expressions	[130]
	SK-LU-1 cell line	Cisplatin (11 and 4 μM) + melatonin (1 or 2 mM)		Melatonin enhanced cisplatin-induced cytotoxicity and apoptosis	Elevating mitochondrial membrane depolarization, activating caspases-3/7, and inducing cell cycle arrest in the S phase	[132]
	SH-SY5Y cells	Melatonin (10 μM, 50 μM) + Oxa (100 μM)		Melatonin protects against the oxaliplatin-induced pain and neuropathic deficits	Preventing the loss of mitochondrial membrane potential (Ψm), inhibiting Bcl-2/Bax ratio and releasing sequestered cytochrome c, and promoting neuritogenesis	[136]
	HT-29 cells	Oxa (0-50 μM) + melatonin (15 and 30 μM)		Melatonin improved mitochondrial electron transport chain function and maintained cellular bioenergetics by improving the ATP levels	Ameliorating nitrooxidative stress and preventing nitrosylation of proteins and loss of antioxidant enzymes	[135]
	SH-SY5Y cells	Oxa (10 μM, 50 μM, and 100 μM) + melatonin (10 μM)		Melatonin attenuated oxaliplatin-induced apoptosis	Inhibition of GSH depletion and Mcl-1 downregulation	[136]
	Male Sprague Dawley rats	Cisplatin (7 mg/kg) + melatonin (5 mg/kg)	Intraperitoneal	Melatonin markedly reduced renal cytotoxicity and DNA fragmentation	Scavenge hydroxyl radical (•OH) directly	[123]
	Male Wistar rats	Melatonin (4 mg/kg, 10 days) + cisplatin (7 mg/kg)	Intraperitoneal	Melatonin suppressed cisplatin-induced nephrotoxicity	Increasing Nrf2 accumulation in the nuclear fraction and increasing the expression of HO-1	[122]
	Female Swiss mice	Melatonin (5, 10, or 20 mg/kg) + cisplatin (5 mg/kg)	Intraperitoneal	Melatonin effectively protected the ovaries against cisplatin-induced damage	The MT1 receptor and melatonin antioxidant effects	[125]
	Female CD-1 mice	Cisplatin (2 mg/kg) + melatonin (15 or 30 mg/kg)	Intraperitoneal	Melatonin attenuated cisplatin-induced follicle loss	Preventing the phosphorylation of PTEN/AKT/FOXO3a pathway	[126]

Table 1: Continued.

Chemotherapy agents	Experimental studies	Drugs and doses	Administration route	Outcomes	Underlying mechanisms	References
	Wistar rats	Melatonin (10 mg/kg) + Oxa (4 mg/kg)	Intraperitoneal	Melatonin ameliorated the mitochondrial lipid peroxidation levels and protein carbonyl content	Modulating altered nonenzymatic and enzymatic antioxidants and complex enzymes of mitochondria	[54]
	Male Sprague-Dawley rats	Melatonin (20 mg/kg + Oxa 5 mg/kg)	Intraperitoneal	Melatonin had anti-inflammatory and antiallodynia effects	Melatonin inhibited synthesis of inflammatory mediators	[138]
Antimetabolite	Male Wistar rats	Melatonin (20 and 40 mg/kg) + MTX (7 mg/kg)	Intraperitoneal	Melatonin reduced small intestinal damage and ameliorates MTX-induced enteritis	Attenuating oxidative stress and restoring the activities of the antioxidant enzymes	[141]
	Male Wistar rats	Melatonin (20 and 40 mg/kg) + MTX (7 mg/kg)	Intraperitoneal	Melatonin protected against MTX-induced small intestinal damage	Attenuation of nitrosative stress, protein tyrosine nitration, and PARP activation	[142]
	Male Wistar rats	MTX (7 mg/kg) + melatonin (40 mg/kg)	Intraperitoneal	Melatonin reduced renal damage via antioxidant and anti-inflammatory activities	Reduction of oxidative stress and alteration in the activity of antioxidant enzymes, as well as elevation in myeloperoxidase activity	[143]
	Male Sprague Dawley rats	MTX (13.4 mg/kg) + melatonin (10 mg/kg)	Intraperitoneal	Melatonin prevented MTX-induced hepatotoxicity	Through their antioxidant- and radical-scavenging activities	[145]
Mitotic inhibitors	Sprague Dawley rats, the 50B11 immortalized DRG neuronal stem cell line	Paclitaxel (100 μM) + melatonin (1 μM)	Intraperitoneal	Melatonin protected against neuropathic pain and limits paclitaxel-induced mitochondrial dysfunction in vitro	Limiting the development of mechanical hypersensitivity	[153]
Molecular-targeted agents	Male Sprague-Dawley rats	Trastuzumab (10 mg/kg) + melatonin (10 mg/kg, 2 days)	Intraperitoneal	Melatonin was effective in preventing trastuzumab-induced cardiotoxicity	Reversing oxidative stress markers	[156]

Abbreviations: CAT, catalase; CP, cyclophosphamide; DOX, doxorubicin; GSH, glutathione; MEC, mechlorethamin; MTX, methotrexate; Oxa, oxaliplatin; PARP, poly(ADP-ribose)-polymerase.

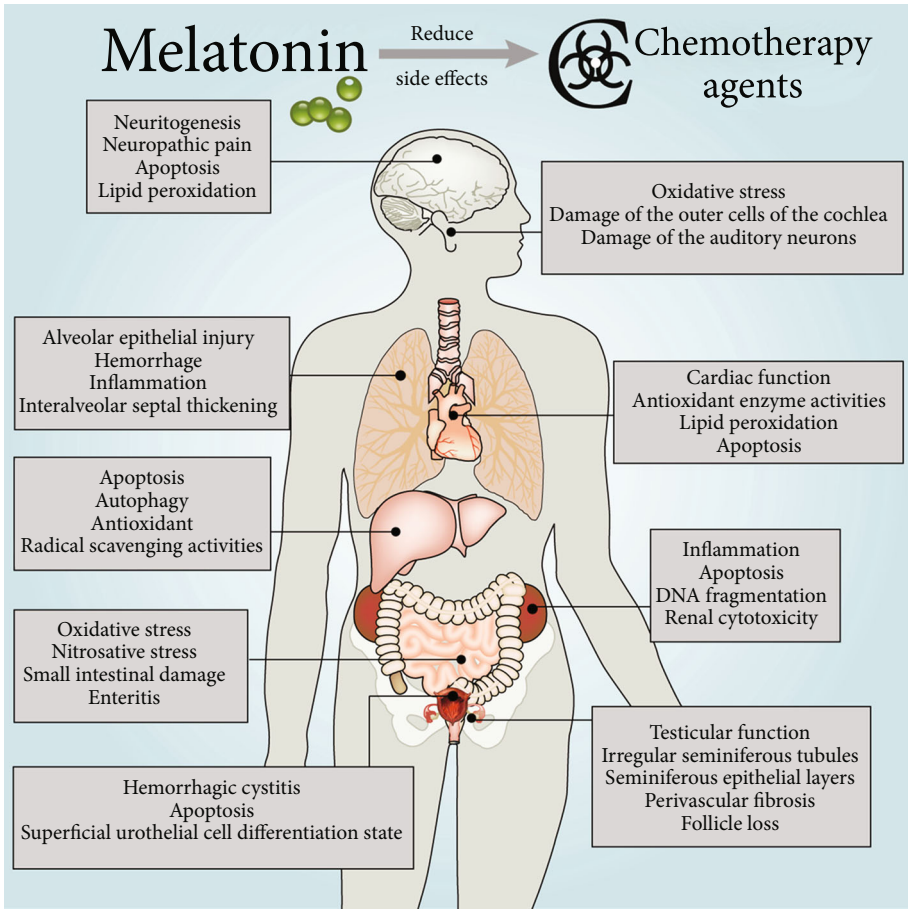

Figure 2: Protection of melatonin against chemotherapy drug-induced damage in various organs.

activity more than vitamin E [98]. DOX causes serious injury when extravasated. Kesik et al. found that melatonin ameliorated DOX-induced skin necrosis in rats. Moreover, it could enhance the sensitivity of tumor to DOX *in vivo* [22, 99]. Melatonin administered in parallel with DNR reduced the proportion of apoptotic cardiomyocytes [100]. Epirubicin increased nitrosative stress only in heart tissue, and the cardioprotective effect of melatonin partially resulted from its suppression of epirubicin-induced nitrosative stress [101]. These results reveal that melatonin has a protective effect against epirubicin-induced cardiotoxicity [101].

6. The Role of Melatonin in Alkylating Agent-Induced Organ Failure

6.1. Cyclophosphamide. CP is most widely used an alkylating agent, and its antineoplastic and immunomodulating activities have been approved for early and advanced breast cancer [102]. CP alkylates DNA, forming DNA-DNA cross-links; thus, it inhibits DNA synthesis and causes cell death [103]. It was also shown that CP exerts its toxic effect via enhancing free radicals and other reactive oxygen species that cause lipid peroxidation and cell damage while melatonin provided an antioxidant defense with a highly chemoprophylactic effect on CP-induced cytotoxicity [104, 105]. Oxidative stress markers and the corresponding adaptability of the antioxidant defense system were increased after CP administration, indicating that oxidative stress plays a central role in CP-induced injury to the lung. Melatonin prevents CP-induced oxidative toxicity in pulmonary tissue [106]. Furthermore, by reducing bladder oxidative stress and blocking the production of nitric oxide synthase and peroxynitrite, melatonin upregulates heme oxygenase-1 (HO-1) and downregulates substance P (SP) expression, significantly improving bladder symptoms and lowering histological damage in CP-induced cystitis in rats (Table 1) [107, 108]. Another work reported that melatonin administration decreased bladder injury and apoptosis due to the upregulation of Nrf2 and nuclear transcription factor NF-κB expression [109]. Moreover, melatonin cotreatment inhibited the development of hyperplastic urothelium, statistically significantly reduced cell proliferation and apoptosis index, and promoted the differentiation of superficial urothelial cells after CP treatment (Figure 2) [110]. CP caused spermatic tubule malformation, reduced the epithelium of spermatic tubules, and caused significant maturation stagnation and perivascular fibrosis [58]. Melatonin significantly improved the histopathologic appearance of a CP-damaged testis, indicating that the protective effect of melatonin on CP-induced testicular injury may be due to

the antioxidant properties of indoleamine [58, 111]. Additionally, melatonin had potent antigenotoxic effects and suppressed chromosome aberrations against CP-induced toxicity in mice, which may relate to the scavenging of free radicals and elevated antioxidant status [112, 113]. Interestingly, the treatment of CP-induced hemorrhagic cystitis in rats with melatonin is characterized by the increased activity of the global autonomic nervous system (ANS) and a significant predominance of sympathetic tone, suggesting that melatonin may regulate autonomic activity through nonreceptor mechanisms [114].

6.2. Nitrogen Mustard. Nitrogen mustards, also known as DNA alkylating agents, are an important class of drugs for cancer treatment [115]. These anticancer drugs are used effectively in myelogenic leukemia; Hodgkin disease; lung, testicle, ovarian, and breast cancers; and several lymphomas [116]. Nonetheless, nitrogen mustards are highly reactive and lack selectivity; thus, they produce several adverse side effects [115]. Accumulation of inflammatory cells and increased proinflammatory cytokines, reactive oxygen species, nitric oxide, and peroxynitrite contribute to the pathogenesis of mustard-induced toxicity. Mechlorethamin (MEC), a nitrogen mustard, can result in alveolar epithelial injury, hemorrhage, inflammation, edema, and interalveolar septal thickening in lung tissues. Melatonin has anti-inflammatory properties, has the documented ability to alleviate mustard-induced toxicity, and acts as an iNOS inhibitor and a peroxynitrite scavenger in the lungs [117, 118]. Moreover, both inflammation and oxidative stress may be mechanisms in MEC-induced nephrotoxicity. TNF-α and IL-1β levels enhanced markedly with MEC application; melatonin ameliorated these increases and elevated NOx levels in kidney tissue. This supports the opinion that melatonin has anti-inflammatory and antioxidant properties [119]. Suppression of the mitochondrial pathway by melatonin significantly inhibited mustard-induced anoikis, indicating that suppression of caspase-dependent mitochondrial permeability transition preserves airway epithelial cells from mustard-induced apoptosis [120].

7. The Role of Melatonin in Platinum-Induced Organ Failure

7.1. Cisplatin. Cisplatin is widely used as a chemotherapeutic agent for the treatment of various malignant tumors in pediatric and adult patients, including non-small-cell lung cancer (NSCLC) and breast, testicular, and ovarian carcinomas [121]. However, the use of cisplatin is limited by its serious side effects such as nephrotoxicity and ototoxicity [122]. The decrease of antioxidant status induced by cisplatin results in the disorders of antioxidant defense against free radical damage [122]. Melatonin and its metabolites protect against cisplatin toxicity [123]. Melatonin directly scavenges the highly toxic hydroxyl radicals (•OH) and significantly attenuates renal cytotoxicity and DNA fragmentation induced by cisplatin [123, 124]. Melatonin treatment promoted the accumulation of Nrf2 and increased the expression of HO-1 in the cytosolic fraction, indicating that melatonin inhibits cisplatin-induced nephrotoxicity by activating the Nrf2/HO-1 pathway (Table 1) [122]. Cisplatin exhausts the dormant follicle pool in mouse ovaries via excessive activation of the primordial follicles without inducing follicular apoptosis. Pretreatment with melatonin effectively preserved the ovaries from cisplatin-induced injury, an effect mediated by the MT1 membrane melatonin receptor [125]. Furthermore, melatonin reduces cisplatin-induced follicle loss via blocking the phosphorylation of the PTEN/AKT/-FOXO3a pathway (Figure 2) [126]. Cisplatin-treatment markedly impaired testicular function, but combined treatment with melatonin prevented the testicular toxicity in rats [111, 127]. Thus, melatonin is a potential therapeutic agent for protecting the reproductive system during chemotherapy.

The mechanism of the ototoxicity caused by cisplatin molecular damage is based on the generation of ROS, which interferes with the physiology of the organ of Corti. As an antioxidant and immune modulator, melatonin has been used to treat cisplatin ototoxicity using transtympanic local application in low doses [128, 129]. Melatonin attenuates cisplatin-induced cell death and reduced phosphorylated p53 apoptotic protein, cleaved caspase 3, and Bax levels, while enhancing the antiapoptotic Bcl-2 gene and protein expression [130]. It also reversed the effects of cisplatin through inhibiting the overexpression of mTOR and ERCC 1 and increasing the expression levels of Beclin-1 and microtubule-associated protein-light chain3-II, bringing about the development of intracellular autophagosomes [130]. These findings suggest that melatonin alleviated cisplatin-induced cell death in HepG2 cells by balancing the roles of apoptotic- and autophagy-related proteins [130].

Chemotherapy with cisplatin also has various vascular side effects. A recent report indicates that melatonin treatment protects the aorta during cisplatin-based chemotherapy [131]. Melatonin increased cisplatin-induced cytotoxicity and apoptosis in human lung adenocarcinoma cells [132]. Melatonin combined with chemotherapy had no effect on survival and adverse events in patients with advanced NSCLC, but showed a trend of improving health-related quality of life [133], which suggests that melatonin has the potential to treat NSCLC in combination with cisplatin.

7.2. Oxaliplatin. Oxaliplatin is a third-generation platinum compound which is active against colorectal growth, but its clinical application is limited attributed to peripheral neuropathy progression [134]. Mitochondrial dysfunction has been considered to be the main pathological mechanism of oxaliplatin-induced neurotoxicity, and the suppression of autophagy may also aggravate the death of neurons [135]. Melatonin has neuroprotective roles in oxaliplatin-induced peripheral neuropathy [135]. Moreover, melatonin protects against the oxaliplatin-induced pain and neuropathic deficits in rats [54, 135]. Melatonin suppressed the loss of mitochondrial membrane potential and Bcl-2/Bax ratio, as well as the release of sequestered cytochrome c, while promoting neuritogenesis in oxaliplatin-stimulated neuro-2a cells [135, 136]. Melatonin lowered oxaliplatin-induced mitochondrial lipid peroxidation levels and protein carbonyl content and regulated the changes of mitochondrial nonenzymatic and

enzymatic antioxidants and complex respiratory enzymes [54]. It also improved oxaliplatin-mediated nitrooxidative stress to prevent nitrosylation of proteins and loss of antioxidant enzymes; thus, it ameliorates the function of the mitochondrial electron transport chain and maintains the biological energy of cells by increasing ATP levels [135]. The protective effects of melatonin are also partially due to the prevention of oxaliplatin-induced neuronal apoptosis via promoting the autophagy pathway of the peripheral and dorsal root ganglia (DRG) [135]. Melatonin was also found to inhibit proteolytic activation of caspase 3, inactivation of poly(ADP-ribose) polymerase, and DNA damage, thus allowing SH-SY5Y cells resistant to apoptotic cell death [136]. A recent study shows that melatonin reduces oxaliplatin-induced apoptosis via preventing GSH depletion and Mcl-1 downregulation in renal carcinoma Caki cells [137]. It has been documented that the neuroinflammatory response in the dorsal horn of the spinal cord is a key factor in oxaliplatin-induced pain. Melatonin has been reported to have anti-inflammatory and antiallodynia effects in preclinical and clinical pain studies [138].

8. The Role of Melatonin in Antimetabolite-Induced Organ Failure

MTX, a structural analogue of folic acid, is one of the most effective and potent anticancer drugs used for leukemia and other malignancies [139]. It is an important component in the treatment regime of acute lymphoblastic leukemia, lymphoma, osteosarcoma, and breast cancer, as well as in head and neck cancer [139]. However, its high toxicity, including gastrointestinal, renal, nervous, hepatic, and bone marrow toxicity, limits its use. The main toxic effects of MTX are intestinal injury and enterocolitis resulting in malabsorption and diarrhea [140], which are the major causes of morbidity in children and adults [141]. It is demonstrated that melatonin reduces MTX-induced oxidative stress and small intestinal damage in rats, indicating that supplementation with exogenous melatonin can significantly attenuate MTX-induced intestinal injury, and may be beneficial to the improvement of human enteritis induced by MTX (Figure 2) [141]. Moreover, a preclinical study reported that melatonin protected against MTX-induced small intestinal damage through reducing nitrosative stress, protein tyrosine nitration, and poly(ADP-ribose)-polymerase (PARP) activation (Table 1) [142]. Melatonin pretreatment attenuated MTX-induced oxidative stress, changed antioxidant enzyme activity, and improved myeloperoxidase activity, suggesting that melatonin may decrease renal damage via antioxidant and anti-inflammatory actions [143, 144]. Melatonin prevents MTX-induced hepatotoxicity through antioxidant- and radical-scavenging activities in male rats [145]. MTX treatment brings about enhanced malondialdehyde levels and myeloperoxidase activity and reduces GSH levels in the blood, liver, and kidney. These effects were reversed by melatonin, suggesting that melatonin may have a high therapeutic benefit when used with MTX [146].

9. The Role of Melatonin in Mitotic Inhibitor-Induced Organ Failure

Taxanes, including paclitaxel and docetaxel, are commonly used chemotherapeutic agents for a variety of malignancies [147, 148]. Paclitaxel has a wide range of anticancer effects. In the process of cell division, paclitaxel inhibits cell cycle and induces cell death by stabilizing microtubules and interfering with microtubule disassembly [149]. In addition to ameliorating disease-specific outcomes, taxanes also can cause considerable morbidity. The most common and particularly troublesome toxicity is taxane-induced peripheral neuropathy [150]. Melatonin plays a beneficial role in taxane-related neuropathy [151, 152]. Patients treated with melatonin during taxane chemotherapy had a lower incidence of neuropathy, suggesting that melatonin may be useful in preventing or reducing taxane-induced neuropathy and in maintaining quality of life [151]. Moreover, melatonin protected rats from paclitaxel-induced neuropathic pain and mitochondrial dysfunction *in vitro* (Figure 2) [153]. Mitochondrial dysfunction associated with oxidative stress in peripheral nerves has been considered as a potential mechanism [153]. The potential of melatonin to decrease mitochondrial injury and neuropathic pain due to paclitaxel has been documented [153].

10. The Role of Melatonin in Molecular-Targeted Agent-Induced Organ Failure

Trastuzumab, a humanized monoclonal antibody that can be used against the extracellular domain of human epidermal growth factor receptor 2 (HER2), is an important component of the adjuvant therapy and metastasis therapy for HER2-positive breast cancers. The herceptin adjuvant study reported that adjuvant trastuzumab treatment for 1 year improves disease-free survival and overall survival in patients with HER2-positive early breast cancer [154]. However, its side effects limit the use of adjuvant trastuzumab treatment, including cardiotoxicity, fever and chills, shortness of breath, muscle weakness, cutaneous rash, diarrhea, and headache [155]. Trastuzumab is an effective agent for the treatment of various neoplastic diseases. Oxidative stress markers and serum CK-MB levels were highly enhanced after treatment with trastuzumab; these changes were also reversed by melatonin treatment which resulted in near normal levels, which suggested that melatonin is effective in preventing trastuzumab-induced cardiotoxicity (Table 1) [156].

11. Melatonin Enhances the Efficacy of Chemotherapy Agents against Tumors

Mounting evidence indicates that melatonin exerts a variety of anticancer properties at different stages of tumor progression and metastasis [157–160]. Moreover, the combination of melatonin and chemotherapies has been reported to improve the effectiveness of anticancer drugs [23, 161]. Melatonin significantly enhanced the cytotoxicity of the

chemotherapy drugs against cancer cells. Consistently, each of the chemotherapy drugs with melatonin increased the ratio of cells entering mitochondrial apoptosis due to ROS overproduction, mitochondrial membrane depolarization, and highly expanded DNA fragmentation [162, 163]. It was also reported that melatonin does not interfere with the action of DOX on cancer cells but actually enhances the action of the anticancer drug possibly by inhibiting the outflow of P-glycoprotein-mediated DOX from cancer cells [23]. Melatonin potentiates cisplatin-induced apoptosis and cell cycle arrest in human lung adenocarcinoma cells [132]. Costimulation of HeLa cells with cisplatin in the presence of melatonin further increased cellular apoptosis, improved the mitochondrial structure and function, and significantly increased caspase-9-dependent mitochondrial apoptosis [161]. Melatonin inactivated mitophagy via blocking c-Jun-N-terminal kinases (JNK)/Parkin, resulting in the suppression of antiapoptotic mitophagy, indicating that melatonin enhances human cervical cancer HeLa cell apoptosis induced by cisplatin through inhibiting the JNK/Parkin/mitophagy axis [161, 164]. Furthermore, melatonin substantially augmented the 5-FU-mediated inhibition of cell proliferation, colony formation, cell migration, and invasion of colon cancer cells [165]. It was shown that melatonin and 5-FU synergistically induced cell cycle arrest by activating the caspase/PARP-dependent apoptosis pathway [165]. Furthermore, melatonin exaggerated the antitumor role of 5-FU by inhibiting the phosphorylation of the phosphatidylinositol 3-kinase (PI3K)/AKT/iNOS signaling pathways or promoting the translocation of NF-κB p50/p65 from the nuclei to the cytoplasm, abrogating their binding to the iNOS promoter; thus, it inhibits iNOS signaling [165, 166]. Additionally, melatonin intensified the antitumor actions of paclitaxel in the endoplasmic reticulum endometrial cancer cell line, which express MT1 melatonin receptors [167].

12. Potential Future Directions and Conclusions

Senescence is a process of gradual functional deterioration of physiological mechanisms as time goes on. About half of human deaths are linked to ageing-related chronic diseases, including neurological disorders, diabetes, cardiovascular diseases, and cancer [168, 169]. Mitochondrial dysfunction is the main driver of these processes, which occur in ageing and age-related disorders; they were also found in chemotherapy treatment [40]. Mitochondria are major production sites of free radicals and related toxic species [170]. Abnormal mitochondrial function, increased ROS production, damaged mitochondrial DNA, decreased respiratory complex activities, and augmented electron leakage and mPTP opening played key roles in the pathophysiology of chemotherapy agent-induced toxicity in ageing [30]. Consistent with the amphiphilic nature of melatonin, it easily crosses all biological barriers and gains access to all compartments of the cell, and it is highly concentrated in mitochondria, indicating its ability to resist mitochondrial oxidative damage [171, 172]. Melatonin was first implicated in modulating nuclear SIRT1 during the biological process of cancer [173, 174]. SIRT3 indirectly reduces cellular ROS to prevent the cardiac hypertrophic response [175]. Moreover, both MnSOD and catalase levels of SIRT3 transgenic mice were increased, implying that SIRT3 was partly responsible for the enhancement of the antioxidant defense mechanisms of the heart [175]. These evidences potentially indicate that melatonin may have the ability to regulate mitochondrial sirtuins during DOX-induced cardiotoxicity [176]. It is demonstrated that mtDNA lesions caused by ROS or ERK1/2 activation directly induced by DOX, followed by elevated phosphorylation of p53, upregulated genes such as Bax [177]. After melatonin pretreatment, ERK2, phosphorylated p38, HSP-70, phosphorylated p53, c-Jun, and other crucial stress protein levels returned to normal [178]. Additionally, excessive DNA damage and enhanced ROS production induced by DOX, resulting in PARP hyperactivation and energy depletion, promotes necroptosis [179, 180].

Melatonin also activates mitochondrial STAT3 via the SAFE pathway of decreasing myocardial IR damage [181–183]. In cultured neonatal rat cardiomyocytes and isolated rat hearts, melatonin precondition alleviates IR-induced mitochondrial oxidative damage by activating the JAK2/-STAT3 signaling pathway, as well as enhances mitochondrial mitophagy via activating the AMPK-OPA1 signaling pathways [184–187]. Thus, melatonin may protect against chemotherapy agent-induced mitochondrial oxidative damage through similar pathways. Apart from melatonin as an effective free radical scavenger, it also maintains a healthy mitochondrial network by regulating mitochondrial biogenesis, dynamics, and mitophagy [188]. Melatonin has multiple mitochondrial benefits in Alzheimer's disease, by significantly reducing ROS-mediated mitochondrial fission, mitochondrial membrane potential depolarization, and mitochondrial tardiness, thereby stabilizing cardiolipin; collectively, these actions reduce enhanced mitochondria-mediated cell death [189].

It is well documented that DOX causes endoplasmic reticulum (ER) dilation, indicating that DOX may also affect ER function apart from actions in the mitochondrion [190]. ER is involved in protein folding, calcium homeostasis, and lipid biosynthesis [191]. ER stress refers to the accumulation of unfolded proteins induced by oxidative stress, ischemic injury, calcium homeostasis disorders, and/or enhanced expression of folded defective proteins [191]. DOX stimulates the ER transmembrane stress sensor, activating transcription factor 6, while suppressing X-box binding protein 1 expression, a gene downstream of activating transcription factor 6 [190]. The reduced expression of X-box binding protein 1 lowered the ER chaperone glucose-regulated protein 78 level that is crucial in adaptive responses to ER stress [190]. The results of this study revealed that DOX promoted the apoptosis response induced by ER stress without inducing the ER chaperone glucose-regulated protein 78, further elevating ER stress in the hearts (Figure 1). Moreover, doxorubicin activated caspase-12, an ER membrane-resident apoptotic molecule, which leads to cardiomyocyte apoptosis and cardiac dysfunction [190]. Melatonin reverses tunicamycin-induced ER stress by preventing the PI3K/AKT pathway, and it promotes cytotoxic response to DOX via enhancing C/EBP-homologous protein (CHOP) as well as

decreasing surviving in human hepatocellular carcinoma cells [192, 193]. Therefore, in addition to protecting mitochondrial homeostasis, maintaining ER homeostasis may also be an important mechanism for melatonin to participate in antichemotherapeutic drug injury. This is an area where more intensive investigation is warranted.

A number of clinical studies have shown that melatonin treatment improves the efficacy and decreases the side roles of chemotherapy, prolongs survival time, and promotes quality of life for patients [82, 90, 194, 195]. The beneficial effects of melatonin administration are partially results from its direct free radical-scavenging activity and its indirect antioxidant properties [30]. Increasing reports on the role of melatonin in animal experiments and clinical trials will undoubtedly deepen our understanding of the protective and beneficial mechanisms of melatonin during chemotherapy. One clinical trial included 70 cancer patients (advanced NSCLC) who were treated with a combination of cisplatin plus etoposide or the chemotherapy drugs plus melatonin. On the basis of complete and partial tumor response rate, melatonin enhanced the effect of cisplatin plus etoposide, and improved the 1-year survival rate. Furthermore, the incidences of myelosuppression, neuropathy, and cachexia were significantly reduced, indicating that patients treated with melatonin had better tolerance to chemotherapy [23]. Another clinical trial treated a total of 250 patients with metastatic solid tumors who were given a variety of different chemotherapies alone or in combination with melatonin [23]. The objective tumor regression rate and the 1-year survival rate were again improved by melatonin cotreatment. Moreover, melatonin significantly alleviated the incidence of thrombocytopenia, neurotoxicity, cardiotoxicity, stomatitis, and asthenia [23]. The patients included in these studies were in the advanced stages of disease where any one treatment is likely to have little effect. Therefore, any benefit of melatonin therapy seems exceptional and applying melatonin therapy in the early stages of cancer seems reasonable, with the promise of greater benefits [23]. Although other clinical trials (NCT01557478, Phase 3; NCT02454855, Phase 3) related to melatonin alleviating the toxicity and improving the efficacy of chemotherapy have yet to be published, it seems necessary to use it more widely given the molecule's apparently beneficial properties and low toxicity. It is suggested that the therapeutic value of melatonin in chemotherapy-induced toxicity and its relationship with mitochondrial dysfunction in further double-blind placebo-controlled studies be evaluated; we anticipate a bounty of additional beneficial findings on the actions of melatonin cotreatment with chemotherapy agents in the next decade.

Conflicts of Interest

The authors declare no competing interests regarding the publication of this manuscript.

Authors' Contributions

YXL, HJ, and LXF designed the study. MZQ, XLQ, and LD searched the literature and wrote the manuscript. ZXY, DSY, LWM, and ZJ searched the literature and made the table, and MZQ drew the figures. RJR helped to revise the grammar and sentences. All authors read and approved the final manuscript. Zhiqiang Ma, Liqun Xu, and Dong Liu contributed equally to this work.

Acknowledgments

This work was supported by the National Natural Science Foundation of China (81572252, 81871866), Natural Science Foundation of Shaanxi Province (2016SF-308; 2019SF-033), the Project of Tangdu Hospital, The Fourth Military Medical University (2015 Key Talents; 2018 Key Talents), and the Excellent Doctoral Support Project of the Fourth Military Medical University (2018D09).

References

[1] M. Majidinia, R. J. Reiter, S. K. Shakouri, and B. Yousefi, "The role of melatonin, a multitasking molecule, in retarding the processes of ageing," *Ageing Research Reviews*, vol. 47, pp. 198–213, 2018.

[2] N. Kubben and T. Misteli, "Shared molecular and cellular mechanisms of premature ageing and ageing-associated diseases," *Nature Reviews Molecular Cell Biology*, vol. 18, no. 10, pp. 595–609, 2017.

[3] Z. Ma, Z. Xin, W. Hu et al., "Forkhead box O proteins: crucial regulators of cancer EMT," *Seminars in Cancer Biology*, vol. 50, pp. 21–31, 2018.

[4] Z. Ma, X. Zhang, L. Xu et al., "Pterostilbene: mechanisms of its action as oncostatic agent in cell models and in vivo studies," *Pharmacological Research*, vol. 145, article 104265, 2019.

[5] F. S. Liu, "Mechanisms of chemotherapeutic drug resistance in cancer therapy—a quick review," *Taiwanese Journal of Obstetrics and Gynecology*, vol. 48, no. 3, pp. 239–244, 2009.

[6] V. da Silva-Diz, L. Lorenzo-Sanz, A. Bernat-Peguera, M. Lopez-Cerda, and P. Muñoz, "Cancer cell plasticity: impact on tumor progression and therapy response," *Seminars in Cancer Biology*, vol. 53, pp. 48–58, 2018.

[7] K. Sak, "Chemotherapy and dietary phytochemical agents," *Chemotherapy Research and Practice*, vol. 2012, Article ID 282570, 11 pages, 2012.

[8] X. Z. Wu, "A new classification system of anticancer drugs – based on cell biological mechanisms," *Medical Hypotheses*, vol. 66, no. 5, pp. 883–887, 2006.

[9] D. W. Lamson and M. S. Brignall, "Antioxidants in cancer therapy; their actions and interactions with oncologic therapies," *Alternative Medicine Review*, vol. 4, no. 5, pp. 304–329, 1999.

[10] H. Ma, T. Das, S. Pereira et al., "Efficacy of dietary antioxidants combined with a chemotherapeutic agent on human colon cancer progression in a fluorescent orthotopic mouse model," *Anticancer Research*, vol. 29, no. 7, pp. 2421–2426, 2009.

[11] M. K. Kanwar, J. Yu, and J. Zhou, "Phytomelatonin: recent advances and future prospects," *Journal of Pineal Research*, vol. 65, no. 4, article e12526, 2018.

[12] Y. Xia, S. Chen, S. Zeng et al., "Melatonin in macrophage biology: current understanding and future perspectives," *Journal of Pineal Research*, vol. 66, no. 2, article e12547, 2019.

[13] D. J. Kennaway, "A critical review of melatonin assays: past and present," *Journal of Pineal Research*, article e12572, 2019.

[14] R. J. Reiter, S. Rosales-Corral, D. X. Tan, M. J. Jou, A. Galano, and B. Xu, "Melatonin as a mitochondria-targeted antioxidant: one of evolution's best ideas," *Cellular and Molecular Life Sciences*, vol. 74, no. 21, pp. 3863–3881, 2017.

[15] Y. T. Chen, C. C. Yang, P. L. Shao, C. R. Huang, and H. K. Yip, "Melatonin-mediated downregulation of ZNF746 suppresses bladder tumorigenesis mainly through inhibiting the AKT-MMP-9 signaling pathway," *Journal of Pineal Research*, vol. 66, no. 1, article e12536, 2019.

[16] D. I. Sánchez, B. González-Fernández, I. Crespo et al., "Melatonin modulates dysregulated circadian clocks in mice with diethylnitrosamine-induced hepatocellular carcinoma," *Journal of Pineal Research*, vol. 65, no. 3, article e12506, 2018.

[17] S. Xiang, R. T. Dauchy, A. E. Hoffman et al., "Epigenetic inhibition of the tumor suppressor ARHI by light at night-induced circadian melatonin disruption mediates STAT3-driven paclitaxel resistance in breast cancer," *Journal of Pineal Research*, no. article e12586, 2019.

[18] R. Sharma, P. Sahota, and M. M. Thakkar, "Melatonin promotes sleep in mice by inhibiting orexin neurons in the perifornical lateral hypothalamus," *Journal of Pineal Research*, vol. 65, no. 2, article e12498, 2018.

[19] J. Schaper, E. Meiser, and G. Stammler, "Ultrastructural morphometric analysis of myocardium from dogs, rats, hamsters, mice, and from human hearts," *Circulation Research*, vol. 56, no. 3, pp. 377–391, 1985.

[20] R. Ventura-Clapier, A. Garnier, and V. Veksler, "Energy metabolism in heart failure," *The Journal of Physiology*, vol. 555, no. 1, pp. 1–13, 2004.

[21] P. Mi, Q. P. Zhang, S. B. Li et al., "Melatonin protects embryonic development and maintains sleep/wake behaviors from the deleterious effects of fluorene-9-bisphenol in zebrafish (*Danio rerio*)," *Journal of Pineal Research*, vol. 66, no. 1, article e12530, 2019.

[22] C. Ma, L. X. Li, Y. Zhang et al., "Protective and sensitive effects of melatonin combined with adriamycin on ER+ (estrogen receptor) breast cancer," *European Journal of Gynaecological Oncology*, vol. 36, no. 2, pp. 197–202, 2015.

[23] R. J. Reiter, D. X. Tan, R. M. Sainz, J. C. Mayo, and S. Lopez-Burillo, "Melatonin: reducing the toxicity and increasing the efficacy of drugs," *Journal of Pharmacy and Pharmacology*, vol. 54, no. 10, pp. 1299–1321, 2002.

[24] J. H. Lee, C. W. Yun, Y. S. Han et al., "Melatonin and 5-fluorouracil co-suppress colon cancer stem cells by regulating cellular prion protein-Oct4 axis," *Journal of Pineal Research*, vol. 65, no. 4, article e12519, 2018.

[25] S. Tengattini, R. J. Reiter, D. X. Tan, M. P. Terron, L. F. Rodella, and R. Rezzani, "Cardiovascular diseases: protective effects of melatonin," *Journal of Pineal Research*, vol. 44, pp. 16–25, 2008.

[26] J. J. García, L. López-Pingarrón, P. Almeida-Souza et al., "Protective effects of melatonin in reducing oxidative stress and in preserving the fluidity of biological membranes: a review," *Journal of Pineal Research*, vol. 56, no. 3, pp. 225–237, 2014.

[27] F. Y. Lee, C. K. Sun, P. H. Sung et al., "Daily melatonin protects the endothelial lineage and functional integrity against the aging process, oxidative stress, and toxic environment and restores blood flow in critical limb ischemia area in mice," *Journal of Pineal Research*, vol. 65, no. 2, article e12489, 2018.

[28] M. M. Anwar and A. R. M. A. Meki, "Oxidative stress in streptozotocin-induced diabetic rats: effects of garlic oil and melatonin," *Comparative Biochemistry and Physiology Part A: Molecular & Integrative Physiology*, vol. 135, no. 4, pp. 539–547, 2003.

[29] F. Gultekin, N. Delibas, S. Yasar, and I. Kilinc, "In vivo changes in antioxidant systems and protective role of melatonin and a combination of vitamin C and vitamin E on oxidative damage in erythrocytes induced by chlorpyrifos-ethyl in rats," *Archives of Toxicology*, vol. 75, no. 2, pp. 88–96, 2001.

[30] J. Govender, B. Loos, E. Marais, and A. M. Engelbrecht, "Mitochondrial catastrophe during doxorubicin-induced cardiotoxicity: a review of the protective role of melatonin," *Journal of Pineal Research*, vol. 57, no. 4, pp. 367–380, 2014.

[31] R. J. Reiter, D. Tan, S. Rosales-Corral, A. Galano, X. Zhou, and B. Xu, "Mitochondria: central organelles for melatonin's antioxidant and anti-aging actions," *Molecules*, vol. 23, no. 2, p. 509, 2018.

[32] S. M. Armstrong and J. R. Redman, "Melatonin: a chronobiotic with anti-aging properties?," *Medical Hypotheses*, vol. 34, no. 4, pp. 300–309, 1991.

[33] M. R. Ramis, S. Esteban, A. Miralles, D. X. Tan, and R. J. Reiter, "Caloric restriction, resveratrol and melatonin: role of SIRT1 and implications for aging and related-diseases," *Mechanisms of Ageing and Development*, vol. 146-148, pp. 28–41, 2015.

[34] D. R. Green, L. Galluzzi, and G. Kroemer, "Mitochondria and the autophagy–inflammation–cell death axis in organismal aging," *Science*, vol. 333, no. 6046, pp. 1109–1112, 2011.

[35] R. Hardeland, "Melatonin and the theories of aging: a critical appraisal of melatonin's role in antiaging mechanisms," *Journal of Pineal Research*, vol. 55, no. 4, pp. 325–356, 2013.

[36] W. Pierpaoli and W. Regelson, "Pineal control of aging: effect of melatonin and pineal grafting on aging mice," *Proceedings of the National Academy of Sciences of the United States of America*, vol. 91, no. 2, pp. 787–791, 1994.

[37] W. Pierpaoli and D. Bulian, "The pineal aging and death program: life prolongation in pre-aging pinealectomized mice," *Annals of the New York Academy of Sciences*, vol. 1057, no. 1, pp. 133–144, 2005.

[38] I. Carreca and L. Balducci, "Cancer chemotherapy in the older cancer patient," *Urologic Oncology: Seminars and Original Investigations*, vol. 27, no. 6, pp. 633–642, 2009.

[39] J. N. Vega, J. Dumas, and P. A. Newhouse, "Cognitive effects of chemotherapy and cancer-related treatments in older adults," *The American Journal of Geriatric Psychiatry*, vol. 25, no. 12, pp. 1415–1426, 2017.

[40] A. V. Kudryavtseva, G. S. Krasnov, A. A. Dmitriev et al., "Mitochondrial dysfunction and oxidative stress in aging and cancer," *Oncotarget*, vol. 7, no. 29, pp. 44879–44905, 2016.

[41] M. C. Pinder, Z. Duan, J. S. Goodwin, G. N. Hortobagyi, and S. H. Giordano, "Congestive heart failure in older women treated with adjuvant anthracycline chemotherapy for breast cancer," *Journal of Clinical Oncology*, vol. 25, no. 25, pp. 3808–3815, 2007.

[42] J. Wen, M. Zeng, Y. Shu et al., "Aging increases the susceptibility of cisplatin-induced nephrotoxicity," *Age*, vol. 37, no. 6, p. 112, 2015.

[43] T. A. Ahles, A. J. Saykin, B. C. McDonald et al., "Longitudinal assessment of cognitive changes associated with adjuvant treatment for breast cancer: impact of age and cognitive reserve," *Journal of Clinical Oncology*, vol. 28, no. 29, pp. 4434–4440, 2010.

[44] C. M. Schilder, C. Seynaeve, L. V. Beex et al., "Effects of tamoxifen and exemestane on cognitive functioning of postmenopausal patients with breast cancer: results from the neuropsychological side study of the tamoxifen and exemestane adjuvant multinational trial," *Journal of Clinical Oncology*, vol. 28, no. 8, pp. 1294–1300, 2010.

[45] J. H. Doroshow, "Anthracycline antibiotic-stimulated superoxide, hydrogen peroxide, and hydroxyl radical production by NADH dehydrogenase," *Cancer Research*, vol. 43, no. 10, pp. 4543–4551, 1983.

[46] T. Li, I. Danelisen, and P. K. Singal, "Early changes in myocardial antioxidant enzymes in rats treated with adriamycin," *Molecular and Cellular Biochemistry*, vol. 232, no. 1-2, pp. 19–26, 2002.

[47] G. Takemura and H. Fujiwara, "Doxorubicin-induced cardiomyopathy: from the cardiotoxic mechanisms to management," *Progress in Cardiovascular Diseases*, vol. 49, no. 5, pp. 330–352, 2007.

[48] Y. W. Zhang, J. Shi, Y. J. Li, and L. Wei, "Cardiomyocyte death in doxorubicin-induced cardiotoxicity," *Archivum Immunologiae et Therapiae Experimentalis*, vol. 57, no. 6, pp. 435–445, 2009.

[49] D. B. Zorov, M. Juhaszova, and S. J. Sollott, "Mitochondrial reactive oxygen species (ROS) and ROS-induced ROS release," *Physiological Reviews*, vol. 94, no. 3, pp. 909–950, 2014.

[50] A. Musatov and N. C. Robinson, "Susceptibility of mitochondrial electron-transport complexes to oxidative damage. Focus on cytochrome c oxidase," *Free Radical Research*, vol. 46, no. 11, pp. 1313–1326, 2012.

[51] J. H. Doroshow, G. Y. Locker, and C. E. Myers, "Enzymatic defenses of the mouse heart against reactive oxygen metabolites: *alterations produced by doxorubicin*," *The Journal of Clinical Investigation*, vol. 65, no. 1, pp. 128–135, 1980.

[52] P. K. Singal, N. Iliskovic, T. Li, and D. Kumar, "Adriamycin cardiomyopathy: pathophysiology and prevention," *The FASEB Journal*, vol. 11, no. 12, pp. 931–936, 1997.

[53] J. Y. Tang, A. A. Farooqi, F. Ou-Yang et al., "Oxidative stress-modulating drugs have preferential anticancer effects - involving the regulation of apoptosis, DNA damage, endoplasmic reticulum stress, autophagy, metabolism, and migration," *Seminars in Cancer Biology*, 2018.

[54] M. Waseem, H. Tabassum, and S. Parvez, "Neuroprotective effects of melatonin as evidenced by abrogation of oxaliplatin induced behavioral alterations, mitochondrial dysfunction and neurotoxicity in rat brain," *Mitochondrion*, vol. 30, pp. 168–176, 2016.

[55] A. Galano and R. J. Reiter, "Melatonin and its metabolites vs oxidative stress: from individual actions to collective protection," *Journal of Pineal Research*, vol. 65, no. 1, article e12514, 2018.

[56] T. Gao, Z. Wang, Y. Dong et al., "Role of melatonin in sleep deprivation-induced intestinal barrier dysfunction in mice," *Journal of Pineal Research*, no. article e12574, 2019.

[57] L. Sagrillo-Fagundes, E. M. Assunção Salustiano, R. Ruano, R. P. Markus, and C. Vaillancourt, "Melatonin modulates autophagy and inflammation protecting human placental trophoblast from hypoxia/reoxygenation," *Journal of Pineal Research*, vol. 65, no. 4, article e12520, 2018.

[58] A. Chabra, M. Shokrzadeh, F. Naghshvar, F. Salehi, and A. Ahmadi, "Melatonin ameliorates oxidative stress and reproductive toxicity induced by cyclophosphamide in male mice," *Human & Experimental Toxicology*, vol. 33, no. 2, pp. 185–195, 2014.

[59] R. J. Reiter, D. X. Tan, C. Osuna, and E. Gitto, "Actions of melatonin in the reduction of oxidative stress," *Journal of Biomedical Science*, vol. 7, no. 6, pp. 444–458, 2000.

[60] D. Mukherjee, A. K. Ghosh, M. Dutta et al., "Mechanisms of isoproterenol-induced cardiac mitochondrial damage: protective actions of melatonin," *Journal of Pineal Research*, vol. 58, no. 3, pp. 275–290, 2015.

[61] S. M. Nair, R. M. A. Rahman, A. N. Clarkson et al., "Melatonin treatment following stroke induction modulates L-arginine metabolism," *Journal of Pineal Research*, vol. 51, no. 3, pp. 313–323, 2011.

[62] M. J. Jou, T. I. Peng, and R. J. Reiter, "Protective stabilization of mitochondrial permeability transition and mitochondrial oxidation during mitochondrial Ca^{2+} stress by melatonin's cascade metabolites C3-OHM and AFMK in RBA1 astrocytes," *Journal of Pineal Research*, vol. 66, no. 1, article e12538, 2019.

[63] H. H. Chen, Y. T. Chen, C. C. Yang et al., "Melatonin pretreatment enhances the therapeutic effects of exogenous mitochondria against hepatic ischemia–reperfusion injury in rats through suppression of mitochondrial permeability transition," *Journal of Pineal Research*, vol. 61, no. 1, pp. 52–68, 2016.

[64] M. Beer, T. Seyfarth, J. Sandstede et al., "Absolute concentrations of high-energy phosphate metabolites in normal, hypertrophied, and failing human myocardium measured noninvasively with ^{31}P-SLOOP magnetic resonance spectroscopy," *Journal of the American College of Cardiology*, vol. 40, no. 7, pp. 1267–1274, 2002.

[65] W. Hu, Z. Ma, S. Jiang et al., "Melatonin: the dawning of a treatment for fibrosis?," *Journal of Pineal Research*, vol. 60, no. 2, pp. 121–131, 2016.

[66] A. Galano, D. X. Tan, and R. J. Reiter, "On the free radical scavenging activities of melatonin's metabolites, AFMK and AMK," *Journal of Pineal Research*, vol. 54, no. 3, pp. 245–257, 2013.

[67] D. X. Tan, R. Hardeland, L. C. Manchester, A. Galano, and R. J. Reiter, "Cyclic-3-hydroxymelatonin (C3HOM), a potent antioxidant, scavenges free radicals and suppresses oxidative reactions," *Current Medicinal Chemistry*, vol. 21, no. 13, pp. 1557–1565, 2014.

[68] X. Liu, Z. Chen, C. C. Chua et al., "Melatonin as an effective protector against doxorubicin-induced cardiotoxicity," *American Journal of Physiology-Heart and Circulatory Physiology*, vol. 283, no. 1, pp. H254–H263, 2002.

[69] N. Siveski-Iliskovic, M. Hill, D. A. Chow, and P. K. Singal, "Probucol protects against adriamycin cardiomyopathy without interfering with its antitumor effect," *Circulation*, vol. 91, no. 1, pp. 10–15, 1995.

[70] D.-X. Tan, L. C. Manchester, R. J. Reiter et al., "Melatonin directly scavenges hydrogen peroxide: a potentially new metabolic pathway of melatonin biotransformation," *Free Radical Biology & Medicine*, vol. 29, no. 11, pp. 1177–1185, 2000.

[71] M. Martin, M. Macias, G. Escames et al., "Melatonin-induced increased activity of the respiratory chain complexes I and IV can prevent mitochondrial damage induced by ruthenium red in vivo," *Journal of Pineal Research*, vol. 28, no. 4, pp. 242–248, 2000.

[72] T. W. Fischer, K. Kleszczynski, L. H. Hardkop, N. Kruse, and D. Zillikens, "Melatonin enhances antioxidative enzyme gene expression (CAT, GPx, SOD), prevents their UVR-induced depletion, and protects against the formation of DNA damage (8-hydroxy-2′-deoxyguanosine) in ex vivo human skin," *Journal of Pineal Research*, vol. 54, no. 3, pp. 303–312, 2013.

[73] Y. Urata, S. Honma, S. Goto et al., "Melatonin induces γ-glutamylcysteine synthetase mediated by activator protein-1 in human vascular endothelial cells," *Free Radical Biology & Medicine*, vol. 27, no. 7-8, pp. 838–847, 1999.

[74] V. Jiménez-Ortega, P. Cano, D. P. Cardinali, and A. I. Esquifino, "24-Hour variation in gene expression of redox pathway enzymes in rat hypothalamus: effect of melatonin treatment," *Redox Report*, vol. 14, no. 3, pp. 132–138, 2009.

[75] D. Pozo, R. J. Reiter, J. R. Calvo, and J. M. Guerrero, "Inhibition of cerebellar nitric oxide synthase and cyclic GMP production by melatonin via complex formation with calmodulin," *Journal of Cellular Biochemistry*, vol. 65, no. 3, pp. 430–442, 1997.

[76] F. Ortiz, J. A. García, D. Acuña-Castroviejo et al., "The beneficial effects of melatonin against heart mitochondrial impairment during sepsis: inhibition of iNOS and preservation of nNOS," *Journal of Pineal Research*, vol. 56, no. 1, pp. 71–81, 2014.

[77] J. A. Boga, B. Caballero, Y. Potes et al., "Therapeutic potential of melatonin related to its role as an autophagy regulator: a review," *Journal of Pineal Research*, vol. 66, no. 1, article e12534, 2019.

[78] R. B. Weiss, "The anthracyclines: will we ever find a better doxorubicin?," *Seminars in Oncology*, vol. 19, no. 6, pp. 670–686, 1992.

[79] K. M. Lee, I. C. Lee, S. H. Kim et al., "Melatonin attenuates doxorubicin-induced testicular toxicity in rats," *Andrologia*, vol. 44, Supplement 1, pp. 796–803, 2012.

[80] Y. Zhang, L. Li, C. Xiang, Z. Ma, T. Ma, and S. Zhu, "Protective effect of melatonin against adriamycin-induced cardiotoxicity," *Experimental and Therapeutic Medicine*, vol. 5, no. 5, pp. 1496–1500, 2013.

[81] J. L. Quiles, J. R. Huertas, M. Battino, J. Mataix, and M. C. Ramírez-Tortosa, "Antioxidant nutrients and adriamycin toxicity," *Toxicology*, vol. 180, no. 1, pp. 79–95, 2002.

[82] E. Sahna, H. Parlakpinar, M. K. Ozer, F. Ozturk, F. Ozugurlu, and A. Acet, "Melatonin protects against myocardial doxorubicin toxicity in rats: role of physiological concentrations," *Journal of Pineal Research*, vol. 35, no. 4, pp. 257–261, 2003.

[83] D. LIU, Z. Ma, S. Di et al., "AMPK/PGC1α activation by melatonin attenuates acute doxorubicin cardiotoxicity *via* alleviating mitochondrial oxidative damage and apoptosis," *Free Radical Biology & Medicine*, vol. 129, pp. 59–72, 2018.

[84] A. Bilginoğlu, D. Aydin, Ş. Ozsoy, and H. Aygün, "Protective effect of melatonin on adriamycin-induced cardiotoxicity in rats," *Turk Kardiyoloji Dernegi Arsivi-Archives of the Turkish Society of Cardiology*, vol. 42, no. 3, pp. 265–273, 2014.

[85] A. I. Othman, M. A. El-Missiry, M. A. Amer, and M. Arafa, "Melatonin controls oxidative stress and modulates iron, ferritin, and transferrin levels in adriamycin treated rats," *Life Sciences*, vol. 83, no. 15-16, pp. 563–568, 2008.

[86] P. Dziegiel, E. Murawska-Cialowicz, Z. Jethon et al., "Melatonin stimulates the activity of protective antioxidative enzymes in myocardial cells of rats in the course of doxorubicin intoxication," *Journal of Pineal Research*, vol. 35, no. 3, pp. 183–187, 2003.

[87] I. Morishima, K. Okumura, H. Matsui et al., "Zinc accumulation in adriamycin-induced cardiomyopathy in rats: Effects of melatonin, a cardioprotective antioxidant," *Journal of Pineal Research*, vol. 26, no. 4, pp. 204–210, 1999.

[88] M. F. Xu, S. Ho, Z. M. Qian, and P. L. Tang, "Melatonin protects against cardiac toxicity of doxorubicin in rat," *Journal of Pineal Research*, vol. 31, no. 4, pp. 301–307, 2001.

[89] G. Kocak, K. M. Erbil, I. Ozdemir et al., "The protective effect of melatonin on adriamycin-induced acute cardiac injury," *The Canadian Journal of Cardiology*, vol. 19, no. 5, pp. 535–541, 2003.

[90] E. Öz, D. Erbaş, H. S. Sürücü, and E. Düzgün, "Prevention of doxorubicin-induced cardiotoxicity by melatonin," *Molecular and Cellular Biochemistry*, vol. 282, no. 1-2, pp. 31–37, 2006.

[91] E. Goormaghtigh, P. Chatelain, J. Caspers, and J. M. Ruysschaert, "Evidence of a complex between adriamycin derivatives and cardiolipin: possible role in cardiotoxicity," *Biochemical Pharmacology*, vol. 29, no. 21, pp. 3003–3010, 1980.

[92] E. Goormaghtigh, P. Huart, R. Brasseur, and J. M. Ruysschaert, "Mechanism of inhibition of mitochondrial enzymatic complex I–III by adriamycin derivatives," *Biochimica et Biophysica Acta (BBA) - Biomembranes*, vol. 861, no. 1, pp. 83–94, 1986.

[93] G. Paradies, G. Petrosillo, V. Paradies, R. J. Reiter, and F. M. Ruggiero, "Melatonin, cardiolipin and mitochondrial bioenergetics in health and disease," *Journal of Pineal Research*, vol. 48, no. 4, pp. 297–310, 2010.

[94] C. GUVEN, E. TASKIN, and H. AKCAKAYA, "Melatonin prevents mitochondrial damage induced by doxorubicin in mouse fibroblasts through AMPK-PPAR gamma-dependent mechanisms," *Medical science monitor : international medical journal of experimental and clinical research*, vol. 22, pp. 438–446, 2016.

[95] W. Tan, Z. Zhong, R. P. Carney et al., "Deciphering the metabolic role of AMPK in cancer multi-drug resistance," *Seminars in Cancer Biology*, vol. 56, pp. 56–71, 2018.

[96] A. Pérez-González, R. Castañeda-Arriaga, J. R. Álvarez-Idaboy, R. J. Reiter, and A. Galano, "Melatonin and its metabolites as chemical agents capable of directly repairing oxidized DNA," *Journal of Pineal Research*, vol. 66, no. 2, article e12539, 2019.

[97] G. Anderson, "Linking the biological underpinnings of depression: Role of mitochondria interactions with melatonin, inflammation, sirtuins, tryptophan catabolites, DNA repair and oxidative and nitrosative stress, with consequences for classification and cognition," *Progress in Neuro-Psychopharmacology and Biological Psychiatry*, vol. 80, pp. 255–266, 2018.

[98] M. H. Wahab, E. S. Akoul, and A. A. Abdel-Aziz, "Modulatory effects of melatonin and vitamin E on doxorubicin-induced cardiotoxicity in Ehrlich ascites carcinoma-bearing mice," *Tumori Journal*, vol. 86, no. 2, pp. 157–162, 2000.

[99] V. Kesik, B. Kurt, T. Tunc et al., "Melatonin ameliorates doxorubicin-induced skin necrosis in rats," *Annals of Plastic Surgery*, vol. 65, no. 2, pp. 250–253, 2010.

[100] P. Dziegiel, P. Surowiak, J. Rabczyński, and M. Zabel, "Effect of melatonin on cytotoxic effects of daunorubicin on myocardium and on transplantable Morris hepatoma in rats," *Polish Journal of Pathology*, vol. 53, no. 4, pp. 201–204, 2002.

[101] A. Guven, O. Yavuz, M. Cam, F. Ercan, N. Bukan, and C. Comunoglu, "Melatonin protects against epirubicin-induced cardiotoxicity," *Acta Histochemica*, vol. 109, no. 1, pp. 52–60, 2007.

[102] C. A. Joslin, P. B. Kunkler, I. H. Evans, V. Jones, and K. Wong, "Cyclophosphamide in the management of advanced breast cancer," *Proceedings of the Royal Society of Medicine*, vol. 63, no. 1, pp. 81–84, 1970.

[103] R. A. Fleming, "An overview of cyclophosphamide and ifosfamide pharmacology," *Pharmacotherapy*, vol. 17, no. 5, Part 2, pp. 146s–154s, 1997.

[104] A. L. Al-Malki, "Synergestic effect of lycopene and melatonin against the genesis of oxidative stress induced by cyclophosphamide in rats," *Toxicology and Industrial Health*, vol. 30, no. 6, pp. 570–575, 2014.

[105] H. Kaya, B. Oral, F. Ozgüner, V. Tahan, Y. Babar, and N. Delibaş, "The effect of melatonin application on lipid peroxidation during cyclophosphamide therapy in female rats," *Zentralblatt fur Gynakologie*, vol. 121, no. 10, pp. 499–502, 1999.

[106] M. Shokrzadeh, A. Chabra, F. Naghshvar, A. Ahmadi, M. Jafarinejhad, and Y. Hasani-Nourian, "Protective effects of melatonin against cyclophosphamide-induced oxidative lung toxicity in mice," *Drug Research*, vol. 65, no. 6, pp. 281–286, 2015.

[107] Q. H. Zhang, Z. S. Zhou, G. S. Lu, B. Song, and J. X. Guo, "Melatonin improves bladder symptoms and may ameliorate bladder damage via increasing HO-1 in rats," *Inflammation*, vol. 36, no. 3, pp. 651–657, 2013.

[108] T. Topal, Y. Oztas, A. Korkmaz et al., "Melatonin ameliorates bladder damage induced by cyclophosphamide in rats," *Journal of Pineal Research*, vol. 38, no. 4, pp. 272–277, 2005.

[109] D. N. Tripathi and G. B. Jena, "Effect of melatonin on the expression of Nrf2 and NF-κB during cyclophosphamide-induced urinary bladder injury in rat," *Journal of Pineal Research*, vol. 48, no. 4, pp. 324–331, 2010.

[110] D. ZUPANCIC, G. VIDMAR, and K. JEZERNIK, "Melatonin prevents the development of hyperplastic urothelium induced by repeated doses of cyclophosphamide," *Virchows Archiv : an international journal of pathology*, vol. 454, no. 6, pp. 657–666, 2009.

[111] Y. O. Ilbey, E. Ozbek, A. Simsek, A. Otunctemur, M. Cekmen, and A. Somay, "Potential chemoprotective effect of melatonin in cyclophosphamide- and cisplatin-induced testicular damage in rats," *Fertility and Sterility*, vol. 92, no. 3, pp. 1124–1132, 2009.

[112] M. Shokrzadeh, F. Naghshvar, A. Ahmadi, A. Chabr, and F. Jeivad, "The potential ameliorative effects of melatonin against cyclophosphamide-induced DNA damage in murine bone marrow cells," *European Review for Medical and Pharmacological Sciences*, vol. 18, no. 5, pp. 605–611, 2014.

[113] S. G. Ferreira, R. A. Peliciari-Garcia, S. A. Takahashi-Hyodo et al., "Effects of melatonin on DNA damage induced by cyclophosphamide in rats," *Brazilian Journal of Medical and Biological Research*, vol. 46, no. 3, pp. 278–286, 2013.

[114] L. Dobrek, A. Baranowska, and P. J. Thor, "Indirect autonomic nervous system activity assessment with heart rate variability in rats with cyclophosphamide-induced hemorrhagic cystitis treated with melatonin or agomelatine," *Contemporary Oncology*, vol. 5, no. 5, pp. 368–373, 2015.

[115] P. Saha, C. Debnath, and G. Berube, "Steroid-linked nitrogen mustards as potential anticancer therapeutics: a review," *The Journal of Steroid Biochemistry and Molecular Biology*, vol. 137, pp. 271–300, 2013.

[116] P. D. Lawley, "Alkylation of DNA and its aftermath," *BioEssays*, vol. 17, no. 6, pp. 561–568, 1995.

[117] M. Ucar, A. Korkmaz, R. J. Reiter et al., "Melatonin alleviates lung damage induced by the chemical warfare agent nitrogen mustard," *Toxicology Letters*, vol. 173, no. 2, pp. 124–131, 2007.

[118] E. Macit, H. Yaren, I. Aydin et al., "The protective effect of melatonin and S-methylisothiourea treatments in nitrogen mustard induced lung toxicity in rats," *Environmental Toxicology and Pharmacology*, vol. 36, no. 3, pp. 1283–1290, 2013.

[119] R. Hardeland, "elatonin and inflammation—Story of a double-edged blade," *Journal of Pineal Research*, vol. 65, no. 4, article e12525, 2018.

[120] M. Sourdeval, C. Lemaire, A. Deniaud et al., "Inhibition of caspase-dependent mitochondrial permeability transition protects airway epithelial cells against mustard-induced apoptosis," *Apoptosis*, vol. 11, no. 9, pp. 1545–1559, 2006.

[121] P. Ferroni, D. Della-Morte, R. Palmirotta et al., "Platinum-based compounds and risk for cardiovascular toxicity in the elderly: role of the antioxidants in chemoprevention," *Rejuvenation Research*, vol. 14, no. 3, pp. 293–308, 2011.

[122] U. Kilic, E. Kilic, Z. Tuzcu et al., "Melatonin suppresses cisplatin-induced nephrotoxicity via activation of Nrf-2/HO-1 pathway," *Nutrition & Metabolism*, vol. 10, no. 1, p. 7, 2013.

[123] M. Hara, M. Yoshida, H. Nishijima et al., "Melatonin, a pineal secretory product with antioxidant properties, protects against cisplatin-induced nephrotoxicity in rats," *Journal of Pineal Research*, vol. 30, no. 3, pp. 129–138, 2001.

[124] M. Majidinia, A. Sadeghpour, S. Mehrzadi, R. J. Reiter, N. Khatami, and B. Yousefi, "Melatonin: a pleiotropic molecule that modulates DNA damage response and repair pathways," vol. 63, no. 1, article e12416, 2017.

[125] R. S. Barberino, V. G. Menezes, A. E. A. S. Ribeiro et al., "Melatonin protects against cisplatin-induced ovarian damage in mice via the MT1 receptor and antioxidant activity," *Biology of Reproduction*, vol. 96, no. 6, pp. 1244–1255, 2017.

[126] H. Jang, O. H. Lee, Y. Lee et al., "Melatonin prevents cisplatin-induced primordial follicle loss via suppression of PTEN/AKT/FOXO3a pathway activation in the mouse ovary," vol. 60, pp. 336–347, 2016.

[127] P. Madhu, K. P. Reddy, and P. S. Reddy, "Role of melatonin in mitigating chemotherapy-induced testicular dysfunction in Wistar rats," *Drug and Chemical Toxicology*, vol. 39, no. 2, pp. 137–146, 2016.

[128] M. A. Lopez-Gonzalez, J. M. Guerrero, F. Rojas, and F. Delgado, "Ototoxicity caused by cisplatin is ameliorated by melatonin and other antioxidants," *Journal of Pineal Research*, vol. 28, no. 2, pp. 73–80, 2000.

[129] M. G. Demir, N. Altintoprak, S. Aydin, E. Kosemihal, and K. Basak, "Effect of transtympanic injection of melatonin on cisplatin-induced ototoxicity," *The Journal of International Advanced Otology*, vol. 11, no. 3, pp. 202–206, 2015.

[130] K. Bennukul, S. Numkliang, and V. Leardkamolkarn, "Melatonin attenuates cisplatin-induced HepG2 cell death via the regulation of mTOR and ERCC1 expressions," *World Journal of Hepatology*, vol. 6, no. 4, pp. 230–242, 2014.

[131] K. E. Atalik, B. Keles, Y. Uyar, M. A. Dündar, M. Öz, and H. H. Esen, "Vasoprotection by melatonin and quercetin in rats treated with cisplatin," *Indian Journal of Experimental Biology*, vol. 48, pp. 1188–1193, 2010.

[132] P. Plaimee, N. Weerapreeyakul, S. Barusrux, and N. P. Johns, "Melatonin potentiates cisplatin-induced apoptosis and cell cycle arrest in human lung adenocarcinoma cells," *Cell Proliferation*, vol. 48, no. 1, pp. 67–77, 2015.

[133] A. Sookprasert, N. P. Johns, A. Phunmanee et al., "Melatonin in patients with cancer receiving chemotherapy: a randomized, double-blind, placebo-controlled trial," *Anticancer Research*, vol. 34, no. 12, pp. 7327–7337, 2014.

[134] A. A. Argyriou, P. Polychronopoulos, G. Iconomou, E. Chroni, and H. P. Kalofonos, "A review on oxaliplatin-induced peripheral nerve damage," *Cancer Treatment Reviews*, vol. 34, no. 4, pp. 368–377, 2008.

[135] A. Areti, P. Komirishetty, M. Akuthota, R. A. Malik, and A. Kumar, "Melatonin prevents mitochondrial dysfunction and promotes neuroprotection by inducing autophagy during oxaliplatin-evoked peripheral neuropathy," *Journal of Pineal Research*, vol. 62, no. 3, 2017.

[136] M. Waseem, U. Sahu, M. Salman et al., "Melatonin pretreatment mitigates SHSY-5Y cells against oxaliplatin induced mitochondrial stress and apoptotic cell death," *PLoS One*, vol. 12, no. 7, article e0180953, 2017.

[137] H. J. Um and T. K. Kwon, "Protective effect of melatonin on oxaliplatin-induced apoptosis through sustained Mcl-1 expression and anti-oxidant action in renal carcinoma Caki cells," *Journal of Pineal Research*, vol. 49, no. 3, pp. 283–290, 2010.

[138] Y. S. Wang, Y. Y. Li, W. Cui et al., "Melatonin attenuates pain hypersensitivity and decreases astrocyte-mediated spinal neuroinflammation in a rat model of oxaliplatin-induced pain," *Inflammation*, vol. 40, no. 6, pp. 2052–2061, 2017.

[139] V. K. Kolli, P. Abraham, and S. Rabi, "Methotrexate-induced nitrosative stress may play a critical role in small intestinal damage in the rat," *Archives of toxicology*, vol. 82, no. 10, pp. 763–770, 2008.

[140] P. Fazzi, "Pharmacotherapeutic management of pulmonary sarcoidosis," *American Journal of Respiratory Medicine*, vol. 2, no. 4, pp. 311–320, 2003.

[141] V. K. Kolli, P. Abraham, B. Isaac, and N. Kasthuri, "Preclinical efficacy of melatonin to reduce methotrexate-induced oxidative stress and small intestinal damage in rats," *Digestive Diseases and Sciences*, vol. 58, no. 4, pp. 959–969, 2013.

[142] V. K. Kolli, I. Kanakasabapathy, M. Faith et al., "A preclinical study on the protective effect of melatonin against methotrexate-induced small intestinal damage: effect mediated by attenuation of nitrosative stress, protein tyrosine nitration, and PARP activation," *Cancer Chemotherapy and Pharmacology*, vol. 71, no. 5, pp. 1209–1218, 2013.

[143] P. Abraham, V. K. Kolli, and S. Rabi, "Melatonin attenuates methotrexate-induced oxidative stress and renal damage in rats," *Cell Biochemistry and Function*, vol. 28, no. 5, pp. 426–433, 2010.

[144] E. Oguz, S. Kocarslan, S. Tabur, H. Sezen, Z. Yilmaz, and N. Aksoy, "Effects of lycopene alone or combined with melatonin on methotrexate-induced nephrotoxicity in rats," *Asian Pacific Journal of Cancer Prevention*, vol. 16, no. 14, pp. 6061–6066, 2015.

[145] A. O. S. Montasser, H. Saleh, O. A. Ahmed-Farid, A. Saad, and M. A. S. Marie, "Protective effects of *Balanites aegyptiaca* extract, melatonin and ursodeoxycholic acid against hepatotoxicity induced by methotrexate in male rats," *Asian Pacific Journal of Tropical Medicine*, vol. 10, no. 6, pp. 557–565, 2017.

[146] H. Çevik, A. Ö. Şehirli, B. Ç. Yeğen, and G. Şener, "Melatonin prevents methotrexate-induced hepatorenal oxidative injury in rats," *Journal of Pineal Research*, vol. 34, no. 4, pp. 282–287, 2003.

[147] D. Ghersi, N. Wilcken, and R. J. Simes, "A systematic review of taxane-containing regimens for metastatic breast cancer," *British Journal of Cancer*, vol. 93, no. 3, pp. 293–301, 2005.

[148] C. N. Frederiks, S. W. Lam, H. J. Guchelaar, and E. Boven, "Genetic polymorphisms and paclitaxel- or docetaxel-induced toxicities: a systematic review," *Cancer Treatment Reviews*, vol. 41, no. 10, pp. 935–950, 2015.

[149] D. Zhang, R. Yang, S. Wang, and Z. Dong, "Paclitaxel: new uses for an old drug," *Drug Design, Development and Therapy*, vol. 8, pp. 279–284, 2014.

[150] B. P. Schneider, D. L. Hershman, and C. Loprinzi, "Symptoms: chemotherapy-induced peripheral neuropathy," in *Improving Outcomes for Breast Cancer Survivors*, P. Ganz, Ed., vol. 862 of Advances in experimental medicine and biology, pp. 77–87, Springer, Cham, 2015.

[151] Z. Nahleh, J. Pruemer, J. Lafollette, and S. Sweany, "Melatonin, a promising role in taxane-related neuropathy," *Clinical Medicine Insights: Oncology*, vol. 4, 2010.

[152] H. Lee, H. J. Lee, J. H. Jung, E. A. Shin, and S. H. Kim, "Melatonin disturbs SUMOylation-mediated crosstalk between c-Myc and nestin via MT1 activation and promotes the sensitivity of paclitaxel in brain cancer stem cells," *Journal of Pineal Research*, vol. 65, no. 2, article e12496, 2018.

[153] H. F. Galley, B. Mccormick, K. L. Wilson, D. A. Lowes, L. Colvin, and C. Torsney, "Melatonin limits paclitaxel-induced mitochondrial dysfunction in vitro and protects against paclitaxel-induced neuropathic pain in the rat," *Journal of Pineal Research*, vol. 63, no. 4, article e12444, 2017.

[154] L. Gianni, U. Dafni, R. D. Gelber et al., "Treatment with trastuzumab for 1 year after adjuvant chemotherapy in patients with HER2-positive early breast cancer: a 4-year follow-up of a randomised controlled trial," *The Lancet Oncology*, vol. 12, no. 3, pp. 236–244, 2011.

[155] E. A. Ghani, I. Kerr, and R. Dada, "Grade 3 trastuzumab-induced neutropenia in breast cancer patient," *Journal of Oncology Pharmacy Practice*, vol. 20, no. 2, pp. 154–157, 2014.

[156] M. Ozturk, M. Ozler, Y. G. Kurt et al., "Efficacy of melatonin, mercaptoethylguanidine and 1400W in doxorubicin- and trastuzumab-induced cardiotoxicity," *Journal of Pineal Research*, vol. 50, no. 1, pp. 89–96, 2011.

[157] R. Reiter, S. Rosales-Corral, D. X. Tan et al., "Melatonin, a full service anti-cancer agent: inhibition of initiation, progression

and metastasis," *International Journal of Molecular Sciences*, vol. 18, no. 4, p. 843, 2017.

[158] J. C. Mayo, D. Hevia, I. Quiros-Gonzalez et al., "IGFBP3 and MAPK/ERK signaling mediates melatonin-induced antitumor activity in prostate cancer," *Journal of Pineal Research*, vol. 62, no. 1, article e12373, 2017.

[159] K. H. Lu, S. C. Su, C. W. Lin et al., "Melatonin attenuates osteosarcoma cell invasion by suppression of C-C motif chemokine ligand 24 through inhibition of the c-Jun N-terminal kinase pathway," *Journal of Pineal Research*, vol. 65, no. 3, article e12507, 2018.

[160] Z. Ma, D. Liu, S. Di et al., "Histone deacetylase 9 downregulation decreases tumor growth and promotes apoptosis in non-small cell lung cancer after melatonin treatment," *Journal of Pineal Research*, no. article e12587, 2019.

[161] L. Chen, L. Liu, Y. Li, and J. Gao, "Melatonin increases human cervical cancer HeLa cells apoptosis induced by cisplatin via inhibition of JNK/Parkin/mitophagy axis," *In vitro Cellular & Developmental Biology Animal*, vol. 54, no. 1, pp. 1–10, 2018.

[162] A. C. Uguz, B. Cig, J. Espino et al., "Melatonin potentiates chemotherapy-induced cytotoxicity and apoptosis in rat pancreatic tumor cells," *Journal of Pineal Research*, vol. 53, no. 1, pp. 91–98, 2012.

[163] R. Pariente, J. A. Pariente, A. B. Rodríguez, and J. Espino, "Melatonin sensitizes human cervical cancer HeLa cells to cisplatin-induced cytotoxicity and apoptosis: effects on oxidative stress and DNA fragmentation," *Journal of Pineal Research*, vol. 60, no. 1, pp. 55–64, 2016.

[164] H. Zhou, W. Du, Y. Li et al., "Effects of melatonin on fatty liver disease: the role of NR4A1/DNA-PKcs/p53 pathway, mitochondrial fission, and mitophagy," *Journal of Pineal Research*, vol. 64, no. 1, 2018.

[165] Y. Gao, X. Xiao, C. Zhang et al., "Melatonin synergizes the chemotherapeutic effect of 5-fluorouracil in colon cancer by suppressing PI3K/AKT and NF-κB/iNOS signaling pathways," *Journal of Pineal Research*, vol. 62, no. 2, 2016.

[166] Q. Yang, W. Jiang, and P. Hou, "Emerging role of PI3K/AKT in tumor-related epigenetic regulation," *Seminars in Cancer biology*, 2019.

[167] E. J. Sanchez-Barcelo, M. D. Mediavilla, C. Alonso-Gonzalez, and R. J. Reiter, "Melatonin uses in oncology: breast cancer prevention and reduction of the side effects of chemotherapy and radiation," *Expert Opinion on Investigational Drugs*, vol. 21, no. 6, pp. 819–831, 2012.

[168] D. Liu, L. Xu, X. Zhang et al., "Snapshot: implications for mTOR in aging-related ischemia/reperfusion injury," *Aging and Disease*, vol. 10, no. 1, pp. 116–133, 2019.

[169] Z. Ma, D. Liu, W. Li et al., "STYK1 promotes tumor growth and metastasis by reducing SPINT2/HAI-2 expression in non-small cell lung cancer," *Cell Death & Disease*, vol. 10, no. 6, 2019.

[170] S. C. Su, M. J. Hsieh, W. E. Yang, W. H. Chung, R. J. Reiter, and S. F. Yang, "Cancer metastasis: mechanisms of inhibition by melatonin," *Journal of Pineal Research*, vol. 62, no. 1, article e12370, 2017.

[171] L. C. Manchester, A. Coto-Montes, J. A. Boga et al., "Melatonin: an ancient molecule that makes oxygen metabolically tolerable," *Journal of Pineal Research*, vol. 59, no. 4, pp. 403–419, 2015.

[172] C. Venegas, J. A. García, G. Escames et al., "Extrapineal melatonin: analysis of its subcellular distribution and daily fluctuations," *Journal of Pineal Research*, vol. 52, no. 2, pp. 217–227, 2012.

[173] B. Jung-Hynes, R. J. Reiter, and N. Ahmad, "Sirtuins, melatonin and circadian rhythms: building a bridge between aging and cancer," *Journal of Pineal Research*, vol. 48, no. 1, pp. 9–19, 2010.

[174] B. Jung-Hynes, T. L. Schmit, S. R. Reagan-Shaw, I. A. Siddiqui, H. Mukhtar, and N. Ahmad, "Melatonin, a novel Sirt1 inhibitor, imparts antiproliferative effects against prostate cancer in vitro in culture and in vivo in TRAMP model," *Journal of Pineal Research*, vol. 50, no. 2, pp. 140–149, 2011.

[175] M. B. Scher, A. Vaquero, and D. Reinberg, "SirT3 is a nuclear NAD^+-dependent histone deacetylase that translocates to the mitochondria upon cellular stress," *Genes & Development*, vol. 21, no. 8, pp. 920–928, 2007.

[176] S. Zhu, Z. Dong, X. Ke et al., "The roles of sirtuins family in cell metabolism during tumor development," *Seminars in Cancer Biology*, 2018.

[177] J. S. KIM, L. He, and J. J. Lemasters, "Mitochondrial permeability transition: a common pathway to necrosis and apoptosis," *Biochemical and Biophysical Research Communications*, vol. 304, no. 3, pp. 463–470, 2003.

[178] D. Mukherjee, A. K. Ghosh, A. Bandyopadhyay et al., "Melatonin protects against isoproterenol-induced alterations in cardiac mitochondrial energy-metabolizing enzymes, apoptotic proteins, and assists in complete recovery from myocardial injury in rats," *Journal of Pineal Research*, vol. 53, no. 2, pp. 166–179, 2012.

[179] X. Xu, C. C. Chua, M. Zhang et al., "The role of PARP activation in glutamate-induced necroptosis in HT-22 cells," *Brain Research*, vol. 1343, pp. 206–212, 2010.

[180] S. W. Yu, H. Wang, M. F. Poitras et al., "Mediation of poly(-ADP-ribose) polymerase-1-dependent cell death by apoptosis-inducing factor," *Science*, vol. 297, no. 5579, pp. 259–263, 2002.

[181] F. Nduhirabandi, K. Lamont, Z. Albertyn, L. H. Opie, and S. Lecour, "Role of toll-like receptor 4 in melatonin-induced cardioprotection," *Journal of Pineal Research*, vol. 60, no. 1, pp. 39–47, 2016.

[182] H. Zhou and Q. Ma, "Protective role of melatonin in cardiac ischemia-reperfusion injury: from pathogenesis to targeted therapy," *Journal of Pineal Research*, vol. 64, no. 3, 2018.

[183] D. Han, Y. Wang, J. Chen et al., "Activation of melatonin receptor 2 but not melatonin receptor 1 mediates melatonin-conferred cardioprotection against myocardial ischemia/reperfusion injury," *Journal of Pineal Research*, no. article e12571, 2019.

[184] Y. Yang, W. Duan, Z. Jin et al., "JAK2/STAT3 activation by melatonin attenuates the mitochondrial oxidative damage induced by myocardial ischemia/reperfusion injury," *Journal of Pineal Research*, vol. 55, no. 3, pp. 275–286, 2013.

[185] Y. Zhang, Y. Wang, J. Xu et al., "Melatonin attenuates myocardial ischemia-reperfusion injury via improving mitochondrial fusion/mitophagy and activating the AMPK-OPA1 signaling pathways," *Journal of Pineal Research*, vol. 66, no. 2, article e12542, 2019.

[186] A. Lochner, E. Marais, and B. Huisamen, "Melatonin and cardioprotection against ischaemia/reperfusion injury: what's

new? A review," *Journal of Pineal Research*, vol. 65, no. 1, article e12490, 2018.

[187] Z. Zhao, C. Lu, T. Li et al., "The protective effect of melatonin on brain ischemia and reperfusion in rats and humans: in vivo assessment and a randomized controlled trial," *Journal of Pineal Research*, vol. 65, no. 4, article e12521, 2018.

[188] B. Jayaraman, A. M. Smith, J. D. Fernandes, and A. D. Frankel, "Oligomeric viral proteins: small in size, large in presence," *Critical Reviews in Biochemistry and Molecular Biology*, vol. 51, no. 5, pp. 379–394, 2016.

[189] C. W. Hsiao, T. I. Peng, A. C. Peng et al., "Long-term Aβ exposure augments mCa^{2+}-independent mROS-mediated depletion of cardiolipin for the shift of a lethal transient mitochondrial permeability transition to its permanent mode in NARP cybrids: a protective targeting of melatonin," *Journal of Pineal Research*, vol. 54, no. 1, pp. 107–125, 2013.

[190] H. Y. Fu, S. Sanada, T. Matsuzaki et al., "Chemical endoplasmic reticulum chaperone alleviates doxorubicin-induced cardiac dysfunction," *Circulation Research*, vol. 118, no. 5, pp. 798–809, 2016.

[191] T. Minamino, I. Komuro, and M. Kitakaze, "Endoplasmic reticulum stress as a therapeutic target in cardiovascular disease," *Circulation Research*, vol. 107, no. 9, pp. 1071–1082, 2010.

[192] L. Fan, G. Sun, T. Ma et al., "Melatonin reverses tunicamycin-induced endoplasmic reticulum stress in human hepatocellular carcinoma cells and improves cytotoxic response to doxorubicin by increasing CHOP and decreasing Survivin," *Journal of Pineal Research*, vol. 55, no. 2, pp. 184–194, 2013.

[193] H. J. Park, J. Y. Park, J. W. Kim et al., "Melatonin improves the meiotic maturation of porcine oocytes by reducing endoplasmic reticulum stress during in vitro maturation," *Journal of Pineal Research*, vol. 64, no. 2, article e12458, 2018.

[194] C. Kim, N. Kim, H. Joo et al., "Modulation by melatonin of the cardiotoxic and antitumor activities of adriamycin," *Journal of Cardiovascular Pharmacology*, vol. 46, no. 2, pp. 200–210, 2005.

[195] H. H. Ahmed, F. Mannaa, G. A. Elmegeed, and S. H. Doss, "Cardioprotective activity of melatonin and its novel synthesized derivatives on doxorubicin-induced cardiotoxicity," *Bioorganic & Medicinal Chemistry*, vol. 13, no. 5, pp. 1847–1857, 2005.

[196] Z. I. Kunak, E. Macit, H. Yaren et al., "Protective effects of melatonin and S-methylisothiourea on mechlorethamine induced nephrotoxicity," *The Journal of Surgical Research*, vol. 175, no. 1, pp. e17–e23, 2012.

Hindawi
Oxidative Medicine and Cellular Longevity
Volume 2019, Article ID 2075614, 51 pages
https://doi.org/10.1155/2019/2075614

Review Article

Medicinal Plants in the Prevention and Treatment of Colon Cancer

Paola Aiello,[1,2] Maedeh Sharghi,[3] Shabnam Malekpour Mansourkhani,[4] Azam Pourabbasi Ardekan,[5] Leila Jouybari,[6] Nahid Daraei,[7] Khadijeh Peiro,[8] Sima Mohamadian,[9] Mahdiyeh Rezaei,[9] Mahdi Heidari,[5] Ilaria Peluso,[1] Fereshteh Ghorat,[10] Anupam Bishayee,[11] and Wesam Kooti[5]

[1]*Council for Agricultural Research and Economics, Research Centre for Food and Nutrition, Via Ardeatina 546, 00178 Rome, Italy*
[2]*Department of Physiology and Pharmacology "V. Erspamer", La Sapienza University of Rome, Rome, Italy*
[3]*Nursing and Midwifery School, Guilan University of Medical Sciences, Rasht, Iran*
[4]*Department of Biology, School of Science, Shiraz University, Shiraz, Iran*
[5]*Lung Diseases and Allergy Research Center, Research Institute for Health Development, Kurdistan University of Medical Sciences, Sanandaj, Iran*
[6]*Nursing Research Center, Golestan University of Medical Sciences, Gorgan, Iran*
[7]*Student Research Committee, Ahvaz Jundishapur University of Medical Sciences, Ahvaz, Iran*
[8]*Department of Biology, Faculty of Sciences, Shahid Chamran University, Ahvaz, Iran*
[9]*Faculty of Pharmacy and Pharmaceutical Sciences, Tehran Medical Sciences, Islamic Azad University, Tehran, Iran*
[10]*Traditional and Complementary Medicine Research Center, Sabzevar University of Medical Sciences, Sabzevar, Iran*
[11]*Lake Erie College of Osteopathic Medicine, 5000 Lakewood Ranch Boulevard, Bradenton, FL 34211, USA*

Correspondence should be addressed to Anupam Bishayee; abishayee@gmail.com and Wesam Kooti; wesamkooti@gmail.com

Received 8 March 2019; Accepted 3 July 2019; Published 4 December 2019

Guest Editor: Ana S. Fernandes

The standard treatment for cancer is generally based on using cytotoxic drugs, radiotherapy, chemotherapy, and surgery. However, the use of traditional treatments has received attention in recent years. The aim of the present work was to provide an overview of medicinal plants effective on colon cancer with special emphasis on bioactive components and underlying mechanisms of action. Various literature databases, including Web of Science, PubMed, and Scopus, were used and English language articles were considered. Based on literature search, 172 experimental studies and 71 clinical cases on 190 plants were included. The results indicate that grape, soybean, green tea, garlic, olive, and pomegranate are the most effective plants against colon cancer. In these studies, fruits, seeds, leaves, and plant roots were used for *in vitro* and *in vivo* models. Various anticolon cancer mechanisms of these medicinal plants include induction of superoxide dismutase, reduction of DNA oxidation, induction of apoptosis by inducing a cell cycle arrest in S phase, reducing the expression of PI3K, P-Akt protein, and MMP as well; reduction of antiapoptotic Bcl-2 and Bcl-xL proteins, and decrease of proliferating cell nuclear antigen (PCNA), cyclin A, cyclin D1, cyclin B1 and cyclin E. Plant compounds also increase both the expression of the cell cycle inhibitors p53, p21, and p27, and the BAD, Bax, caspase 3, caspase 7, caspase 8, and caspase 9 proteins levels. In fact, purification of herbal compounds and demonstration of their efficacy in appropriate *in vivo* models, as well as clinical studies, may lead to alternative and effective ways of controlling and treating colon cancer.

1. Introduction

An uncontrolled growth of the body's cells can lead to cancer. Cancer of the large intestine (colon) is one of the main cause of death due to cancer. While the numbers for colon cancer are somewhat equal in women (47,820) and men (47,700), it will be diagnosed in (16,190) men (23,720) more than women. Multiple factors are involved in the development of colorectal cancer, such as lack of physical activity [1], excessive alcohol consumption [2], old age [3], family history [4], high-fat diets with no fiber and red meat, diabetes [5], and inflammatory bowel diseases, including ulcerative colitis and Crohn's disease [6].

Prevention of colorectal cancer usually depends on screening methods to diagnose adenomatous polyps which are precursor lesions to colon cancer [7]. The standard treatment for cancer is generally based on using cytotoxic drugs, radiotherapy, chemotherapy, and surgery [8]. Apart from these treatments, antiangiogenic agents are also used for the treatment and control of cancer progression [9].

Colon cancer has several stages: 0, I, II, III, and IV. Treatment for stages 0 to III typically involves surgery, while for stage IV and the recurrent colon cancer both surgery and chemotherapy are the options [10]. Depending on the cancer stage and the patient characteristics, several chemotherapeutic drugs and diets have been recommended for the management of colorectal cancer. Drugs such as 5-fluorouracil (5-FU), at the base of the neoadjuvant therapies folfox and folfiri, are used together with bevacizumab, panitumumab, or cetuximab [7].

Chemotherapy works on active cells (live cells), such as cancerous ones, which grow and divide more rapidly than other cells. But some healthy cells are active too, including blood, gastrointestinal tract, and hair follicle ones. Side effects of chemotherapy occur when healthy cells are damaged. Among these side effects, fatigue, headache, muscle pain, stomach pain, diarrhea and vomiting, sore throat, blood abnormalities, constipation, damage to the nervous system, memory problems, loss of appetite, and hair loss can be mentioned [11].

Throughout the world, early diagnosis and treatment of cancer usually increase the individual's chances of survival. But in developing countries, access to effective and modern diagnostic methods and facilities is usually limited for most people, especially in rural areas [12]. Accordingly, the World Health Organization (WHO) has estimated that about 80% of the world population use traditional treatments [13]. One of these treatments is phytotherapy, also known as phytomedicine, namely, the use of plants or a mixture of plant extracts for the treatment of diseases. The use of medicinal plants can restore the body's ability to protect, regulate, and heal itself, promoting a physical, mental, and emotional well-being [14–16]. Various studies have shown the therapeutic effects of plants on fertility and infertility [17], hormonal disorders, hyperlipidemia [18], liver diseases [19], anemia [20], renal diseases [21], and neurological and psychiatric diseases [22]. Therefore, due to all the positive effects showed by medicinal plants, their potential use in cancer prevention and therapy has been widely suggested [23–25].

Since the current treatments usually have side effects, plants and their extracts can be useful in the treatment of colon cancer with fewer side effects. The aims of this review are to present and analyse the evidence of medicinal plants effective on colon cancer, to investigate and identify the most important compounds present in these plant extracts, and to decipher underlying molecular mechanisms of action.

2. Literature Search Methodology

This is a narrative review of all research (English full text or abstract) studies conducted on effective medicinal plants in the treatment or prevention of colon cancer throughout the world. Keywords, including colon cancer, extract, herbs, plant extracts, and plants, were searched separately or combined in various literature databases, such as Web of Science, PubMed, and Scopus. Only English language articles published until July 2018 were considered.

In the current narrative review, studies (published papers) were accepted on the basis of inclusion and exclusion criteria. The inclusion criterion was English language studies, which demonstrated an effective use of whole plants or herbal ingredients, as well as studies which included standard laboratory tests. *In vivo* and *in vitro* studies that were published as original articles or short communications were also included. The exclusion criteria included irrelevancy of the studies to the subject matter, not sufficient data in the study, studies on mushrooms or algae, and the lack of access to the full text. Reviews, case reports/case series, and letters to editors were also excluded but used to find appropriate primary literature.

The abstracts of the studies were reviewed independently by two reviewers (authors of this study) on the basis of the inclusion and exclusion criteria. In case of any inconsistency, both authors reviewed the results together and solved the discrepancy. Data extracted from various articles were included in the study and entered into a check list after the quality was confirmed. This check list included some information: authors' name, year of publication, experimental model, type of extract and its concentration or dose, main components, and mechanisms of action (if reported).

3. Results

3.1. Medicinal Plants and Colon Cancer. Overall, 1,150 articles were collected in the first step and unrelated articles were excluded later on according to title and abstract evaluation. Moreover, articles that did not have complete data along with congress and conference proceedings were excluded. Accordingly, a total of 1,012 articles were excluded in this step. Finally, 190 articles fulfilled the criteria and were included in this review. These papers were published within 2000-2017. A total of 190 plants were

included in this study. Based on literature search, 172 experimental studies and 71 clinical cases were included.

Overall, results indicate that grape, soybean, green tea, garlic, olive, and pomegranate are the most effective plants against colon cancer. In these studies, fruits, seeds, leaves, and plant roots were used for *in vitro* and *in vivo* studies.

3.1.1. In Vitro Studies. Out of 172 studies, 75 were carried out on HT-29, 60 on HCT116, and 24 on Caco-2 cells (Table 1). On HT-29 cells, both *Allium sativum* root extracts and *Camellia sinensis* leaf extracts induced cell apoptosis by two different mechanisms, respectively. In fact, the former showed inhibition of the PI3K/Akt pathway, upregulation of PTEN, and downregulation of Akt and p-Akt expression, while the latter was involved in attenuation of COX-2 expression and modulation of NFκB, AP-1, CREB, and/or NF-IL-6. Moreover, an antiproliferative activity has also been detected in *Olea europaea* fruit extracts, which increased caspase 3-like activity and were involved in the production of superoxide anions in mitochondria. An antiproliferative activity, by means of a blockage in the G2/M phase, has also been reported in Caco-2 cells by *Vitis vinifera* fruit extracts. Concerning HCT116 cells, several plants, such as *American ginseng* and *Hibiscus cannabinus*, induced cell cycle arrest in different checkpoints.

3.1.2. Studies in Animal Models. The most used animal model is the murine one (Tables 2(a) and 2(b)). In particular, studies were carried out above all on HT-29 and HCT116 cells. The effects of the different medicinal plants and their extracts are essentially the same detected in *in vitro* studies. In particular, plant extracts were able to induce apoptosis and inhibit proliferation and tumor angiogenesis by regulating p53 levels and checkpoint proteins with consequent cell cycle arrest and antiproliferative and antiapoptotic effects on cancerous cells.

The main mechanisms of action of medicinal plants are summarized in Figure 1.

In *in vitro* studies, it has been found that grapes, which contain substantial amounts of flavonoids and procyanidins, play a role in reducing the proliferation of cancer cells by increasing dihydroceramides and p53 and p21 (cell cycle gate keeper) protein levels. Additionally, grape extracts triggered antioxidant response by activating the transcriptional factor nuclear factor erythroid 2-related factor 2 (Nrf2) [27].

Grape seeds contain polyphenolic and procyanidin compounds, and their reducing effects on the activity of myeloperoxidase have been shown in *in vitro* and *in vivo* studies. It has been suggested that grape seeds could inhibit the growth of colon cancer cells by altering the cell cycle, which would lead eventually to exert the caspase-dependent apoptosis [180].

Another plant that attracted researchers' attention was soybean, which contain saponins. After 72 h of exposure of colon cancer cells to the soy extract, it was found that this extract inhibited the activity and expression of protein kinase C and cyclooxygenase-2 (COX-2) [34]. The density of the cancer cells being exposed to the soy extract significantly decreased. Soybeans can also reduce the number of cancer cells and increase their mortality, which may be due to increased levels of Rab6 protein [216].

Green tea leaves have also attracted the researchers' attention in these studies. Green tea leaves, with high levels of catechins, increased apoptosis in colon cancer cells and reduced the expression of the vascular endothelial growth factor (VEGF) and its promoter activity in *in vitro* and *in vivo* studies. The extract increased apoptosis (programmed cell death) by 1.9 times in tumor cells and 3 times in endothelial cells compared to the control group [182]. In another *in vitro* study, the results showed that green tea leaves can be effective in the inhibition of matrix metalloproteinase 9 (MMP-9) and in inhibiting the secretion of VEGF [183].

Garlic was another effective plant in this study. Its roots have allicin and organosulfur compounds. In an *in vitro* study, they inhibited cancer cell growth and induced apoptosis through the inhibition of the phosphoinositide 3-kinase/Akt pathway. They can also increase the expression of phosphatase and tensin homolog (PTEN) and reduce the expression of Akt and p-Akt [32]. Garlic roots contain S-allylcysteine and S-allylmercaptocysteine, which are known to exhibit anticancer properties. The results of a clinical trial on 51 patients, whose illness was diagnosed as colon cancer through colonoscopy, and who ranged in age from 40 to 79 years, suggest that the garlic extract has an inhibitory effect on the size and number of cancer cells. Possible mechanisms suggested for the anticancer effects of the garlic extract are both the increase of detoxifying enzyme soluble adenylyl cyclase (SAC) and an increased activity of glutathione S-transferase (GST). The results suggest that the garlic extract stimulates mouse spleen cells, causes the secretion of cytokines, such as interleukin-2 (IL2), tumor necrosis factor-α (TNF-α), and interferon-γ, and increases the activity of natural killer (NK) cells and phagocytic peritoneal macrophages [200].

The results of *in vitro* studies on olive fruit showed that it can increase peroxide anions in the mitochondria of HT-29 cancer cells due to the presence of 73.25% of maslinic acid and 25.75% of oleanolic acid. It also increases caspase 3-like activity up to 6 times and induces programmed cell death through the internal pathway [217]. Furthermore, the olive extract induces the production of reactive oxygen species (ROS) and causes a quick release of cytochrome c from mitochondria to cytosol.

The pomegranate fruit contains numerous phytochemicals, such as punicalagins, ellagitannins, ellagic acid, and other flavonoids, including quercetin, kaempferol, and luteolin glycosides. The results of an *in vitro* study indicate the anticancer activity of this extract through reduction of phosphorylation of the p65 subunit and subsequent inhibition of nuclear factor-κB (NFκB). It also inhibits the activity of TNF receptor induced by Akt, which is needed for the activity of NFκB. The fruit juice can considerably inhibit the expression of TNF-α-inducing proteins (Tipα) in the COX-2 pathway in cancer cells [43]. The effective and important compounds in pomegranate identified in these 104 studies are flavonoids, polyphenol compounds, such as caffeic acid, catechins, saponins, polysaccharides, triterpenoids,

Table 1: Cytotoxic effects of medicinal plants on colon cancer in *in vitro* models.

Scientific name	Parts used	Cell line	Conc.	Type of extract	Important compounds	Cellular effect	Mechanisms	References
Vitis vinifera	Fruit	HCT116	NM	*Lyophilized*	Hydroxycinnamic acids, proanthocyanidins, stilbenoids	Increase of dihydroceramides, sphingolipid mediators involved in cell cycle arrest, and reduction of the proliferation rate	(i) Increase of p53 and p21 cell cycle gate keepers (ii) Activation of the transcriptional factor Nrf2	[26, 27]
	Fruit	Caco-2	365 mg/g	*Methanolic*	Catechin, epicatechin, quercetin, gallic acid	Antiproliferative activity and direct initiation of cell death	Blockage in the G2/M phase	[28, 29]
	Seed	Caco-2	10–25 μg/mL	*Aqueous*	Procyanidins	(i) Increased crypt depth (ii) Inhibited cell viability and decreased histological damage score	Reduced MPO (myeloperoxidase) activity	[29]
	Skin	NM	7.5, 30, 60 μg/mL	*Methanolic*	4′-Geranyloxyferulic acid	NM	NM	[30]
	Seed	Colon cancer stem cells	6.25, 12.5, 25 μg/mL	*NM*	(+)-catechin, (−)-epicatechin	NM	(i) Increment of p53, Bax/Bcl-2 ratio, and cleaved PARP (ii) Inhibition of Wnt/β-catenin signaling	[31]
Allium sativum	Root	HT-29	20, 50, 100 mg/mL	*Ethanolic*	NM	Induction of apoptosis and cell cycle arrest	(i) Inhibition of the PI3K/Akt pathway (ii) Upregulation of PTEN and downregulation of Akt and p-Akt expression	[32]
Glycine max	Seed	Caco-2, SW620, HT-29	12.5 μg/mL	*Aqueous*	Anthoxanthin	Cell death and significant reduction of cell density	Enhancement of Rab6 protein levels	[33]
	Seed	HT-29	240, 600 ppm	*Crude*	Saponin		Suppression of PKC activation and increase of alkaline phosphatase activity	[33]
	Seed	HT-29	NM	*Crude*	Saponin	NM	(i) Suppression of the degradation of IκBα in PMA-stimulated cells (ii) Downregulation of COX-2 and PKC expressions	[34]

Table 1: Continued.

Scientific name	Parts used	Cell line	Conc.	Type of extract	Important compounds	Cellular effect	Mechanisms	References
Camellia sinensis	Leaf	HT-29	0, 10, 30, 50 μM	*Aqueous*	Catechin, epigallocatechin gallate	1.9-fold increase in tumor cell apoptosis and a 3-fold increase in endothelial cell apoptosis	(i) Suppression of ERK-1 and ERK-2 activation (ii) Suppression of VEGF expression	[35]
	Leaf	Caco-2, HT-29	300 μM	*Aqueous*	Theaflavins (TF-2T, F-3, TF-1)	Human colon cancer cell apoptosis induction	Modulation of NFκB, AP-1, CREB, and/or IL-6	[36]
	Leaf	HT-29	68-80 0.73 μg/mL	*Hot water extract*	Flavan-3-ol (catechin & tannin) & polyphenols (teadenol B)	Inhibition of proliferation of HT-29 cells	Increased expression levels of caspases 3/7, 8, and 9	[35]
Olea europaea	Fruit	HT-29	150, 55.5 200 and 74 μmol/L	*Methanolic and chloroform*	Maslinic acid, oleanolic acid	Antiproliferative activity	(i) Increased caspase 3-like activity to 6-fold (ii) Production of superoxide anions in the mitochondria	[37]
	Fruit, leaf	SW480 and HT-29	100–400 m/z	*Methanolic & hexane*	Oleic acid, linoleic acid, gamma-linolenic acid, lignans, flavonoids, secoiridoids	Reduced cell growth in both cell lines	(i) Limited G2M cell cycle (ii) Depressed cyclooxygenase-2 expression in HT-29 cells (iii) Suppression of β-catenin/TCF signaling in SW480 cells (iv) Promotion of the entry into subG1 phase	[38]
	Fruit	Caco-2	50 μM	*Aqueous*	Phenolic compounds, authentic hydroxyl tyrosol (HT)	Reduced proliferation of Caco-2 cells	Reduction of the methylation levels of CNR1 promoter	[39]
	Fruit	HT115	25 μg/mL	*Hydroethanolic*	Phenolic compounds (p-hydroxyphenyl ethanol, pinoresinol & dihydroxyphenyl ethanol)	NM	Inhibition by reduced expression of a range of α5 & β1	[40]
	Olive mill wastewater	HT-29, HCT116, CT26	NM	*Methanolic*	Hydroxytyrosol	(i) Inhibited proliferation (ii) Inhibited migration and invasion	(i) Reduced sprout formation (ii) Inhibited VEGF and IL-8 levels	[41]
	Fruit	Caco-2	0-2,000 μg/mL	*Ethanolic*	Tyrosol, hydroxytyrosol, oleuropein, rutin, quercetin and glucoside forms of luteolin and apigenin	NM	(i) Induction of the cell cycle arrest in S-phase	[42]
Punica granatum	Juice	HT-29	50 mg/L	*Aqueous*	Ellagitannins, punicalagin	Inhibition of cancer cell proliferation	(i) Suppressed TNFR-induced COX-2 protein expression (ii) Reduced phosphorylation of the p65 subunit and binding to the NFκB response element	[43]
	Seed	LS174	63.2 μg/mL	*Supercritical fluid*	Punicic acid, γ-tocopherol, α-tocopherol	Cytotoxic activity	(i) Slightly decreased development of tubules from elongated cell bodies (ii) Reduction of the number of cell connections	[44]

Table 1: Continued.

Scientific name	Parts used	Cell line	Conc.	Type of extract	Important compounds	Cellular effect	Mechanisms	References
Glycyrrhiza glabra	Root	HT-29	12.2 and 31 μg/mL	*Ethanolic*	Licochalcone	NM	Increase of the protein levels of proapoptotic Bax	[37]
Opuntia ficus-indica	Fruit	Caco-2	115 μM	*Aqueous*	Betalain pigment indicaxanthin	Apoptosis of proliferating cells	(i) Demethylation of the tumor suppressor p16INK4a gene promoter (ii) Reactivation of the silenced mRNA expression and accumulation of p16INK4a	[38]
	Fruit	HT-29 & Caco-2 & NIH 3 T3 (as control)	Against HT-29 (4.9 μg/mL) against Caco-2 (8.2 μg/mL)	*Alkaline hydrolysis with NaOH*	Isorhamnetin glycosides (IG5 and IG6)-phenol	Cell death through apoptosis and necrosis	Increased activity of caspase 3/7	[45]
Piper betle	Leaf	HT-29 and HCT116	200.0 μg/mL	*Aqueous*	Hydroxychavicol	Antioxidant capacity and induction of a greater apoptotic effect	(i) Scavenging activity (ii) Formation of electrophilic metabolites	[41, 46]
Fragaria×ananassa	Fruit	HT-29	0.025, 0.05, 0.25, 0.5%	*Ethanolic*	Ascorbate, ellagic acid	Decreased proliferation of HT-29 cells	Increase in the levels of 8OHA and decrease in the levels of 8OHG	[40]
Sasa quelpaertensis	Leaf	HT-29 HCT116	0, 100, 200, 300 mg/L	*Ethanolic*	p-Coumaric acid, tricin	Inhibited colony formation	Nonadherent sphere formation suppressed CD133+ & CD44+ population	[41]
Salvia chinensis	Stem	HCT116, COLO 205	10, 20, 40,60, 80, 100 mg/L	*Polyphenolic*	Terpenoids, phenolic acid, flavonoids, dibenzylcyclooctadiene	Apoptosis & loss of mitochondrial membrane	Induced G0/G1 cell cycle	[42]
Rubus idaeus L.	Fruit	HT-29, HT-115, Caco-2	3.125, 6.25, 12.5, 25, 50 mg/L	*Acetate*	Polyphenol, anthocyanin, ellagitannin	NM	Decreased population of cells in G1 phase	[47]
		LoVo	50 μL	*Aqueous*	NM	Inhibited proliferation of LoVo	Suppression of the NFκB pathway	[48]
Curcuma longa	Root	HT-29, HCT15, DLD1, HCT116	(i) Short-term assay: four 10-fold dilutions (100 to 0.1 mg/L) (ii) Long-term assay: 5, 10, 20 mg/L	*Ethanolic*	Curcumin (diferuloylmethane)	Inhibited formation of HCT116 spheroids	NM	[49]

Table 1: Continued.

Scientific name	Parts used	Cell line	Conc.	Type of extract	Important compounds	Cellular effect	Mechanisms	References
Eleutherococcus senticosus	Root	HCT116	12.5, 25, 50, 100	*Methanolic*	Eleutherosides, triterpenoid saponins, glycans	NM	Activation of natural killer cells and thus enhancement of immune function	[50]
Tabernaemontana divaricata L.	Leaf	HT-29, HCT15	10, 30, 100 mg/L	*Ethyl acetate, chloroform, methanolic*	Alkaloids	NM	Inhibited the unwinding of supercoiled DNA	[45]
Millingtonia hortensis	Root, flower, leaf	RKO	50, 100, 200, 400, 800 mg/L	*Aqueous*	Phenylethanoid glycoside, squalene, salidroside, 2-phenyl rutinoside	Apoptosis induction	(i) Increase of fragmented DNA (ii) Decrease of the expression of antiapoptotic proteins, Bcl-xL and p-BAD	[46]
	Powder	RKO	200, 400, 800 μg/mL	*Aqueous*	Water soluble compounds	Antiproliferative effect	NM	[51]
Thai purple rice	Seed	Caco-2, Cat. No. HTB-37	16.11 μg/mL	*Methanol acidified*	Cyanidin-3-glucoside and peonidin-3-glucoside, anthocyanins, phenolic compounds	(i) Antioxidation of anthocyanins and phenols (ii) Antiproliferation of colon cancer cells	NM	[52]
Annona muricata	Leaf	HCT116, HT-29	11.43 ± 1.87 μg/ml and 8.98 ± 1.24 μg/ml	*Ethanolic*	Alkaloids, acetogenins, essential oils	Block of the migration and invasion of HT-29 and HCT116 cells	(i) Cell cycle arrest at G1 phase (ii) Disruption of MMP, cytochrome c leakage and activation	[53]
	NM	HT-29, HCT116	<4, <20 μg/mL	*EtOAc*	Annopentocin A, annopentocin B, annopentocin C, cis- and trans-annomuricin-D-ones, annomuricin E	NM	Suppression of ATP production and NADH oxidase in cancer cells	[54]
Pistacia lentiscus L. var. *chia*	Leaf	HCT116	NM	*Ethanolic*	Resin, known as Chios mastic gum (CMG)	Causes several morphological changes typical of apoptosis in cell organelles	(i) Induction of cell cycle arrest at G1 phase (ii) Activation of pro-caspases 8, 9, 3	[55]
	Resin	HCT116	100 μg/mL	*Hexane*	Caryophyllene	Induction of the anoikis form of apoptosis in human colon cancer HCT116 cells	(i) Induction of G1 phase arrest (ii) Loss of adhesion to the substrate	[56]
American ginseng (Panax quinquefolius)	Biological constituents	HCT116	0-2.0 mg/mL	*Aqueous*	Ginseng (GE) or its ginsenoside (GF) and polysaccharide (PS)	Proliferation was inhibited by GE, GF, and PS in wild-type and p21 cells	(i) Cells arrest in G0/G1 phase and increment of p53 and p21 proteins (ii) Increment of Bax and caspase 3 proteins expression	[57]

Table 1: Continued.

Scientific name	Parts used	Cell line	Conc.	Type of extract	Important compounds	Cellular effect	Mechanisms	References
Purple-fleshed potatoes	Fruit	Colon cancer stem cells	5.0 μg/mL	*Ethanol, methanol, ethyl acetate*	Anthocyanin, β-catenin, cytochrome c	Critical regulator of CSC proliferation and its downstream proteins (c-Myc and cyclin D1) and elevated Bax and cytochrome c	(i) Cytochrome c levels were elevated regardless of p53 status (ii) Mitochondria-mediated apoptotic pathway (iii) Suppressed levels of cytoplasmic and nuclear β-catenin	[58]
Phaseolus vulgaris	Leaf	HT-29	NM	*Ethanolic*	Polysaccharides, oligosaccharides	Changes in genes involved or linked to cell cycle arrest	(i) Inactivation of the retinoblastoma phosphoprotein (ii) Induction of G1 arrest (iii) Suppression of NF-jB1 (iv) Increase in EGR1 expression	[59]
Opuntia spp.	Fruit	HT-29	5.8 ± 1.0, 7.5 ± 2.0 , 12 ± 1% (V/V)	*Hydroalcoholic*	Betacyanins, flavonoids (isorhamnetin derivatives) and phenolic acids (ferulic acid)	NM	Induced cell cycle arrest at different checkpoints—G1, G2/M, and S	[60]
Suillus luteus	NM	HCT15	400 μg/mL	*Methanolic*	Protocatechuic acid, cinnamic acid, α-tocopherol, β-tocopherol, mannitol, trehalose, polyunsaturated fatty acids, monounsaturated fatty acids, saturated fatty acids	(i) Increase in the cellular levels of p-H2A.X, which is suggestive of DNA damage	(i) Inhibition of cell proliferation in G1 phase (ii) Increase in the cellular levels of p-H2A.X	[61]
Poncirus trifoliata	Leaf	HT-29	0.63 μM	*Aqueous (in acetone)*	β-Sitosterol, 2-hydroxy-1,2,3-propanetricarboxylic acid 2-methyl ester	Arrest of cell growth was observed with β-sitosterol	NM	[62]
Rosmarinus officinalis L.	Leaf	SW 620, DLD-1	0-120 μg/mL	*Methanolic*	Polyphenols	Antiproliferative effect of 5-FU	Downregulation of TYMS and TK1, enzymes related to 5-FU resistance	[63]
	Leaf	HT-29	SC-RE 30 μg/mL and CA 12.5 μg/mL	*Ethanolic*	Polyphenols (carnosic acid (CA) and carnosol)	(i) Upregulation of VLDLR gene as the principal contributor to the observed cholesterol accumulation in SC-RE-treated cells (ii) Downregulation of several genes involved in G1-S	Activation of Nrf2 transcription factor and common regulators, such as XBP1 (Xbp1) gene related to the unfolded protein response (UPR)	[64]

Table 1: Continued.

Scientific name	Parts used	Cell line	Conc.	Type of extract	Important compounds	Cellular effect	Mechanisms	References
	NM	HT-29	10, 20, 30, 40, 50, 60, 70 μg/mL	*NM*	Carnosic acid, carnosol, rosmarinic acid, rosmanol	NM	NM	[65]
	Leaf	HGUE-C-1, HT-29, and SW480	20–40 mg/mL	*CO2-supercritical fluid extract*	Carnosic acid, carnosol, and betulinic acid	NM	(i) Prooxidative capability by increasing the intracellular generation of ROS (ii) Activation of Nrf2	[66]
Glehnia littoralis	Leaf	HT-29	50 mg/mL	*Methanolic*	Bergapten, isoimpinellin, xanthotoxin, imperatorin, panaxydiol, falcarindiol, falcarinol	Induced apoptosis by the decreased expression of the antiapoptotic Bcl-2 mRNA	(i) Reduced expression of Bcl-2 (ii) Reduced expression levels of iNOS and COX-2	[67]
Verbena officinalis	Leaf	HCT116	20 mg/mL	*Aqueous*	Phenylethanoid glycosides, diacetyl-O-isoverbascoside, diacetyl-O-betonyoside A, and diacetyl-O-betonyoside A	(i) Substantial tumor cell growth inhibitory activity (ii) Time-dependent cytotoxicity against both cell lines	(i) Increased lipophilicity of molecules seemed to be responsible for enhanced cytotoxicity (ii) Antiproliferative activity is determined by the number of acetyl groups and also by their position in the aliphatic rings	[68]
Mentha spicata	Leaf	RCM-1	12.5 μg/mL	*N-Hexane*	Acetic acid 3-methylthio propyl ester (AMTP), methyl thio propionic acid ethyl ester (MTPE)	Exhibited antimutagenic activity	Auraptene (7-geranyloxycoumarin) having a monoterpene moiety and β-cryptoxanthin (one of the tetraterpenes) increased antibody production	[69]
Euphoria longana Lam.	Seed	SW 480	0–100 μg/mL	*Ethanolic*	Corilagin, gallic acid, ellagic acid	(i) Antiangiogenetic properties (ii) All fractions showed the anti-VEGF secretion activity	Release and expression of VEGF indicated that all fractions showed the anti-VEGF secretion activity	[70]
Sutherlandia frutescens	Flower	Caco-2	1/50 dilution of the ethanolic extract	*Ethanolic*	Amino acids, including L-arginine and L-canavanine, pinitol, flavonoids, and triterpenoid saponins as well as hexadecanoic acid and γ-sitosterol	Disruption of the key molecules in the PI3K pathway thereby inducing apoptosis	Decrease in cell viability and increment in pyknosis as well as loss in cellular membrane integrity	[71]
Melissa officinalis	Leaf	HT-29, T84	346, 120 μg/mL	*Ethanolic*	Phenolic acids (rosmarinic acid, coumaric acid, caffeic acid, protocatechuic acid, ferulic acid, chlorogenic acid), flavonoids, sesquiterpenes, monoterpenes, triterpenes	(i) Inhibited proliferation of colon carcinoma cells (ii) Induced apoptosis through formation of ROS	(i) G2/M cell cycle arrest (ii) Cleavage of caspases 3 and 7 (iii) Induced phosphatidylserine externalization in colon carcinoma cells (iv) Induced formation of ROS in colon carcinoma cells	[72]

Table 1: Continued.

Scientific name	Parts used	Cell line	Conc.	Type of extract	Important compounds	Cellular effect	Mechanisms	References
Sargassum cristaefolium	Leaf	HT-29	500 mg/mL	*Ethanolic*	Fucoidans	(i) Reduction of free radicals (ii) DPPH radical scavenging	Accumulation of cells in G0/G1 phase	[73]
Hedyotis diffusa	NM	HT-29	400 mg/mL	*Ethanolic and then DMSO*	Octadecyl (E)-p-coumarate, P-E-methoxy-cinnamic acid, ferulic acid, scopoletin, succinic acid, aurantiamide acetate, rubiadin	Suppress tumor cell growth and induce the apoptosis of human CRC cells	(i) Block G1/S progression (ii) Induce the activation of caspases 9 and 3 (iii) Inhibit IL-6-mediated STAT3 activation (iv) Downregulate the mRNA and protein expression levels of cyclin D1, CDK4, Bcl-1, and Bax	[74]
Zingiber officinale Roscoe	Peel	LoVo	100 mg/mL	*Ethanolic*	Linoleic acid methyl ester, α-zingiberene, and zingiberone	Interesting antiproliferative activity against colorectal carcinoma	NM	[75]
Scutellaria barbata	Leaf	LoVo	413.3 mg/L	*Methanolic*	Scutellarein, scutellarin, carthamidin, isocarthamidin, wogonin	Induce cell death in the human colon cancer cell line	Increase in the sub-G1 phase and inhibition of cell growth	[76]
Pistacia atlantica, Pistacia lentiscus	Resin	HCT116	100 μg/mL	*Hexane extract*	Caryophyllene	Induce the anoikis form of apoptosis in human colon cancer HCT116 cells	(i) Induce G1 phase arrest (ii) Loss of adhesion to the substrate	[56]
Citrus reticulata	Peel	SNU-C4	100 μg/mL	*Methanolic*	Limonene, geranial, neral, geranyl acetate, geraniol, β-caryophyllene, nerol, neryl acetate	Induce the apoptosis on SNU-C4, human colon cancer cells	Expression of proapoptotic gene, Bax, and major apoptotic gene, caspase 3	[77]
Echinacea pallida, Echinacea angustifolia, Echinacea purpurea	Root	COLO320	150 mg/mL	*Hexanic*	Caffeic acid derivatives, alkylamides, polyacetylenes, polysaccharides	Induce apoptosis and promote nuclear DNA fragmentation	(i) Induce apoptosis by increasing caspase 3/7 activity (ii) Promote nuclear DNA fragmentation	[78]
Nasturtium officinale	Leaf	HT-29	50 μL/mL	*Methanolic*	Phenethyl isothiocyanate, 7-methylsulfinylheptyl, 8-methylsulfinyl	(i) Inhibition of initiation, proliferation, and metastasis	(i) Inhibited DNA damage (ii) Accumulation of cells in S phase of the cell cycle	[79]

Table 1: Continued.

Scientific name	Parts used	Cell line	Conc.	Type of extract	Important compounds	Cellular effect	Mechanisms	References
Polysiphonia	NM	SW480, HCT15, HCT116, DLD-1	20 and 40 μg/mL	*Methanolic*	2,5-Dibromo-3,4-dihydroxybenzyl n-propyl ether	Potentially could be used as a chemopreventive agent against colon cancer	(i) Inhibited Wnt/β-catenin pathway (ii) Repressed CRT in colon cancer cells (iii) Downregulated cyclin D1 (iv) Activated the NFκB pathway	[80]
Aristolochia debilis Sieb. et Zucc.	Stem	HT-29	200 μg/mL	*Methanolic*	Aristolochic acid, nitrophenanthrene carboxylic acids	Inhibition of proliferation and induction of apoptosis in HT-29 cells	(i) Induction of sub-G1 cell cycle (ii) Generation of ROS and decrease of the MMP (iii) Bax overexpression and increase of Bax/Bcl-2 ratio	[81]
Myrtaceae	Leaf	HCT116	100 μg/mL (in vitro), 200 and 100 μg/disc (*in vivo*)	*Methanolic*	Phenols, flavonoid, betulinic acid	Strong inhibition of microvessel outgrowth	(i) Inhibition of tube formation on Matrigel matrix (ii) Inhibition of HUVECS migration (*in vitro*) (iii) Decreased nutrient and oxygen supply	[82]
Spica prunellae	Leaf	HT-29	200 mg/mL (*in vitro*), 600 mg/mL (*in vivo*)	*Ethanolic*	Rosmarinic acid	Inhibits CRC cell growth	(i) Suppresses STAT3 phosphorylation (ii) Regulates the expression of Bcl-2, Bax, cyclin D1, CDK4, VEGF-A, and VEGFR-2	[83]
Phytolacca americana	Root	HCT116	3200 μg/mL	*Ethanolic*	Jaligonic acids, kaempferol, quercetin, quercetin 3-glucoside, isoquercitrin, ferulic acid	Control of growth and spread of cancer cells	Reduction in the expressions of MYC, PLAU, and TEK	[84]
Morus alba	Leaf	HCT15	13.8 μg/mL	*Methanolic*	Epicatechin, myricetin, quercetin hydrate, luteolin, kaempferol, ascorbic acid, gallic acid, pelargonidine, p-coumaric acid	Cytotoxic effect on human colon cancer cells (HCT15)	(i) Apoptosis induction also involved in the downregulation of iNOS (ii) Fragmentation of DNA (iii) Upregulation of caspase 3 activity	[85]
Rhodiola imbricata	Leaf	HT-29	200 μg/mL	*Acetone and methanolic*	Phenols, tannins, and flavonoids	(i) Antioxidant activity (ii) Inhibited proliferation of HT-29 cells	(i) Scavenge free radicals (ii) DPPH radical scavenging activity (iii) Increased metal chelating activity	[86]
Asiasarum heterotropoides F.	Dried *A. radix*	HCT116	20 mg/mL	*Ethanolic*	Asarinin and xanthoxylol	Inhibition of the growth of HCT116 cells	(i) Caspase-dependent apoptosis (ii) Regulation of p53 expression at transcription level	[87]

Table 1: Continued.

Scientific name	Parts used	Cell line	Conc.	Type of extract	Important compounds	Cellular effect	Mechanisms	References
Podocarpus elatus	Fruit	HT-29	500 mg/mL	*Methanolic*	Phenolic and anthocyanin	Reduction of proliferation of colon cancer cells	(i) Cell cycle delay in S phase (ii) 93% downregulation of telomerase activity and decrease in telomere length (iii) Induced morphological alterations to HT-29 cells	[88]
Echinacea purpurea	Flower	Caco-2, HCT116	0–2,000 mg/mL	*Hydroethanolic*	Cichoric acid	(i) Inhibition of proliferation (ii) Decreased telomerase activity in HCT116 cells	(i) Decreased telomerase activity (ii) Activation of caspase 9 (iii) Cleavage of PARP (iv) Downregulation of β-catenin	[89]
	Root	COLO320	150 mg/mL	*Hexanic*	Caffeic acid derivatives, alkylamides, polyacetylenes, polysaccharides	Induce apoptosis by increasing significantly caspase 3/7 activity and promote nuclear DNA fragmentation	(i) Increase significantly caspase 3/7 activity (ii) Promote nuclear DNA fragmentation	[78]
Hop (Humulus lupulus L.), Franseria artemisioides	Leaf	NM	100 mg/kg b.w./day	*Aqueous*	Coumarin, lignans, quinones	30% reduction of tumor-induced neovascularization	NM	[90]
	NM	Caco-2	NM	*Ethanolic*	Phenolic compounds, flavonoid, diterpenes	Digestive, gastroprotective, antiseptic, anti-inflammatory, and antiproliferative activity	NM	[91]
	Fruit	NL-17	0, 50, 100, 150 μg/mL	*Methanolic*	α-Mangostin (xanthone)	NM	(i) Induction of caspase 3 and caspase 9 activation (ii) Induced cell cycle arrest at G1/G0 phase	[92]
	Stem, bark	HT-29	50 μg/mL	*Chloroform-soluble*	β-Mangostin, garcinone D, cratoxyxanthone	Cytotoxic activity against HT-29 human colon cancer	Inhibition of p50 and p65 activation	[93]
Annona squamosa Linn	Leaf	HCT116	8.98 μg/mL	*Crude, Aq ethyl acetate*	Acetogenins (annoreticuin & isoannoreticuin) and alkaloids dopamine, salsolinol, and coclaurine	Inhibition of growth and proliferation of tumor cells	(i) Reactive oxygen species (ROS) formation, lactate dehydrogenase (LDH) release (ii) Activation of caspases 3/7, 8, and 9	[94]
Derris scandens	Stem	HT-29	5-15 μg/mL	*Ethanolic*	Benzyls and isoflavones (genistein, coumarins, scandinone)	Apoptosis and mitotic catastrophe of human colon cancer HT-29 cells	(i) Inhibition of α-glucosidase activity (ii) Scavenge free radicals	[95]

Table 1: Continued.

Scientific name	Parts used	Cell line	Conc.	Type of extract	Important compounds	Cellular effect	Mechanisms	References
Eupatorium cannabinum	Aerial parts	HT-29	25 μg/mL	*Ethanolic*	Pyrrolizidine alkaloids (senecionine, senkirkine, monocrotaline, echimidine)	Induced alteration of colony morphology	(i) Upregulation of p21 and downregulation of NCL, FOS, and AURKA (ii) Mitotic disruption and nonapoptotic cell death via upregulation of Bcl-xL, limited TUNEL labeling, and nuclear size increase	[96]
Sorghum bicolor	The dermal layer of stalk	HCT116 & colon cancer stem cells	>16 and 103 μg/mL	*Phenolic-rich ethanolic, acetone*	Apigeninidin & luteolinidin	Antiproliferative	Target p53-dependent and p53-independent pathways	[97]
	Dermal and seed head	CCSC	NM	*Methanolic*	Apigeninidin, luteolinidin, malvidin 3-O-glucoside, apigenin, luteolin, naringenin, naringenin 7-O-glucoside, eriodictyol 5-glucoside, taxifolin, catechins	NM	(i) Elevation of caspase 3/7 activity (ii) Decrease in β-catenin, cyclin D1, c-Myc, and survivin protein levels (iii) Suppression of Wnt/β-catenin signaling in a p53-dependent (dermal layer) and partial p53-dependent (seed head) manner	[98]
Hibiscus cannabinus	Seed	HCT116	KSE (15.625 μg/mL to 1,000 μg/mL)	*Ethanolic*	Gallic acid, p-hydroxybenzoic acid, caffeic acid, vanillic acid, syringic acid, and p-coumaric and ferulic acids	Cytotoxic activity against human colon cancer HCT116 cells	Apoptosis via blockade of mid G1-late G1-S transition thereby causing G1 phase cell cycle arrest	[99]
Salix aegyptiaca L.	Bark	HCT116 & HT-29	300 μg/mL	*Ethanolic*	Catechin, salicin, catechol and smaller amounts of gallic acid, epigallocatechin gallate (EGCG), quercetin, coumaric acid, rutin, syringic acid, and vanillin	Anticarcinogenic effects in colon cancer cells	Apoptosis via inhibition of phosphatidylinositol 3-kinase/protein kinase B and mitogen-activated protein kinase signaling pathways	[100]
Rubus coreanum	Fruit	HT-29	400 μg/mL	*Aqueous*	Polyphenols, gallic acid, sanguine	Induction of apoptosis	(i) Induced activity of caspases 3, 7, and 9 (ii) Cleavage of poly(adenosine diphosphate-ribose) polymerase	[101]
Codonopsis lanceolata	Root	HT-29	200 μg/mL	*N-Butanol fraction*	Tannins, saponins, polyphenolics, alkaloids	Apoptosis in human colon tumor HT-29 cells	(i) Induced G0/G1 arrest (ii) Enhancement of expression of caspase 3 and p53 and of the Bax/Bcl-2 ratio	[102]

Table 1: Continued.

Scientific name	Parts used	Cell line	Conc.	Type of extract	Important compounds	Cellular effect	Mechanisms	References
Gleditsia sinensis	Thorn	HCT116	800 μg/mL	*Aqueous*	Flavonoid, lupine acid, ellagic acid glycosides	(i) Increase in p53 levels (ii) Downregulation of the checkpoint proteins, cyclin B1, Cdc2, and Cdc25c	Inhibition of proliferation of colon cancer cells	[90]
	Thorn	HCT116	600 μg/mL	*Ethanolic*	NM	Inhibitory effect on proliferation of human colon cancer HCT116 cells	(i) Caused cell cycle arrest at G2/M phase together with a decrease of cyclin B1 and Cdc2 (ii) Progression from G2/M phase	[91]
Ligustrum lucidum	Fruit	DLD-1	50 μg/mL	*Aqueous*	Oleanolic acid, ursolic acid	Inhibited proliferation	(i) Reduction of Tbx3 rescued the dysregulated P14ARF-P53 signaling	[94]
Zingiber officinale	Rhizome	HCT116	5 μM	*Ethanolic*	6-Paradol, 6- and 10-dehydrogingerdione, 6- and 10-gingerdione, 4-, 6-, 8-, and 10-gingerdiol, 6-methylgingerdiol, zingerone, 6-hydroxyshogaol, 6-, 8-, 10-dehydroshogaol, diarylheptanoids	Inhibitory effects on the proliferation of human colon cancer cells	(i) Arrest at G0/G1 phase (ii) Reduced DNA synthesis	[103]
Grifola frondosa	Fruit	HT-29	10 ng/mL	*Aqueous*	Phenolic compounds (pyrogallol, caffeic acid, myricetin, protocatechuic acid)	Inhibition of TNBS-induced rat colitis	Induced cell cycle progression in G0/G1 phase	[104]
Cucumaria frondosa	The enzymatically hydrolyzed epithelium of the edible	HCT116	<150 μg/mL	*Hydroalcoholic*	Monosulphated triterpenoid glycoside frondoside A, the disulphated glycoside frondoside B, the trisulphated glycoside frondoside C	Inhibition of human colon cancer cell growth	(i) Inhibition at S and G2-M phases with a decrease in Cdc25c and increase in p21WAF1/CIP (ii) Apoptosis associated with H2AX phosphorylation and caspase 2	[105]
Rolandra fruticosa	Leaf & twigs	HT-29	10 and 5 mg/kg/day	*Methanolic*	Sesquiterpene lactone (13-acetoxyrolandrolide)	Antiproliferative effect against human colon cancer cells	Inhibition of the NFκB pathway, NFκB subunit p65 (RelA), upstream mediators IKKβ and oncogenic K-ras	[106]

Table 1: Continued.

Scientific name	Parts used	Cell line	Conc.	Type of extract	Important compounds	Cellular effect	Mechanisms	References
Cydonia oblonga Miller	Leaf & Fruit	Caco-2	250–500 μg/mL	*Methanolic*	Phenolic compound (flavonol and flavone heterosides, 5-O-caffeoylquinic acid)	Antiproliferative effect against human kidney and colon cancer cells	(i) Suppression of factor activation, nuclear factor-kB (NFκB) activation, protein-1 (AP-1) transcription factor, mitogen protein kinases (MAPKs), protein kinases (PKs), namely, PKC, growth-factor receptor- (GFR-) mediated pathways and angiogenesis (ii) Cell cycle arrest and induction of apoptosis, antioxidant, and anti-inflammatory effects	[107]
Morchella esculenta	Fruits	HT-29	820 mg/mL	*Methylene chloride*	Steroids (mainly ergosterol derivatives) & polysaccharides & galactomannan	Antioxidant activity in HT-29 colon cancer cells	Inhibition of NF-B activation in the NF-B assay	[108]
Sedum kamtschaticum	Aerial part	HT-29	0–0.5 mg/mL	*Methanolic*	Buddlejasaponin IV	Induced apoptosis in HT-29 human colon cancer cells	Induction of apoptosis via mitochondrial pathway by downregulation of Bcl-2 protein levels, caspase 3 activation, and subsequent PARP cleavage	[109]
Ginseng and Glycyrrhiza glabra	Leaf	HT-29	500 μL	*Aqueous*	Uracil, adenine, adenosine, Li-glycyrrhetinic acid, quiritin	NM	Antiproliferative effect determination of the protein levels of p21, cyclin D1, PCNA, and cdk-2, which are the key regulators for cell cycle progression	[110]
Orostachys japonicus	Leaf & stem	HT-29	2 mg/mL	*Aqueous*	Flavonoids, triterpenoids, 4-hydroxybenzoic acid, 3,4-dihydroxybenzoic acid, polysaccharide	Antiproliferation in HT-29 colon cancer cells	Inhibited proliferation at G2 point of the cell cycle and apoptosis via tumor suppressor protein p53	[111]
Ginkgo biloba	Fruit & leaf	HT-29	20–320mg/L	*Aqueous*	Terpene lactones and flavonoid glycosides	(i) Inhibited progression of human colon cancer cells (ii) Induced HT-29 cell apoptosis	Increase in caspase 3 activities and elevation in p53 MRN reduction in Bcl-2 mRNA	[112]
Oryza sativa	Seed	HT-29, SW 480, HCEC	100 μg/mL	*Ethyl acetate*	Phenolic compound (tricin, ferulic acid, caffeic acid, and methoxycinnamic acid)	Inhibition of the human colon cancer cell growth	(i) Induced apoptosis by enhanced activation of caspases 8 and 3 (ii) Decrease of the number of viable SW480 and HCEC cells (iii) Reduced colony-forming ability of these cells	[113]

Table 1: Continued.

Scientific name	Parts used	Cell line	Conc.	Type of extract	Important compounds	Cellular effect	Mechanisms	References
Cnidium officinale Makino	Root	HT-29	305.024/mL	*Ethanolic*	Osthole, auraptenol, imperatorin	Inhibited proliferation of human colon cancer cells (HT-29)	Inhibition of the cellular proliferation via G0/G1 phase arrest of the cell cycle and induced apoptosis	[114]
Cnidium officinale Makino	Root	HT-29	0.1-5 mg/mL	*Aqueous*	N-(3-(Aminomethyl)benzyl)acetamidine	Inhibited the invasiveness of cytokine-treated HT-29 cells through the Matrigel-coated membrane in a concentration-dependent manner	(i) Reduction of HT-29 cell invasion through the Matrigel (ii) Inhibited cytokine-mediated NO production, iNOS expression, and invasiveness of HT-29 cells (iii) Inhibited MMP-2 activity	[115]
Long pepper (PLX)	Fruit	HT-29 and HCT116	0.10 mg/mL	*Ethanolic*	Piperidine alkaloids, piperamides, piperlongumine	(i) Induction of apoptosis, following DNA fragmentation in HT-29 colon cancer cells in a time-dependent manner (ii) Induced caspase-independent apoptosis	Induced whole cell ROS production	[116]
Achyranthes aspera	Root	COLO 205	50-100 and 150-200 μg/mL	*Ethanolic (EAA) and aqueous (AAA) root extracts* *Aqueous*	Phenolic compounds	(i) Enhanced growth inhibitory effects of AAA towards COLO 205 cells in contrast to EAA (ii) Stimulatory role of AAA in the activation of cell cycle inhibitors	(i) Triggered mitochondrial apoptosis pathway and S phase cell cycle arrest (ii) Increased levels of caspase 9, caspase 3, and caspase 3/7 activity	[117]
Thymus vulgaris	Leaf	HCT116	0.2, 0.4, 0.6, 0.8 mg/mL		Carvacrol and thymol	Inhibited proliferation, adhesion, migration, and invasion of cancer cells		[118]
Dictyopteris undulata	NM	SW480	40 μg/mL	*Ethanolic*	Cyclozonarone benzoquinone	NM	Induced apoptosis by reducing Bcl-2 levels, upregulating Bax, and disrupting the mitochondrial membrane potential, leading to the activation of caspases 3 and 9	[119]

Table 1: Continued.

Scientific name	Parts used	Cell line	Conc.	Type of extract	Important compounds	Cellular effect	Mechanisms	References
Dendrobium microspermae	NM	HCT116	0.25, 0.5, 1.0 mg/mL	*Methanolic*	NM	NM	Upregulation of Bax and caspases 9 and 3 and downregulation of Bcl-2 expression of genes	[120]
Cannabis sativa	Dry flower & leaf	DLD-1 and HCT116	0.3–5 μM	*Methanolic*	Cannabidiol, phytocannabinoids	Reduced cell proliferation in a CB1-sensitive	(i) Reduced AOM-induced preneoplastic lesions and polyps (ii) Inhibited colorectal cancer cell proliferation via CB1 and CB2 receptor activation	[121]
Phoenix dactylifera L.	Fruit	Caco-2	0.2 mg/mL	*Aqueous*	Phenolic acids (gallic, protocatechuic, hydroxybenzoic, vanillic, isovanillic, syringic, caffeic, ferulic, sinapic, p-coumaric, isoferulic), flavonoid glycosides (quercetin, luteolin, apigenin, and kaempferol), and anthocyanidins	Increasing beneficial bacterial growth and inhibition of proliferation of colon cancer cells	NM	[122]
Melia toosendan	Fruit	SW480, CT26	0, 10, 20, 30, 40, 50 μg/mL	*Ethanolic*	Triterpenoids, flavonoids, polysaccharide, limonoids	NM	(i) Inhibited cell proliferation of SW480 and CT26 by promoting apoptosis as indicated by nuclear chromatin condensation and DNA fragmentation (ii) Induced caspase 9 activity which further activated caspase 3 and poly(ADP-ribose) polymerase cleavage, leading the tumor cells to apoptosis	[123]
Crocus sativus L.	Flower	HCT116	0.25, 0.5, 1, 2, 4 μg/mL	*Ethanolic*	Carotenoid, pigment, crocin, crocetin	Induced DNA damage and apoptosis	(i) Induction of a p53 pattern-dependent caspase 3 activation with a full G2/M stop (ii) Induced remarkable delay in S/G2 phase transit with entry into mitosis	[124]
	Tepals and leaf	Caco-2	0.42 mg/mL	*NM*	Polyphenols, glycosides of kaempferol, luteolin, and quercetin	Proliferation of Caco-2 cells was greatly inhibited	NM	[125]
Luffa echinata	Fruit	HT-29	50, 100, and 200 μg/mL	*Methanolic*	Amariin, echinatin, saponins, hentriacontane, gypsogenin, cucurbitacin B, datiscacin, 2-*O*-β-D-glucopyranosyl cucurbitacin B, and 2-*O*-β-D-glucopyranosyl cucurbitacin S	Increase in the population of apoptotic cells	(i) Inhibited the cellular proliferation of HT-29 cells via G2/M phase arrest of the cell cycle (ii) Induced apoptotic cell death via ROS generation (iii) Accumulation of caspase 3 transcripts of HT-29 cells	[126]

Table 1: Continued.

Scientific name	Parts used	Cell line	Conc.	Type of extract	Important compounds	Cellular effect	Mechanisms	References
Vitis aestivalis hybrid	Fruits (wine)	CCD-18Co	25, 50, 100 μg/mL	NM	Polyphenolics	NM	(i) Decreased mRNA expression of lipopolysaccharide- (LPS-) induced inflammatory mediators NFκB, ICAM-1, VCAM-1, and PECAM-1 (ii) Enhanced expression of miR-126 (iii) Decreased gene expression and reduced activation of the NFκB transcription factor, NFκB-dependent (iv) Decrease in ROS 113MAH	[127]
Xylopia aethiopica	Dried fruit	HCT116	0, 5, 10, 15, 20, 25, 30 μg/mL	*Ethanolic*	Ent-15-oxokaur-16-en-19-oic acid (EOKA)	NM	(i) Induced DNA damage, cell cycle arrest in G1 phase, and apoptotic cell death	[128]
Sorghum	Grain	ER-β; nonmalignant young adult mouse colonocytes	1, 5, 10, 100 μg/mL	*Aqueous*	Flavones (luteolin and apigenin), 3-deoxyanthocyanins naringenin (eriodictyol and naringenin)	Reduced cell growth via apoptosis	Increased caspase 3 activity	[129]
	NM	HT-29, HCT116	0.9-2.0 mg/mL	*Hydroethanolic*	Procyanidin B1, delphinidin-3-O-glucoside, tannin, cyanidin-3-O glucoside	(i) Significantly arrested HT-29 cells in G1 (ii) Highest growth inhibition (iii) Increased percentage of apoptotic cells	(i) Downregulation of apoptotic proteins, such as cIAP-2, livin, survivin, and XIAP, was seen in HCT116 cells (ii) Inhibition of tyrosine kinase	[130]
Panax notoginseng (Burk.) F.H. Chen	Root	LoVo and Caco-2	0, 100, 250, and 500 μg/mL	*Alcoholic*	Saponin, ginsenoside	NM	Delay in progression of the G0/G1, S, or G2/M cell cycle phases	[131]
Brassica oleracea L. var. *italica*	Broccoli florets	HCT116	0, 1, 2.5, 5, 10 μg/mL	*Ethanolic*	Glucoiberin, 3 hydroxy,4(α-L-rhamnopyranosyloxy), benzyl glucosinolate 4-vinyl-3-pyrazolidinone 4-(methyl sulphinyl), butyl thiourea, β-thioglucoside N-hydroxysulphates	NM	NM	[132]

Table 1: Continued.

Scientific name	Parts used	Cell line	Conc.	Type of extract	Important compounds	Cellular effect	Mechanisms	References
Cistanche deserticola	Dried stem	SW480	*In vivo:* 0.4 g/kg/day *In vitro:* 100 μg/mL	*Aqueous*	Polysaccharides, phenylethanoid glycosides	(i) Decreased number of mucosal hyperplasia and intestinal helicobacter infection (ii) Increased number of splenic macrophage, NK cells, and splenic macrophages	Decreased frequency of hyperplasia and *Helicobacter hepaticus* infection of the intestine	[133]
Chaenomeles japonica	Fruit	Caco-2 and HT-29	10, 25, 50, 75, 100, 125, 150 μM CE	NM	Procyanidins	NM	NM	[134]
Prunus mume	Fruit	SW480, COLO, and WiDr	150, 300, and 600 μg/mL	*Hydrophobic*	Triterpenoid saponins	NM	(i) Inhibited growth and lysed SW480, COLO, and WiDr (ii) Induction of massive cytoplasmic vacuoles	[135]
Solanum lyratum	NM	COLO 205	50, 100, 200, 300, 400 μg/mL	*EtOH*	β-Lycotetraosyl	Induced S phase arrest and apoptosis	(i) Induced DNA fragments (ii) Increased the levels of p27, p53, cyclin B1, active-caspase 3, and Bax (iii) Decreased the levels of Cdk1, pro-caspase 9, Bcl-2 and NF-ÎB, p65, and p50	[136]
Onopordum cynarocephalum	Aerial parts	HCT116, HT-29	0, 0.04, 0.12, 0.2, 0.4, 1.2 mg/mL 0, 0.2, 0.4, 1.2, 2.0, 3.0 mg/mL	*Aqueous*	Flavonoids, lignans, and sesquiterpene lactones	NM	(i) Increase in the expression of proapoptotic proteins such as p53, p21, and Bax (ii) Inhibition of the antiapoptotic protein Bcl-2 (iii) Decrease in cyclin D1 protein	[137]
Eleutherine palmifolia	Bulbs	SW480	2.5, 5, 10 μg/mL	*MeOH*	Eleutherin, isoeleutherin	NM	(i) Inhibited the transcription of TCF/β-catenin (ii) Decrease in the level of nuclear β-catenin protein	[138]
Asparagus officinalis	Spears	HCT116	76 μg/mL	*Acetone*	Steroidal saponins (HTSA-1, HTSAP-2, HTSAP-12, HTSAP-6, HTSAP-8)	NM	(i) Inhibition of Akt, p70S6K, and ERK phosphorylation (ii) Induction of caspase 3 activity, PARP-1 cleavage, DNA fragmentation, G0/G1 cell cycle arrest by reducing the expression of cyclins D, A, and E	[139]

Table 1: Continued.

Scientific name	Parts used	Cell line	Conc.	Type of extract	Important compounds	Cellular effect	Mechanisms	References
Phyllanthus emblica L.	Seed, pulp	HCCSCs, HCT116	200 μg/mL	*Methanolic*	Trigonelline, naringin, kaempferol, embinin, catechin, isorhamnetin, quercetin	(i) Suppressed proliferation (ii) Induced apoptosis independent from p53 stemness property (in HCCSCs) (iii) Antiproliferative properties	(i) Suppressed cell proliferation and expression of c-Myc and cyclin D1 (ii) Induced intrinsic mitochondrial apoptotic signaling pathway	[140]
Red grape	NM	HT-29, HCT116	0.9-2.0 mg/mL	*Hydroethanolic*	Delphinidin glycosides, quercetin derivatives, delphinidin-3-O-glucoside (high), cyanidin-3-O-glucoside	(i) Highest growth inhibition (ii) Increased the percentage of apoptotic cells	(i) Downregulation of apoptotic proteins, such as cIAP-2, livin, survivin, and XIAP (ii) Inhibition of tyrosine kinase	[130]
Black lentil	NM	HT-29, HCT116	0.9-2.0 mg/mL	*Hydroethanolic*	Delphinidin glycosides, procyanidin B1, delphinidin-3-O-glucoside (high), cyanidin-3-O-glucoside	(i) Significantly arrested HT-29 cells in G1 (ii) Highest growth inhibition (iii) Increased percentage of apoptotic cells	(i) Downregulation of apoptotic proteins, such as cIAP-2, livin, survivin, and XIAP (ii) Inhibition of tyrosine kinase	[130]
Graptopetalum paraguayense	Leaf	Caco-2, BV-2	0.2, 0.4, 0.6, 0.8, 1.0 mg/mL	*Hydroethanolic*	Oxalic acid, hydroxybutanedioic acid, gallic acid, quercetin, chlorogenic acid glucans with fucose, xylose, ribose (GW100) arabino-rhamnogalactans (GW100E)	(i) Great potential in antiproliferation (ii) Significant immunomodulatory activities on BV-2 cells and interleukin-6 (IL-6) (GW100)	(i) Scavenging α, α-diphenyl-β-picrylhydrazyl radicals (DPPH) (GW100E excelled in scavenging DPPH), 2,2-azino-bis [3-ethylbenzothiazoline-6-sulfonic acid] radicals (ABTS), superoxide anions (O2) (GW100) (ii) Significant inhibition of tumor necrosis factor-a (TNF-a), scavenging ABTS and O2	[141]
Butea monosperma	Flower	SW480	200, 370 μg/mL	*Floral*	n-Butanol	Significant antiproliferative effect	(i) Significantly downregulated the expression of Wnt signaling proteins such as β-catenin, APC, GSK-3β, cyclin D1, and c-Myc (ii) Increased intracellular level of ROS	[142]

Table 1: Continued.

Scientific name	Parts used	Cell line	Conc.	Type of extract	Important compounds	Cellular effect	Mechanisms	References
Rehmannia glutinosa	NM	CT26	5, 20, 80 μM	*NM*	Catalpol	Inhibited proliferation and growth invasion of colon cancer cells	(i) Downregulated MMP-2 and MMP-9 protein expressions (ii) Reduction in the angiogenic markers secretions	[143]
Telectadium dongnaiense	Bark	HCT116	1.5, 2.0 μg/mL	*MeOH extract*	4-Dicaffeoylquinic acid, quercetin 3-rutinoside, periplocin	NM	(i) Inhibition of β-catenin/TCF transcriptional activity and effects on Wnt/β-catenin (ii) Downregulation of the expression of Wnt target genes	[144]
Gloriosa superba	Root	SW620	30 ng/mL	*Protein hydrolysate extract*	Protein hydrolysate	NM	(i) Upregulation of p53 (ii) Downregulation of NFκB	[145]
Boswellia serrata	Resin	HT-29	100, 150 μg	*Methanolic*	Boswellic acid	Decreased cell viability	(i) Reduction in mPGES-1, VEGF, CXCR4, MMP-2, MMP-9, HIF-1, PGE2 expression (ii) Increment in the caspase 3 activity (iii) Inhibition of cell migration and vascular sprout formation	[146]
Typhonium flagelliforme	Leaf	WiDr	70 μg/mL	*Ethyl acetate*	Glycoside flavonoid, isovitexin, alkaloids	NM	Inhibition of COX-2 expression	[28]
Diospyros kaki	Fruit	HT-29	2,000 μg/mL	*Hydroacetone extract*	Polyphenol	Impaired cell proliferation and invasion	NM	[147]
Carpobrotus edulis	Leaf	HCT116	1,000 mg/mL	*Hydroethanolic*	Gallic acid, quercetin, sinapic acid, ferulic acid, luteolin 7-o-glucoside, hyperoside, isoquercitrin, ellagic acid, isorhamnetin 3-O-rutinoside	Inhibited proliferation	(i) Possession of high DPPH scavenging activity and effective capacity for iron binding (ii) Inhibition of NO radical, linoleic acid peroxidation, protein glycation, and oxidative damage	[148]
Piper methysticum	Root	HT-29	10, 20, 30, 40, 50 μg/mL	*Aqueous*	11-Hydroxy-12-methoxydihydrokavain, 11-hydroxy-12-methoxydihydrokavain, prenyl caffeate, pinostrobin chalcone, 11-methoxytetrahydroyangonin, awaine, methysticin, dihydromethysticin, 5,6,7,8-tetrahydroyangonin, kavain, 7,8-dihydrokavain, yangonin, desmethoxyyangonin, flavokawain B	Inhibited the growth	NM	[26]

Table 1: Continued.

Scientific name	Parts used	Cell line	Conc.	Type of extract	Important compounds	Cellular effect	Mechanisms	References
Salvia ballotiflora	Ground aerial parts	CT26	6.76 μg/mL	*Hexane-washed chloroform extract*	19-Deoxyicetexone, 7,20-dihydroanastomosine, icetexone, 19-deoxyisoicetexone	Cytotoxic activity	NM	[149]
Tinospora cordifolia	Stem	HCT116	1, 10, 30, 50 μM	*Hydroalcoholic*	Clerodane furano diterpene glycoside, cordifoliosides A and B, sitosterol, ecdysterone, 2β,3β:15,16-diepoxy-4α, 6β-dihydroxy-13(16),14-clerodadiene-17,12:18,1-diolide	Induced chromatin condensation and fragmentation of nuclei of few cells	(i) Considerable loss of MMP (ii) Decreased in mitochondria function (iii) Increased cytochrome c in the cytosol (iv) Induced ROS/oxidative stress (v) Increased autophagy	[150]
Euterpe oleracea	Fruit	NM	35 μg/mL	*Hydroethanolic*	Vanillic acid, orientin, isoorientin	NM	(i) Scavenging capacity towards ROO and HOCl (ii) Inhibition of nitroso compound formation	[151]
Salvia miltiorrhiza	NM	HCT116	7.4 ± 1.0, 4.4 ± 0.5 μg/mL	*Ethanolic*	Diterpene quinone	NM	Decreased levels of pro-caspases 3 and 9	[152]
Coffea	Bean	HCT116	1 mg/mL	*Aqueous*	Chlorogenic acid complex (CGA7)	NM	(i) DNA fragmentation, PARP-1 cleavage, caspase 9 activation, downregulation of Bcl-2 and upregulation of Bax	[153]
Illicium verum	Fruit	HCT116	10 mg/mL	*Ethanolic*	Gallic acid quercetin	Induction of apoptosis and inhibition of key steps of metastasis	NM	[154]
Garcinia propinqua Craib	Leaf	HCT116	NM	*CH2Cl2 extract*	Benzophenones, xanthones, and caged xanthones	Potent inhibitory cytotoxicities	NM	[155]
	Stem, bark	HCT116	14.23, 23.95 μM	*MeOH, CH_2Cl_2, and EtOAc extract*	Xerophenone A, doitunggarcinones A and B, sampsonione, 7β-H-11-benzoyl-5α-ydroxy-6, 10-tetramethyl-1-(3-methyl-2-butenyl)-tetracyclotetradecane-2,12,14-trione, hypersampsone M, assiguxanthone A (cudraxanthone Q), 40 10-O-methylmacluraxanthone (16), 41- and 5-O-methylxanthone V1	NM	NM	[156]

Table 1: Continued.

Scientific name	Parts used	Cell line	Conc.	Type of extract	Important compounds	Cellular effect	Mechanisms	References
Malus pumila Miller cv. Annurca	Fruit	Caco-2	400 mg/L	*Methanolic*	Chlorogenic acid, (+)catechin, (−)epicatechin, isoquercetin, rutin, phloridzin, procyanidin B2, phloretin, quercetin	WNT inhibitors and reduced WNT activity elicited by WNT5A	NM	[157]
Malus domestica cv. Limoncella	Fruit	Caco-2	400 mg/L	*Methanolic*	Chlorogenic acid, (+)catechin, (−)epicatechin, isoquercetin, rutin, phloridzin, procyanidin B2, phloretin, quercetin	WNT inhibitors and reduced WNT activity elicited by WNT5A	NM	[157]
Coix lacryma-jobi var. *ma-yuen*	Leaf	HCT116	0.5, 1 mg/mL	*Aqueous*	Coixspirolactam A, coixspirolactam B, coixspirolactam C, coixlactam, methyl dioxindole-3-acetate	NM	Inhibited migration, invasion, and adhesion via repression of the ERK1/2 and Akt pathways under hypoxic conditions	[158]
Mesua ferrea	Stem, bark	HCT116, HT-29	3.3, 6.6, and 11.8 μg/mL	*NM*	Fractions (α-amyrin, SF-3, n-Hex)	Downregulation of multiple tumor promoter	Upregulation of p53, Myc/Max, and TGF-β signaling pathways	[159]
Taraxacum	Root	SGC7901, BGC823	3 mg/mL	*Aqueous*	NM	NM	Proliferation and migration through targeting lncRNA-CCAT1	[160]
Portulaca oleracea	Leaf	HT-29 CSCs	2.25 μg/mL	*Alcoholic*	Oxalic, malic acid	NM	Inhibited expression of the Notch1 and β-catenin genes, regulatory and target genes that mediate the Notch signal transduction pathway	[161]
Hordeum vulgare L.	NM	HT-29	NM	*Aqueous & juice*	Protein, dietary fiber, the B vitamins, niacin, vitamin B6, manganese, phosphorus, carbohydrates	(i) Inhibited proliferation of cancer cells (ii) Cytotoxic activity	Free radical scavenging activity	[162]
Paraconiothyrium sp.	NM	COLO 205 and KM12	12.5 μM	*Methyl ethyl ketone extract*	n-Hexane, CH_2Cl_2, EtOAc, and MeOH fractions (A–D)	(i) Growth inhibitory activity (ii) Antiproliferative effect	NM	[163]
Mentha×piperita	Leaf	HCT116	5, 10, 20, 30, 40, 50 μg/mL	*Aqueous*	Polyphenols	NM	Inhibited replication of DNA and transcription of RNA which induce the ROS	[164]

Table 1: Continued.

Scientific name	Parts used	Cell line	Conc.	Type of extract	Important compounds	Cellular effect	Mechanisms	References
Mammea longifolia Planch. and Triana	Fruit	SW480	25, 50, 100 μg/mL	*Methanolic*	NM	NM	Mitochondria-related apoptosis and activation of p53	[165]
Rollinia mucosa (Jacq.) Baill.	NM	HCT116, SW-480	<4, <20 μg/mL	*EtOH*	Rollitacin, jimenezin, membranacin, desacetyluvaricin, laherradurin	Cytotoxic activity	NM	[54]
Annona diversifolia Saff.	NM	SW-480	0.5 μg/mL	NM	Cherimolin-2	Cytotoxic activity	NM	[54]
A. purpurea Moc. & Sessé ex Dunal	NM	HT-29	1.47 μg/mL	*$CHCl_3$-MeOH*	Purpurediolin, purpurenin, annoglaucin, annonacin A	Cytotoxic activity	NM	[54]
Viguiera decurrens (A.Gray) A. Gray	NM	NM	3.6 μg/mL	*Hex; EtOAc; MeOH*	β-Sitosterol-3-O-β-D-glucopyranoside; β-D-glucopyranosyl oleanolate; β-sitosterol-3-O-β-D-glucopyranoside, and oleanolic acid-3-O-methyl-β-D-glucuronopyranoside ronoate	Cytotoxic activity	NM	[54]
Helianthella quinquenervis (Hook.) A. Gray	NM	HT-29	2-10 μg/mL	NM	Demethylencecalin	Cytotoxic activity	NM	[54]
Smallanthus maculatus (Cav.) H. Rob.	NM	HCT15	<20 μg/mL	*Acetone*	Fraction F-4, fraction F-5, ursolic acid	Cytotoxic activity	NM	[54]
Bursera fagaroides (Kunth) Engl.	NM	HF6	1.8×10^{-4} to 2.80 μg/mL	*Hydroalcoholic*	Podophyllotoxin, β-peltatin-A methyl ether, 5′-desmethoxy-β-peltatin-A methyl ether, desmethoxy-yatein, deoxypodophyllotoxin, burseranin, acetyl podophyllotoxin	NM	(i) Inhibitor of microtubules (ii) Ability to arrest cell cycle in metaphase	[54]
Viburnum jucundum C.V. Morton	NM	HCT15	<20 μg/mL	*Acetone*	Ursolic acid	Cytotoxic activity	NM	[54]
Hemiangium excelsum (Kunth) A.C.Sm.	NM	HCT15	<10 (μg/mL)	*MeOH*	*PE, EtOAc, MeOH*	Cytotoxic activity	NM	[54]

Table 1: Continued.

Scientific name	Parts used	Cell line	Conc.	Type of extract	Important compounds	Cellular effect	Mechanisms	References
Hyptis pectinata (L.) Poit.	NM	Col2	<4, <20 μg/mL	NM	Pectinolide A, pectinolide B, pectinolide C, α-pyrone, boronolide, deacetylepiol-guine	Cytotoxic activity	NM	[54]
H. verticillata Jacq.	NM	Col2	<4,<20 μg/mL	NM	Dehydro-β-peltatin, methyl ether dibenzylbutyrolactone, (-)-yatein, 4′-demethyl-deoxypodophyllotoxin	Nonspecific cytotoxic activity	NM	[54]
H. suaveolens (L.)	NM	HF6	2.8-12 μg/mL	*Chloroform and butanol*	β-Apopicropodophyllin	Nonspecific cytotoxic activity	NM	[54]
Salvia leucantha Cav.	Leaf, root, stem	HF6, HT-29, HCT15	14.9, 12.7, 9.9 μg/mL	$CHCl_3$	NM	Cytotoxic activity	NM	[54]
Vitex trifolia L.	NM	HCT15	3.5 to <1 (μg/mL)	*Hexane and dichloromethane*	Salvileucalin B, Hex: leaf, Hex: stem, DCM: leaf, DCM: stem	Cytotoxic activity	NM	[54]
Persea americana Mill.	NM	HT-29	<4 μg/mL and <20 μg/mL	*Ethanolic*	1,2,4-trihydroxynonadecan, 1,2,4-trihydroxyheptadec-16-ene, 1,2,4-trihydroxyheptadec-16-yne	Cytotoxic activity	NM	[54]
Linum scabrellum	Roots, aerial parts	HF6	0.2, 0.5, 2.3 μg/mL	*Chloroform and butanol*	DCM: MeOH, 6MPTOXPTOX	NM	(i) Induction of cell cycle arrest in G2/M (ii) Inhibition of tubulin polymerization	[54]
Phoradendron reichenbachianum (Seem.) Oliv.	NM	HCT15	3.6, 3.9, and 4.3 μg/mL	NM	Moronic acid	Cytotoxic activity	NM	[54]
Cuphea aequipetala Cav.	NM	HCT15	18.70 μg/mL	*Acetone*	NM	Cytotoxic inactivity	NM	[54]
Galphimia glauca Cav.	NM	HCT15	0.63, 0.50, 1.99 μg/mL	*EtOH, MeOH, aqueous*	NM	Cytotoxic activity	NM	[54]
Mimulus glabratus Kunth	NM	HF6	12.64 μg/mL	*MeOH*	NM	Cytotoxic activity	NM	[54]
Picramnia antidesma Sw.	NM	HCT15	0.6 to 4.5 μM	NM	10-Epi-uveoside, uveoside, picramnioside E, picramnioside D	Cytotoxic activity	NM	[54]

Table 1: Continued.

Scientific name	Parts used	Cell line	Conc.	Type of extract	Important compounds	Cellular effect	Mechanisms	References
Penstemon barbatus (Cav.) Roth	NM	HF6	15.19 μg/mL	*MeOH*	NM	Cytotoxic activity	NM	[54]
P. campanulatus (Cav.) Willd.	NM	HF6	6.74 μg/mL	*MeOH*	NM	Cytotoxic activity	NM	[54]
Veronica americana Schwein. ex Benth.	NM	HF6	0.169 and 1.46 μg/mL	*MeOH*	NM	Cytotoxic activity	NM	[54]
Zea mays L.	NM	HCT116, SW-480, SW-620	NM	NM	13-Hydroxy-10-oxo-trans-11-octadecenoic acid	Cytotoxic activity	NM	[54]
Colubrina macrocarpa (Cav.) G. Don	NM	HCT15	10, 2.1, 9.1 μg/mL	*PE, EtOAc, MeOH*	NM	Cytotoxic activity	NM	[54]
Coix lacryma-jobi	Seed, endosperm, and hull	HT-29	0.1–1,000 μg/mL	*Methanolic, hexane*	Phytosterols (campesterol, stigmasterol, and β-sitosterol), gamma-linolenic acid (GLA), arachidonic acid (AA), eicosapentaenoicacid (EPA) and docosahexaenoic acid (DHA), linoleic acid	NM	(i) Influence of signal transduction pathways that involve the membrane phospholipids (ii) Enhancement of ROS generation and decrease of cell antioxidant capacity	[166]
Abutilon indicum	Leaf	HT-29	210 μg/mL	*Aqueous*	Flavonoids (4H-pyran-4-one, 2,3-dihydro-3,5-dihydroxy-6-methyl, 2-ethoxy-4-vinylphenol, N,N′-dimethylglycine, lup-20(29)-en-3-one, linolenin, 1-mono-, 9-hexadecanoic acid methyl ester, linolenic acid methyl ester), phenolic (amino acids, terpenoids, fatty acids, methyl palmitoleate)	NM	(i) Increase in the levels of reactive oxygen species and simultaneous reduction in cellular antioxidant, mitochondrial membrane loss, DNA damage, and G1/S phase cell cycle arrest	[167]
Galla rhois	NM	HCT116, HT-29	12.5, 25, 50, 100, 200 μg/mL	*Aqueous with steaming process*	Gallotannins	Increased contents of gallic acid and ellagic acid	(i) Induced apoptosis through the activation of caspases 3, 8, 9 (ii) Modulated activation of mitogen and protein kinases, p38, and c-Jun NH2-terminal kinase	[168]

Table 1: Continued.

Scientific name	Parts used	Cell line	Conc.	Type of extract	Important compounds	Cellular effect	Mechanisms	References
Artemisia annua Linné	Powder	HCT116	20, 30, 40, 60, 80, 100 μg/mL	*Ethanolic*	Phenolic compounds	Inhibited cell viability and increased LDH release	(i) PTEN/p53/PDK1/Akt signal pathways through PTEN/p53 induce apoptosis (ii) Increased apoptotic bodies, caspase 3 and 7 activation (iii) Regulated cytochrome c translocation to the cytoplasm and Bax translocation to the mitochondrial membrane	[169]
Nelumbo nucifera stamen	Powder	HCT116	100, 200, 400 μg/mL	*Ethanolic crude*	NM	NM	(i) Increased the sub-G1 population, mRNA levels of caspases 3 and 8, levels of IκBα and caspase 9 (ii) Modulated the Bcl-2 family mRNA expression (iii) Reduced the mRNA levels of NFκB	[170]
Corn silk	NM	LoVo, HCT116	1.25, 2.5, 5, 10, 20 μg/mL	*Aqueous*	Proteins, polysaccharides, flavonoid, vitamins, tannins, alkaloids, mineral salts, steroids	NM	(i) Increase in the Bax, cytochrome c, caspases 3 and 9 levels	[171]
Lycium barbarum L.	Powder	HT-29	1, 2, 3, 4, 5 μg/mL	*NM*	Neoxanthin, all-trans-β-cryptoxanthin, polysaccharides, carotenoids, flavonoids	NM	(i) Upregulation of p53 and p21 expression (ii) Downregulation of the CDK2, CDK1, cyclin A, and cyclin B expression (iii) Arrest in the G2/M phase of cell cycle	[172]
Chrysobalanus icaco L.	Freeze-dried fruit	HT-29	1, 2.5, 5, 10, 20 μg/mL	*Crude ethyl acetate*	Delphinidin, cyanidin, petunidin, and peonidin	NM	(i) Increased intracellular ROS production (ii) Decreased TNF-α, IL-1β, IL-6, and NFκB1 expressions	[173]
Zanthoxylum piperitum De Candolle	Fruit	Caco-2, DLD-1	200 μg/mL	*Aqueous*	NM	NM	(i) Increased the phosphorylation of c-Jun N-terminal kinase (JNK)	[174]
Celtis aetnensis (Tornab.) Strobl (Ulmaceae)	Twigs	Caco-2	5, 50, 100, 250, or 500 μg/mL	*Methanolic*	Flavonoid and triterpenic compounds	NM	(i) Increase in the levels of ROS (ii) Decrease in RSH levels and expression of HO-1	[175]

Table 1: Continued.

Scientific name	Parts used	Cell line	Conc.	Type of extract	Important compounds	Cellular effect	Mechanisms	References
Rosa canina	Peel and pulp	Caco-2	62.5, 125, 250, 500 μg/mL	*Total extract (fraction 1), vitamin C (fraction 2), neutral polyphenols (fraction 3), and acidic polyphenols (fraction 4)*	Polyphenols	Decreased production of reactive oxygen species (ROS)	NM	[176]
Rhazya stricta	Leaf	HCT116	47, 63, 79, and 95 μg/cm^2	*Crude alkaloid*	Alkaloids	NM	(i) Downregulated DNA-binding and transcriptional activities of NFκB and AP-1 proteins (ii) Increase in Bax, caspases 3/7 and 9, p53, p21 and Nrf-2 levels (iii) Decrease in expression of ERK MAPK, Bcl-2, cyclin D1, CDK-4, survivin, and VEGF	[177]
Green coffee	NM	Caco-2	10-1,000 μg/mL	*NM*	5-Caffeoylquinic acid (5-CQA), 3,5-dicaffeoylquinic acid (3,5-DCQA), ferulic acid (FA), caffeic acid (CA), dihydrocaffeic acid (DHCA), dihydroferulic acid (DHFA)	Reduced viability of cancer cells	NM	[178]
Flourensia microphylla	Leaf	HT-29	NM	*Ethanolic and acetone*	Phenolic compounds	NM	(i) Inhibition of IL-8 (ii) Activation of apoptosis by the increment of the Bax/Bcl-2 ratio and expression of TNF family	[179]

*NM: not mentioned.

Table 2

(a) Efficacy of medicinal plants on colon cancer in *in vivo* models

Scientific name	Parts used	Model		Dose	Type of extract	Important compounds	Cellular effect	Mechanisms	References
Vitis vinifera	Seed	*In vivo* (murine)	Caco-2	*In vivo*: 400–1,000 mg/kg In vitro: 10–25 μg/mL	*Aqueous*	Procyanidins	(i) Increased crypt depth and growth-inhibitory effects (ii) Inhibited cell viability (iii) Significantly decreased the histological damage score	Reduced MPO (myeloperoxidase) activity	[180]
	Seed	*In vivo*	HT-29, SW480	5 mg/kg	*Aqueous*	NM	NM	Decreased VEGF, TNF, MMP-1, MMP-3, MMP-7, MMP-8, MMP-9, and MMP-13 protein expression	[181]
	Skin	*In vivo*	NM	7.5, 30, 60 μg/mL	*Methanolic*	4′-Geranyloxyferulic acid	NM	NM	[30]
	Seed	*In vivo* (murine)	NM	0.12% *w*/*w*	*NM*	Catechin, epicatechin	NM	(i) Suppressed proliferation, sphere formation, nuclear translocation of β-catenin and Wnt/β-catenin signaling (ii) Elevated p53, Bax/Bcl-2 ratio, and cleaved PARP and mitochondrial-mediated apoptosis	[31]
Camellia sinensis	Leaf	*In vivo* (murine)	HT-29	In vitro: 0, 10, 30, 50 μM In vivo: 1.5 mg per day	*Aqueous*	Catechin, epigallocatechin gallate	1.9-fold increase in tumor endothelial cell apoptosis	Inhibited the ERK-1 and ERK-2 activation, VEGF expression, and VEGF promoter	[182]
		In vivo (murine)	HCT116	0.5%	NM	NM	Reduced basement membrane	Inhibition of MMP-9 and VEGF secretion	[183]
		In vivo (murine)	Caco-2, HT-29	300 μM	*Aqueous*	Theaflavins (TF-2, TF-3, TF-1)	Induced apoptosis of human colon cancer cells	Inhibition of edema formation correlated to attenuation of COX-2 expression and promoter analysis revealed	[36]

Table 2: Continued.

Scientific name	Parts used	Model		Dose	Type of extract	Important compounds	Cellular effect	Mechanisms	References
								modulation of NFκB, AP-1, CREB, and/or NF-Il-6 (C/EBP) Inhibition via reduced expression of a range of α5 & β1	
		In vivo (murine)	HT115	25 μg/mL	*Hydroethanolic*	Phenolic compounds (p-hydroxyphenyl ethanol, pinoresinol & dihydroxyphenyl ethanol)	NM		[184]
Sasa quelpaertensis	Leaf	*In vivo*	HT-29, HCT116	0, 100, 200, 300 mg/L	*Ethanolic*	p-Coumaric acid, tricin	Inhibition of colony formation	(i) Nonadherent sphere formation suppressed CD133+ & CD44+ population (ii) Downregulated expression of cancer stem cell markers	[41]
Anoectochilus	NM	*In vivo*	CT26	Oral dose of 50 & 10 mg/mouse per day	*Aqueous*	Kinsenoside	Stimulated proliferation of lymphoid tissues	Activation of phagocytosis of peritoneal macrophages	[185]
Purple-fleshed potatoes	Fruit	*In vivo*	Colon cancer stem cells	5.0 μg/mL	*Ethanol, methanol, ethyl acetate*	Anthocyanin, β-catenin, cytochrome c	Reduction in colon CSCs number and tumor incidence	(i) Increase in cytochrome c levels from p53 status and maybe mitochondria-mediated apoptosis (ii) Suppressed levels of cytoplasmic and nuclear β-catenin	[58]
Phaseolus vulgaris	Leaf	*In vivo*	HT-29	Nm	*Ethanolic*	Polysaccharides, oligosaccharides	Induction of apoptosis and inhibit proliferation	(i) Inactivation of the retinoblastoma phosphoprotein (ii) Induced G1 arrest (iii) Suppression of NF-jb1 (iv) Increase in EGR1 expression	[59]

Table 2: Continued.

Scientific name	Parts used	Model		Dose	Type of extract	Important compounds	Cellular effect	Mechanisms	References
Rosmarinus officinalis L.	Leaf	*In vivo*	HT-29	SC-RE 30 μg/mL and CA 12.5 μg/mL	*Ethanolic*	Polyphenols (carnosic acid (CA) and carnosol)		(i) Activation of Nrf2 transcription factor (ii) Activated common regulators, such as XBP1 (Xbp1) gene, SREBF1/SREBF2 (Srebp1/2), CEBPA and NR1I2 (Pxr) genes	
	Leaf	*In vivo* (rat)	NM	NM	*Ethanolic*	Rosmanol and its isomers, carnosol, rosmadial, carnosic acid, and 12-methoxycarnosic acid, carnosic acid, carnosol	Interactions with the gut microbiota and by a direct effect on colonocytes with respect to the onset of cancer or its progression	NM	
Wasabia japonica	Rhizomes	*In vivo*	COLO 205	5 mg/mL	*Methanolic*	6-(Methylsulfinyl)hexyl isothiocyanate	Anticolon cancer properties through the induction of apoptosis and autophagy	(i) Activation of TNF-α, Fas-L, caspases (ii) Truncated Bid and cytochrome c (iii) Decreased phosphorylation of Akt and Mtor (iv) Promoted expression of microtubule-associated protein 1 light chain 3-II and AVO formation	[186]
Zingiberaceae	Rhizome	HT-29	HT-29	5 g/kg	*Dichloromethanic*	Turmerone	Suppressed the proliferation of HT-29 colon cancer cells	(i) LDH release (ii) ROS generation (iii) Collapse in mitochondrial membrane potential (iv) Cytochrome c leakage (v) Activation of caspase 9 and caspase 3	[187]

Table 2: Continued.

Scientific name	Parts used	Model		Dose	Type of extract	Important compounds	Cellular effect	Mechanisms	References
Panax quinquefolius	Root	*In vivo* (murine)	NM	30 mg/kg	*Ethanolic*	Ginsenosides (protopanaxadiol or protopanaxatriol)	Attenuated azoxymethane/DSS-induced colon carcinogenesis by reducing the colon tumor number and tumor load	(i) Reduced experimental colitis (ii) Attenuated on AOM/DSS-induced colon carcinogenesis (iii) Proinflammatory cytokines activation (iv) Suppressed DSS (v) Downregulated inflammatory cytokine gene expression	[188]
Myrtaceae	Leaf	*In vivo* (murine)	HCT116	100 μg/mL (*in vitro*) 200 and 100 μg/disc (*in vivo*)	*Methanolic*	Phenolics, flavonoids, betulinic acid	Inhibition of tumor angiogenesis	(i) Inhibition of angiogenesis of tube formation on Matrigel matrix and HUVECS migration (*in vitro*) (ii) Decreased nutrient and oxygen supply and consequently tumor growth and tumor size (*in vivo*) (iii) Increased extent of tumor necrosis	[82]
Spica prunellae	Leaf	*In vivo*	HT-29	200 mg/mL (*in vitro*), 600 mg/mL (*in vivo*)	*Ethanolic*	Rosmarinic acid	Induction of apoptosis and inhibition of cell proliferation and tumor angiogenesis	(i) Induced apoptosis (ii) Inhibited cancer cell proliferation and angiogenesis STAT3 phosphorylation (iii) Regulated expression of Bcl-2, Bax, cyclin D1, CDK4, VEGF-A, and VEGFR-2 (*in vivo*)	[83]
Gymnaster koraiensis	Aerial part	*In vivo* (murine)	NM	500 μmol/kg	*Ethanolic*	Gymnasterkoreaynes B, C, E, 2,9,16-heptadecatrien-4,6-dyne-8-ol	Anti-inflammatory and cancer preventive activities	(i) Significant decrease in expression of COX-2 (ii) Increase in serum IL-6	[189]

Table 2: Continued.

Scientific name	Parts used	Model		Dose	Type of extract	Important compounds	Cellular effect	Mechanisms	References
Allium fistulosum	Edible portions	*In vivo* (murine)	CT26	50 mg/kg b.w.	*Hot water*	p-Coumaric acid, ferulic acid, sinapic acid, quercitrin, isoquercitrin, quercetol, kaempferol	Suppression of tumor growth and enhanced survival rate of test mice	(i) Decreased expression of inflammatory molecular markers (ii) Downregulated expression of MMP-9 and ICAM (iii) Metabolite profiling and candidate active phytochemical components	[190]
Annona squamosa Linn	Leaf	*In vivo* (animal)	HCT116	8.98 μg/mL	*Crude ethyl acetate*	Acetogenins (annoreticuin & isoannoreticuin) and alkaloids dopamine, salsolinol, and coclaurine	(i) Inhibited growth and proliferation of tumor cells	Reactive oxygen species (ROS) formation, lactate dehydrogenase (LDH) release, and caspases 3/7, 8, 9 activation	[191]
Eupatorium cannabinum	Aerial parts	*In vivo* (murine)	HT-29	25 μg/mL	*Ethanolic*	Pyrrolizidine alkaloids (senecionine, senkirkine, monocrotaline, echimidine)	Cytotoxicity against colon cancer cells	(i) Upregulation of p21 and downregulation of NCL, FOS, and AURKA, indicating reduced proliferation capacity (ii) Mitotic disruption and nonapoptotic cell death via upregulation of Bcl-xL	[96]
Flacourtia indica	Aerial parts	*In vivo* (murine)	HCT116	500 μg/mL	*Methanolic*	Phenolic glucoside (flacourticin, 4′ -benzoylpoliothrysoside)	Antiproliferative and proapoptotic effects in HCT116 cells	Apoptosis via generation of ROS and activation of caspases (PARP)	[192]
Sorghum bicolor	The dermal layer of stalk	*In vivo* (murine)	HCT116 & colon cancer stem cells	>16 and 103 μg/mL	*Phenolic, acetone*	Apigeninidin & luteolinidin	Antiproliferative effect	(i) Target p53-dependent and p53-independent pathways	[97]

Table 2: Continued.

Scientific name	Parts used	Model		Dose	Type of extract	Important compounds	Cellular effect	Mechanisms	References
Gleditsia sinensis	Thorn	*In vivo* (murine)	HCT116	800 μg/mL	*Aqueous*	Flavonoid, lupine acid, ellagic acid glycosides	Inhibited proliferation of colon cancer	(i) Increased p53 levels (ii) Downregulation of the checkpoint proteins, cyclin B1, Cdc2, and Cdc25c	[90]
	Thorn	*In vivo* (murine)	HCT116	600 μg/mL	*Ethanolic*	NM	Inhibitory effect on the proliferation of human colon cancer HCT116 cells	(i) Caused G2/M phase cell cycle arrest	[91]
Zingiber officinale	Rhizome	*In vitro/in vivo* (murine)	HCT116	5 μM	*Ethanolic*	6-Paradol, 6- and 10-dehydrogingerdione, 6- and 10-gingerdione, 4-, 6-, 8-, and 10-gingerdiol, 6-methylgingerdiol, zingerone, 6-hydroxyshogaol, 6-, 8-, 10-dehydroshogaol, diarylheptanoids	Inhibitory effects on the proliferation of human colon cancer cells	(i) Arrest of G0/G1 phase (ii) Reduced DNA synthesis (iii) Induced apoptosis	[103]
Cucumaria frondosa	The enzymatically hydrolyzed epithelium of the edible	*In vivo* (murine)	HCT116	<150 μg/mL	*Hydroalcoholic*	Monosulphated triterpenoid glycoside frondoside A, the disulphated glycoside frondoside B, the trisulphated glycoside frondoside C	(i) Inhibition at S and G2-M phase with a decrease in Cdc25c (ii) Increase in p21WAF1/CIP	(i) Inhibition the growth of human colon (ii) Apoptosis associated with H2AX phosphorylation and caspase 2	[105]
Rolandra fruticosa	Leaf & twigs	*In vivo* (murine)	HT-29	10 and 5 mg/kg/day	*Methanolic*	Sesquiterpene lactone (13-acetoxyrolandrolide)	Antiproliferative effect against human colon cancer cells	(i) Inhibition of the NFκB pathway, subunit p65 (RelA) and upstream mediators IKKβ and oncogenic K-ras	[106]
Cydonia oblonga Miller	Leaf & fruit	*In vivo* (murine)	Caco-2	250–500 μg/mL	*Methanolic*	Phenolic compound (flavonol and flavone heterosides, 5-O-caffeoylquinic acid)	Antiproliferative effect against human kidney and colon cancer cells	(i) Suppression of NFκB activation, activator (AP-1), mitogen-activated protein kinases, namely, PKC, (GFR)-mediated pathways (ii) Cell cycle arrest (iii) Induction of apoptosis, antioxidant, and anti-inflammatory effects	[107]

Table 2: Continued.

Scientific name	Parts used	Model		Dose	Type of extract	Important compounds	Cellular effect	Mechanisms	References
Sedum kamtschaticum	Aerial part	*In vivo* (murine)	HT-29	0–0.5 mg/mL	*Methanolic*	Buddlejasaponin IV	Induced apoptosis in HT-29 human colon cancer cells	(i) Induced apoptosis via mitochondrial-dependent pathway triggered by downregulation of Bcl-2 protein levels, caspase 3 activation, and subsequent PARP cleavage	[109]
Ganoderma lucidum	Caps & stalks	*In vivo* (murine)	HT-29	0-0.1 mg/mL	*Triterpene extract (hot water) extract*	Polysaccharides (mainly glucans & glycoproteins), triterpenes (ganoderic acids, ganoderic alcohols, and their derivatives)	Cytokine expression inhibited during early inflammation in colorectal carcinoma	Induced autophagy through inhibition of p38 mitogen-activated kinase and activation of farnesyl protein transferase (FPT)	[193]
Ginkgo biloba	Fruit & leaf	*In vivo* (murine)	HT-29	20–320 mg/L	*Aqueous*	Terpene lactones and flavonoid glycosides	Inhibited progression of human colon cancer cells induced HT-29 cell apoptosis	(i) Activation in caspase 3, reduction in Bcl-2 expression, and elevation in p53 expression	[112]
Rubus occidentalis	Fruit	*In vivo* (murine)	JB6 Cl 41	25 μg/mL	*Methanolic*	β-Carotene, α-carotene, ellagic acid, ferulic acid, coumaric acid	Inhibited tumor development	(i) Impaired signal transduction pathways leading to activation of AP-1 and NFB RU-ME fraction	[194]
Oryza sativa	Seed	*In vivo* (murine)	HT-29, SW 480, HCEC	100 μg/mL	*Ethyl acetate extract*	Phenolic compound (tricin, ferulic acid, caffeic acid, and methoxycinnamic acid)	Inhibited growth of human colon cancer cells	(i) Induction of apoptosis by enhanced activation of caspases 8 and 3 (ii) Decreased the number of viable SW480 and HCEC cells	[113]
Cistanche deserticola	Dried stem	*In vivo* (murine)	SW480	In vivo: 0.4 g/kg/day In vitro: 100 mg/mL	*Aqueous*	Polysaccharides, phenylethanoid glycosides	Decreased mucosal hyperplasia and helicobacter infection	(i) Increased number of splenic macrophages and NK cells (ii) Decreased frequency of hyperplasia and *H. hepaticus* infection of the intestine	[133]

Table 2: Continued.

Scientific name	Parts used	Model		Dose	Type of extract	Important compounds	Cellular effect	Mechanisms	References
Rehmannia glutinosa	NM	*In vivo* (male C57BL6 mice and Sprague-Dawley rats)	CT26	28 mg/kg	*NM*	Catalpol	(i) Inhibited proliferation, growth, and expression of angiogenic markers	(i) VEGF, VEGFR2, HIF-1α, bFGF inhibited the expressions of inflammatory factors such as IL-1β, IL-6, and IL-8	[143]
	Olive mill wastewater	*In vivo* (murine)	NM	NM	*Methanolic*	Hydroxytyrosol	Interferes with tumor cell growth	NM	[195]
Olea europaea	Leaf	*In vivo* (xenograft model) (murine)	HCT116, HCT8	0, 5, 10, 20, 30, 50, and 70 μg/mL	*Phenolic*	Oleuropein and hydroxytyrosol	NM	(i) Activation of caspases 3, 7, and 9 (ii) Decrease of mitochondrial membrane potential and cytochrome c release (iii) Increase in intracellular Ca2+ concentration	[196]
Ginkgo biloba L.	Leaf	*In vivo* (rat)	NM	0.675 and 1.35 g/kg	*Methanolic*	Flavonoid glycosides, terpene lactones, and ginkgolic acids	(i) Suppressed tumor cell proliferation, promoted apoptosis, and mitigated inflammation	NM	[197]
Rhus trilobata Nutt.	NM	*In vivo* (hamster)	NM	400 mg/kg, 100 mg/kg	*Aqueous*	Tannic acid, gallic acid	Cytotoxic activity	NM	[54]
Annona diversifolia Saff.	NM	*In vivo* (mice)	SW-480	1.5, 7.5 mg/kg/day	NM	Laherradurin	Cytotoxic activity	NM	[54]
A. muricata L.	NM	*In vivo* (rat)	NM	250/500 mg/kg	*EtOAc*	A, B, and C, and cis- and trans-annomuricin-D-ones	Cytotoxic activity	NM	[54]
Plumeria acutifolia Poir.	NM	*In vivo* (hamster)	NM	400 mg/kg/day	*Aqueous*	NM	Cytotoxic activity	NM	[54]
Lasianthaea podocephala (A. Gray) K. M. Becker	NM	*In vivo* (hamster)	NM	200 mg/kg/day	*Aqueous*	NM	Cytotoxic activity	NM	[54]

Table 2: Continued.

Scientific name	Parts used	Model		Dose	Type of extract	Important compounds	Cellular effect	Mechanisms	References
Flourensia cernua DC.	NM	*In vivo* (hamster)	NM	350 mg/kg/day	*Aqueous*	Flavonoids, sesquiterpenoids, monoterpenoids, acetylenes, p-acetophenones, benzopyrans, benzofurans	Cytotoxic activity	NM	[54]
Ambrosia ambrosioides (Cav.) W. W. Payne	NM	*In vivo* (hamster)	NM	400 mg/kg/day	*Aqueous*	NM	Cytotoxic activity	NM	[54]
Alnus jorullensis Kunth	NM	*In vivo* (hamster)	NM	175 mg/kg/day	*Aqueous*	NM	Cytotoxic activity	NM	[54]
Dimorphocarpa wislizeni (Engelm.) Rollins	NM	*In vivo* (hamster)	NM	100 mg/kg/day	*Aqueous*	NM	Cytotoxic activity	NM	[54]
Euphorbia pulcherrima Willd. ex Klotzsch	NM	*In vivo* (hamster)	NM	200 mg/kg/day	*Aqueous*	NM	Cytotoxic activity	NM	[54]
Acalypha monostachya Cav.	NM	*In vivo* (hamster)	NM	400 mg/kg/day	*Aqueous*	NM	Cytotoxic activity	NM	[54]
Crotalaria longirostrata Hook. & Arn.	NM	*In vivo* (hamster)	NM	400 mg/kg/day, 350 mg/kg/day	*EtOH-$CHCl_3$*	NM	Cytotoxic activity	NM	[54]
Asterohyptis stellulata (Benth.) Epling	NM	*In vivo* (hamster)	NM	50 mg/kg/day	*Aqueous*	NM	Cytotoxic activity	NM	[54]
Acacia constricta A. Gray	NM	*In vivo* (hamster)	NM	400 mg/kg/day	*Aqueous*	NM	Cytotoxic activity	NM	[54]
Holodiscus dumosus A. Heller	NM	*In vivo* (hamster)	NM	350 mg/kg/day	*Aqueous*	NM	Cytotoxic activity	NM	[54]
Butea monosperma	Flower	*In vivo* (rat)	HT-29	150 mg/kg	*n-Butanol extract*	Isocoreopsin, butrin, and isobutrin	Free radical scavenging and anticancer activities	NM	[198]

Table 2: Continued.

Scientific name	Parts used	Model		Dose	Type of extract	Important compounds	Cellular effect	Mechanisms	References
Taraxacum spp.	Root	*In vivo* (xenograft murine model)	HT-29, HCT116	40 mg/kg/day	*Aqueous*	α-Amyrin, β-amyrin, lupeol, and taraxasterol	Induced programmed cell death	NM	[199]

*NM: not mentioned.

(b) Other effects of medicinal plants in *in vivo* models

Scientific name	Parts used	Model		Dose	Type of extract	Important compounds	Cellular effect	Mechanisms	References
Allium sativum	Root	*In vivo* (murine)	NM	2.4 mL of daily	*Ethanolic*	Allicin, S-allylmercaptocysteine	Significantly suppressed both the size and number of colon adenomas	Enhancement of detoxifying enzymes: SAC and GST activity	[200]
Olea europaea	Fruit	*In vivo*	Caco-2	50 μM	*Aqueous*	Phenolic compounds, authentic hydroxyl tyrosol (HT)	(i) Effect of OPE and HT on CB1 associated with reduced proliferation of Caco-2 cells (ii) Increase in CB1 expression in the colon of rats receiving dietary EVOO	Increase in Cnr1 gene expression, CB1 protein levels	[201]
		In vivo (murine)	HT115	25 μg/mL	*Hydroethanolic*	Phenolic compounds (p-hydroxyphenyl ethanol, pinoresinol & dihydroxyphenyl ethanol)	NM	Inhibition via reduced expression of a range of α5 & β1	[184]
Origanum vulgare L.	Leaf	*In vivo* (murine)	NM	20, 40, 60 mg·kg^{-1}	*Aqueous*	Rosmarinic acid, caffeic acid, flavonoids	Antioxidant status	(i) Increased LPO products and activity of SOD and CAT enzymes and GST and GPx activity (ii) Antioxidant and anticarcinogenic effect	[202]
Hazelnut	Skin	*In vivo*	NM	The flow rate 0.21 mL/min and injection volume 9.4 μL	*Aqueous*	Flavan-3-ols, in monomeric and polymeric forms, and phenolic acids	(i) Decreased circulating levels of free fatty acids and triglycerides (ii) Higher excretion of bile acid	Increase of the total antioxidant capacity of plasma	[203]
Apples and apple juice	Fruit	*In vivo*	NM	90 mg/L	*Aqueous*	Phenolic acids, flavonoids, tannins, stilbenes, curcuminoids	NM	NM	[204]

Table 2: Continued.

Scientific name	Parts used	Model		Dose	Type of extract	Important compounds	Cellular effect	Mechanisms	References
Grifola frondosa	Fruit	*In vivo* (murine)	HT-29	10 ng/mL	*Aqueous*	Phenolic compounds (pyrogallol, caffeic acid, myricetin, protocatechuic acid, etc.)	Inhibition of TNBS-induced rat colitis	(i) Induced cell cycle progression in G0/G1 phase and apoptotic death	[104]
Ruta chalepensis	Leaf	*In vivo* (human)	NM	250 μg/mL	*Ethanolic*	Rutin, gallic acid, catechin hydrate, naringin	Oxidative profile in patients with colon cancer	NM	[205]
Cannabis sativa	Dry flower & leaf	*In vivo* (murine)	DLD-1 and HCT116	0.3–5 μM	*Methanolic*	Cannabidiol, phytocannabinoids	NM	(i) Reduced cell proliferation in a CB1-sensitive and AOM-induced preneoplastic lesions and polyps (ii) Inhibition of colorectal cancer cell proliferation via CB1and CB2 receptor activation	[121]
Melia toosendan	Fruit	*In vivo* (murine)	SW480, CT26	0, 10, 20, 30, 40, 50 μg/mL	*Ethanolic*	Triterpenoids, flavonoids, polysaccharide, limonoids	NM	(i) Inhibited cell proliferation of SW480 and CT26 by promoting apoptosis as indicated by nuclear chromatin condensation and DNA fragmentation (ii) Induced caspase 9 activity which further activated caspase 3 and poly(ADP-ribose) polymerase cleavage, leading the tumor cells to apoptosis	[123]
Smallanthus sonchifolius	Root	*In vivo* (murine)	NM	73.90, 150.74, 147.65, and 123.26 mg/kg	*Aqueous*	Fructans	NM	Reduction incidence of colon tumors expressing altered β-catenin	[206]
Punica granatum	Peel	*In vivo* (adult male Wistar rats)	NM	4.5 g/kg	*Methanolic*	Gallic acid, protocatechuic acid, cateachin, rutin, ellagic acid, punicalagin	NM	(i) Reduction in TGF-β, Bcl-2, EGF, CEA, CCSA-4, MMP-7 and in COX-2, cyclin D1, survivin content (ii) Downregulated expression of β-catenin, K-ras, c-Myc genes	[207]
Linum usitatissimum	Seed	*In vivo* (male Sprague-Dawley rats)	NM	500 mg/kg	*Alkaline*	Secoisolariciresinol diglucoside, carbohydrates, proteins, and tannins	Reduced the serum fasting glucose levels	Significantly reduced the HbA1c, insulin levels, and proinflammatory cytokines	[208]
Diospyros kaki	Fruit	*In vivo* (male	NM	15 mg/kg	*Hydroacetone*	Polyphenol	(i) Decreased attenuation of colon length in	Decreased expression of COX-2 and iNOS in the colonic tissue	[147]

Table 2: Continued.

Scientific name	Parts used	Model		Dose	Type of extract	Important compounds	Cellular effect	Mechanisms	References
		CD-1 mice)					diarrhea severity (ii) Reduced mortality rate (iii) Reduction of the extent of visible injury (ulcer formation) and of mucosal hemorrhage		
Muntingia calabura	Leaf	*In vivo* (rat)	NM	50, 250, 500 mg/kg	*Methanolic*	Rutin, gallic acid, ferulic acid, and pinocembrin	Reduction of the colonic oxidative stress, increasing the antioxidants levels possibly via the synergistic action of several flavonoids	NM	[209]
Portulaca oleracea	NM	*In vivo* (murine)	HT-29 CSCs	2.25 μg/mL	*Alcoholic*	NM	Regulatory and target genes that mediate the Notch signal transduction pathway	Inhibition of expression of the Notch1 and β-catenin genes	[161]
Aloe vera	Gel	*In vivo* (murine)	NM	400 mg/kg/day	*Gel*	Polysaccharides	NM	(i) Via inhibition of the cell cycle progression (ii) Induction of cellular factors, such as extracellular signal-regulated kinases 1/2, cyclin-dependent kinase 4, and cyclin D1; on the other hand, PAG increased the expression of caudal-related homeobox transcription factor 2	[210]
Artemisia annua Linné	Powder	*In vivo* (xenograft murine model)	HCT116	20, 40 mg/kg/day	*Ethanolic*	Phenolic compounds	NM	(i) Induced apoptosis via PTEN/p53/PDK1/Akt signal pathways through PTEN/p53 (ii) Inhibited cell viability and increased LDH release and apoptotic bodies, caspase 3 and 7 activation, and reduced mitochondria membrane potential (iii) Regulated cytochrome c translocation to the cytoplasm and Bax translocation to the mitochondrial membrane (iv) Regulation of proteins	[169]

Table 2: Continued.

Scientific name	Parts used	Model		Dose	Type of extract	Important compounds	Cellular effect	Mechanisms	References
Hordeum vulgare	Powder	*In vivo* (xenograft murine model)	HT-29	2 g/kg and 1 g/kg	*Aqueous (fermented)*	*β*-Glucan, protein, amino acids, phenolic compounds	NM	(i) Promoted tumor apoptosis by upregulating the mRNA expression of Bax and caspase 3 and downregulating the mRNA expression of Bcl-2 and cyclin D1 (ii) Decreased mRNA expression of Bcl-2 and cyclin D1 (iii) Upregulated expressions levels of Bax and caspase 3	[211]
Dendrophthoe pentandra	Leaf	*In vivo* (murine)	NM	125, 250, 500 mg/kg	*Ethanolic*	Quercetin-3-rhamnose	NM	(i) Decreased the levels of IL-22, MPO levels, proliferation of epithelial cells (ii) Inhibited S phase of the cell cycle (iii) Upregulated p53 wild-type gene expression	[212]
Aquilaria crassna	Stem, bark	*In vivo* (murine)	HCT116	2,000 mg/kg/day 100, 200 mg/kg	*NM*	Resin and essential oils	NM	NM	[213]
Berberis integerrima	NM	*In vivo* (murine)	NM	50 and 100 mg/kg	*Hydroalcoholic*	NM	NM	NM	[214]
Salix aegyptiaca	Bark	*In vivo* (murine)	NM	100 and 400 mg/kg	*Ethanolic*	Catechin, catechol, and salicin	NM	Decreased level of EGFR, nuclear *β*-catenin, and COX-2	[215]

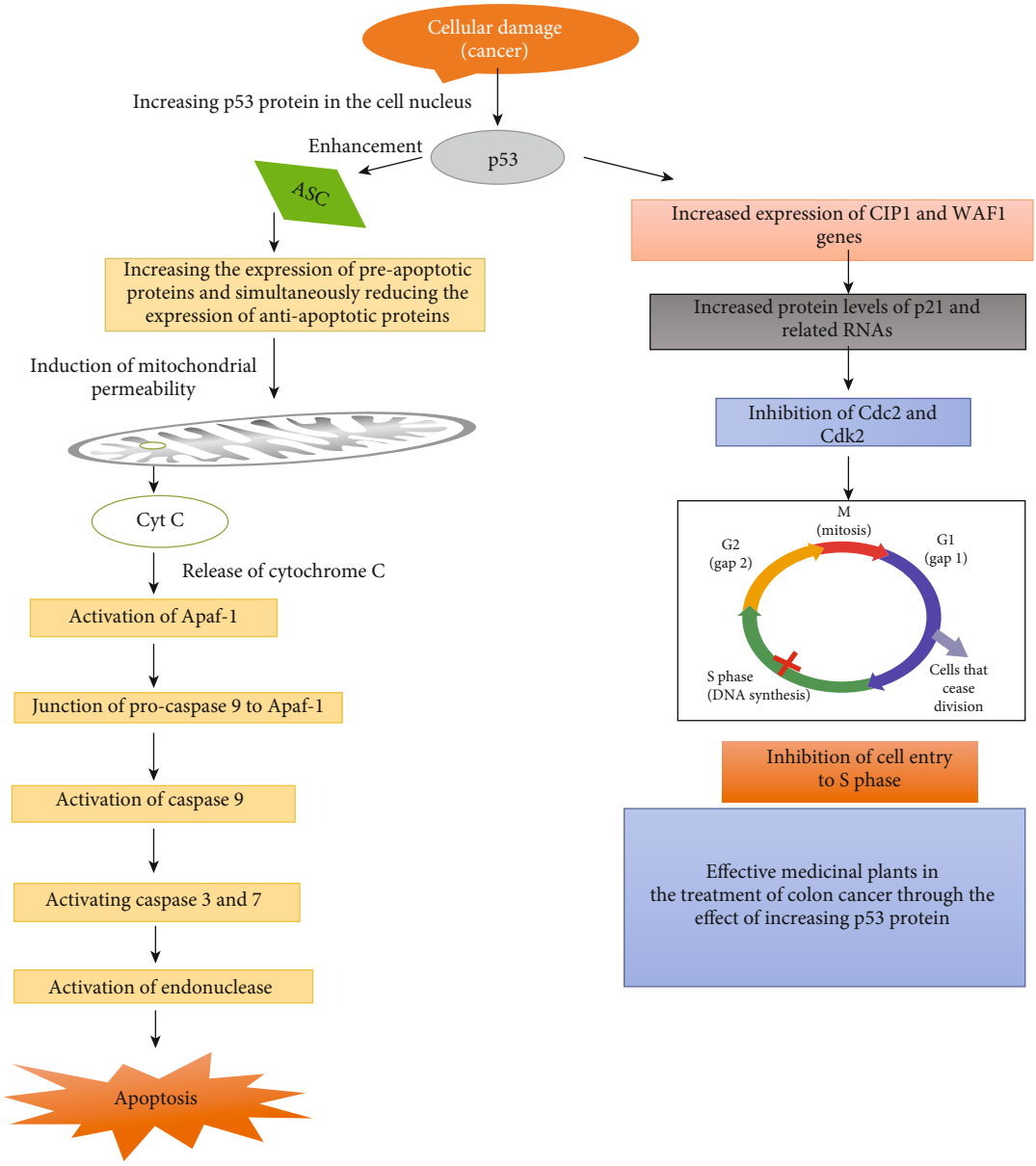

Figure 1: Cell damage and cancer trigger p53 activation. The p53 protein activates the apoptotic protein Bax. Bax inhibits the antiapoptotic protein Bcl-2. During apoptosis, cytochrome c is released from mitochondria. To activate the Apaf-1 protein, the interaction between these proteins and cytochrome C is necessary. Pro-caspase 9 attaches to Apaf-1 and activates caspase 9. Caspase 9 activates caspases 3 and 7 and apoptosis occurs.

alkaloids, glycosides, and phenols, such as quercetin and luteolin, and kaempferol and luteolin glycosides.

In a systematic review of the plants being studied, some mechanisms were mainly common, including the induction of apoptosis by means of an increase of expression and levels of caspase 2, caspase 3, caspase 7, caspase 8, and caspase 9 in cancer cells, increasing the expression of the proapoptotic protein Bax and decreasing the expression of the antiapoptotic proteins.

Many herbal extracts block specific phase of the cell cycle. For instance, the extract prepared from the leaves of *Annona muricata* inhibits the proliferation of colon cancer cells and induces apoptosis by arresting cells in the G1 phase [53]. They can also prevent the progress of the G1/S phase in cancer cells [74]. In general, the herbal extracts reported here have been able to stop cancer cells at various stages, such as G2/M, G1/S, S phase, G0/G1, and G1 phase, and could prevent their proliferation and growth.

Other important anticancer mechanisms are the increase of both p53 protein levels and transcription of its gene. Even the increase of p21 expression is not without effect [137]. In an *in vitro* study on the *Garcinia mangostana* roots, the results were indicative of the inhibitory effect of the extract of this plant on p50 and P65 activation [93]. Moreover, reduction of cyclin D1 levels and increase of p21 levels are among these mechanisms [137], as well as inhibition of NFκB

and reduction of the transcription of its genes, which contribute to reduce the number of cancerous cells [127]. Other important anticancer mechanisms are the inhibition of COX-2, as well as the reduction of the protein levels in this pathway [34]. In addition to this, in some cases, the inhibition of MMP-9 can be mentioned as the significant mechanism of some herbal extracts to kill cancer cells [183].

4. Conclusion and Perspectives

The findings of this review indicate that medicinal plants containing various phytochemicals, such as flavonoids, polyphenol compounds, such as caffeic acid, catechins, saponins, polysaccharides, triterpenoids, alkaloids, glycosides, and phenols, such as quercetin and luteolin, and kaempferol and luteolin glycosides, can inhibit tumor cell proliferation and also intduce apoptosis.

Plants and their main compounds affect transcription and cell cycle via different mechanisms. Among these pathways, we can point to induction of superoxide dismutase to eliminate free radicals, reduction of DNA oxidation, induction of apoptosis by inducing a cell cycle arrest in S phase, reduction of PI3K, P-Akt protein, and MMP expression, reduction of antiapoptotic Bcl-2, Bcl-xL proteins, and decrease of proliferating cell nuclear antigen (PCNA), cyclin A, cyclin D1, cyclin B1, and cyclin E. Plant compounds also increase the expression of both cell cycle inhibitors, such as p53, p21, and p27, and BAD, Bax, caspase 3, caspase 7, caspase 8, and caspase 9 proteins levels. In general, this study showed that medicinal plants are potentially able to inhibit growth and proliferation of colon cancer cells. But the clinical usage of these results requires more studies on these compounds in *in vivo* models. Despite many studies' *in vivo* models, rarely clinical trials were observed among the studies. In fact, purification of herbal compounds and demonstration of their efficacy in appropriate *in vivo* models, as well as clinical studies, may lead to alternative and effective ways of controlling and treating colon cancer.

Conflicts of Interest

There is no conflict of interest regarding the publication of this paper.

Authors' Contributions

Dr. Paola Aiello and Maedeh Sharghi contributed equally to this work. Shabnam Malekpour Mansourkhani and Azam Pourabbasi Ardekan contributed equally to this work.

Acknowledgments

The authors appreciate and thank Dr. Moahammad Firouzbakht for his cooperation in draft editing.

References

[1] A. J. M. Watson and P. D. Collins, "Colon cancer: a civilization disorder," *Digestive Diseases*, vol. 29, no. 2, pp. 222–228, 2011.

[2] R. R. Huxley, A. Ansary-Moghaddam, P. Clifton, S. Czernichow, C. L. Parr, and M. Woodward, "The impact of dietary and lifestyle risk factors on risk of colorectal cancer: a quantitative overview of the epidemiological evidence," *International Journal of Cancer*, vol. 125, no. 1, pp. 171–180, 2009.

[3] D. J. Schultz, N. S. Wickramasinghe, M. M. Ivanova et al., "Anacardic acid inhibits estrogen receptor α–DNA binding and reduces target gene transcription and breast cancer cell proliferation," *Molecular Cancer Therapeutics*, vol. 9, no. 3, pp. 594–605, 2010.

[4] L. E. Johns and R. S. Houlston, "A systematic review and meta-analysis of familial colorectal cancer risk," *The American Journal of Gastroenterology*, vol. 96, no. 10, pp. 2992–3003, 2001.

[5] J. A. Meyerhardt, P. J. Catalano, D. G. Haller et al., "Impact of diabetes mellitus on outcomes in patients with colon cancer," *Journal of Clinical Oncology*, vol. 21, no. 3, pp. 433–440, 2003.

[6] J. Terzić, S. Grivennikov, E. Karin, and M. Karin, "Inflammation and colon cancer," *Gastroenterology*, vol. 138, no. 6, pp. 2101–2114.e5, 2010.

[7] H. J. Schmoll, E. van Cutsem, A. Stein et al., "ESMO consensus guidelines for management of patients with colon and rectal cancer. A personalized approach to clinical decision making," *Annals of Oncology*, vol. 23, no. 10, pp. 2479–2516, 2012.

[8] M. S. O'Reilly, T. Boehm, Y. Shing et al., "Endostatin: an endogenous inhibitor of angiogenesis and tumor growth," *Cell*, vol. 88, no. 2, pp. 277–285, 1997.

[9] E. Pasquier, M. Carré, B. Pourroy et al., "Antiangiogenic activity of paclitaxel is associated with its cytostatic effect, mediated by the initiation but not completion of a mitochondrial apoptotic signaling pathway," *Molecular Cancer Therapeutics*, vol. 3, no. 10, pp. 1301–1310, 2004.

[10] Board PDQATE, *Colon Cancer Treatment (PDQ(R)): Health Professional Version. PDQ Cancer Information Summaries*, National Cancer Institute (US), Bethesda, MD, USA, 2002.

[11] http://www.cancer.net/navigating-cancer-care/how-cancer-treated/chemotherapy/side-effects-chemotherapy.

[12] A. D. Edgar, R. Levin, C. E. Constantinou, and L. Denis, "A critical review of the pharmacology of the plant extract of *Pygeum africanum* in the treatment of LUTS," *Neurourology and Urodynamics*, vol. 26, no. 4, pp. 458–463, 2007.

[13] J. W. Holaday and B. A. Berkowitz, "Antiangiogenic drugs: insights into drug development from endostatin, avastin and thalidomide," *Molecular Interventions*, vol. 9, no. 4, pp. 157–166, 2009.

[14] W. Kooti and N. Daraei, "A review of the antioxidant activity of celery (*Apium graveolens* L)," *Journal of Evidence-Based Complementary & Alternative Medicine*, vol. 22, no. 4, pp. 1029–1034, 2017.

[15] H. Z. Marzouni, N. Daraei, N. Sharafi-Ahvazi, N. Kalani, and W. Kooti, "The effect of aqueous extract of celery leaves (*Apium graveolens*) on fertility in female rats," *World Journal of Pharmacy and Pharmaceutical Sciences*, vol. 5, no. 5, pp. 1710–1714, 2016.

[16] R. Sharma and S. Jain, "Cancer tretment: an overview of herbal medicines," *World Journal of Pharmacy and Pharmaceutical Sciences*, vol. 3, no. 8, pp. 222–230, 2014.

[17] M. Ghasemiboron, E. Mansori, M. Asadi-Samani et al., "Effect of ointment with cabbage, pomegranate peel, and common plantain on wound healing in male rat," *Journal of Shahrekord Uuniversity of Medical Sciences*, vol. 15, no. 6, pp. 92–100, 2014.

[18] W. Kooti, M. Ghasemiboroon, M. Asadi-Samani et al., "The effects of hydro-alcoholic extract of celery on lipid profile of rats fed a high fat diet," *Advances in Environmental Biology*, vol. 8, no. 9, pp. 325–330, 2014.

[19] A. L. Zahoor, L. Yaqoob, S. K. Shaukat, A. W. Aijaz, and I. R. Mohd, "Hepatoprotective medicinal plants used by the Gond and Bhill tribals of District Raisen Madhya Pradesh, India," *Journal of Medicinal Plants Research*, vol. 9, no. 12, pp. 400–406, 2015.

[20] E. Mansouri, W. Kooti, M. Bazvand et al., "The effect of hydro-alcoholic extract of Foeniculum vulgare Mill on leukocytes and hematological tests in male rats," *Jundishapur Journal of Natural Pharmaceutical Products*, vol. 10, no. 1, article e18396, 2015.

[21] S.-Y. Wu, J.-L. Shen, K.-M. Man et al., "An emerging translational model to screen potential medicinal plants for nephrolithiasis, an independent risk factor for chronic kidney disease," *Evidence-Based Complementary and Alternative Medicine*, vol. 2014, Article ID 972958, 7 pages, 2014.

[22] K. Saki, M. Bahmani, M. Rafieian-Kopaei et al., "The most common native medicinal plants used for psychiatric and neurological disorders in Urmia city, northwest of Iran," *Asian Pacific Journal of Tropical Disease*, vol. 4, pp. S895–S901, 2014.

[23] M. Asadi-Samani, W. Kooti, E. Aslani, and H. Shirzad, "A systematic review of Iran's medicinal plants with anticancer effects," *Journal of Evidence-Based Complementary & Alternative Medicine*, vol. 21, no. 2, pp. 143–153, 2016.

[24] A. Bishayee and G. Sethi, "Bioactive natural products in cancer prevention and therapy: progress and promise," *Seminars in Cancer Biology*, vol. 40-41, pp. 1–3, 2016.

[25] K. I. Block, C. Gyllenhaal, L. Lowe et al., "Designing a broad-spectrum integrative approach for cancer prevention and treatment," *Seminars in Cancer Biology*, vol. 35, pp. S276–S304, 2015.

[26] L. S. Einbond, A. Negrin, D. M. Kulakowski et al., "Traditional preparations of kava (*Piper methysticum*) inhibit the growth of human colon cancer cells in vitro," *Phytomedicine*, vol. 24, pp. 1–13, 2017.

[27] P. Signorelli, C. Fabiani, A. Brizzolari et al., "Natural grape extracts regulate colon cancer cells malignancy," *Nutrition and Cancer*, vol. 67, no. 3, pp. 494–503, 2015.

[28] A. Setiawati, H. Immanuel, and M. T. Utami, "The inhibition of *Typhonium flagelliforme* Lodd. Blume leaf extract on COX-2 expression of WiDr colon cancer cells," *Asian Pacific Journal of Tropical Biomedicine*, vol. 6, no. 3, pp. 251–255, 2016.

[29] M. J. Jara-Palacios, D. Hernanz, T. Cifuentes-Gomez, M. L. Escudero-Gilete, F. J. Heredia, and J. P. E. Spencer, "Assessment of white grape pomace from winemaking as source of bioactive compounds, and its antiproliferative activity," *Food Chemistry*, vol. 183, pp. 78–82, 2015.

[30] S. Genovese, F. Epifano, G. Carlucci, M. C. Marcotullio, M. Curini, and M. Locatelli, "Quantification of 4′-geranyloxyferulic acid, a new natural colon cancer chemopreventive agent, by HPLC-DAD in grapefruit skin extract," *Journal of Pharmaceutical and Biomedical Analysis*, vol. 53, no. 2, pp. 212–214, 2010.

[31] L. Reddivari, V. Charepalli, S. Radhakrishnan et al., "Grape compounds suppress colon cancer stem cells in vitro and in a rodent model of colon carcinogenesis," *BMC Complementary and Alternative Medicine*, vol. 16, no. 1, p. 278, 2016.

[32] M. Dong, G. Yang, H. Liu et al., "Aged black garlic extract inhibits HT29 colon cancer cell growth via the PI3K/Akt signaling pathway," *Biomedical Reports*, vol. 2, no. 2, pp. 250–254, 2014.

[33] Y. J. Oh and M. K. Sung, "Soybean saponins inhibit cell proliferation by suppressing PKC activation and induce differentiation of HT-29 human colon adenocarcinoma cells," *Nutrition and Cancer*, vol. 39, no. 1, pp. 132–138, 2001.

[34] H.-Y. Kim, R. Yu, J.-S. Kim, Y.-K. Kim, and M.-K. Sung, "Antiproliferative crude soy saponin extract modulates the expression of IκBα, protein kinase C, and cyclooxygenase-2 in human colon cancer cells," *Cancer Letters*, vol. 210, no. 1, pp. 1–6, 2004.

[35] F. Hajiaghaalipour, M. S. Kanthimathi, J. Sanusi, and J. Rajarajeswaran, "White tea (*Camellia sinensis*) inhibits proliferation of the colon cancer cell line, HT-29, activates caspases and protects DNA of normal cells against oxidative damage," *Food Chemistry*, vol. 169, pp. 401–410, 2015.

[36] A. Gosslau, D. L. En Jao, M.-T. Huang et al., "Effects of the black tea polyphenol theaflavin-2 on apoptotic and inflammatory pathways in vitro and in vivo," *Molecular Nutrition & Food Research*, vol. 55, no. 2, pp. 198–208, 2011.

[37] S. Y. Park, E. J. Kim, H. J. Choi et al., "Anti-carcinogenic effects of non-polar components containing licochalcone A in roasted licorice root," *Nutrition Research and Practice*, vol. 8, no. 3, pp. 257–266, 2014.

[38] F. Naselli, L. Tesoriere, F. Caradonna et al., "Anti-proliferative and pro-apoptotic activity of whole extract and isolated indicaxanthin from *Opuntia ficus-indica* associated with re-activation of the onco-suppressor $p16^{INK4a}$ gene in human colorectal carcinoma (Caco-2) cells," *Biochemical and Biophysical Research Communications*, vol. 450, no. 1, pp. 652–658, 2014.

[39] P. L. Ng, N. F. Rajab, S. M. Then et al., "*Piper betle* leaf extract enhances the cytotoxicity effect of 5-fluorouracil in inhibiting the growth of HT29 and HCT116 colon cancer cells," *Journal of Zhejiang University-SCIENCE B*, vol. 15, no. 8, pp. 692–700, 2014.

[40] M. E. Olsson, C. S. Andersson, S. Oredsson, R. H. Berglund, and K. E. Gustavsson, "Antioxidant levels and inhibition of cancer cell proliferation in vitro by extracts from organically and conventionally cultivated strawberries," *Journal of Agricultural and Food Chemistry*, vol. 54, no. 4, pp. 1248–1255, 2006.

[41] S. J. Min, J. Y. Lim, H. R. Kim, S. J. Kim, and Y. Kim, "*Sasa quelpaertensis* leaf extract inhibits colon cancer by regulating cancer cell stemness in vitro and in vivo," *International Journal of Molecular Sciences*, vol. 16, no. 12, pp. 9976–9997, 2015.

[42] Q. Zhao, X. C. Huo, F. D. Sun, and R. Q. Dong, "Polyphenol-rich extract of Salvia chinensis exhibits anticancer activity in different cancer cell lines, and induces cell cycle arrest at the

G0/G1-phase, apoptosis and loss of mitochondrial membrane potential in pancreatic cancer cells," *Molecular Medicine Reports*, vol. 12, no. 4, pp. 4843–4850, 2015.

[43] L. S. Adams, N. P. Seeram, B. B. Aggarwal, Y. Takada, D. Sand, and D. Heber, "Pomegranate juice, total pomegranate ellagitannins, and punicalagin suppress inflammatory cell signaling in colon cancer cells," *Journal of Agricultural and Food Chemistry*, vol. 54, no. 3, pp. 980–985, 2006.

[44] S. Đurđević, K. Šavikin, J. Živković et al., "Antioxidant and cytotoxic activity of fatty oil isolated by supercritical fluid extraction from microwave pretreated seeds of wild growing *Punica granatum* L.," *The Journal of Supercritical Fluids*, vol. 133, no. 1, pp. 225–232, 2018.

[45] T. S. Thind, S. K. Agrawal, A. K. Saxena, and S. Arora, "Studies on cytotoxic, hydroxyl radical scavenging and topoisomerase inhibitory activities of extracts of *Tabernaemontana divaricata* (L.) R.Br. ex Roem. and Schult," *Food and Chemical Toxicology*, vol. 46, no. 8, pp. 2922–2927, 2008.

[46] S. Tansuwanwong, H. Yamamoto, K. Imai, and U. Vinitketkumnuen, "Antiproliferation and apoptosis on RKO colon cancer by *Millingtonia hortensis*," *Plant Foods for Human Nutrition*, vol. 64, no. 1, pp. 11–17, 2009.

[47] E. M. Coates, G. Popa, C. I. R. Gill et al., "Colon-available raspberry polyphenols exhibit anti-cancer effects on in vitro models of colon cancer," *Journal of Carcinogenesis*, vol. 6, no. 1, p. 4, 2007.

[48] J. God, P. L. Tate, and L. L. Larcom, "Red raspberries have antioxidant effects that play a minor role in the killing of stomach and colon cancer cells," *Nutrition Research*, vol. 30, no. 11, pp. 777–782, 2010.

[49] K. Dimas, C. Tsimplouli, C. Houchen et al., "An ethanol extract of Hawaiian turmeric: extensive in vitro anticancer activity against human colon cancer cells," *Alternative Therapies in Health and Medicine*, vol. 21, Supplement 2, pp. 46–54, 2015.

[50] S. A. Cichello, Q. Yao, A. Dowell, B. Leury, and X. Q. He, "Proliferative and inhibitory activity of Siberian ginseng (Eleutherococcus senticosus) extract on cancer cell lines; A-549, XWLC-05, HCT-116, CNE and Beas-2b," *Asian Pacific Journal of Cancer Prevention*, vol. 16, no. 11, pp. 4781–4786, 2015.

[51] S. Tansuwanwong, Y. Hiroyuki, I. Kohzoh, and U. Vinitketkumnuen, "Induction of apoptosis in RKO colon cancer cell line by an aqueous extract of *Millingtonia hortensis*," *Asian Pacific Journal of Cancer Prevention*, vol. 7, no. 4, pp. 641–644, 2006.

[52] R. Chatthongpisut, S. J. Schwartz, and J. Yongsawatdigul, "Antioxidant activities and antiproliferative activity of Thai purple rice cooked by various methods on human colon cancer cells," *Food Chemistry*, vol. 188, pp. 99–105, 2015.

[53] S. Z. Moghadamtousi, H. Karimian, E. Rouhollahi, M. Paydar, M. Fadaeinasab, and H. Abdul Kadir, "*Annona muricata* leaves induce G_1 cell cycle arrest and apoptosis through mitochondria-mediated pathway in human HCT-116 and HT-29 colon cancer cells," *Journal of Ethnopharmacology*, vol. 156, pp. 277–289, 2014.

[54] N. J. Jacobo-Herrera, F. E. Jacobo-Herrera, A. Zentella-Dehesa, A. Andrade-Cetto, M. Heinrich, and C. Perez-Plasencia, "Medicinal plants used in Mexican traditional medicine for the treatment of colorectal cancer," *Journal of Ethnopharmacology*, vol. 179, pp. 391–402, 2016.

[55] K. V. Balan, J. Prince, Z. Han et al., "Antiproliferative activity and induction of apoptosis in human colon cancer cells treated in vitro with constituents of a product derived from *Pistacia lentiscus* L. var. *chia*," *Phytomedicine*, vol. 14, no. 4, pp. 263–272, 2007.

[56] K. V. Balan, C. Demetzos, J. Prince et al., "Induction of apoptosis in human colon cancer HCT116 cells treated with an extract of the plant product, Chios mastic gum," *In Vivo*, vol. 19, no. 1, pp. 93–102, 2005.

[57] M. L. King and L. L. Murphy, "Role of cyclin inhibitor protein p21 in the inhibition of HCT116 human colon cancer cell proliferation by American ginseng (*Panax quinquefolius*) and its constituents," *Phytomedicine*, vol. 17, no. 3-4, pp. 261–268, 2010.

[58] V. Charepalli, L. Reddivari, S. Radhakrishnan, R. Vadde, R. Agarwal, and J. K. P. Vanamala, "Anthocyanin-containing purple-fleshed potatoes suppress colon tumorigenesis via elimination of colon cancer stem cells," *The Journal of Nutritional Biochemistry*, vol. 26, no. 12, pp. 1641–1649, 2015.

[59] R. Campos-Vega, R. G. Guevara-Gonzalez, B. L. Guevara-Olvera, B. Dave Oomah, and G. Loarca-Piña, "Bean (*Phaseolus vulgaris* L.) polysaccharides modulate gene expression in human colon cancer cells (HT-29)," *Food Research International*, vol. 43, no. 4, pp. 1057–1064, 2010.

[60] A. T. Serra, J. Poejo, A. A. Matias, M. R. Bronze, and C. M. M. Duarte, "Evaluation of *Opuntia* spp. derived products as antiproliferative agents in human colon cancer cell line (HT29)," *Food Research International*, vol. 54, no. 1, pp. 892–901, 2013.

[61] T. dos Santos, C. Tavares, D. Sousa et al., "*Suillus luteus* methanolic extract inhibits cell growth and proliferation of a colon cancer cell line," *Food Research International*, vol. 53, no. 1, pp. 476–481, 2013.

[62] G. K. Jayaprakasha, K. K. Mandadi, S. M. Poulose, Y. Jadegoud, G. A. Nagana Gowda, and B. S. Patil, "Inhibition of colon cancer cell growth and antioxidant activity of bioactive compounds from *Poncirus trifoliata* (L.) Raf," *Bioorganic & Medicinal Chemistry*, vol. 15, no. 14, pp. 4923–4932, 2007.

[63] M. González-Vallinas, S. Molina, G. Vicente et al., "Antitumor effect of 5-fluorouracil is enhanced by rosemary extract in both drug sensitive and resistant colon cancer cells," *Pharmacological Research*, vol. 72, pp. 61–68, 2013.

[64] A. Valdés, G. Sullini, E. Ibáñez, A. Cifuentes, and V. García-Cañas, "Rosemary polyphenols induce unfolded protein response and changes in cholesterol metabolism in colon cancer cells," *Journal of Functional Foods*, vol. 15, pp. 429–439, 2015.

[65] A. Valdes, K. A. Artemenko, J. Bergquist, V. Garcia-Canas, and A. Cifuentes, "Comprehensive proteomic study of the antiproliferative activity of a polyphenol-enriched rosemary extract on colon cancer cells using nanoliquid chromatography–orbitrap MS/MS," *Journal of Proteome Research*, vol. 15, no. 6, pp. 1971–1985, 2016.

[66] A. Pérez-Sánchez, N. Sánchez-Marzo, M. Herranz-López, E. Barrajón-Catalán, and V. Micol, "Rosemary (*Rosmarinus officinalis L*) extract increases ROS and modulates Nrf2 pathway in human colon cancer cell lines," *Free Radical Biology & Medicine*, vol. 108, p. S79, 2017.

[67] Y. R. Um, C.-S. Kong, J. I. Lee, Y. A. Kim, T. J. Nam, and Y. Seo, "Evaluation of chemical constituents from *Glehnia littoralis* for antiproliferative activity against HT-29 human colon cancer cells," *Process Biochemistry*, vol. 45, no. 1, pp. 114–119, 2010.

[68] M. A. Encalada, S. Rehecho, D. Ansorena, I. Astiasarán, R. Y. Cavero, and M. I. Calvo, "Antiproliferative effect of phenylethanoid glycosides from *Verbena officinalis* L. on colon cancer cell lines," *LWT - Food Science and Technology*, vol. 63, no. 2, pp. 1016–1022, 2015.

[69] Y. Nakamura, Y. Hasegawa, K. Shirota et al., "Differentiation-inducing effect of piperitenone oxide, a fragrant ingredient of spearmint (*Mentha spicata*), but not carvone and menthol, against human colon cancer cells," *Journal of Functional Foods*, vol. 8, pp. 62–67, 2014.

[70] A. Panyathep, T. Chewonarin, K. Taneyhill, Y.-J. Surh, and U. Vinitketkumnuen, "Effects of dried longan seed (*Euphoria longana* Lam.) extract on VEGF secretion and expression in colon cancer cells and angiogenesis in human umbilical vein endothelial cells," *Journal of Functional Foods*, vol. 5, no. 3, pp. 1088–1096, 2013.

[71] G. Leisching, B. Loos, T. Nell, and A. M. Engelbrecht, "*Sutherlandia frutescens* treatment induces apoptosis and modulates the PI3-kinase pathway in colon cancer cells," *South African Journal of Botany*, vol. 100, pp. 20–26, 2015.

[72] C. Weidner, M. Rousseau, A. Plauth et al., "*Melissa officinalis* extract induces apoptosis and inhibits proliferation in colon cancer cells through formation of reactive oxygen species," *Phytomedicine*, vol. 22, no. 2, pp. 262–270, 2015.

[73] C.-Y. Wang, T.-C. Wu, S.-L. Hsieh, Y.-H. Tsai, C.-W. Yeh, and C.-Y. Huang, "Antioxidant activity and growth inhibition of human colon cancer cells by crude and purified fucoidan preparations extracted from *Sargassum cristaefolium*," *Journal of Food and Drug Analysis*, vol. 23, no. 4, pp. 766–777, 2015.

[74] J. Lin, Q. Li, H. Chen, H. Lin, Z. Lai, and J. Peng, "Hedyotis diffusa Willd. extract suppresses proliferation and induces apoptosis via IL-6-inducible STAT3 pathway inactivation in human colorectal cancer cells," *Oncology Letters*, vol. 9, no. 4, pp. 1962–1970, 2015.

[75] M. Marrelli, F. Menichini, and F. Conforti, "A comparative study of *Zingiber officinale* Roscoe pulp and peel: phytochemical composition and evaluation of antitumour activity," *Natural Product Research*, vol. 29, no. 21, pp. 2045–2049, 2015.

[76] D. Goh, Y. H. Lee, and E. S. Ong, "Inhibitory effects of a chemically standardized extract from *Scutellaria barbata* in human colon cancer cell lines, LoVo," *Journal of Agricultural and Food Chemistry*, vol. 53, no. 21, pp. 8197–8204, 2005.

[77] S. A. Kang, H. J. Park, M.-J. Kim, S.-Y. Lee, S.-W. Han, and K.-H. Leem, "Citri Reticulatae Viride Pericarpium extract induced apoptosis in SNU-C4, human colon cancer cells," *Journal of Ethnopharmacology*, vol. 97, no. 2, pp. 231–235, 2005.

[78] A. Chicca, B. Adinolfi, E. Martinotti et al., "Cytotoxic effects of *Echinacea* root hexanic extracts on human cancer cell lines," *Journal of Ethnopharmacology*, vol. 110, no. 1, pp. 148–153, 2007.

[79] L. A. Boyd, M. J. McCann, Y. Hashim, R. N. Bennett, C. I. R. Gill, and I. R. Rowland, "Assessment of the anti-genotoxic, anti-proliferative, and anti-metastatic potential of crude watercress extract in human colon cancer cells," *Nutrition and Cancer*, vol. 55, no. 2, pp. 232–241, 2006.

[80] J. Gwak, S. Park, M. Cho et al., "Polysiphonia japonica extract suppresses the Wnt/β-catenin pathway in colon cancer cells by activation of NF-κB," *International Journal of Molecular Medicine*, vol. 17, pp. 1005–1010, 2006.

[81] C. Li and M.-H. Wang, "*Aristolochia debilis* Sieb. *et* Zucc. induces apoptosis and reactive oxygen species in the HT-29 human colon cancer cell line," *Cancer Biotherapy and Radiopharmaceuticals*, vol. 28, no. 10, pp. 717–724, 2013.

[82] A. F. A. Aisha, Z. Ismail, K. M. Abu-Salah, J. M. Siddiqui, G. Ghafar, and A. M. S. Abdul Majid, "*Syzygium campanulatum* korth methanolic extract inhibits angiogenesis and tumor growth in nude mice," *BMC Complementary and Alternative Medicine*, vol. 13, no. 1, 2013.

[83] W. Lin, L. Zheng, Q. Zhuang et al., "*Spica prunellae* promotes cancer cell apoptosis, inhibits cell proliferation and tumor angiogenesis in a mouse model of colorectal cancer via suppression of stat3 pathway," *BMC Complementary and Alternative Medicine*, vol. 13, no. 1, 2013.

[84] L. Maness, I. Goktepe, H. Chen, M. Ahmedna, and S. Sang, "Impact of *Phytolacca americana* extracts on gene expression of colon cancer cells," *Phytotherapy Research*, vol. 28, no. 2, pp. 219–223, 2014.

[85] M. Deepa, T. Sureshkumar, P. K. Satheeshkumar, and S. Priya, "Antioxidant rich *Morus alba* leaf extract induces apoptosis in human colon and breast cancer cells by the downregulation of nitric oxide produced by inducible nitric oxide synthase," *Nutrition and Cancer*, vol. 65, no. 2, pp. 305–310, 2013.

[86] R. Senthilkumar, T. Parimelazhagan, O. P. Chaurasia, and R. B. Srivastava, "Free radical scavenging property and antiproliferative activity of *Rhodiola imbricata* Edgew extracts in HT-29 human colon cancer cells," *Asian Pacific Journal of Tropical Medicine*, vol. 6, no. 1, pp. 11–19, 2013.

[87] S.-M. Oh, J. Kim, J. Lee et al., "Anticancer potential of an ethanol extract of Asiasari radix against HCT-116 human colon cancer cells in vitro," *Oncology Letters*, vol. 5, no. 1, pp. 305–310, 2013.

[88] E. L. Symonds, I. Konczak, and M. Fenech, "The Australian fruit Illawarra plum (*Podocarpus elatus* Endl., Podocarpaceae) inhibits telomerase, increases histone deacetylase activity and decreases proliferation of colon cancer cells," *British Journal of Nutrition*, vol. 109, no. 12, pp. 2117–2125, 2013.

[89] Y. L. Tsai, C. C. Chiu, J. Yi-Fu Chen, K. C. Chan, and S. D. Lin, "Cytotoxic effects of *Echinacea purpurea* flower extracts and cichoric acid on human colon cancer cells through induction of apoptosis," *Journal of Ethnopharmacology*, vol. 143, no. 3, pp. 914–919, 2012.

[90] S.-J. Lee, K. Park, S.-D. Ha, W.-J. Kim, and S.-K. Moon, "Gleditsia sinensis thorn extract inhibits human colon cancer cells: the role of ERK1/2, G2/MPhase cell cycle arrest and p53 expression," *Phytotherapy Research*, vol. 24, no. 12, pp. 1870–1876, 2010.

[91] S. J. Lee, Y. H. Cho, H. Kim et al., "Inhibitory effects of the ethanol extract of Gleditsia sinensis thorns on human colon cancer HCT116 cells in vitro and in vivo," *Oncology Reports*, vol. 22, no. 6, pp. 1505–1512, 2009.

[92] N. Kosem, K. Ichikawa, H. Utsumi, and P. Moongkarndi, "In vivo toxicity and antitumor activity of mangosteen extract," *Journal of Natural Medicines*, vol. 67, no. 2, pp. 255–263, 2013.

[93] A.-R. Han, J.-A. Kim, D. D. Lantvit et al., "Cytotoxic xanthone constituents of the stem bark of *Garcinia mangostana* (mangosteen)," *Journal of Natural Products*, vol. 72, no. 11, pp. 2028–2031, 2009.

[94] J.-f. Zhang, M.-l. He, Qi Dong et al., "Aqueous extracts of Fructus Ligustri Lucidi enhance the sensitivity of human

colorectal carcinoma DLD-1 cells to doxorubicin-induced apoptosis via Tbx3 suppression," *Integrative Cancer Therapies*, vol. 10, no. 1, pp. 85–91, 2011.

[95] A. Hematulin, K. Ingkaninan, N. Limpeanchob, and D. Sagan, "Ethanolic extract from Derris scandens Benth mediates radiosensitzation via two distinct modes of cell death in human colon cancer HT-29 cells," *Asian Pacific Journal of Cancer Prevention*, vol. 15, no. 4, pp. 1871–1877, 2014.

[96] E. Ribeiro-Varandas, F. Ressurreição, W. Viegas, and M. Delgado, "Cytotoxicity of *Eupatorium cannabinum L.* ethanolic extract against colon cancer cells and interactions with bisphenol A and doxorubicin," *BMC Complementary and Alternative Medicine*, vol. 14, no. 1, 2014.

[97] A. R. Massey, L. Reddivari, and J. Vanamala, "The dermal layer of sweet sorghum (*Sorghum bicolor*) stalk, a byproduct of biofuel production and source of unique 3-deoxyanthocyanidins, has more antiproliferative and proapoptotic activity than the pith in p53 variants of HCT116 and colon cancer stem cells," *Journal of Agricultural and Food Chemistry*, vol. 62, no. 14, pp. 3150–3159, 2014.

[98] A. R. Massey, L. Reddivari, S. Radhakrishnan et al., "Pro-apoptotic activity against cancer stem cells differs between different parts of sweet sorghum," *Journal of Functional Foods*, vol. 23, pp. 601–613, 2016.

[99] Y. H. Wong, W. Y. Tan, C. P. Tan, K. Long, and K. L. Nyam, "Cytotoxic activity of kenaf (*Hibiscus cannabinus* L.) seed extract and oil against human cancer cell lines," *Asian Pacific Journal of Tropical Biomedicine*, vol. 4, Supplement 1, pp. S510–S515, 2014.

[100] S. Enayat, M. S. Ceyhan, A. A. Basaran, M. Gursel, and S. Banerjee, "Anticarcinogenic effects of the ethanolic extract of *Salix aegyptiaca* in colon cancer cells: involvement of Akt/PKB and MAPK pathways," *Nutrition and Cancer*, vol. 65, no. 7, pp. 1045–1058, 2013.

[101] E. J. Kim, Y.-J. Lee, H.-K. Shin, and J. H. Y. Park, "Induction of apoptosis by the aqueous extract of *Rubus coreanum* in HT-29 human colon cancer cells," *Nutrition*, vol. 21, no. 11-12, pp. 1141–1148, 2005.

[102] L. Wang, M. L. Xu, J. H. Hu, S. K. Rasmussen, and M.-H. Wang, "*Codonopsis lanceolata* extract induces G0/G1 arrest and apoptosis in human colon tumor HT-29 cells – involvement of ROS generation and polyamine depletion," *Food and Chemical Toxicology*, vol. 49, no. 1, pp. 149–154, 2011.

[103] S. Sang, J. Hong, H. Wu et al., "Increased growth inhibitory effects on human cancer cells and anti-inflammatory potency of shogaols from Zingiber officinale relative to gingerols," *Journal of Agricultural and Food Chemistry*, vol. 57, no. 22, pp. 10645–10650, 2009.

[104] J. S. Lee, S.-Y. Park, D. Thapa et al., "Grifola frondosa water extract alleviates intestinal inflammation by suppressing TNF-α production and its signaling," *Experimental and Molecular Medicine*, vol. 42, no. 2, pp. 143–154, 2010.

[105] N. B. Janakiram, A. Mohammed, Y. Zhang et al., "Chemopreventive effects of Frondanol A5, a Cucumaria frondosa extract, against rat colon carcinogenesis and inhibition of human colon cancer cell growth," *Cancer Prevention Research*, vol. 3, no. 1, pp. 82–91, 2010.

[106] L. Pan, D. D. Lantvit, S. Riswan et al., "Bioactivity-guided isolation of cytotoxic sesquiterpenes of Rolandra fruticosa," *Phytochemistry*, vol. 71, no. 5-6, pp. 635–640, 2010.

[107] M. Carvalho, B. M. Silva, R. Silva, P:. Valentão, P. B. Andrade, and M. L. Bastos, "First report on Cydonia oblonga Miller anticancer potential: differential antiproliferative effect against human kidney and colon cancer cells," *Journal of Agricultural and Food Chemistry*, vol. 58, no. 6, pp. 3366–3370, 2010.

[108] J. A. Kim, E. Lau, D. Tay, and E. J. C. de Blanco, "Antioxidant and NF-κB inhibitory constituents isolated from Morchella esculenta," *Natural Product Research*, vol. 25, no. 15, pp. 1412–1417, 2011.

[109] J. E. Kim, W. Y. Chung, K. S. Chun et al., "*Pleurospermum kamtschaticum* extract induces apoptosis via mitochondrial pathway and NAG-1 expression in colon cancer cells," *Bioscience, Biotechnology, and Biochemistry*, vol. 74, no. 4, pp. 788–792, 2014.

[110] S. C. W. Sze, K. L. Wong, W. K. Liu et al., "Regulation of p21, MMP-1, and MDR-1 expression in human colon carcinoma HT29 cells by Tian Xian Liquid, a Chinese medicinal formula, in vitro and in vivo," *Integrative Cancer Therapies*, vol. 10, no. 1, pp. 58–69, 2011.

[111] D. S. Ryu, G. O. Baek, E. Y. Kim, K. H. Kim, and D. S. Lee, "Effects of polysaccharides derived from Orostachys japonicus on induction of cell cycle arrest and apoptotic cell death in human colon cancer cells," *BMB Reports*, vol. 43, no. 11, pp. 750–755, 2010.

[112] X.-H. Chen, Y.-X. Miao, X.-J. Wang et al., "Effects of *Ginkgo biloba* extract EGb761 on human colon adenocarcinoma cells," *Cellular Physiology and Biochemistry*, vol. 27, no. 3-4, pp. 227–232, 2011.

[113] E. A. Hudson, P. A. Dinh, T. Kokubun, M. S. Simmonds, and A. Gescher, "Characterization of potentially chemopreventive phenols in extracts of brown rice that inhibit the growth of human breast and colon cancer cells," *Cancer Epidemiology, Biomarkers & Prevention*, vol. 9, pp. 1163–1170, 2000.

[114] J. de la Cruz, D. H. Kim, and S. G. Hwang, "Anti cancer effects of Cnidium officinale Makino extract mediated through apoptosis and cell cycle arrest in the HT-29 human colorectal cancer cell line," *Asian Pacific Journal of Cancer Prevention : APJCP*, vol. 15, no. 13, pp. 5117–5121, 2014.

[115] K.-S. Nam, B. G. Ha, and Y. H. Shon, "Effect of Cnidii Rhizoma on nitric oxide production and invasion of human colorectal adenocarcinoma HT-29 cells," *Oncology Letters*, vol. 9, no. 1, pp. 483–487, 2015.

[116] P. Ovadje, D. Ma, P. Tremblay et al., "Evaluation of the efficacy & biochemical mechanism of cell death induction by Piper longum extract selectively in in-vitro and in-vivo models of human cancer cells," *PLoS One*, vol. 9, no. 11, article e113250, 2014.

[117] S. Arora and S. Tandon, "Achyranthes aspera root extracts induce human colon cancer cell (COLO-205) death by triggering the mitochondrial apoptosis pathway and S phase cell cycle arrest," *The Scientific World Journal*, vol. 2014, Article ID 129697, 15 pages, 2014.

[118] A. al-Menhali, A. al-Rumaihi, H. al-Mohammed et al., "Thymus vulgaris (thyme) inhibits proliferation, adhesion, migration, and invasion of human colorectal cancer cells," *Journal of Medicinal Food*, vol. 18, no. 1, pp. 54–59, 2015.

[119] K. A. Kang, J. K. Kim, Y. J. Jeong, S.-Y. Na, and J. W. Hyun, "Dictyopteris undulata extract induces apoptosis via induction of endoplasmic reticulum stress in human colon cancer cells," *Journal of Cancer Prevention*, vol. 19, no. 2, pp. 118–124, 2014.

[120] X. Zhao, P. Sun, Y. Qian, and H. Suo, "D. candidum has in vitro anticancer effects in HCT-116 cancer cells and exerts

in vivo anti-metastatic effects in mice," *Nutrition Research and Practice*, vol. 8, no. 5, pp. 487–493, 2014.

[121] B. Romano, F. Borrelli, E. Pagano, M. G. Cascio, R. G. Pertwee, and A. A. Izzo, "Inhibition of colon carcinogenesis by a standardized Cannabis sativa extract with high content of cannabidiol," *Phytomedicine*, vol. 21, no. 5, pp. 631–639, 2014.

[122] N. Eid, S. Enani, G. Walton et al., "The impact of date palm fruits and their component polyphenols, on gut microbial ecology, bacterial metabolites and colon cancer cell proliferation," *Journal of Nutritional Science*, vol. 3, no. 46, pp. 1–9, 2014.

[123] X.-L. Tang, X. Y. Yang, Y. C. Kim et al., "Protective effects of the ethanolic extract of Melia toosendan fruit against colon cancer," *Indian Journal of Biochemistry & Biophysics*, vol. 49, no. 3, pp. 173–181, 2012.

[124] K. Bajbouj, J. Schulze-Luehrmann, S. Diermeier, A. Amin, and R. Schneider-Stock, "The anticancer effect of saffron in two p53 isogenic colorectal cancer cell lines," *BMC Complementary and Alternative Medicine*, vol. 12, no. 1, 2012.

[125] R. Sánchez-Vioque, O. Santana-Méridas, M. Polissiou et al., "Polyphenol composition and in vitro antiproliferative effect of corm, tepal and leaf from Crocus sativus L. on human colon adenocarcinoma cells (Caco-2)," *Journal of Functional Foods*, vol. 24, pp. 18–25, 2016.

[126] L.-H. Shang, C.-M. Li, Z.-Y. Yang, D.-H. Che, J.-Y. Cao, and Y. Yu, "Luffa echinata Roxb. induces human colon cancer cell (HT-29) death by triggering the mitochondrial apoptosis pathway," *Molecules*, vol. 17, no. 5, pp. 5780–5794, 2012.

[127] G. Angel-Morales, G. Noratto, and S. Mertens-Talcott, "Red wine polyphenolics reduce the expression of inflammation markers in human colon-derived CCD-18Co myofibroblast cells: potential role of microRNA-126," *Food & Function*, vol. 3, no. 7, pp. 745–752, 2012.

[128] A. T. Choumessi, M. Danel, S. Chassaing et al., "Characterization of the antiproliferative activity of Xylopia aethiopica," *Cell Division*, vol. 7, no. 1, pp. 8–8, 2012.

[129] L. Yang, K. F. Allred, B. Geera, C. D. Allred, and J. M. Awika, "Sorghum phenolics demonstrate estrogenic action and induce apoptosis in nonmalignant colonocytes," *Nutrition and Cancer*, vol. 64, no. 3, pp. 419–427, 2012.

[130] C. Mazewski, K. Liang, and E. Gonzalez de Mejia, "Comparison of the effect of chemical composition of anthocyanin-rich plant extracts on colon cancer cell proliferation and their potential mechanism of action using in vitro, in silico, and biochemical assays," *Food Chemistry*, vol. 242, pp. 378–388, 2018.

[131] N.-W. He, Y. Zhao, L. Guo, J. Shang, and X.-B. Yang, "Antioxidant, antiproliferative, and pro-apoptotic activities of a saponin extract derived from the roots of *Panax notoginseng* (Burk.) F.H. Chen," *Journal of Medicinal Food*, vol. 15, no. 4, pp. 350–359, 2012.

[132] F. A. Hashem, H. Motawea, A. E. el-Shabrawy, K. Shaker, and S. el-Sherbini, "Myrosinase hydrolysates of Brassica oleraceae L. var. *italica* reduce the risk of colon cancer," *Phytotherapy Research*, vol. 26, no. 5, pp. 743–747, 2012.

[133] Y. Jia, Q. Guan, Y. Guo, and C. du, "Reduction of inflammatory hyperplasia in the intestine in colon cancer-prone mice by water-extract of Cistanche deserticola," *Phytotherapy Research*, vol. 26, no. 6, pp. 812–819, 2012.

[134] S. Gorlach, W. Wagner, A. Podsędek, K. Szewczyk, M. Koziołkiewicz, and J. Dastych, "Procyanidins from Japanese quince (Chaenomeles japonica) fruit induce apoptosis in human colon cancer Caco-2 cells in a degree of polymerization-dependent manner," *Nutrition and Cancer*, vol. 63, no. 8, pp. 1348–1360, 2011.

[135] S. Mori, T. Sawada, T. Okada, T. Ohsawa, M. Adachi, and K. Keiichi, "New anti-proliferative agent, MK615, from Japanese apricot "Prunus mume" induces striking autophagy in colon cancer cells in vitro," *World Journal of Gastroenterology*, vol. 13, no. 48, pp. 6512–6517, 2007.

[136] S. C. Hsu, J. H. Lu, C. L. Kuo et al., "Crude extracts of Solanum lyratum induced cytotoxicity and apoptosis in a human colon adenocarcinoma cell line (Colo 205)," *Anticancer Research*, vol. 28, no. 2A, pp. 1045–1054, 2008.

[137] N. el-Najjar, N. Saliba, S. Talhouk, and H. Gali-Muhtasib, "Onopordum cynarocephalum induces apoptosis and protects against 1,2 dimethylhydrazine-induced colon cancer," *Oncology Reports*, vol. 17, no. 6, pp. 1517–1523, 2007.

[138] X. Li, T. Ohtsuki, T. Koyano, T. Kowithayakorn, and M. Ishibashi, "New Wnt/β-catenin signaling inhibitors isolated from *Eleutherine palmifolia*," *Chemistry*, vol. 4, no. 4, pp. 540–547, 2009.

[139] S. Jaramillo, F. J. G. Muriana, R. Guillen, A. Jimenez-Araujo, R. Rodriguez-Arcos, and S. Lopez, "Saponins from edible spears of wild asparagus inhibit AKT, p70S6K, and ERK signalling, and induce apoptosis through G0/G1 cell cycle arrest in human colon cancer HCT-116 cells," *Journal of Functional Foods*, vol. 26, pp. 1–10, 2016.

[140] R. Vadde, S. Radhakrishnan, H. Eranda Karunathilake Kurundu, L. Reddivari, and J. K. P. Vanamala, "Indian gooseberry (*Emblica officinalis* Gaertn.) suppresses cell proliferation and induces apoptosis in human colon cancer stem cells independent of p53 status via suppression of c-Myc and cyclin D1," *Journal of Functional Foods*, vol. 25, pp. 267–278, 2016.

[141] L. Ai, Y.-C. Chung, K.-C. G. Jeng et al., "Antioxidant hydrocolloids from herb Graptopetalum paraguayense leaves show anti-colon cancer cells and anti-neuroinflammatory potentials," *Food Hydrocolloids*, vol. 73, pp. 51–59, 2017.

[142] N. Polachi, B. Subramaniyan, P. Nagaraja, K. Rangiah, and M. Ganeshan, "Extract from *Butea monosperma* inhibits β-catenin/Tcf signaling in SW480 human colon cancer cells," *Gene Reports*, vol. 10, pp. 79–89, 2018.

[143] P. Zhu, Y. Wu, A. Yang, X. Fu, M. Mao, and Z. Liu, "Catalpol suppressed proliferation, growth and invasion of CT26 colon cancer by inhibiting inflammation and tumor angiogenesis," *Biomedicine & Pharmacotherapy*, vol. 95, pp. 68–76, 2017.

[144] W. K. Kim, D. H. Bach, H. W. Ryu et al., "Cytotoxic activities of Telectadium dongnaiense and its constituents by inhibition of the Wnt/β-catenin signaling pathway," *Phytomedicine*, vol. 34, pp. 136–142, 2017.

[145] P. Budchart, A. Khamwut, C. Sinthuvanich, S. Ratanapo, Y. Poovorawan, and N. P. T-Thienprasert, "Partially purified Gloriosa superba peptides inhibit colon cancer cell viability by inducing apoptosis through p53 upregulation," *The American Journal of the Medical Sciences*, vol. 354, no. 4, pp. 423–429, 2017.

[146] T. Ranjbarnejad, M. Saidijam, S. Moradkhani, and R. Najafi, "Methanolic extract of Boswellia serrata exhibits anti-cancer activities by targeting microsomal prostaglandin E synthase-1 in human colon cancer cells," *Prostaglandins & Other Lipid Mediators*, vol. 131, pp. 1–8, 2017.

[147] R. Direito, A. Lima, J. Rocha et al., "Dyospiros kaki phenolics inhibit colitis and colon cancer cell proliferation, but not gelatinase activities," *The Journal of Nutritional Biochemistry*, vol. 46, pp. 100–108, 2017.

[148] J. Hafsa, K. M. Hammi, M. R. B. Khedher et al., "Inhibition of protein glycation, antioxidant and antiproliferative activities of Carpobrotus edulis extracts," *Biomedicine & Pharmacotherapy*, vol. 84, pp. 1496–1503, 2016.

[149] N. Campos-Xolalpa, Á. J. Alonso-Castro, E. Sánchez-Mendoza, M. Á. Zavala-Sánchez, and S. Pérez-Gutiérrez, "Cytotoxic activity of the chloroform extract and four diterpenes isolated from Salvia ballotiflora," *Revista Brasileira de Farmacognosia*, vol. 27, no. 3, pp. 302–305, 2017.

[150] N. Sharma, A. Kumar, P. R. Sharma et al., "A new clerodane furano diterpene glycoside from Tinospora cordifolia triggers autophagy and apoptosis in HCT-116 colon cancer cells," *Journal of Ethnopharmacology*, vol. 211, pp. 295–310, 2018.

[151] T. F. F. da Silveira, T. C. L. de Souza, A. V. Carvalho, A. B. Ribeiro, G. G. C. Kuhnle, and H. T. Godoy, "White açaí juice (*Euterpe oleracea*): phenolic composition by LC-ESI-MS/MS, antioxidant capacity and inhibition effect on the formation of colorectal cancer related compounds," *Journal of Functional Foods*, vol. 36, pp. 215–223, 2017.

[152] S. Li, L. Zhaohuan, Z. Guangshun, X. Guanhua, and Z. Guangji, "Diterpenoid Tanshinones, the extract from Danshen (*Radix Salviae Miltiorrhizae*) induced apoptosis in nine human cancer cell lines," *Journal of Traditional Chinese Medicine*, vol. 36, no. 4, pp. 514–521, 2016.

[153] K. Gouthamchandra, H. V. Sudeep, B. J. Venkatesh, and K. Shyam Prasad, "Chlorogenic acid complex (CGA7), standardized extract from green coffee beans exerts anticancer effects against cultured human colon cancer HCT-116 cells," *Food Science and Human Wellness*, vol. 6, no. 3, pp. 147–153, 2017.

[154] M. Asif, A. H. S. Yehya, M. A. al-Mansoub et al., "Anticancer attributes of Illicium verum essential oils against colon cancer," *South African Journal of Botany*, vol. 103, pp. 156–161, 2016.

[155] T. Sriyatep, C. Tantapakul, R. J. Andersen et al., "Resolution and identification of scalemic caged xanthones from the leaf extract of Garcinia propinqua having potent cytotoxicities against colon cancer cells," *Fitoterapia*, vol. 124, pp. 34–41, 2018.

[156] T. Sriyatep, R. J. Andersen, B. O. Patrick et al., "Scalemic caged xanthones isolated from the stem bark extract of *Garcinia propinqua*," *Journal of Natural Products*, vol. 80, no. 5, pp. 1658–1667, 2017.

[157] G. Riccio, M. Maisto, S. Bottone et al., "WNT inhibitory activity of Malus pumila Miller cv Annurca and Malus domestica cv Limoncella apple extracts on human colonrectal cells carrying familial adenomatous polyposis mutations," *Nutrients*, vol. 9, no. 11, p. 1262, 2017.

[158] E. S. Son, Y. O. Kim, C. G. Park et al., "Coix lacryma-jobi var. ma-yuen Stapf sprout extract has anti-metastatic activity in colon cancer cells in vitro," *BMC Complementary and Alternative Medicine*, vol. 17, no. 1, p. 486, 2017.

[159] M. Asif, A. Shafaei, A. S. Abdul Majid et al., "Mesua ferrea stem bark extract induces apoptosis and inhibits metastasis in human colorectal carcinoma HCT 116 cells, through modulation of multiple cell signalling pathways," *Chinese Journal of Natural Medicines*, vol. 15, no. 7, pp. 505–514, 2017.

[160] H. Zhu, H. Zhao, L. Zhang et al., "Dandelion root extract suppressed gastric cancer cells proliferation and migration through targeting lncRNA-CCAT1," *Biomedicine & Pharmacotherapy*, vol. 93, pp. 1010–1017, 2017.

[161] H. Jin, L. Chen, S. Wang, and D. Chao, "*Portulaca oleracea* extract can inhibit nodule formation of colon cancer stem cells by regulating gene expression of the Notch signal transduction pathway," *Tumour Biology*, vol. 39, no. 7, 2017.

[162] A. Czerwonka, K. Kawka, K. Cykier, M. K. Lemieszek, and W. Rzeski, "Evaluation of anticancer activity of water and juice extracts of young Hordeum vulgare in human cancer cell lines HT-29 and A549," *Annals of Agricultural and Environmental Medicine : AAEM*, vol. 24, no. 2, pp. 345–349, 2017.

[163] N. Cho, T. T. Ransom, J. Sigmund et al., "Growth inhibition of colon cancer and melanoma cells by versiol derivatives from a Paraconiothyrium species," *Journal of Natural Products*, vol. 80, no. 7, pp. 2037–2044, 2017.

[164] C. Yang, M. Wang, J. Zhou, and Q. Chi, "Bio-synthesis of peppermint leaf extract polyphenols capped nano-platinum and their in-vitro cytotoxicity towards colon cancer cell lines (HCT 116)," *Materials Science and Engineering: C*, vol. 77, pp. 1012–1016, 2017.

[165] C. Li, Y. Jeong, and M. Kim, "*Mammea longifolia* Planch. and Triana fruit extract induces cell death in the human colon cancer cell line, SW480, via mitochondria-related apoptosis and activation of p53," *Journal of Medicinal Food*, vol. 20, no. 5, pp. 485–490, 2017.

[166] A. Manosroi, M. Sainakham, C. Chankhampan, W. Manosroi, and J. Manosroi, "In vitro anti-cancer activities of Job's tears (Coix lachryma-jobi Linn.) extracts on human colon adenocarcinoma," *Saudi Journal of Biological Sciences*, vol. 23, no. 2, pp. 248–256, 2016.

[167] R. Mata, J. R. Nakkala, and S. R. Sadras, "Polyphenol stabilized colloidal gold nanoparticles from Abutilon indicum leaf extract induce apoptosis in HT-29 colon cancer cells," *Colloids and Surfaces B: Biointerfaces*, vol. 143, pp. 499–510, 2016.

[168] N. H. Yim, M. J. Gu, Y. H. Hwang, W. K. Cho, and J. Y. Ma, "Water extract of Galla Rhois with steaming process enhances apoptotic cell death in human colon cancer cells," *Integrative Medicine Research*, vol. 5, no. 4, pp. 284–292, 2016.

[169] E. J. Kim, G. T. Kim, B. M. Kim, E. G. Lim, S. Y. Kim, and Y. M. Kim, "Apoptosis-induced effects of extract from *Artemisia annua* Linne by modulating PTEN/p53/PDK1/Akt/ signal pathways through PTEN/p53-independent manner in HCT116 colon cancer cells," *BMC Complementary and Alternative Medicine*, vol. 17, no. 1, p. 236, 2017.

[170] X. Zhao, X. Feng, C. Wang, D. Peng, K. Zhu, and J. L. Song, "Anticancer activity of Nelumbo nucifera stamen extract in human colon cancer HCT-116 cells in vitro," *Oncology Letters*, vol. 13, no. 3, pp. 1470–1478, 2017.

[171] H. Guo, H. Guan, W. Yang et al., "Pro-apoptotic and antiproliferative effects of corn silk extract on human colon cancer cell lines," *Oncology Letters*, vol. 13, no. 2, pp. 973–978, 2017.

[172] H. J. Hsu, R. F. Huang, T. H. Kao, B. S. Inbaraj, and B. H. Chen, "Preparation of carotenoid extracts and nanoemulsions from Lycium barbarum L. and their effects on growth of HT-29 colon cancer cells," *Nanotechnology*, vol. 28, no. 13, article 135103, 2017.

[173] V. P. Venancio, P. A. Cipriano, H. Kim, L. M. G. Antunes, S. T. Talcott, and S. U. Mertens-Talcott, "Cocoplum (*Chrysobalanus icaco* L.) anthocyanins exert anti-inflammatory activity in human colon cancer and non-malignant colon cells," *Food & Function*, vol. 8, no. 1, pp. 307–314, 2017.

[174] R. Nozaki, T. Kono, H. Bochimoto et al., "Zanthoxylum fruit extract from Japanese pepper promotes autophagic cell death in cancer cells," *Oncotarget*, vol. 7, no. 43, pp. 70437–70446, 2016.

[175] R. Acquaviva, V. Sorrenti, R. Santangelo et al., "Effects of an extract of Celtis aetnensis (Tornab.) Strobl twigs on human colon cancer cell cultures," *Oncology Reports*, vol. 36, no. 4, pp. 2298–2304, 2016.

[176] S. Jimenez, S. Gascon, A. Luquin, M. Laguna, C. Ancin-Azpilicueta, and M. J. Rodriguez-Yoldi, "Rosa canina extracts have antiproliferative and antioxidant effects on Caco-2 human colon cancer," *PLoS One*, vol. 11, no. 7, article e0159136, 2016.

[177] A. I. Elkady, R. A. Hussein, and S. M. El-Assouli, "Harmal extract induces apoptosis of HCT116 human colon cancer cells, mediated by inhibition of nuclear factor-κB and activator protein-1 signaling pathways and induction of cytoprotective genes," *Asian Pacific Journal of Cancer Prevention : APJCP*, vol. 17, no. 4, pp. 1947–1959, 2016.

[178] M. Amigo-Benavent, S. Wang, R. Mateos, B. Sarria, and L. Bravo, "Antiproliferative and cytotoxic effects of green coffee and yerba mate extracts, their main hydroxycinnamic acids, methylxanthine and metabolites in different human cell lines," *Food and Chemical Toxicology*, vol. 106, Part A, pp. 125–138, 2017.

[179] D. J. de Rodríguez, D. A. Carrillo-Lomelí, N. E. Rocha-Guzmán et al., "Antioxidant, anti-inflammatory and apoptotic effects of Flourensia microphylla on HT-29 colon cancer cells," *Industrial Crops and Products*, vol. 107, pp. 472–481, 2017.

[180] K. Y. Cheah, G. S. Howarth, and S. E. P. Bastian, "Grape seed extract dose-responsively decreases disease severity in a rat model of mucositis; Concomitantly Enhancing Chemotherapeutic Effectiveness in Colon Cancer Cells," *PLoS ONE*, vol. 9, no. 1, article e85184, 2014.

[181] M. M. Derry, K. Raina, R. Agarwal, and C. Agarwal, "Characterization of azoxymethane-induced colon tumor metastasis to lung in a mouse model relevant to human sporadic colorectal cancer and evaluation of grape seed extract efficacy," *Experimental and Toxicologic Pathology*, vol. 66, no. 5-6, pp. 235–242, 2014.

[182] Y. D. Jung, M. S. Kim, B. A. Shin et al., "EGCG, a major component of green tea, inhibits tumour growth by inhibiting VEGF induction in human colon carcinoma cells," *British Journal of Cancer*, vol. 84, no. 6, pp. 844–850, 2001.

[183] M. W. Roomi, V. Ivanov, T. Kalinovsky, A. Niedzwiecki, and M. Rath, "In vivo antitumor effect of ascorbic acid, lysine, proline and green tea extract on human colon cancer cell HCT 116 xenografts in nude mice: evaluation of tumor growth and immunohistochemistry," *Oncology Reports*, vol. 13, no. 3, pp. 421–425, 2005.

[184] Y. Z. H.-Y. Hashim, J. Worthington, P. Allsopp et al., "Virgin olive oil phenolics extract inhibit invasion of HT115 human colon cancer cells in vitro and in vivo," *Food & Function*, vol. 5, no. 7, pp. 1513–1519, 2014.

[185] C. C. Tseng, H. F. Shang, L. F. Wang et al., "Antitumor and immunostimulating effects of Anoectochilus formosanus Hayata," *Phytomedicine*, vol. 13, no. 5, pp. 366–370, 2006.

[186] S.-W. Hsuan, C.-C. Chyau, H.-Y. Hung, J.-H. Chen, and F.-P. Chou, "The induction of apoptosis and autophagy by Wasabia japonica extract in colon cancer," *European Journal of Nutrition*, vol. 55, no. 2, pp. 491–503, 2016.

[187] E. Rouhollahi, S. Zorofchian Moghadamtousi, M. Paydar et al., "Inhibitory effect of *Curcuma purpurascens* BI. rhizome on HT-29 colon cancer cells through mitochondrial-dependent apoptosis pathway," *BMC Complementary and Alternative Medicine*, vol. 15, no. 1, p. 15, 2015.

[188] C. Yu, X.-D. Wen, Z. Zhang et al., "American ginseng attenuates azoxymethane/dextran sodium sulfate-induced colon carcinogenesis in mice," *Journal of Ginseng Research*, vol. 39, no. 1, pp. 14–21, 2015.

[189] S. M. Butler, M. A. Wallig, C. W. Nho et al., "A polyacetylene-rich extract from Gymnaster koraiensis strongly inhibits colitis-associated colon cancer in mice," *Food and Chemical Toxicology*, vol. 53, pp. 235–239, 2013.

[190] P. Arulselvan, C.-C. Wen, C.-W. Lan, Y.-H. Chen, W.-C. Wei, and N.-S. Yang, "Dietary administration of scallion extract effectively inhibits colorectal tumor growth: cellular and molecular mechanisms in mice," *PloS One*, vol. 7, no. 9, article e44658, 2012.

[191] D. S. Wang, G. H. Rizwani, H. Guo et al., "*Annona squamosa* Linn: cytotoxic activity found in leaf extract against human tumor cell lines," *Pakistan Journal of Pharmaceutical Sciences*, vol. 27, no. 5, pp. 1559–1563, 2014.

[192] K.-W. Park, J. Kundu, I. G. Chae, S. C. Bachar, J.-W. Bae, and K.-S. Chun, "Methanol Extract of *Flacourtia indica* Aerial Parts Induces Apoptosis via Generation of ROS and Activation of Caspases in Human Colon Cancer HCT116 Cells," *Asian Pacific Journal of Cancer Prevention*, vol. 15, no. 17, pp. 7291–7296, 2014.

[193] A. Thyagarajan, A. Jedinak, H. Nguyen et al., "Triterpenes from Ganoderma lucidum induce autophagy in colon cancer through the inhibition of p38 mitogen-activated kinase (p38 MAPK)," *Nutrition and Cancer*, vol. 62, no. 5, pp. 630–640, 2010.

[194] C. Huang, Y. Huang, J. Li et al., "Inhibition of benzo(a)pyrene diol-epoxide-induced transactivation of activated protein 1 and nuclear factor κB by black raspberry extracts," *Cancer Research*, vol. 62, no. 23, pp. 6857–6863, 2002.

[195] B. Bassani, T. Rossi, D. de Stefano et al., "Potential chemopreventive activities of a polyphenol rich purified extract from olive mill wastewater on colon cancer cells," *Journal of Functional Foods*, vol. 27, pp. 236–248, 2016.

[196] W. Zeriouh, A. Nani, M. Belarbi et al., "Phenolic extract from oleaster (*Olea europaea* var. Sylvestris) leaves reduces colon cancer growth and induces caspase-dependent apoptosis in colon cancer cells via the mitochondrial apoptotic pathway," *PloS One*, vol. 12, no. 2, article e0170823, 2017.

[197] H. H. Ahmed, H. S. El-Abhar, E. A. K. Hassanin, N. F. Abdelkader, and M. B. Shalaby, "*Ginkgo biloba* L. leaf extract offers multiple mechanisms in bridling N-methylnitrosourea - mediated experimental colorectal cancer," *Biomedicine & Pharmacotherapy*, vol. 95, pp. 387–393, 2017.

[198] B. Subramaniyan, N. Polachi, and G. Mathan, "Isocoreopsin: an active constituent of n-butanol extract of *Butea monosperma* flowers against colorectal cancer (CRC)," *Journal of Pharmaceutical Analysis*, vol. 6, no. 5, pp. 318–325, 2016.

[199] P. Ovadje, S. Ammar, J. A. Guerrero, J. T. Arnason, and S. Pandey, "Dandelion root extract affects colorectal cancer proliferation and survival through the activation of multiple

death signalling pathways," *Oncotarget*, vol. 7, no. 45, pp. 73080–73100, 2016.

[200] S. Tanaka, K. Haruma, M. Yoshihara et al., "Aged garlic extract has potential suppressive effect on colorectal adenomas in humans," *The Journal of Nutrition*, vol. 136, no. 3, pp. 821S–826S, 2006.

[201] A. di Francesco, A. Falconi, C. di Germanio et al., "Extravirgin olive oil up-regulates CB1 tumor suppressor gene in human colon cancer cells and in rat colon via epigenetic mechanisms," *The Journal of Nutritional Biochemistry*, vol. 26, no. 3, pp. 250–258, 2015.

[202] T. Srihari, M. Sengottuvelan, and N. Nalini, "Dose-dependent effect of oregano (Origanum vulgare L.) on lipid peroxidation and antioxidant status in 1,2-dimethylhydrazine-induced rat colon carcinogenesis," *The Journal of Pharmacy and Pharmacology*, vol. 60, no. 6, pp. 787–794, 2008.

[203] A. Caimari, F. Puiggròs, M. Suárez et al., "The intake of a hazelnut skin extract improves the plasma lipid profile and reduces the lithocholic/deoxycholic bile acid faecal ratio, a risk factor for colon cancer, in hamsters fed a high-fat diet," *Food Chemistry*, vol. 167, pp. 138–144, 2015.

[204] L. Pan, F. Will, N. Frank, H. Dietrich, H. Bartsch, and C. Gerhauser, "Natural cloudy apple juice and polyphenol-enriched apple juice extract prevent intestinal adenoma formation in the APCMin/+ model for colon cancer prevention," *European Journal of Cancer Supplements*, vol. 4, no. 1, pp. 55-56, 2006.

[205] R. Acquaviva, L. Iauk, V. Sorrenti et al., "Oxidative profile in patients with colon cancer: effects of *Ruta chalepensis* L," *European Review for Medical and Pharmacological Sciences*, vol. 15, no. 2, pp. 181–191, 2011.

[206] N. A. de Moura, B. F. Caetano, K. Sivieri et al., "Characterization of potentially chemopreventive phenols in extracts of brown rice that inhibit the growth of human breast and colon cancer cells," *Food and Chemical Toxicology*, vol. 50, no. 8, pp. 2902–2910, 2012.

[207] H. H. Ahmed, H. S. El-Abhar, E. A. K. Hassanin, N. F. Abdelkader, and M. B. Shalaby, "Punica granatum suppresses colon cancer through downregulation of Wnt/β-catenin in rat model," *Revista Brasileira de Farmacognosia*, vol. 27, no. 5, pp. 627–635, 2017.

[208] N. R. Shah and B. M. Patel, "Secoisolariciresinol diglucoside rich extract of L. usitatissimum prevents diabetic colon cancer through inhibition of CDK4," *Biomedicine & Pharmacotherapy*, vol. 83, pp. 733–739, 2016.

[209] N. L. Md Nasir, N. E. Kamsani, N. Mohtarrudin, F. Othman, S. F. Md Tohid, and Z. A. Zakaria, "Anticarcinogenic activity of *Muntingia calabura* leaves methanol extract against the azoxymethane-induced colon cancer in rats involved modulation of the colonic antioxidant system partly by flavonoids," *Pharmaceutical Biology*, vol. 55, no. 1, pp. 2102–2109, 2016.

[210] S. A. Im, J. W. Kim, H. S. Kim et al., "Prevention of azoxymethane/dextran sodium sulfate-induced mouse colon carcinogenesis by processed Aloe vera gel," *International Immunopharmacology*, vol. 40, pp. 428–435, 2016.

[211] F. Yao, J. Y. Zhang, X. Xiao, Y. Dong, and X. H. Zhou, "Antitumor activities and apoptosis-regulated mechanisms of fermented barley extract in the transplantation tumor model of human HT-29 cells in nude mice," *Biomedical and Environmental Sciences*, vol. 30, no. 1, pp. 10–21, 2017.

[212] A. T. Endharti, A. Wulandari, A. Listyana, E. Norahmawati, and S. Permana, "Dendrophthoe pentandra (L.) Miq extract effectively inhibits inflammation, proliferation and induces p53 expression on colitis-associated colon cancer," *BMC Complementary and Alternative Medicine*, vol. 16, no. 1, p. 374, 2016.

[213] S. S. Dahham, L. E. A. Hassan, M. B. K. Ahamed, A. S. A. Majid, A. M. S. A. Majid, and N. N. Zulkepli, "In vivo toxicity and antitumor activity of essential oils extract from agarwood (Aquilaria crassna)," *BMC Complementary and Alternative Medicine*, vol. 16, no. 1, p. 236, 2016.

[214] M. R. Malayeri, A. Dadkhah, F. Fatemi et al., "Chemotherapeutic effect of Berberis integerrima hydroalcoholic extract on colon cancer development in the 1,2-dimethyl hydrazine rat model," *Zeitschrift für Naturforschung C*, vol. 71, no. 7-8, pp. 225–232, 2016.

[215] A. Bounaama, S. Enayat, M. S. Ceyhan, H. Moulahoum, B. Djerdjouri, and S. Banerjee, "Ethanolic extract of bark from Salix aegyptiaca ameliorates 1,2-dimethylhydrazine-induced colon carcinogenesis in mice by reducing oxidative stress," *Nutrition and Cancer*, vol. 68, no. 3, pp. 495–506, 2016.

[216] Q. Zhu, J. Meisinger, D. H. V. Thiel, Y. Zhang, and S. Mobarhan, "Effects of soybean extract on morphology and survival of Caco-2, SW620, and HT-29 cells," *Nutrition and Cancer*, vol. 42, no. 1, pp. 131–140, 2002.

[217] M. E. Juan, U. Wenzel, V. Ruiz-Gutierrez, H. Daniel, and J. M. Planas, "Olive fruit extracts inhibit proliferation and induce apoptosis in HT-29 human colon cancer cells," *The Journal of Nutrition*, vol. 136, no. 10, pp. 2553–2557, 2006.

Hindawi
Oxidative Medicine and Cellular Longevity
Volume 2019, Article ID 5820415, 20 pages
https://doi.org/10.1155/2019/5820415

Research Article

Tetramethylpyrazine Attenuates the Endotheliotoxicity and the Mitochondrial Dysfunction by Doxorubicin *via* 14-3-3γ/Bcl-2

Bin Yang,[1] Hongwei Li,[2] Yang Qiao,[2] Qing Zhou,[2] Shuping Chen,[2] Dong Yin,[3] Huan He,[2] and Ming He[1,2]

[1]*Jiangxi Provincial Institute of Hypertension, the First Affiliated Hospital of Nanchang University, Nanchang 330006, China*
[2]*Jiangxi Provincial Key Laboratory of Basic Pharmacology, Nanchang University School of Pharmaceutical Science, Nanchang 330006, China*
[3]*Jiangxi Provincial Key Laboratory of Molecular Medicine, the Second Affiliated Hospital, Nanchang University, Nanchang 330006, China*

Correspondence should be addressed to Huan He; hehuan0118@ncu.edu.cn and Ming He; jxhm56@hotmail.com

Received 26 May 2019; Revised 28 August 2019; Accepted 11 September 2019; Published 3 December 2019

Guest Editor: Patrícia Rijo

Doxorubicin (Dox) with cardiotoxicity and endotheliotoxicity limits its clinical application for cancer. The toxicitic mechanism involves excess ROS generation. 14-3-3s have the protective effects on various injured tissues and cells. Tetramethylpyrazine (TMP) is an alkaloid extracted from the rhizome of Ligusticum wallichii and has multiple bioactivities. We hypothesize that TMP has the protective effects on vascular endothelium by upregulating 14-3-3γ. To test the hypothesis, Dox-induced endotheliotoxicity was used to establish vascular endothelium injury models in mice and human umbilical vein endothelial cells. The effects of TMP were assessed by determining thoracic aortic strips' endothelium-dependent dilation (EDD), as well as LDH, CK, caspase-3, SOD, CAT, GSH-Px activities and MDA level in serum, apoptotic rate, and histopathological changes of vascular tissue (*in vivo*). Also, cell viability, LDH and caspase-3 activities, ROS generation, levels of NAD^+/NADH and GSH/GSSG, MMP, mPTP opening, and apoptotic rate were evaluated (*in vitro*). The expression of 14-3-3γ and Bcl-2, as well as phosphorylation of Bad (S112), were determined by Western blot. Our results showed that Dox-induced injury to vascular endothelium was decreased by TMP *via* upregulating 14-3-3γ expression in total protein and Bcl-2 expression in mitochondria, activating Bad (S112) phosphorylation, maintaining EDD, reducing LDH, CK, and caspase-3 activities, thereby causing a reduction in apoptotic rate, and histopathological changes of vascular endothelium (*in vivo*). Furthermore, TMP increased cell viability and MMP levels, maintained NAD^+/NADH, GSH/GSSG balance, decreased LDH and caspase-3 activities, ROS generation, mPTP opening, and apoptotic rate (*in vitro*). However, the protective effects to vascular endothelium of TMP were significantly canceled by pAD/14-3-3γ-shRNA, an adenovirus that caused knockdown 14-3-3γ expression, or ABT-737, a specific Bcl-2 inhibitor. In conclusion, this study is the first to demonstrate that TMP protects the vascular endothelium against Dox-induced injury via upregulating 14-3-3γ expression, promoting translocation of Bcl-2 to the mitochondria, closing mPTP, maintaining MMP, inhibiting RIRR mechanism, suppressing oxidative stress, improving mitochondrial function, and alleviating Dox-induced endotheliotoxicity.

1. Introduction

Doxorubicin (Dox) is a broad-spectrum, high efficiency, low cost and convenient use of anticancer antibiotic [1]. However, its dose-dependent cardiotoxicity greatly limits its clinical application [2]. In recent years, the damage of Dox to vascular endothelium, and so-called endotheliotoxicity has also attracted considerable attention [3].

Many studies have found that there are various reasons for Dox's cardiotoxicity or endotheliotoxicity [3, 4]. However, one of the most important reason is that Dox itself may induce oxidative stress, resulting in excessive reactive

oxygen species (ROS) generation [3–6]. In previous studies, we have shown that Dox toxicity can cause excessive ROS generation, resulting in severe myocardial damage [7, 8]. However, inhibiting oxidative stress and reducing ROS generation may alleviate cardiotoxicity or endotheliotoxicity induced by Dox [9–13]. Phytochemicals are candidate subjects [7, 8, 10–13].

Tetramethylpyrazine (TMP), an alkaloid extracted from the roots of Ligusticum chuanxiong Hort (LC; Umbelliferae), a traditional Chinese medicine [14], it has multiple targets and many biological functions, such as anti-oxidation, anti-platelet, anti-inflammation, anti-apoptosis and so on [15–17]. Many studies have shown that TMP has protective effects on the myocardium, brain, and vascular endothelium, suggesting that TMP has an excellent application prospect in the prevention and treatment of cardiocerebrovascular diseases [16–19]. Recently, we have found that TMP could up-regulate 14-3-3γ expression, improve mitochondrial function, and reduce apoptosis induced by LPS to cardiomyocytes [20].

14-3-3s is a highly conserved acidic protein family composed of seven isoforms [21]. Through phosphorylation, it interacts with the partner protein and participates in almost all life activities in cells [22]. Our previous studies found that 14-3-3η and 14-3-3γ participate in acute myocardial injury and protection. 14-3-3η participates in ischemia/hypoxia injury and protection, while 14-3-3γ mainly involves infection or inflammatory injury and protection [20, 23–29]. Recently, we found that curcumin and quercetin could up-regulate 14-3-3γ expression, improve mitochondrial function, and protect the myocardium against Dox's cardiotoxicity [7, 8].

Therefore, the aims of the current study were to investigate by *in vivo* and *in vitro* 1) Whether TMP protected vascular endothelium against endotheliotoxicity induced by Dox; 2) Whether up-regulation of 14-3-3γ expression, phosphorylation of Bad (S112) and subsequent translocation of Bcl-2 to the mitochondria were involved in the protection of TMP against endotheliotoxicity induced by Dox; 3) Whether the change of 14-3-3γ/Bcl-2 caused by TMP could affect mitochondrial oxidative stress that vascular endothelium induced by Dox endotheliotoxicity; 4) Whether improvement of mitochondrial function mediated by 14-3-3γ/Bcl-2 was involved in TMP protecting vascular endothelium against endotheliotoxicity induced by Dox.

2. Materials and Methods

2.1. Materials, Cells and Animals. Adenovirus pAD/14-3-3γ-shRNA and negative control (pAD/scrRNAi) were from GeneChem Co., Ltd (Shanghai, China). TMP, Dox, phenylephrine (PE), sodium nitroprusside (SNP), acetylcholine (Ach), atractyloside (Atr), and ciclosporin A (CsA) were purchased from Sigma-Aldrich (Cat. No. 95162, D1515, P1240000, PHR1423, PHR1546, A6882, C1832, St. Louis, MO, USA). Mitoquinone (MitoQ) was from MedChemExpress (Cat. No. HY-100116, Shanghai, China). ABT-737 was from Selleck (Cat. No. S1002, Houston, TX, USA). Antibodies directed against 14-3-3γ was purchased from Santa Cruz (Cat. No. sc-69955, Santa Cruz, CA, USA). Antibodies directed against Bcl-2, Bad phospho-S112, eNOS, eNOS phospho-S1177, cytochrome C (*cyt C*), COX4, and β-actin were purchased from Abcam (Cat. No. ab196495, ab129192, ab5589, ab184154, ab16381, ab33985, ab8229, Cambridge, UK). Horseradish peroxidase-conjugated IgG was from Jackson Immuno Research (Cat. No. 107-035-142, West Grove, PA, USA).

Human umbilical vein endothelial cells (HUVECs) were purchased from the China infrastructure of cell line resources (Shanghai, China). Male Kunming mice (8-10 weeks old, weighing 20-22 g) were provided by the Animal Center of Nanchang University (Nanchang, China).

All experimental protocols were performed in accordance with the National Institutes of Health (NIH) Guidelines for the Care and Use of Laboratory Animals (NIH Publication No. 85-23, revised 1996), and approved by the Ethics Committee of Nanchang University (No. 2019-0006).

2.2. In Vivo Experiments. Mice were housed (two per cage) in a controlled environment at a temperature of 22°C, humidity of 50%, and a 12-hour light/dark cycle. Water was provided to animals *ad libitum*.

2.2.1. Experimental Grouping In Vivo. As shown in Figure 1, 75 mice were randomly divided into five groups: the Dox group, mice were routinely fed for 3 weeks; then intraperitoneally injected with six injections of 2.5 mg/kg Dox over 3 weeks for a cumulative dose of 15 mg/kg [7]; the TMP + Dox group, mice were administered 6 mg/kg TMP [30], once daily for 6 weeks via intragastric administration, an hour before Dox administration; the TMP + Dox + pAD/14-3-3γ-shRNA group, mice were treated with a regimen similar to the TMP + Dox group for 4 weeks, then injected with pAD/14-3-3γ-shRNA adenovirus; the TMP + Dox + ABT-737 group, mice were treated with a regimen similar to the TMP + Dox group for 5 weeks, then followed by a once daily intraperitoneal injection with ABT-737 (20 μg/kg) [31], an hour before TMP administration, for 1 week; and the Control group, mice were given an equal volume of phosphate buffered saline (PBS) using a regimen similar to the TMP + Dox group.

2.2.2. Gene Delivery via Tail Vein. The 14-3-3γ knockdown model was constructed in Kunming mice *via* tail vein injection of a recombinant adenovirus containing the shRNA of 14-3-3γ gene (Genbank ID 22628, target sequence: GCTT CTGAGGCAGC GTATA) as previously described [32]. Briefly, pAD/14-3-3γ-shRNA adenovirus (2×10^{11} plaque-forming units/ml, 200 μl) was injected into the tail vein. Two weeks post-injection, mice were killed.

2.2.3. Collection of Blood and Tissue. At the end of the experiment, mice were anesthetized using an intraperitoneal injection with ketamine (100 mg/kg) and xylazine (8 mg/kg). Then, blood was collected in heparinized capillary tubes via a cardiac puncture and immediately centrifuged for 10 min at 3000 rpm and 25°C for serum separation. Thoracic aorta rings were harvested in ice-cold physiologic saline solution (PSS: 0.288 g NaH_2PO_4, 1.802 g glucose, 0.44 g sodium

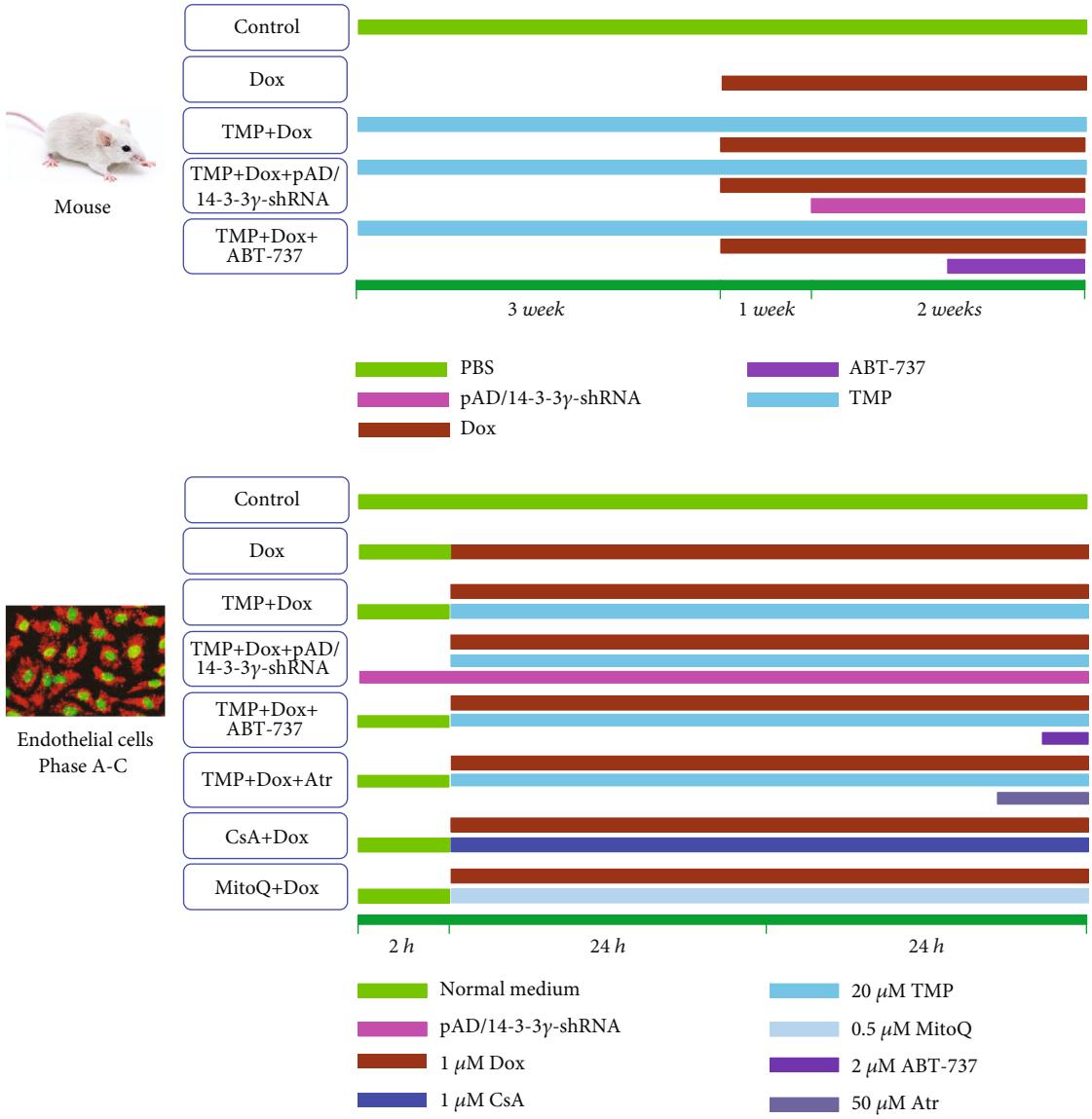

Figure 1: Schematic representation of the experimental design *in vivo* and *in vitro*. *In vivo,* 75 mice were randomly divided into five different groups: Dox group, mice were routinely fed for 3 weeks; then intraperitoneal injected with six injections of 2.5 mg/kg Dox over 3 weeks for a cumulative dose of 15 mg/kg; TMP + Dox group, mice were administered 6 mg/kg TMP, once daily for 6 weeks via intragastric administration, an hour before Dox administration; TMP + Dox + pAD/14-3-3γ-shRNA group, mice were treated with a regimen similar to the TMP + Dox group for 4 weeks, then injected with pAD/14-3- 3γ-shRNA adenovirus; TMP + Dox + ABT-737 group, mice were treated with a regimen similar to the TMP + Dox group for 5 weeks, followed by a once daily intraperitoneal injection with ABT-737(20 μg/kg), an hour before TMP administration, for 1 week; Control group: mice were given an equal volume of PBS using a regimen similar to the TMP + Dox group. For the *in vitro* experimental groupings: HUVECs in the control group were cultured under normal conditions (37°C, 95% O_2 and 5% CO_2) over the entire experiment; HUVECs in the Dox group were treated with 1 μM Dox for 48 hours; HUVECs in the TMP + Dox group were treated similar to the Dox group, but cells were also co-incubated with 20 μM TMP for 48 hours, whereas HUVECs in the TMP + Dox + pAD/14-3-3γ-shRNA group were treated with pAD/14-3-3γ-shRNA for 2 hours before TMP treatment; HUVECs in the TMP + Dox + ABT-737 group were treated in a manner similar to the TMP + Dox group, but these cells were also co-incubated with 2 μM ABT-737 for an hour; HUVECs in the TMP + Dox + Atr group were treated in a manner similar to HUVECs in the TMP + Dox group, but were also co-incubated for 2 hours with 50 μM Atr; HUVECs in the Dox + CsA/MitoQ groups were treated in a manner similar to the Dox group, but the cells were also co-incubated with 1 μM CsA/0.5 μM MitoQ for 48 hours, respectively. HUVECs that underwent these treatments were combined to form Phase A-C (See the 2.3.2 in the text).

pyruvate, 20.0 g BSA, 21.48 g NaCl, 0.875 g KCl, 0.7195 g $MgSO_4$ $7H_20$, 13.9 g MOPS sodium salt, and 0.185 g EDTA per liter solution at pH 7.4) and evaluated for vascular reactivity as described previously [33].

2.2.4. Determination of Biochemical and Tissues Injury Indexes. As a biomarker of tissue injury, the activities of serum lactate dehydrogenase (LDH), and creatine kinase (CK) were measured by a microplate reader (Bio-rad 680,

Hercules, CA, USA) according to the specifications of their respective assay kit (Nanjing Jiancheng Bioengineering Institute Co. Ltd., Nanjing, China).

The ferric reducing antioxidant power (FRAP) assay (Cell Biolabs, Inc. Santiago, CA, USA), which is based on reduction of the ferric tripyridyltriazine (Fe^{3+}-TPTZ) complex to ferrous (Fe^{2+}-TPTZ), was used to evaluate the antioxidant potential of the serum of mice at an absorption of 560 nm [29, 34]. In brief, 5 μl serum and 15 μl deionized water were mixed with 75 μl FRAP color solution. The mixture was incubated for 30 min at 25°C and its OD was measured at a wavelength of 560 nm by a spectrophotometer. A ferrous chloride standard was used to prepare the standard curve. The concentration of samples, indicating antioxidant potential, was obtained using the equation of the standard curve.

Malondialdehyde (MDA), superoxide dismutase (SOD), catalase (CAT), and glutathione peroxidase (GSH-Px) are vital indexes for estimating oxidative stress [29, 35]. The antioxidant enzyme activities and lipid peroxidation levels in mice serum were determined according to the manufacturer's instructions. In brief, collected supernatants were measured using a microplate reader. Kits for measuring MDA level, SOD, CAT, and GSH-Px activities were purchased from Nanjing Jiancheng Bioenginering Institute Co. Ltd. (Nanjing, China).

2.2.5. Hematoxylin–Eosin (H&E) Staining and the Terminal Deoxynucleotidyl Transferase-Mediated Nick End Labeling (TUNEL) Assay. Freshly harvested thoracic aortas were fixed in 10% buffered formalin solution embedded in paraffin and sectioned into 5 μm thick sections that were mounted onto glass slides. To evaluate morphological changes, H&E staining was performed. In addition, to detect apoptosis, TUNEL (Promega, Madison, WI, USA) staining method was performed according to the manufacturer's guidelines [7].

2.2.6. Vascular Reactivity. Vascular contractility and relaxation were determined as previously described [33, 36]. Briefly, thoracic aortas were placed in pressure myograph chambers (DMT Inc., Atlanta, GA, USA), containing warm PSS, cannulated and secured onto glass micropipettes, and equilibrated at an intraluminal pressure of 50 mmHg for an hour at 37°C. First, we confirmed that arteries maintained constriction to phenylephrine (PE: 10^{-10}-10^{-4} M) for the duration of the experiment until no spontaneous dilatation occurred during the constriction period (i.e. 5-12 min). Then, the samples were constricted by increasing doses of PE (10^{-6} M, about EC_{50}), immediately followed by a dose-response with endothelium-dependent dilator acetylcholine (ACh: 10^{-9}-10^{-4} M). After a washout period and after pre-constriction to PE (10^{-6} M), a dose-response to the endothelium-independent dilator sodium nitroprusside (SNP: 10^{-10}-10^{-4} M) was performed. The percent of dilation was calculated based on the maximal luminal diameter of each artery.

2.2.7. Determination of Nitric Oxide (NO) Contents. The NO content in mice's serum or the culture medium was indirectly reflected by the contents of nitrite and nitrate [37]. Nitrate is converted to nitrite by aspergillus nitrite reductase, and the total level of nitrite was measured using the Griess reagent (G4410, Sigma-Aldrich), for which the absorbance was determined at 540 nm. The NO content in samples was presented as the amounts of nitrite and nitrate (μM) per gram protein of serum or per liter of culture medium.

2.2.8. Western Blot Analysis. The total amount of protein from thoracic aortas samples, as well as total amount of protein and the mitochondrial proteins from HUVECs, were extracted using a protein extraction kit (Applygen Technologies Inc, Beijing, China), respectively. The protein concentration was determined by Bradford method. A total of 50 μg of protein was separated by denaturing SDS-polyacrylamide gel electrophoresis and transferred to polyvinylidene fluoride membranes. Membranes were then blocked with 5% skim milk, washed, incubated with primary antibodies directed against 14-3-3γ (1 : 1000), Bcl-2 (1 : 500), Bad phospho-S112 (1 : 500), eNOS (1 : 1000), eNOS phospho-S1177 (1 : 1000), *cyt C* (1 : 1000), β-actin (1 : 2000), and COX4 (1 : 1000), then incubated with Horseradish peroxidase-conjugated secondary antibody. Subsequently, membranes were incubated with an enhanced chemiluminescence reagent for 2 min at room temperature, and protein bands were visualized using an enhanced chemiluminescence method and analyzed with Quantity One software (Bio-Rad, Hercules, CA, USA) [7].

2.3. Experiments In Vitro

2.3.1. Endothelial Cell Culture and Adenovirus Transfection. For transfection assays, HUVECs were cultivated in high-glucose Dulbecco's modified Eagle medium (DMEM, Gibco-BRL, Grand Island, NY, USA) supplemented with 10% heat- inactivated fetal bovine serum (FBS, Gibco-BRL), penicillin (100 U/mL), and streptomycin (100 μg/mL) and cultured at 37°C in a humidified atmosphere at 5% CO_2.

Adenovirus pAD/14-3-3γ-shRNA and negative control-pAD/scrRNAi (shRNA of 14-3-3γ gene, the target sequence: GCTTCTGAGGCAGCGTATA and the negative control sequence: TTCTCCGAACGTGTCACGT) were transfected into HUVECs cultured in fresh DMEM supplemented with 15% FBS. Transfection efficiency was roughly 85% after 48 hours. Transfected cells were incubated at 37°C, 95% O_2, and 5% CO_2 for 2 hours before use in the experiments.

2.3.2. Experimental Design (Figure 1)

(1) Phase A. Firstly, we investigated whether TMP-treated HUVECs confirmed protective effects against the endotheliotoxicity induced by Dox. As well, the optimal concentration of TMP-treated was determined.

Cells were randomly divided into the following experimental groups: HUVECs in the control group were cultured under normal conditions (37°C, 95% O_2 and 5% CO_2) over the entire experiment; HUVECs in the Dox group were treated with 1 μM Dox for 48 hours [7]; HUVECs in the TMP + Dox group were treated similar to the Dox group, but cells were also co-incubated with different concentrations

of TMP (10, 20, 40, or 80 μM) for 48 hours. At the end of the experiments, cell viability and LDH activity were determined.

(2) Phase B. Next, we further confirmed whether 14-3-3γ expression and Bcl-2 activity could affect the protective effects of TMP on Dox's endotheliotoxicity.

Cells were randomly divided into five groups. Thereinto, the control, and the Dox group were treated with the above (1). HUVECs in the TMP + Dox group were treated similar to the Dox group, but cells were also co-incubated with 20 μM TMP for 48 hours, whereas cells in the TMP + Dox + pAD/14-3-3γ-shRNA groups were treated with pAD/14-3-3γ-shRNA for 2 hours before TMP treatment; HUVECs in the TMP + Dox + ABT-737 group were treated similar to the TMP + Dox group, but these cells were also co-incubated with 2 μM ABT-737 for an hour [31]. At the end of the experiments, cell viability, apoptosis, LDH and caspase 3 activities, NO levels in the culture medium, the expression of 14-3-3γ, Bad phospho-S112, eNOS, and eNOS phospho-S1177 in the lysate of HUVECs, and Bcl-2 expression in mitochondria were determined.

(3) Phase C. Finally, we investigated how TMP-treated HUVECs maintain mitochondrial function and possible mechanisms.

In brief, HUVECs were randomly divided into six groups. Thereinto, HUVECs in the control, the Dox, and the TMP + Dox group were treated with the above (2). HUVECs in the TMP + Dox + Atr group were treated similar to cells in the TMP + Dox group, but were also co-incubated for 2 hours with 50 μM Atr [38]; HUVECs in the Dox + CsA/MitoQ groups were treated similar to the Dox group, but the cells were also co-incubated with 1 μM CsA/0.5 μM MitoQ for 48 hours, respectively [39, 40].

At the end of the experiments, cell viability and LDH activity, oxygen consumption rate (OCR), extracellular acidification rate (ECAR), intracellular and mitochondrial ROS generation, levels of NAD^+, NADH, GSH, and GSSG in mitochondria/intracellular, mitochondrial membrane potential (MMP), mitochondria permeability transition pore (mPTP) opening, and *cyt C* release from mitochondria to cytoplasm in HUVECs were determined.

2.3.3. 3-(4,5-Dimethylthiazol-2-Yl)-5-(3-Carboxymethoxyphenyl)-2-(4-Sulfophenyl)-2H -Tetrazolium (MTS) Assay. Cells were plated in 96-well plates at a density of 1×10^4 cells/well, incubated at 37°C with 20 μl MTS (5 mg/ml, Promega, Madison, WI, USA) in 100 μl of DMEM medium for 2 hours. Next, the absorbance of each well was measured at 490 nm by a microplate reader (Bio-Rad680). The absorbance was directly proportional to the number of live cells.

2.3.4. Measurement of LDH and Caspase-3 Activities. In HUVECs, LDH is an intracellular enzyme that is released into the culture medium upon cell damage [7]. In this study, at the end of the experiment, the supernatant was collected, and the LDH activity was determined by a microplate reader (Bio-rad 680) according to the specifications of the LDH assay kit (Nanjing Jiancheng Bioengineering Institute Co. Ltd.).

Caspase-3 activity was measured in the cytosolic fraction of isolated HUVECs as described previously [7]. Briefly, caspase-3 activity was determined by measuring the cleavage of a caspase-3-specific substrate [acetyl-Asp-Glu-Val-Asp(DEVD)-p-nitroanilide (pNA)(DEVD-pNA)] using a caspase-3 activity assay kit (R&D Systems, Minneapolis, MN, USA) according to the manufacturer's instructions.

2.3.5. Assessment of Endothelial Apoptosis Using Annexin V-FITC and PI. Assessment of apoptosis of HUVECs was performed using an Annexin V-EGFP/PI apoptosis detection kit (BD Biosciences, San Diego, CA, USA). Annexin V-stained cells were analyzed using a Cytomics FC500 flow cytometer (Beckman Coulter, Brea, CA, USA) and DCF fluorescence was determined, which is an index of cellular damage [7].

2.3.6. Measurement of Intracellular and Mitochondrial ROS. Intracellular and mitochondrial ROS generation was measured using a DCFH-DA or mitoSOX probe as previously method [41]. In brief, cells were harvested and washed with serum-free DMEM media. Then, cells were mixed with serum-free media containing 10 μM DCFH-DA probe (Molecular Probes, Eugene, OR, USA) or 5 μM mitoSOX probe (Thermo Fisher Scientific, Waltham, MA, USA) and incubated at 37°C in the dark for 30 min with slight agitation every 5 min. Subsequently, cell pellets were collected, washed three times with PBS, and resuspended in 500 μL PBS for flow cytometry analysis (Cytomics FC500). The induced green fluorescence from 10,000 cells was documented at 488 or 510 nm. Flow Jo software was used to analyze the average fluorescence intensity.

2.3.7. Evaluation of OCR and ECAR. Mitochondrial respiration is an indicator of the functional bioenergetics capacity of the mitochondria and overall cellular health [29, 42]. In the present study, we used an XFp Extracellular Flux Analyzer (Seahorse Biosciences, North Billerica, MA, USA) to evaluate the OCR, which was measured as a function of time. In brief, HUVECs were seeded in Seahorse XFp cell cultured miniplates at a density of 5,000 cells/well and subjected to the corresponding treatment. After analysis of basal respiration, oligomycin (complex V inhibitor, 10 μM), carbonyl-cyanide-4-(trifluoromethoxy) phenylhydrazone (FCCP, permeabilizes the inner mitochondrial membrane for protons, 2 μM), rotenone/antimycin A (inhibitors of complex I and III, 0.5 μM/0.5 μM) were added sequentially. Wells without cells served as background and were used to normalize the reading of each well to the background noise of the plate. OCR was normalized to total protein per well.

To monitor glycolytic function, ECAR, expressed as mpH/min, was determined. The measurement procedure was similar to that of OCR described above. After measurement of basal ECAR, glucose solution (80 mM), oligomycin (5 mM), and 2-DG (100 mM) were added sequentially to determine glycolysis, glycolytic capacity, and the glycolytic reserve, respectively [42].

2.3.8. Isolation of Mitochondrial Fractions and Assessment of Nicotinamide Adenine Dinucleotide Mitochondrial. At the end of the experiments, HUVECs were collected and washed twice with cold PBS. The cells were resuspended in 1 × Cytosol Extraction Buffer Mix and homogenized on ice. The mixture was left on ice for 15 min and centrifuged at 1,300 × g for 5 min at 4°C. The supernatant was then transferred into a new tube and spun at 17,000 × g for 10 min at 4°C to precipitate the mitochondria. This pellet was resuspended in 15% Percoll (Cat. No. P4937, Sigma- Aldrich), and layered onto a preformed gradient of 22% Percoll, then layered onto 50% Percoll. The Percoll density gradient was centrifuged at 17,000 × g for 10 min at 4°C, and purified mitochondria were collected at the interface between the 50% and 22% gradients. The purified mitochondrial sample was centrifuged at 7,000 × g for 10 min at 4°C [27, 43].

Nicotinamide adenine dinucleotide exists in an oxidized (NAD^+) form and a reduced (NADH) form. Total NAD^+ and NADH levels in the purified mitochondrial samples were quantified using an NAD^+/NADH quantification kit according to the manufacturer's instructions (Biovision, Milpitas, CA, USA) [43]. Total NAD^+/NADH levels were assessed by converting all NAD^+ in the samples to NADH using the NAD Cycling Enzyme Mix and NADH Developer included in the kit. Nicotinamide adenine dinucleotide reduced-only concentrations were achieved by heating the mitochondrial samples to 60°C for 30 min to decompose NAD^+. Reduced nicotinamide adenine dinucleotide was measured at OD 450 nm using a spectrophotometer microplate reader (Bio-Tek Instruments, Winooski, VT, USA). Known concentrations of purified NADH were used to generate standard curves and to calculate mitochondrial concentration. Values of NAD^+ were generated by subtracting the NADH-only value from the total NAD^+/NADH value.

2.3.9. Assessment of Intracellular GSH, GSSG, and GSH/GSSG Ratio. Reduced glutathione is the most abundant intracellular thiol. The intracellular redox state is reflected by the levels of oxidized (GSSG) and reduced (GSH) glutathione. The GSH/GSSG ratio is also an essential indicator of cellular health [44, 45]. Measurements were performed according to the manufacturer's instructions using supernatants from cells lysed after treatment. GSH, GSSG, and GSH/GSSG ratio assay kits were purchased from Beyotime Institute of Biotechnology (Haimen, Jiangsu, China).

2.3.10. Assessment of MMP. Flow cytometry analysis was used to assess the loss of MMP using the fluorescent indicator, JC-1 (5, 5', 6, 6'-tetrachloro-1,1',3,3'-tetraethyl-benzimidazole carbocyanine iodide, Invitrogen, Carlsbad, CA, USA). HUVECs were harvested and the cell suspension was incubated with JC-1 (200 μM) at 37°C for 20 min followed by two rounds of washing with PBS to remove the remaining reagents. Fluorescence was measured with a Cytomics FC500 flow cytometer with initial excitation and emission wavelengths (ex/em) of 530 and 580 nm (red), followed by ex/em at 485/530 nm (green). The ratio of red to green fluorescence intensity of cells indicated the level of MMP [7].

2.3.11. Opening of mPTP. In cell apoptosis, mPTP opening plays a major role and the Ca^{2+} induced mitochondria swelling assay can be used to determine mPTP opening. The isolated mitochondria were resuspended in swelling buffer (KCl 120 mM, Tris-HCl 10 mM, MOPS 20 mM, KH_2PO_4 5 mM), and poured into a 96-well microtiter plate. The addition of 40 μl of $CaCl_2$ solution (200 nM) to each well served as a stimulant of mPTP opening and resulted in a steady decline in mitochondrial density. The absorbance at 520 nm was measured every minute until stable values were observed. To measure the extent of mPTP opening, changes in absorbance were calculated [7].

2.4. Statistical Analysis. All values were expressed as the means ± standard error of mean (SEM). One-way analysis of variance (ANOVA) was employed to test the significance of differences in the biochemical data across groups, followed by post hoc testing for individual differences. The results were considered significant at a value of $P < 0.05$.

3. Results

3.1. TMP-Treated Alleviates Vascular tissue's Damage Induced by Dox Toxicity in Mice. As shown in Figure 2(a), as expected, the activities of serum LDH and CK in the Dox group were significantly increased ($P < 0.01$), which were significantly decreased following TMP-treated ($P < 0.01$), and restored mostly when combined with pAD/14-3-3γ-shRNA or ABT-737 ($P < 0.01$), indicating that Dox had caused tissue and/or organ damage in mice, TMP could effectively resist it, but which depended on 14-3-3γ expression and Bcl-2 activity.

Histopathological examination of mice's thoracic aortas also confirmed the protective effects of TMP on Dox-induced vascular toxicity. As shown in Figure 2(c), in the Dox's mice, some inflammatory changes, such as inflammatory infiltration, and cell swelling, were found in the thoracic aorta's tissue. However, tissue injury was significantly reduced with TMP-treated. Further, the apoptosis of thoracic aorta's tissue was assayed using TUNEL staining (Figure 2(d)). In microscopy, the Dox group clearly promoted apoptosis of the thoracic aorta's tissue, which was significantly reversed by TMP-treated. However, when combined with pAD/14-3-3γ-shRNA or ABT-737, the above protective effects of TMP were mostly canceled.

As illustrated in Figure 2(b), the serum contents of NO in the Dox's mice were much lower ($P < 0.01$), which were significantly reversed by TMP-treated ($P < 0.01$). This change could be mostly completely counteracted by pAD/14-3-3γ-shRNA or ABT-737 ($P < 0.01$). Furthermore, we detected the expression of eNOS and p-eNOS of the thoracic aorta's tissue in all mice, respectively. As illustrated in Figures 3(c) and 3(g), the aortic tissue in the Dox's mice, the p-eNOS/e-NOS ratio was reduced ($P < 0.01$), which significantly reversed by TMP-treated ($P < 0.01$), but it could be only partly counteracted by pAD/14-3-3γ-shRNA or ABT-737 ($P < 0.01$). The above results indicated that TMP-treated could promote the phosphorylation of eNOS in the aortic

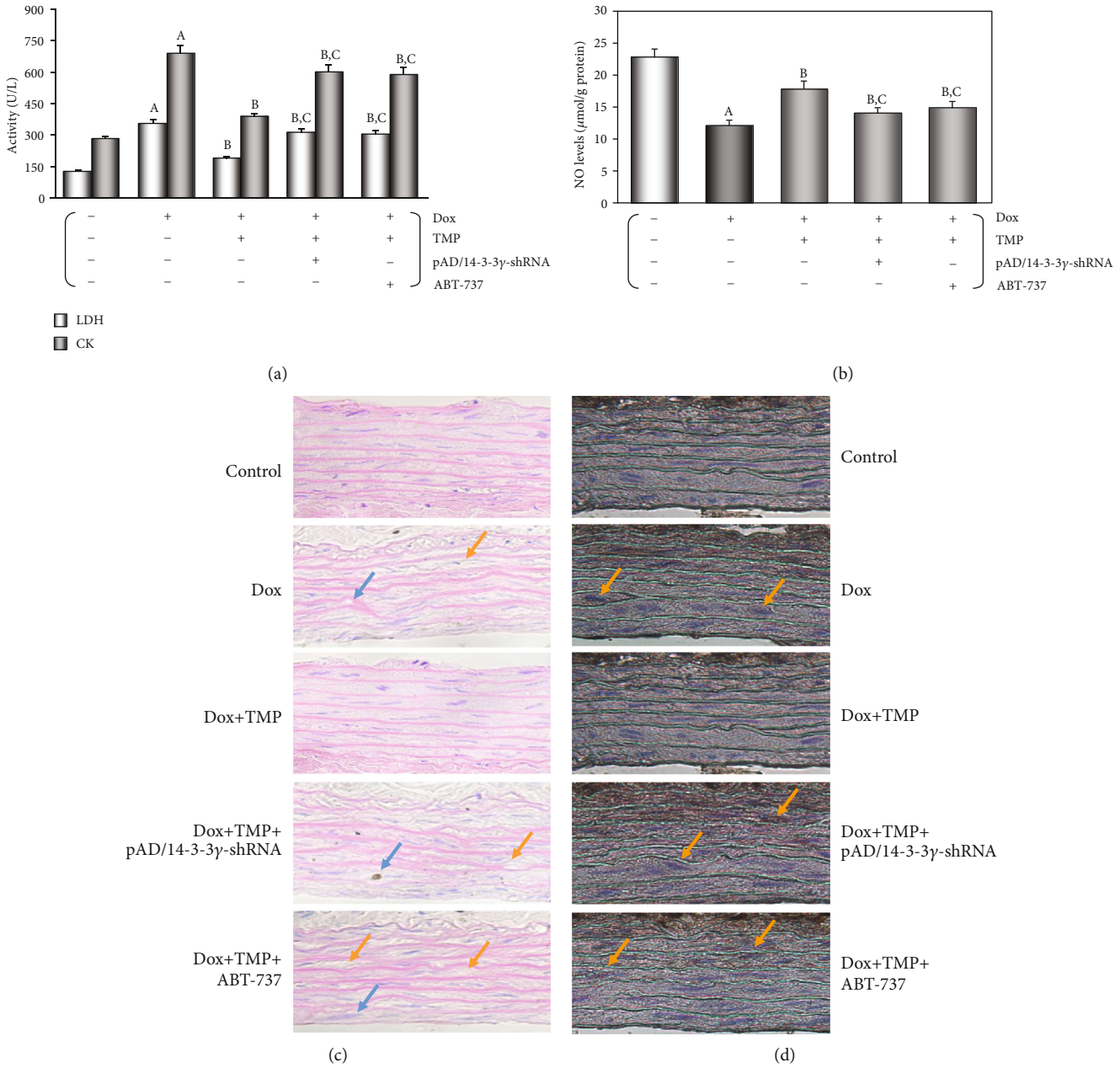

Figure 2: TMP-treated alleviates vascular tissue's damage induced by Dox toxicity in mice. (a) The activities of mice's serum LDH and CK. (b) Serum contents of NO. (c) H&E staining was performed for morphological analysis in the thoracic aortas tissue. Blue arrow: spotty necrosis; Orange arrow: hypertrophy of interstitial cells. (d) TUNEL staining was performed for morphological analysis in the thoracic aortas tissue. Orange arrow: TUNEL-positive cells. Data are presented as the mean ± SEM. for fifteen individual experiments. a: $P < 0.01$, versus control group; b: $P < 0.01$, versus Dox group; c: $P < 0.01$, versus TMP + Dox group.

tissue, increase NO synthesis, which also only partly depended on 14-3-3γ expression and Bcl-2 activity.

3.2. TMP-Treated Protects the Vascular endothelia's Function against the Endotheliotoxicity by Dox in Mice. Generally, the control experiments of endothelium-dependent dilation (EDD) with Ach and endothelium-independent dilation (EID) with SNP are noteworthy criteria for judging whether the vascular endothelium's function normally or not [33]. As shown in Figures 3(a) and 3(b), EDD in the Dox group was markedly impaired ($P < 0.01$), and area under the curve (AUC) of dose-effect relationship decreased to 34.3% of the control group ($P < 0.01$). TMP-treated improved EDD such that dilation was significantly increased at several doses of Ach ($P < 0.01$), and AUC also recovered to 78.6% of the control group ($P < 0.01$), but it could be mostly also reversed by pAD/14-3-3γ-shRNA or ABT-737 to 42.5% and 45.5% of the control group, respectively ($P < 0.01$). Similarly, EID in the Dox group was significantly impaired, and the AUC was 28.3% compared to the control group, TMP-treated improved could also reverse the related changes ($P < 0.01$, Figure S1A and B of the section of Supplementary

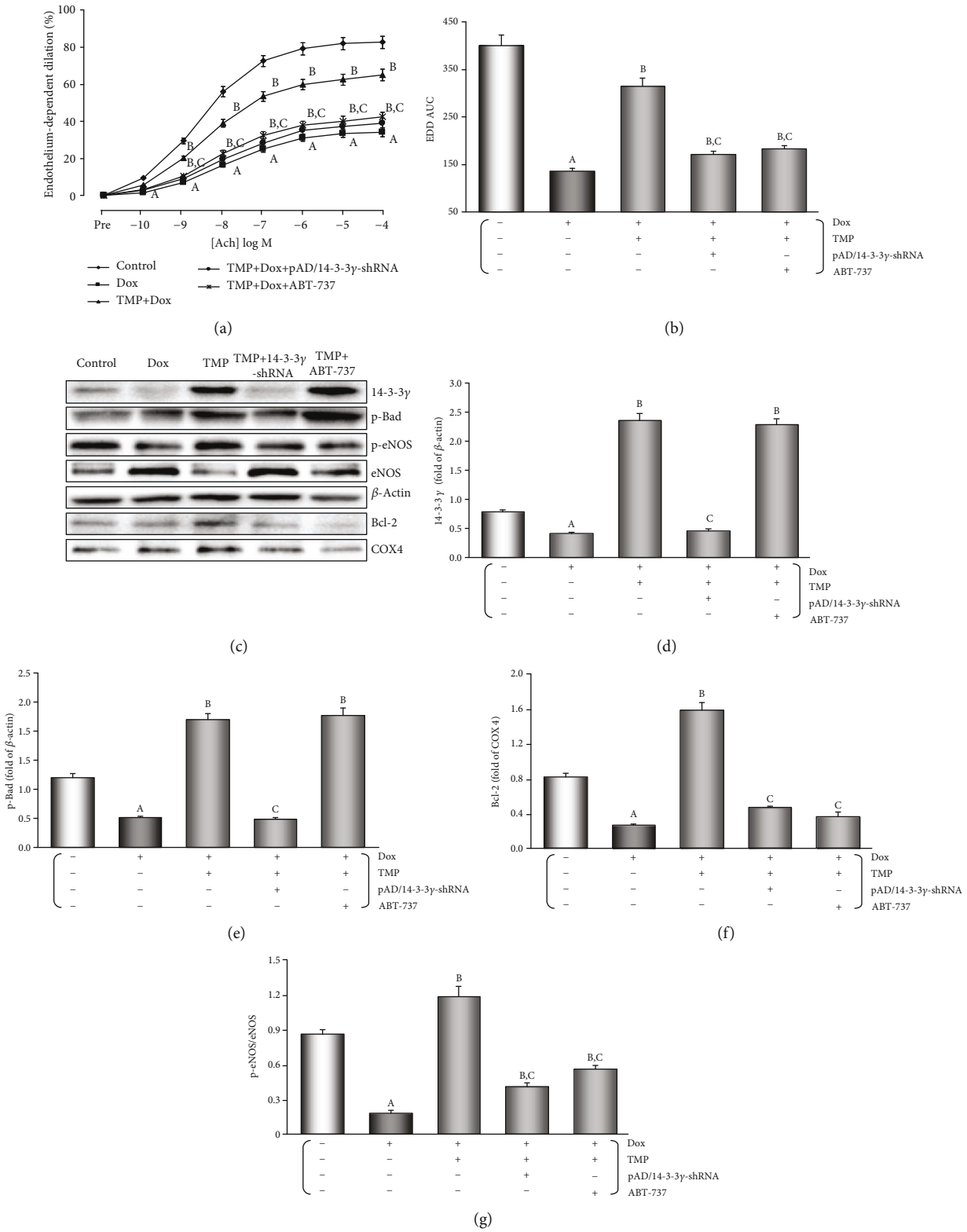

FIGURE 3: TMP-treated protects VECs' function against the endotheliotoxicity by Dox in mice. (a) Endothelium-dependent dilation (EDD) of the thoracic aortic strips. (b) Area under of the curve for EDD of the thoracic aortic strips. (c) Western blot's banding of related proteins in the aortic tissue. (d) Histogram of 14-3-3γ expression in the cytoplasm. (e) Histogram of p-Bad expression in the cytoplasm. (f) Histogram of Bcl-2 expression in the mitochondria. (g) Histogram of p-eNOS/eNOS expression in the cytoplasm. On (c), from left to right, lane 1: control; lane 2: Dox; lane 3: TMP + Dox; lane 4: TMP + Dox + pAD/14-3-3γ-shRNA; lane 5: TMP + Dox + ABT-737. Data are presented as the mean ± SEM. for fifteen individual experiments. a: $P < 0.01$, versus control group; b: $P < 0.01$, versus Dox group; c: $P < 0.01$, versus TMP + Dox group.

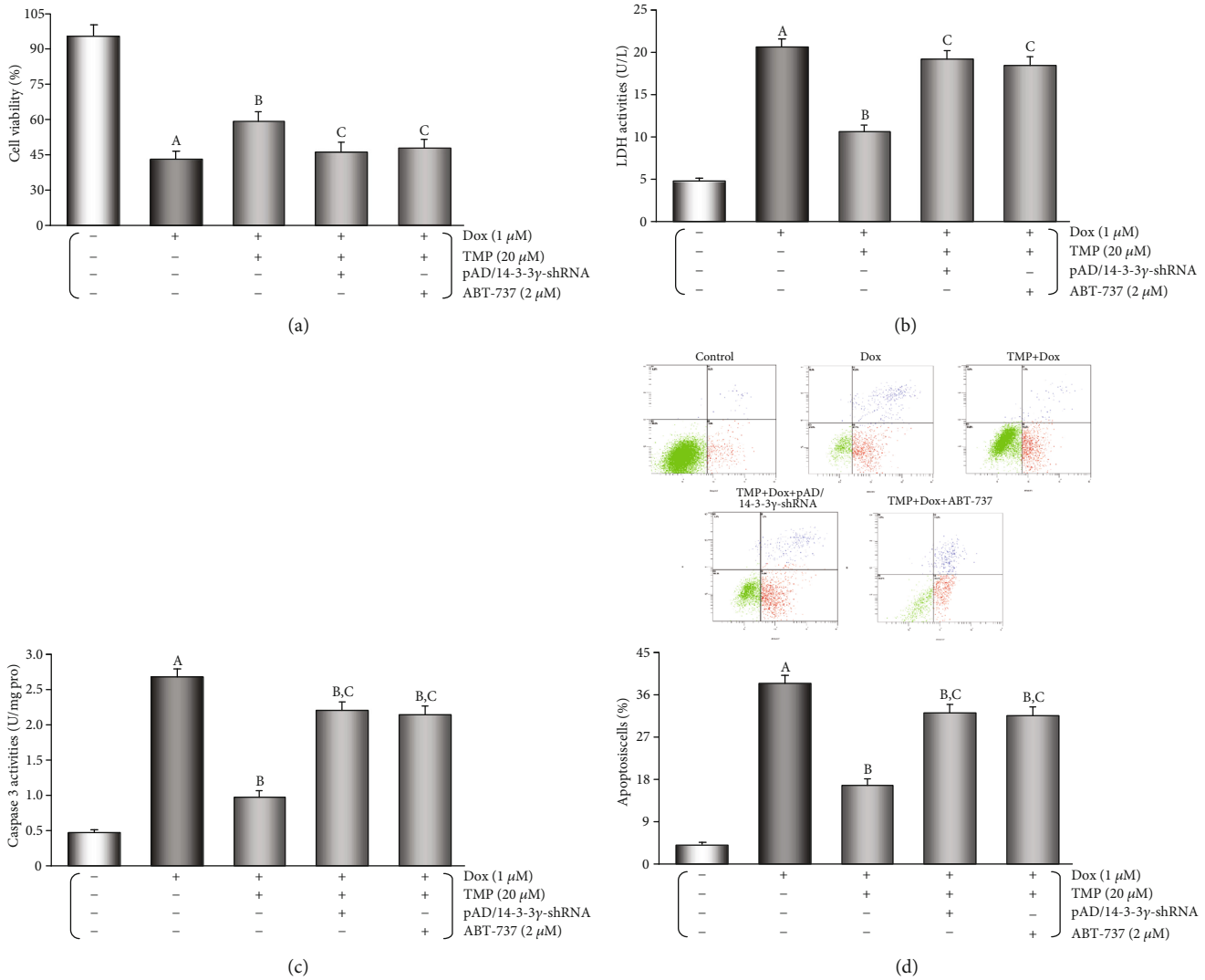

FIGURE 4: TMP-treated protects HUVECs against the endotheliotoxicity induced by Dox. (a) Cell viability of HUVECs. (b) LDH activities in culture media. (c) Histogram of the caspase-3 activity in HUVECs. (d) Flow cytometry dot plots (x-axis: annexin V-staining, y-axis: PI staining), and the quantitation of apoptotic cells. Data are presented as the mean ± SEM. for eight individual experiments. a: $P < 0.01$, versus control group; b: $P < 0.01$, versus Dox group; c: $P < 0.01$, versus TMP + Dox group.

materials). This indicated that TMP-treated could significantly alleviate vascular endothelium's damage by Dox toxicity, it also has considerable to ease harm to vascular smooth muscle, of course, which also depended on 14-3-3γ expression and Bcl-2 activity.

As illustrated in Figures 3(c)–3(f), it was interesting that in the aortic tissue TMP-treated up-regulated 14-3-3γ expression and promoted the phosphorylation of Bad, especially upregulation of mitochondrial Bcl-2 expression ($P < 0.01$). However, ABT-737, a specific Bcl-2 inhibitor [31], did not affect up-regulation of 14-3-3γ expression and Bad phosphorylation by TMP-treated ($P > 0.05$), but could significantly reduce Bcl-2 expression by TMP-treated in mitochondria ($P < 0.01$).

3.3. TMP-Treated Protects HUVECs against the Endotheliotoxicity Induced by Dox. Cell viability and LDH leakage generally serve as indexes of cell injury [7]. To evaluate the effects of TMP-treated, we tested different concentrations of TMP-treated on HUVECs that were subjected to Dox toxicity. As shown in Figure S2A and B of the section of Supplementary materials, HUVECs subjected to Dox toxicity showed a decrease in cell viability ($P < 0.01$) and an increase in LDH activity ($P < 0.01$). TMP-treated significantly increased cell viability and reduced LDH activity ($P < 0.01$) in a concentration-dependent manner. The optimal concentration of TMP-treated was determined to be 20 μM by chosen for subsequent experiments. Interestingly, co-treatment by pAD/14-3-3γ-shRNA or ABT-737 mostly abolished the protective effects of TMP-treated (Figures 4(a) and 4(b), $P < 0.01$).

When compared with the control group, cell viability and LDH activity did not change when using TMP alone, CsA alone, MitoQ alone, pAD/scrRNAi alone, TMP+ pAD/14-3-3γ-shRNA, TMP + pAD/scrRNAi, TMP + ABT-737, and TMP + Atr ($P > 0.05$), however, treatment with pAD/14-3-

3γ-shRNA alone, ABT-737 alone or Atr alone, cell viability was lower and LDH activity was higher compared to that of the control group ($P < 0.01$, Figure S3A and B of the section of Supplementary materials), indicating that 14-3-3γ expression, Bcl-2 activity, and mPTP closing play a vital role in maintaining normal HUVECs function. This was also the case for the pAD/14-3-3γ-shRNA+Dox, the ABT-737 + Dox, and the Atr + Dox groups compared with the Dox group ($P < 0.01$). But cell viability and LDH activity did not change when using pAD/scrRNAi+Dox ($P > 0.05$, Figure S4A and B of the section of Supplementary materials), indicating that could aggravate HUVECs injury using pAD/14-3-3γ-shRNA downregulates 14-3-3γ expression, or ABT-737 inhibits Bcl-2, or Atr opens the mPTP. However, pAD/scrRNAi as a negative control could not affect cell viability and LDH activity.

As shown in Figure 4(c), the caspase-3 activity in the Dox group was significantly increased when compared to that in the control group ($P < 0.01$), whereas TMP-treated significantly inhibited the caspase-3 activity when compared to the Dox group ($P < 0.01$). The caspase-3 activities of increased upon TMP plus pAD/14-3-3γ-shRNA or ABT-737 ($P < 0.01$).

The degree of HUVECs apoptosis was evaluated using Annexin V/PI double staining, then analyzed by flow cytometry (Figure 4(d)). The results showed that when compared with the Dox group, apoptosis by TMP-treated was significantly reduced ($P < 0.01$). However, a higher rate of apoptosis was observed in cells with TMP plus pAD/14-3-3γ-shRNA or ABT-737 ($P < 0.01$).

3.4. TMP-Treated Alters the Expression, Phosphorylation, or Sublocalization, or Metabolism of the Related Active Proteins in HUVECs of Dox Injury. As illustrated in Figures 5(a)-5(d), in HUVECs TMP-treated significantly up-regulated 14-3-3γ expression and promoted the phosphorylation of Bad, especially upregulation of mitochondrial Bcl-2 expression ($P < 0.01$), TMP plus pAD/14-3-3γ-shRNA could completely reverse the above changes. However, ABT-737 had no effect on up-regulation of 14-3-3γ expression and Bad phosphorylation by TMP ($P > 0.05$), but could significantly reduce Bcl-2 expression in mitochondria caused by TMP-treated ($P < 0.01$).

When compared with the control group, 14-3-3γ expression did not change when using pAD/scrRNAi alone-treated, as same as using TMP + pAD/scrRNAi+Dox and TMP + Dox ($P > 0.05$, Figure S5 of the section of Supplementary materials), indicating that pAD/scrRNAi did not affect 14-3-3γ expression as a negative control.

As illustrated in Figures 5(a), 5(e) and 5(f), in HUVECs, the p-eNOS/eNOS ratio increased significantly ($P < 0.01$) after TMP-treated, and NO content increased significantly ($P < 0.01$) as a follow-up result, but pAD/14-3-3γ-shRNA or ABT-737 could partly counteract it ($P < 0.01$). The above results indicated that TMP-treated could promote the phosphorylation of eNOS in HUVECs, increase NO synthesis, which also only partly depended on 14-3-3γ expression and Bcl-2 activity.

3.5. TMP-Treated Preserves the Intracellular/Mitochondrial Balance between ROS Generation and Their Neutralisation in HUVECs. It has previously been shown that oxidative stress plays a key role in Dox toxic injury [7, 8]. First, we found that HUVECs were treated by 1 μM Dox added 1 μM CsA [39], a mPTP closing agent, or 0.5 μM MitoQ [40], a mitochondria-targeted CoQ-10 antioxidant co-incubation, cell viability increased and LDH activity in the culture medium decreased, these results indicated that CsA and MitoQ alleviate caused HUVECs injury by Dox toxicity. However, 50 μM Atr, a potent mPTP opener, could completely reverse the protective effects of 20 μM TMP, that is, it could decrease cell viability and increase LDH activity in the culture medium ($P < 0.01$, Figure S6 A and B of the section of Supplementary materials).

After adding Dox for 48 hours, the peak of intracellular/-mitochondrial ROS in HUVECs was significantly moved to the right, indicating both significant increase in intracellular/mitochondrial ROS generation of the Dox group ($P < 0.01$, Figure 6(a)). Moreover, adding TMP/CsA/MitoQ co-incubation caused a significant shift of the peak of intracellular/mitochondrial ROS in HUVECs to the left, which indicated a significant decrease in intracellular/mitochondrial ROS generation when compared with the Dox group ($P < 0.01$). However, adding Atr co-incubation could reverse TMP's effect ($P < 0.01$), this strongly suggests that mPTP is open or closed and plays an important role in intracellular/-mitochondrial ROS generation.

Several small molecular markers such as NAD^+/NADH [43, 45] and GSH/GSSG [44, 46] in mitochondria/intracellular are useful indexes of redox state and redox balance [47]. In HUVECs, the content of NADH and GSH, GSH/GSSG ratio increased significantly ($P < 0.01$) and the content of NAD^+ and GSSG, NAD^+/NADH ratio decreased ($P < 0.01$) in TMP treatment (Figures 6(b) and 6(c)); these results were similar to that achieved with CsA and MitoQ treatment. This results further confirm that TMP, like CsA or MitoQ, could significantly reduce oxidative stress and ROS generation in mitochondria. The effects were also found to directly relate to mitochondrial mPTP opening as Atr, a potent mPTP opener, could almost completely cancel the effect of 20 μM TMP ($P < 0.01$). This phenomenon was consistent with the changes in cell viability and LDH activity mentioned above.

Usually, in animal serum, MDA content, SOD, CAT, and GSH-Px activities are determined to assess the level of oxidative stress [7, 29], and FRAP assay is used to evaluate the antioxidant potential [29, 34]. In this study, as shown in Table 1, in mice's serum after TMP-treated, SOD, CAT, and GSH-Px activities were significantly increased and MDA content was decreased ($P < 0.01$). Consistent with the lower level of oxidative stress, the FRAP results indicated a high antioxidant potential in the TMP group ($P < 0.01$), however, the above protective effects of TMP-treated could be mostly counteracted by pAD/14-3-3γ-shRNA or ABT-737 ($P < 0.01$).

3.6. TMP-Treated Maintains Mitochondrial Function in HUVECs. To explore the protective effects of TMP on mitochondrial respiration, OCR was measured using a Seahorse

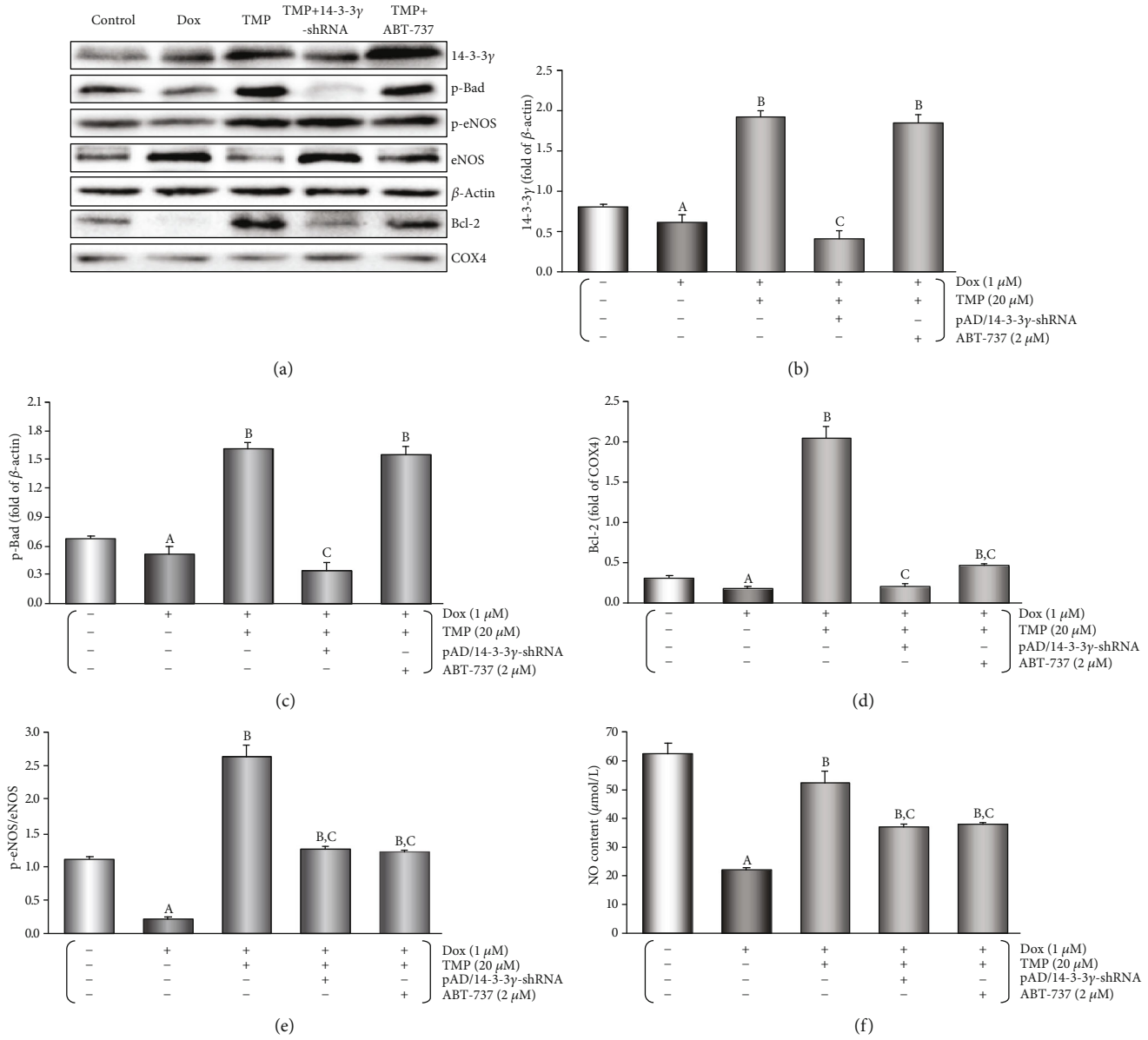

FIGURE 5: TMP-treated alters the expression, phosphorylation, or sublocalization, or metabolism of the related active proteins in HUVECs of Dox injury. (a) Western blot's banding of the related proteins in HUVECs. (b) Histogram of 14-3-3γ expression in the cytoplasm. (c) Histogram of p-Bad expression in the cytoplasm. (d) Histogram of Bcl-2 expression in the mitochondria. (e) Histogram of p-eNOS/eNOS expression in the cytoplasm. (f) The contents of NO in culture medium. On (a), from left to right, lane 1: control; lane 2: Dox; lane 3: TMP + Dox; lane 4: TMP + Dox + pAD/14-3-3γ-shRNA; lane 5: TMP + Dox + ABT-737. Data are presented as the mean ± SEM. for eight individual experiments. a: $P < 0.01$, versus control group; b: $P < 0.01$, versus Dox group; c: $P < 0.01$, versus TMP + Dox group.

XF analyzer in HUVECs. The OCR of cells treated with 20 μM TMP remained higher than those treated with 1 μM Dox ($P < 0.01$, Figure 7(a)). As shown in Figure 7(b), basal respiration before the addition of oligomycin, ATP production after the addition of oligomycin, maximal respiration after the addition of FCCP, and spare respiratory capacity after the addition of rotenone/antimycin A were significantly higher in HUVECs following TMP treatment than Dox treatment. The proton peak was, however, significantly lower with TMP treatment than Dox treatment ($P < 0.01$).

ECAR was used to determine the changes in glycolytic rate in HUVECs. As illustrated in Figure 7(c), the ECAR of TMP-treated cells remained higher than in Dox cells ($P < 0.01$). Basal rates of glycolysis and glycolytic capacity were significantly higher in HUVECs by TMP-treatment following oligomycin injection ($P < 0.01$). In contrast, non-glycolytic acidification increased slightly (Figure 7(d)). These findings suggest that the energetic demand of HUVECs was increased and intracellular acidosis was corrected after TMP treatment due to better maintenance of the mitochondria.

Loss of MMP occurs in the early stages of apoptosis. In live cells, JC-1 accumulates in the mitochondrial matrix and only exists in its monomeric form in apoptotic and dead cells

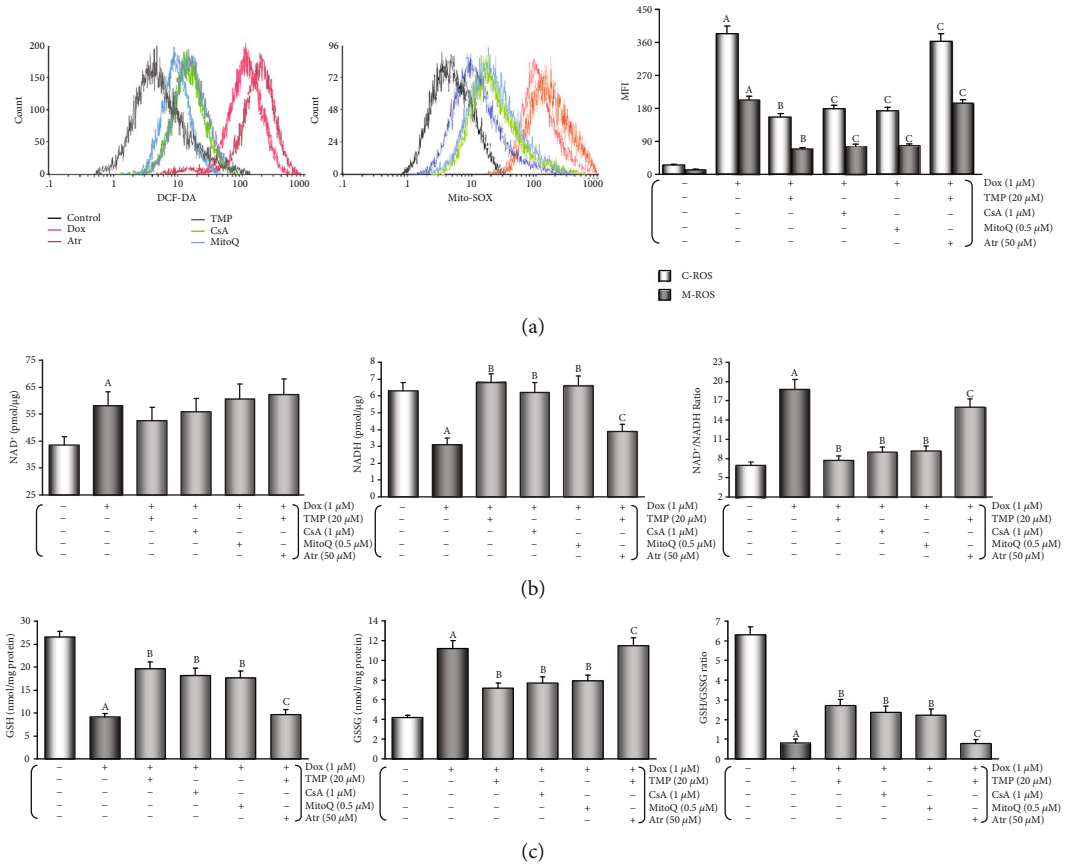

Figure 6: TMP-treated preserves the intracellular/mitochondrial balance between ROS generation and their neutralisation in HUVECs. (a) Intracellular/mitochondrial ROS generation of HUVECs after different treatments. Left: Intracellular ROS generation; middle: mitochondrial ROS generation; right: histogram of the intracellular/mitochondrial ROS generation at various treatments. MFI: mean fluorescence intensity. C-ROS: intracellular ROS. M-ROS: mitochondrial ROS. (b) mitochondrial nicotinamide adenine dinucleotide levels of HUVECs after different treatments. Left: histogram of mitochondrial NAD^+ levels at various treatments; middle: histogram of mitochondrial NADH levels at various treatments; right: histogram of mitochondrial NAD^+/NADH ratio at various treatments. (c) Intracellular glutathione levels of HUVECs after different treatments. left: histogram of intracellular GSH levels at various treatments; middle: histogram of intracellular GSSG levels at various treatments; right: histogram of intracellular GSH/GSSG ratio at various treatments. Data are presented as the mean ± SEM for eight individual experiments. a: $P < 0.01$, versus control group; b: $P < 0.01$, versus Dox group; c: $P < 0.01$, versus TMP + Dox group.

Table 1: TMP preserved the ferric reducing antioxidant power, the activities of antioxidant enzymes and reduced the levels of lipid peroxidation in the mice's serum against Dox's endotheliotoxicity.

Groups	FRAP (mmol Fe^{2+}/L)	SOD activity (U/g protein)	GSH-Px activity (U/g protein)	CAT activity (U/g protein)	MDA content (nmol/g protein)
Control	4.92 ± 0.21	96.1 ± 5.2	26.3 ± 1.8	17.5 ± 1.1	33.2 ± 2.0
Dox	1.56 ± 0.06 [a]	22.8 ± 1.9 [a]	5.2 ± 0.3 [a]	4.7 ± 0.4 [a]	151.6 ± 14.1 [a]
TMP + dox	3.60 ± 0.23 [b]	66.1 ± 3.9 [b]	17.1 ± 1.5 [b]	13.6 ± 1.2 [b]	55.7 ± 5.1 [b]
TMP + dox + pAD/14-3-3γ-shRNA	1.85 ± 0.07 [b,c]	27.3 ± 2.4 [b,c]	8.2 ± 0.5 [b,c]	7.6 ± 0.6 [b,c]	115.2 ± 12.2 [b,c]
TMP + dox + ABT-737	1.95 ± 0.09 [b,c]	29.2 ± 3.1 [b,c]	9.1 ± 0.8 [b,c]	7.9 ± 0.8 [b,c]	102.5 ± 11.5 [b,c]

Values were presented as mean ± SEM. for fifteen individual experiments. a: $P < 0.01$, versus control group; b: $P < 0.01$ versus Dox group; c: $P < 0.01$ versus TMP + Dox group.

because of the loss of MMP [7]. As shown in Figure 8(a), MMP was kept after TMP-treated because the peak of MMP levels significantly shifted to the right ($P < 0.01$). Similarly, CsA or MitoQ treatment also resulted in a significant increase in MMP ($P < 0.01$), but the addition of Atr, co-incubation, resulted a substantial loss in MMP, because of a shift of the peak of MMP to the left ($P < 0.01$).

mPTP opening is a primary cause in cellular apoptosis. The status of mPTP opening was determined by Ca^{2+}-induced swelling of mitochondrial [7]. Figure 8(b) shows that

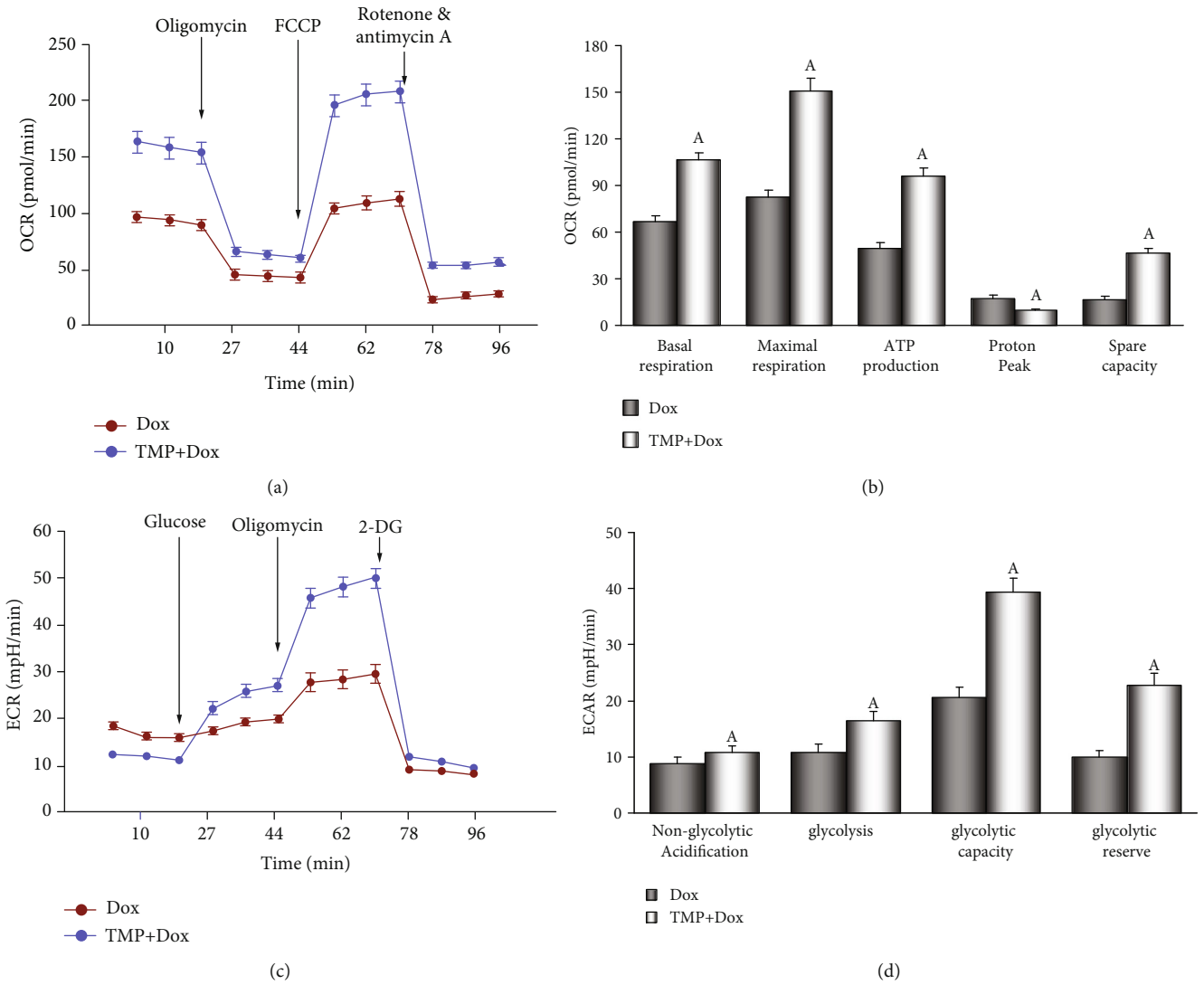

Figure 7: TMP-treated defends mitochondrial respiration and metabolize in HUVECs. (a) Mitochondrial oxygen consumption rate (OCR) curves obtained from different treatme. (b) Histogram of OCR important parameter from different treatme. (c) Mitochondrial extracellular acidification rate (ECAR) curves obtained from different treatme. (d) Histogram of ECAR important parameter from different treatme. Data are presented as the mean ± SEM. for three individual experiments. a: $P < 0.01$, versus Dox group.

when compared with the Dox group opening of the mPTP was inhibited after TMP-treated ($P < 0.01$). CsA or MitoQ treatment also lead to similar effects; however, with the addition of ATR, the effect of TMP-treated on the opening of mPTP was reversed ($P < 0.01$).

On the release of mitochondrial *cyt C* into the cytosol of HUVECs cells were evaluated using Western blot analysis. As shown in Figure 8(c), Dox injury resulted in a significant accumulation of *cyt C* in the cytosol ($P < 0.01$) and *cyt C* in the cytosol was significantly reduced when cells were treated with TMP, or CsA, or MitoQ ($P < 0.01$), but with the addition of ATR, the effect of TMP-treated was canceled ($P < 0.01$).

4. Discussion

Dox is a chemotherapeutic drug to treat, including breast cancer, bladder cancer, Kaposi's sarcoma, lymphoma, and acute lymphocytic leukemia [1]. However, in a dose-dependent manner, Dox could cause the irreversible cardiomyopathy [2, 10–12]. In addition to cardiotoxicity, many kinds of cytotoxicity induced by Dox have gradually attracted great attention, especially endothelial dysfunction [3, 4, 48, 49]. It has been noted that the toxicity of Dox to the myocardium and vascular endothelium is often accompanied by and may even cause and effect each other [3–6]. In this study, we could observe the endotheliotoxicity of Dox on vascular endothelium whether *in vivo* or *in vitro*, whether related enzymatic indexes, endothelial function indexes, cell survival, and apoptotic indexes, or morphological indexes (Figures 2–5).

TMP is a main biologically active ingredient purified from the rhizome of *Ligusticum wallichii* [14]. Recently, people has found abundant TMP in mature vinegar and old vinegar [15]. It had been explored many pharmacologically activities of TMP, such as scavenging free radicals, blocking calcium overload, protecting mitochondria,

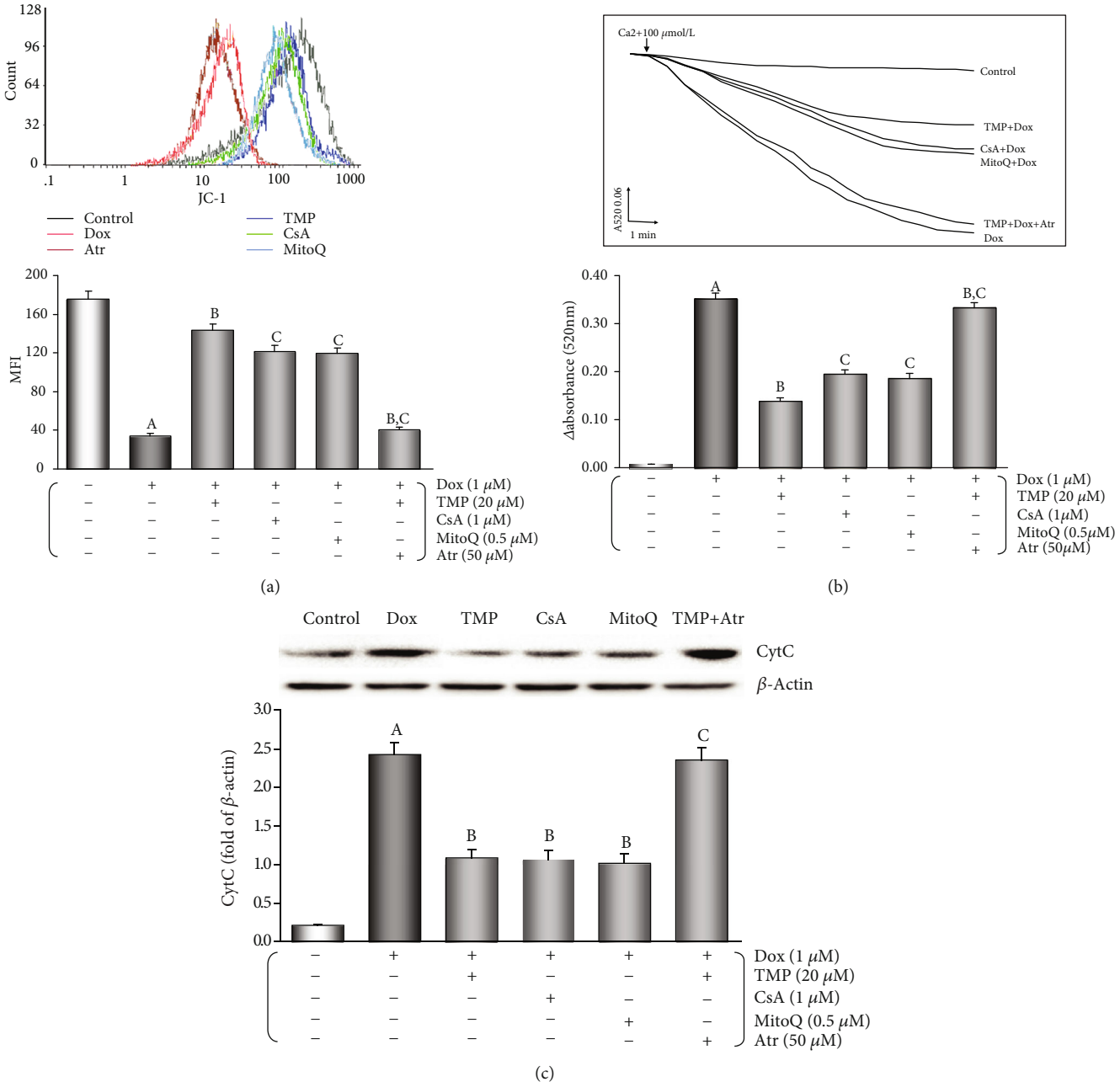

FIGURE 8: TMP-treated maintains mitochondrial function in HUVECs. (a) MMP levels were evaluated by JC-1. The results of the fluorescence peak on the *x*-axis was used to assess the level of MMP. (b) Ca^{2+}-induced swelling of mitochondria was used to determine mPTP opening. The changes in absorbance at 520 nm were detected every 2 minute. The data were accessed by the following equation: $\Delta OD = A520_{0min}$-$A520_{20min}$. (c) Western blot analysis and histogram of *cyt C* expression in the cytosol. From left to right, lane 1: control; lane 2: Dox; lane 3: TMP + Dox; lane 4: CsA + Dox; lane 5: MitoQ+Dox; lane 6: TMP + Dox + Atr. Data are presented as the mean ± SEM. for eight individual experiments. a: $P < 0.01$, versus control group; b: $P < 0.01$, versus Dox group; c: $P < 0.01$, versus TMP + Dox group.

improving energy metabolism, inhibiting cell apoptosis, inducing cytoprotection and so on [15–17]. Many studies have shown that TMP and its derivatives or compatibility with salvianic acid A/resveratrol possess functional cardioprotection/neuroprotection after myocardial ischemia-reperfusion/ischaemic stroke through interfering with PI3K/Akt/GSK3β, PGC1α/Nrf2, BDNF/Akt/CREB pathway, up-regulating Nrf-2 and HO-1 expression, maintaining Ca^{2+} homeostasis, and inhibiting inflammatory reaction, *etc.* [18–20, 50–52]. Some researchers have shown that TMP and prescriptions as mentioned above can attenuate injury Dox-induced cardiotoxicity and nephrotoxicity by inhibiting oxidative stress, cell autophagy and apoptosis [53, 54]. TMP and the prescriptions can also reverse multidrug resistance induced by Dox in breast cancer, bladder cancer, hepatocellular carcinoma through regulating the expression and function of P-gp, MRP2, MRP3, MRP5, MRP1, GST, Bcl-2, and TOPO-II, or directly enhance the

anti-cancer effect of Dox [55–58]. In the study, TMP reversing the vascular endothelium injury induced by Dox-endothelio- toxicity could be confirmed through reducing LDH and CK activities in serum, maintaining EDD, causing a reduction in caspase-3 activity, apoptotic rate, and histopathological changes of vascular endothelium (*in vivo*, Figures 2 and 3). Furthermore, TMP increased cell viability, decreased LDH and caspase-3 activity, and apoptotic rate (*in vitro*, Figures 4 and 5). These results indicate that TMP could reverse or alleviate the damage of Dox toxicity to vascular endothelium *in vivo* and *in vitro*.

Studies have shown that TMP is a multi-target and multi-mechanism ingredient [14], that regulates signaling pathways and affects the expression and activity of specific proteins is one of its prominent mechanisms [14–17]. Our previous work has also found that TMP could up-regulate 14-3-3γ expression, phosphorylate Bad (S112), translocate Bcl-2 to the mitochondria, improve mitochondrial function, and reduce apoptosis ultimately against LPS injury in cardiomyocyte [20]. Coincidentally, in this study, both *in vivo* and *in vitro*, with the protective effects on vascular endothelium, TMP could significantly up-regulate 14-3-3γ expression, phosphorylate Bad (S112), and Bcl-2 expression, especially in mitochondria. However, pAD/14-3-3γ-shRNA, an adenovirus knocking down intracellular 14-3-3γ expression, not only knocked down 14-3-3γ expression and inhibited Bad phosphorylation, but also significantly decreased Bcl-2 expression in mitochondria (Figures 3(c)-3(f) and 5(a)-5(d)). Concurrently, the protective effects of TMP on vascular endothelium were lost (Figures 2–5). Interestingly, ABT-737, a specific inhibitor of Bcl-2, could not change the up-regulation of 14-3-3γ expression and promote Bad phosphorylation. However, it could cancel TMP's effect of Bcl-2 expression in the mitochondria (Figures 3(c)–3(f) and 5(a)–5(d)) and its protective effects on the vascular endothelium (Figures 2–5). Studies have confirmed that Bcl-2 and Bad usually combine to form a complex in the cytoplasm [59]. When stimulated by certain stimuli, at Ser-112 and/or Ser-136 sites, 14-3-3s phosphorylate Bad, Bcl-2 dissociates from the complex and translocate targeting to mitochondria to exert corresponding physiological effects [60]. Combining with the above results of predecessors and ourselves, we could conclude that TMP can significantly up-regulate 14-3-3γ expression. Owing to Dox toxicity, 14-3-3γ phosphorylates Bad, releases Bcl-2, and translocates targeting mitochondria, reverses or alleviates the vascular endothelial damage. In other words, TMP against the endotheliotoxicity of Dox depends on the 14-3-3γ expression and Bcl-2 activity. In addition, some studies have found TMP induces the phosphorylation of eNOS Ser1177 and protects the myocardium [61], in the study, pAD/14-3-3γ-shRNA or ABT-737 could not completely inhibit or cancel the effects of TMP on improving p-eNOS/eNOS ratio and NO content (Figures 2(b), 3(g) and 5(e), 5(f)), or that part of the effect of TMP did not depend entirely on14-3-3γ expression and Bcl-2 activity.

A growing evidence demonstrate that in Dox-induced cytotoxicity ROS generation caused by triggers subsequent pathophysiological changes [3–6, 10–12]. Studies have shown that Dox accumulates through the reduction of the redox cycling in complex I of electron transport chain (ETC) in mitochondria, thereby increasing ROS generation [62]. Furthermore, mitochondrial NADH-dependent enzymes reduce Dox to corresponding semiquinone radicals, which undergo redox cycles to form superoxide radicals and hydrogen peroxide [63]. In this study, we found that mice after injected Dox, the antioxidant potential was weakened (Table 1, FRAP), the level of oxidative stress was enhanced (Table 1, MDA content, SOD, CAT, and GSH-Px activities). In HUVECs that were treated by Dox, both intracellular/mitochondrial ROS generation significantly increased, NAD^+, GSSG, and NAD^+/NADH increased, NADH, GSH, and GSH/GSSG decreased, MitoQ, a mitochondria-targeted CoQ-10 antioxidant, could completely reverse the above changes (Figure 6), indicating that increased oxidative stress was responsible for HUVECs damage, moreover, it provides an experimental basis for "excessive ROS comes from mitochondria" [62]. This result is consistent with the mainstream literature reports. Subsequently, TMP could significantly reverse the increase of oxidative stress induced by Dox, resulting in the antioxidant potential was enhanced, the level of oxidative stress was weakened (*in vivo*, Table 1), a significant decrease in both intracellular/mitochondrial ROS generation, a significant increase in NADH, GSH, and GSH/GSSG, and a significant decrease in NAD^+, GSSG, and NAD^+/-NADH (*in vitro*, Figure 6). More interestingly, the above effects of TMP are very similar to those of MitoQ, and CsA, a mPTP closing agent, and can be completely reversed by Atr, a potent mPTP opener (Figure 6). It is generally believed that TMP has a certain antioxidant capacity in the cytoplasm [12, 17]. There is no evidence that TMP can scavenge free radicals in mitochondria like MitoQ. Therefore, it is inappropriate to explain the above effects of TMP by its direct antioxidant capacity. Considering the similarity between TMP and CsA, and the reversal of the above effects of TMP after opening mPTP with Atr, we can use the "ROS-induced ROS release" (RIRR) hypothesis to explain it. The hypothesis [64] suggests that when mitochondrial ROS increases, MMP becomes unstable and mPTP opens continuously, then mitochondria swell and rupture, irreversibly damaging mitochondria. Therefore, ROS are released from its matrix into the cytosol and absorbed rapidly by adjacent normal mitochondria, which induces similar changes in adjacent mitochondria, and cascade-like positive feedback amplification, which ultimately leads to apoptosis [65]. Therefore, mPTP openness plays an important role in RIRR, and ROS is the most important stimulus for mPTP opening [66], which forms a vicious circle. TMP could promote the translocation of Bcl-2 to mitochondria. Like CsA, TMP could close mPTP, stabilize MMP, suppress RIRR mechanism, inhibit ROS burst (Figures 6 and 8), terminate vicious cycle, attenuate ultimately the injury of vascular endothelium induced by Dox.

Mitochondria are multifunctional organelles, and can actively or passively drive cellular dysfunction or demise [29, 67]. Indeed, its structural and functional integrity is fundamental to cellular life [29, 68]. In the study, when TMP helps Bcl-2 to translocate in mitochondria, mitochondrial function improves markedly. These include: increased mitochondrial

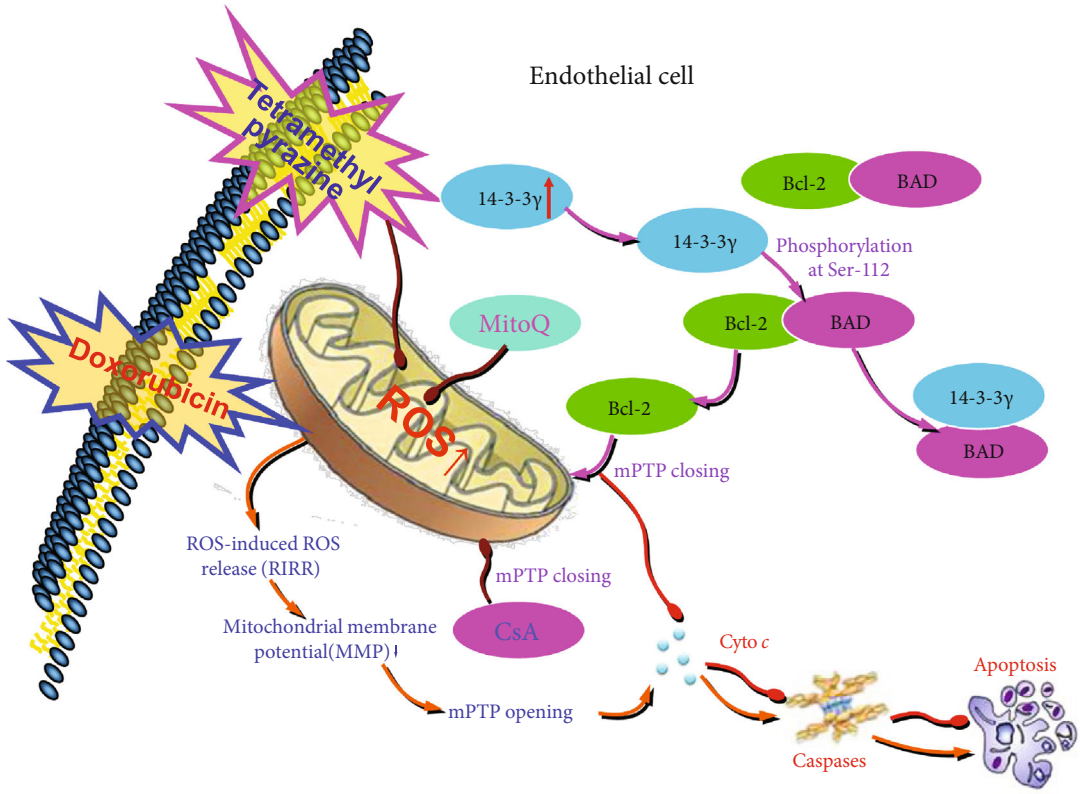

Figure 9: Diagram exhibiting a new mechanism of TMP protects mitochondrial function via 14-3-3γ/Bcl-2 in Dox-induced endotheliotoxicity. Dox induced excessive mitochondrial ROS generation, activating RIRR mechanism, weakening MMP, opening mPTP, induce ROS burst, leading to mitochondrial dysfunction, which in turn damages vascular endothelium. TMP upregulated 14-3-3γ expression of vascular endothelium, promoted the translocation of Bcl-2 into mitochondria, closed mPTP, keeped MMP, inhibited RIRR mechanism, thereby suppressed oxidative stress, improved mitochondrial function, and alleviated Dox-induced endotheliotoxicity.

respiration and glycolytic function (the abilities of oxidative phosphorylation and ATP production), corrected intracellular acidosis, normalized energy metabolism (Figure 7), stable MMP, inhibited mPTP opening, and markedly reduced *cyt C* release into the cytoplasm (Figure 8). Therefore, we can conclude that mitochondria are the ultimate target organelles for TMP to protect vascular endothelium from Dox toxicity.

5. Conclusion

In summary, Dox-induced excessive mitochondrial ROS generation, activating RIRR mechanism, weakening MMP, opening mPTP, inducing ROS burst, leading to mitochondrial dysfunction, which in turn damages vascular endothelium. TMP upregulated 14-3-3γ expression of vascular endothelium, promoted the translocation of Bcl-2 into mitochondria, closed mPTP, kept MMP, inhibited RIRR mechanism, suppressed oxidative stress, thereby improved mitochondrial function, and alleviated Dox-induced endotheliotoxicity (Figure 9).

Abbreviations

ACh: Acetylcholine
ANOVA: Analysis of variance
Atr: Atractyloside
AUC: Area under the curve
CAT: Catalase
CK: Creatine kinase
CsA: Ciclosporin a
cyt C: Cytochrome C
DCFH-DA: 6-carboxy-2`-7`- Dichlorodihydro-flurescein diacetate
DMEM: dulbecco's modified eagle medium
Dox: Doxorubicin
ECAR: Extracelluar acidification rate
EDD: Endothelium-dependent dilation
EID: Endothelium-independent dilation
eNOS: Endothelial nitric oxide synthase
FBS: Fetal bovine serum
FRAP: Ferric reducing antioxidant power
GSH: Reduced glutathione
GSH-Px: Glutathione peroxidase
GSSG: Oxidized glutathione
H&E: Hematoxylin-eosin staining
HUVECs: Human umbilical vein endothelial cells
JC-1: 5, 5', 6, 6'-tetrachloro-1,1',3,3'-tetraethyl-benzimidazolo carbocyanine iodide
LDH: Lactate dehydrogenase
LPS: Lipopolysaccharide
MDA: Malondialdehyde
MitoQ: Mitoquinone

MMP: Mitochondrial membrane potential
mPTP: Mitochonondria permeability transition pore
NAD^+: Oxidized nicotinamide adenine dinucleotide
NADH: Reduced nicotinamide adenine dinucleotide
NO: Nitric oxide
OCR: Oxygen consumption rate
PBS: Phosphate buffered saline
PE: Phenylephrine
PSS: Physiologic saline solution
RIRR: ROS-induced ROS release
ROS: Reactive oxygen species
SEM: Standard error of mean
SFN: Sulforaphane
SNP: Sodium nitroprusside
SOD: Superoxide dismutase
TUNEL: Terminal deoxynucleotidyl transferase d UTP nick-end labeling
TMP: Tetramethylpyrazine.

Data Availability

The data used to support the findings of this study are included within the article.

Conflicts of Interest

The authors declared no conflict of interest.

Acknowledgments

This research was supported by grants from the Natural Science Foundation of China (№: 21467017, 81660538, 81803534) and Jiangxi applied research and cultivation program (20181BBG78059).

Supplementary Materials

Figure S1: Effects of TMP on vascular reactivity of mice's thoracic aortas (endothelium-independent dilation, EID). (A) Endothelium-independent dilation (EID) of the thoracic aortic strips. (B) Area under of the curve for EID of the thoracic aortic strips. Data are presented as the mean ± SEM. for fifteen individual experiments. a: P<0.01, versus control group; b: P<0.01, versus Dox group; c: P<0.01, versus TMP+Dox group. Figure S2: TMP protects HUVECs against the endotheliotoxicity induced by Dox. TMP-treated significantly increased cell viability and reduced LDH activity (P<0.01) in a concentration-dependent manner. (A) Histogram of the cell viability. (B) Histogram of the LDH activity. Data are presented as the mean ± SEM for eight individual experiments. Data are presented as the mean ± SEM for eight individual experiments. a: P<0.01, versus control group; b: P<0.01, versus prior dosage. Figure S3: Effects of TMP/CsA/MitoQ, or downregulated 14-3-3γ expression, or inhibited Bcl-2 activity on the cell viability and LDH activity of normal HUVECs. Cell viability and LDH activity did not change by using MP alone, CsA alone, MitoQ alone, pAD/scrRNAi alone, TMP+pAD/14-3-3γ-shRNA, TMP+pAD/scrRNAi, TMP+ABT-737, and TMP +Atr when compared with the control group (P>0.05). However, the cell viability of treatment with pAD/14-3-3γ-shRNA alone, ABT-737 alone or Atr alone were lower and the LDH activity was higher compared to that of the control group (P<0.01), indicating that 14-3-3γ expression, Bcl-2 activity, and mPTP closing play an important role in maintaining normal cell function, and pAD/scrRNAi as a negative control couldn't affect cell viability and LDH activity. (A) Histogram of the cell viability. (B) Histogram of the LDH activity. Data are presented as the mean ± SEM for eight individual experiments. Data are presented as the mean ± SEM for eight individual experiments. a: P<0.01, versus control group. Figure S4: Effects of downregulated 14-3-3γ expression, or inhibited Bcl-2 activity on the cell viability and LDH activity of HUVECs by Dox injury. The cell viability of treatment with pAD/14-3-3γ-shRNA +Dox, ABT-737+Dox, and Atr+Dox were lower and the LDH activity was higher compared to that of the Dox group (P<0.01) , however, cell viability and LDH activity did not change when using pAD/scrRNAi+Dox (P>0.05), indicating that treatment with pAD/14-3-3γ-shRNA downregulated the expression of 14-3-3γ, or using ABT-737 inhibited Bcl-2, or allowing Atr to open the mPTP, thereby aggravating HUVECs injury, and pAD/scrRNAi as a negative control couldn't affect cell viability and LDH activity. (A) Histogram of the cell viability. (B) Histogram of the LDH activity. Data are presented as the mean ± SEM for eight individual experiments. a: P<0.01, versus control group. Figure S5: Effects of TMP, pAD/14-3-3γ-shRNA and pAD/scrRNAi on 14-3-3γ expression of normal HUVECs. TMP could significantly up-regulated 14-3-3γ expression of normal HUVECs, pAD/14-3-3γ-shRNA could selectively silence 14-3-3 expression effectively, and pAD/scrRNAi as a negative control couldn't affect 14-3-3 expression. Data are presented as the mean ± SEM for five individual experiments. a: P<0.01, versus control group, b: P<0.01, versus TMP group Figure S6: Effects of TMP/CsA/-MitoQ, or TMP added 50 μM Atr on the cell viability and LDH activity of HUVECs injuried by 1 μM Dox. TMP/CsA/MitoQ with 1 μM Dox co-treat HUVECs, the cell viability increased and LDH activity decreased, however added 50 μM Atr could reverse the related effects of TMP. (A) Histogram of the cell viability. (B) Histogram of the LDH activity. Data are presented as the mean ± SEM for eight individual experiments. a: P<0.01, versus control group; b: P<0.01, versus Dox group; c: P<0.01, versus TMP+Dox group. *(Supplementary Materials)*

References

[1] G. Bonadonna, S. Monfardini, M. De Lena, and F. Fossati-Bellani, "Clinical evaluation of adriamycin, a new antitumour antibiotic," *British Medical Journal*, vol. 3, no. 5669, pp. 503–506, 1969.

[2] P. Vejpongsa and E. T. Yeh, "Prevention of anthracycline-induced cardiotoxicity: challenges and opportunities," *Journal of the American College of Cardiology*, vol. 64, no. 9, pp. 938–945, 2014.

[3] A. Soultati, G. Mountzios, C. Avgerinou et al., "Endothelial vascular toxicity from chemotherapeutic agents: preclinical

evidence and clinical implications," *Cancer Treatment Reviews*, vol. 38, no. 5, pp. 473–483, 2012.

[4] D. Cappetta, F. Rossi, E. Piegari et al., "Doxorubicin targets multiple players: a new view of an old problem," *Pharmacological Research*, vol. 127, pp. 4–14, 2018.

[5] Y. Octavia, C. G. Tocchetti, K. L. Gabrielson, S. Janssens, H. J. Crijns, and A. L. Moens, "Doxorubicin-induced cardiomyopathy: from molecular mechanisms to therapeutic strategies," *Journal of Molecular and Cellular Cardiology*, vol. 52, no. 6, pp. 1213–1225, 2013.

[6] T. Wojcik, E. Szczesny, and S. Chlopicki, "Detrimental effects of chemotherapeutics and other drugs on the endothelium: a call for endothelial toxicity profiling," *Pharmacological Reports*, vol. 67, no. 4, pp. 811–817, 2015.

[7] H. He, Y. Luo, Y. Qiao et al., "Curcumin attenuates doxorubicin-induced cardiotoxicity via suppressing oxidative stress and preventing mitochondrial dysfunction mediated by 14-3-3γ," *Food & Function*, vol. 9, no. 8, pp. 4404–4418, 2018.

[8] X. Chen, X. Peng, Y. Luo et al., "Quercetin protects cardiomyocytes against doxorubicin-induced toxicity by suppressing oxidative stress and improving mitochondrial function via 14-3-3γ," *Toxicology Mechanisms and Methods*, vol. 29, no. 5, pp. 344–354, 2019.

[9] E. Mira, L. Carmona-Rodríguez, B. Pérez-Villamil et al., "SOD3 improves the tumor response to chemotherapy by stabilizing endothelial HIF-2α," *Nature Communications*, vol. 9, p. 575, 2018.

[10] A. I. Abushouk, A. M. A. Salem, A. Saad et al., "Mesenchymal stem cell therapy for doxorubicin-induced cardiomyopathy: potential mechanisms, governing factors, and implications of the heart stem cell debate," *Frontiers in Pharmacology*, vol. 10, p. 635, 2019.

[11] M. M. Abdel-Daim, O. E. Kilany, H. A. Khalifa, and A. A. M. Ahmed, "Allicin ameliorates doxorubicin-induced cardiotoxicity in rats via suppression of oxidative stress, inflammation and apoptosis," *Cancer Chemotherapy and Pharmacology*, vol. 80, no. 4, pp. 745–753, 2017.

[12] A. I. Abushouk, A. Ismail, A. M. A. Salem, A. M. Afifi, and M. M. Abdel-Daim, "Cardioprotective mechanisms of phytochemicals against doxorubicin-induced cardiotoxicity," *Biomedicine & Pharmacotherapy*, vol. 90, pp. 935–946, 2017.

[13] X. Wang, L. Chen, T. Wang et al., "Ginsenoside Rg3 antagonizes adriamycin-induced cardiotoxicity by improving endothelial dysfunction from oxidative stress _via_ upregulating the Nrf2-ARE pathway through the activation of akt," *Phytomedicine*, vol. 22, no. 10, pp. 875–884, 2015.

[14] P. O. Donkor, Y. Chen, L. Ding, and F. Qiu, "Locally and traditionally used *Ligusticum* species - A review of their phytochemistry, pharmacology and pharmacokinetics," *Journal of Ethnopharmacology*, vol. 194, pp. 530–548, 2016.

[15] J. Chen, J. Tian, H. Ge, R. Liu, and J. Xiao, "Effects of tetramethylpyrazine from Chinese black vinegar on antioxidant and hypolipidemia activities in HepG2 cells," *Food and Chemical Toxicology*, vol. 109, Part 2, pp. 930–940, 2017.

[16] G. Zhang, F. Zhang, T. Zhang et al., "Tetramethylpyrazine Nitrone improves neurobehavioral functions and confers neuroprotection on rats with traumatic brain injury," *Neurochemical Research*, vol. 41, no. 11, pp. 2948–2957, 2016.

[17] H. P. Chen, M. He, Q. R. Huang, G. H. Zeng, and D. Liu, "Delayed protection of tetramethylpyrazine on neonatal rat cardiomyocytes subjected to anoxia-reoxygenation injury," *Basic & Clinical Pharmacology & Toxicology*, vol. 100, no. 6, pp. 366–371, 2007.

[18] Y. Zhao, Y. Liu, and K. Chen, "Mechanisms and clinical application of Tetramethylpyrazine (an interesting natural compound isolated from Ligusticum Wallichii): current status and perspective," *Oxidative Medicine and Cellular Longevity*, vol. 2016, Article ID 2124638, 9 pages, 2016.

[19] G. Zhang, T. Zhang, N. Li et al., "Tetramethylpyrazine nitrone activates the BDNF/Akt/CREB pathway to promote post-ischaemic neuroregeneration and recovery of neurological functions in rats," *British Journal of Pharmacology*, vol. 175, no. 3, pp. 517–531, 2018.

[20] B. Huang, J. You, Y. Qiao et al., "Tetramethylpyrazine attenuates lipopolysaccharide-induced cardiomyocyte injury via improving mitochondrial function mediated by 14-3-3γ," *European Journal of Pharmacology*, vol. 832, pp. 67–74, 2018.

[21] A. Aitken, "14-3-3 proteins: a historic overview," *Seminars in Cancer Biology*, vol. 16, no. 3, pp. 162–172, 2006.

[22] M. J. van Hemert, H. Y. Steensma, and G. P. van Heusden, "14-3-3 proteins: key regulators of cell division, signalling and apoptosis," *BioEssays*, vol. 23, no. 10, pp. 936–946, 2001.

[23] M. He, J. X. Zhang, L. J. Shao et al., "Upregulation of 14-3-3 isoforms in acute rat myocardial injuries induced by burn and lipopolysaccharide," *Clinical and Experimental Pharmacology and Physiology*, vol. 33, no. 4, pp. 374–380, 2006.

[24] H. P. Chen, M. He, Y. L. Xu et al., "Anoxic preconditioning upregulates 14-3-3 protein expression in neonatal rat cardiomyocytes through extracellular signal-regulated protein kinase 1/2," *Life Sciences*, vol. 81, no. 5, pp. 372–379, 2007.

[25] J. Huang, Z. Liu, P. Xu et al., "Capsaicin prevents mitochondrial damage, protects cardiomyocytes subjected to anoxia/reoxygenation injury mediated by 14-3-3η/Bcl-2," *European Journal of Pharmacology*, vol. 819, pp. 43–50, 2018.

[26] Z. Liu, L. Yang, J. Huang et al., "Luteoloside attenuates anoxia/reoxygenation-induced cardiomyocytes injury via mitochondrial pathway mediated by 14-3-3η protein," *Phytotherapy Research*, vol. 32, no. 6, pp. 1126–1134, 2018.

[27] Z. Y. Zhang, H. He, Y. Qiao et al., "TanshinoneIIA pretreatment protects H9c2 cells against anoxia/reoxygenation injury: involvement of the translocation of Bcl-2 to mitochondria mediated by 14-3-3η," *Oxidative Medicine and Cellular Longevity*, vol. 2018, Article ID 3583921, 13 pages, 2018.

[28] D. Liu, B. Yi, Z. Liao et al., "14-3-3γ protein attenuates lipopolysaccharide-induced cardiomyocytes injury through the Bcl-2 family/mitochondria pathway," *International Immunopharmacology*, vol. 21, no. 2, pp. 509–515, 2014.

[29] Y. Luo, Q. Wan, M. Xu et al., "Nutritional preconditioning induced by astragaloside IV on isolated hearts and cardiomyocytes against myocardial ischemia injury via improving Bcl-2-mediated mitochondrial function," *Chemico-Biological Interactions*, vol. 309, article 108723, 2019.

[30] J. R. Sheu, G. Hsiao, Y. M. Lee, and M. H. Yen, "Antithrombotic effects of tetramethylpyrazine in in vivo experiments," *International Journal of Hematology*, vol. 73, no. 3, pp. 393–398, 2001.

[31] C. Chen, H. He, Y. Luo, M. Zhou, D. Yin, and M. He, "Involvement of Bcl-2 signal pathway in the protective effects of Apigenin on anoxia/Reoxygenation- induced myocardium

injury," *Journal of Cardiovascular Pharmacology*, vol. 67, no. 2, pp. 152–163, 2016.

[32] C. Chen, Y. Weifeng, W. Shan et al., "Crosstalk between Connexin 32 and mitochondrial apoptotic signaling pathway plays a pivotal role in renal ischemia reperfusion-induced acute kidney injury," *Antioxidants & Redox Signaling*, vol. 30, no. 12, pp. 1521–1538, 2018.

[33] D. M. Lee, M. L. Battson, D. K. Jarrell et al., "SGLT2 inhibition via dapagliflozin improves generalized vascular dysfunction and alters the gut microbiota in type 2 diabetic mice," *Cardiovascular Diabetology*, vol. 17, p. 62, 2018.

[34] A. Rapacz, J. Sapa, K. Pytka et al., "Antiarrhythmic activity of new 2-methoxyphenylpiperazine xanthone derivatives after ischemia/reperfusion in rats," *Pharmacological Reports*, vol. 67, no. 6, pp. 1163–1167, 2015.

[35] D. Qu, J. Han, H. Ren et al., "Cardioprotective effects of astragalin against myocardial ischemia/ reperfusion injury in isolated rat heart," *Oxidative Medicine and Cellular Longevity*, vol. 2016, Article ID 8194690, 11 pages, 2016.

[36] J. Wu, Z. Jiang, H. Zhang et al., "Sodium butyrate attenuates diabetes-induced aortic endothelial dysfunction via P300-mediated transcriptional activation of *Nrf2*," *Free Radical Biology & Medicine*, vol. 124, pp. 454–465, 2018.

[37] Y. Wu, J. J. Zhang, T. B. Li et al., "Phosphorylation of non-muscle myosin light chain promotes endothelial injury in Hyperlipidemic rats through a mechanism involving down-regulation of Dimethylarginine Dimethylaminohydrolase 2," *Journal of Cardiovascular Pharmacology and Therapeutics*, vol. 21, no. 6, pp. 536–548, 2016.

[38] X. G. Zhang, L. Zhao, Y. Zhang et al., "Extracellular Cl^--free-induced cardioprotection against hypoxia/reoxygenation is associated with attenuation of mitochondrial permeability transition pore," *Biomedicine & Pharmacotherapy*, vol. 86, pp. 637–644, 2017.

[39] G. Teixeira, M. Abrial, K. Portier et al., "Synergistic protective effect of cyclosporin A and rotenone against hypoxia- reoxygenation in cardiomyocytes," *Journal of Molecular and Cellular Cardiology*, vol. 56, pp. 55–62, 2013.

[40] Y. Imai, B. D. Fink, J. A. Promes, C. A. Kulkarni, R. J. Kerns, and W. I. Sivitz, "Effect of a mitochondrial-targeted coenzyme Q analog on pancreatic β-cell function and energetics in high fat fed obese mice," *Pharmacology Research & Perspectives*, vol. 6, no. 3, article e00393, 2018.

[41] Y. H. Zuo, Q. B. Han, G. T. Dong et al., "*Panax ginseng* polysaccharide protected H9c2 cardiomyocyte from hypoxia/Reoxygenation injury through regulating mitochondrial metabolism and RISK pathway," *Frontiers in Physiology*, vol. 15, p. 699, 2018.

[42] Y. Pan, W. Zhao, D. Zhao et al., "Salvianolic acid B improves mitochondrial function in 3T3-L1 adipocytes through a pathway involving PPARγ coactivator-1α (PGC-1α)," *Frontiers in Pharmacology*, vol. 15, p. 671, 2018.

[43] K. C. Morris-Blanco, C. H. Cohan, J. T. Neumann, T. J. Sick, and M. A. Perez-Pinzon, "Protein kinase C epsilon regulates mitochondrial pools of Nampt and NAD following resveratrol and ischemic preconditioning in the rat cortex," *Journal of Cerebral Blood Flow & Metabolism*, vol. 34, no. 6, pp. 1024–1032, 2014.

[44] G. M. Enns and T. M. Cowan, "Glutathione as a redox biomarker in mitochondrial disease–implications for therapy," *Journal of Clinical Medicine*, vol. 6, no. 5, article E50, 2017.

[45] T. S. Blacker and M. R. Duchen, "Investigating mitochondrial redox state using NADH and NADPH autofluorescence," *Free Radical Biology & Medicine*, vol. 100, pp. 53–65, 2016.

[46] M. Marí, A. Morales, A. Colell, C. García-Ruiz, and J. C. Fernández-Checa, "Mitochondrial glutathione, a key survival antioxidant," *Antioxidants & Redox Signaling*, vol. 11, no. 11, pp. 2685–2700, 2009.

[47] A. J. Kowaltowski, "Strategies to detect mitochondrial oxidants," *Redox Biology*, vol. 21, article 101065, 2019.

[48] A. Pugazhendhi, T. N. J. I. Edison, B. K. Velmurugan, J. A. Jacob, and I. Karuppusamy, "Toxicity of doxorubicin (dox) to different experimental organ systems," *Life Sciences*, vol. 200, pp. 26–30, 2018.

[49] M. B. Wolf and J. W. Baynes, "The anti-cancer drug, doxorubicin, causes oxidant stress-induced endothelial dysfunction," *Biochimica et Biophysica Acta*, vol. 1760, no. 2, pp. 267–271, 2006.

[50] H. Chen, J. Cao, Z. Zhu et al., "A novel Tetramethylpyrazine derivative protects against glutamate-induced cytotoxicity through PGC1α/Nrf2 and PI3K/Akt signaling pathways," *Frontiers in Neuroscience*, vol. 12, p. 567, 2018.

[51] S. Hu, H. Hu, S. Mak et al., "A novel Tetramethylpyrazine derivative prophylactically protects against glutamate-induced excitotoxicity in primary neurons through the blockage of N-methyl-D-aspartate receptor," *Frontiers in Pharmacology*, vol. 9, p. 73, 2018.

[52] X. Luo, Y. Yu, Z. Xiang et al., "Tetramethylpyrazine nitrone protects retinal ganglion cells against N-methyl-d-aspartate-induced excitotoxicity," *Journal of Neurochemistry*, vol. 141, no. 3, pp. 373–386, 2017.

[53] F. Tang, X. Zhou, L. Wang et al., "A novel compound DT-010 protects against doxorubicin-induced cardiotoxicity in zebrafish and H9c2 cells by inhibiting reactive oxygen species-mediated apoptotic and autophagic pathways," *European Journal of Pharmacology*, vol. 820, pp. 86–96, 2018.

[54] C. Y. Cheng, Y. M. Sue, C. H. Chen et al., "Tetramethylpyrazine attenuates adriamycin-induced apoptotic injury in rat renal tubular cells NRK-52E," *Planta Medica*, vol. 72, no. 10, pp. 888–893, 2006.

[55] L. Wang, J. Y. Chan, X. Zhou et al., "A novel agent enhances the chemotherapeutic efficacy of doxorubicin in MCF-7 breast Cancer cells," *Frontiers in Pharmacology*, vol. 7, p. 249, 2016.

[56] S. Wang, T. Lei, and M. Zhang, "The reversal effect and its mechanisms of Tetramethylpyrazine on multidrug resistance in human bladder Cancer," *PLoS One*, vol. 11, no. 7, article e0157759, 2016.

[57] X. B. Wang, S. S. Wang, Q. F. Zhang et al., "Inhibition of tetramethylpyrazine on P-gp, MRP2, MRP3 and MRP5 in multidrug resistant human hepatocellular carcinoma cells," *Oncology Reports*, vol. 23, no. 1, pp. 211–215, 2010.

[58] Y. Zhang, X. Liu, T. Zuo, Y. Liu, and J. H. Zhang, "Tetramethylpyrazine reverses multidrug resistance in breast cancer cells through regulating the expression and function of P-glycoprotein," *Medical Oncology*, vol. 29, no. 2, pp. 534–538, 2012.

[59] J. Fan, G. Xu, D. J. Nagel, Z. Hua, N. Zhang, and G. Yin, "A model of ischemia and reperfusion increases JNK activity, inhibits the association of BAD and 14-3-3, and induces apoptosis of rabbit spinal neurocytes," *Neuroscience Letters*, vol. 473, no. 3, pp. 196–201, 2010.

[60] M. Pozuelo-Rubio, "Proteomic and biochemical analysis of 14-3-3-binding proteins during C2-ceramide-induced apoptosis," *FEBS Journal*, vol. 277, no. 16, pp. 3321–3342, 2010.

[61] W. Huang, Y. Yang, Z. Zeng, M. Su, Q. Gao, and B. Zhu, "Effect of Salvia miltiorrhiza and ligustrazine injection on myocardial ischemia/reperfusion and hypoxia/reoxygenation injury," *Molecular Medicine Reports*, vol. 14, no. 5, pp. 4537–4544, 2016.

[62] K. Renu, V. G. Abilash, P. B. Tirupathi Pichiah, and S. Arunachalam, "Molecular mechanism of doxorubicin-induced cardiomyopathy - An update," *European Journal of Pharmacology*, vol. 818, pp. 241–253, 2018.

[63] S. Shabalala, C. J. F. Muller, J. Louw, and R. Johnson, "Polyphenols, autophagy and doxorubicin-induced cardiotoxicity," *Life Sciences*, vol. 180, pp. 160–170, 2017.

[64] D. B. Zorov, M. Juhaszova, and S. J. Sollott, "Mitochondrial ROS-induced ROS release: an update and review," *Biochimica et Biophysica Acta (BBA) - Bioenergetics*, vol. 1757, no. 5-6, pp. 509–517, 2006.

[65] N. R. Brady, A. Hamacher-Brady, H. V. Westerhoff, and R. A. Gottlieb, "A wave of reactive oxygen species (ROS)-induced ROS release in a sea of excitable mitochondria," *Antioxidants & Redox Signaling*, vol. 8, no. 9-10, pp. 1651–1665, 2006.

[66] J. J. Lemasters, A. L. Nieminen, T. Qian et al., "The mitochondrial permeability transition in cell death: a common mechanism in necrosis, apoptosis and autophagy," *Biochimica et Biophysica Acta (BBA) - Bioenergetics*, vol. 1366, no. 1-2, pp. 177–196, 1998.

[67] X. Tang, Y. X. Luo, H. Z. Chen, and D. P. Liu, "Mitochondria, endothelial cell function, and vascular diseases," *Frontiers in Physiology*, vol. 5, p. 175, 2014.

[68] A. Szewczyk, W. Jarmuszkiewicz, A. Koziel et al., "Mitochondrial mechanisms of endothelial dysfunction," *Pharmacological Reports*, vol. 67, no. 4, pp. 704–710, 2015.

Hindawi
Oxidative Medicine and Cellular Longevity
Volume 2019, Article ID 1805635, 19 pages
https://doi.org/10.1155/2019/1805635

Research Article

Polyphyllin VII Promotes Apoptosis and Autophagic Cell Death via ROS-Inhibited AKT Activity, and Sensitizes Glioma Cells to Temozolomide

Dejiang Pang,[1,2] **Chao Li**,[1,3] **Chengcheng Yang**,[1,3] **Yuanfeng Zou**,[3,4] **Bin Feng**,[5] **Lixia Li**,[3,4] **Wentao Liu**,[1,3] **Yi Geng**,[3] **Qihui Luo**,[1,3] **Zhengli Chen**,[1,3] **and Chao Huang**[1,3]

[1]*Laboratory of Experimental Animal Disease Model, College of Veterinary Medicine, Sichuan Agricultural University, Chengdu 611130, China*
[2]*Neuroscience & Metabolism Research, State Key Laboratory of Biotherapy, West China Hospital, Sichuan University and Collaborative Innovation Center, Chengdu 610041, China*
[3]*Key Laboratory of Animal Disease and Human Health of Sichuan Province, College of Veterinary Medicine, Sichuan Agricultural University, Chengdu 611130, China*
[4]*Natural Medicine Research Center, College of Veterinary Medicine, Sichuan Agricultural University, Chengdu 611130, China*
[5]*Animal Nutrition Institute, Sichuan Agricultural University, Chengdu 611130, China*

Correspondence should be addressed to Zhengli Chen; chzhli75@163.com and Chao Huang; huangchao@sicau.edu.cn

Dejiang Pang, Chao Li, and Chengcheng Yang contributed equally to this work.

Received 5 April 2019; Revised 7 July 2019; Accepted 23 September 2019; Published 14 November 2019

Guest Editor: Milica Pesic

The high recurrence frequency of gliomas but deficiency of effective treatment and prevalent chemoresistance have elicited interests in exploring and developing new agents. Paris polyphyllins are monomers extracted from rhizome of Paris polyphylla var. yunnanensis. Here, we first reported that polyphyllin VII (PP7) exhibited cytotoxic effect on glioma cells. PP7 significantly suppressed the viability and induced cell death of U87-MG and U251 cells after 24 h, with the IC50 values $4.24 \pm 0.87\,\mu$M and $2.17 \pm 0.14\,\mu$M, respectively. Both apoptotic and autophagic processes were involved in the cytotoxic effect of PP7, as PP7 activated the Bcl2/Bax pathway and the inhibition of autophagy partly rescued the toxicity of PP7 in glioma cells. In addition, an inhibition of AKT/mTORC1 activity was found after PP7 administration, and it seemed that the overproduction of reactive oxygen species (ROS) was responsible for this effect. Namely, the removal of ROS by NAC treatment mitigated PP7-induced cell death, autophagy, and its effect on the AKT/mTORC1 signaling. Additionally, a combination assay of PP7 with temozolomide (TMZ), the most used chemotherapy for glioma patients, was performed resulting in synergism, while PP7 reduced TMZ resistance through inhibition of MGMT expression. Thus, our study reports PP7 as a potential agent for glioma treatment and reveals its underlying mechanisms of action.

1. Introduction

Gliomas are the most common type of primary tumors in the brain, accounting for 30% of all brain and central nervous system tumors and 80% of all the malignant brain tumors [1]. The recurrence and mortality rates of gliomas are quite high, resulting in poor prognosis. Despite progresses in neurosurgery and radio- and chemotherapy, the fatality rate of glioma patients is still high according to recent reports [2, 3]. The median survival time of glioma patients is 12–15 months, the rate of high-grade glioma patients survival over 1 year is lower than 30%, and the 5-year survival rate after diagnosis is 5% [4, 5]. The alkylating agent temozolomide (TMZ) is the most used treatment for glioma after surgical resection and radiotherapy [4]. TMZ methylates DNA at the O^6 position of guanine, which may cause mismatch

pairing of guanines with thymines rather than cytosines resulting in hypermutation and genomic instability that finally leads to cell death [6]. However, the side effects of TMZ were widely reported, such as low white blood cell counts, fever, swollen gums, trouble breathing, and many others according to the Electronic Medicines Compendium (UK) [7, 8]. Previous data showed that TMZ-induced hypermutation was associated with drug resistance [9]. Therefore, mounting efforts need to be done to explore and develop more effective agents for the glioma treatment, or for to define new combined treatments with TMZ to reduce its side effects [10].

Polyphyllins are a class of saponins isolated from the rhizome of a traditional Chinese herb—Paris polyphylla var. yunnanensis (so-called Rhizoma paridis) [11]. Various polyphyllins have been identified by previous studies, including polyphyllin I (PPI), polyphyllin II (PPII), polyphyllin C (PPC), polyphyllin D (PPD), polyphyllin VI (PP6), and polyphyllin VII (PP7), and a wide range of pharmacological effects of these saponins were also reported, such as anti-inflammatory, immunity-enhancing, and especially antitumor activity [12, 13]. It has been demonstrated that PPI suppressed the proliferation rate of tumor cells, such as non-small-cell lung cancer cells, hepatocellular carcinoma cells, ovarian cancer cells, and osteosarcoma cells [14–17]. PPD inhibited growth of breast cancer cells in vitro and decreased the volume of xenografts formed by these cells [18]. Both PPI and PPD were able to increase the apoptosis of glioma cells [19, 20]. The mechanisms underlying the antitumor properties of polyphyllins are diverse, and previous studies have demonstrated that increased ROS production, autophagy, activated cell death processes, and disrupted cell cycle distribution contribute to the polyphyllin mechanisms of action probably in an associated manner [15, 21].

Polyphyllin VII (PP7) is an active pennogenyl saponin with larger molecular weight than other identified polyphyllins. Researchers have recently focused on its bioactivities in cancer treatment, and effective anticancer property of PP7 was found in liver, lung, breast, and colorectal cancer cells [21–24]. However, the anticancer activity of PP7 and its underlying mechanism against gliomas are still unexplored and not well defined. In this work, we aim to investigate the sensitivity of glioma cells to PP7 *in vitro*, evaluate the possibility of its combination with TMZ, and further reveal the molecular mechanisms behind these processes. Our study is aimed at displaying a new perspective for PP7 application in glioma treatment, which could be beneficial for glioma patients.

2. Materials and Methods

2.1. Reagents. PP7 was purchased from Chengdu Must Bio-Technology Co., Ltd. (Chengdu, China), and the purity of PPI was ≥98%. N-acetyl-L-cysteine (NAC) was purchased from Sigma-Aldrich (Merck KGaA, Darmstadt, Germany). Insulin-like growth factor 1 (IGF-1) and epidermal growth factor (EGF) were purchased from PeproTech (Rocky Hill, USA). 3-methyladenine (3-MA, S2767) and bafilomycin A1 (Baf-A1, S1413) were from Selleck Chemicals (Houston, TX, USA). TMZ was supplied by Tasly Pharmaceutical Co., Ltd. (Tianjin, China). The Cell Counting Kit-8 (CCK-8) was purchased from Dojindo Molecular Technologie (Kumamoto, Japan). Hoechst33342/PI kit, cell mitochondrial isolation kit, and dihydroethidium were supplied by Beyotime Institute of Biotechnology (Haimen, China).

2.2. Cell Culture. The glioma cell lines U87-MG and U251 were obtained from the Shanghai Institutes of Biological Sciences, Chinese Academy of Sciences (Shanghai, China). U87-MG and U251 cells were cultured in Dulbecco's modified Eagle's medium (DMEM; HyClone, GE Healthcare Life Sciences, Logan, UT, USA) supplemented with 10% fetal bovine serum (FBS; Gibco; Thermo Fisher Scientific, Inc., Waltham, MA, USA) and 1% penicillin-streptomycin (Invitrogen; Thermo Fisher Scientific, Inc., Waltham, MA, USA). Cells were maintained at 37°C in a humidified atmosphere (5% CO_2).

2.3. Cell Viability Assay. Cell viability was determined by CCK-8 assay as reported before [1]. The cells were seeded with a density of 5×10^3 cells/well in 96-well plates and incubated, at 37°C, in complete medium (DMEM with 10% FBS) with serial dilutions of PP7 for 24 h. CCK-8 was added to each well of the 96-well plate (CCK-8, plus fresh medium at a fixed ratio of 1 : 10, 100 μl/well), followed by further incubation for 1 h. The absorbance was measured at 450 nm using a microplate reader (Thermo Fisher Scientific, Inc.). The half-maximal inhibitory concentration (IC50), defined as the drug dose at which cell growth is inhibited by 50%, was measured using GraphPad Prism software version 5.0 (GraphPad Software, Inc., La Jolla, CA, USA). The formula was used as follows:

$$\text{Cell viability rate}\,(\%) = \frac{\text{Absorbance of test sample} - \text{Absorbance of blank}}{\text{Absorbance of control} - \text{Absorbance of blank}} \times 100\%. \quad (1)$$

2.4. Hoechst 33342/Propidium Iodide (PI) Staining. Hoechst 33342 and propidium iodide (PI) double staining were performed according to the manufacturer's instructions. Briefly, U87-MG or U251 glioma cells were plated in 12-well plates with a density of 5×10^4 cells/well and treated with PP7 at 37°C for 24 h. The cells were washed in PBS three times and incubated in Hoechst33342/propidium iodide (PI) solution (10 μg/ml) for 30 min at 4°C. Finally, fluorescence microscopy was used to observe the PI and Hoechst-positive signals of U87-MG or U251 glioma

cells in 15 nonoverlapping fields, and the cell death rate was calculated by the ration of PI-positive cells to Hoechst 33342-positive cells. For each treatment group, ≥1000 cells were analyzed in triplicate.

2.5. Reactive Oxygen Species (ROS) Detection. ROS assay kit purchased from Beyotime Institute of Biotechnology was used according to the manufacturer's instructions and previous report [25]. Dihydroethidium was prepared as a 10 mM solution. U251 and U87-MG glioma cells were treated with PP7 at 37°C for 24 h. Then, cells were incubated with 10 μM dihydroethidium (Eth) in DMEM at 37°C for 30 minutes. Finally, fluorescence microscopy was used to observe the ROS production of U251 glioma cells. The fluorescence intensity of Eth was analyzed by Image-Pro Plus software, and then the fluorescence intensity value of each experimental group was compared with the fluorescence intensity value of the control group to get a relative value and quantified by GraphPad Prism software version 5.0 (GraphPad Software, Inc., La Jolla, CA, USA).

2.6. Western Blotting Analysis. Western blotting was performed according to standard procedures as reported before [1]. To extract protein from cultured cells was sonicated in lysis buffer (2% SDS with proteinase inhibitors and phosphatase inhibitor). The protein concentration of each extract was measured using the BCA Protein Assay kit (Thermo Scientific Pierce). Equal amounts of protein from each extract were loaded into each lane of a gel and separated by SDS PAGE. The proteins were transferred onto PVDF membranes using standard procedures. The membranes were then blocked with 5% nonfat dry milk in TBST (TBS with 0.1% Tween 20, pH 7.6) for 1 hour at room temperature (RT) and incubated overnight with respected primary antibody at 4°C. After 3 washes with TBST at RT for 10 minutes each wash, the membranes were incubated 1 hour with a 1 : 10,000 dilution of appropriate secondary antibodies diluted in TBST at RT. The membranes were washed another 3 times with TBST at RT for 10 minutes each wash, proteins were then detected with ECL reagent (Thermo Scientific Pierce), and the membranes were exposed to film (Kodak). The antibodies in our experiments include Bax (Abcam, ab232479, 1 : 1000 dilution), Bcl-2 (Abcam, ab32124, 1 : 1000 dilution), caspase-3 (Abcam, ab197202, 1 : 1000 dilution), cleaved caspase-3 (Abcam, ab32042, 1 : 300 dilution), cytochrome C (Abcam, ab133504, 1 : 1000 dilution), prohibitin (Abcam, ab75766, 1 : 2000 dilution), AKT (Cell Signaling Technology, 9272S, 1 : 2000 dilution), pAKT (S473) (Cell Signaling Technology, 4060S, 1 : 2000 dilution), pAKT (T308) (Cell Signaling Technology, 2965S, 1 : 2000 dilution), pS6 (S240/244) (Cell Signaling Technology, 2215S, 1 : 2000 dilution), p4EBP1 (T37/46) (Cell Signaling Technology, 9459, 1 : 1000 dilution), pS6K (T389) (Cell Signaling Technology, 9205, 1 : 1000 dilution), SQSTM1/P62 (Abcam, ab91526, 1 : 2000 dilution), LC3B (Abcam, ab192890, 1 : 500 dilution), GAPDH (Millipore, MAB374, 1 : 2000 dilution), β-actin (Boster,BM0627, 1 : 1000 dilution), Goat anti-Rabbit IgG (H+L) Secondary Antibody (Pierce, 31460 1 : 10,000 dilution), and Goat anti-Mouse IgG (H+L) Secondary Antibody (Pierce, 31430 1 : 10,000 dilution). We used ImageJ software to quantitate western blots. Firstly, we measured the grey value of blots by using ImageJ. Secondly, normalized each sample using a normalizer (housekeeping protein such as GAPDH or β-actin, as mentioned above) and then the normalized value of each experimental group was compared with the normalized value of the control group to get a relative value. Finally, we used GraphPad software to make a histogram.

2.7. Cell Mitochondria Isolation. We used a cell mitochondrial isolation kit (Beyotime Biotechnology, C3601) for mitochondrial isolation of U87-MG cells and U251 cells. Firstly, we washed the cells with PBS, cells were harvested with trypsin-EDTA solution, centrifuged at 100-200 g for 5-10 minutes at room temperature, and the cells were collected. Secondly, we added 1-2.5 ml mitochondrial separation reagent per 20-50 million cells and then cells were gently suspended and placed on ice for 10-15 minutes. Thirdly, the cell suspension was transferred to a glass homogenizer of appropriate size, homogenizing the cells about 10-30 times. Fourthly, after homogenization, the cell suspension was centrifuged for 10 min at 600g at 4°C. Fifthly, the supernatant was carefully transferred to a new tube and centrifuged for 10 min at 11,000g at 4°C. The precipitate was the isolated mitochondria of the cells. Next, the supernatant was carefully transferred to a new tube and centrifuged for 10 min at 12,000 g at 4°C. The supernatant was the cytoplasmic protein that removed mitochondria. Both cytoplasmic protein and mitochondria were finally lysed for WB detection.

2.8. GFP-LC3 Puncta Imaging. We first constructed the GFP-LC3 vector. The cDNA encoding human LC3B (Gene ID: 81631) was obtained by PCR from U251 cDNA. Primer sequences used were as follows: LC3B forward, 5′-GCG TCG ACCA TGC CGT CGG AGA AGAC-3′ and reverse, 5′-GCG CGG CCG CTT ACA CTG ACA ATT TCAT-3′. The forward primers included Sal1 restriction endonuclease restriction site and the reverse primers included Not1 restriction endonuclease restriction site. Firstly, using U251 cDNA as template, LC3B coding sequences were cloned by adding Taq2x mix enzyme and a pair of primers in the PCR amplification system. Secondly, the PCR products were subjected to nucleic acid electrophoresis and LC3B cDNA were purified from the nucleic acid gel. Thirdly, LC3B cDNA and pEGFP-C1 vector were subjected to Sal1/Not1 double restriction enzyme digestion, and then the LC3B cDNA were inserted into the pEGFP-C1 vector by T4 DNA ligase. Fourthly, the ligation products of the previous step were transformed into *E. coli* competent cells, and then the clone was selected and the plasmid was extracted to obtain the GFP-LC3 plasmid. Finally, sequencing was performed to identify the plasmid.

U251 cells and U87-MG cells were seeded with a density of 2×10^5 cells/well in 12-well plates and incubated in complete medium (DMEM with 10% FBS) for overnight and then were transfected with GFP-LC3 plasmid using Lipofectamine™ 2000 (Invitrogen). Briefly, for each well of 12-well plates, we diluted 2 μg GFP-LC3 plasmid into 50 μl medium without serum in tube A and diluted 2 μl of Lipofectamine™

2000 into 50 μl medium without serum in tube B, and incubated for 5 min at room temperature. Then, we added 50 μl of the tube B to tube A, mixed gently, and incubated at room temperature for 20 min to allow DNA-Lipofectamine™ 2000 complexes to form. This DNA-Lipofectamine™ 2000 complex (100 μl) was added directly into each well of the plates containing cells and mixed gently. Twenty-four hours after transfection, corresponding treatments were performed for 8 h. Finally, fluorescence microscopy was preformed to observe the GFP-LC3 puncta of U251 glioma cells as described before [26]. The number of GFP-LC3B puncta per cells was assessed in 10 nonoverlapping fields and measured by Image-Pro Plus software, and then we calculated the average LC3 puncta per cells in these 10 nonoverlapping fields and made the graph by GraphPad Prism software. For the treatment of 3-MA, U251 and U87-MG cells were treated with PP7 (2 μM and 4 μM to U251 cells, 3 μM and 6 μM to U87-MG cells) for 8 h, 3-MA (5 mM) was added into U251 and U87-MG cells 3 hours after adding PP7, and then the puncta were evaluated. In CCK-8 assay, U251 and U87-MG cells were treated with PP7 (4 μM to U251 cells, 6 μM to U87-MG cells) alone or in combination with 3-MA (5 mM) for 24 h. For the treatment of bafilomycin A1, U251 and U87-MG cells were treated with PP7 (4 μM to U251 cells, 6 μM to U87-MG cells) alone or together with bafilomycin A1 (10 nM) for 24 h.

2.9. Real-Time PCR. Total RNA was extracted from the U251 cells and U87-MG cells using TRIzol reagent (Invitrogen; Thermo Fisher Scientific, Inc.), according to the manufacturer's instructions after being treated with indicated concentrations of PP7 or TMZ. In each group, 2 μg RNA was reverse transcribed into cDNA using the Revert Aid First Strand cDNA Synthesis kit (Thermo Fisher Scientific, Inc.) for RT-PCR as described before [1]. One microliter cDNA was added to a total volume of 20 μl. PCR amplification system qPCR was performed using the SYBR Premix Ex Taq™ II kit (Takara Biotechnology, Co., Ltd., Dalian, China). Relative fold levels were determined using GAPDH gene as normalizer control. The qPCR results were analyzed by Bio-Rad CFX Manager 3.0 software, and the normalized value of each experimental group was compared with the normalized value of the control group to get a relative value. Threshold cycle (Ct) values should be within the range mean ± 1 for each reference gene across all samples to ensure similar cDNA yield from each RT reaction. Primer sequences used were as follows: MGMT mRNA forward, 5′- ACC GTT TGC GAC TTG GTA CTT-3′ and reverse, 5′- GGA GCT TTA TTT CGT GCA GACC-3′. GAPDH mRNA forward, 5′- GGA GCG AGA TCC CTC CAA AAT -3′ and reverse, 5′- GGC TGT TGT CAT ACT TCT CAT GG -3′.

2.10. Statistical Analysis. Statistical evaluation was conducted using SPSS 19.0 (SPSS, Inc., Chicago, IL, USA) for Windows package software. Data from western blots, LC3 punctum quantifications are presented as the mean ± standard deviation, while the others are presented as mean ± standard error of mean. Differences among multiple groups were compared by one-way analysis of variance, and differences between two groups were compared by the Student t -test. $p < 0.05$ was considered to indicate a statistically significant difference.

3. Results

3.1. PP7 Decreases the Viability of U87-MG and U251 Cells. To evaluate the cytotoxic effect of PP7, two human glioma cell lines (U87-MG and U251) were exposed to PP7 at different concentrations for 12, 24, and 36 h before CCK-8 assay. As shown in Figures 1(a) and 1(b), cell viability of both U87-MG and U251 cells was suppressed by PP7, while the most pronounced dose-dependent effect was achieved after 24 h with IC50 values 4.24 μM ± 0.87 μM and 2.17 ± 0.14 μM, respectively. According to these IC50 values, concentrations of 3 μM and 6 μM PP7 for U87-MG cells, as well as 2 μM and 4 μM PP7 for U251 cells, were chosen for most of the following experiments. The decrease in cell viability of U87-MG and U251 cells after PP7 treatment resulted from cell death induction according to the experiments performed by Hoechst33342/propidium iodide (PI) double staining (Figures 1(c)–1(e)). To discriminate the cell death type, we analyzed the expression of Bcl-2 family proteins as well as cleaved caspase 3 and found that PP7 reduced the protein levels of Bcl-2, which was accompanied with an increase of Bax and cleaved caspase-3 levels in U87-MG and U251 cells (Figures 1(f)–1(k)). In addition, the sublocalizations of Bax and cytochrome C were compared between mitochondria and cytoplasm, showing significant enrichment of Bax in mitochondria while cytochrome C was more abundant in cytoplasm fraction (Figures 1(l)–1(o)). All these results demonstrated that PP7 decreased the viability of glioma cells is mediated by the induction of apoptosis.

3.2. PP7 Promotes Reactive Oxygen Species (ROS) Production in U87-MG and U251 Cells. Potential anticancer compounds able to promote ROS production in cancer cells have a good prospect for further preclinical investigations. In our study, we found significantly increased ROS accumulation in U87-MG and U251 cells after PP7 treatment, which was measured by fluorescent dihydroethidium (Eth) labeling (Figures 2(a) left, 2(b), and 2(c)). To study the relationship between ROS production and cytotoxic effect induced by PP7, we further performed ROS clearance with the common antioxidant N-acetylcysteine (NAC). As shown by Eth labeling, ROS accumulation was decreased after NAC treatment (Figures 2(a) right, 2(b), and 2(c)). In addition, significantly increased cell viability was detected by CCK-8 assay in U87-MG and U251 cells exposed to NAC/PP7 combined treatment (Figures 2(d) and 2(e)). These results indicated that overproduction of ROS was involved in PP7 cytotoxicity of glioma cells.

3.3. ROS Generated from PP7 Treatment Induces Autophagy in U87-MG and U251 Cells. To investigate whether the overproduction of ROS in PP7-treated glioma cells induced cellular autophagy, the protein levels of widely used autophagy markers—LC3 and SQSTM1 (p62)—were analyzed. In our study, SQSTM1 (p62) protein levels were significantly

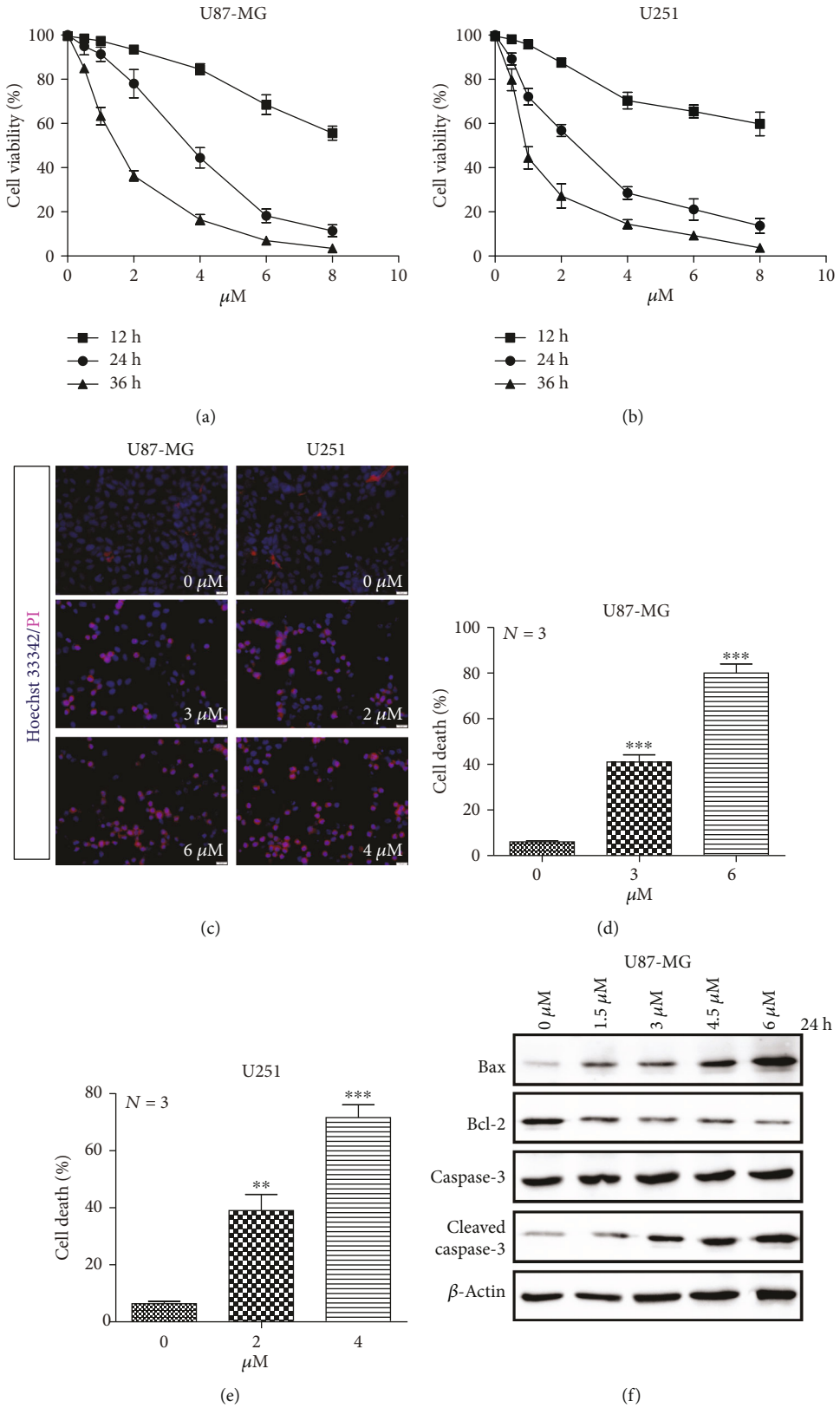

Figure 1: Continued.

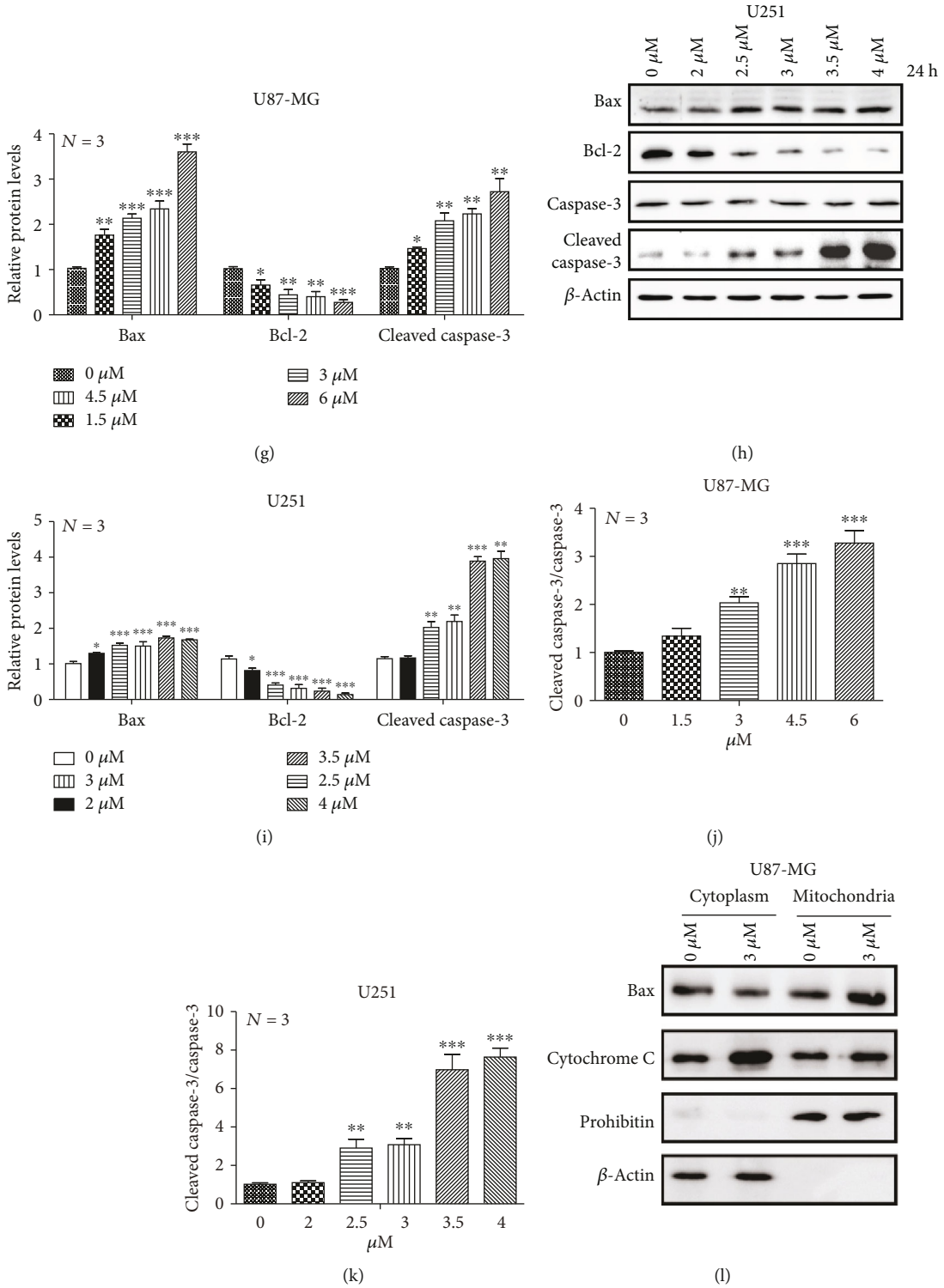

Figure 1: Continued.

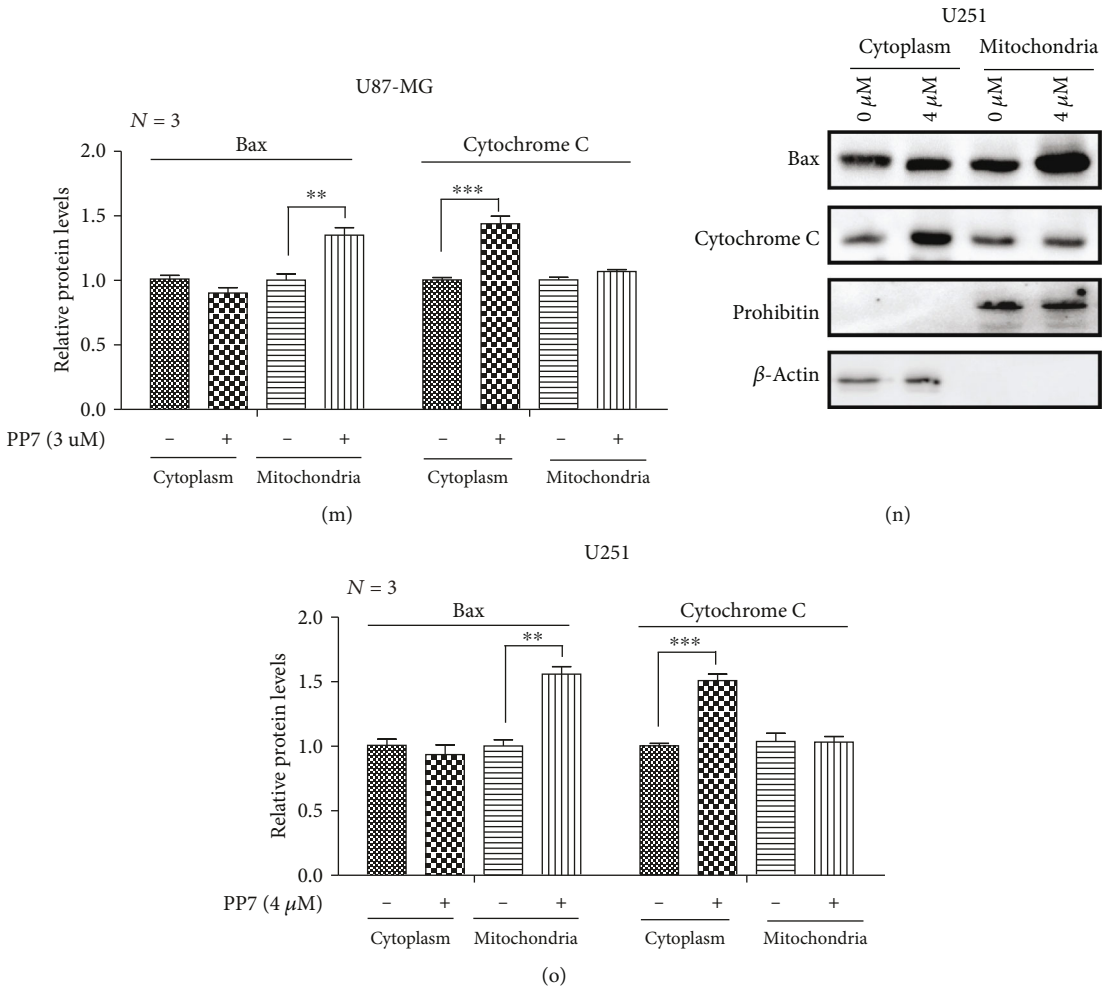

Figure 1: PP7 cytotoxicity in U87-MG and U251 cells. (a, b) The cell viability of U87-MG and U251 cells treated with different concentrations of PP7 was assessed after 12, 24, and 36 h. (c–e) Representative images and quantifications display increased cell death of U87-MG and U251 cells under PP7 treatment for 24 h, labeled with Hoechst33342/PI. Arrows indicate dead cells. (f, g) Western blots and their quantification show increased Bax and cleaved caspase-3 protein levels but decreased Bcl-2 levels in a dose-dependent manner in U87-MG cells and (h, i) in U251 cells. (j, k) Quantifications of the ratio of cleaved caspase-3 to total caspase-3 in U87-MG and U251 cells after PP7 treatment. (l, m) Western blots and their quantification show increased Bax protein levels in mitochondria as well as increased cytochrome C protein levels in cytoplasm after PP7 treatment in U87-MG cells and (n, o) in U251 cells. Prohibitin was selected as loading control for mitochondrial fraction, while β-actin was an internal control for the cytoplasmic fraction. Solvent controls are presented as 0 μM groups, while N stands for the repetition of experiments. $^{*}p < 0.05$, $^{**}p < 0.01$, $^{***}p < 0.001$.

reduced, while increased LC3 II/LC3 I ratio was observed in U251 and U87-MG cells under a series of PP7 increasing concentrations and at different time points (Figures 3(a)–3(l)). To further corroborate this finding, GFP-LC3 plasmids were transfected into U251 and U87-MG cells. We observed large amounts of fluorescent puncta formed in the cytoplasm of U87-MG and U251 cells after PP7 treatment, displaying the presence of LC3 conjugation that is considered as a hallmark event in the autophagic process (Figures 3(m) left and 3(n) left). These results indicated that PP7 indeed induces autophagy in glioma cells. To investigate the role of ROS in PP7-induced autophagy, we further performed the ROS clearance experiment with the administration of NAC. We found that the formation of GFP-LC3 puncta induced by PP7 could be easily suppressed by the treatment of NAC, suggesting that the PP7-stimulated ROS overproduction was implicated in the subsequent autophagic process (Figures 3(m) right, 3(n) right, 3(o), and 3(p)).

3.4. Autophagy Contributes to PP7 Cytotoxic Effect in Glioma Cells. To evaluate whether autophagy was also implicated in PP7-suppressed glioma cells viability, 3-methyladenine (3-MA) was applied as an autophagy inhibitor. We found that PP7-induced autophagy could be inhibited by 3-MA both in U87-MG and U251 cells, as shown by increased SQSTM1 (p62), decreased LC3II protein levels, and the decrease in LC3 II/LC3 I ratio (Figures 4(a)–4(f)). Moreover, significantly less LC3 puncta were observed in both glioma cell lines exposed to PP7 and 3-MA combined treatment (Figures 4(g)–4(i)). Most importantly, cytotoxicity induced by PP7 was partly rescued by 3-MA treatment in U87-MG and U251 cells (Figures 4(j) and 4(k)). To

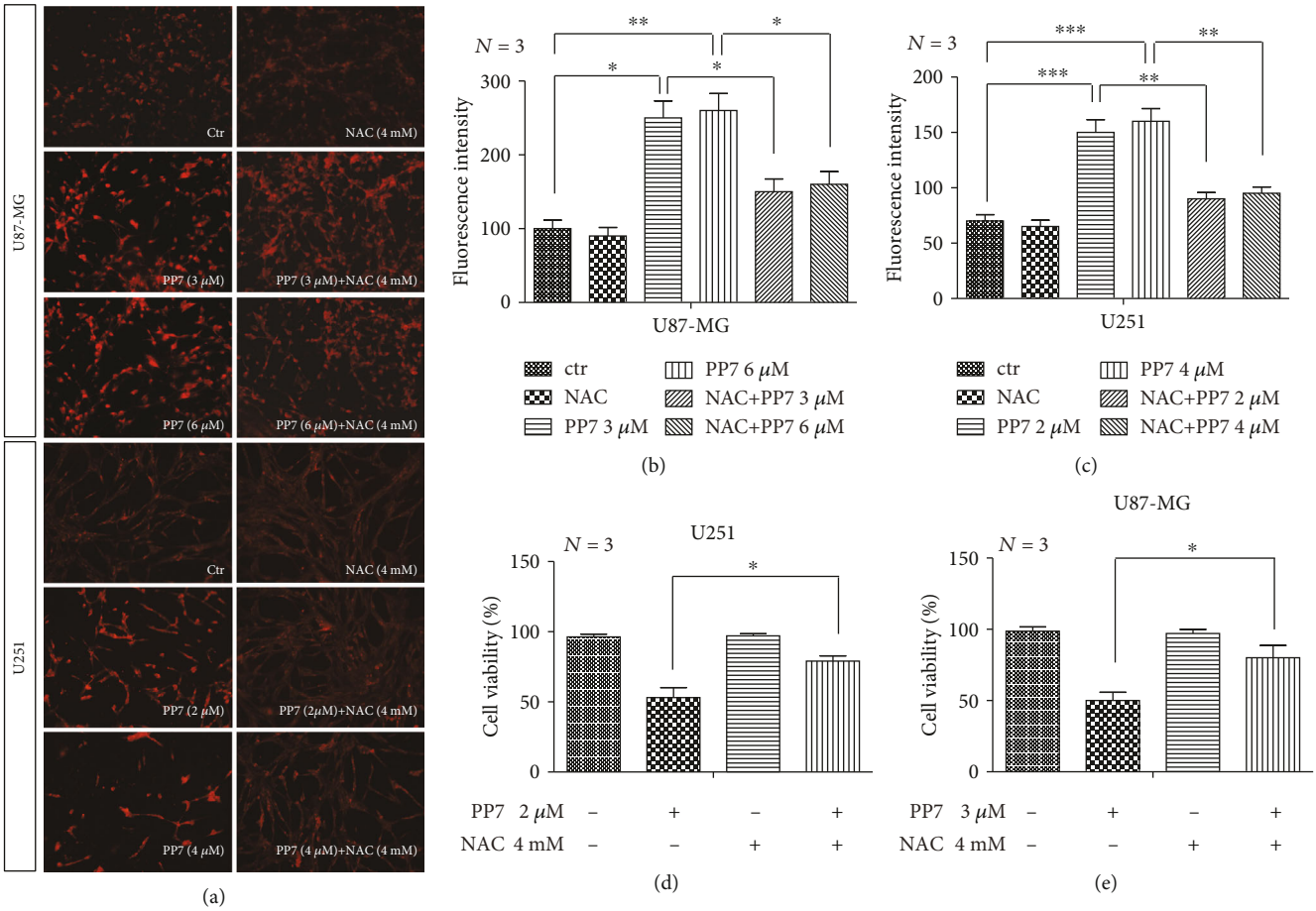

Figure 2: PP7 promotes ROS production in U87-MG and U251 cells. (a–c) Representative images and quantification analysis of PP7 effect on ROS production in U87-MG and U251 cells, assessed by dihydroethidium labeling (a, left) and clearance of ROS after NAC treatment (a, right). (d, e) Quantification of CCK-8 assay shows that NAC administration increases cell viability of PP7-treated U251 and U87-MG cells. Ctr represents cells treated with solvent, while N stands for the repetition of experiments. $^{*}p < 0.05$, $^{**}p < 0.01$, $^{***}p < 0.001$.

strengthen our observations, we further performed the experiments with another widely used autophagy inhibitor—bafilomycin A1 (Baf-A1) in U87-MG and U251 cells. The results showed that PP7 cytotoxic effect was also partly rescued by bafilomycin A1 treatment (Figures 4(l) and 4(m)). Therefore, the autophagic cell death, along with apoptosis, is involved in the antiglioma effect of PP7.

3.5. PP7 Inhibits the AKT/mTORC1 Signaling Pathway in U251 and U87-MG Cells. Taking into consideration that AKT promotes antiapoptotic and protumorigenic activities, we investigated the effect of PP7 on AKT activation. The treatment of U251 cells with PP7 resulted in a notable decreased phosphorylation levels of AKT, while the total levels of AKT remained unchanged, which suggested that PP7 suppresses the activity of AKT pathway (Figures 5(a) and 5(b)). Furthermore, we showed that suppressed AKT phosphorylation could be rescued by growth factors (IGF-1 and EGF) (Figures 5(c) and 5(d)). AKT signaling is involved in the regulation of mTORC1 activity; thus, the effect of PP7 on mTORC1 activity was further analyzed. We found that suppressed AKT activity after PP7 treatment caused the inhibition of the mTORC1 complex activity, as illustrated by the decreased phosphorylation levels of mTORC1 effectors, 4E-BP1, pS6K, and S6 (Figures 5(e) and 5(f)). In addition, we further evaluated the effects of PP7 on AKT/mTORC1 signaling in U87-MG cells and found the same pattern as in U251 cells (Figures 5(g) and 5(h)). In order to investigate whether the inhibitory response on AKT/mTORC1 signaling was also dependent on ROS, NAC was administrated in combination with PP7, resulting in recovered phosphorylation levels of both mTORC1 effectors and AKT (Figures 5(i) and 5(j)). Therefore, our work demonstrated that AKT/mTORC1 signaling pathway is involved in PP7 antiglioma effect.

3.6. Synergistic Cytotoxic Effect of PP7 and TMZ Combination in U251 and U87-MG Cells. Temozolomide (TMZ) is the main chemotherapy utilized for glioma treatment with serious side effects. Therefore, the agents that could secure the efficacy of TMZ when applied in combination and reduce its side effects due to the decreased effective dose will be valuable for glioma treatment. In order to evaluate the potential of PP7 in glioma treatment combined with TMZ, low ineffective concentrations of PP7 (0.2 μM and 0.4 μM for U251, 0.4 μM and 0.8 μM for U87-MG) were combined with

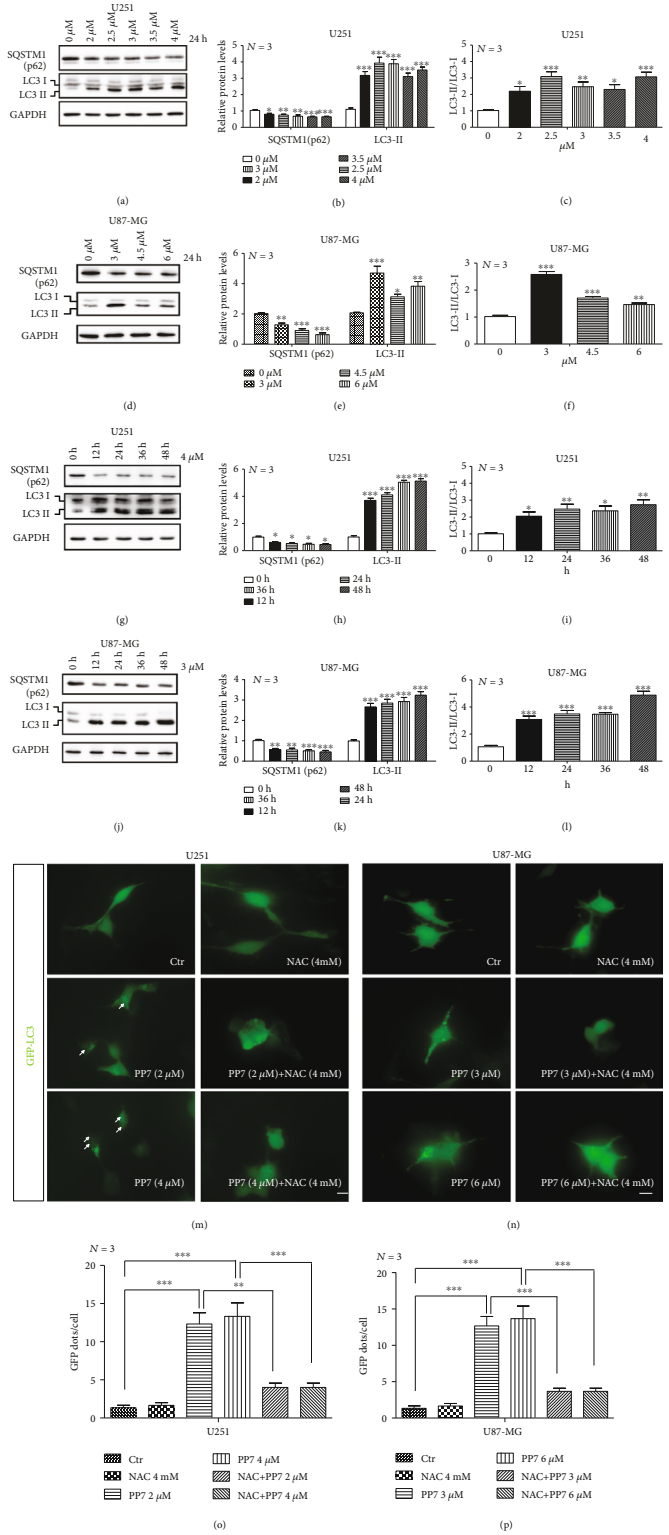

Figure 3: PP7 induces autophagy in U87-MG and U251 cells. (a–c) Western blots and their quantification show PP7 concentration-dependent decreased SQSTM1 (p62) protein levels and increased LC3II levels accompanied with the increase in LC3 II/LC3 I ratio in U251 cells as well as (d–f) in U87-MG cells. Solvent-treated cells are presented as the 0 μM control groups. (g–i) Western blots and their quantification show time-dependent decreased SQSTM1 (p62) protein levels and increased LC3II levels accompanied with the increase in LC3 II/LC3 I ratio in U251 cells treated with 4 μM PP7 as well as (j–l) in U87-MG cells treated with 3 μM PP7. (m–p) Representative images and quantification analysis display that PP7 promotes the formation of GFP-LC3 puncta in U251 and U87-MG cells, and this process could be inhibited by NAC treatment. Ctr stands for the cells treated with solvent. Arrows indicate the LC3 puncta. N stands for the repetition of experiments. $^{*}p < 0.05$, $^{**}p < 0.01$, $^{***}p < 0.001$.

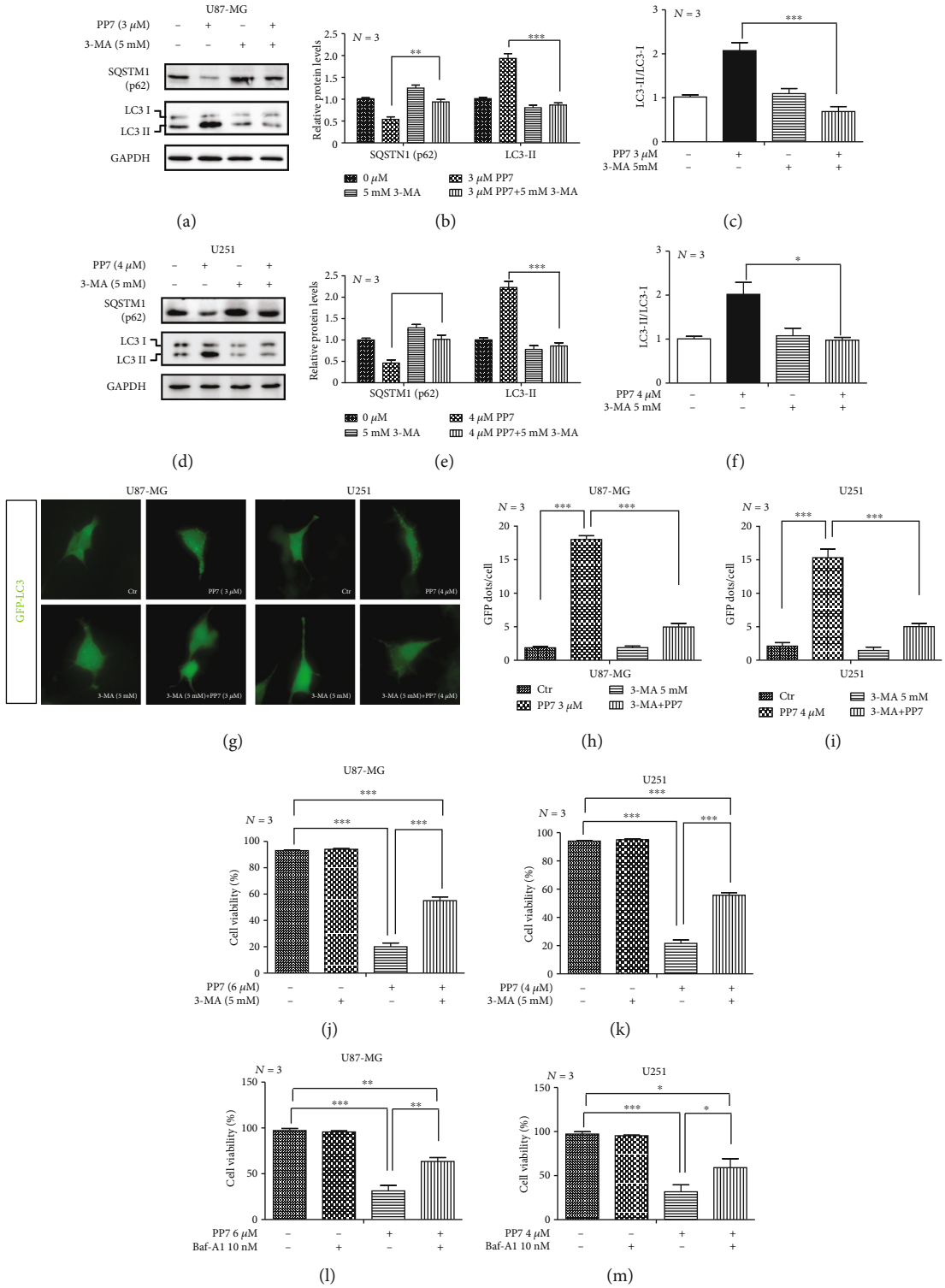

FIGURE 4: Autophagy is involved in the antiglioma effect of PP7. (a–c) Western blots and corresponding quantification analysis show the effect of 3-MA in respect to increased SQSTM1 (p62), decreased LC3II protein levels, and the decrease in LC3 II/LC3 I ratio in U87-MG cells and (d–f) in U251 cells. U87-MG and U251 cells were subsequently treated with 3 μM PP7 and 3 μM PP7, respectively, and with 5 mM 3-MA. 3-MA was added 3 h after adding PP7, while the overall treatment lasted 8 h. (g–i) Representative images and quantification analysis display decrease in LC3 puncta after PP7 and 3-MA combined treatment in U251 and U87-MG cells. Ctr represents cells treated only with solvent. (j, k) Cytotoxic effect induced by PP7 was partly rescued by 3-MA treatment in U87-MG and U251 cells. U87-MG and U251 cells were treated with 6 μM and 4 μM PP7, respectively, alone or in combination with 3-MA (5 mM) for 24 h. (l, m) Cytotoxic effect induced by PP7 was partly rescued by Baf-A1 treatment in U87-MG and U251 cells. U251 and U87-MG cells were treated with 4 μM and 6 μM PP7, respectively, alone or in combination with bafilomycin A1 (10 nM) for 24 h. *N* stands for the repetition of experiments. $^{*}p < 0.05$, $^{**}p < 0.01$, $^{***}p < 0.001$.

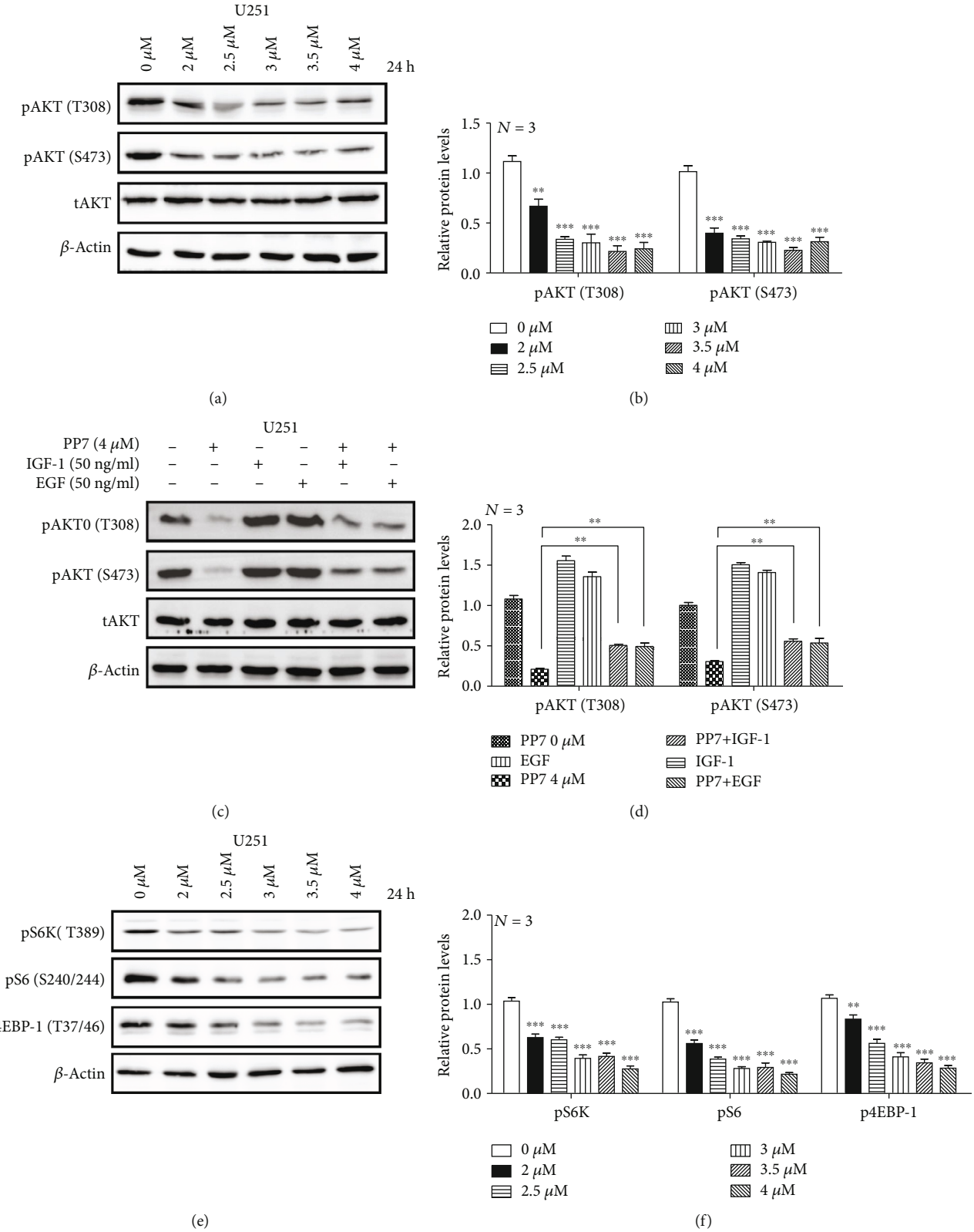

Figure 5: Continued.

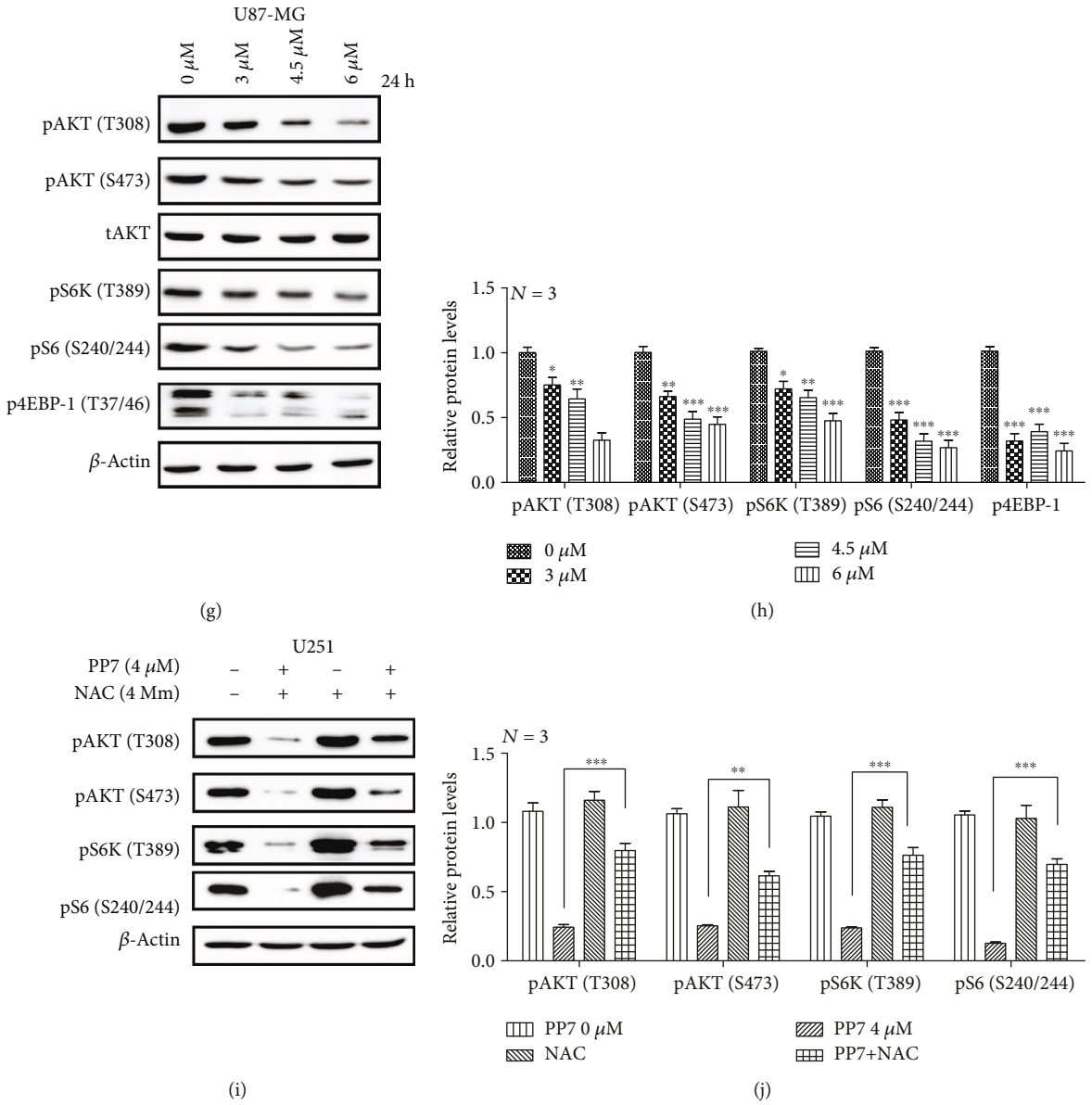

Figure 5: PP7 inhibits the AKT/mTORC1 pathway in U251 and U87-MG cells. (a, b) Western blots and corresponding quantification analysis show decreased phosphorylation levels of AKT in PP7-treated U251cells. Solvent-treated cells are presented as 0 μM control. (c, d) Western blots and corresponding quantification analysis show the effects of growth factors' application on phosphorylation levels of AKT after PP7 treatment in U251cells. (e, f) Western blots and corresponding quantification analysis show decreased phosphorylation levels of mTORC1 effectors, 4E-BP1, p70S6K, and S6, in U251 cells treated with PP7. (g, h) Western blots and corresponding quantification analysis show that PP7 inhibits the AKT/mTORC1 pathway in U87-MG. Solvent-treated cells are represented as 0 μM control. (i, j) Western blots and corresponding quantification show that the NAC administration recovers the phosphorylation levels of AKT and mTORC1 effectors induced by PP7 treatment in U251cells. N stands for the repetition of experiments. $^{**}p < 0.01$, $^{***}p < 0.001$.

different concentration gradients of TMZ, which displayed no statistically significant cytotoxicity to U251 and U87-MG cells (Figures 6(a), 6(b), 6(e), and 6(f)). The combined treatments lasted 24 h. We found that the combination of PP7 and TMZ significantly increased the cytotoxicity in U251 and U87-MG cells, especially when 0.4 μM PP7 were applied in combination with TMZ in U251 cells (Figures 6(c) and 6(d)) and 0.8 μM in U87-MG cells (Figures 6(g) and 6(h)). Besides, Hoechst 33342/PI staining confirmed the synergy of PP7 and TMZ in glioma cell death induction (0.4 μM PP7 with 90 μM for U251 and 0.8 μM PP7 with 150 μM for U87-MG) (Figures 6(i)–6(l)). These data indicated that even low concentrations of PP7 can increase the cytotoxicity of TMZ, which offers a broad application prospect for PP7.

3.7. PP7 Reduces TMZ Resistance in U251 and U87-MG Cells by Suppressing the Expression of MGMT. In addition to the

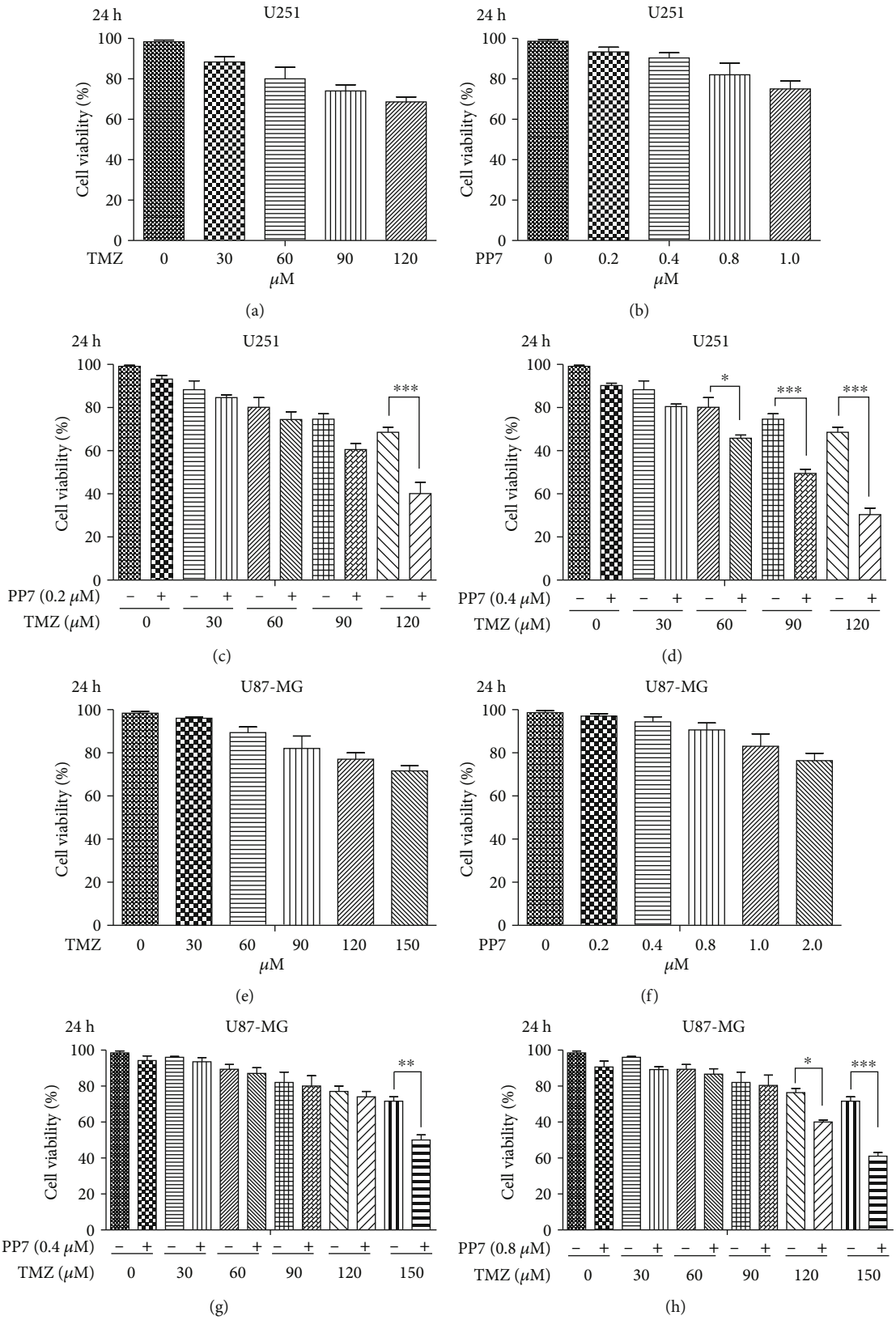

Figure 6: Continued.

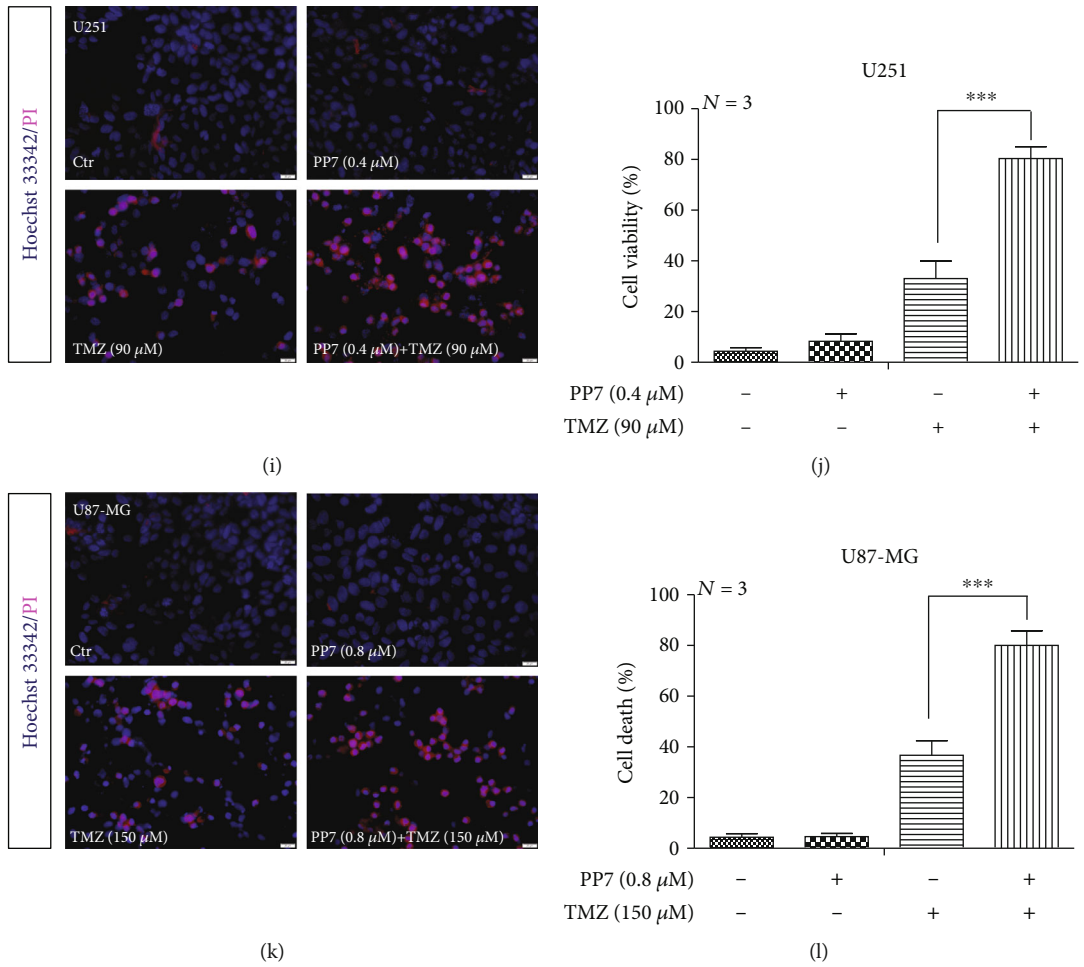

Figure 6: Synergistic cytotoxic effect of PP7 and TMZ combination in U251 and U87-MG cells. (a, b) Cell viability of U251 cells treated with ineffective concentrations of PP7 or TMZ separately for 24 h ($N = 3$). (c, d) Cell viability of U251 cells treated with combinations of PP7 and TMZ for 24 h ($N = 4$). (e, f) Cell viability of U87-MG cells treated with ineffective concentrations of PP7 or TMZ separately for 24 h ($N = 3$). (g, h) Cell viability of U87-MG cells treated with combinations of PP7 and TMZ for 24 h ($N = 4$). (i, j) Representative images and quantification analysis show that low concentration of PP7, combined with TMZ, induced cell death in U251 cells. Solvent controls are represented as 0 μM. $^{*}p < 0.05$, $^{***}p < 0.001$. (k, l) Representative images and quantification analysis show that low concentration of PP7, combined with TMZ, induced cell death in U87-MG cells. Solvent controls are represented as 0 μM. N stands for the repetition of experiments. $^{*}p < 0.05$, $^{***}p < 0.001$.

side effects, TMZ resistance resulting from abnormal expression of MGMT is also an important factor affecting the treatment of gliomas. In our study, we found the induction of MGMT expression in U251 and U87-MG cells after TMZ treatment, and this induction could be suppressed by the combined treatment of PP7 with TMZ (Figures 7(a)–7(d)). As the AKT pathway was proven to be involved in the transcriptional regulation of MGMT, we further investigated the effects of PP7 on AKT phosphorylation which was increased by TMZ treatment in U251 and U87-MG cells (Figures 7(e)–7(h)). These results suggested that drug resistance will be suppressed if PP7 is applied in combination with TMZ.

4. Discussions

PP7 has been reported to exhibit strong anticancer activities in some cancer types. Zhang et al. reported that PP7 induced HepG2 cells death through an inhibition of the PI3K/AKT/mTOR pathway [22], while Lin et al. found an induction of G2/M cell cycle arrest and apoptosis in PP7-treated lung cancer cells [21]. In glioma cells, polyphyllin D (PPD) has been reported to induce apoptosis in U87 cells through the JNK pathway [20], and PP1 has been reported to induce cell cycle arrest and apoptosis in U251 cells also via the JNK pathway [19]. However, the anticancer activity of PP7 in glioma cells and its mechanism have not been defined. In this present work, we displayed that PP7-induced ROS production suppressed the activity of AKT signaling to induce cell death in U251 and U87-MG cells. Apoptosis is one of the major cell death-related pathways, and Bcl-2 family is responsible for the release of proapoptotic factors, such as cytochrome C, to trigger mitochondria-related and caspase-3 dependent apoptosis [27]. Antiapoptotic Bcl-2 proteins (e.g., Bcl-2 and BCL-xL) function to directly bind and inhibit the proapoptotic BCL-2 proteins (e.g., Bax) [28].

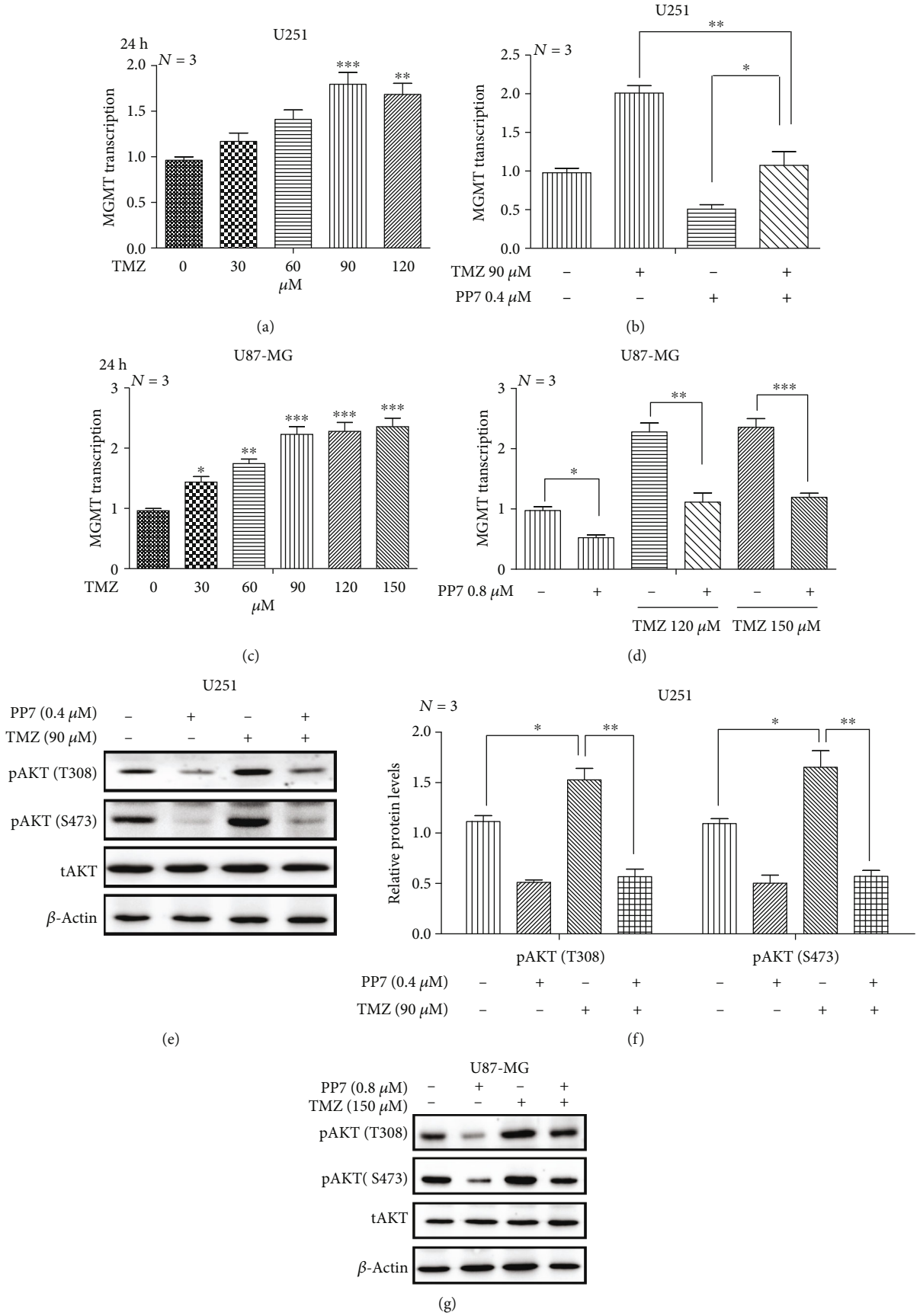

Figure 7: Continued.

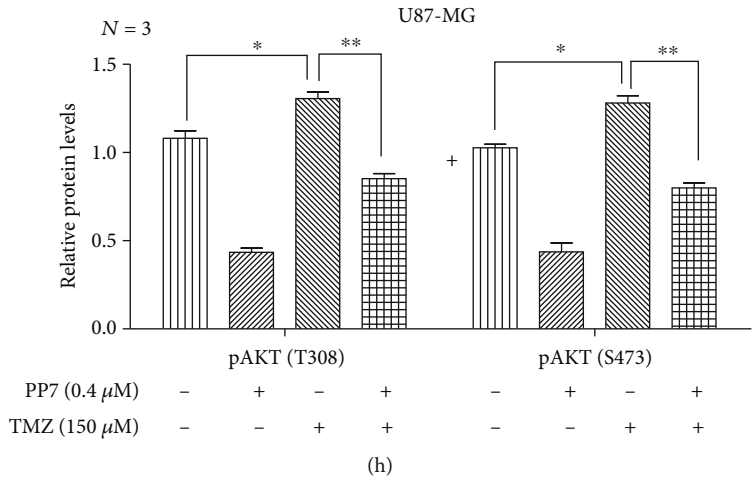

Figure 7: PP7 reduces TMZ resistance in U251 and U87-MG cells by suppressing the expression of MGMT. (a) Quantified mRNA expression of MGMT after TMZ treatment in U251 cells ($N = 3$). (b) PP7 suppresses the expression of MGMT induced by TMZ treatment in U251 cells ($N = 3$). (c) Quantified mRNA expression of MGMT after TMZ treatment in U87-MG cells ($N = 3$). (d) PP7 suppresses the expression of MGMT induced by TMZ treatment in U87-MG cells ($N = 3$). (e, f) Western blots and corresponding quantification analysis show that TMZ activates the phosphorylation of AKT, which could be inhibited by PP7 in U251 cells ($N = 3$). (g, h) Western blots and corresponding quantification show that TMZ activates the phosphorylation of AKT, which could be inhibited by PP7 in U87-MG cells ($N = 3$). Solvent controls are represented as 0 μM. N stands for the repetition of experiments. $^{*}p < 0.05$, $^{**}p < 0.01$, $^{***}p < 0.001$.

Autophagy is a regulated lysosomal pathway critical for the long-lived proteins and organelle degradation and recycling [29]. The roles of autophagy in cancers are complex, and controversial studies were published [30, 31]. However, lots of works supported an anticancer property for autophagy, as the autophagy gene Beclin-1 was proven to be a tumor suppressor, while the tumor suppressor genes p53 and PTEN were demonstrated to induce autophagy [32–34]. In our study, we found increased Bax levels, cytochrome C release, and induction of autophagy in PP7-treated glioma cells, which suggested that PP7-induced glioma cells death may be resulted from increased apoptosis and autophagic cell death. Meanwhile, the U251 cells were more sensitive to PP7 than U87-MG cells, which may be due to different expressions of critical genes between them. For example, U87-MG express WT p53, while U251 contained mutant p53, and the expression of glutathione S-transferase omega-1, a member of glutathione S-transferase super family that is implicated in the drug resistance of cancer cells, is higher in U87-MG cells than that in U251 cells [35, 36].

Physiologically, ROS are normal by-products generated from metabolic or enzymatic processes [1]. Compelling evidences have indicated that ROS function as a critical regulator not only in normal cells but also in many cancer cells for multiple cellular signaling pathways [1]. In order to keep high proliferation metabolic rates, cancer cells maintain much more ROS than normal ones. Although numerous physiological roles of ROS have been reported, especially as signaling molecules involved in cell growth, differentiation, and tumor progression. The redox balance in cancer cells is of critical importance, and excessive ROS accumulations are catastrophic for cancer cells [37]. Besides, the antitumor property of ROS has elicited interests in recent years. Researchers have reported that ROS were implicated in selective killing of cancer cells [38], but a clear understanding of the mechanisms underlying these processes is still elusive. The AKT/mTOR pathway plays a crucial role in regulating cellular proliferation, cell cycle, survival, and metabolism [39]. The impact of ROS on AKT/mTOR was widely investigated, yielding conflicting results. Some studies reported the amplification of AKT/mTOR activity by ROS through an inactivation of PTEN [40–42], whereas the others found that ROS were capable of modulating AKT itself with an inhibitory effect, especially under high doses [43–46]. In our study, we found the phosphorylation of AKT and mTORC1 downstream effectors were dramatically downregulated by PP7 administration, and this response could be reversed by NAC treatment. These results were in concert with the recent publications regarding negative redox regulation of AKT/mTORC1 and provided evidence that PP7 mediated AKT/mTORC1 inhibition via an ROS-dependent mechanism [43–46].

The relationship between autophagy and tumorigenesis has been well established. Autophagy could provide cancer cells with additional energy or nutrients in some specific periods, and it also functions as a cell death and tumor suppressor mechanism [47]. Although physiological level of autophagy is essential for cellular homeostasis maintenance under various stress conditions, excessive or uncontrolled level of that is able to induce autophagic cell death [30]. Furthermore, as different classifications of cell death, apoptosis and autophagic cell death display intricate interrelationships between each other. Under some conditions, synergetic effects of apoptosis and autophagy could be found, whereas in other situations, autophagy can be triggered only when apoptosis is suppressed, indicating that different types of cell death may develop concomitantly to response to different stress conditions [47, 48]. Meanwhile, the relationship between ROS accumulation and

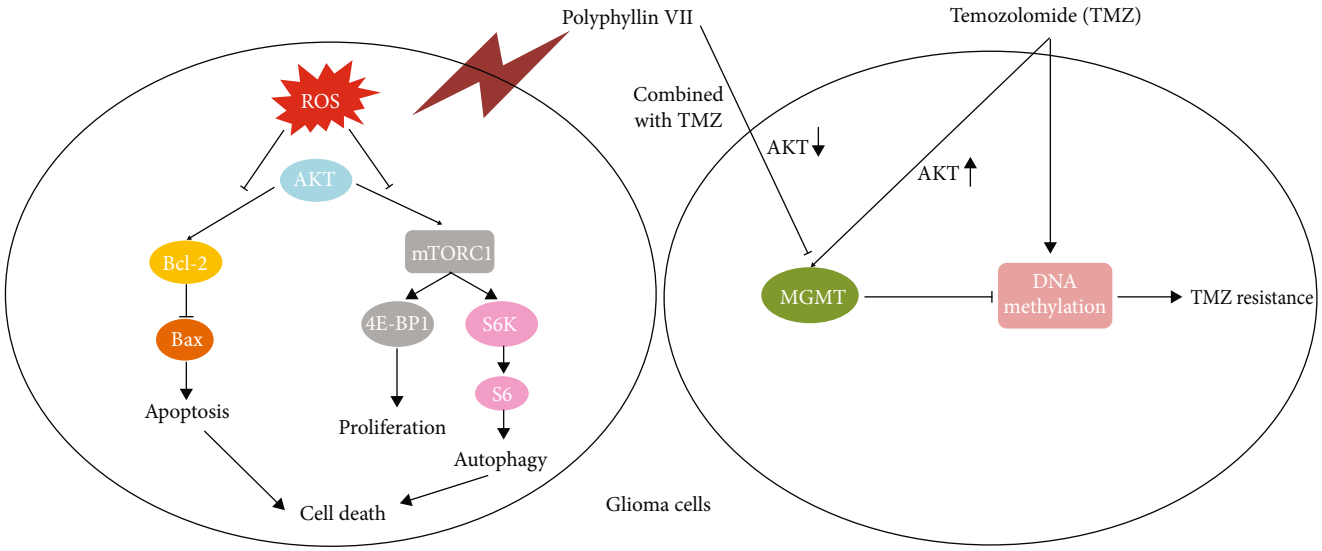

Figure 8: Schematic illustration of signals involved in cytotoxicity induced by PP7 (left) and by combination of PP7 with TMZ (right).

autophagy has been widely studied in the recent years, and it is believed that ROS are an important inducer of autophagy [29]. In our study, we found that PP7 could induce both apoptosis and autophagy in glioma cells, which was dependent on the generation of ROS. In addition to the coordination of energy, and growth signals, mTORC1 has been proven to modulate cellular autophagy [49]. Expectedly, the suppressed mTORC1 activity resulted in an induction of autophagy in glioma cells, as demonstrated by the accumulation of LC3 and decreased p62 levels in PP7-treated cells. Moreover, the LC3 accumulation was further proven by detection of autophagic puncta in GFP-LC3 transfected glioma cells treated with PP7. Our study also found that the cell death present in PP7-treated glioma cells could be partly rescued by 3-MA and Baf-A1, inhibitors of autophagy [50, 51], thus providing clear evidences for the autophagy role in PP7-induced glioma cell death.

Surgical resection, radiotherapy, and TMZ chemotherapy are the standard therapy for glioma patients, but seriously, side effects [52] and the resistance to TMZ due to the expression of MGMT resulted in limiting efficacy of this treatment. O^6 methylguanine-DNA methyltransferase (MGMT) is an enzyme that is able to transfer the methyl-adduct from O^6 guanine to cysteine residue, which effectively repair the DNA alteration in tumor cells prior to replication [53]. Therefore, the presence of MGMT is considered to be the main reason for the resistance of tumor cells to alkylating agents. Li et al. have previously demonstrated that TMZ could induce the transcription of MGMT in glioma cells [54]. Some MGMT inhibitors, such as PaTrin-2, O^6-benzylguanine, and streptozotocin, were analyzed in a combination treatment with TMZ, resulting in less activity of MGMT but with serious drug reactions or systematic toxicity [54–56]. Therefore, there is an urgent need to develop agents which combined with TMZ can inhibit the activity of MGMT and reduce the TMZ resistance. In the present study, PP7 was demonstrated to be efficient in a combination treatment with TMZ, by suppressing the expression of MGMT induced by TMZ treatment alone, and this effect may also through the modulating of AKT signaling, as AKT pathway was proven to be involved in the transcriptional regulation of MGMT [54, 57]. Our data suggested that the combination of PP7 with TMZ can be considered as an effective treatment for gliomas, but further works are still needed to prove the anti-glioma effect of PP7 *in vivo*.

In conclusion, we provide for the first-time evidence that PP7 capably induces cell death in glioma cells, through the induction of apoptosis and autophagic cell death via ROS-induced AKT/mTORC1 activity inhibition (Figure 8, left). Moreover, combined treatments of PP7 with TMZ resulted in more effective cytotoxicity and decreased MGMT expression, which can be foreseen as a strategy to attenuate the ability of glioma cells to repair the TMZ-induced DNA methylation and therefore reduce the resistance of TMZ (Figure 8, right). Thus, our results suggest a novel therapeutic strategy based on PP7 treatment in gliomas. However, limitations are still present. First, it is unclear how PP7 stimulates the generation of ROS in glioma cells. Then, further evidence needs to be provided to understand whether the combined usage of PP7 and TMZ is effective in other glioma cell lines.

Data Availability

The data used to support the findings of this study are available from the corresponding author upon request.

Conflicts of Interest

The authors declare that they have no conflicts of interest.

Authors' Contributions

Dejiang Pang, Chao Li, and Chengcheng Yang contributed equally to this work.

Acknowledgments

This research was supported by grants from the National Key Technology Support Program (2014BAI03B01 to Z.C) and in part by the National Natural Science Foundation of China (31501200 to C.H) and the Key Research Project from Sichuan Provincial Department of Education, China (16ZA0029 to C.H).

References

[1] J. Hu, X. Cao, D. Pang et al., "Tumor grade related expression of neuroglobin is negatively regulated by PPARγ and confers antioxidant activity in glioma progression," *Redox Biology*, vol. 12, pp. 682–689, 2017.

[2] K. Rock, O. McArdle, P. Forde et al., "A clinical review of treatment outcomes in glioblastoma multiforme—the validation in a non-trial population of the results of a randomised phase III clinical trial: has a more radical approach improved survival?," *The British Journal of Radiology*, vol. 85, no. 1017, pp. e729–e733, 2012.

[3] Y. Wang and T. Jiang, "Understanding high grade glioma: molecular mechanism, therapy and comprehensive management," *Cancer Letters*, vol. 331, no. 2, pp. 139–146, 2013.

[4] R. Stupp, W. P. Mason, M. J. van den Bent et al., "Radiotherapy plus concomitant and adjuvant temozolomide for glioblastoma," *The New England Journal of Medicine*, vol. 352, no. 10, pp. 987–996, 2005.

[5] Q. T. Ostrom, H. Gittleman, G. Truitt, A. Boscia, C. Kruchko, and J. S. Barnholtz-Sloan, "CBTRUS statistical report: primary brain and other central nervous system tumors diagnosed in the United States in 2011-2015," *Neuro-Oncology*, vol. 20, Supplement 4, pp. iv1–iv86, 2018.

[6] P. Daniel, S. Sabri, A. Chaddad et al., "Temozolomide induced hypermutation in glioma: evolutionary mechanisms and therapeutic opportunities," *Frontiers in Oncology*, vol. 9, p. 41, 2019.

[7] A. T. Faje, L. Nachtigall, D. Wexler, K. K. Miller, A. Klibanski, and H. Makimura, "Central diabetes insipidus: a previously unreported side effect of temozolomide," *The Journal of Clinical Endocrinology & Metabolism*, vol. 98, no. 10, pp. 3926–3931, 2013.

[8] E. M. Compendium, "Summary of product characteristics," in *Via Electronic Medicines Compendium (eMC)*, Datapharm, 2015, http://www.medicines.org.uk.

[9] R. J. Head, M. F. Fay, L. Cosgrove, K. Y. C. Fung, D. Rundle-Thiele, and J. H. Martin, "Persistence of DNA adducts, hypermutation and acquisition of cellular resistance to alkylating agents in glioblastoma," *Cancer Biology & Therapy*, vol. 18, no. 12, pp. 917–926, 2017.

[10] J. N. Sarkaria, G. J. Kitange, C. D. James et al., "Mechanisms of chemoresistance to alkylating agents in malignant glioma," *Clinical Cancer Research*, vol. 14, no. 10, pp. 2900–2908, 2008.

[11] Z. Liu, N. Li, W. Gao, S. Man, S. Yin, and C. Liu, "Comparative study on hemostatic, cytotoxic and hemolytic activities of different species of *Paris* L.," *Journal of Ethnopharmacology*, vol. 142, no. 3, pp. 789–794, 2012.

[12] D. Deng, D. Lauren, J. Cooney et al., "Antifungal saponins fromParis polyphyllaSmith," *Planta Medica*, vol. 74, no. 11, pp. 1397–1402, 2008.

[13] S. A. Shah, P. B. Mazumder, and M. D. Choudhury, "Medicinal properties of Paris polyphylla Smith: a review," *Journal of Herbal Medicine and Toxicology*, vol. 6, pp. 27–33, 2012.

[14] L. Li, J. J. Wu, F. Zheng, Q. Tang, W. Y. Wu, and S. S. Hann, "Inhibition of EZH2 via activation of SAPK/JNK and reduction of p65 and DNMT1 as a novel mechanism in inhibition of human lung cancer cells by polyphyllin I," *Journal of Experimental & Clinical Cancer Research*, vol. 35, no. 1, p. 112, 2016.

[15] Y.-M. Shi, L. Yang, Y.-D. Geng, C. Zhang, and L.-Y. Kong, "Polyphyllin I induced-apoptosis is enhanced by inhibition of autophagy in human hepatocellular carcinoma cells," *Phytomedicine*, vol. 22, no. 13, pp. 1139–1149, 2015.

[16] L. Gu, J. Feng, H. Xu, M. Luo, and D. Su, "Polyphyllin I inhibits proliferation and metastasis of ovarian cancer cell line HO-8910PM *in vitro*," *Journal of Traditional Chinese Medicine*, vol. 33, no. 3, pp. 325–333, 2013.

[17] J. Chang, H. Wang, X. Wang et al., "Molecular mechanisms of polyphyllin I-induced apoptosis and reversal of the epithelial-mesenchymal transition in human osteosarcoma cells," *Journal of Ethnopharmacology*, vol. 170, pp. 117–127, 2015.

[18] M. S. Lee, J. Y. W. Chan, S. K. Kong et al., "Effects of polyphyllin D, a steroidal saponin inParis polyphylla, in growth inhibition of human breast cancer cells and in xenograft," *Cancer Biology & Therapy*, vol. 4, no. 11, pp. 1248–1254, 2005.

[19] J. Liu, Y. Zhang, L. Chen et al., "Polyphyllin I induces G2/M phase arrest and apoptosis in U251 human glioma cells via mitochondrial dysfunction and the JNK signaling pathway," *Acta Biochimica et Biophysica Sinica*, vol. 49, no. 6, pp. 479–486, 2017.

[20] Q. Yu, Q. Li, P. Lu, and Q. Chen, "Polyphyllin D induces apoptosis in U87 human glioma cells through the c-Jun NH2-terminal kinase pathway," *Journal of Medicinal Food*, vol. 17, no. 9, pp. 1036–1042, 2014.

[21] Z. Lin, Y. Liu, F. Li et al., "Anti-lung cancer effects of polyphyllin VI and VII potentially correlate with apoptosis in vitro and in vivo," *Phytotherapy Research*, vol. 29, no. 10, pp. 1568–1576, 2015.

[22] C. Zhang, X. Jia, K. Wang et al., "Polyphyllin VII induces an autophagic cell death by activation of the JNK pathway and inhibition of PI3K/AKT/mTOR pathway in HepG2 cells," *PLoS One*, vol. 11, no. 1, 2016.

[23] D. X. He, G. H. Li, X. T. Gu et al., "A new agent developed by biotransformation of polyphyllin VII inhibits chemoresistance in breast cancer," *Oncotarget*, vol. 7, no. 22, pp. 31814–31824, 2016.

[24] L. Fan, Y. Li, Y. Sun et al., "Paris saponin VII inhibits metastasis by modulating matrix metalloproteinases in colorectal cancer cells," *Molecular Medicine Reports*, vol. 11, no. 1, pp. 705–711, 2015.

[25] L. Wei, Y. Zhou, C. Qiao et al., "Oroxylin A inhibits glycolysis-dependent proliferation of human breast cancer via promoting SIRT3-mediated SOD2 transcription and HIF1α destabilization," *Cell Death & Disease*, vol. 6, no. 4, p. e1714, 2015.

[26] H.-M. Ni, A. Bockus, A. L. Wozniak et al., "Dissecting the dynamic turnover of GFP-LC3 in the autolysosome," *Autophagy*, vol. 7, no. 2, pp. 188–204, 2011.

[27] T. Rossé, R. Olivier, L. Monney et al., "Bcl-2 prolongs cell survival after Bax-induced release of cytochrome *c*," *Nature*, vol. 391, no. 6666, pp. 496–499, 1998.

[28] J. E. Chipuk, G. P. McStay, A. Bharti et al., "Sphingolipid metabolism cooperates with BAK and BAX to promote the mitochondrial pathway of apoptosis," *Cell*, vol. 148, no. 5, pp. 988–1000, 2012.

[29] M. B. Azad, Y. Chen, and S. B. Gibson, "Regulation of autophagy by reactive oxygen species (ROS): implications for cancer progression and treatment," *Antioxidants & Redox Signaling*, vol. 11, no. 4, pp. 777–790, 2009.

[30] Y. Liu and B. Levine, "Autosis and autophagic cell death: the dark side of autophagy," *Cell Death & Differentiation*, vol. 22, no. 3, pp. 367–376, 2015.

[31] M. M. Hippert, P. S. O'Toole, and A. Thorburn, "Autophagy in cancer: good, bad, or both?," *Cancer Research*, vol. 66, no. 19, pp. 9349–9351, 2006.

[32] S. Arico, A. Petiot, C. Bauvy et al., "The tumor suppressor PTEN positively regulates macroautophagy by inhibiting the phosphatidylinositol 3-kinase/protein kinase B pathway," *Journal of Biological Chemistry*, vol. 276, no. 38, pp. 35243–35246, 2001.

[33] Z. Feng, H. Zhang, A. J. Levine, and S. Jin, "The coordinate regulation of the p53 and mTOR pathways in cells," *Proceedings of the National Academy of Sciences of the United States of America*, vol. 102, no. 23, pp. 8204–8209, 2005.

[34] Z. Yue, S. Jin, C. Yang, A. J. Levine, and N. Heintz, "Beclin 1, an autophagy gene essential for early embryonic development, is a haploinsufficient tumor suppressor," *Proceedings of the National Academy of Sciences of the United States of America*, vol. 100, no. 25, pp. 15077–15082, 2003.

[35] K. Camphausen, B. Purow, M. Sproull et al., "From the cover: influence of in vivo growth on human glioma cell line gene expression: convergent profiles under orthotopic conditions," *Proceedings of the National Academy of Sciences of the United States of America*, vol. 102, no. 23, pp. 8287–8292, 2005.

[36] H. Li, B. Lei, W. Xiang et al., "Differences in protein expression between the U251 and U87 cell lines," *Turkish Neurosurgery*, vol. 27, no. 6, pp. 894–903, 2017.

[37] M. Schieber and N. S. Chandel, "ROS function in redox signaling and oxidative stress," *Current Biology*, vol. 24, no. 10, pp. R453–R462, 2014.

[38] L. Raj, T. Ide, A. U. Gurkar et al., "Selective killing of cancer cells by a small molecule targeting the stress response to ROS," *Nature*, vol. 475, no. 7355, pp. 231–234, 2011.

[39] B. D. Manning and L. C. Cantley, "AKT/PKB signaling: navigating downstream," *Cell*, vol. 129, no. 7, pp. 1261–1274, 2007.

[40] S. Yalcin, D. Marinkovic, S. K. Mungamuri et al., "ROS-mediated amplification of AKT/mTOR signalling pathway leads to myeloproliferative syndrome in Foxo3$^{-/-}$ mice," *The EMBO Journal*, vol. 29, no. 24, pp. 4118–4131, 2010.

[41] C. T. Shearn, R. L. Smathers, B. J. Stewart et al., "Phosphatase and tensin homolog deleted on chromosome 10 (PTEN) inhibition by 4-hydroxynonenal leads to increased Akt activation in hepatocytes," *Molecular Pharmacology*, vol. 79, no. 6, pp. 941–952, 2011.

[42] P. Chiarugi, "ReviewPTPs versus PTKs: the redox side of the coin," *Free Radical Research*, vol. 39, no. 4, pp. 353–364, 2005.

[43] H. Murata, Y. Ihara, H. Nakamura, J. Yodoi, K. Sumikawa, and T. Kondo, "Glutaredoxin exerts an antiapoptotic effect by regulating the redox state of Akt," *Journal of Biological Chemistry*, vol. 278, no. 50, pp. 50226–50233, 2003.

[44] P. Makhov, K. Golovine, E. Teper et al., "Piperlongumine promotes autophagy via inhibition of Akt/mTOR signalling and mediates cancer cell death," *British Journal of Cancer*, vol. 110, no. 4, pp. 899–907, 2014.

[45] C. T. Shearn, K. S. Fritz, P. Reigan, and D. R. Petersen, "Modification of Akt2 by 4-hydroxynonenal inhibits insulin-dependent Akt signaling in HepG2 cells," *Biochemistry*, vol. 50, no. 19, pp. 3984–3996, 2011.

[46] M. Li, L. Zhao, J. Liu et al., "Multi-mechanisms are involved in reactive oxygen species regulation of mTORC1 signaling," *Cellular Signalling*, vol. 22, no. 10, pp. 1469–1476, 2010.

[47] D. Gozuacik and A. Kimchi, "Autophagy as a cell death and tumor suppressor mechanism," *Oncogene*, vol. 23, no. 16, pp. 2891–2906, 2004.

[48] L. Ouyang, Z. Shi, S. Zhao et al., "Programmed cell death pathways in cancer: a review of apoptosis, autophagy and programmed necrosis," *Cell Proliferation*, vol. 45, no. 6, pp. 487–498, 2012.

[49] J. A. Martina, Y. Chen, M. Gucek, and R. Puertollano, "MTORC1 functions as a transcriptional regulator of autophagy by preventing nuclear transport of TFEB," *Autophagy*, vol. 8, no. 6, pp. 903–914, 2012.

[50] Y.-T. Wu, H.-L. Tan, G. Shui et al., "Dual role of 3-methyladenine in modulation of autophagy via different temporal patterns of inhibition on class I and III phosphoinositide 3-kinase," *Journal of Biological Chemistry*, vol. 285, no. 14, pp. 10850–10861, 2010.

[51] M. Redmann, G. A. Benavides, T. F. Berryhill et al., "Inhibition of autophagy with bafilomycin and chloroquine decreases mitochondrial quality and bioenergetic function in primary neurons," *Redox Biology*, vol. 11, pp. 73–81, 2017.

[52] G. P. Margison, M. F. Santibanez Koref, and A. C. Povey, "Mechanisms of carcinogenicity/chemotherapy by O6-methylguanine," *Mutagenesis*, vol. 17, no. 6, pp. 483–487, 2002.

[53] C. H. Fan, W. L. Liu, H. Cao, C. Wen, L. Chen, and G. Jiang, "O^6-methylguanine DNA methyltransferase as a promising target for the treatment of temozolomide-resistant gliomas," *Cell Death & Disease*, vol. 4, no. 10, 2013.

[54] M. Li, R. F. Liang, X. Wang, Q. Mao, and Y. H. Liu, "BKM120 sensitizes C6 glioma cells to temozolomide via suppression of the PI3K/Akt/NF-κB/MGMT signaling pathway," *Oncology Letters*, vol. 14, no. 6, pp. 6597–6603, 2017.

[55] J. A. Quinn, S. X. Jiang, D. A. Reardon et al., "Phase II trial of temozolomide plus o6-benzylguanine in adults with recurrent, temozolomide-resistant malignant glioma," *Journal of Clinical Oncology*, vol. 27, no. 8, 1267 pages, 2009.

[56] M. Turriziani, P. Caporaso, L. Bonmassar et al., "O^6-(4-bromothenyl)guanine (PaTrin-2), a novel inhibitor of O^6-alkylguanine DNA alkyl-transferase, increases the inhibitory activity of temozolomide against human acute leukaemia cells in vitro," *Pharmacological Research*, vol. 53, no. 4, pp. 317–323, 2006.

[57] L.-H. Zhang, A.-A. Yin, J.-X. Cheng et al., "TRIM24 promotes glioma progression and enhances chemoresistance through activation of the PI3K/Akt signaling pathway," *Oncogene*, vol. 34, no. 5, pp. 600–610, 2015.

Hindawi
Oxidative Medicine and Cellular Longevity
Volume 2019, Article ID 9165784, 13 pages
https://doi.org/10.1155/2019/9165784

Research Article

An Evaluation of the DNA-Protective Effects of Extracts from *Menyanthes trifoliata* L. Plants Derived from *In Vitro* Culture Associated with Redox Balance and Other Biological Activities

Tomasz Kowalczyk,[1] **Przemysław Sitarek**,[2] **Ewa Skała**,[2] **Patricia Rijo**,[3,4] **Joana M. Andrade**,[3] **Ewelina Synowiec**,[5] **Janusz Szemraj**,[6] **Urszula Krajewska**,[7] **and Tomasz Śliwiński**[5]

[1]*Department of Molecular Biotechnology and Genetics, University of Lodz, Banacha 12/16, 90-237 Lodz, Poland*
[2]*Department of Biology and Pharmaceutical Botany, Medical University of Lodz, Muszynskiego 1, 90-151 Lodz, Poland*
[3]*Center for Research in Biosciences and Health Technologies (CBIOS), Universidade Lusófona de Humanidades e Tecnologias, 1749-024 Lisbon, Portugal*
[4]*Instituto de Investigação do Medicamento (iMed.ULisboa), Faculdade de Farmácia, Universidade de Lisboa, 1649-003 Lisbon, Portugal*
[5]*Laboratory of Medical Genetics, Faculty of Biology and Environmental Protection, University of Lodz, Pomorska 141/143, 90-236 Lodz, Poland*
[6]*Department of Medical Biochemistry, Medical University of Lodz, Mazowiecka 6/8, 92-215 Lodz, Poland*
[7]*Department of Pharmaceutical Biochemistry, Molecular Biology Laboratory, Medical University of Lodz, Muszynskiego 1, 90-151 Lodz, Poland*

Correspondence should be addressed to Tomasz Kowalczyk; tomasz.kowalczyk@biol.uni.lodz.pl

Received 4 March 2019; Accepted 24 August 2019; Published 16 October 2019

Academic Editor: Gabriele Saretzki

Menyanthes trifoliata L. is a valuable medical plant found in Europe, North America, and Asia, which grows on peat bogs and swamps. It has long been used in folk medicine as a remedy for various ailments. This is the first report to demonstrate the protective antioxidant and anti-inflammatory properties of aqueous methanolic extracts derived from the aerial parts (MtAPV) and roots (MtRV) of *in vitro* grown plants on human umbilical vein endothelial cells (HUVECs). It describes the influence of the tested extracts on the expression of antioxidant (HO-1, NQO1, *NRF2*, *kEAP1*, and *GCLC*) and inflammation-related genes (*IL-1α*, *IL-1β*, *IL-6*, *TNF-α*, and *IFN-γ*) in cells stimulated with H_2O_2 or LPS, respectively. In addition, *M. trifoliata* extracts were found to moderately affect the growth of certain bacterial and fungal pathogens, with the strongest antibacterial effect found against *Pseudomonas aeruginosa* and *Enterococcus faecalis*. *M. trifoliata* extracts demonstrated protective effects against mitochondrial DNA (mtDNA) and nuclear DNA (nDNA) damage caused by ROS, decreasing the numbers of mtDNA lesions in the *ND1* and *ND2* genes and nDNA damage in the *TP53* and *HPRT1* genes and reducing cleavage in PARP1- and γ-H2A.X-positive cells. The root extract of *in vitro M. trifoliata* (MtRV) appears to have better anti-inflammatory, antioxidant, antimicrobial, and protective properties than the extract from the aerial part (MtAPV). These differences in biological properties may result from the higher content of selected phenolic compounds and betulinic acid in the MtRV than in the MtAPV extract.

1. Introduction

Health-promoting properties of plants have been used in the prevention and therapy of many human diseases for thousands of years. Currently, it is estimated that 300,000 plant species exist worldwide [1]; however, relatively few have confirmed therapeutic or protective properties. Fortunately, modern methods and equipment allow much faster and

more accurate analyses of the resources hidden in plants. It is well known that they synthesize a large number of metabolites which play important roles, including defense against herbivores, other plants, or pathogens, and some can be successfully used in general health care [2–5]. One such group of extremely valuable plant secondary metabolites is the polyphenols, which allow the plant to respond to stress agents. When assimilated through the diet in fruits, vegetables, tea, or medicinal and culinary herbs, these natural compounds play a key role in the antioxidant protection of the human body and are believed to have a significant impact on reducing the risk of cancer or cardiovascular disease [6]. Therefore, there is a need to identity rich sources of these compounds in nature and study their biological properties.

Menyanthes trifoliata L., Menyanthaceae, offers a lot of promise. This medicinal plant, commonly known as Bogbean, occurs in the northern hemisphere, mainly in the circumpolar temperate zone of Europe, North America, and Asia [7]. In traditional and folk medicine, its leaves are used to treat lack of appetite, scurvy, fevers, and skin disorders. Extracts obtained from *in vitro* cultures of this plant have also been found to induce apoptosis in glioma cells [8]. Studies have examined the biological properties of its metabolites [9, 10], and their results indicate that *M. trifoliata* is a source of phenolics or flavonols [11], some of which, such as phenolic acids, scopoletin, rutin, or loganin, may have potential medical applications [12–14].

The aim of this work is to determine the antioxidant, anti-inflammatory, antimicrobial, and DNA-protective effects of the aerial part and root extracts from *Menyanthes trifoliata* plants grown in *in vitro* culture on Schenk and Hildebrandt (SH) medium together with various other biological properties.

2. Materials and Methods

2.1. Plant Material. *In vitro* shoots of *M. trifoliata* were established from seeds as described previously [8]. In the present study, young leaves, roots, and stems were used for shoot regeneration. The explants were cultured on 0.8% agar-solidified Schenk and Hildebrandt (SH) medium supplemented with 1.0 mg/L 6-benzyladenine (6-BA) and 0.1 mg/L α-naphthaleneacetic acid (NAA) under the following conditions: 16/8-hour light/dark photoperiod; light intensity, 40 μmol m^{-2} s^{-1}; and temperature, 26°C. Light green calli were observed after 14 days on the surface of explants; these were then transferred to SH medium with 4.0 mg/L 6-BA and 0.3 mg/L NAA for shoot induction. After four weeks, the shoots obtained from calli were transferred to SH rooting medium supplemented with 0.3 mg/L 6-BA and 1.0 mg/L NAA. After two weeks, rooted young plants were transferred to solid SH medium without growth regulators and cultured under the conditions described above. In *M. trifoliata in vitro*, propagation steps are shown in Figures 1(a)–1(d).

2.2. M. trifoliata Aerial Part and Root Extract Preparation. The plant extracts from aerial parts and roots of *M. trifoliata* plants grown *in vitro* were prepared according to Sitarek et al. [15]. Briefly, 10 g of dry weight of aerial parts and roots was used for extraction. The plant material was extracted for 15 minutes with 80% (*v*/*v*) aqueous methanol (500 mL) at 35°C using an ultrasonic bath and then for 15 minutes with 300 mL of the same solvent. Finally, the extracts were filtered, evaporated under reduced pressure, lyophilized to dryness, and then kept dry in the dark until further use. The yields (*w*/*w*) of the extracts were 52.8% and 50.4% of initial plant dry weight for aerial parts (MtAPV) and roots (MtRV) of *M. trifoliata* plants, respectively.

2.3. Phytochemical Analysis of Extracts of M. trifoliata Aerial Parts and Roots. The phenolic compounds and betulinic acid were examined in MtAPV and MtRV extracts by HPLC (Dionex, Sunnyvale, USA) according to Kowalczyk et al. [8].

2.4. Cell Cultures. All experiments were performed on human umbilical vein endothelial cells (HUVECs). These cells were purchased from Gibco (Cascade Biologics®, catalog number C0035C) and cultured in Medium 200 (Gibco, catalog number M-200-500) supplemented with Low Serum G Growth Supplement Kit (LSGS Kit; Gibco, catalog number S003K) at 37°C and 5% CO_2 in an incubator (Galaxy® 170 R-CO_2 Incubator, New Brunswick Scientific) under a humidified atmosphere.

2.5. Cell Viability. The MTT assay was employed to measure the viability of HUVECs treated with different concentrations of LPS or H_2O_2 and the MtRV and MtAPV extracts of *M. trifoliata* plants grown *in vitro*. Briefly, cells were seeded at 1×10^4 cells per well in 96-well culture plates and were left overnight before being treated for attachment. The cells were incubated for 24 hours with MtRV and MtAPV extracts over the concentration ranges 0-5 mg/mL. The inflammatory process was initiated with 1 μg/mL LPS, and separately, the antioxidant response was stimulated with 50 μM H_2O_2. In the next experiment, the cells were incubated with 1 mg/mL MtRV and MtAPV extracts or pretreated with LPS or H_2O_2 for one hour and then treated with plant extracts for 24 hours. After completing the incubation, the cells were washed once and incubated with 0.5 mg/mL of 3-(4,5-dimethylthiazol-2-yl)-2,5-diphenyl tetrazolium bromide (MTT) at 37°C for four hours. The MTT was then carefully removed and DMSO (100 μL) added to each well. The mixture was vortexed at low speed for five minutes to fully dissolve the blue crystals. Absorbance was measured at 570 nm with a reference at 630 nm using a BioTek Synergy HT Microplate Reader (BioTek Instruments, Winooski, VT, USA). Independent experiments were repeated in triplicate. Cell viability was expressed as a percentage relative to the untreated (control) cells, which was defined as 100%.

2.6. Gene Expression. HUVECs were first incubated in the presence of LPS or H_2O_2 for one hour and then with 1 mg/mL MtRV and MtAPV extracts for 24 hours. Total RNA was then extracted using an ISOLATE II RNA Mini Kit, according to the manufacturer's instructions. cDNA was synthesized from total RNA using a High-Capacity cDNA Reverse Transcription Kit. A sample of 1 ng total RNA was used as a template in a total volume of 10 μL,

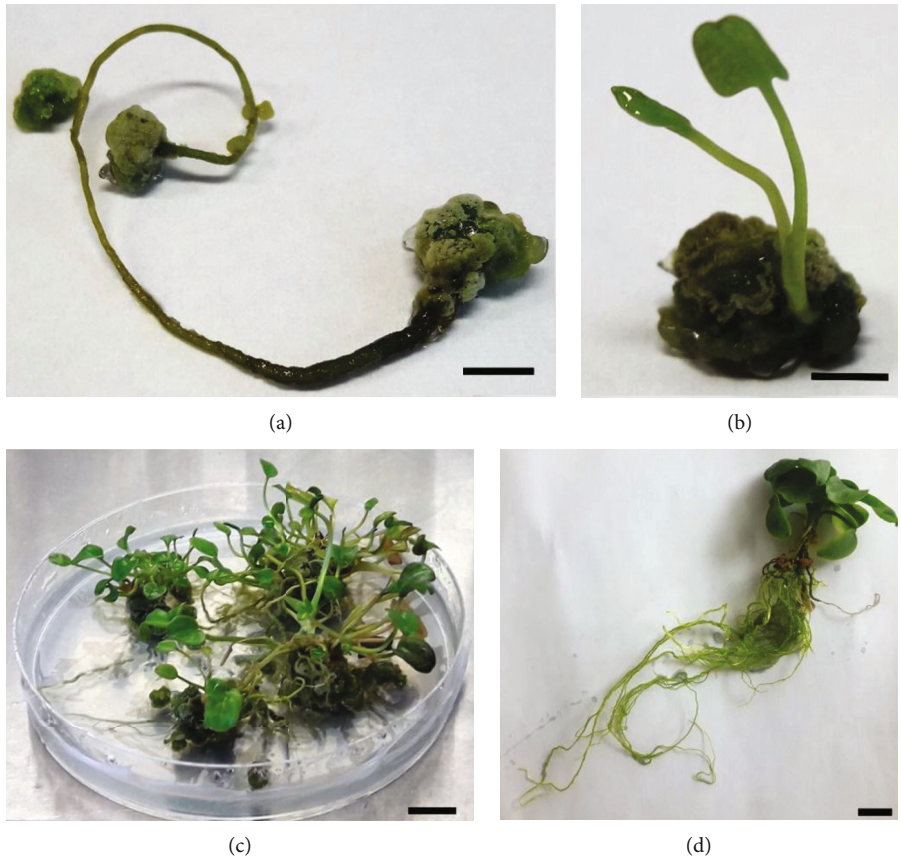

Figure 1: Subsequent stages of *Menyanthes trifoliata* regeneration. (a) Callus formation on the root after 20-day incubation on SH medium with 1.0 mg/L (6-BA) and 0.1 mg/L (NAA). (b) Regenerated shoot formed on SH medium with 4.0 mg/L 6-BA and 0.3 mg/L NAA. Fourth week of incubation. (c) Rooted young plants grown on SH medium supplemented with 0.3 mg/L 6-BA and 1.0 mg/L NAA before transfer to fresh solid SH medium. (d) Regenerated plant grown on solid SH medium without growth regulators after five weeks. Bar = 1 cm.

following the manufacturer's instructions. Next, gene expression was analyzed by TaqMan Probe-Based Real-Time PCR Assay. TaqMan probes (Life Technologies) were used to analyze 10 genes (*HO-1*, *NQO1, kAEP1*, *GCLC*, *IL-1α*, *IL-1β*, *IL-6*, *TNF-α*, and *IFN-γ*), and beta actin (*ACTB*) was included as the reference gene. qRT-PCR was performed using TaqMan® Real-Time PCR Master Mix (Life Technologies) and a CFX96™ Real-Time PCR Detection System (Bio-Rad Laboratories, Hercules, CA, USA) working on CFX Manager™ Software (version 3.1). The thermal cycling conditions were as follows: 10 minutes of polymerase activation at 95°C, followed by 40 cycles of 30 s denaturation at 95°C and 60 s annealing/extension at 60°C. Each sample was run in triplicate. The basal expression level was calculated using the C_t method [16].

2.7. Determination of Nuclear DNA (nDNA) Damage and Mitochondrial DNA (mtDNA) Damage. Total genomic DNA (nuclear and mitochondrial) was isolated from cells treated with 1 mg/mL MtRV and MtAPV extracts for 24 h and then treated with 50 μM H_2O_2 for one hour using a QIAamp DNA Mini Kit (Qiagen, Valencia, CA, USA) according to the manufacturer's instructions. DNA concentrations were determined by spectrophotometric measurement of absorbance at 260 nm, and the purities were calculated by the A260/A280 ratio using a BioTek Synergy HT Microplate Reader (BioTek Instruments, Winooski, VT, USA). The semilong run quantitative RT-PCR (SLR-qRT-PCR) was used to assess mitochondrial DNA (mtDNA) and nuclear DNA (nDNA) damage, as described previously, with some modifications [17]. All conditions were described previously [18].

2.8. Cytoplasmic ROS and Mitochondrial ROS Detection. The cells were incubated with 1 mg/mL MtRV or MtAPV for 24 hours and then with 50 μM H_2O_2 for one hour. DCFDA (molecular probe, Life Technologies) staining was used to detect cytoplasmic ROS. DCFDA was diluted to a 5 μmol/L final concentration with Hanks' balanced salt solution (HBSS), which was incubated with the cells at 37°C for 30 minutes. A MitoSOX Red mitochondrial superoxide indicator was used to measure mitochondrial ROS production. The indicator was diluted to a 5 μmol/L final concentration with HBSS, which was applied to incubate cells at 37°C for 30 minutes. The cells were washed three times with HBSS. The fluorescence emission was measured using a BioTek Synergy HT Microplate Reader. Each sample was run in triplicate.

2.9. Analysis of Cellular Phosphorylated H2A.X and Cleaved PARP Levels. HUVECs were plated in a six-well plate at a density of 2×10^5 viable cells. The following day, the cells were treated with MtRV and MtAPV extracts (1 mg/mL) for 24 h and then incubated with 50 μM H_2O_2 for one hour. After incubation, the cells were collected, and phosphorylated H2A.X- and cleaved PARP-positive cells were detected using the Apoptosis, DNA Damage and Cell Proliferation Kit (BD Pharmingen, 562253) according to the protocol given by the manufacturer. The cells were analyzed with a FACSCanto II cytometer (Becton Dickinson, San Jose, California, USA).

2.10. Antimicrobial Activity. The following strains were tested: *Staphylococcus aureus* (ATCC 25923), *Enterococcus faecalis* (ATCC29212), *Escherichia coli* (ATCC 25922), *Pseudomonas aeruginosa* (ATCC 27853), and the yeasts *Candida albicans* (ATCC 10231) and *Saccharomyces cerevisiae* (ATCC 2601). The growth conditions of all the tested microorganisms were described previously by Sitarek el al. [19]. MtRV and MtAPV extracts were used in this study. The minimum inhibitory concentration (MIC) and the Minimum Bactericidal/Fungicidal Concentration (MBC or MFC) of the tested extract were determined as detailed previously [19].

2.11. Data Analysis. The statistical analysis was performed using GraphPad Prism 5. All experimental values presented in this study were expressed as mean ± standard deviation (SD). The Shapiro-Wilk test to analyze the normality of the distribution of results was used. Next, the results were analyzed for equality of variance using Levene's test. Significant differences were identified using the ANOVA test for multiple comparisons, followed by the Dunnet *post hoc* test.

3. Results

3.1. Chemical Composition of Aerial Part (MtAPV) and Root Extracts (MtRV) of M. trifoliata Plants. The following phenolic compounds have previously been identified in MtRV and MtAPV extracts: chlorogenic acid (177 and 258 μg/g dry weight, respectively), ellagic acid (518 and 451 μg/g dry weight, receptively), sinapinic acid (146 and 71 μg/g dry weight, respectively), syringic acid (114 μg/g dry weight and not detected, respectively), rutin (256 and 153 μg/g dry weight, respectively), and also pentacyclic triterpene-betulinic acid (5437 and 395 μg/g dry weight, respectively) [8]. The main components of the plant extracts are presented in Table 1.

3.2. Effects of MtAPV and MtRV Extracts on Cell Viability. Our results showed that the MtRV and MtAPV extracts of *M. trifoliata* plants did not present any cytotoxic effect on the human umbilical vein endothelial cells (HUVECs) in the tested concentrations (0-5 mg/mL) after 24-hour incubation (Figure 2).

In further experiments, 1 μg/mL LPS or 50 μM H_2O_2 was used: these values did not exhibit 50% growth inhibition (IC_{50} value) of cells and were used for the induction of inflammation or antioxidant effect, respectively (data not shown). In addition, the effect on cell viability was determined for both extracts of *M. trifoliata* in combination with LPS or H_2O_2. It was found that the HUVECs demonstrated no significant difference in cell viability following treatment with MtRV or MtAPV extracts alone, MtRV or MtAPV in combination with H_2O_2, and also MtRV or MtAPV in combination with LPS (Figure 3).

Table 1: Chosen secondary metabolites of aerial parts (MtAPV) and roots (MtRV) of *Menyanthes trifoliata* plants grown *in vitro* [8].

Compounds	MtRV	MtAPV
	μg/g dry weight	
Betulinic acid	5437.15 ± 141.33	395.31 ± 14.50
Chlorogenic acid	177.34 ± 9.57	257.9 ± 14.70
Ellagic acid	518.11 ± 26.46	450.65 ± 14.22
Rutin	256.20 ± 3.24	152.99 ± 6.24
Sinapinic acid	146.53 ± 7.03	71.16 ± 3.34
Syringic acid	113.80 ± 0.80	n.d.

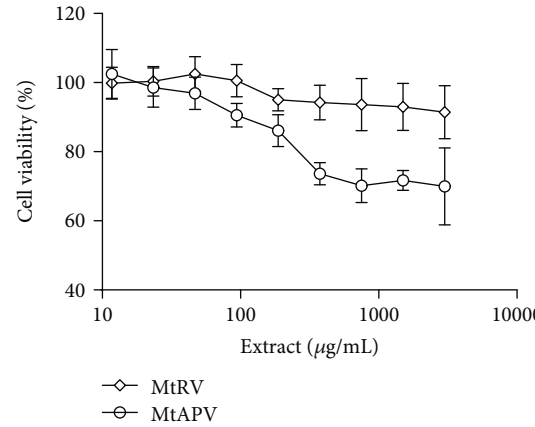

Figure 2: Cell viability after 24-hour treatment of MtRV and MtAPV extracts of *M. trifoliata* plants at concentrations of 0-5 mg/mL on HUVECs. Data are presented as mean ± SD.

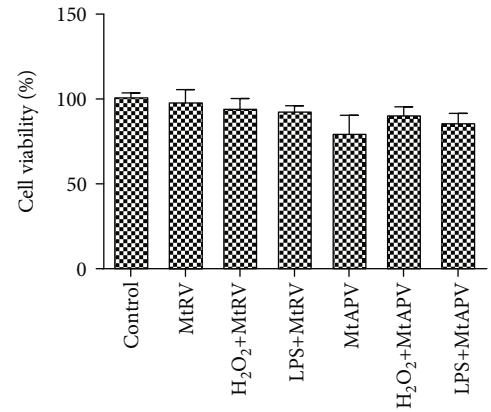

Figure 3: Cell viability after 24-hour treatment of HUVECs with 1 mg/mL of *M. trifoliata* MtRV and MtAPV extracts and pretreatment with LPS and H_2O_2. Data are presented as mean ± SD.

3.3. Gene Expression. Quantitative real-time RT-PCR was used to measure mRNA levels of the antioxidant genes HO-1, NQO1, *NRF2*, *kAEP1*, and *GCLC* and inflammation genes *IL-1α*, *IL-1β*, *IL-6*, *TNF-α*, and *IFN-γ* after treatment with 50 μM H_2O_2 or 1 μg/mL LPS for one hour and after treatment with the MtRV or MtAPV extract of *M. trifoliata* for 24 hours. Our results demonstrated that treatment with both extracts at a concentration of 1 mg/mL was able to change the level of antioxidant genes in H_2O_2-stimulated HUVECs compared to the controls. Similar results were obtained for inflammatory genes. All the tested genes in the LPS-stimulated cells demonstrated changes in expression following treatment with either extract compared to controls, but better anti-inflammatory properties were observed for the MtRV extract. The results are shown in Figures 4(a) and 4(b).

3.4. Quantification of Nuclear DNA (nDNA) and Mitochondrial DNA (mtDNA) Damage. mtDNA and nDNA damage was examined by SLR-qRT-PCR amplification of DNA isolated from HUVECs exposed to MtRV or MtAPV extracts for 24 hours and then 50 μM H_2O_2 for one hour. The cells exposed to 50 μM H_2O_2 demonstrated a significant increase in lesion rate in the *ND1* and *ND5* regions: about five lesions per 10 kb DNA. Similarly, the same cells demonstrated an increase in lesion rate in the *HPRT1* and *TP53* regions of nDNA: about five lesions per 10 kb DNA were observed. In the cells, 24-hour treatment with MtRV or MtAPV extracts was found to bestow a protective effect against mtDNA and nDNA damage by decreasing the mtDNA lesion number in the *ND1* and *ND5* genes and nDNA damage in the *TP53* and *HPRT1* genes (Figures 5(a)–5(d)).

3.5. Cytoplasmic ROS and Mitochondrial Superoxide Generation Detection. Cytoplasmic and mitochondrial ROS levels were measured after 24-hour treatment with MtRV and MtAPV (1 mg/mL) extracts and then one-hour treatment with 50 μM H_2O_2. Following 24-hour treatment with either tested extract, decreased cytoplasmic and mitochondrial ROS levels were observed compared to the cells treated with only H_2O_2, indicating the presence of a protective effect (Figures 6(a) and 6(b)).

3.6. Assessment of PARP1- and γ-H2A.X-Positive Cell Levels by Flow Cytometry after Treatment with MtAPV and MtRV Extracts. The levels of γH2A.X- and cleaved poly (ADP-ribose) polymerase 1- (PARP1-) positive cells were evaluated to determine the protective effect of MtRV and MtAPV extracts on HUVECs induced by 50 μM H_2O_2. It was found that the HUVECs treated with 50 μM H_2O_2 generated a higher level of γH2A.X- and cleaved PARP1-positive cells than untreated cells. In turn, 24-hour incubation of cells with MtRV and MtAPV extracts demonstrated a protective effect on cells following treatment with 50 μM H_2O_2, reflecting a significantly lower percentage of γH2A.X- and cleaved PARP1-positive cells. Although both extracts demonstrated a protective effect, better results were observed for the MtRV extract (Figures 7(a) and 7(b)).

3.7. Assessment of Antimicrobial Activity of MtAPV and MtRV Extracts. The antimicrobial activity of MtRV and MtAPV extracts against *Staphylococcus aureus*, *Pseudomonas aeruginosa*, *Escherichia coli*, *Enterococcus faecalis*, *Saccharomyces cerevisiae*, and *Candida albicans* was screened using MIC and MBC/MFC methods. Both the tested extracts showed moderate antimicrobial activity (Table 2) against various strains at a range of MIC values (150-925 μg/mL) and for MBC/MFC (500-2500 μg/mL). The MtRV extract showed better activity than the MtAPV extract against *P. aeruginosa* and *E. faecalis*, with a MIC value of 150 μg/mL. The MtRV extract demonstrated also better antifungal activity than the MtAPV extract for *C. albicans* and *S. cerevisiae*, with MIC values of 625 μg/mL and 725 μg/mL, respectively, and with MFC values of 625 μg/mL and 1500 μg/mL, respectively.

4. Discussion

Plants are well-known to have beneficial effects on human health. Their extraordinary wealth of biologically active compounds makes them indispensable for human life and allow the prevention of many civilization diseases. One plant species that contains many valuable biologically active compounds is *Menyanthes trifoliata*. Extracts and infusions of this plant are used as anti-inflammatory, diuretic, or cleansing agents, becoming an important element of phytomedicine [20].

This work is the first to demonstrate the protective properties of *M. trifoliata* extracts derived from aerial parts and roots of plants cultivated *in vitro*. It examines the anti-inflammatory and antioxidant properties of *M. trifoliata* extracts (MtRV and MtAPV extracts) in human umbilical vein endothelial cells (HUVECs) which had previously been treated with LPS or H_2O_2. Inflammation is a very complex physiological phenomenon developing in the tissue under the influence of different stimuli and is mediated by a wide range of specific components. It involves interactions between signal molecules produced by leukocytes, macrophages, and mast cells, as well as by the activation of complements [21–23]. A range of studies describe the anti-inflammatory properties of plant extracts against a wide spectrum of normal and cancer cells [24–26].

One of the aims of the study was to investigate the anti-inflammatory properties of *M. trifoliata* extracts on HUVECs following stimulation by lipopolysaccharide (LPS) for 24 hours. LPS is the main component of the outer membrane of Gram-negative bacteria. It activates mononuclear phagocytes and other cell types by toll-like receptor 4 to promote the secretion of inflammatory mediators including TNF-α, IL-6, and IL-1β [27]. It was found that the aerial part (MtAPV) and root (MtRV) extracts of *in vitro*-derived *M. trifoliata* exhibit an anti-inflammatory effect by decreasing the expression of selected genes encoding inflammation-associated cytokines (IL-1α, IL-1β, IL-6, TNF-α, and IFN-γ).

Many reports indicate that *M. trifoliata* is a source of phenolic compounds such as coumarins, flavonols, or iridoids [11]. Our previous study also showed the presence of various phenolic compounds in the extracts of *in vitro*- and

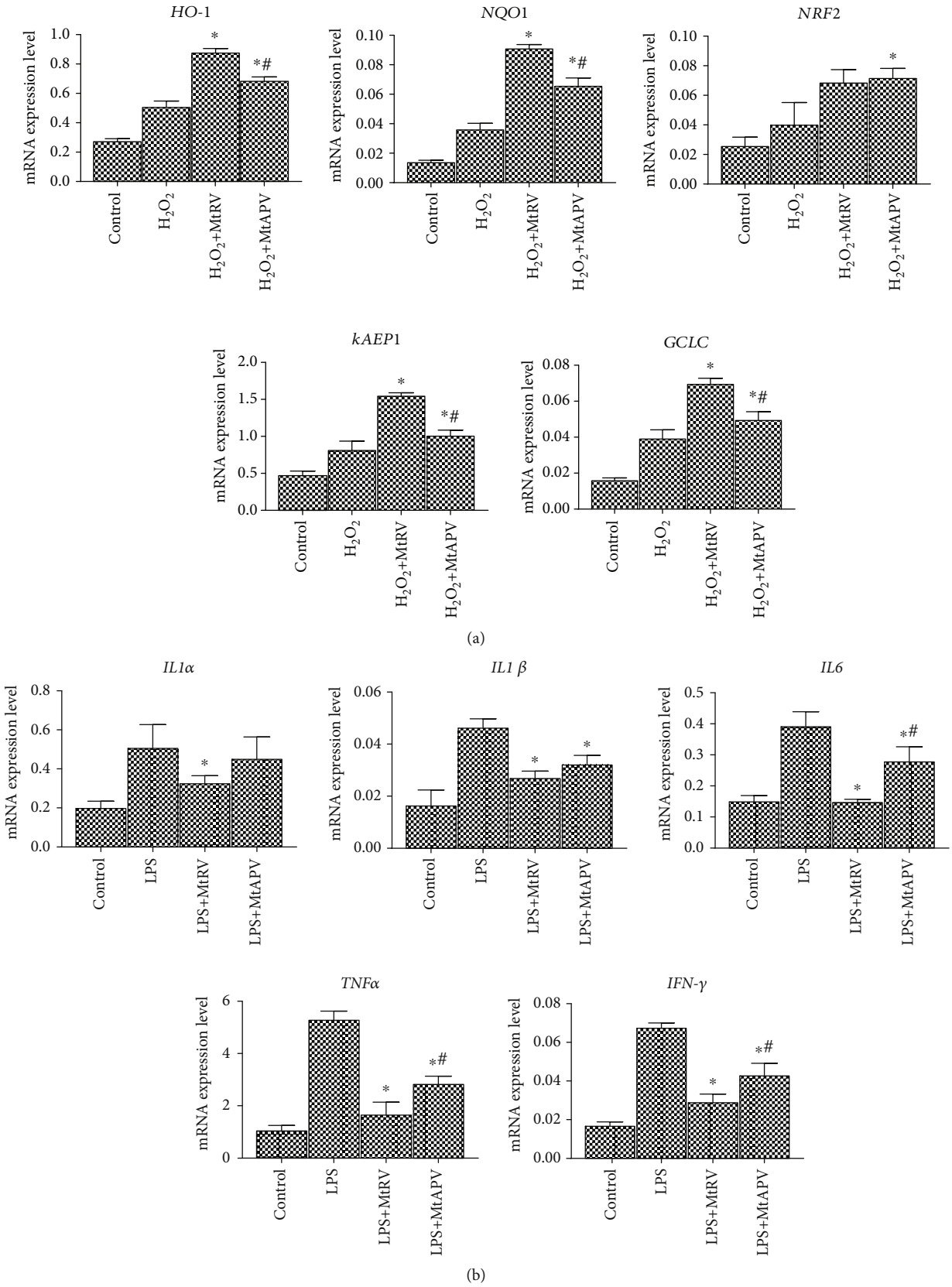

Figure 4: (a) mRNA expression of antioxidant genes after 24-hour treatment of MtRV and MtAPV extracts (1 mg/mL) of *M. trifoliata* plants and stimulation with 50 μM H_2O_2. (b) mRNA expression of inflammatory genes after 24-hour treatment with MtRV and MtAPV extracts of *M. trifoliata* plants and 1 μg/mL LPS. *For comparison control vs. MtAPV and MtRV extracts. #For comparison MtAPV vs. MtRV extracts. *ACTB* served as the reference gene. Data are presented as mean ± SD ($n = 3$).

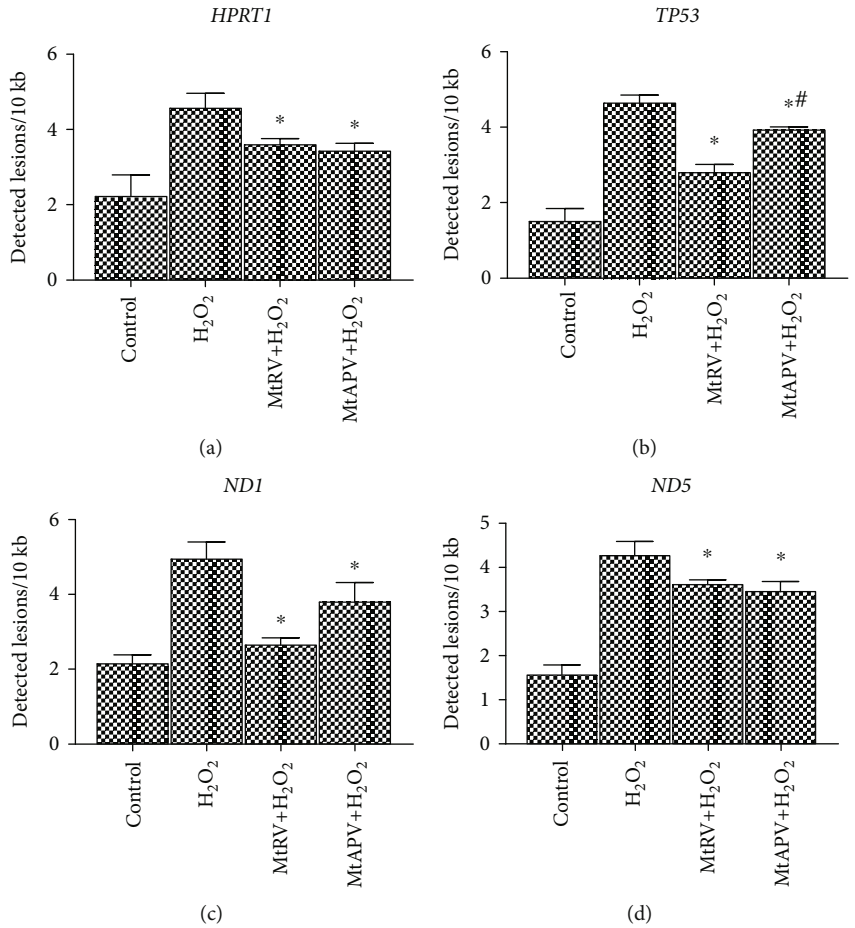

Figure 5: Quantification of nuclear DNA (nDNA) (a, b) and mitochondrial DNA (mtDNA) (c, d) lesion frequency per 10 kb DNA by SLR-qRT-PCR amplification of total DNA from human umbilical vein endothelial cells exposed to MtRV and MtAPV (1 mg/mL) extracts for 24 hours followed by 50 μM H_2O_2 for one hour. *For comparison control vs. MtAPV and MtRV extracts. #For comparison MtAPV vs. MtRV extracts. Data represent the mean ± SD of three replicates.

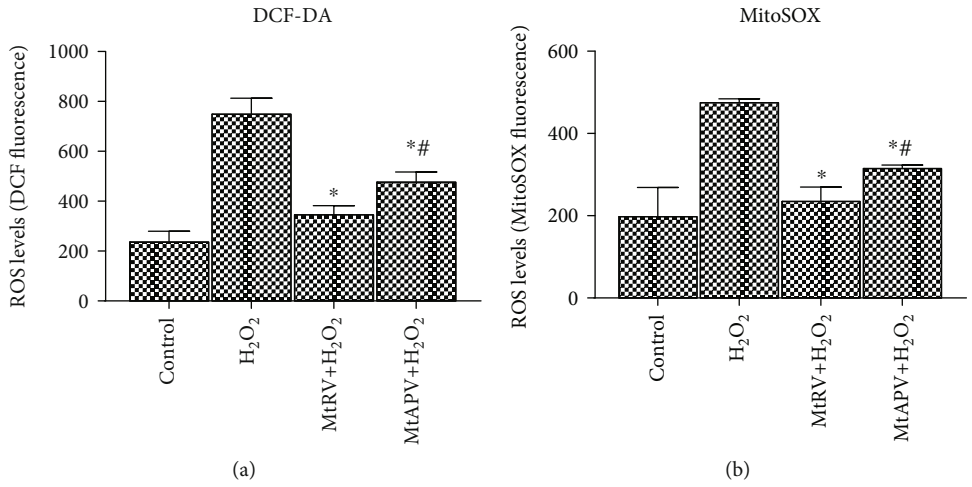

Figure 6: The production of ROS in human umbilical vein endothelial cells exposed to MtRV and MtAPV extracts of *M. trifoliata* (1 mg/mL) for 24 hours followed by 50 μM H_2O_2 for one hour, measured using the probes: DCFDA (a) and MitoSOX (b). *For comparison control vs. MtAPV and MtRV extracts. #For comparison MtAPV vs. MtRV extracts. Results represent means ± SD.

in vivo-derived *M. trifoliata* plants, with the content of ellagic acid (299-518 μg/g dry weight), chlorogenic acid (129-258 μg/g dry weight), and rutin (82-256 μg/g dry weight) varying according to the plant part and growth conditions. Betulinic acid, a pentacyclic triterpene, was found at its highest concentrations in the roots of plants derived from

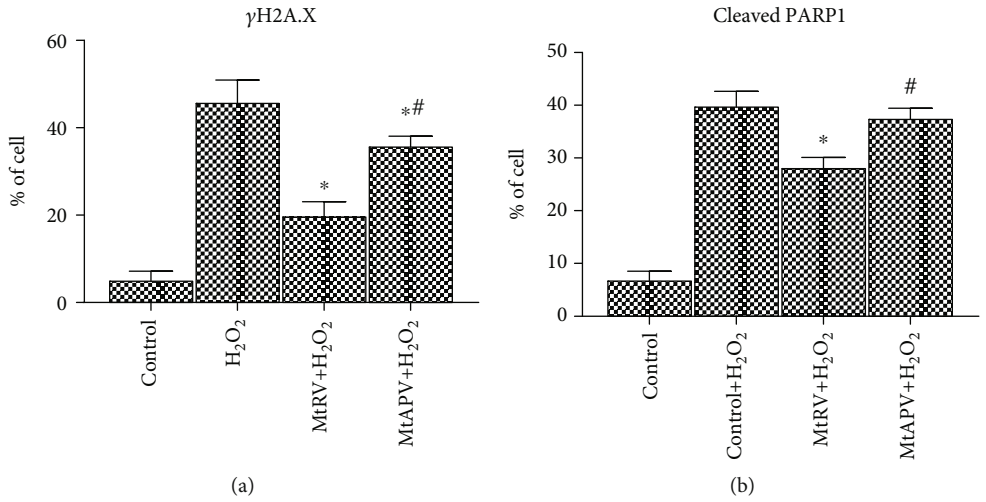

Figure 7: Diagrams presented percentage of H2A.X phosphorylation- (a) and cleaved PARP1- (b) positive human umbilical vein endothelial cells after 24-hour exposure to MtRV and MtAPV extracts followed by 50 μM H_2O_2 for one hour. *For comparison control vs. MtAPV and MtRV extracts. #For comparison MtAPV vs. MtRV extracts. The values represent mean ± SD of three independent experiments.

Table 2: Antimicrobial activity of MtRV and MtAPV extracts of *M. trifoliata*. Van: vancomycin; NOR: norfloxacin; ANF: amphotericin B. Data represent the median values in triplicate.

Plant material	*Staphylococcus aureus*		*Pseudomonas aeruginosa*		*Escherichia coli*		*Enterococcus faecalis*		*Saccharomyces cerevisiae*		*Candida albicans*	
	MIC (μg/mL)	MBC	MIC (μg/mL)	MBC	MIC (μg/mL)	MBC	MIC (μg/mL)	MBC	MIC (μg/mL)	MFC	MIC (μg/mL)	MFC
Mt RV extract	**225**	**>500**	**150**	**>500**	**250**	**>500**	**150**	**>500**	**725**	**625**	**625**	**1500**
Mt APV extract	**250**	**>500**	**250**	**>500**	**250**	**>500**	**250**	**>500**	**725**	**725**	**925**	**2500**
Positive control	**7.82** VAN	**>500**	**<0.48** NOR	**>500**	**0.98** NOR	**>500**	**1.95** VAN	**>500**	**<0.48** ANF	**>5000**	**<0.48** ANF	**>5000**

in vitro cultures. The anti-inflammatory and antioxidant activity of this plant compound is also well documented in literature [28–30].

Our present findings indicated that the tested *M. trifoliata* extracts bestow a DNA-protective effect on the tested cell line. We speculate that betulinic acid and the identified phenolic acids (syringic acid, sinapinic acid, ellagic acid, and chlorogenic acid) may be responsible for this positive effect, especially as betulinic acid and sinapinic acid have been found to suppress inflammatory cytokines such as IL-6 or TNF-α [31, 32]. Betulinic acid (lupane-type triterpene) exhibits a protective effect on mice exposed to lethal doses of LPS and causes a reduction of LPS-induced TNF-α production. In addition, betulinic acid is also known as an inhibitor of IFN-γ production [33]. Kim et al. report the compound to be an anti-inflammatory agent acting via inhibition of the nuclear factor-κB (NF-κB) pathway. Similarly, suppression of tumor necrosis factor-α (TNF-α), interleukin-6 (IL-6), and interleukin-1β (IL-1β) was demonstrated in LPS-activated RAW 264.7 macrophages after betulinic acid treatment [34]. Similar properties have also been described for sinapinic acid [35–37], ellagic acid [38], or chlorogenic acid [39].

The present study also analyzes the influence of the two *M. trifoliata* extracts on oxidative stress-related gene expression. Changes in the expression of genes encoding heme oxygenase 1 (HO-1), quinone dehydrogenase 1 (NQO1), nuclear factor (erythroid-derived-2)-like-2 (NRF2), Kelch-like ECH-associated protein 1 (kEAP1), or glutamate-cysteine ligase catalytic subunit (GCLC) cast light on the protective role played by the components of the tested extract in H_2O_2-stimulated cells. The MtRV and MtAPV extracts, administered at 1 mg/mL, were found to influence the expression of *HO-1*, *NRF2*, *kEAP1*, *NQO1*, and *GCLC* genes in H_2O_2-stimulated HUVECs, with the MtRV extract demonstrating better protective properties than the MtAPV.

Previous studies provide a wealth of information describing the cytoprotective effect of plant phenolic compounds on HUVECs [40–42]. Some affect the expression of oxidative stress-related genes; for example, those contained in the green tea extract increase the mRNA level of heme oxygenase-1 (HO-1) in human aortic endothelial cells [43], while the polyphenolic antioxidant fraction from *Nymphaea nouchali* leaves increases HO-1 and Nrf2 level in RAW 264.7 cells [44]. Recently, special attention has been paid to the

close relationship between inflammation and oxidative stress. The appearance of an excessive amount of free radicals reacts with cell membrane fatty acids, proteins, or DNA, leading to mutation and consequently to the development of many diseases. In this context, searching for natural components that protect cells from adverse changes is extremely desirable.

The present study also tested cytoplasmic and mitochondrial ROS levels in H_2O_2-stimulated HUVECs after treatment with MtRV and MtAPV extracts. Our results, obtained with dichloro-dihydro-fluorescein diacetate and red mitochondrial superoxide indicator (MitoSOX), found the plant extracts to exert a protective effect by decreasing cytoplasmic and mitochondrial ROS levels in cells. The MtRV extract demonstrated a stronger antioxidant effect than the MtAPV extract. It is known that ROS are produced in epithelial cells by many enzymes, including nicotinamide adenine dinucleotide phosphate oxidase (NOX), nitric oxide synthase (NOS), or xanthine oxidase (XOD), as well as the respiratory chain complex [45]. ROS are extremely important elements that play a crucial role in the initiation of inflammatory processes. Elevated levels of ROS produced by polymorph nuclear neutrophils (PMN) at the site of inflammation can lead to epithelial cell dysfunction and consequent tissue damage [46]. A considerable body of evidence indicates that the excessive cellular production of ROS may be closely related to the induction of inflammation and consequently affect the development of diseases such as Alzheimer's, Parkinson's, or cancer [47]. Our findings confirm that *M. trifoliata* extracts exhibit protective antioxidant properties, probably due to the presence of identified phenolic compounds and pentacyclic triterpenes, such as betulinic acid, which is consistent with literature data [48]. It should also be noted that the MtRV extract appears to offer the strongest cytoprotective effects.

Nuclear and mitochondrial DNA damage was also quantified by SLR-qRT-PCR amplification of DNA from HUVECs exposed to plant extracts followed by 50 μM H_2O_2. Both extracts were found to have a protective effect, resulting in a decrease in the lesion rate for all the tested nuclear and mitochondrial DNA regions after incubation with MtRV and MtAPV extracts compared to cells incubated only with 50 μM H_2O_2. Although mitochondrial and nuclear DNA damage, and hence the protective effects of the tested extracts, can be detected by various methods such as Southern blot analysis or comet assay, the present study used a semilong run RT-PCR-based assay. Also, the MtRV extract demonstrated a stronger protective potential against ROS-derived DNA damage than the MtAPV extract.

Plant phenolic compounds are known to bestow a protective effect on DNA against various physical or chemical factors [49–51]. A similar study investigating the protective effect of *Salvia officinalis* and *Thymus vulgaris* extracts on the DNA of HepG2 cells was performed by Kozics et al. [52]. Their results indicate that H_2O_2-induced DNA damage was significantly reduced in cells pretreated with both the tested plant extracts, which were also found to contain phenolic compounds and betulinic acid. Another study examined the effect of a purified *Eugenia jambolan* leaf and fruit extract on HepG2 cells; the extracts were found to be rich sources of many phenolic compounds and betulinic acid and to exhibit antigenotoxic and antimutagenic effects [53].

Other studies have shown that phenolic compounds, including phenolic acids, can reduce the level of oxidative DNA damage in a variety of cell types [54, 55]. However, the present study is first to report the ability of the *in vitro*-derived *M. trifoliata* plant extract to protect cells against DNA damage. As noted in previous studies, our results suggest that the protective effect demonstrated by the examined extracts is related to its phenolic compound content, including betulinic acid, and the synergy between extract components.

Flow cytometric analysis showed that *M. trifoliata* extracts had a protective effect on the tested cells. HUVECs treated with H_2O_2 generated a higher level of γH2A.X- and cleaved PARP1-positive cells than untreated cells. On the other hand, 24-hour incubation with the studied MtRV and MtAPV extracts exhibited a protective effect against pretreatment with H_2O_2 by reducing the number of γH2A.X- and cleaved PARP1-positive cells. Poly (ADP-ribose) polymerase 1 (PARP1) is responsible for the ADP-ribosylation process (PARylation), which is a common posttranslational modification of DNA damage. This modification regulates many other biological processes, including the reorganization of chromatin or DNA damage response (DDR). In addition, PARP is a substrate for caspases and is cleaved during apoptosis into 86 and 24 kDa fragments [56, 57]. For this reason, PARP1 acts as a good DNA damage sensor [58]. Similarly, the H2A.X protein is a key factor in the repair of damaged DNA and can be phosphorylated on the 139th serine residue in the presence of DNA damage [59]. Phosphorylated protein causes a conformational change in the DNA-H2A.X complex, which allows recruitment of proteins needed to repair DNA injury [60].

Our results clearly show that *M. trifoliata* extracts from plants derived from *in vitro* cultures play an important role in DNA protection of the tested cells. This is consistent with other literature data showing that polyphenol-rich natural products also inhibit the increases in cleaved PARP level [61, 62]. Similarly, the level of phosphorylated H2A.X, another determinant of DNA damage, has previously been found to be reduced under the influence of the black tea or *Camptosorus sibiricus* extract [63] in other cells. It is most likely that the phenolic compounds and pentacyclic triterpene present in the MtRV and MtAPV extracts may be responsible for the biological effect observed in the present study.

The study also examines the antibacterial and antifungal properties of *M. trifoliata* extracts. The tested MtRV and MtAPV extracts demonstrated stronger antibacterial than antifungal action. It was also shown that the MtRV extract possessed a stronger effect against the tested microorganisms than MtAPV. The best bacterial growth inhibitory effects were obtained against *Pseudomonas aeruginosa* (ATCC 27853) and *Enterococcus faecalis* (ATCC29212) for the MtRV extract (MIC = 150 μg/mL). Similar effects were demonstrated for the MtAPV extract against all the tested bacteria (MIC = 250 μg/mL). Also, better fungal growth inhibition was exhibited by the MtRV extract than the MtAPV extract

against *Candida albicans* (ATCC 10231) and *Saccharomyces cerevisiae* (ATCC 2601), where the MIC for *Candida albicans* was 625 μg/mL. Many plant species naturally produce compounds with antimicrobial or antifungal properties [64–66]. Ivanišová et al. [67] examined the antimicrobial activity of *M. trifoliata* leaf extracts, rich sources of polyphenols and flavonoids, and extracts from other plants against three Gram-negative bacteria and two Gram-positive species. The *M. trifoliata* extract demonstrated the strongest antibacterial activity against *Escherichia coli*, *Salmonella enterica* subsp. *enterica*, *Bacillus thuringiensis*, *Staphylococcus aureus* subsp. *aureus*, and *Pseudomonas aeruginosa*, which corresponds to our results. This study found *M. trifoliata* to be the richest source of polyphenols, flavonoids, and phenolic acids among all the analyzed wild plants in the study. The antibacterial and antifungal properties of *M. trifoliata* extracts have also been investigated by Paudel et al. [68] by testing their influence on pathogenic microorganisms such as *S. aureus*, *E. coli*, and *C. albicans*. In this case, the plant extracts were active only against *S. aureus*. The authors attribute these differences in antimicrobial activity to variations in antimicrobial metabolites among the tested samples.

The search for new antibacterial compounds has recently become an extremely important issue due to emerging resistance of pathogens to traditional medicines; in this sense, plant-derived compounds can play a potentially important role. They often have specific chemical structures that can inhibit bacterial growth through new mechanisms of action [69]; however, this group of secondary metabolites may also be of great importance in the development of new compounds against human pathogens. Based on data obtained in previous studies [70–72], it is likely that betulinic acid may be chiefly responsible for the antibacterial and antifungal effects of the tested extracts [70, 73]. Additionally, we suspect that phenolic acids may have a similar effect and show synergistic effects with other components, particularly since the MtRV extract showed the best antimicrobial properties. Generally, the antibacterial and antifungal mechanism of action of many phenolic compounds is not yet fully understood [69]. Some studies indicate that they interact with a range of targets such as DNA, DNA gyrase [74], protein kinases [75], and helicase, among others [69]. Attempts should be made to identify new antimicrobial components, especially as increasing numbers of multidrug-resistant strains are appearing in the environment [76].

5. Conclusion

The results of our study demonstrate for the first time that MtRV and MtAPV extracts from *M. trifoliata* plants derived from *in vitro* cultures showed antioxidant and anti-inflammatory effects on human umbilical vein endothelial cells (HUVECs) stimulated by H_2O_2 or LPS, and of the two, the MtRV extract demonstrated the strongest activities. Additionally, the protective effect was observed which was associated with a decrease in DNA damage, reductions in cytoplasmic and mitochondrial ROS levels, and reduced γH2A.X- and cleaved PARP1-positive HUVEC numbers. Furthermore, the tested extracts demonstrated moderate antimicrobial activities against various pathogenic bacterial and fungal strains. Therefore, this plant may play a potential role in the therapy and prevention of many civilization diseases.

Data Availability

All data are available at the request of the reviewer or other interested persons.

Conflicts of Interest

The authors declare no competing interests.

Acknowledgments

This study was funded by University of Lodz Statutory Funding Grant Number B1711000000201.01.

References

[1] C. Mora, D. P. Tittensor, S. Adl, A. G. B. Simpson, and B. Worm, "How many species are there on earth and in the ocean?," *PLoS Biology*, vol. 9, no. 8, article e1001127, 2011.

[2] X. Liu, K. Vrieling, and P. G. L. Klinkhamer, "Interactions between plant metabolites affect herbivores: a study with pyrrolizidine alkaloids and chlorogenic acid," *Frontiers in Plant Science*, vol. 8, p. 903, 2017.

[3] S. Latif, G. Chiapusio, and L. A. Weston, "Allelopathy and the role of allelochemicals in plant defence," *Advances in Botanical Research*, vol. 82, pp. 19–54, 2017.

[4] J. Reichling, "Plant-Microbe Interactions and Secondary Metabolites with Antibacterial, Antifungal and Antiviral Properties," in *Functions and biotechnology of plant secondary metabolites, vol. 39*, pp. 214–347, Blackwell, Oxford, UK, 2nd edition, 2010.

[5] A. G. Atanasov, B. Waltenberger, E. M. Pferschy-Wenzig et al., "Discovery and resupply of pharmacologically active plant-derived natural products: a review," *Biotechnology Advances*, vol. 33, no. 8, pp. 1582–1614, 2015.

[6] H. Yang, T. Tian, D. Wu, D. Guo, and J. Lu, "Prevention and treatment effects of edible berries for three deadly diseases: cardiovascular disease, cancer and diabetes," *Critical Reviews in Food Science and Nutrition*, vol. 59, no. 12, pp. 1903–1912, 2019.

[7] F. L. Thompson, L. A. Hermanutz, and D. J. Innes, "The reproductive ecology of island populations of distylous *Menyanthes trifoliata* (Menyanthaceae)," *Canadian Journal of Botany*, vol. 76, no. 5, pp. 818–828, 1998.

[8] T. Kowalczyk, P. Sitarek, E. Skała et al., "Induction of apoptosis by in vitro and in vivo plant extracts derived from *Menyanthes trifoliata* L. in human cancer cells," *Cytotechnology*, vol. 71, no. 1, pp. 165–180, 2019.

[9] J. Kuduk-Jaworska, J. Szpunar, K. Gąsiorowski, and B. Brokos, "Immunomodulating polysaccharide fractions of Menyanthes trifoliata L.," *Zeitschrift für Naturforschung C*, vol. 59, no. 7-8, pp. 485–493, 2004.

[10] H. Tunón, L. Bohlin, and G. Öjteg, "The effect of *Menyanthes trifoliata* L. on acute renal failure might be due to PAF-inhibition," *Phytomedicine*, vol. 1, no. 1, pp. 39–45, 1994.

[11] F. Martz, M. Turunen, R. Julkunen-Tiitto, K. Lakkala, and M. L. Sutinen, "Effect of the temperature and the exclusion of UVB radiation on the phenolics and iridoids in *Menyanthes trifoliata* L. leaves in the subarctic," *Environmental Pollution*, vol. 157, no. 12, pp. 3471–3478, 2009.

[12] S. H. Lim, E. S. Jeon, J. Lee, S. Y. Han, and H. Chae, "Pharmacognostic outlooks on medical herbs of Sasang typology," *Integrative Medicine Research*, vol. 6, no. 3, pp. 231–239, 2017.

[13] R. Gautam, M. Singh, S. Gautam, J. K. Rawat, S. A. Saraf, and G. Kaithwas, "Rutin attenuates intestinal toxicity induced by methotrexate linked with anti-oxidative and anti-inflammatory effects," *BMC Complementary and Alternative Medicine*, vol. 16, no. 1, p. 99, 2016.

[14] L. Wang, H. L. Wu, X. L. Yin, Y. Hu, H. W. Gu, and R. Q. Yu, "Simultaneous determination of umbelliferone and scopoletin in Tibetan medicine *Saussurea laniceps* and traditional Chinese medicine *Radix angelicae pubescentis* using excitation-emission matrix fluorescence coupled with second-order calibration method," *Spectrochimica Acta Part A: Molecular and Biomolecular Spectroscopy*, vol. 170, pp. 104–110, 2017.

[15] P. Sitarek, E. Skała, M. Toma et al., "Transformed root extract of *Leonurus sibiricus* induces apoptosis through intrinsic and extrinsic pathways in various grades of human glioma cells," *Pathology Oncology Research*, vol. 23, no. 3, pp. 679–687, 2017.

[16] T. D. Schmittgen and K. J. Livak, "Analyzing real-time PCR data by the comparative C_T method," *Nature Protocols*, vol. 3, no. 6, pp. 1101–1108, 2008.

[17] O. Rothfuss, T. Gasser, and N. Patenge, "Analysis of differential DNA damage in the mitochondrial genome employing a semi-long run real-time PCR approach," *Nucleic Acids Research*, vol. 38, no. 4, article e24, 2010.

[18] P. Sitarek, E. Synowiec, T. Kowalczyk, T. Śliwiński, and E. Skała, "An in vitro estimation of the cytotoxicity and genotoxicity of root extract from *Leonurus sibiricus* L. overexpressing AtPAP1 against different cancer cell lines," *Molecules*, vol. 23, no. 8, article 2049, 2018.

[19] P. Sitarek, P. Rijo, C. Garcia et al., "Antibacterial, anti-inflammatory, antioxidant, and antiproliferative properties of essential oils from hairy and normal roots of *Leonurus sibiricus* L. and their chemical composition," *Oxidative Medicine and Cellular Longevity*, vol. 2017, Article ID 7384061, 12 pages, 2017.

[20] H. Tunón, C. Olavsdotter, and L. Bohlin, "Evaluation of anti-inflammatory activity of some Swedish medicinal plants. Inhibition of prostaglandin biosynthesis and PAF-induced exocytosis," *Journal of Ethnopharmacology*, vol. 48, no. 2, pp. 61–76, 1995.

[21] J. D. Rosenblat, D. S. Cha, R. B. Mansur, and R. S. McIntyre, "Inflamed moods: a review of the interactions between inflammation and mood disorders," *Progress in Neuro-Psychopharmacology & Biological Psychiatry*, vol. 53, pp. 23–34, 2014.

[22] N. P. Babu, P. Pandikumar, and S. Ignacimuthu, "Anti-inflammatory activity of *Albizia lebbeck* Benth., an ethnomedicinal plant, in acute and chronic animal models of inflammation," *Journal of Ethnopharmacology*, vol. 125, no. 2, pp. 356–360, 2009.

[23] A. U. Ahmed, "An overview of inflammation: mechanism and consequences," *Frontiers of Biology in China*, vol. 6, p. 274, 2011.

[24] A.'a. Al-Bakheit, S. Abu-Romman, A. Sharab, and M. Al Shhab, "Anti-inflammatory effect of *Varthemia iphionoides* extracts against prostate cancer *in vitro*," *European Journal of Inflammation*, vol. 15, no. 1, pp. 8–14, 2017.

[25] C. Ma, L. Zhu, J. Wang et al., "Anti-inflammatory effects of water extract of *Taraxacum mongolicum hand.-Mazz* on lipopolysaccharide-induced inflammation in acute lung injury by suppressing PI3K/Akt/mTOR signaling pathway," *Journal of Ethnopharmacology*, vol. 168, pp. 349–355, 2015.

[26] S. A. Adebayo, J. P. Dzoyem, L. J. Shai, and J. N. Eloff, "The anti-inflammatory and antioxidant activity of 25 plant species used traditionally to treat pain in southern African," *BMC Complementary and Alternative Medicine*, vol. 15, no. 1, p. 159, 2015.

[27] H. Fang, R. A. Pengal, X. Cao et al., "Lipopolysaccharide-induced macrophage inflammatory response is regulated by SHIP," *Journal of Immunology*, vol. 173, no. 1, pp. 360–366, 2004.

[28] P. Mizgier, A. Z. Kucharska, A. Sokół-Łętowska, J. Kolniak-Ostek, M. Kidoń, and I. Fecka, "Characterization of phenolic compounds and antioxidant and anti-inflammatory properties of red cabbage and purple carrot extracts," *Journal of Functional Foods*, vol. 21, pp. 133–146, 2016.

[29] M. J. Rodrigues, V. Neves, A. Martins et al., "*In vitro* antioxidant and anti-inflammatory properties of *Limonium algarvense* flowers' infusions and decoctions: a comparison with green tea (*Camellia sinensis*)," *Food Chemistry*, vol. 200, pp. 322–329, 2016.

[30] M. H. Grace, D. Esposito, M. A. Timmers et al., "Chemical composition, antioxidant and anti-inflammatory properties of pistachio hull extracts," *Food Chemistry*, vol. 210, pp. 85–95, 2016.

[31] J. J. Yoon, Y. J. Lee, J. S. Kim, D. G. Kang, and H. S. Lee, "Protective role of betulinic acid on TNF-α-induced cell adhesion molecules in vascular endothelial cells," *Biochemical and Biophysical Research Communications*, vol. 391, no. 1, pp. 96–101, 2010.

[32] W. T. Wu, M. C. Mong, Y. C. Yang, Z. H. Wang, and M. C. Yin, "Aqueous and ethanol extracts of daylily flower (*Hemerocallis fulva* L.) protect HUVE cells against high glucose," *Journal of Food Science*, vol. 83, no. 5, pp. 1463–1469, 2018.

[33] B. Zdzisińska, W. Rzeski, R. Paduch et al., "Differential effect of betulin and betulinic acid on cytokine production in human whole blood cell cultures," *Polish Journal of Pharmacology*, vol. 55, no. 2, pp. 235–238, 2003.

[34] K. S. Kim, D. S. Lee, D. C. Kim et al., "Anti-inflammatory effects and mechanisms of action of coussaric and betulinic acids isolated from *diospyros kaki* in lipopolysaccharide-stimulated RAW 264.7 macrophages," *Molecules*, vol. 21, no. 9, article 1206, 2016.

[35] X. Huang, Q. Pan, Z. Mao et al., "Sinapic acid inhibits the IL-1β-induced inflammation via MAPK downregulation in rat chondrocytes," *Inflammation*, vol. 41, no. 2, pp. 562–568, 2018.

[36] K. J. Yun, D. J. Koh, S. H. Kim et al., "Anti-inflammatory effects of sinapic acid through the suppression of inducible nitric oxide synthase, cyclooxygase-2, and proinflammatory cytokines expressions via nuclear factor-κB inactivation," *Journal of Agricultural and Food Chemistry*, vol. 56, no. 21, pp. 10265–10272, 2008.

[37] M. Jayachandran, R. Vinayagam, R. R. Ambati, B. Xu, and S. S. M. Chung, "Guava leaf extract diminishes hyperglycemia and oxidative stress, prevents β-cell death, inhibits inflammation, and regulates NF-κB signaling pathway in STZ induced

diabetic rats," *BioMed Research International*, vol. 2018, Article ID 4601649, 14 pages, 2018.

[38] J. H. Lee, J. H. Won, J. M. Choi et al., "Protective effect of ellagic acid on concanavalin A-induced hepatitis via toll-like receptor and mitogen-activated protein kinase/nuclear factor κb signaling pathways," *Journal of Agricultural and Food Chemistry*, vol. 62, no. 41, pp. 10110–10117, 2014.

[39] S. J. Hwang, Y. W. Kim, Y. Park, H. J. Lee, and K. W. Kim, "Anti-inflammatory effects of chlorogenic acid in lipopolysaccharide-stimulated RAW 264.7 cells," *Inflammation Research*, vol. 63, no. 1, pp. 81–90, 2014.

[40] V. A. Kostyuk, A. I. Potapovich, T. O. Suhan, C. De Luca, and L. G. Korkina, "Antioxidant and signal modulation properties of plant polyphenols in controlling vascular inflammation," *European Journal of Pharmacology*, vol. 658, no. 2-3, pp. 248–256, 2011.

[41] M. De La Luz Cádiz-Gurrea, I. Borrás-Linares, J. Lozano-Sánchez, J. Joven, S. Fernández-Arroyo, and A. Segura-Carretero, "Cocoa and grape seed byproducts as a source of antioxidant and anti-inflammatory proanthocyanidins," *International Journal of Molecular Sciences*, vol. 18, no. 2, p. 376, 2017.

[42] M. S. Karimian, M. Pirro, M. Majeed, and A. Sahebkar, "Curcumin as a natural regulator of monocyte chemoattractant protein-1," *Cytokine and Growth Factor Reviews*, vol. 33, pp. 55–63, 2017.

[43] P. Pullikotil, H. Chen, R. Muniyappa et al., "Epigallocatechin gallate induces expression of heme oxygenase-1 in endothelial cells via p38 MAPK and Nrf-2 that suppresses proinflammatory actions of TNF-α," *The Journal of Nutritional Biochemistry*, vol. 23, no. 9, pp. 1134–1145, 2012.

[44] V. K. Bajpai, M. B. Alam, M. K. Ju et al., "Antioxidant mechanism of polyphenol-rich Nymphaea nouchali leaf extract protecting DNA damage and attenuating oxidative stress-induced cell death via Nrf2-mediated heme-oxygenase-1 induction coupled with ERK/p38 signaling pathway," *Biomedicine & Pharmacotherapy*, vol. 103, pp. 1397–1407, 2018.

[45] A. I. Casas, V. T. V. Dao, A. Daiber et al., "Reactive oxygen-related diseases: therapeutic targets and emerging clinical indications," *Antioxidants & Redox Signaling*, vol. 23, no. 14, pp. 1171–1185, 2015.

[46] M. Mittal, M. R. Siddiqui, K. Tran, S. P. Reddy, and A. B. Malik, "Reactive oxygen species in inflammation and tissue injury," *Antioxidants & Redox Signaling*, vol. 20, no. 7, pp. 1126–1167, 2014.

[47] S. Manoharan, G. J. Guillemin, R. S. Abiramasundari, M. M. Essa, M. Akbar, and M. D. Akbar, "The role of reactive oxygen species in the pathogenesis of Alzheimer's disease, Parkinson's disease, and Huntington's disease: a mini review," *Oxidative Medicine and Cellular Longevity*, vol. 2016, Article ID 8590578, 15 pages, 2016.

[48] F. Festa, T. Aglitti, G. Duranti, R. Ricordy, P. Perticone, and R. Cozzi, "Strong antioxidant activity of ellagic acid in mammalian cells in vitro revealed by the comet assay," *Anticancer Research*, vol. 21, no. 6A, pp. 3903–3908, 2001.

[49] K. Sevgi, B. Tepe, and C. Sarikurkcu, "Antioxidant and DNA damage protection potentials of selected phenolic acids," *Food and Chemical Toxicology*, vol. 77, pp. 12–21, 2015.

[50] S. R. Abbas, S. M. Sabir, S. D. Ahmad, A. A. Boligon, and M. L. Athayde, "Phenolic profile, antioxidant potential and DNA damage protecting activity of sugarcane (*Saccharum officinarum*)," *Food Chemistry*, vol. 147, pp. 10–16, 2014.

[51] P. Singh, S. P. Vishwakarma, and R. L. Singh, "Antioxidant, oxidative DNA damage protective and antimicrobial activities of the plant *Trigonella foenum-graecum*," *Journal of the Science of Food and Agriculture*, vol. 94, no. 12, pp. 2497–2504, 2014.

[52] K. Kozics, V. Klusová, A. Srančíková et al., "Effects of *Salvia officinalis* and *Thymus vulgaris* on oxidant-induced DNA damage and antioxidant status in HepG2 cells," *Food Chemistry*, vol. 141, no. 3, pp. 2198–2206, 2013.

[53] A. C. Dametto, D. Agustoni, T. F. Moreira et al., "Chemical composition and *in vitro* chemoprevention assessment of *Eugenia jambolana* Lam. (Myrtaceae) fruits and leaves," *Journal of Functional Foods*, vol. 36, pp. 490–502, 2017.

[54] S. Schaefer, M. Baum, G. Eisenbrand, H. Dietrich, F. Will, and C. Janzowski, "Polyphenolic apple juice extracts and their major constituents reduce oxidative damage in human colon cell lines," *Molecular Nutrition & Food Research*, vol. 50, no. 1, pp. 24–33, 2006.

[55] F. Guglielmi, C. Luceri, L. Giovannelli, P. Dolara, and M. Lodovici, "Effect of 4-coumaric and 3,4-dihydroxybenzoic acid on oxidative DNA damage in rat colonic mucosa," *The British Journal of Nutrition*, vol. 89, no. 5, pp. 581–587, 2003.

[56] C. H. Tsai, S. F. Tzeng, S. C. Hsieh et al., "A standardized *Wedelia chinensis* extract overcomes the feedback activation of HER2/3 signaling upon androgen-ablation in prostate cancer," *Frontiers in Pharmacology*, vol. 8, p. 721, 2017.

[57] C. Soldani and A. I. Scovassi, "Poly(ADP-ribose) polymerase-1 cleavage during apoptosis: an update," *Apoptosis*, vol. 7, no. 4, pp. 321–328, 2002.

[58] H. Wei and X. Yu, "Functions of PARylation in DNA damage repair pathways," *Genomics, Proteomics & Bioinformatics*, vol. 14, no. 3, pp. 131–139, 2016.

[59] L. J. Kuo and L. X. Yang, "Gamma-H2AX - a novel biomarker for DNA double-strand breaks," *In Vivo*, vol. 22, no. 3, pp. 305–309, 2008.

[60] M. Hausmann, E. Wagner, J. H. Lee et al., "Super-resolution localization microscopy of radiation-induced histone H2AX-phosphorylation in relation to H3K9-trimethylation in HeLa cells," *Nanoscale*, vol. 10, no. 9, pp. 4320–4331, 2018.

[61] C. Y. Lin, P. N. Chen, Y. S. Hsieh, and S. C. Chu, "Koelreuteria formosana extract impedes in vitro human LDL and prevents oxidised LDL-induced apoptosis in human umbilical vein endothelial cells," *Food Chemistry*, vol. 146, pp. 299–307, 2014.

[62] H. Chang, W. Yuan, H. Wu, X. Yin, and H. Xuan, "Bioactive components and mechanisms of Chinese poplar propolis alleviates oxidized low-density lipoprotein-induced endothelial cells injury," *BMC Complementary and Alternative Medicine*, vol. 18, no. 1, p. 142, 2018.

[63] S. He, R. Ou, W. Wang et al., "Camptosorus sibiricus rupr aqueous extract prevents lung tumorigenesis via dual effects against ROS and DNA damage," *Journal of Ethnopharmacology*, vol. 220, pp. 44–56, 2018.

[64] R. S. Carvalho, C. A. Carollo, J. C. de Magalhães et al., "Antibacterial and antifungal activities of phenolic compound-enriched ethyl acetate fraction from *Cochlospermum regium* (mart. Et. Schr.) Pilger roots: mechanisms of action and synergism with tannin and gallic acid," *South African Journal of Botany*, vol. 114, pp. 181–187, 2018.

[65] R. R. Chand, A. D. Jokhan, R. D. Gopalan, and T. Osborne, "Antibacterial and antifungal activities of essential oils from medicinal plants found in the South Pacific," *The South Pacific*

Journal of Natural and Applied Sciences, vol. 35, no. 1, pp. 10–19, 2017.

[66] K. Bashir Dar, A. Hussain Bhat, S. Amin et al., "Evaluation of antibacterial, antifungal and phytochemical screening of *Solanum nigrum*," *Biochemistry & Analytical Biochemistry*, vol. 6, no. 1, p. 309, 2017.

[67] E. Ivanišová, T. Krajčovič, M. Tokár, Š. Dráb, A. Kántor, and M. Kačániová, "Potential of wild plants as a source of bioactive compounds," *Animal Science & Biotechnologies*, vol. 50, pp. 109–114, 2017.

[68] B. Paudel, H. D. Bhattarai, I. C. Kim et al., "Estimation of antioxidant, antimicrobial activity and brine shrimp toxicity of plants collected from Oymyakon region of the republic of Sakha (Yakutia), Russia," *Biological Research*, vol. 47, no. 1, p. 10, 2014.

[69] C. S. Rempe, K. P. Burris, S. C. Lenaghan, and C. N. Stewart, "The potential of systems biology to discover antibacterial mechanisms of plant phenolics," *Frontiers in Microbiology*, vol. 8, p. 422, 2017.

[70] H. O. B. Oloyede, H. O. Ajiboye, M. O. Salawu, and T. O. Ajiboye, "Influence of oxidative stress on the antibacterial activity of betulin, betulinic acid and ursolic acid," *Microbial Pathogenesis*, vol. 111, pp. 338–344, 2017.

[71] G. M. Woldemichael, M. P. Singh, W. M. Maiese, and B. N. Timmermann, "Constituents of antibacterial extract of Caesalpinia paraguariensis Burk," *Zeitschrift für Naturforschung C*, vol. 58, no. 1-2, pp. 70–75, 2003.

[72] C. Chandramu, R. D. Manohar, D. G. L. Krupadanam, and R. V. Dashavantha, "Isolation, characterization and biological activity of betulinic acid and ursolic acid from *Vitex negundo* L," *Phytotherapy Research*, vol. 17, no. 2, pp. 129–134, 2003.

[73] L. Catteau, L. Zhu, F. Van Bambeke, and J. Quetin-Leclercq, "Natural and hemi-synthetic pentacyclic triterpenes as antimicrobials and resistance modifying agents against *Staphylococcus aureus*: a review," *Phytochemistry Reviews*, vol. 17, no. 5, pp. 1129–1163, 2018.

[74] T. Wu, X. Zang, M. He, S. Pan, and X. Xu, "Structure–activity relationship of flavonoids on their anti-Escherichia coli activity and inhibition of DNA gyrase," *Journal of Agricultural and Food Chemistry*, vol. 61, no. 34, pp. 8185–8190, 2013.

[75] S. Khan, T. Ur-Rehman, B. Mirza, I. Ul-Haq, and M. Zia, "Antioxidant, antimicrobial, cytotoxic and protein kinase inhibition activities of fifteen traditional medicinal plants from Pakistan," *Pharmaceutical Chemistry Journal*, vol. 51, no. 5, pp. 391–398, 2017.

[76] C. Willyard, "The drug-resistant bacteria that pose the greatest health threats," *Nature*, vol. 543, no. 7643, p. 15, 2017.

Hindawi
Oxidative Medicine and Cellular Longevity
Volume 2019, Article ID 3685264, 16 pages
https://doi.org/10.1155/2019/3685264

Review Article

Medicinal Plants from Brazilian Cerrado: Antioxidant and Anticancer Potential and Protection against Chemotherapy Toxicity

José Tarcísio de Giffoni de Carvalho, Débora da Silva Baldivia, Daniel Ferreira Leite, Laura Costa Alves de Araújo, Priscilla Pereira de Toledo Espindola, Katia Avila Antunes, Paola Santos Rocha, Kely de Picoli Souza, and Edson Lucas dos Santos

Research Group on Biotechnology and Bioprospecting Applied to Metabolism, Federal University of Grande Dourados, Dourados, Brazil

Correspondence should be addressed to Edson Lucas dos Santos; edsonsantosphd@gmail.com

Received 8 March 2019; Revised 16 June 2019; Accepted 15 July 2019; Published 25 August 2019

Guest Editor: Patrícia Rijo

The use of natural antioxidants in cancer therapy has increased: first, due to the potential of natural antioxidants to kill tumour cells and second, because of their capacity to protect healthy cells from the damage caused by chemotherapy. This review article discusses the antioxidant properties of extracts obtained from medicinal plants from the Brazilian Cerrado and the cell death profile induced by each of these extracts in malignant cells. Next, we describe the capacity of other medicinal plants from the Cerrado to protect against chemotherapy-induced cell toxicity. Finally, we focus on recent insights into the cell death profile induced by extracts from Cerrado plants and perspectives for future therapeutic approaches.

1. Introduction

Natural products or their derivatives represent approximately 60% of all chemotherapeutic agents approved by the Food and Drug Administration (FDA), including vincristine, vinblastine, and Taxol [1–3]. However, the search for medicinal plants with anticancer properties has intensified in recent years since chemotherapeutic agents are limited by a high rate of drug resistance and by severe side effects. Additionally, some of the current drugs used in cancer therapy are very expensive to produce [2, 4]. Therefore, there is great interest in the discovery and identification of effective anticancer compounds and molecules with low production costs and high target cell selectivity [5–7].

Brazil is considered to be the territory with the richest biodiversity in the world [8–11]; the Cerrado is the second main biome, exhibiting a great diversity of natural plants [9, 12, 13]. The Cerrado is located in the middle west of Brazil, encompassing almost 2 million km^2 that covers 21% of the Brazilian territory [14, 15].

Numerous studies have evaluated the biological effects of extracts from medicinal plants from the Cerrado. These extracts include *Stryphnodendron adstringens*, popularly known as barbatimão, which has displayed antiulcerogenic and antifungal effects [16], and *Campomanesia adamantium*, popularly known as Guavira, which has presented antidiabetic properties, anti-inflammatory, and diuretic actions [17]. Another plant from the Brazilian Cerrado is *Senna velutina*; little is known about its biological effects, but an important study investigated its antitumour activity in a leukaemia cell lineage [18]. In addition, the *Jacaranda* [19] and *Harconia* [20] genera are other examples of medicinal plants from the Cerrado commonly used in folk

medicine and with some described biological properties, mainly antioxidant activity. Finally, *Schinus terebinthifolius* and *Guazuma ulmifolia* are used in traditional medicine to treat ulcers, diarrhoea, arthritis, and infections [21] and inflammation, gastrointestinal diseases, and diabetes [22], respectively. The botanical features and geographical distribution of plants from the Brazilian Cerrado are outlined in Table 1.

This review article discusses the antioxidant properties of extracts obtained from medicinal plants from the Brazilian Cerrado and the cell death profile induced by these extracts in malignant cells. Next, we describe the capacity of other medicinal plants from the Cerrado to protect against chemotherapy-induced cell toxicity.

2. Redox Balance Potential

Natural antioxidants are molecules that protect cells from the damage induced by reactive oxidative species (ROS) [4, 66]. These ROS, including superoxide anion ($O_2^{\bullet}-$) and hydrogen peroxide (H_2O_2), are involved in various cellular processes (host immune defence, cell signaling, cellular respiration process, and others); however, if they are not properly regulated by the antioxidant system, ROS initiate a number of deleterious effects, which may cause the oxidation of biomolecules [67, 68]. For example, excessive ROS results in lipid peroxidation, a process in which free radicals attack polyunsaturated fatty acids, a lipid present in the cell membrane, resulting in membrane rupture and the production of toxic molecules, especially malondialdehyde (MDA), associated with cell damage and mutagenicity [68–70].

Superoxide is generated from diverse metabolic pathways in cells, including the mitochondrial respiratory chain and the enzymatic action of cytochrome p450 and NADPH oxidases [71, 72]. The superoxide that results from these reactions can undergo dismutation to generate water (H_2O) by superoxide dismutase (SOD), an enzyme in the antioxidant system or can react with nitric oxide ($NO^{\bullet}$), to generate reactive nitrogen species, such as peroxynitrite ($ONOO^{-}$), the most powerful oxidant [67, 69].

Superoxide dismutase catalyses the dismutation of $O_2^{\bullet-}$ to hydrogen peroxide (H_2O_2), which is a less reactive species and a substrate for other enzymes involved in the antioxidant system. Successively, in a Fenton reaction, H_2O_2 can be modified to a toxic hydroxyl radical (OH^{-}) in the presence of transmission metals, such as iron (Fe^{2+}), and therefore should be decomposed to H_2O. For this step, the most efficient enzymatic antioxidants are catalase (CAT) and/or glutathione peroxidase enzymes (GPx) [73, 74]. GPx reduce peroxides to water (or alcohol) through oxidation of selenol residue to selenenic acid (RSe-OH) groups which are converted back to selenols by the tripeptide glutathione (GSH). Oxidazed gluthatione (GSSH) is oxidazed back to GSH by glutatione reductase [67, 69, 73].

Numerous studies have evaluated the antioxidant potential of extracts from plants from the Cerrado. Campos et al. [18] studied the effects of *S. velutina* on radical scavenging activity. Extracts prepared from the leaves of *S. velutina* in an ethanol solvent were found to be very potent inhibitors of radical scavenging activity by the DPPH (2,2′-diphenyl-1-picrylhydrazyl) method, and the concentration necessary for the 50% inhibition (IC_{50}) of DPPH of these extracts was lower than that of the commercial antioxidant butylated hydroxytoluene (BHT) (6.3 ± 1.3 versus $21.3 \pm 1.2\,\mu$g/mL). Similarly, Dos Santos et al. [46] evaluated the antioxidant capacity of a leaf extract of *Hancornia speciosa* in an ethanolic solvent and also observed a potential activity by the DPPH method and improved IC_{50} values in relation to BHT (9.4 ± 0.8 versus $66.1 \pm 23.6\,\mu$g/mL).

Espindola et al. [38] found that an extract prepared from the root of *C. adamantium* in an aqueous solvent and BHT had similar antioxidant capacities by the DPPH method (IC_{50} : 37.3 ± 4.1 versus $36.1 \pm 9.1\,\mu$g/mL) [38]. Baldivia et al. [16] evaluated the antioxidant effects of an extract from the stem bark of *S. adstringens* by the DPPH and ABTS methods (2,2′-azino-bis(3-ethylbenzothiazoline-6-sulfonic acid)). The antioxidant efficacy of *S. adstringens* is similar to that of ascorbic acid according to both methods (DPPH IC_{50}, 3.81 ± 0.02 versus $2.65 \pm 0.03\,\mu$g/mL; ABTS IC_{50}, 1.83 ± 0.15 versus $1.34 \pm 0.01\,\mu$g/mL).

These results demonstrate that the extracts obtained from *S. velutina*, *H. speciosa*, *C. adamantium*, and *S. adstringens* may directly react with free radicals by electron donation radical scavenging, thereby inhibiting ROS-induced damage. These actions can be attributed to the presence of phenolic compounds. The antioxidant efficiency of a phenolic compound depends on the capacity of a hydrogen atom in a hydroxyl group on an aromatic structure to be donated to a free radical [75, 76]. Among the phenolic compounds described as major potential antioxidants, gallic acid is a well-described phenolic compound with antioxidant and antihaemolytic activities in human erythrocytes [77–79]. Procyanidins are also excellent antioxidants capable of protecting erythrocytes from oxidative haemolysis [80, 81]. Furthermore, flavonoids known as catechins [82, 83], rutin [84, 85], and quercetin [86, 87] are among the most abundant and important chemical constituents of plant species and are described as lipid peroxidation inhibitors. The phenolic compounds identified in extracts of *C. adamantium*, *S. velutina*, and *S. adstringens* are listed in Table 2.

The extracts from these plants also showed antioxidant activity and demonstrated lipid peroxidation prevention in 2,2′-azobis(-amidinopropane) dihydrochloride- (AAPH-) induced erythrocyte haemolysis as evidenced by MDA production. Importantly, MDA is related to cell damage and mutagenicity and the inhibition of this process can restore cell homeostasis and prevent the development of oxidative stress-related disease [88].

Casagrande et al. [19] evaluated the activities of SOD, CAT, and GPx antioxidant enzymes in human erythrocyte lysates and found that a hydroethanolic extract of *Jacaranda decurrens subsp. symmetrifoliolata* leaves increased the enzyme activity of glutathione peroxidase and reduced the activity of superoxide dismutase and catalase. Rocha et al. [21] showed that the enzymatic activity of SOD and GPx enzymes increased upon treatment of human erythrocytes

Table 1: Biological activities, botanical features, and geographical distribution of plants from Brazilian Cerrado.

Name	Family	Biological activities	Botanical features	Geographical distribution
Stryphnodendron adstringens Mart. Coville	Fabaceae	The roots and stem bark extract (h) have wound healing [23, 24], anti-inflammatory (w) [25], antigastric ulcer (e) [26], and antidiabetic (e) [27] effects, and fractions from stem bark extract have antimicrobial activity against *Cryptococcus neoformans* (aw-F/etacF) [28], *Candida albicans* (aw-F/etacF) [29, 30], herpes virus (etacF) [31], and gram-positive bacteria (e, h, and b) [32].	Trees in this genus are medium-sized, the trunk does not have ramifications, and the stem usually has a rusty, coarse, and rust-colored bark. Species can be differentiated by their leaf structure; *S. adstringens* has 5–7 pairs of leaflets in an opposite sense with 5–6 pairs of second-order leaflets alternately inserted, different from other species [33].	Distribution of gender is limited to the area between Nicaragua and the southern regions of Brazil. S. adstringens more specifically is distributed in Brazilian states: Tocantins, Bahia, Distrito Federal, Goiás, Mato Grosso, Minas Gerais, São Paulo, and Paraná [33].
Campomanesia adamantium O. Berg	Myrtaceae	The peel extract (e : w–70/30%) was found to have antiplatelet and anti-inflammatory effects [34]; the seed extract (w) has an antinociceptive effect [35, 36]; the peel extract (e : w–70/30%) has antidiarrhoeal activity [37]; and the leaf extract (w) has hypolipidaemic [38] effects.	They are shrubs with elliptical branches, growing from 1.5 m to 3 m in height with a disorganized crown. The trunk is tortuous and branched from the base with yellowish bark. The leaves are simple, opposing, oblong (longer than broad), and glabrescent (with almost no hair on the mature leaf), and the dimensions of the leaf range are from 4.5 to 6.8 cm in length by 1.5 to 2.3 cm wide [39].	Endemic distribution in some Brazilian states such as Minas Gerais, Mato Grosso do Sul, and Santa Catarina and arriving in some adjacent regions in Argentina and Paraguay [39].
Hancornia speciosa Gomes	Apocynaceae	The bark extract has antidiabetic, antiobesity, antimicrobial, and gastroprotective activities (he) [40]; the latex has anti-inflammatory activity [41]; and the leaf extract (e) was found to have antihypertensive [42], vasodilatory (e) [43, 44], and antidiabetic (e) [45] activities.	*H. speciosa* is a tree that has a medium-sized (2-10 m), tortuous, and rough trunk. The leaves are simple, alternating, and opposite and varied in shapes and sizes. The flowers are white and have an elongated shape. The small fruit has a shape similar to that of the pear [46].	Widely distributed throughout the Brazilian territory and described in other countries such as Paraguay, Peru, Bolivia, and Venezuela [46].
Schinus terebinthifolius Raddi	Anacardiaceae	The leaf extract (e) has antidiabetic activity [47]. The leaf extracts (me) can treat neuropathic pain [48] and have antihypertensive (meF) [49] and antiarthritis (he) [50] effects. The essential oil from twigs and leaf extract (c : m) showed activity against *Enterococcus faecium* and *Streptococcus agalactiae* [51], and the essential oil from leaves (e) has anti-inflammatory and wound healing effects [52]. Isolated endophytic fungi showed activity against *Staphylococcus aureus* and *Pseudomonas aeruginosa* [53]. The stem bark extract has activity against herpes simplex virus type 1 (he and mef) [54]; the bark extract has activity against the Candida genus (a) [55]; and the leaves and fruits extracts (e) have activity against *Escherichia coli* [56].	*S. terebinthifolius* is a tree that is almost 8 m in height, and the diameter of the trunk can reach up to 60 cm. The leaves are composite by leaflets measuring 3 to 5 cm, and the plant has small flowers in a pyramidal structure and red fruits [57].	More frequently seen along the Brazilian coast from the north to the south and found in other regions such as Mato Grosso do Sul and Minas Gerais. It probably covers most of South America and was largely introduced in other countries, including the United States, as ornamental plants [57].

Table 1: Continued.

Name	Family	Biological activities	Botanical features	Geographical distribution
Jacaranda decurrens subsp. *symmetrifoliolata* Farias & Proenca	Bignoniaceae	The leaf extract (he) is described to have antiobesity, hypocholesterolemic, and hypolipidaemic [58] activities and the roots (he) has anti-inflammatory [59] activity.	The species measures 50-150 cm. Its leaf is biped, with leaflets elliptical to oblong, and its fruit is an oblong-obovate capsule, extremely woody, brown, and glabrous with a nonwavy margin in the dehiscence [60].	This is an endemic species of the southern State of Mato Grosso [60].
Guazuma ulmifolia Lam.	Malvaceae	The stem bark and leaf extracts (w) have antidiabetic potential [61]. The stem bark extract (a) has hypotensive, vasorelaxant [62], and gastroprotective [63, 64] effects.	The leaves *of G. ulmifolia* display as an ovoid structure; the flowers have long filiform appendages; and the black fruits have a capsular form of two to three centimeters [65].	*G. ulmifolia* is a tree that is distributed from Mexico to Brazil [65].

Legend. Solvent: e: ethanol; h: hexane; w: water; a: acetate; m: methanol; e : w: ethanol : water; h : e: hydro : ethanol; c : m: chloroform : methanol. Fraction: aw-F: acetate water; etacF: ethyl acetate fraction; meF: methanol fraction.

Table 2: Cytotoxic potential and compounds identified from extracts of Cerrado plants.

Plant species	Parts used	Model	Cytotoxic features	Compounds identified	Ref.
S. adstringens	Stem bark	B16F10-Nex2	Mitochondrial depolarization, caspase-3 activation, and ROS production	Gallic acid, procyanidins, and catechins	Baldivia et al. [16]
	Stem bark	HeLa, SiHa, and C33A	Intense oxidative stress, mitochondrial damage, increased Bax/BCL-2 ratio, and increased caspase-9 and caspase-3 expression	Proanthocyanidin polymer-rich fraction	Kaplum et al. [146]
		MCF-7 and MDA-MB-435	Increased Bax/BCL-2 ratio and increased caspase-9, active caspase-3, caspase-8, LC-3, and beclin-1 expression	Gallic acid, procyanidins, and catechins	Sabino et al. [147]
C. adamantium	Leaves	K562 cells	Caspase-3 and caspase-9 activation, cell cycle arrest at the S and G2 phases, and calcium influx	O-Pentoside and O-deoxyhexoside myricetin, quercetin O-pentoside, and myricetin-O-(O-galloyl)-pentoside	Campos et al. [17]
	Roots			O-Pentoside, O-methyl ellagic acid, O-hexoside, O-deoxyhexoside, O-methyl ellagic acid, and gallic acid	
	Leaves	PC-3	Inhibited prostate cancer cell proliferation, DNA fragmentation, and decreased NFkB1 expression	Chalcone cardamonin	Pascoal et al. [144]
		MCF-7, HeLa, and M059J	Inhibited cancer cell proliferation	β-Myrcene, spathulenol, germacrene-B, β-caryophyllene oxide, β-caryophyllene, α-pinene, viridiflorol, limonene, and (Z,E)-farnesol (6.51%)	Alves et al. [145]
S. velutina	Leaves	Jurkat/K562 cells	Caspase-3 activation, mitochondrial depolarization, cell cycle arrest at the S and G2 phases, and calcium influx	Epigallocatechin, epicatechin, rutin, kaempferol glycosides, and dimeric and trimeric proanthocyanidins	Campos et al. [18]
	Roots	B16F10nex2 cells and mouse C57b1/6	Increased intracellular ROS levels, induced mitochondrial membrane potential dysfunction, activated caspase-3, and impaired pulmonary metastasis *in vitro*	Flavonoid derivatives of catechin and piceatannol (active metabolite of resveratrol) groups and dimeric tetrahydroanthracene derivatives	Castro et al. [142]
J. decurrens	Leaves	K562 cells	Mitochondrial depolarization, Caspase-3 activation, necrosis and late apoptosis	Phenolic compounds and flavonoids	Casagrande et al. [19]
H. speciosa	Leaves	Kasumi-1 cells	Necroptosis and cathepsin release	Bornesitol, quinic acid, chlorogenic acid, and flavonoids derived from kaempferol and rutin	Dos Santos et al. [46]

Table 2: Continued.

Plant species	Parts used	Model	Cytotoxic features	Compounds identified	Ref.
G. ulmifolia	Stem bark	K562 cells and mouse C57b1/6	Protected against the doxorubicin-induced cardiotoxicity and reduced oxidative haemolysis *in vitro*	Citric and quinic acids	Dos Santos et al. [22]
	Leaves			O-Pentosyl and di-O-deoxyhesosyl-hesosyl quercetin, O-deoxyhexosyl hexosyl luteolin, and di-O-deoxyhexosyl hexosyl kaempferol	
S. terebinthifolius	Leaves	K562 cells and mouse C57b1/6	Protected against doxorubicin-induced cardiotoxicity and reduced oxidative haemolysis *in vitro*	Phenolic compounds, flavonoid, tannin, and ascorbic acid [21] and α-pinene, limonene, carene, and phellandrene [159]	Rocha et al. [21] and Carneiro et al. [159]

with an extract prepared from the leaves of *S. terebinthifolius* in methanol solvent. Based on these results, it seems that *J. decurrens* and *S. terebinthifolius* may modulate the endogenous antioxidant system.

Extracts of *C. adamantium*, in addition to scavenging activity, were described to reduce MDA *in vitro* and *in vivo* [38]. The capacity of *C. adamantium* to present *in vivo* antioxidant effects represents a major advantage for the development of new products. In many cases, *in vitro* findings are not reproduced in an organism due to various factors, such as enzyme inactivation, poor absorption, and tissue distribution [89, 90]. This finding suggests that the *C. adamantium* extract showed a bioavailability profile suitable for use *in vivo*.

These results demonstrated that these extracts are very potent antioxidants due to their radical scavenging capacity and their capacity to protect the cell against lipid peroxidation. Furthermore, the synthetic antioxidants commonly used are reported to be mutagenic and cause liver injury [91]. The search for new antioxidants that are more effective and have a better toxicity profile than current antioxidants is desirable, and the plants described here may represent interesting targets for this purpose.

3. Antioxidants and Cancer

Cancer is a multistage process resulting in an uncontrolled cell cycle and cell division and apoptosis resistance and is one of the main diseases that cause mortality worldwide [92]. Carcinogenesis is a process that involves multiple steps, including an initiation phase that can occur after exposure to a carcinogenic agent, and commonly results in increased production of ROS [93, 94]. The initialization of cancer cells commonly depends on mutations in genes related to the regulation of the cell cycle, apoptosis, and/or growth factor signalling pathways, which can be induced by ROS-mediated DNA mutations [95, 96].

The interaction between antioxidants and cancer cells can occur in at least three ways:

(i) Prevention: the ability of antioxidants to protect cells from ROS-induced DNA damage is the basis of the association of antioxidants with cancer prevention [97–99]

(ii) Protects against chemotherapy toxicity: chemotherapy commonly increases the production of ROS, which induces oxidative stress in cancer cells and other tissues. Excessive ROS may cause a disruption in cellular homeostasis, which can lead to toxicity. Therefore, to improve the clinical response to chemotherapy, combination approaches with antioxidants are being investigated by providing protection against toxic side effects [100, 101]

(iii) New anticancer molecules: recent evidence has suggested that antioxidants can also be used to eliminate cancer cells. Over the last few decades, antioxidant extracts from medicinal plants have shown a great cytotoxic potential [102, 103]

4. Cell Death Pathway in Cancer Cells

Currently, cell death continues to be considered a complex process that results in a variety of pathways [104–106]. The fact that cells die through different death pathways and that cancer cells can be resistant to each cell death signalling pathway is a relevant aspect in the development of new drugs for anticancer therapy [107, 108]. To date, knowledge of the cell death pathway induced by medicinal plants from the Cerrado is still scarce [109, 110].

4.1. Classical Cell Death. Apoptosis is a regulated and controlled process accompanied by a series of hallmarks, including cell shrinkage, chromatin condensation, DNA fragmentation, and apoptotic body formation, which is dependent on the activation of a protease enzyme family called caspases [111, 112]. In apoptosis, a change in the membrane of the cell marks the cell for recognition and phagocytosis by macrophages [113, 114].

Despite the modulation of apoptosis by drugs in cancer cells, the activation of the intrinsic pathway is a critical step [109, 115]. In response to insults, the opening of pores occurs in the mitochondrial membrane and the release of proapoptotic factors, such as cytochrome c, then forms an apoptosome complex in the cytosol together with the apoptosis inductor factor and pro-caspase-9, leading to caspase-9 activation. Caspase-9 then activates effector caspases such as caspase-3, resulting in the cleavage of several cellular targets involved in all aspects of apoptosis. The release of proapoptotic factors from mitochondria is regulated by proapoptotic (BAX) and antiapoptotic (Bcl-2) proteins [116–118].

In addition to the Bcl-2 family, the intrinsic pathway can also be modulated by intracellular calcium [119–121] and the ROS generated by mitochondria [71, 72, 122]. The ROS generated by mitochondria, or elsewhere in the cells, can activate p53, which activates proapoptotic Bcl-2 proteins that can inhibit the functions of antiapoptotic proteins [71, 122–124]. Moreover, ROS cause mitochondrial membrane depolarization and/or open Bax/Bak channels on the mitochondrial membrane, which allows for the release of apoptosis-inducing factor, endonuclease G, cytochrome c, and Smac/Diablo into the cytosol [72, 124]. Furthermore, the perturbation of intracellular Ca^{2+} homeostasis is also associated with cell death. Endoplasmic reticulum stress responses can induce lesions that affect membrane integrity and the release of Ca^{2+} [120, 121, 125]. Following Ca^{2+} efflux into the cytoplasm, the proapoptotic proteins Bak and Bax, which are located in both the reticulum and mitochondria, may be delivered to the cytosol. Calcium overload can induce mitochondrial dysfunction and cell death accompanied by membrane rupture, a process called necrosis [119, 125].

4.2. Alternative Cell Death Pathway. For several decades, apoptosis was depicted as programmed cell death in malignant and healthy cells and as a pivotal target for new therapies. Recently, other forms of cell death have also been increasingly noted [111, 126]. Discovering novel therapeutic strategies that may induce alternative cell death pathways

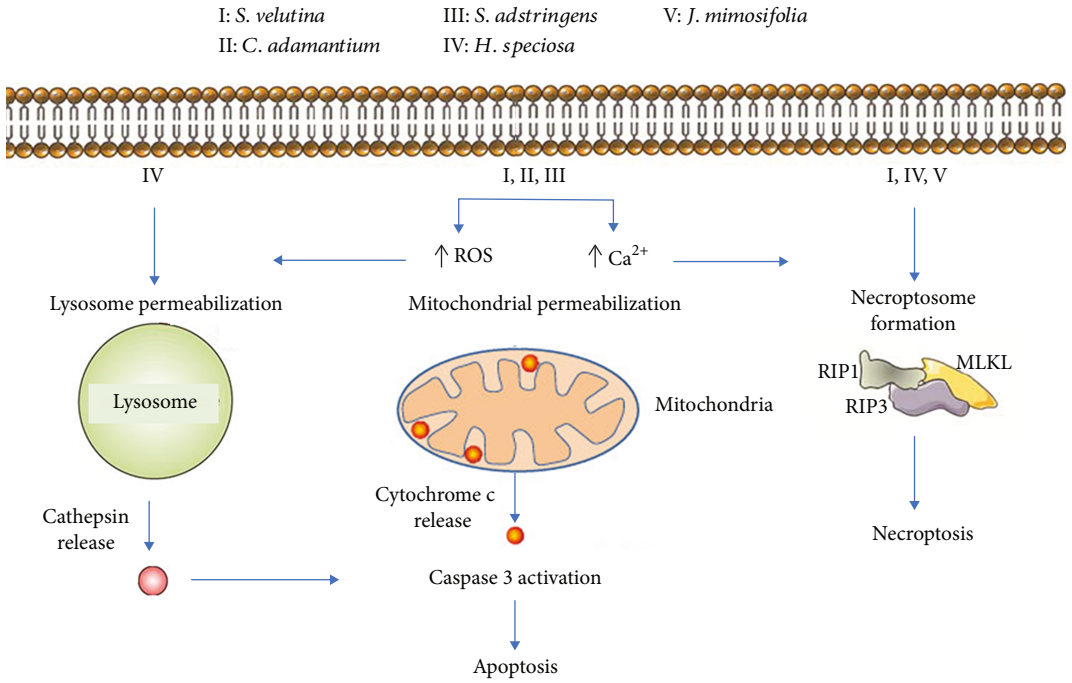

Figure 1: Cell death profile induced by extracts and/or compounds from medicinal plants of Cerrado.

appears to be especially useful for opposing malignant cell resistance to caspase-dependent apoptosis [127].

Necroptosis is a form of necrosis that occurs under caspase-deficient conditions [128, 129]. At the molecular level, necroptosis depends on the activation of serine/threonine receptor-interacting protein kinases 1 and 3 (RIPK1 and RIPK3) by death receptor ligands, which leads to the activation of mixed lineage kinase domain-like pseudokinase (MLKL) [130–132], allowing for a cascade of intracellular events involving Ca^{2+} influx, ROS production, and membrane rupture [133]. Moreover, accumulating evidence has shown that necroptosis promotes an anticancer immune response [134].

Lysosome-dependent cell death is initiated by perturbations of intracellular homeostasis and is demarcated by the permeabilization of lysosomal membranes [135–137]. Upon lysosomal stress, lysosome-dependent cell death proceeds through membrane permeabilization, resulting in the release of proteolytic enzymes from the cathepsin family to the cytoplasm, which activates death signalling pathways. More commonly, ROS play a prominent causal role in lysosomal permeabilization. The production of hydroxyl radicals by Fenton reactions destabilizes the lysosomal membrane upon lipid peroxidation, but an increase in cytoplasmic Ca^{2+} is also a key regulator reportedly involved in the activation of lysosomal cell death [138, 139]. Moreover, lysosomal dysregulation may be associated with alterations in autophagy and the role of ROS in homeostasis and cell death [137]. Autophagy is a self-digestive process that involves lysosomal fusion to degrade unnecessary or dysfunctional cellular components [140]. The role of autophagy in cancer is controversial; thus, the modulation of autophagy depends on each subtype of malignant cells and an improved understanding of this pathway in the cancer environment [141].

5. Cell Death Profile Induced by Plants from the Cerrado

Several reports from our group [16–19] have demonstrated the potential anticancer properties of medicinal Cerrado plants. Assessing the cell death profile induced by these extracts, through cell death inhibitors and/or caspase detection indicated the involvement of different cell death pathways for each plant extract. For example, many studies have demonstrated the antitumour potential of plant extracts through caspase-independent cell death, including *H. speciosa* [20] and *J. decurrens* [19], while others such as *C. adamantium* [17], *S. velutina* [18], and *S. adstringens* [16] killed malignant haematologic cells or melanoma cells through apoptosis (Figure 1 and Table 2).

Campos et al. [18] studied the effect of an extract from the leaves of *S. velutina* in two leukaemia cell lines: Jurkat cells, acute T cell leukaemia cells, and K562, Philadelphia chromosome-positive cells. Jurkat cells were found to be more sensitive to the cytotoxic effect of *S. velutina* than K562 cells, and this effect was accompanied by caspase-3 activation, mitochondrial depolarization, and cell cycle arrest at the S and G2 phases. Furthermore, these features were reversed by chelation of calcium, demonstrating the involvement of calcium as the main regulator of cell death mediated by *S. velutina*. Castro et al. [142] evaluated the effect of an extract from the roots of *S. velutina* on a melanoma cell line B16F10-Nex2 and also evaluated the antimetastatic effect of this extract using models of tumour volume progression and pulmonary nodule formation in C57Bl/6 mice. The extract reduced cell viability and promoted apoptotic cell death, caspase-3 activation, with increased intracellular calcium and ROS levels, and cell cycle arrest at the sub-G0/G1 phase. *In vivo*, the tumour volume

progression and pulmonary metastasis of *S. velutina*-treated mice decreased by over 50%. Taken together, these results show that *S. velutina* had *in vitro* and *in vivo* antitumour effects, predominantly through apoptosis, thus demonstrating its promising potential as a therapeutic agent in the treatment of melanoma, leukaemia, and possibly other types of cancer.

Other studies have identified the *in vitro* antiproliferative activity of the extract from leaves of *C. adamantium* in many cell lineages, including murine melanoma cells (B16-F10) [143], prostate cancer cells (PC-3) [144], breast adenocarcinoma cells (MCF-7), cervical adenocarcinoma cells (HeLa), and glioblastoma cells (M059J) [145]. However, none of these studies evaluated the cell death profile induced by extract of *C. adamantium*. In another study, Campos et al. [17] studied the cell death profile induced in Jurkat cells by an extract prepared from the leaves and roots of *C. adamantium*. A dose-dependent inhibition of viability occurred in cells incubated with the leaves and roots of *C. adamantium*. This effect was dependent on the accumulation of cytosolic Ca^{2+} and on cell cycle arrest at the S phase. In addition, the cell death induced by extracts was likely mediated by the intrinsic apoptotic pathway, since both extracts induced the activation of caspase-9 and caspase-3, and cell death was reversed after incubation with a general caspase inhibitor.

Baldivia et al. [16] found a similar profile of cell death in a study evaluating the effect of a hydroethanolic extract of the stem bark from *S. adstringens* on the melanoma cell line B16. *S. adstringens* increased the production of ROS, which may have induced the disruption in mitochondrial membrane potential that caused the apoptotic cell death observed in melanoma cells. These *in vitro* experiments demonstrated that *S. adstringens* is a potent cytotoxic extract that induces apoptosis-mediated cell death [16]. Kaplum et al. [146] investigated the *in vitro* anticancer activity of a proanthocyanidin polymer-rich fraction of the stem bark from *S. adstringens* (extracted in acetone : water) in cervical cancer cell lines, including HeLa (HPV18-positive), SiHa (HPV16-positive), and C33A (HPV-negative) cells, and evaluated *in vivo* anticancer activity. HeLa and SiHa cells treated with the extract exhibited intense oxidative stress, mitochondrial damage, and increased Bax/BCL-2 ratio and caspase-9 and caspase-3 expression. The inhibition of ROS production by N-acetylcysteine significantly suppressed oxidative stress in both cell lines. *In vivo*, the extract significantly reduced tumour volume and weight of Ehrlich solid tumours and significantly increased lipoperoxidation, indicating that it also induced oxidative stress in the *in vivo* model. These findings indicate that the proanthocyanidin polymer-rich fraction of *S. adstringens* may be a potential chemotherapeutic candidate for cancer treatment. Sabino et al. [147] investigated the *in vitro* anticancer activity of a fraction isolated from an aqueous leaf extract of *S. adstringens* in breast cancer cell lines. The fraction was cytotoxic against two human breast cancer cell lines: the estrogen receptor-positive cell line MCF-7 and the triple-negative cell line MDA-MB-435. Treatment with the fraction increased the expression of Bax, caspase-9, active caspase-3, caspase-8, LC-3, and beclin-1 and decreased the expression of Bcl-2, caspase-3, and pro-caspase-8 in cancer cells. Taken together, these results show that *S. adstringens* had *in vitro* and *in vivo* antitumour effects, predominantly through apoptosis, thus demonstrating its promising potential as a therapeutic agent in the treatment of melanoma, cervical cancer, breast cancer, and possibly other types of cancer.

Despite the benefits of the pharmacological cancer therapies, the high toxicity of chemotherapeutic drugs is one of the main identified problems. Importantly, in this context, *S. adstringens* and *C. adamantium* show less toxicity against healthy normal cells and peripheral blood mononuclear cells (PBMCs) than tumour cells. In particular, extracts made from the leaves of *C. adamantium* did not change the viability of PBMCs at the evaluated concentrations but exhibited an IC_{50} of 40 μg/mL in Jurkat cells. Although there was a cytotoxic effect of *S. adstringens* on PBMCs, this effect only occurred at the highest concentration evaluated ($\geq$200 μg/mL), which is comparable to the IC_{50} (65 μg/mL) exhibited against B16 cells, suggesting a high therapeutic index. These experiments indicate that these plants show selective effects against cancer cells and possibly do not confer any toxicity to healthy normal cells. New targeted therapies with low toxicity and limited side effects are promising for the development of new anticancer agents [148].

Dos Santos et al. [46] evaluated the cell death profile of an extract from *H. speciosa* in an acute myeloid leukaemia cell line, Kasumi-1. The extract from *H. speciosa* promoted caspase-independent apoptosis because the pancaspase inhibitor did not inhibit the cytotoxic activity of these extracts. This extract killed Kasumi-1 through the involvement of cathepsins and necroptosis and consequently, an alternative pathway of cell death. Cell signalization dependent on lysosomal degradation remains not yet understood, and it seems to modulate autophagic flux [137]. Thus, additional studies evaluating the modulation of autophagic flux mediated by *H. speciosa* are desirable.

Casagrande et al. [19] evaluated the cell death profile induced by extracts from *J. decurrens* in K562 erythroleukaemia cells. These researchers found concentration-dependent cytotoxic activity against the malignant cells studied, which occurred through late apoptosis and necrosis, the activation of caspase-3, and a decrease in mitochondrial membrane potential. Clinically, this cell death pathway (necrosis and necroptosis) is promising for the development of new anticancer compounds against malignant cells resistant to apoptosis [149, 150]. Moreover, accumulating evidence has shown that necroptosis promotes an anticancer immune response [134]. The great potential of necroptosis induced by *H. speciosa* and *J. decurrens* suggests further evaluation of the immunogenicity capacity of these medicinal plants.

Many phenolic compounds derived from Cerrado plants have demonstrated potential anticancer properties. At high concentrations, the phenolic compounds can act as prooxidants and impair the redox balance of malignant cells [151–155]. Gallic acid is a phenolic compound found in both *C. adamantium* and *S. adstringens*. Gallic acid induces death in various cell lines via the intrinsic apoptotic pathway

[79–81]. *S. velutina* also has a large number of phenolic compounds; specifically, the phytochemical analysis of roots identified flavonoid-like molecules, such as epigallocatechin, epicatechin, rutin, kaempferol glycosides, and dimeric and trimeric proanthocyanidins [18], and identified the main compounds to be the flavonoid derivatives of catechin and piceatannol (active metabolite of resveratrol) groups and dimeric tetrahydroanthracene derivatives [142].

Accordingly, several flavonoids, such as luteolin, jacaranone, triterpenes, ursolic acid, and oleanolic acid, have been identified in the genus *Jacaranda* and their cytotoxic activities have been described [155–158]. Further studies to isolate and identify the compounds in the medicinal plants *H. speciosa*, *J. decurrens*, *S. velutina*, *C. adamantium*, and *S. adstringens* and clinical trials to study these extracts and/or isolated compounds have potential to facilitate the development of alternative therapeutic strategies and the design and selection of new drugs for cancer therapy.

6. Protection against Chemical Toxicity by Plants from the Cerrado

Chemotherapy commonly increases the production of ROS, which induces oxidative stress in cancer cells and other tissues [160, 161]. Excessive ROS may disrupt cellular homeostasis, leading to toxicity [162–164]. In fact, after chemotherapy treatment, oncology patients exhibit signs of lipid peroxidation in plasma, reduced levels of antioxidant vitamins in the blood, and decreased levels of GSH in tissues [165]. For example, drugs such as taxanes (paclitaxel and docetaxel) and vinca alkaloids (vincristine and vinblastine) induce cell death by cytochrome c release from mitochondria and interfering with the electron transport chain, resulting in the production of superoxide radicals [166]. Other drugs, such as anthracyclines (for example, doxorubicin), also generate extremely high ROS levels [167].

Combinatory approaches with antioxidants can protect the health tissues against toxic side effects, improving the clinical response of chemotherapy [164, 168–170]. Regardless of the role of plant antioxidants from the Cerrado in chemotherapy, two recent studies evaluated the effect of doxorubicin on chemotherapy using *in vitro* and *in vivo* models. Dos Santos et al. [22] evaluated the capacity of *G. ulmifolia* extract to protect against doxorubicin injury *in vitro* and *in vivo*. The oxidative stress markers in human erythrocytes exposed to doxorubicin, including haemolysis and MDA, were reduced by the combined use of *G. ulmifolia* extract and doxorubicin. *G. ulmifolia* extract also induced cardioprotection in rats treated with doxorubicin. *G. ulmifolia* extract was able to prevent MDA production in the cardiac tissue of animals treated with doxorubicin. Similarly, Rocha et al. [21] described the potential of *S. terebinthifolius* to protect against doxorubicin injury *in vitro* and *in vivo*. The treatment of C57Bl/6 mice with a *S. terebinthifolius* leaf extract protected against doxorubicin-induced cardiotoxicity, corroborating the results of the reduced oxidative haemolysis *in vitro*. The cotreatment of doxorubicin with *G. ulmifolia* or *S. terebinthifolius* did not attenuate cytotoxicity in erythroleukaemic cells, confirming that these antioxidants do not specifically interfere with the cytotoxic efficacy of this anticancer agent. In conclusion, *G. ulmifolia* and *S. terebinthifolius* have been found to be capable of protecting against the damage caused by doxorubicin and can offer a therapeutic opportunity for treating cancer.

Other studies have evaluated the antimutagenic potential of some plants from the Cerrado. As discussed previously, carcinogenesis initiation, progression, and promotion are processes related to increased intracellular ROS. Martello et al. [171] described the antimutagenic activities of *C. adamantium* hydroethanolic extract in Swiss mice treated with cyclophosphamide. When the extract was administered in combination with cyclophosphamide, the micronucleus frequency and apoptosis were reduced. Extract components might affect cyclophosphamide metabolism, which possibly leads to the increased clearance of this chemotherapeutic agent. Thus, caution should be exercised when consuming these extracts, especially when received in combination with other drugs. de Oliveira et al. [172] investigated the capacity of *C. adamantium* fruits to protect HepG2 cells (hepatocytes) from carbon tetrachloride- (CCl_4-) induced toxicity. Carbon tetrachloride (CCl_4) is a highly toxic chemical that is used to investigate hepatotoxicity. Pretreatment of HepG2 cells with pulp or peel/seed hydroalcoholic extract significantly protected against the cytotoxicity induced by CCl_4. Additionally, the cells treated with both extracts (both at 1000 μg/mL) showed normal morphology (general and nuclear), in contrast to the apoptotic characteristics of the cells only exposed to CCl_4 [172].

In another study, using a similar model, Abdou et al. [173] found that the administration of an ethanol extract of leaves from *S. terebinthifolius* significantly protected against CCl_4 liver damage in Wistar rats. Interestingly, *S. terebinthifolius* extract inhibited hepatocyte apoptosis as revealed by an approximate 20-time downregulation in caspase-3 expression compared with the CCl_4-untreated group. Endringer et al. [97] investigated the capacity of *H. speciosa* to induce antioxidant response element (ARE) activation in HepG2 cells transfected with ARE-luciferase plasmid. ARE is a regulatory enhancer gene encoding protective proteins, including phase II detoxification enzymes such as NAD(P)H:quinone oxidoreductase and antioxidant enzymes such as glutathione (GSH) S-transferases (GST). Extracts and fractions (methanol and methanol : water (1 : 1)) caused ARE induction.

7. Conclusion

The evidence discussed in this review indicates that the medicinal plants from the Cerrado show antioxidant activity, anticancer activity, and protective effects against chemical toxicity. These plants are potential candidates for the identification of effective pharmacological compounds. Therefore, the in vivo assay followed by clinical trials may provide clear evidence on the potential benefits of these extracts and/or isolated compounds and may facilitate the development of alternative therapeutic strategies and the design and selection of new drugs for cancer therapy.

Conflicts of Interest

The authors declare that they have no conflicts of interest.

Acknowledgments

This work was supported by grants from Universidade Federal da Grande Dourados (UFGD); Fundação de Apoio ao Desenvolvimento do Ensino, Ciência e Tecnologia do Estado de Mato Grosso do Sul (FUNDECT); Coordenação de Aperfeiçoamento de Pessoal de Nível Superior (CAPES); Conselho Nacional de Desenvolvimento Científico e Tecnológico (CNPq); and Financiadora de Estudos e Projetos (FINEP).

References

[1] L. Katz and R. H. Baltz, "Natural product discovery: past, present, and future," *Journal of Industrial Microbiology & Biotechnology*, vol. 43, no. 2-3, pp. 155–176, 2016.

[2] D. J. Newman and G. M. Cragg, "Natural products as sources of new drugs from 1981 to 2014," *Journal of Natural Products*, vol. 79, no. 3, pp. 629–661, 2016.

[3] S. Florian and T. J. Mitchison, "Anti-microtubule drugs," in *Mitotic Spindle Methods Protoc*, P. Chang and R. Ohi, Eds., pp. 403–421, Springer New York, New York, NY, 2016, cited 2019 Feb 28.

[4] D.-P. Xu, Y. Li, X. Meng et al., "Natural antioxidants in foods and medicinal plants: extraction, assessment and resources," *International Journal of Molecular Sciences*, vol. 18, no. 1, p. 96, 2017.

[5] N. Khansari, Y. Shakiba, and M. Mahmoudi, "Chronic inflammation and oxidative stress as a major cause of age-related diseases and cancer," *Recent Patents on Inflammation & Allergy Drug Discovery*, vol. 3, no. 1, pp. 73–80, 2009.

[6] A. Lichota and K. Gwozdzinski, "Anticancer activity of natural compounds from plant and marine environment," *International Journal of Molecular Sciences*, vol. 19, no. 11, p. 3533, 2018.

[7] S. Habtemariam and G. Lentini, "Plant-derived anticancer agents: lessons from the pharmacology of geniposide and its aglycone, genipin," *Biomedicines*, vol. 6, no. 2, p. 39, 2018.

[8] R. C. Dutra, M. M. Campos, A. R. S. Santos, and J. B. Calixto, "Medicinal plants in Brazil: pharmacological studies, drug discovery, challenges and perspectives," *Pharmacological Research*, vol. 112, pp. 4–29, 2016.

[9] M. Valli, H. M. Russo, and V. S. Bolzani, "The potential contribution of the natural products from Brazilian biodiversity to bioeconomy," *Anais da Academia Brasileira de Ciências*, vol. 90, 1 suppl 1, pp. 763–778, 2018.

[10] A. C. Pilon, M. Valli, A. C. Dametto et al., "NuBBEDB: an updated database to uncover chemical and biological information from Brazilian biodiversity," *Scientific Reports*, vol. 7, no. 1, p. 7215, 2017.

[11] C. J. R. Alho, "The value of biodiversity," *Brazilian Journal of Biology*, vol. 68, 4 suppl, pp. 1115–1118, 2008.

[12] E. E. Sano, A. A. Rodrigues, E. S. Martins et al., "Cerrado ecoregions: a spatial framework to assess and prioritize Brazilian savanna environmental diversity for conservation," *Journal of Environmental Management*, vol. 232, pp. 818–828, 2019.

[13] V. C. da Silva and C. M. Rodrigues, "Natural products: an extraordinary source of value-added compounds from diverse biomasses in Brazil," *Chemical and Biological Technologies in Agriculture*, vol. 1, no. 1, p. 14, 2014.

[14] D. C. Savi, R. Aluizio, and C. Glienke, "Brazilian plants: an unexplored source of endophytes as producers of active metabolites," *Planta Medica*, vol. 85, no. 08, pp. 619–636, 2019.

[15] G. Damasco, C. Fontes, R. Françoso, and R. Haidar, "The Cerrado biome: a forgotten biodiversity hotspot," *Frontiers for Young Minds*, vol. 6, 2018.

[16] D. Baldivia, D. Leite, D. Castro et al., "Evaluation of in vitro antioxidant and anticancer properties of the aqueous extract from the stem bark of Stryphnodendron adstringens," *International Journal of Molecular Sciences*, vol. 19, no. 8, p. 2432, 2018.

[17] J. F. Campos, P. P. T. Espindola, H. F. V. Torquato et al., "Leaf and root extracts from Campomanesia adamantium (Myrtaceae) promote apoptotic death of leukemic cells via activation of intracellular calcium and caspase-3," *Frontiers in Pharmacology*, vol. 8, p. 466, 2017.

[18] J. F. Campos, D. T. H. de Castro, M. J. Damião et al., "The Chemical Profile ofSenna velutinaLeaves and Their Antioxidant and Cytotoxic Effects," *Oxidative Medicine and Cellular Longevity*, vol. 2016, Article ID 8405957, 12 pages, 2016.

[19] J. C. Casagrande, L. F. B. Macorini, K. A. Antunes et al., "Antioxidant and cytotoxic activity of hydroethanolic extract from Jacaranda decurrens leaves," *PLoS One*, vol. 9, no. 11, 2014.

[20] U. P. Santos, J. F. Campos, H. F. V. Torquato et al., "Antioxidant, antimicrobial and cytotoxic properties as well as the phenolic content of the extract from Hancornia speciosa Gomes," *PloS One*, vol. 11, no. 12, 2016.

[21] P. dos Santos da Rocha, J. F. Campos, V. Nunes-Souza et al., "Antioxidant and protective effects of Schinus terebinthifolius Raddi against doxorubicin-induced toxicity," *Applied Biochemistry and Biotechnology*, vol. 184, no. 3, pp. 869–884, 2018.

[22] J. M. dos Santos, T. M. Alfredo, K. Á. Antunes et al., "Guazuma ulmifoliaLam. Decreases Oxidative Stress in Blood Cells and Prevents Doxorubicin-Induced Cardiotoxicity," *Oxidative Medicine and Cellular Longevity*, vol. 2018, Article ID 2935051, 16 pages, 2018.

[23] L. M. Ricardo, B. M. Dias, F. L. B. Mügge, V. V. Leite, and M. G. L. Brandão, "Evidence of traditionality of Brazilian medicinal plants: the case studies of Stryphnodendron adstringens (Mart.) Coville (barbatimão) barks and Copaifera spp. (copaíba) oleoresin in wound healing," *Journal of Ethnopharmacology*, vol. 219, pp. 319–336, 2018.

[24] S. C. Pinto, F. Bueno, G. Panizzon et al., "Stryphnodendron adstringens: clarifying wound healing in Streptozotocin-induced diabetic rats," *Planta Medica*, vol. 81, no. 12/13, pp. 1090–1096, 2015.

[25] B. O. Henriques, O. Corrêa, E. P. C. Azevedo et al., "In vitro TNF-α inhibitory activity of Brazilian plants and anti-inflammatory effect of Stryphnodendron adstringens in an acute arthritis model," *Evidence-based Complementary and Alternative Medicine*, vol. 2016, Article ID 9872598, 15 pages, 2016.

[26] E. A. Audi, D. P. Toledo, P. G. Peres et al., "Gastric antiulcerogenic effects ofStryphnodendron adstringens in rats," *Phytotherapy Research*, vol. 13, no. 3, pp. 264–266, 1999.

[27] P. De Souza, P. de Sales, L. Simeoni, E. Silva, D. Silveira, and P. de Oliveira Magalhães, "Inhibitory Activity ofα-Amylase andα-Glucosidase by Plant Extracts from the Brazilian Cerrado," *Planta Medica*, vol. 78, no. 04, pp. 393–399, 2012.

[28] K. Ishida, S. Rozental, J. C. de Mello, and C. V. Nakamura, "Activity of tannins from Stryphnodendron adstringens on Cryptococcus neoformans: effects on growth, capsule size and pigmentation," *Annals of Clinical Microbiology and Antimicrobials*, vol. 8, no. 1, p. 29, 2009.

[29] A. L. D. de Freitas, V. Kaplum, D. C. P. Rossi et al., "Proanthocyanidin polymeric tannins from Stryphnodendron adstringens are effective against Candida spp. isolates and for vaginal candidiasis treatment," *Journal of Ethnopharmacology*, vol. 216, pp. 184–190, 2018.

[30] K. Ishida, J. C. P. de Mello, D. A. G. Cortez, B. P. D. Filho, T. Ueda-Nakamura, and C. V. Nakamura, "Influence of tannins from Stryphnodendron adstringens on growth and virulence factors of Candida albicans," *J Antimicrob Chemother*, vol. 58, no. 5, pp. 942–949, 2006.

[31] A. M. M. Felipe, V. P. Rincão, F. J. Benati et al., "Antiviral effect of Guazuma ulmifolia and Stryphnodendron adstringens on poliovirus and bovine herpesvirus," *Biological & Pharmaceutical Bulletin*, vol. 29, no. 6, pp. 1092–1095, 2006.

[32] E. M. Pereira, R. Gomes, N. Freire, E. Aguiar, M. Brandão, and V. Santos, "In vitroAntimicrobial Activity of Brazilian Medicinal Plant Extracts against Pathogenic Microorganisms of Interest to Dentistry," *Planta Medica*, vol. 77, no. 04, pp. 401–404, 2011.

[33] T. M. Souza-Moreira, G. M. Queiroz-Fernandes, and R. C. L. R. Pietro, "Stryphnodendron species known as "barbatimão": a comprehensive report," *Molecules*, vol. 23, no. 4, p. 910, 2018.

[34] C. H. Lescano, F. Freitas de Lima, C. B. Mendes-Silvério et al., "Effect of polyphenols from Campomanesia adamantium on platelet aggregation and inhibition of cyclooxygenases: molecular docking and in vitro analysis," *Frontiers in Pharmacology*, vol. 9, p. 617, 2018.

[35] D. Zuntini Viscardi, J. S. Arrigo, C. A. C. Correia et al., "Seed and peel essential oils obtained from Campomanesia adamantium fruit inhibit inflammatory and pain parameters in rodents," *PloS One*, vol. 12, no. 2, 2017.

[36] L. C. Ferreira, A. Grabe-Guimarães, C. A. de Paula et al., "Anti-inflammatory and antinociceptive activities of Campomanesia adamantium," *Journal of Ethnopharmacology*, vol. 145, no. 1, pp. 100–108, 2013.

[37] C. H. Lescano, I. P. de Oliveira, T. Zaminelli et al., "Campomanesia adamantium peel extract in antidiarrheal activity: the ability of inhibition of heat-stable enterotoxin by polyphenols," *PloS One*, vol. 11, no. 10, p. e0165208, 2016.

[38] P. P. de Toledo Espindola, P. dos Santos da Rocha, C. A. Carollo et al., "Antioxidant and Antihyperlipidemic Effects ofCampomanesia adamantiumO. Berg Root," *Oxidative Medicine and Cellular Longevity*, vol. 2016, Article ID 7910340, 8 pages, 2016.

[39] C. M. L. Cardozo, A. Inada, G. Marcelino et al., "Therapeutic potential of Brazilian Cerrado Campomanesia species on metabolic dysfunctions," *Molecules*, vol. 23, no. 9, p. 2336, 2018.

[40] T. de Mello Moraes, C. M. Rodrigues, H. Kushima et al., "Hancornia speciosa: indications of gastroprotective, healing and anti-Helicobacter pylori actions," *Journal of Ethnopharmacology*, vol. 120, no. 2, pp. 161–168, 2008.

[41] D. G. Marinho, D. S. Alviano, M. E. Matheus, C. S. Alviano, and P. D. Fernandes, "The latex obtained from Hancornia speciosa Gomes possesses anti-inflammatory activity," *Journal of Ethnopharmacology*, vol. 135, no. 2, pp. 530–537, 2011.

[42] G. C. Silva, F. C. Braga, M. P. Lima, J. L. Pesquero, V. S. Lemos, and S. F. Cortes, "Hancornia speciosa Gomes induces hypotensive effect through inhibition of ACE and increase on NO," *Journal of Ethnopharmacology*, vol. 137, no. 1, pp. 709–713, 2011.

[43] H. C. Ferreira, C. P. Serra, D. C. Endringer, V. S. Lemos, F. C. Braga, and S. F. Cortes, "Endothelium-dependent vasodilation induced by Hancornia speciosa in rat superior mesenteric artery," *Phytomedicine*, vol. 14, no. 7-8, pp. 473–478, 2007.

[44] H. C. Ferreira, C. P. Serra, V. S. Lemos, F. C. Braga, and S. F. Cortes, "Nitric oxide-dependent vasodilatation by ethanolic extract of Hancornia speciosa via phosphatidyl-inositol 3-kinase," *Journal of Ethnopharmacology*, vol. 109, no. 1, pp. 161–164, 2007.

[45] A. C. Pereira, A. B. D. Pereira, C. C. L. Moreira et al., "Hancornia speciosa Gomes (Apocynaceae) as a potential anti-diabetic drug," *Journal of Ethnopharmacology*, vol. 161, pp. 30–35, 2015.

[46] U. P. Dos Santos, G. S. Tolentino, J. S. Morais, K. de Picoli Souza, L. M. Estevinho, and E. L. dos Santos, "Physicochemical Characterization, Microbiological Quality and Safety, and Pharmacological Potential ofHancornia speciosa-Gomes," *Oxidative Medicine and Cellular Longevity*, vol. 2018, Article ID 2976985, 17 pages, 2018.

[47] P. dos Santos da Rocha, A. P. de Araújo Boleti, M. do Carmo Vieira et al., "Microbiological quality, chemical profile as well as antioxidant and antidiabetic activities of Schinus terebinthifolius Raddi," *Comparative Biochemistry and Physiology Part C: Toxicology & Pharmacology*, vol. 220, pp. 36–46, 2019.

[48] T. Scheid, M. S. Moraes, T. P. Henriques et al., "Effects of Methanol Fraction from Leaves ofSchinus terebinthifolius-Raddi on Nociception and Spinal-Cord Oxidative Biomarkers in Rats with Neuropathic Pain," *Evidence-Based Complementary and Alternative Medicine*, vol. 2018, Article ID 5783412, 11 pages, 2018.

[49] L. de Lima Glória, M. B. de Souza Arantes, S. M. de Faria Pereira et al., "Phenolic compounds present Schinus terebinthifolius Raddi influence the lowering of blood pressure in rats," *Molecules*, vol. 22, no. 10, p. 1792, 2017.

[50] E. C. Rosas, L. B. Correa, T. A. Pádua et al., "Anti-inflammatory effect of Schinus terebinthifolius Raddi hydroalcoholic extract on neutrophil migration in zymosan-induced arthritis," *Journal of Ethnopharmacology*, vol. 175, pp. 490–498, 2015.

[51] A. Ennigrou, H. Casabianca, E. Vulliet, B. Hanchi, and K. Hosni, "Assessing the fatty acid, essential oil composition, their radical scavenging and antibacterial activities of Schinus terebinthifolius Raddi leaves and twigs," *Journal of Food Science and Technology*, vol. 55, no. 4, pp. 1582–1590, 2018.

[52] L. R. M. Estevão, R. S. Simões, P. Cassini-Vieira et al., "Schinus terebinthifolius Raddi (Aroeira) leaves oil attenuates inflammatory responses in cutaneous wound healing in

mice," *Acta Cirúrgica Brasileira*, vol. 32, no. 9, pp. 726–735, 2017.

[53] F. Tonial, B. H. L. N. S. Maia, J. A. Gomes-Figueiredo et al., "Influence of culturing conditions on bioprospecting and the antimicrobial potential of endophytic fungi from Schinus terebinthifolius," *Current Microbiology*, vol. 72, no. 2, pp. 173–183, 2016.

[54] S. R. Nocchi, G. F. de Moura-Costa, C. R. Novello et al., "In vitro cytotoxicity and anti-herpes simplex virus type 1 activity of hydroethanolic extract, fractions, and isolated compounds from stem bark of Schinus terebinthifolius Raddi," *Pharmacognosy Magazine*, vol. 12, no. 46, pp. 160–164, 2016.

[55] K. Torres, S. Lima, and S. Ueda, "Activity of the aqueous extract of Schinus terebinthifolius Raddi on strains of the Candida genus," *Revista Brasileira de Ginecologia e Obstetrícia / RBGO Gynecology and Obstetrics*, vol. 38, no. 12, pp. 593–599, 2016.

[56] J. H. S. da Silva, N. K. Simas, C. S. Alviano et al., "Anti-Escherichia coli activity of extracts from Schinus terebinthifolius fruits and leaves," *Natural Product Research*, vol. 32, no. 11, pp. 1365–1368, 2018.

[57] D. M. Pilatti, A. M. T. Fortes, T. C. M. Jorge, and N. P. Boiago, "Comparison of the phytochemical profiles of five native plant species in two different forest formations," *Brazilian Journal of Biology*, vol. 79, no. 2, pp. 233–242, 2019.

[58] K. A. Antunes, D. S. Baldivia, P. S. da Rocha et al., "Antiobesity Effects of Hydroethanolic Extract ofJacaranda decurrensLeaves," *Evidence-Based Complementary and Alternative Medicine*, vol. 2016, Article ID 4353604, 8 pages, 2016.

[59] J. A. Santos, A. Arruda, M. A. Silva et al., "Anti-inflammatory effects and acute toxicity of hydroethanolic extract of Jacaranda decurrens roots in adult male rats," *Journal of Ethnopharmacology*, vol. 144, no. 3, pp. 802–805, 2012.

[60] R. U. Y. J. V. ALVES, N. L. B. E. R. G. DA SILVA, A. L. U. S. I. O. J. FERNANDES JUNIOR, and A. L. E. S. S. A. N. D. R. A. R. GUIMARAES, "Longevity of the Brazilian underground tree Jacaranda decurrens Cham," *Anais da Academia Brasileira de Ciências*, vol. 85, no. 2, pp. 671–678, 2013.

[61] A. J. Alonso-Castro and L. A. Salazar-Olivo, "The anti-diabetic properties of Guazuma ulmifolia Lam are mediated by the stimulation of glucose uptake in normal and diabetic adipocytes without inducing adipogenesis," *Journal of Ethnopharmacology*, vol. 118, no. 2, pp. 252–256, 2008.

[62] C. Caballero-George, P. M. Vanderheyden, T. de Bruyne et al., "In VitroInhibition of [3H]-Angiotensin II Binding on the Human AT1Receptor by Proanthocyanidins fromGuazuma ulmifoliaBark," *Planta Medica*, vol. 68, no. 12, pp. 1066–1071, 2002.

[63] B. Berenguer, C. Trabadela, S. Sánchez-Fidalgo et al., "The aerial parts of Guazuma ulmifolia Lam. protect against NSAID-induced gastric lesions," *Journal of Ethnopharmacology*, vol. 114, no. 2, pp. 153–160, 2007.

[64] M. Hör, H. Rimpler, and M. Heinrich, "Inhibition of Intestinal Chloride Secretion by Proanthocyanidins fromGuazuma ulmifolia," *Planta Medica*, vol. 61, no. 03, pp. 208–212, 1995.

[65] H. R. A. Pires, A. C. Franco, M. T. F. Piedade, V. V. Scudeller, B. Kruijt, and C. S. Ferreira, "Flood tolerance in two tree species that inhabit both the Amazonian floodplain and the dry Cerrado savanna of Brazil," *AoB PLANTS*, vol. 10, 2018.

[66] M. Valko, D. Leibfritz, J. Moncol, M. T. D. Cronin, M. Mazur, and J. Telser, "Free radicals and antioxidants in normal physiological functions and human disease," *The International Journal of Biochemistry & Cell Biology*, vol. 39, no. 1, pp. 44–84, 2007.

[67] A. Chandrasekaran, M. P. S. Idelchik, and J. A. Melendez, "Redox control of senescence and age-related disease," *Redox Biology*, vol. 11, pp. 91–102, 2017.

[68] P. Poprac, K. Jomova, M. Simunkova, V. Kollar, C. J. Rhodes, and M. Valko, "Targeting free radicals in oxidative stress-related human diseases," *Trends in Pharmacological Sciences*, vol. 38, no. 7, pp. 592–607, 2017.

[69] O. Firuzi, R. Miri, M. Tavakkoli, and L. Saso, "Antioxidant therapy: current status and future prospects," *Current Medicinal Chemistry*, vol. 18, no. 25, pp. 3871–3888, 2011.

[70] A. Srivastava and A. Srivastava, "Oxidative stress-mediated human diseases," in *Oxidative Stress: Diagnostic Methods and Applications in Medical Science*, P. K. Maurya and P. Chandra, Eds., Springer, Singapore, 2017.

[71] M. A. Babizhayev, "Mitochondria induce oxidative stress, generation of reactive oxygen species and redox state unbalance of the eye lens leading to human cataract formation: disruption of redox lens organization by phospholipid hydroperoxides as a common basis for cataract disease," *Cell Biochemistry and Function*, vol. 29, no. 3, pp. 183–206, 2011.

[72] M. Redza-Dutordoir and D. A. Averill-Bates, "Activation of apoptosis signalling pathways by reactive oxygen species," *Biochimica et Biophysica Acta (BBA) - Molecular Cell Research*, vol. 1863, no. 12, pp. 2977–2992, 2016.

[73] E. Birben, U. M. Sahiner, C. Sackesen, S. Erzurum, and O. Kalayci, "Oxidative stress and antioxidant defense," *World Allergy Organization Journal*, vol. 5, no. 1, pp. 9–19, 2012.

[74] V. Lubrano and S. Balzan, "Enzymatic antioxidant system in vascular inflammation and coronary artery disease," *World Journal of Experimental Medicine*, vol. 5, no. 4, pp. 218–224, 2015.

[75] M. Daglia, A. Di Lorenzo, S. F. Nabavi, Z. S. Talas, and S. M. Nabavi, "Polyphenols: well beyond the antioxidant capacity: gallic acid and related compounds as neuroprotective agents: you are what you eat!," *Current Pharmaceutical Biotechnology*, vol. 15, no. 4, pp. 362–372, 2014.

[76] C. G. Fraga, K. D. Croft, D. O. Kennedy, and F. A. Tomás-Barberán, "The effects of polyphenols and other bioactives on human health," *Food & Function*, vol. 10, no. 2, pp. 514–528, 2019.

[77] M. Suwalsky, J. Colina, M. J. Gallardo et al., "Antioxidant capacity of gallic acid in vitro assayed on human erythrocytes," *The Journal of Membrane Biology*, vol. 249, no. 6, pp. 769–779, 2016.

[78] S. Choubey, S. Goyal, L. R. Varughese, V. Kumar, A. K. Sharma, and V. Beniwal, "Probing gallic acid for its broad spectrum applications," *Mini Reviews in Medicinal Chemistry*, vol. 18, no. 15, pp. 1283–1293, 2018.

[79] S. Choubey, L. R. Varughese, V. Kumar, and V. Beniwal, "Medicinal importance of gallic acid and its ester derivatives: a patent review," *Pharmaceutical Patent Analyst*, vol. 4, no. 4, pp. 305–315, 2015.

[80] S. Li, M. Xu, Q. Niu et al., "Efficacy of procyanidins against in vivo cellular oxidative damage: a systematic review and meta-analysis," *PLoS One*, vol. 10, no. 10, article e0139455, 2015.

[81] Q. Y. Zhu, D. D. Schramm, H. B. Gross et al., "Influence of cocoa flavanols and procyanidins on free radical-induced human erythrocyte hemolysis," *Clinical & Developmental Immunology*, vol. 12, no. 1, pp. 27–34, 2005.

[82] M. Grzesik, K. Naparło, G. Bartosz, and I. Sadowska-Bartosz, "Antioxidant properties of catechins: comparison with other antioxidants," *Food Chemistry*, vol. 241, pp. 480–492, 2018.

[83] J. V. Higdon and B. Frei, "Tea catechins and polyphenols: health effects, metabolism, and antioxidant functions," *Critical Reviews in Food Science and Nutrition*, vol. 43, no. 1, pp. 89–143, 2003.

[84] S. P. Boyle, V. L. Dobson, S. J. Duthie, D. C. Hinselwood, J. A. Kyle, and A. R. Collins, "Bioavailability and efficiency of rutin as an antioxidant: a human supplementation study," *European Journal of Clinical Nutrition*, vol. 54, no. 10, pp. 774–782, 2000.

[85] S. Habtemariam, "Antioxidant and rutin content analysis of leaves of the common buckwheat (Fagopyrum esculentum Moench) grown in the United Kingdom: a case study," *Antioxidants*, vol. 8, no. 6, p. 160, 2019.

[86] *A review of quercetin: chemistry, antioxidant properties, and bioavailability*Avaliable from: https://www.jyi.org/.

[87] M. Zhang, S. G. Swarts, L. Yin et al., "Antioxidant properties of quercetin," *Advances in Experimental Medicine and Biology*, vol. 701, pp. 283–289, 2011.

[88] G. Barrera, "Oxidative stress and lipid peroxidation products in cancer progression and therapy," *ISRN Oncology*, vol. 2012, Article ID 137289, 21 pages, 2012.

[89] T. Brodniewicz and G. Grynkiewicz, "Preclinical drug development," *Acta Poloniae Pharmaceutica*, vol. 67, pp. 578–585, 2010.

[90] M. R. Fielden and K. L. Kolaja, "The role of early in vivo toxicity testing in drug discovery toxicology," *Expert Opinion on Drug Safety*, vol. 7, no. 2, pp. 107–110, 2008.

[91] K. Pavithra and S. Vadivukkarasi, "Evaluation of free radical scavenging activity of various extracts of leaves from Kedrostis foetidissima (Jacq.) Cogn," *Food Science and Human Wellness*, vol. 4, no. 1, pp. 42–46, 2015.

[92] F. Bray, J. Ferlay, I. Soerjomataram, R. L. Siegel, L. A. Torre, and A. Jemal, "Global cancer statistics 2018: GLOBOCAN estimates of incidence and mortality worldwide for 36 cancers in 185 countries," *CA: a Cancer Journal for Clinicians*, vol. 68, no. 6, pp. 394–424, 2018.

[93] G. E. Forcados, D. B. James, A. B. Sallau, A. Muhammad, and P. Mabeta, "Oxidative stress and carcinogenesis: potential of phytochemicals in breast cancer therapy," *Nutrition and Cancer*, vol. 69, no. 3, pp. 365–374, 2017.

[94] J. E. Klaunig and Z. Wang, "Oxidative stress in carcinogenesis," *Current Opinion in Toxicology*, vol. 7, pp. 116–121, 2018.

[95] A. Nagarajan, P. Malvi, and N. Wajapeyee, "Oncogene-directed alterations in cancer cell metabolism," *Trends in Cancer*, vol. 2, no. 7, pp. 365–377, 2016.

[96] T. Fatemian and E. Chowdhury, "Targeting oncogenes and tumor suppressors genes to mitigate chemoresistance," *Current Cancer Drug Targets*, vol. 14, no. 7, pp. 599–609, 2014.

[97] D. C. Endringer, Y. M. Valadares, P. R. V. Campana et al., "Evaluation of Brazilian plants on cancer chemoprevention targetsin vitro," *Phytotherapy Research*, vol. 24, no. 6, pp. n/a–n33, 2009.

[98] Y. J. Surh, "NF-κB and Nrf2 as potential chemopreventive targets of some anti-inflammatory and antioxidative phytonutrients with anti-inflammatory and antioxidative activities," *Asia Pacific Journal of Clinical Nutrition*, vol. 17, no. S1, pp. 269–272, 2008.

[99] S. Nair, W. Li, and A.-N. T. Kong, "Natural dietary anticancer chemopreventive compounds: redox-mediated differential signaling mechanisms in cytoprotection of normal cells versus cytotoxicity in tumor cells," *Acta Pharmacologica Sinica*, vol. 28, no. 4, pp. 459–472, 2007.

[100] D. Delmas and J. Xiao, "EDITORIAL (Hot Topic: Natural Polyphenols Properties: Chemopreventive and Chemosensitizing Activities)," *Anti-Cancer Agents in Medicinal Chemistry*, vol. 12, no. 8, p. 835, 2012.

[101] F. Ghiringhelli, C. Rebe, A. Hichami, and D. Delmas, "Immunomodulation and anti-inflammatory roles of polyphenols as anticancer agents," *Anti-Cancer Agents in Medicinal Chemistry*, vol. 12, no. 8, pp. 852–873, 2012.

[102] M. Greenwell and P. K. S. M. Rahman, "Medicinal plants: their use in anticancer treatment," *International Journal of Pharmaceutical Sciences and Research*, vol. 6, no. 10, pp. 4103–4112, 2015.

[103] A. M. L. Seca and D. C. G. A. Pinto, "Plant secondary metabolites as anticancer agents: successes in clinical trials and therapeutic application," *International Journal of Molecular Sciences*, vol. 19, no. 1, p. 263, 2018.

[104] R. C. Taylor, S. P. Cullen, and S. J. Martin, "Apoptosis: controlled demolition at the cellular level," *Nature Reviews. Molecular Cell Biology*, vol. 9, no. 3, pp. 231–241, 2008.

[105] G. Ichim and S. W. G. Tait, "A fate worse than death: apoptosis as an oncogenic process," *Nature Reviews. Cancer*, vol. 16, no. 8, pp. 539–548, 2016.

[106] D. Hanahan and R. A. Weinberg, "The hallmarks of cancer," *Cell*, vol. 100, no. 1, pp. 57–70, 2000.

[107] R. E. Martell, D. Sermer, K. Getz, and K. I. Kaitin, "Oncology drug development and approval of systemic anticancer therapy by the U.S. Food and Drug Administration," *The Oncologist*, vol. 18, no. 1, pp. 104–111, 2013.

[108] J. Sun, Q. Wei, Y. Zhou, J. Wang, Q. Liu, and H. Xu, "A systematic analysis of FDA-approved anticancer drugs," *BMC Systems Biology*, vol. 11, Suppl 5, p. 87, 2017.

[109] C. Pfeffer and A. Singh, "Apoptosis: a target for anticancer therapy," *International Journal of Molecular Sciences*, vol. 19, no. 2, p. 448, 2018.

[110] H. Gali-Muhtasib, R. Hmadi, M. Kareh, R. Tohme, and N. Darwiche, "Cell death mechanisms of plant-derived anticancer drugs: beyond apoptosis," *Apoptosis*, vol. 20, no. 12, pp. 1531–1562, 2015.

[111] Q. Chen, J. Kang, and C. Fu, "The independence of and associations among apoptosis, autophagy, and necrosis," *Signal Transduction and Targeted Therapy*, vol. 3, no. 1, p. 18, 2018.

[112] S. Elmore, "Apoptosis: a review of programmed cell death," *Toxicologic Pathology*, vol. 35, no. 4, pp. 495–516, 2007.

[113] C. Feig and M. . E. Peter, "How apoptosis got the immune system in shape," *European Journal of Immunology*, vol. 37, Suppl 1, pp. S61–S70, 2007.

[114] J. T. Opferman, "Apoptosis in the development of the immune system," *Cell Death and Differentiation*, vol. 15, no. 2, pp. 234–242, 2008.

[115] S. Baig, I. Seevasant, J. Mohamad, A. Mukheem, H. Z. Huri, and T. Kamarul, "Potential of apoptotic pathway-targeted

cancer therapeutic research: where do we stand?," *Cell Death & Disease*, vol. 7, article e2058, 2016.

[116] J. Berthelet and L. Dubrez, "Regulation of apoptosis by inhibitors of apoptosis (IAPs)," *Cell*, vol. 2, no. 1, pp. 163–187, 2013.

[117] J. Silke and D. Vucic, "IAP family of cell death and signaling regulators," *Methods in Enzymology*, vol. 545, pp. 35–65, 2014.

[118] D. Vasudevan and H. D. Ryoo, "Regulation of cell death by IAPs and their antagonists," *Current Topics in Developmental Biology*, vol. 114, pp. 185–208, 2015.

[119] W.-T. Chiu, H. A. Chang, Y. H. Lin et al., "Bcl-2 regulates store-operated Ca^{2+} entry to modulate ER stress-induced apoptosis," *Cell Death Discovery*, vol. 4, no. 1, 2018.

[120] B. Zhivotovsky and S. Orrenius, "Calcium and cell death mechanisms: a perspective from the cell death community," *Cell Calcium*, vol. 50, no. 3, pp. 211–221, 2011.

[121] S. Orrenius, V. Gogvadze, and B. Zhivotovsky, "Calcium and mitochondria in the regulation of cell death," *Biochemical and Biophysical Research Communications*, vol. 460, no. 1, pp. 72–81, 2015.

[122] S. W. G. Tait and D. R. Green, "Mitochondria and cell death: outer membrane permeabilization and beyond," *Nature Reviews. Molecular Cell Biology*, vol. 11, no. 9, pp. 621–632, 2010.

[123] L. Galluzzi, O. Kepp, and G. Kroemer, "Mitochondrial regulation of cell death: a phylogenetically conserved control," *Microbial Cell*, vol. 3, no. 3, pp. 101–108, 2016.

[124] P. E. Czabotar, G. Lessene, A. Strasser, and J. M. Adams, "Control of apoptosis by the BCL-2 protein family: implications for physiology and therapy," *Nature Reviews. Molecular Cell Biology*, vol. 15, no. 1, pp. 49–63, 2014.

[125] H. M. Heath-Engel, N. C. Chang, and G. C. Shore, "The endoplasmic reticulum in apoptosis and autophagy: role of the BCL-2 protein family," *Oncogene*, vol. 27, no. 50, pp. 6419–6433, 2008.

[126] S. J. Martin and C. M. Henry, "Distinguishing between apoptosis, necrosis, necroptosis and other cell death modalities," *Methods*, vol. 61, no. 2, pp. 87–89, 2013.

[127] E. Bobrovnikova-Marjon and J. B. Hurov, "Targeting metabolic changes in cancer: novel therapeutic approaches," *Annual Review of Medicine*, vol. 65, no. 1, pp. 157–170, 2014.

[128] C. Liu, K. Zhang, H. Shen, X. Yao, Q. Sun, and G. Chen, "Necroptosis: a novel manner of cell death, associated with stroke (review)," *International Journal of Molecular Medicine*, vol. 41, no. 2, pp. 624–630, 2018.

[129] A. Najafov, H. Chen, and J. Yuan, "Necroptosis and cancer," *Trends Cancer.*, vol. 3, no. 4, pp. 294–301, 2017.

[130] P. Vandenabeele, L. Galluzzi, T. Vanden Berghe, and G. Kroemer, "Molecular mechanisms of necroptosis: an ordered cellular explosion," *Nature Reviews. Molecular Cell Biology*, vol. 11, no. 10, pp. 700–714, 2010.

[131] D. E. Christofferson and J. Yuan, "Necroptosis as an alternative form of programmed cell death," *Current Opinion in Cell Biology*, vol. 22, no. 2, pp. 263–268, 2010.

[132] X. Yu, Q. Deng, W. Li et al., "Neoalbaconol induces cell death through necroptosis by regulating RIPK-dependent autocrine TNF*α* and ROS production," *Oncotarget*, vol. 6, no. 4, pp. 1995–2008, 2015.

[133] W. Sun, X. Wu, H. Gao et al., "Cytosolic calcium mediates RIP1/RIP3 complex-dependent necroptosis through JNK activation and mitochondrial ROS production in human colon cancer cells," *Free Radical Biology & Medicine*, vol. 108, pp. 433–444, 2017.

[134] N. Lalaoui and G. Brumatti, "Relevance of necroptosis in cancer," *Immunology and Cell Biology*, vol. 95, no. 2, pp. 137–145, 2017.

[135] A. Serrano-Puebla and P. Boya, "Lysosomal membrane permeabilization as a cell death mechanism in cancer cells," *Biochemical Society Transactions*, vol. 46, no. 2, pp. 207–215, 2018.

[136] A.-C. Johansson, H. Appelqvist, C. Nilsson, K. Kågedal, K. Roberg, and K. Öllinger, "Regulation of apoptosis-associated lysosomal membrane permeabilization," *Apoptosis*, vol. 15, no. 5, pp. 527–540, 2010.

[137] F. Wang, A. Salvati, and P. Boya, "Lysosome-dependent cell death and deregulated autophagy induced by amine-modified polystyrene nanoparticles," *Open Biology*, vol. 8, no. 4, p. 170271, 2018.

[138] F. Wang, R. Gómez-Sintes, and P. Boya, "Lysosomal membrane permeabilization and cell death," *Traffic*, vol. 19, no. 12, pp. 918–931, 2018.

[139] A. B. Pupyshev, "Lysosomal membrane permeabilization as apoptogenic factor," *Tsitologiia*, vol. 53, no. 4, pp. 313–324, 2011.

[140] S. Kaushik and A. M. Cuervo, "The coming of age of chaperone-mediated autophagy," *Nature Reviews Molecular Cell Biology*, vol. 19, no. 6, pp. 365–381, 2018.

[141] I. Dikic and Z. Elazar, "Mechanism and medical implications of mammalian autophagy," *Nature Reviews. Molecular Cell Biology*, vol. 19, no. 6, pp. 349–364, 2018.

[142] D. T. H. Castro, J. F. Campos, M. J. Damião et al., "Ethanolic Extract ofSenna velutinaRoots: Chemical Composition,In VitroandIn VivoAntitumor Effects, and B16F10-Nex2 Melanoma Cell Death Mechanisms," *Oxidative Medicine and Cellular Longevity*, vol. 2019, Article ID 5719483, 14 pages, 2019.

[143] M. C. B. Lima e Silva, D. Bogo, C. A. F. Alexandrino et al., "Antiproliferative activity of extracts ofCampomanesia adamantium(Cambess.) O. Berg and isolated compound dimethylchalcone against B16-F10 murine melanoma," *Journal of Medicinal Food*, vol. 21, no. 10, pp. 1024–1034, 2018.

[144] A. C. R. F. Pascoal, C. A. Ehrenfried, B. G. C. Lopez et al., "Antiproliferative activity and induction of apoptosis in PC-3 cells by the chalcone cardamonin from *Campomanesia adamantium* (Myrtaceae) in a bioactivity-guided study," *Molecules*, vol. 19, no. 2, pp. 1843–1855, 2014.

[145] C. C. F. Alves, J. D. Oliveira, E. B. B. Estevam et al., "Antiproliferative activity of essential oils from three plants of the Brazilian Cerrado: *Campomanesia adamantium* (Myrtaceae), *Protium ovatum* (Burseraceae) and *Cardiopetalum calophyllum* (Annonaceae)," *Brazilian Journal of Biology*, 2019.

[146] V. Kaplum, A. C. Ramos, M. E. L. Consolaro et al., "Proanthocyanidin polymer-rich fraction of Stryphnodendron adstringens promotes in vitro and in vivo cancer cell death via oxidative stress," *Frontiers in Pharmacology*, vol. 9, p. 694, 2018.

[147] A. P. L. Sabino, L. M. S. Eustáquio, A. C. F. Miranda, C. Biojone, T. N. Mariosa, and C. M. C. P. Gouvêa, "Stryphnodendron adstringens ("barbatimão") leaf fraction: chemical characterization, antioxidant activity, and cytotoxicity towards human breast cancer cell lines," *Applied*

Biochemistry and Biotechnology, vol. 184, no. 4, pp. 1375–1389, 2018.

[148] F. Kroschinsky, F. Stölzel, S. von Bonin et al., "New drugs, new toxicities: severe side effects of modern targeted and immunotherapy of cancer and their management," *Critical Care*, vol. 21, no. 1, p. 89, 2017.

[149] X. Yu, Q. Deng, A. M. Bode, Z. Dong, and Y. Cao, "The role of necroptosis, an alternative form of cell death, in cancer therapy," *Expert Review of Anticancer Therapy*, vol. 13, no. 7, pp. 883–893, 2013.

[150] D. Chen, J. Yu, and L. Zhang, "Necroptosis: an alternative cell death program defending against cancer," *Biochimica et Biophysica Acta (BBA) - Reviews on Cancer*, vol. 1865, no. 2, pp. 228–236, 2016.

[151] P. G. Anantharaju, P. C. Gowda, M. G. Vimalambike, and S. R. V. Madhunapantula, "An overview on the role of dietary phenolics for the treatment of cancers," *Nutrition Journal*, vol. 15, no. 1, p. 99, 2016.

[152] L. F. Călinoiu and D. C. Vodnar, "Whole grains and phenolic acids: a review on bioactivity, functionality, health benefits and bioavailability," *Nutrients*, vol. 10, no. 11, article 1615, 2018.

[153] T. Costea, A. Hudiță, O. A. Ciolac et al., "Chemoprevention of colorectal cancer by dietary compounds," *International Journal of Molecular Sciences*, vol. 19, no. 12, article 3787, 2018.

[154] K. W. J. Wahle, I. Brown, D. Rotondo, and S. D. Heys, "Plant phenolics in the prevention and treatment of cancer," *Advances in Experimental Medicine and Biology*, vol. 698, pp. 36–51, 2010.

[155] C. Kandaswami, L. T. Lee, P. P. Lee et al., "The antitumor activities of flavonoids," *In Vivo*, vol. 19, no. 5, pp. 895–909, 2005.

[156] A. Taleghani and Z. Tayarani-Najaran, "Potent cytotoxic natural flavonoids: the limits of perspective," *Current Pharmaceutical Design*, vol. 24, no. 46, pp. 5555–5579, 2019.

[157] F. N. Iheagwam, O. O. Ogunlana, O. E. Ogunlana, I. Isewon, and J. Oyelade, "Potential anti-cancer flavonoids isolated from *Caesalpinia bonduc* young twigs and leaves: molecular docking and in silico studies," *Bioinformatics and Biology Insights*, vol. 13, 2019.

[158] H. Zhang, X. Wu, J. Wang et al., "Flavonoids from the leaves of *Epimedium Koreanum* Nakai and their potential cytotoxic activities," *Natural Product Research*, vol. 19, pp. 1–8, 2019.

[159] F. B. Carneiro, P. Q. Lopes, R. C. Ramalho, M. T. Scotti, S. G. Santos, and L. A. L. Soares, "Characterization of leaf extracts of *Schinus terebinthifolius* Raddi by GC-MS and chemometric analysis," *Pharmacognosy Magazine*, vol. 13, no. 51, pp. 672–675, 2017.

[160] V. Fuchs-Tarlovsky, "Role of antioxidants in cancer therapy," *Nutrition*, vol. 29, no. 1, pp. 15–21, 2013.

[161] A. Thyagarajan and R. P. Sahu, "Potential contributions of antioxidants to cancer therapy: immunomodulation and radiosensitization," *Integrative Cancer Therapies*, vol. 17, no. 2, pp. 210–216, 2018.

[162] J. N. Moloney and T. G. Cotter, "ROS signalling in the biology of cancer," *Seminars in Cell & Developmental Biology*, vol. 80, pp. 50–64, 2018.

[163] C. Gorrini, I. S. Harris, and T. W. Mak, "Modulation of oxidative stress as an anticancer strategy," *Nature Reviews Drug Discovery*, vol. 12, no. 12, pp. 931–947, 2013.

[164] J. Fang, T. Seki, and H. Maeda, "Therapeutic strategies by modulating oxygen stress in cancer and inflammation," *Advanced Drug Delivery Reviews*, vol. 61, no. 4, pp. 290–302, 2009.

[165] A. Glasauer and N. S. Chandel, "Targeting antioxidants for cancer therapy," *Biochemical Pharmacology*, vol. 92, no. 1, pp. 90–101, 2014.

[166] S. Saeidnia and M. Abdollahi, "Antioxidants: friends or foe in prevention or treatment of cancer: the debate of the century," *Toxicology and Applied Pharmacology*, vol. 271, no. 1, pp. 49–63, 2013.

[167] J. Watson, "Oxidants, antioxidants and the current incurability of metastatic cancers," *Open Biology*, vol. 3, no. 1, article 120144, 2013.

[168] H. Yang, R. M. Villani, H. Wang et al., "The role of cellular reactive oxygen species in cancer chemotherapy," *Journal of Experimental & Clinical Cancer Research*, vol. 37, no. 1, article 266, 2018.

[169] A. J. Montero and J. Jassem, "Cellular redox pathways as a therapeutic target in the treatment of cancer," *Drugs*, vol. 71, no. 11, pp. 1385–1396, 2011.

[170] J. Fang, H. Nakamura, and A. K. Iyer, "Tumor-targeted induction of oxystress for cancer therapy," *Journal of Drug Targeting*, vol. 15, no. 7-8, pp. 475–486, 2007.

[171] M. D. Martello, N. David, R. Matuo et al., "*Campomanesia adamantium* extract induces DNA damage, apoptosis, and affects cyclophosphamide metabolism," *Genetics and Molecular Research*, vol. 15, no. 2, 2016.

[172] T. de Oliveira Fernandes, R. I. de Ávila, S. S. de Moura, G. de Almeida Ribeiro, M. M. V. Naves, and M. C. Valadares, "*Campomanesia adamantium* (Myrtaceae) fruits protect HEPG2 cells against carbon tetrachloride-induced toxicity," *Toxicology Reports*, vol. 2, pp. 184–193, 2015.

[173] R. H. Abdou, S. Y. Saleh, and W. F. Khalil, "Toxicological and biochemical studies on Schinus terebinthifolius concerning its curative and hepatoprotective effects against carbon tetrachloride-induced liver injury," *Pharmacognosy Magazine*, vol. 11, Suppl 1, pp. S93–101, 2015.

Hindawi
Oxidative Medicine and Cellular Longevity
Volume 2019, Article ID 9719730, 12 pages
https://doi.org/10.1155/2019/9719730

Research Article

Ocoxin Modulates Cancer Stem Cells and M2 Macrophage Polarization in Glioblastoma

Esther Hernández-SanMiguel,[1] Ricardo Gargini,[2] Teresa Cejalvo,[3] Berta Segura-Collar,[1] Paula Núñez-Hervada,[1] Rafael Hortigüela,[1] Juan M. Sepúlveda-Sánchez,[3] Aurelio Hernández-Laín,[3] Angel Pérez-Núñez,[3] Eduardo Sanz,[4] and Pilar Sánchez-Gómez[1]

[1]*Neurooncology Unit, Instituto de Salud Carlos III-UFIEC, Madrid, Spain*
[2]*Centro de Biología Molecular, CSIC, Madrid, Spain*
[3]*Unidad Multidisciplinar de Neurooncología, Hospital Universitario 12 de Octubre, Madrid, Spain*
[4]*Catalysis S.L., Madrid, Spain*

Correspondence should be addressed to Pilar Sánchez-Gómez; psanchezg@isciii.es

Received 8 February 2019; Revised 17 April 2019; Accepted 5 May 2019; Published 5 August 2019

Guest Editor: Ana S. Fernandes

Glioblastoma (GBM) is the most common and devastating primary brain tumor. The presence of cancer stem cells (CSCs) has been linked to their therapy resistance. Molecular and cellular components of the tumor microenvironment also play a fundamental role in the aggressiveness of these tumors. In particular, high levels of hypoxia and reactive oxygen species participate in several aspects of GBM biology. Moreover, GBM contains a large number of macrophages, which normally behave as immunosuppressive tumor-supportive cells. In fact, the presence of both, hypoxia and M2-like macrophages, correlates with malignancy and poor prognosis in gliomas. Antioxidant agents, as nutritional supplements, might have antitumor activity. Ocoxin® oral solution (OOS), in particular, has anti-inflammatory and antioxidant properties, as well as antitumor properties in several neoplasia, without known side effects. Here, we describe how OOS affects stem cell properties in certain GBMs, slowing down their tumor growth. In parallel, OOS has a direct effect on macrophage polarization *in vitro* and *in vivo*, inhibiting the protumoral features of M2 macrophages. Therefore, OOS could be a feasible candidate to be used in combination therapies during GBM treatment because it can target the highly resilient CSCs as well as their supportive immune microenvironment, without adding toxicity to conventional treatments.

1. Introduction

Glioblastomas (GBMs) are the most aggressive form of primary brain tumors. Histologically, they are characterized by pronounced hypercellularity, aberrant vasculature, and necrotic regions [1]. Standard treatment of GBM consists of maximal safe surgical resection followed by focal, fractionated radiotherapy, in combination with concurrent and adjuvant chemotherapy with the DNA alkylating agent temozolomide (TMZ) [2]. In any case, the prognosis is still grim, with less than 10% of GBM patients surviving 5 years after diagnosis, so novel treatment modalities are urgently required.

GBM cancer stem cells (CSCs) are able to self-renew, differentiate and repopulate the whole bulk of the tumor, and they have been associated with tumor relapse after treatment [3]. Maintenance of an undifferentiated state of GBM CSCs seems to be controlled by cues from their niches, mainly vascularized areas and hypoxic regions [4, 5]. Paradoxically, hypoxia is associated with an increase in reactive oxygen species (ROS) [6]. In fact, molecules that induce a decrease in endogenous ROS levels have been recently associated with the inhibition of CSC-like properties in GBM [7, 8].

Dietary supplements (including antioxidants) are widely used among patients with cancer, with the potential to be anticancer and antitoxic agents, reducing side effects. Whereas some authors have reported undesirable interactions with conventional therapies, others have suggested a synergistic effect [9, 10]. Ocoxin® oral solution (OOS)

is a nutritional supplement with recognized antioxidant, anti-inflammatory and immunomodulatory properties. The solution is composed, among others, of green tea extract, glyzyrrhicic acid, and vitamins C, B6 and B12, which have undergone a molecular activation process that boosts their antioxidant and biological activities. It was synthesized by combining two products, Viusid® and Ocoxin®. The Viusid component has shown beneficial effects in patients suffering from chronic hepatitis C and cirrhosis, showing antioxidant and immunomodulatory effects [11, 12]. OOS has also been tested in several cancer clinical trials, resulting in a significant improvement in the quality of life of patients, better tolerance to conventional therapies, and an increase in the survival index [13] (NCT01392131). Moreover, OOS antitumor effects have been validated *in vitro* and *in vivo* in preclinical breast cancer [14] and acute myeloid leukemia models [15], playing an inhibitory role for the liver metastasis of colorectal carcinoma [16, 17]. In all cases, when administered to animal models, OOS showed no detrimental effects. In fact, it even improved the overall health state of the mice.

Here, we have tested the effect of OOS in GBM models. For that we have used primary cell lines, derived from patient samples. We have observed that OOS has a dual function, it reduces tumor growth in some GBM through the modulation of CSC properties, and it shows a striking capacity to inhibit M2-like macrophage polarization, both *in vitro* and in the tumor environment. Moreover, pretreatment with OOS reduces the protumoral function of M2 macrophages. Therefore, OOS could be a good candidate to be used in combination therapies during GBM treatment, especially if we consider that it has been marketed for years without any report of adverse effects.

2. Materials and Methods

2.1. GBM Cell Culture. GBM1 (L0627) was provided by Rosella Galli (San Raffaele Scientific Institute, Milan, Italy); GBM2 (12O15) and GBM3 (12O01) were obtained by dissociation of human GBM surgical specimens from patients treated at Hospital Universitario 12 de Octubre (Madrid, Spain). We obtained an informed consent for study participation from both patients. None of them was under the age of 18. The study was performed with the approval and following the guidelines of the Research Ethics Committee of Hospital 12 de Octubre (CEI 14/023). Primary GBM cells were cultured in Neurobasal medium (Invitrogen) supplemented with B27 (1 : 50, Invitrogen), Glutamax (1 : 100, Invitrogen), penicillin-streptomycin (1 : 100, Lonza), 0.4% heparin (Sigma-Aldrich), 40 ng/ml EGF (PeproTech), and 20 ng/ml $bFGF_2$ (PeproTech) and passaged after enzymatic disaggregation using Accumax (Millipore), as previously described [18].

2.2. GBM In Vitro Assays. For viability assays, 5000 cells were seeded in triplicate wells of a 96-multiwell plate coated with Matrigel (Becton-Dickinson, 15 mg/ml stock solution diluted 1 : 100 in DMEM medium (Lonza)). 24 h later, cells were treated with OOS (1 : 100) (Catalysis S.L.) and viability was measured after 72 h of treatment. For that, cells were incubated with Hoechst 33342 (1 : 200, Sigma-Aldrich) and propidium iodide (1 : 1000, Merck) and fluorescence was measured in a Cytell Cell Imaging System (GE Healthcare Life Sciences). Wells containing nontreated cells were considered as 100% viability for each tested cell line. For self-renewal assays, GBM neurospheres were disaggregated into single cells and plated in fresh medium in the absence of OOS at a clonal density of 2.5 cells/μl in triplicate wells of a 96-multiwell plate. 24 hours later, GBM cell lines were treated with OOS (1 : 100). The percentage of self-renewing cells was determined 6 days after treatment by counting the number of individual neurospheres that originated from plated cells. Nontreated cells were used as a control.

2.3. Macrophage Isolation and Culture. Peritoneal macrophages were isolated as described in [19]. In brief, for macrophage isolation, 2.5 ml of 3% thioglycollate (Sigma-Aldrich) was injected into the peritoneum of C57BL/6 mice. Four days later, peritoneal cells were harvested and 15000 cells/well were seeded in a 96-multiwell plate for viability and ROS assays. Otherwise, 2.5×10^6 cells/well were seeded in a 6-multiwell plate for RNA isolation. Cells were cultured in RPMI 1640 (Fisher Scientific) with 10% of heat-inactivated fetal bovine serum (FBS, Fisher Scientific) and penicillin-streptomycin (1 : 100, Lonza) for 3 h. The amount of FBS was then reduced to 2% for overnight cell starvation. After overnight starvation, cells were treated with or without 1 : 100 OOS, in the presence of the differentiation inducers: LPS (200 ng/ml, InvivoGen), IL4 (20 ng/ml, PeproTech) or GBM1 conditioned medium (CM, 1 : 1) (obtained after 72 h incubation of GBM1 cells in neurosphere media). Control cells were maintained in 2% FBS medium. After 24 h, LPS and IL4 were removed but OOS was maintained for another 24 h before macrophage analysis.

2.4. Macrophage In Vitro Assays. Macrophage viability was assessed using AlamarBlue reagent (Fisher Scientific). The reagent was added to the media (1 : 10) and incubated for 4 h at 37°C and 5% CO_2, protected from light. Fluorescence of the samples was measured (excitation at 560 nm and emission at 600 nm) in an Infinite 200 PRO microplate reader (Tecan). Wells containing only culture media were used as a background control for all the samples measured, and wells containing nontreated cells were considered as 100% viability. ROS measurement was performed using dihydroethidium (DHE) reagent (Cayman Chemical). DHE was added to the media (1 : 800) and incubated for 1 h at 37°C and 5% CO_2, protected from light. Fluorescence of the samples was measured in a Cytell Cell Imaging System. Wells containing only culture media were used as a background control for all the samples measured, and wells containing nontreated cells were considered as 100% ROS. For the coculture experiment, 2.5×10^6 macrophages were seeded per 6-multiwell plate. After the overnight starvation, cells were treated with or without 1 : 100 OOS, in the presence of IL4 (20 ng/ml, PeproTech). Control macrophages were maintained in 2% FBS medium. After 24 h, IL4 was removed but OOS was

maintained for another 24 h. After OOS removal, macrophages were washed and freshly dissociated GBM1 cells (expressing the luciferase reporter) (250000 cells) were added on top of the macrophages (in GBM media without growth factors). Three days later, luciferin was added (150 μg/ml) and luminiscence was measured in an IVIS equipment (Perkin Elmer).

2.5. Mouse Xenograft Assays. Animal care and experimental procedures were performed in accordance with the European Union and National Guidelines for the use of animals in research and were reviewed and approved by the Research Ethics and Animal Welfare Committee at our institution (Instituto de Salud Carlos III, Madrid) (PROEX 244/14). Heterotopic and orthotopic xenografts were performed as previously described [20]. For heterotopic xenografts, 1×10^6 cells were resuspended in culture media with Matrigel (1 : 10, BD) and then subcutaneously injected into athymic nude *Foxn1*^{nu} mice (Harlan Iberica). When the subcutaneous tumors were noticeable (around 4 mm in diameter), OOS or water was orally administered to the mice (100 μl/day, 5 days/week). During the treatments, tumors were measured with a caliper twice a week until mice sacrifice. Tumor volume was calculated as 1/2 (length $\times$ width^2). Relative tumor growth was calculated in relation to tumor volume at day 1 of treatment. For orthotopic xenografts, stereotactically guided intracranial injections in athymic nude *Foxn1*^{nu} mice were performed by administering 0.5×10^5 GBM1 cells resuspended in 2 μl of culture media. The injections were made into the striatum (coordinates: A-P, –0.5 mm; M-L, +2 mm; and D-V, –3 mm; related to the bregma) using a Hamilton syringe. Mice were orally treated with OOS or water (200 μl/day, 5 days/week) 3 weeks after the intracranial injections until mice were sacrificed at the onset of symptoms.

2.6. Tumor Tissue Analysis. At the endpoint, subcutaneous tumors or brain tumors were dissected and the tissue was fresh frozen for molecular analysis, dissociated for flow cytometry analysis or fixed o/n in 4% paraformaldehyde (Merck) and embedded in paraffin. Paraffin-embedded tissue was cut with a microtome (Leica Microsystems) (3 μm sections), and sections were stained with hematoxylin-eosin (H&E) or incubated with specific antibodies for immunohistochemical- (IHC-) DAB staining.

2.7. Western Blot (WB). For immunoblot analysis, cells were collected and rinsed in cold PBS. Samples were resuspended in 0.1% SDS-RIPA buffer supplemented with a protease inhibitor cocktail (Roche), incubated 20 minutes on ice and centrifuged at 14000 rpm for 15 min at 4°C. Protein concentration was determined using a commercially available colorimetric assay (Pierce BCA Protein Assay Kit, Thermo Scientific). Approximately 20 μg of protein were resolved by 12% SDS-PAGE and transferred onto a nitrocellulose membrane. Membranes were blocked for 1 h at room temperature in 5% BSA in TBS-T (10 mM Tris-HCl, pH 7.5, 100 mM NaCl and 0.1% Tween-20) and then incubated o/n at 4°C with the corresponding primary antibody diluted in 5% BSA in TBS-T. After washing 3 times with TBS-T, membranes were incubated for 1 hour at room temperature with their corresponding secondary antibody diluted in TBS-T. Detection was done by enhanced chemiluminescence with ECL (Millipore). Primary and secondary antibodies are shown in Supp. Table S1 and S2, respectively.

2.8. Quantitative Real-Time PCR (qRT-PCR). RNA was extracted from both frozen pellets of cells or frozen tissue sections with the High Pure RNA Isolation Kit (Roche) following the manufacturer's instructions. Total RNA (1 μg) was reverse transcribed with the PrimeScript RT Reagent Kit (TAKARA) in a total volume of 20 μl. The product of this retrotranscription was tenfold diluted for quantitative PCR analysis. Quantitative real-time PCR (qRT-PCR) was performed using the Light Cycler 480 (Roche) with SYBR Premix Ex Taq (TAKARA) in LightCycler® 480 Multiwell Plates using 10 μM of forward and reverse primers and 2 μl of cDNA template (tenfold diluted). Cycling conditions included an initial denaturation for 10 minutes at 95°C, followed by 45 cycles of 10 s at 95°C, 10 s at primer hybridization temperature and 10 s at 72°C. Quantification of gene expression was performed by the delta-delta Ct method, and Ct values were calculated following the manufacturer's instructions (LightCycler Software, Roche). The expression of the housekeeping genes *Actin* or *RPII* was used as an internal expression control. Primers used are indicated in Supp. Table S3.

2.9. Flow Cytometry Analysis. Tumor cells were disaggregated into individual cells with Accumax (5 min, RT) and erythrocytes were lysed with Quicklysis (15 min, RT; Cytognos) before staining. Cells were stained with anti-CD44-FITC (ImmunoTools, Supplementary Table S1) diluted in PBS +0.5% BSA+2 mM EDTA (staining buffer) for 20 min on ice and treated with PI (5 μg/ml, Sigma-Aldrich) for 5 min on ice. After staining, cells were washed with staining buffer and analyzed by flow cytometry (FACSCalibur, Becton Dickinson) using the FlowJo software.

2.10. Immunohistochemical Analysis (IHC). Tumors were fixed o/n at 4°C in 4% paraformaldehyde (PFA, Merck), rinsed with 0.1 M phosphate buffer (PB), and dehydrated by an ethanol gradient before embedding in paraffin for microtome sectioning. Tumors were cut with a microtome (Leica Microsystems), and paraffin sections (3 μm) were dewaxed and rehydrated. Antigen retrieval was achieved by microwaving the sections in 10 mM sodium citrate (pH 6.0) and endogenous peroxidase was blocked with 0.3% hydrogen peroxide. Tissue sections were blocked with 5% BSA+10% FBS in PB-Triton X-100 (0.1%) and incubated o/n at 4°C with anti-Activated Caspase 3 in blocking buffer. Sections were incubated with a secondary antibody labelled with biotin (2 hours at room temperature) before incubation with ABC-Peroxidase Solution (Thermo Scientific) for 30 min at room temperature. The peroxidase activity was developed with DAB (Vector) and sections were counterstained with hematoxylin. Images were acquired with a Leica DM4B microscope and analyzed by using ImageJ software. The

primary and secondary antibodies used are indicated in Supp. Table S1 and S2, respectively.

2.11. Statistical Analysis. The survival of nude mice was analyzed by the Kaplan-Meier method and evaluated with a two-sided log-rank test. Student's *t*-test was performed for statistical analysis of *in vitro* studies. Data in graphs are presented as means ± SEM. $^{*}P \leq 0.05$; $^{**}P \leq 0.01$; $^{***}P \leq 0.001$. Statistical values of $P > 0.05$ were not considered significant.

3. Results

3.1. OOS Inhibits the Self-Renewal Capacity of Some GBM CSCs. To explore the antitumor activity of OOS we used three different primary GBM cell lines derived from human samples, grown in the absence of serum and in the presence of growth factors, in the form of floating neurospheres enriched in CSCs [21]. Three days' incubation in the presence of OOS (1 : 100) did not produce a significant change in cell viability (Figure 1(a)). However, the same concentration of OOS inhibited the capacity of GBM1 and GBM2 cells to grow at highly diluted conditions (self-renewal assay) (Figure 1(b)), which is a feature related to CSCs and tumor-initiating properties [22]. Interestingly, we did not observe a significant effect of OOS on the self-renewal capacity of GBM3 cells. In agreement with these results, we observed a significant inhibition of CSC-related markers in GBM1 cells treated with OOS for 24 h (Figure 1(c)), whereas the supplement did not change the expression of these genes in GBM3 cells (Figure 1(d)).

GBM is a very heterogeneous group of tumors. In fact, we know that the behavior of GBM1 and GBM2 differs from GBM3 as the first two grow in a highly angiogenic manner in the mouse's brain, whereas the third one generates very invasive tumors (Gargini et al., manuscript in preparation) [23]. We have also observed differences in the metabolic profile of GBM3 cells, in comparison with GBM1 and GBM2 cells, with a clear upregulation of glycolytic enzyme *LDHC1* (Lactate-dehydrogenase-C1) expression and a significant reduction in the expression of the mitochondrial enzyme *ACSS1* (Acyl-CoA synthetase short-chain family-member1) (Figure 1(e)). Moreover, OOS induced the expression of several antioxidant enzymes in GBM1 and GBM2, but not in GBM3 (Figure 1(f)). We also checked the status of the detoxifying Nrf-2 (Nuclear factor erythroid-2-related factor 2) system. Nrf-2 can be modulated in response to redox imbalance [24] and it induces the expression of several antioxidative genes like hemoxygenase-1 (HO-1) and NAD(P)H Quinone Dehydrogenase 1 (NQO-1) [25]. OOS augmented the levels of Nrf-2 protein in the three cell lines, although the expression of its targets was induced in GBM1 and GBM2 cells but not in the GBM3 line, being GBM1 the one that responds to lower levels of OOS at shorter times (Figure 1(g)). All these results reinforce the idea that the metabolic and redox profiles of GBM3 cells, compared to GBM1 and GBM2 cells, are quite different and this might be the cause for their lack of response to OOS. Moreover, the results suggest that the expression of some of these proteins could be used as biomarkers of response to OOS.

3.2. The Growth of Some GBMs Is Impaired by Systemic Administration of OOS. CSCs in GBM have been associated with tumor initiation and growth. In order to test if the inhibition of self-renewal induced by OOS *in vitro* has an effect on tumor growth, we injected the three primary GBM lines into the flanks of immunodeficient (nude) mice. When tumors became visible, animals received intragastric administration of OOS and tumor growth was monitored with a caliper. The results showed that there was a significant reduction in tumor growth in GBM1, a small but not significant inhibition of GBM2 growth, and no reduction in GBM3 tumors (Figures 2(a)–2(c)). Histological analysis of GBM1 tumors showed no changes in the number of mitoses or in the number of Activated Caspase 3-positive cells (Supp. Figure S2), suggesting that OOS does not affect overall tumor growth or survival, which correlates with the lack of effect on cell viability (Figure 1(a)). Moreover, we observed a significan change in GBM1 tumors in the expression of the marker *NESTIN*, associated with GBM CSCs, which was not observed in GBM3 tumors (Figure 2(d)). This reinforces the idea that OOS reduces the stem cell properties of certain GBMs, affecting tumor growth.

With the goal of measuring the effect of OOS in an orthotopic setting, we performed an intracranial injection of GBM1 cells in nude mouse brains. We observed that systemic administration of OOS reduces tumor burden (Figure 3(a)). To further quantify tumor growth, we dissected the right hemispheres from the mouse brains and we measured the expression of *β-tubulin*, with primers that recognize specifically the human sequence. We compared it with the expression of the *RNA polymerase subunit-2* (*RPII*), measured with primers that equally recognize both human and mouse sequences. In the dissected brains, we observed a significant reduction in the human component (Figure 3(b)), confirming that the effects of OOS are visible in the brain. We also dissociated the injected hemispheres and we analyzed the cells using flow cytometry, measuring a strong reduction in the percentage of $CD44^{+}$ cells (Figure 3(c)). CD44 is considered a marker for GBM CSCs [26, 27], reinforcing the idea that OOS affects GBM1 tumor growth by impairing CSCs.

3.3. OOS Stimulates Changes in the Macrophage Component of GBM Tumors. Other authors have suggested that OOS increases the level of inflammatory cytokines [15]. To check if OOS has an effect on the immune component of GBMs, we performed a qRT-PCR analysis of a panel of markers of mouse lymphoid and myeloid cells in the dissected GBM1 and GBM3 tumors. We detected a change in macrophage polarization markers after OOS treatment, with a significant decrease in the expression of M2 (immunosuppressive) genes in GBM1 tumors as well as in GBM3 tumors (Figure 4(a)). We also detected an increase in some M1 (inflammatory) genes after OOS treatment, but only in GBM1 tumors (Figure 4(b)). GBM can contain large amounts of microglia and tumor-infiltrating macrophages, and their density is positively correlated with glioma grade, which suggests that they support tumor progression [28]. In fact, pharmacological or genetic inhibition of macrophage recruitment and M2 polarization blocks glioma growth [29]. Glioma-associated

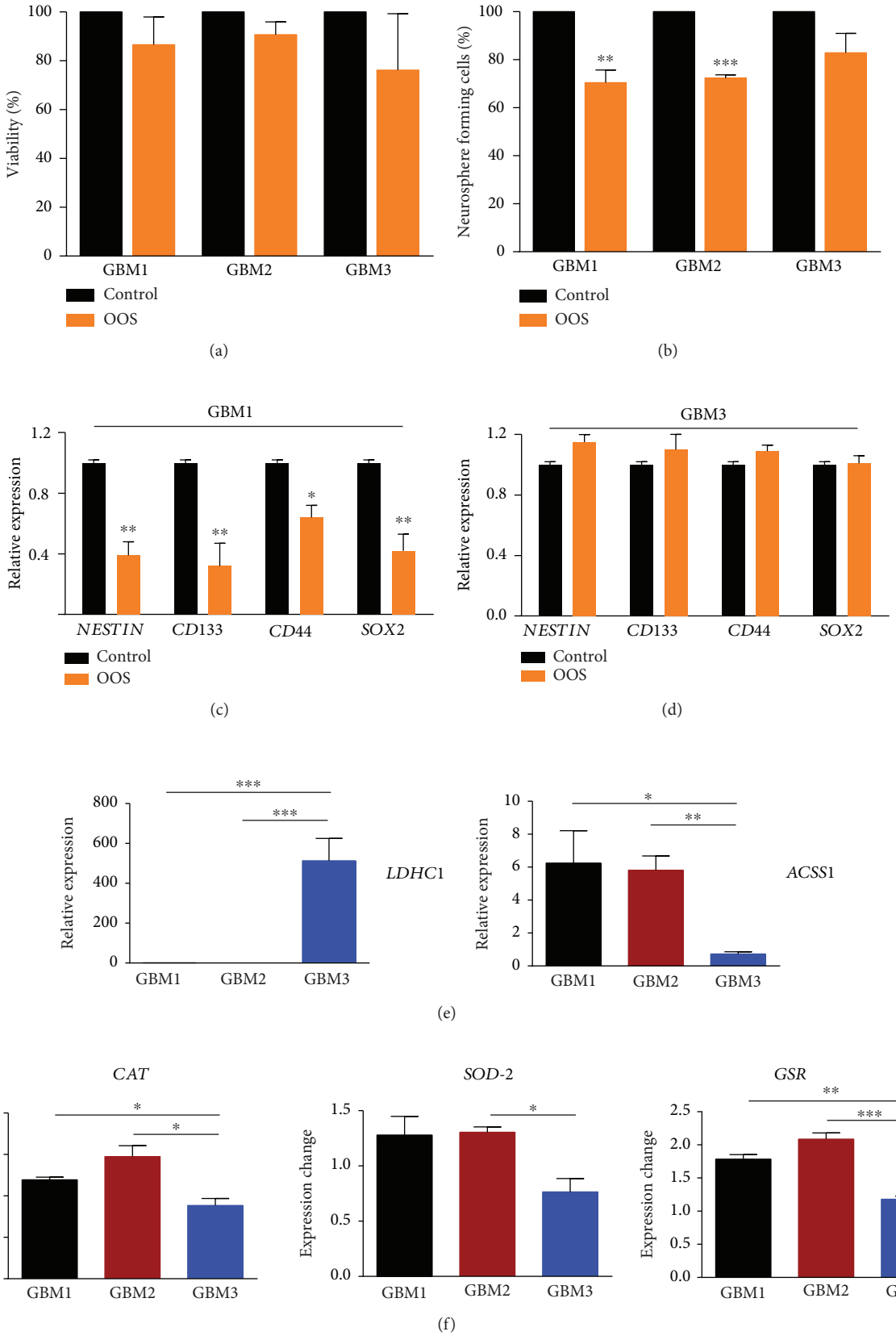

Figure 1: Continued.

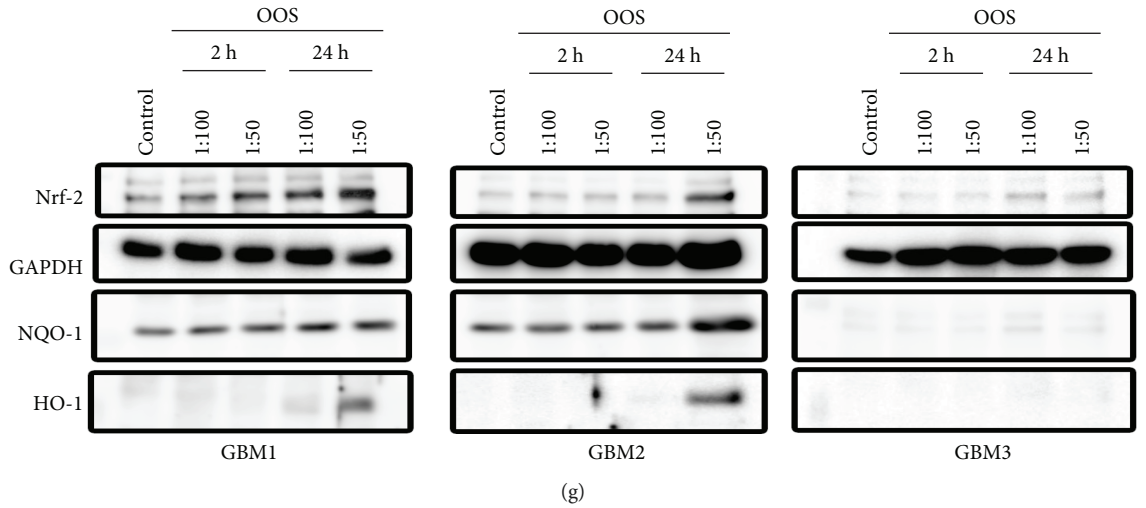

Figure 1: OOS inhibits the self-renewal capacity of GBM cells. (a) Cell viability of GBM cells in response to OOS (3d), $n = 3$. (b) Formation of GBM clonal spheres in the presence of OOS (6d), $n = 3$. (c, d) Relative expression (qRT-PCR) of CSC-related markers in GBM1 (c) and GBM3 (d) cells treated in the absence or in the presence of OOS (24 h), $n = 3$. (e) Relative expression (qRT-PCR) of metabolic markers in the three different GBM lines, $n = 3$. (f) Induction of the expression of several antioxidant enzymes in the presence of OOS (24 h), $n = 3$. *RPII* was used for normalization in all qRT-PCRs. (g) GBM cells were treated with OOS (1 : 100 or 1 : 50) for 2 or 24 h and expression of Nrf-2, NQO-1, and HO-1 was measured by WB. Nontreated spheres were used as a control and the expression of GAPDH as a loading control. The blots in the image were cropped from the same gel (full-length blots are shown in Supp. Figure S1). $^{*}P \leq 0.05$; $^{**}P \leq 0.01$; $^{***}P \leq 0.001$.

macrophages have been associated with proangiogenic, proinvasive and immunosuppressive functions, similar to those of alternatively activated M2 macrophages [30].

In order to decipher if OOS has a direct effect on macrophages, we cultured peritoneal macrophages in the presence and in the absence of the supplement. To induce M1 or M2 polarization, we used LPS (lipopolysaccharide) and IL4 (interleukin 4), respectively. We also incubated the macrophages in the presence of glioma-conditioned media (CM) (from GBM1). It has been shown that glioma cells release several factors that recruit and promote the growth of macrophages [28, 31]. We first determined that the viability of the macrophages was only slightly affected by the presence of OOS, although there was a clear stimulation in the presence of glioma-CM (Figure 5(a)), which was not able to induce M1 differentiation (data not shown). OOS did not significantly change the expression of M1 markers (in the absence or in the presence of LPS) (Figure 5(b)), although a small increment was observed in control-treated cells ($P = 0.12$). However, OOS clearly inhibited the upregulation of M2 markers induced by IL4 incubation and, to a lesser extent, by glioma-CM (Figure 5(c)), suggesting that OOS has a direct effect on these tumor inflammatory cells. Moreover, we observed that OOS was able to reduce the levels of ROS in the macrophages, independently of the differentiation stimuli (Figure 5(d)).

Macrophages that infiltrate glioma tissues are closely involved in the development of the tumor microenvironment by inducing angiogenesis, immunosuppression and invasion [28]. Moreover, it has been suggested that they can promote directly tumor cell proliferation. In order to analyze if the changes in macrophage polarization induced by OOS could affect secondarily glioma cells, we incubated GBM1 cells on top of macrophages that had been previously polarized by IL4, in the presence or in the absence of OOS. Results in Figure 5(e) suggest that there is indeed a protumoral function of M2 macrophages on glioma cells, as they support GBM1 growth even in the absence of growth factors. More importantly, pretreatment with OOS severely impaired this growth induction.

Altogether, these data reinforce the antitumor potential of OOS, as it could target CSCs and their supportive immunosuppressive microenvironment. However, in the xenograft setting, this general change in M2 polarization does not seem to be enough to inhibit tumor growth as OOS had no effect on GBM3 tumors (Figure 2), even though M2 markers were diminished (Figure 4(a)).

4. Discussion

In this study, we have evaluated the antitumor action of OOS in GBM using several human primary cell lines. OOS was able to reduce the *in vivo* growth of some of the GBM lines tested. We did not detect any changes in proliferation or cell death in the most sensitive tumors (GBM1 cells) (Supplementary Figure S1), suggesting that OOS does not have an effect on the overall tumor cell viability, as we had observed in the *in vitro* assays. However, there was a significant decrease in stem cell markers (*NESTIN* or CD44 expression) in response to OOS *in vitro* and *in vivo*. Moreover, the inhibition of the self-renewal capacity of GBM cells further confirmed that OOS inhibits the stem cell properties. Therefore, we cannot discard that OOS could be affecting proliferation or survival in the GBM CSC population.

Glioma CSCs are enriched in areas of high oxidative stress [4, 5]. Paradoxically, it has been suggested that low levels of ROS are required for stem cells to maintain

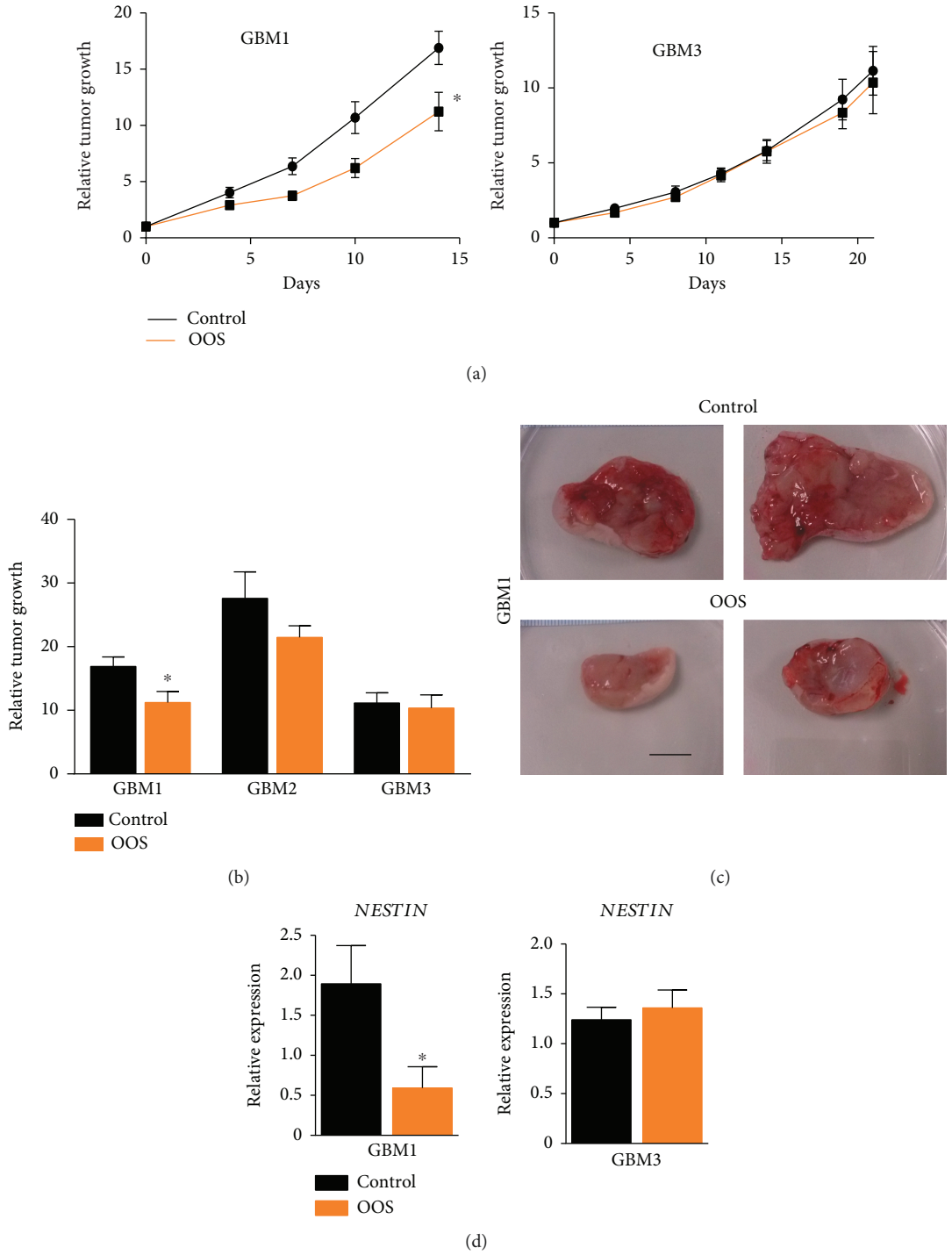

Figure 2: OOS inhibits GBM growth. GBM1-3 cells were injected subcutaneously into the flanks of nude mice; when tumors became visible, animals started receiving daily oral doses of OOS (100 μl/day, 5 days/week) or water (control). Relative tumor growth at different time points (a) or the time of sacrifice (b) is represented, $n = 8$. (c) Representative pictures of the tumors are shown. (d) *NESTIN* expression (qRT-PCR) in flank tumors after OOS treatment, $n = 4$. *RPII* was used for normalization in all qRT-PCRs. $^*P \leq 0.05$. Scale bar = 1 cm.

quiescence and self-renewal, both in normal tissues and tumors [32]. In gliomas, CSCs appear to generate less ROS and have a higher ROS-scavenging capacity than more differentiated tumor cells [33]. In fact, an increase in mitochondrial ROS has also been linked to the loss of stem cell markers [34]. In contrast, our results indicate that the main effect of the antioxidant OOS is a decrease in the stemness properties of GBM. This observation agrees with recent results obtained with several ROS-scavenging compounds [7, 8]. Based on these data, it could be hypothesized that certain levels of ROS may be necessary to maintain CSCs in GBM cells, although too much oxidative stress could be also

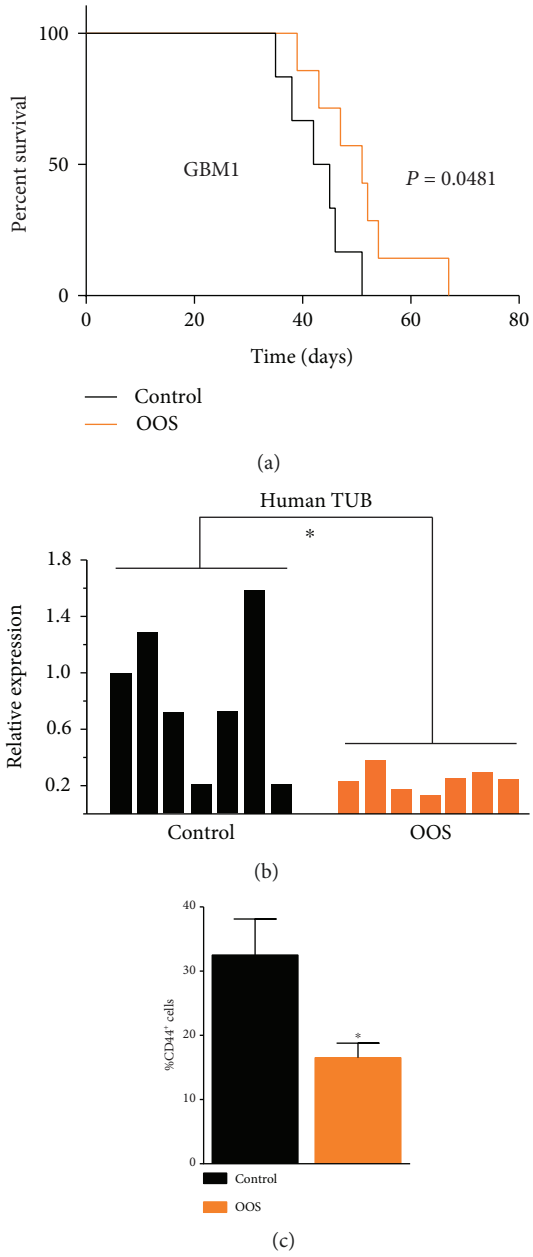

FIGURE 3: OOS inhibits intracranial tumor growth. GBM1 cells were injected into the brains of nude mice. The animals were treated orally with daily doses of OOS (200 μl, 5 days/week) or water (control). (a) Animal survival was evaluated using a Kaplan-Meier survival curve and the differences in survival times were analyzed with a log-rank test, $n = 7$. (b) qRT-PCR analysis of *human* β-*tubulin* (*human TUB*) related to *RPII* (human and mouse) levels in the dissected brains. Each bar represents one tumor. (c) Percentage of $CD44^+$ cells in dissociated brain tumors analyzed by flow cytometry, $n = 3$. $^*P \leq 0.05$.

detrimental. Antioxidants could, therefore, deregulate this oxidative stress equilibrium, affecting stem cell properties and tumor growth.

Not all GBM CSCs seem to be sensitive to OOS. The supplement did not inhibit the clonal growth of GBM3 cells and it did not slow down the growth of GBM3 tumors, suggesting that CSCs from GBM3 are less sensitive to OOS than those from GBM1 or GBM2. It is important to remark that OOS was able to induce the expression of several antioxidant enzymes, but only in GBM1 and GBM2 cells. Moreover, the expression of some metabolic enzymes was very different in GBM3 cells compared to the other two lines, suggesting that the redox and the metabolic status of the glioma cells may determine their response to OOS. It would be interesting to test, in a larger cohort study, if the expression of some of these enzymes could be used as a predictive marker for the efficacy OOS or other antioxidant compounds.

Apart from the direct effect of OOS in GBM tumor cells, our data reflect that there was a change in the inflammatory component of the tumors, with a weaker expression of M2 macrophage markers in tumors treated with OOS. Glioma cells in general, and CSCs in particular, release several factors that recruit and promote the growth of macrophages [28, 31]. Therefore, changes in the properties of CSCs induced by OOS could be affecting the surrounding myeloid cells. Although we cannot discard such indirect effect, our results *in vitro* clearly indicate that OOS affects macrophage polarization in a direct way, reducing the expression of M2 markers in response to a classical inducer like IL4 but also in response to glioma-CM. We also confirmed that OOS reduces the levels of ROS in the macrophages in all the conditions tested. Although ROS production is usually associated with the activation and function of M1 macrophages [28], it has been recently shown that ROS are important in M2 but not in M1 macrophage differentiation. Thus, antioxidants like BHA (butylated hydroxy-anisole) [35], dihydroxycoumarins [36], or caffeic acid [37] inhibit M2 but not M1 polarization and prevent tumor growth and metastasis formation. Furthermore, chlorogenic acid, a product with antibacterial and antioxidant properties, inhibits the growth of GBM through the repolarization of macrophage from M2 to M1 phenotype [38]. Therefore, OOS could exert their antitumorigenic action, at least in part, through the inhibition of M2 differentiation. Other authors have observed an increase in proinflammatory cytokines like IL6 in mouse models of acute leukemia treated with OOS [15], suggesting that the macrophage-polarization effect of OOS could be extended to other cancers. In our hands, however, OOS does not induce a significant increase in the expression of M1 markers in LPS-treated macrophages, although *IL18* (but not *NOS2*) is overexpressed in GBM1 tumors treated with OOS. IL18 is another cytokine secreted by M1 macrophages that participates in the activation of T cell-mediated inflammatory responses [39]. Interestingly, in GBM3 tumors, M2 markers are also inhibited whereas *IL8* expression is not induced in response to OOS. This could participate in the lack of response of these cells to the dietary supplement. Moreover, these results suggest that other components of the glioma (including the tumor cells) might modulate the response of macrophages to OOS, making some tumors more susceptible to these changes than others.

It is important to remark that, in our hands, treatment with OOS does not have any apparent toxic effect since no differences were observed in animal weight or behavior in control and treated mice. Some oncologists avoid the use of

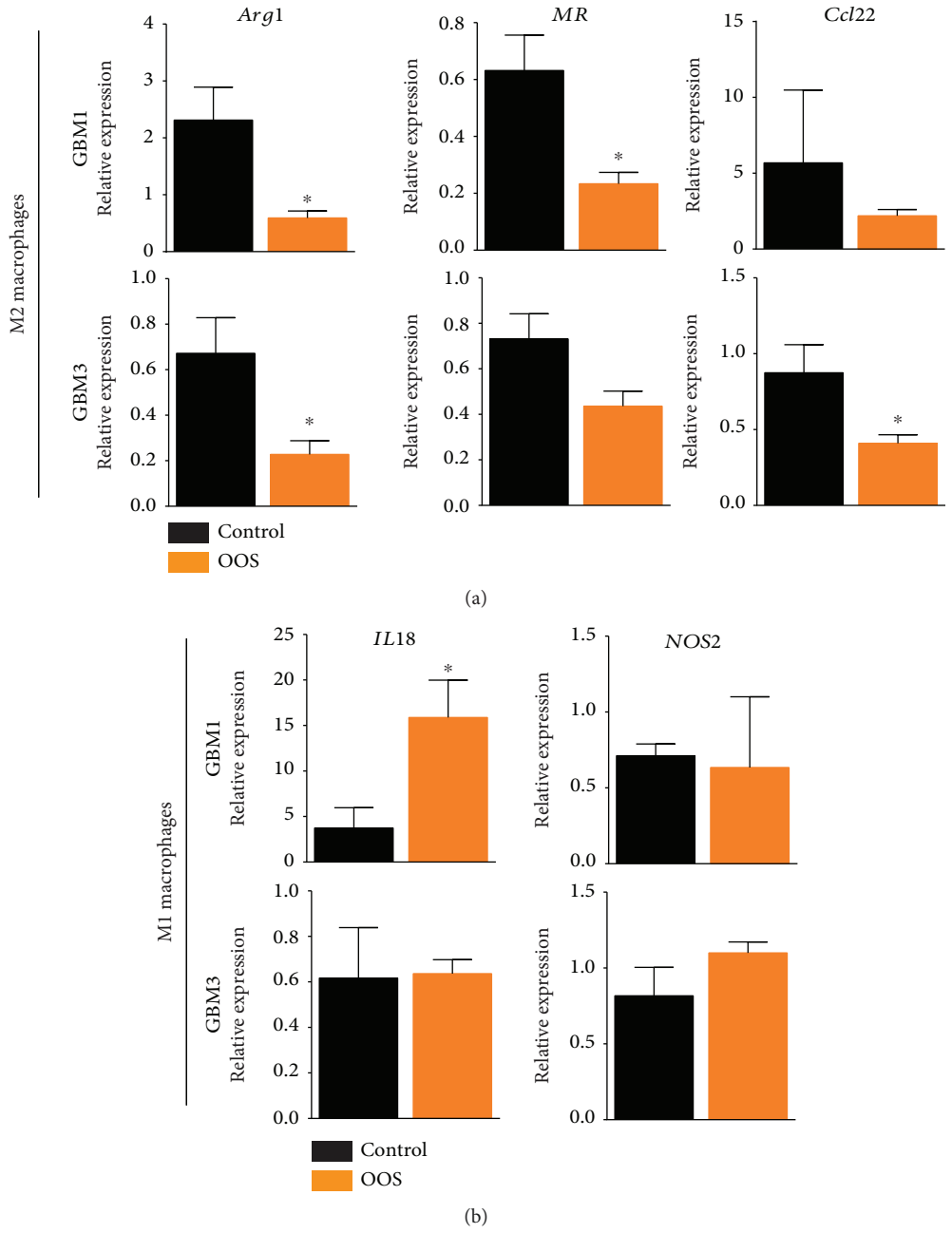

Figure 4: OOS affects macrophage polarization *in vivo*. GBM1 and GBM3 flank tumors were dissociated and the expression of different M2 (a) or M1 (b) markers was determined by qRT-PCR ($n = 6$). Mouse *Actin* was used for normalization. $^*P \leq 0.05$.

antioxidant supplements during treatment because it has been reported that they may have detrimental effects or even undesirable interactions with certain therapies. However, several articles have concluded that antioxidant supplements do not undermine the effectiveness of cytotoxic therapies [10]. Therefore, it would be interesting to find out if there is a synergy between OOS and the conventional chemotherapy (TMZ), as it has been shown in other types of cancer [15, 40]. The fact that OOS has been marketed for years without any report of adverse effects would help in verifying this synergism in the clinic. Moreover, it would be interesting to test whether OOS could have a similar beneficial effect in combination with radiotherapy or even for the novel immunotherapies that are currently in early clinical phases.

5. Conclusions

(i) The presence of Ocoxin® oral solution (OOS) inhibits the self-renewal capacity of a percentage of primary glioblastoma (GBM) cell lines

(ii) Systemic treatment with OOS reduces tumor burden of a percentage of primary GBMs

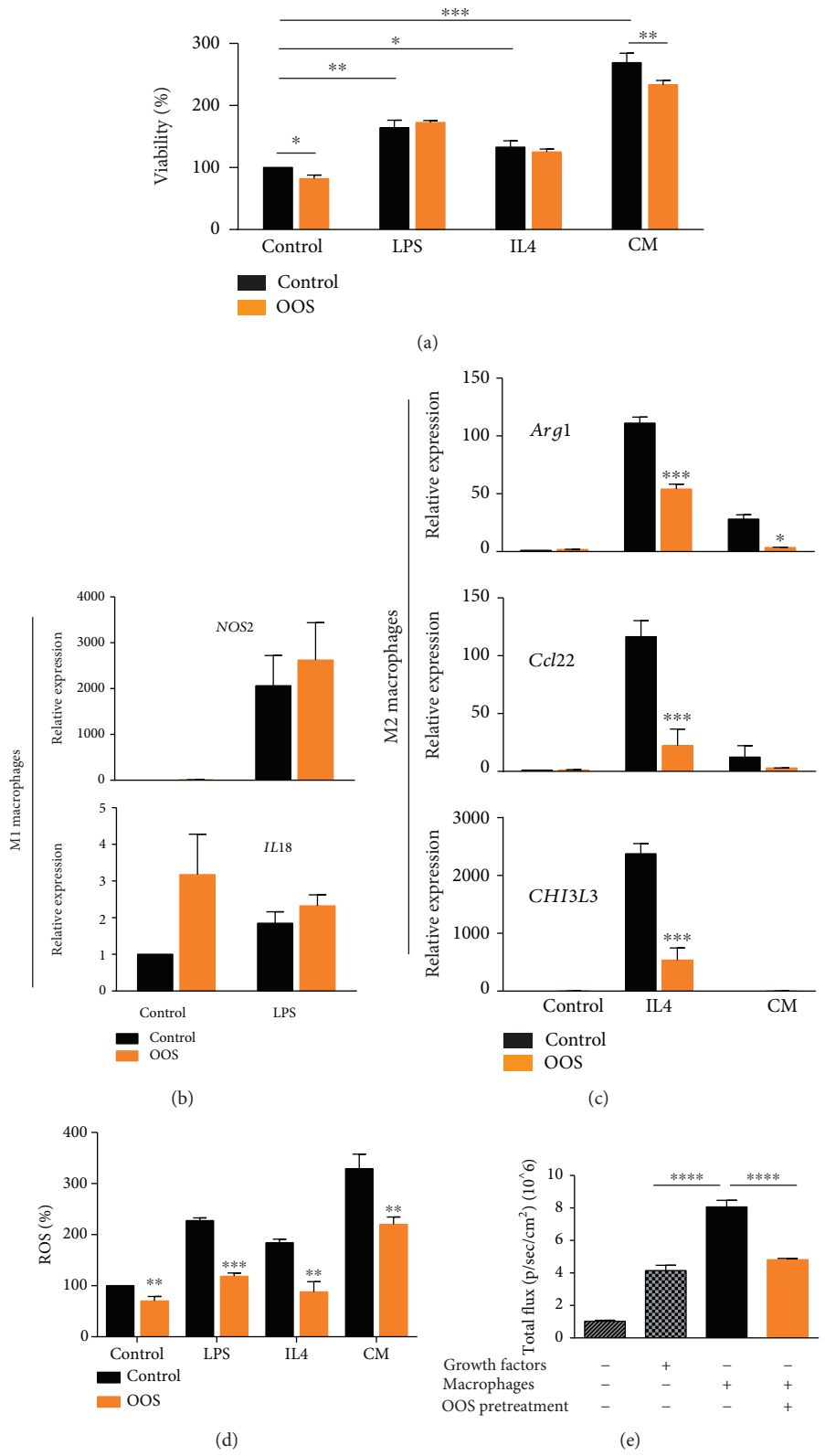

FIGURE 5: OOS affects macrophage polarization *in vitro*. (a) Cell viability was measured in the presence of the different stimuli. (b, c) Macrophage pellets were processed for qRT-PCR analysis of M1 (b) and M2 (c) genes. Mouse *Actin* was used for normalization, $n = 3$. (d) Analysis of ROS levels with DHE reagent in macrophages treated with the different stimuli, with or without OOS, $n = 5$. (e) Peritoneal macrophages were incubated in the presence of IL4 and OOS. After washing the macrophages, GBM1 cells were dissociated and plated on top of the macrophages or in control plates (with or without growth factors). Three days later, luciferase activity was measured in an IVIS equipment, $n = 3$. $^{*}P \leq 0.05$; $^{**}P \leq 0.01$; $^{***}P \leq 0.001$; $^{****}P \leq 0.0001$.

(iii) OOS inhibits M2 protumoral polarization of macrophages *in vitro*

(iv) Systemic treatment with OOS inhibits the M2 protumoral polarization of glioma-associated macrophages

(v) OOS is a feasible candidate to be used in combination therapies during the treatment of GBM patients

Data Availability

The mouse models and the molecular and cellular data used to support the findings of this study are included within the article and within the supplementary information files.

Conflicts of Interest

The authors declare that this work was partially supported by Catalysis S.L. ES is a current employee of Catalysis S.L. The authors declare that there are no other nonfinancial competing interests.

Authors' Contributions

EHS performed most of the *in vitro* and *in vivo* experiments; RG and BS performed the WB analysis of the antioxidant-related molecules; TC performed the flow cytometry analysis; PNH performed some of the IHC and IF analysis of the tumors; RH performed some of the *in vivo* mouse tumor growth analysis; JMS, AHL, and APN developed the primary glioma cell lines; ES provided OOS and helped to write the manuscript; PSG supervised all the experiments and wrote the manuscript.

Acknowledgments

The authors would like to acknowledge Atanasio Pandiella for critical comments on the manuscript, Rosella Galli for donating GBM1, and Jacqueline Gutiérrez, Daniela Moiseev, Daniel Batzan, and Mario Alia for their technical support. RG has been funded by the Fundación Científica Asociación Española Contra el Cáncer. Research has been funded by grants from Fundación Científica Asociación Española Contra el Cáncer (18/006) to JMS; from MINECO: Acción Estratégica en Salud (AES) PI13/01258 to AHL; AES PI17/01621 to JMS; Red Temática de Investigación Cooperativa en Cancer (RTICC) RD12/0036/0027 to AHL, JMS, APN, and PSG; and MINECO-RETOS/FEDER SAF2015-65175 to PSG.

Supplementary Materials

Supplementary Figure S1: full-length blots of Figure 1(g). GBM cells were treated with OOS (1 : 100 or 1 : 50) for 2 or 24 h and expression of Nrf-2 and NQO-1, and HO-1 was measured by WB. Nontreated spheres were used as a control and the expression of GAPDH as a loading control. Supplementary Figure S2: OOS does not induce overall changes in proliferation or cell death in GBM1 tumors. Paraffin sections of GBM1 flank tumors were stained with hematoxylin-eosin to count the number of mitosis (upper panel) or were stained with Activated Caspase 3 antibody to count apoptotic cells (lower panel). In both cases, the graphs represent the number of cells counted in 10 fields per tumor ($n = 10$). Supplementary Table S1: list of primary antibodies for immunohistochemical DAB staining (IHC), flow cytometry (FC) and western blot (WB). Supplementary Table S2: list of secondary antibodies for immunohistochemical DAB staining (IHC) and western blot (WB). Supplementary Table S3: list of primers used for RT-PCR. *(Supplementary Materials)*

References

[1] D. N. Louis, A. Perry, G. Reifenberger et al., "The 2016 World Health Organization classification of tumors of the central nervous system: a summary," *Acta Neuropathologica*, vol. 131, no. 6, pp. 803–820, 2016.

[2] R. Stupp, W. P. Mason, M. van den Bent et al., "Radiotherapy plus concomitant and adjuvant temozolomide for glioblastoma," *The New England Journal of Medicine*, vol. 352, no. 10, pp. 987–996, 2005.

[3] J. D. Lathia, S. C. Mack, E. E. Mulkearns-Hubert, C. L. Valentim, and J. N. Rich, "Cancer stem cells in glioblastoma," *Genes & Development*, vol. 29, no. 12, pp. 1203–1217, 2015.

[4] J. M. Heddleston, M. Hitomi, M. Venere et al., "Glioma stem cell maintenance: the role of the microenvironment," *Current Pharmaceutical Design*, vol. 17, no. 23, pp. 2386–2401, 2011.

[5] N. Colwell, M. Larion, A. J. Giles et al., "Hypoxia in the glioblastoma microenvironment: shaping the phenotype of cancer stem-like cells," *Neuro-Oncology*, vol. 19, no. 7, pp. 887–896, 2017.

[6] S. S. Sabharwal and P. T. Schumacker, "Mitochondrial ROS in cancer: initiators, amplifiers or an Achilles' heel?," *Nature Reviews Cancer*, vol. 14, no. 11, pp. 709–721, 2014.

[7] M. D. Polewski, R. F. Reveron-Thornton, G. A. Cherryholmes, G. K. Marinov, and K. S. Aboody, "*SLC7A11* overexpression in glioblastoma is associated with increased cancer stem cell-like properties," *Stem Cells and Development*, vol. 26, no. 17, pp. 1236–1246, 2017.

[8] N. Jung, H. J. Kwon, and H. J. Jung, "Downregulation of mitochondrial UQCRB inhibits cancer stem cell-like properties in glioblastoma," *International Journal of Oncology*, vol. 52, pp. 241–251, 2018.

[9] X. Wu, J. Cheng, and X. Wang, "Dietary antioxidants: potential anticancer agents," *Nutrition and Cancer*, vol. 69, no. 4, pp. 521–533, 2017.

[10] R. W. Moss, "Do antioxidants interfere with radiation therapy for cancer?," *Integrative Cancer Therapies*, vol. 6, no. 3, pp. 281–292, 2007.

[11] E. V. Gomez, Y. M. Perez, H. V. Sanchez et al., "Antioxidant and immunomodulatory effects of Viusid in patients with chronic hepatitis C," *World Journal of Gastroenterology*, vol. 16, no. 21, pp. 2638–2647, 2010.

[12] E. V. Gomez, Y. S. Rodriguez, A. T. Gonzalez et al., "Viusid, a nutritional supplement, increases survival and reduces disease progression in HCV-related decompensated cirrhosis: a randomised and controlled trial," *BMJ Open*, vol. 1, no. 2, article e000140, 2011.

[13] M. Al-Mahtab, S. M. Akbar, M. S. Khan, and S. Rahman, "Increased survival of patients with end-stage hepatocellular carcinoma due to intake of ONCOXIN(R), a dietary

supplement," *Indian Journal of Cancer*, vol. 52, no. 3, pp. 443–446, 2015.

[14] S. Hernandez-Garcia, V. Gonzalez, E. Sanz, and A. Pandiella, "Effect of Oncoxin oral solution in HER2-overexpressing breast cancer," *Nutrition and Cancer*, vol. 67, no. 7, pp. 1159–1169, 2015.

[15] E. Diaz-Rodriguez, S. Hernandez-Garcia, E. Sanz, and A. Pandiella, "Antitumoral effect of Ocoxin on acute myeloid leukemia," *Oncotarget*, vol. 7, no. 5, pp. 6231–6242, 2016.

[16] J. Marquez, J. Mena, I. Hernandez-Unzueta et al., "Ocoxin® oral solution slows down tumor growth in an experimental model of colorectal cancer metastasis to the liver in Balb/c mice," *Oncology Reports*, vol. 35, no. 3, pp. 1265–1272, 2016.

[17] I. Hernandez-Unzueta, A. Benedicto, E. Olaso et al., "Ocoxin oral solution® as a complement to irinotecan chemotherapy in the metastatic progression of colorectal cancer to the liver," *Oncology Letters*, vol. 13, no. 6, pp. 4002–4012, 2017.

[18] N. Pozo, C. Zahonero, P. Fernández et al., "Inhibition of DYRK1A destabilizes EGFR and reduces EGFR-dependent glioblastoma growth," *The Journal of Clinical Investigation*, vol. 123, no. 6, pp. 2475–2487, 2013.

[19] L. Jimenez-Garcia, S. Herranz, A. Luque, and S. Hortelano, "Critical role of p38 MAPK in IL-4-induced alternative activation of peritoneal macrophages," *European Journal of Immunology*, vol. 45, no. 1, pp. 273–286, 2015.

[20] C. Zahonero, P. Aguilera, C. Ramírez-Castillejo et al., "Preclinical test of dacomitinib, an irreversible EGFR inhibitor, confirms its effectiveness for glioblastoma," *Molecular Cancer Therapeutics*, vol. 14, no. 7, pp. 1548–1558, 2015.

[21] J. Lee, S. Kotliarova, Y. Kotliarov et al., "Tumor stem cells derived from glioblastomas cultured in bFGF and EGF more closely mirror the phenotype and genotype of primary tumors than do serum-cultured cell lines," *Cancer Cell*, vol. 9, no. 5, pp. 391–403, 2006.

[22] D. R. Laks, M. Masterman-Smith, K. Visnyei et al., "Neurosphere formation is an independent predictor of clinical outcome in malignant glioma," *Stem Cells*, vol. 27, no. 4, pp. 980–987, 2009.

[23] N. Garcia-Romero, C. González-Tejedo, J. Carrión-Navarro et al., "Cancer stem cells from human glioblastoma resemble but do not mimic original tumors after *in vitro* passaging in serum-free media," *Oncotarget*, vol. 7, no. 40, pp. 65888–65901, 2016.

[24] M. R. de Oliveira, B. F. de Bittencourt, and C. R. Furstenau, "Sulforaphane promotes mitochondrial protection in SH-SY5Y cells exposed to hydrogen peroxide by an Nrf2-dependent mechanism," *Molecular Neurobiology*, vol. 55, no. 6, pp. 4777–4787, 2017.

[25] P. Basak, P. Sadhukhan, P. Sarkar, and P. C. Sil, "Perspectives of the Nrf-2 signaling pathway in cancer progression and therapy," *Toxicology Reports*, vol. 4, pp. 306–318, 2017.

[26] J. Anido, A. Sáez-Borderías, A. Gonzàlez-Juncà et al., "TGF-β receptor inhibitors target the $CD44^{high}/Id1^{high}$ glioma-initiating cell population in human glioblastoma," *Cancer Cell*, vol. 18, no. 6, pp. 655–668, 2010.

[27] A. Pietras, A. M. Katz, E. J. Ekström et al., "Osteopontin-CD44 signaling in the glioma perivascular niche enhances cancer stem cell phenotypes and promotes aggressive tumor growth," *Cell Stem Cell*, vol. 14, no. 3, pp. 357–369, 2014.

[28] R. Glass and M. Synowitz, "CNS macrophages and peripheral myeloid cells in brain tumours," *Acta Neuropathologica*, vol. 128, no. 3, pp. 347–362, 2014.

[29] S. M. Pyonteck, L. Akkari, A. J. Schuhmacher et al., "CSF-1R inhibition alters macrophage polarization and blocks glioma progression," *Nature Medicine*, vol. 19, no. 10, pp. 1264–1272, 2013.

[30] A. Ellert-Miklaszewska, M. Dabrowski, M. Lipko, M. Sliwa, M. Maleszewska, and B. Kaminska, "Molecular definition of the pro-tumorigenic phenotype of glioma-activated microglia," *Glia*, vol. 61, no. 7, pp. 1178–1190, 2013.

[31] M. Sielska, P. Przanowski, B. Wylot et al., "Distinct roles of CSF family cytokines in macrophage infiltration and activation in glioma progression and injury response," *The Journal of Pathology*, vol. 230, no. 3, pp. 310–321, 2013.

[32] D. Zhou, L. Shao, and D. R. Spitz, "Chapter One - Reactive oxygen species in normal and tumor stem cells," *Advances in Cancer Research*, vol. 122, pp. 1–67, 2014.

[33] S. H. Kim, C. H. Kwon, and I. Nakano, "Detoxification of oxidative stress in glioma stem cells: mechanism, clinical relevance, and therapeutic development," *Journal of Neuroscience Research*, vol. 92, no. 11, pp. 1419–1424, 2014.

[34] S. Yuan, Y. Lu, J. Yang et al., "Metabolic activation of mitochondria in glioma stem cells promotes cancer development through a reactive oxygen species-mediated mechanism," *Stem Cell Research & Therapy*, vol. 6, no. 1, 2015.

[35] Y. Zhang, S. Choksi, K. Chen, Y. Pobezinskaya, I. Linnoila, and Z. G. Liu, "ROS play a critical role in the differentiation of alternatively activated macrophages and the occurrence of tumor-associated macrophages," *Cell Research*, vol. 23, no. 7, pp. 898–914, 2013.

[36] Y. Kimura and M. Sumiyoshi, "Antitumor and antimetastatic actions of dihydroxycoumarins (esculetin or fraxetin) through the inhibition of M2 macrophage differentiation in tumor-associated macrophages and/or G1 arrest in tumor cells," *European Journal of Pharmacology*, vol. 746, pp. 115–125, 2015.

[37] N. Orsolic, M. Kunstic, M. Kukolj, R. Gracan, and J. Nemrava, "Oxidative stress, polarization of macrophages and tumour angiogenesis: efficacy of caffeic acid," *Chemico-Biological Interactions*, vol. 256, pp. 111–124, 2016.

[38] N. Xue, Q. Zhou, M. Ji et al., "Chlorogenic acid inhibits glioblastoma growth through repolarizating macrophage from M2 to M1 phenotype," *Scientific Reports*, vol. 7, no. 1, article 39011, 2017.

[39] P. J. Murray, J. E. Allen, S. K. Biswas et al., "Macrophage activation and polarization: nomenclature and experimental guidelines," *Immunity*, vol. 41, no. 1, pp. 14–20, 2014.

[40] E. Diaz-Rodriguez, A. M. El-Mallah, E. Sanz, and A. Pandiella, "Antitumoral effect of Ocoxin in hepatocellular carcinoma," *Oncology Letters*, vol. 14, no. 2, pp. 1950–1958, 2017.

Hindawi
Oxidative Medicine and Cellular Longevity
Volume 2019, Article ID 8307196, 15 pages
https://doi.org/10.1155/2019/8307196

Research Article

Antioxidant Effects of *Satureja hortensis* L. Attenuate the Anxiogenic Effect of Cisplatin in Rats

Igor Kumburovic,[1] Dragica Selakovic,[1] Tatjana Juric,[2] Nemanja Jovicic,[3] Vladimir Mihailovic,[4] Jelena Katanic Stankovic,[4] Nikola Sreckovic,[4] Davor Kumburovic,[1] Vladimir Jakovljevic,[1,5] and Gvozden Rosic[1]

[1]*Department of Physiology, Faculty of Medical Sciences, University of Kragujevac, Kragujevac, Serbia*
[2]*Faculty of Agriculture, University of Novi Sad, Novi Sad, Serbia*
[3]*Department of Histology and Embryology, Faculty of Medical Sciences, University of Kragujevac, Kragujevac, Serbia*
[4]*Department of Chemistry, Faculty of Science, University of Kragujevac, Kragujevac, Serbia*
[5]*Department of Human Pathology, 1st Moscow State Medical University IM Sechenov, Moscow, Russia*

Correspondence should be addressed to Gvozden Rosic; grosic@medf.kg.ac.rs

Received 5 April 2019; Revised 13 May 2019; Accepted 26 May 2019; Published 29 July 2019

Guest Editor: Patrícia Rijo

Numerous adverse effects of cisplatin-based therapy are usually accompanied by enhanced oxidative damage and cell apoptosis in various tissues. Even neurotoxic manifestations of cisplatin administration, such as the anxiogenic effect, appear along with the increased oxidative stress and apoptotic indicators in certain brain regions. Thirty-five Wistar albino male rats were divided into seven groups: control, cisplatin (received a single dose of cisplatin: 7.5 mg/kg), three groups with oral administration of *Satureja hortensis* L. methanolic extract (SH) (low: 50 mg/kg, middle: 100 mg/kg, and high dose: 200 mg/kg) along with cisplatin application, a group with the extract in high dose alone, and a silymarin group (cisplatin and silymarin: 100 mg/kg), in order to evaluate the antioxidant effects of SH on cisplatin-induced increase in the anxiety level. After completing 10-day pretreatments, behavioral testing was performed in the open field and the elevated plus maze, followed by an investigation of oxidative stress and apoptosis parameters in hippocampal tissue samples. Cisplatin administration resulted in anxiogenic-like behavior, increased lipid peroxidation, and proapoptotic markers accompanied by the decline in antioxidant and antiapoptotic defense. The administration of extract alone did not significantly alter any of the estimated parameters. When applied along with cisplatin, SH in a dose of 100 mg/kg induced the significant anxiolytic effect with concomitant recovery of antioxidant and antiapoptotic activity indicators, while both lower and higher doses of the extract failed to improve the adverse effects of cisplatin administration. The beneficial effects of the middle dose of SH were equivalent to the same dose of silymarin, as a "golden standard." Our results indicate that the antioxidant supplementation with SH in an optimal dose significantly improved the oxidative status and it had antiapoptotic effect in the rat hippocampus disturbed by cisplatin administration, which was accompanied with attenuation of cisplatin-induced anxiogenic effect.

1. Introduction

Generation of reactive oxygen species (ROS) in brain tissue is considered to be the main process linked to the appearance of a broad spectrum of psychiatric disorders [1]. A chemotherapeutic drug, cisplatin, although considered to be one of the most promising chemotherapeutics in the treatment of various malignancies, exerts morphological or behavioral impairments in brain tissue [2]. The primary evidence of neurotoxicity of cisplatin is decreased activity of antioxidant enzymes with concomitant depletion in the glutathione level, elevated lipid membrane peroxidation, and mitochondrial dysfunction. This indicates that cisplatin causes overproduction of ROS and imbalance between oxidant-antioxidant levels, consequently leading to the insufficient level of antioxidants to counteract the raised ROS in tissue [3]. Besides,

cisplatin-induced neurotoxicity has been shown to result in numerous clinical forms. Although the majority of the investigated mechanisms focused on the manifestations of peripheral nerve injury [4], recent investigations have paid more attention to the effects on the central nervous system. Therefore, it has been reported that various protocols of cisplatin administration may affect mood regulation [5], as well as cognitive and perceptual impairments [6]. Furthermore, it has been proposed that the described behavioral alterations are connected with an underlying increase of oxidative stress [7] in specific brain regions involved in the control of those features. Also, Manohar and coworkers demonstrated that cisplatin promotes cell death in the hippocampus by increasing the expression of proapoptotic genes while reducing the expression of antiapoptotic genes [8].

Phytochemicals and plant-based products have been widely applied in treatments of various types of neurological disorders, due to their safety and the absence of side effects [9]. *Satureja hortensis* L. (summer savory, garden savory) is an annual shrub belonging to the genus *Satureja* of the Lamiaceae family. Summer savory is native to North America as well as warmer regions, such as the Mediterranean area and Southern Europe [10]. Due to its flavoring properties, the aerial parts of some *Satureja* species are mostly used as a culinary spice [11], but their medical benefits on human health are also remarkable. In traditional medicine, *S. hortensis* has been widely applied to relieve muscle pain, as a carminative and as a medicament in the treatment of diarrhea and digestion impairments [12]. Modern phytochemical analysis revealed a wide range of bioactive constituents in *S. hortensis*: monoterpenoids, carvacrol, thymol, and *p*-cymene as the main compounds in volatile oil [13] and phenolics, especially a high amount of rosmarinic acid, as major active principles in the extract [14]. Considering the different active compounds that are present in *S. hortensis*, the exceptional potential of essential oil and extracts of summer savory has been reported in *in vitro* and *in vivo* studies. Recent studies showed that *S. hortensis* exhibited notable antioxidant, antimicrobial, antiparasitic, anti-inflammatory, antinociceptive, antiviral, anti-Alzheimer (acetyl- and butyrylcholinesterase inhibitory activity), and hepatoprotective properties [15, 16]. Our earlier study showed the amelioration effect of *S. hortensis* methanolic extract against cisplatin-induced hepatorenal and testicular toxicity [17]. Similarly, it was demonstrated that administration of *S. hortensis* extract could prevent alterations in cisplatin-induced oxidative damage in several tissues [18]. There are no studies on toxicity of *S. hortensis* extract, but Fierascu et al. [15] recently reported that *S. hortensis* tea or infusion can be safely consumed, but essential oil of summer savory may cause mild dermal irritations. Previous investigations showed that rosmarinic acid, the main phenolic compound in *S. hortensis* extract, produced antidepressive and anxiolytic effects [19], and therefore, the following investigations were performed in order to evaluate the effects of *S. hortensis* methanolic extract (SH) on the cisplatin-induced increase in the anxiety level and oxidative stress in hippocampal tissue.

2. Materials and Methods

2.1. Extract Preparation. Aerial parts of *Satureja hortensis* L. were collected during the full flowering period in August 2015 in village Borač (municipality of Kragujevac, Republic of Serbia). A voucher specimen (No. 121/15) was deposited in the Herbarium of the Department of Biology and Ecology, Faculty of Science, University of Kragujevac, Kragujevac, Serbia, after the identification of species. Plant material was air-dried at room temperature. The methanolic extract of *S. hortensis* was prepared according to the previously published procedure [17]. Phytochemical characterization of methanolic extract using HPLC/DAD/(-)HESI-MS/MS analysis was previously published in the study by Boroja and coworkers, and this methanolic extract was investigated in the presented paper, as a part of the same study [17].

2.2. Animals and Treatment. Thirty-five male Wistar albino rats (two months old, 200-250 g, obtained from the Military Medical Academy, Belgrade, Serbia) were included in this study. The animals were housed in groups of five per cage in suitable environmental conditions (23 ± 1°C and 12/12 h light/dark cycles) and had free access to food and tap water. Animals were divided into seven equal groups and underwent pretreatment protocols, as follows: the control group received water for 10 days and a single intraperitoneal (i.p.) application of 0.5 mL normal saline on the 5th day; the CIS group received water for 10 days and a single dose of cisplatin (7.5 mg/kg b.w., i.p.) on the 5th day; the CIS+E50 group received *S. hortensis* extract (50 mg/kg b.w.) orally for 10 days and a single dose of cisplatin (7.5 mg/kg b.w., i.p.) on the 5th day; the CIS+E100 group received *S. hortensis* extract (100 mg/kg b.w.) orally for 10 days and a single dose of cisplatin (7.5 mg/kg b.w., i.p.) on the 5th day; the CIS+E200 group received *S. hortensis* extract (200 mg/kg b.w.) orally for 10 days and a single dose of cisplatin (7.5 mg/kg b.w., i.p.) on the 5th day; the CIS+silymarin group received silymarin (100 mg/kg b.w.) orally for 10 days and a single dose of cisplatin (7.5 mg/kg b.w., i.p.) on the 5th day; and the E200 group received *S. hortensis* extract (200 mg/kg b.w.) orally for 10 days.

The final concentration of extract doses was calculated on the basis of average water intake in the previous 24 hours.

2.3. Behavioral Testing. Twenty-four hours after completing the protocols, the animals were allowed to acclimate in a testing room (approximately at 8 am) for at least 1 h, and behavioral testing was performed in an open field (OF) and the elevated plus maze (EPM), as previously described [20]. The following parameters were estimated in the OF test: cumulative duration in the center zone (CDCZ, in seconds), frequency in the center zone (FCZ), total distance moved (TDM, in cm), the percentage of time moving (%TM), and the number of rearings during 5 minutes of testing. Immediately after completing the OF test, the rats were placed in the EPM in order to obtain different parameters: cumulative duration in open arms (CDOA, in seconds), frequency to open arms (FOA), TDM (in cm), %TM, the number of rearings, the number of head-dippings (HD), and the

number of total exploratory activity (TEA) episodes. Both tests were recorded, and video files were analyzed using EthoVision software (XT 12, Noldus Information Technology, The Netherlands).

After completing behavioral testing, the rats were decapitated following a short-term narcosis induced by intraperitoneal application of ketamine (10 mg/kg) and xylazine (5 mg/kg), the brains were quickly removed, and hippocampal tissue was isolated for further analysis.

2.4. The Estimation of Oxidative Stress Parameters in the Hippocampus. The hippocampus tissue homogenates were prepared in phosphate-buffered saline (PBS, pH 7.4) and centrifuged at 4000 rpm for 15 min at 4°C. The obtained supernatants were used for the determination of catalase (CAT) and superoxide dismutase (SOD) activities, as well as reduced glutathione (GSH) and thiobarbituric acid reactive substance (TBARS) levels. The activity of CAT in tissue homogenates was determined by monitoring the decomposition rate of hydrogen peroxide according to the method described by Beers and Sizer [21]. The measurement of SOD activity in hippocampus tissue homogenates was based on the colorimetric reaction inhibition of adrenochrome formation from adrenalin according to the method of Misra and Fridovich [22]. CAT and SOD activities in tissue homogenates were expressed as unit per milligram of protein (U per mg of proteins). The reduced glutathione (GSH) level in homogenates was estimated by Ellman's procedure and expressed as mg GSH per gram of proteins [23]. The thiobarbituric acid reactive substance (TBARS) level in samples was determined by the method of Ohkawa and coworkers and expressed as nmol MDA per mg of proteins [24]. The Lowry et al.'s method [25] was used for the determination of protein concentrations in tissue homogenates, using bovine serum albumin (BSA) as a standard. All spectrophotometric measurements were performed using a UV-Vis double beam spectrophotometer (model Halo DB-20S, with a temperature controller, Dynamica GmbH, Dietikon, Switzerland).

2.5. RNA Isolation and Real-Time PCR Analysis. Total RNA was extracted from hippocampal tissue using the TRIzol reagent (Invitrogen, CA) according to the manufacturer's instructions. For reverse transcription, a High-Capacity cDNA Reverse Transcription Kit (Applied Biosystems, CA) was used. Quantitative RT-PCR was performed using the Thermo Scientific Luminaris Color HiGreen qPCR Master Mix (Applied Biosystems, CA). Also, mRNA-specific primers for Bax, Bcl-2, caspase-3, and β-actin as a housekeeping gene (Invitrogen, CA) were used (Supplement 1). Quantitative RT-PCR reactions were done in the Mastercycler ep realplex (Eppendorf, Germany), and after data analysis, relative gene expression was calculated according to Livak and Schmittgen [26].

All research procedures were carried out in accordance with the European Directive for the welfare of laboratory animals No. 86/609/EEC and the principles of Good Laboratory Practice (GLP) and in accordance with the ARRIVE guidelines. All experiments were approved by the Ethical Committee of the Faculty of Medical Sciences, University of Kragujevac, Serbia.

2.6. Statistical Analysis. The data were presented as means ± S.E.M. After completing the tests for homogeneity (Levene's) and normality (Shapiro-Wilk), comparisons between groups were performed using one-way ANOVA, followed by Bonferroni post hoc analysis. Simple linear regression analyses were performed to analyze relationships between parameters obtained in behavioral tests and other analyses (oxidative stress and apoptosis indicators). Significance was determined at $p < 0.05$ for all tests. Statistical analysis was performed with SPSS version 20.0 statistical package (IBM SPSS Statistics 20).

3. Results

3.1. Antioxidant Supplementation Attenuates Cisplatin-Induced Anxiogenic Effect. Behavioral testing performed in this study revealed the anxiogenic-like effect of cisplatin in both OF (Figure 1) and EPM (Figure 2) tests. Cisplatin administration significantly decreased the principal indicators of the anxiety level, CDCZ (Figure 1(a)), and FCZ (Figure 1(b)), in the OF test ($F = 6.527$ and 5.530, respectively; df = 6, $p < 0.01$). The similar response to cisplatin, expressed as a significant decline in key parameters for anxiety level estimation in EPM, CDOA, and FOA (Figures 2(a) and 2(b); $F = 8.204$ and 6.027, respectively; df = 6, $p < 0.01$) was observed. Also, the overall locomotor activity in OF was significantly reduced following cisplatin application by means of TDM (Figure 1(c)) and %TM (Figure 1(d)) ($F = 16.064$ and 6.609, respectively; df = 6, $p < 0.01$), as it was in the EPM test, by means of the same parameters (Figures 2(c) and 2(d); $F = 14.693$ and 7.441, respectively; $p < 0.01$). At the same time, the exploratory activity was significantly reduced in OF (Figure 1(e); $F = 8.980$, $p < 0.01$) and EPM (Figures 2(e)–2(g)) that was manifested as decline in the number of HD ($F = 15.590$, $p < 0.01$), rearings ($F = 4.920$, $p < 0.05$), and TEA episodes ($F = 13.437$, $p < 0.01$).

Oral administration of the methanolic extract of *S. hortensis* (200 mg/kg/d), when applied alone, despite the fact that it was not statistically different, decreased all estimated parameters in OF and EPM tests when compared to the control. However, SH, continuously applied before and following cisplatin application in different doses, induced the alteration in cisplatin-induced anxiogenic effect. The attenuation of cisplatin-induced anxiogenic effect in OF and EPM tests was observed only in E100 and was manifested by a significant anxiolytic-like effect when compared to the cisplatin group ($p < 0.01$), reversing CDCZ and FCZ (Figures 1(a) and 1(b)) in OF and CDOA and FOA (Figures 2(a) and 2(b)) in EPM to the control values. SH in the lowest (50 mg/kg/d) and the highest (200 mg/kg/d) applied doses was not sufficient to abolish the anxiogenic effect of cisplatin by means of the principal indicators of anxiety in both tests. The similar consequences of SH were manifested on locomotor activity in both tests. The orally applied extract in a dose of 100 mg/kg/d diminished

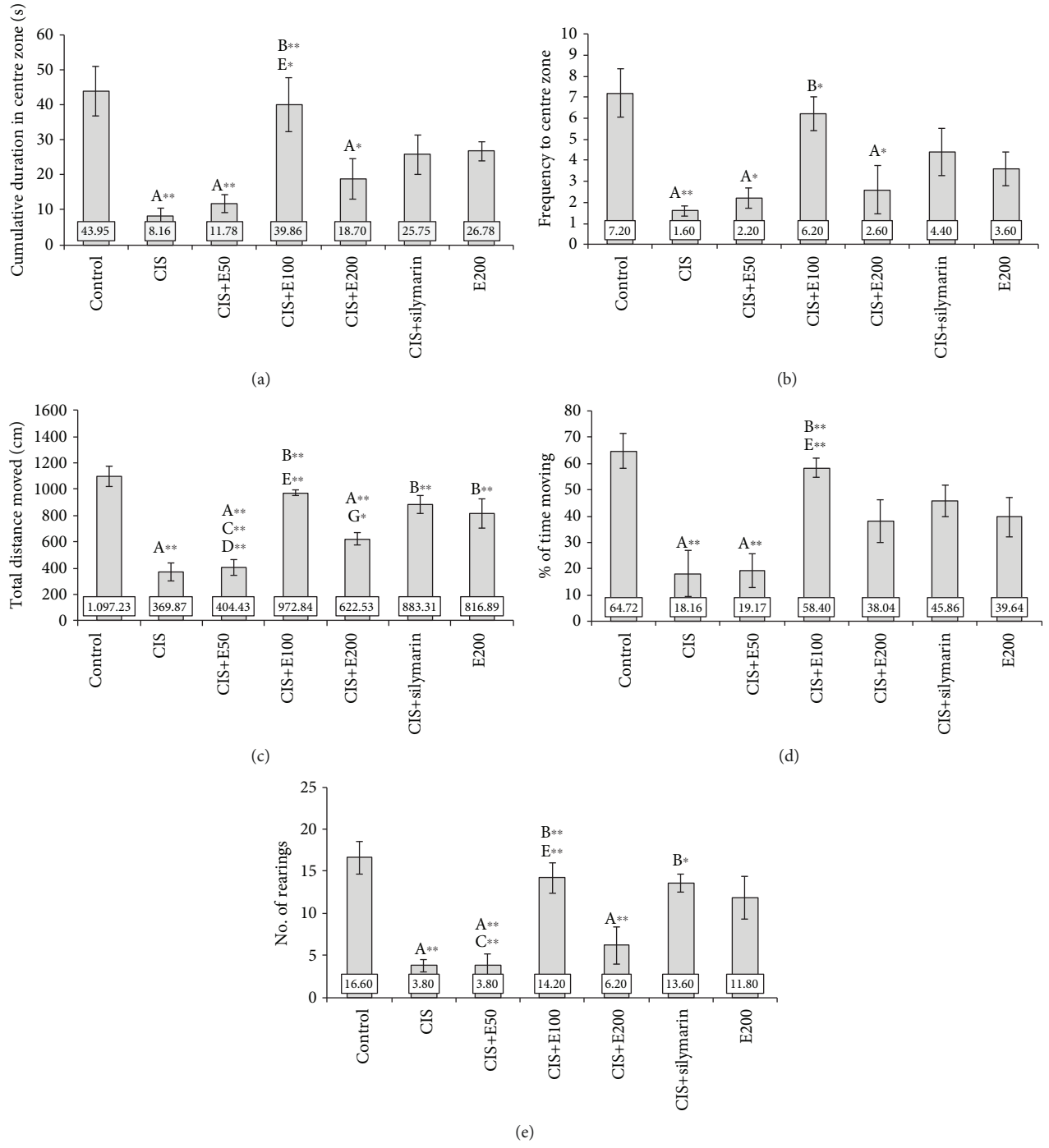

Figure 1: Parameters obtained in the open field (OF) test: (a) the cumulative duration in center zone (CDCZ), (b) the frequency to center zone (FCZ), (c) the total distance moved (TDM), (d) the percentage of time moving (%TM), and (e) the number of rearings. Values are the mean ± standard error of the mean (SEM); $n = 5$ per group. ∗ denotes a significant difference of $p < 0.05$; ∗∗ denotes a significant difference of $p < 0.01$. A: control vs. other groups; B: CIS vs. other groups; C: CIS+silymarin vs. other groups; D: E200 vs. other groups; E: CIS+E50 vs. CIS+E100; F: CIS+E50 vs. CIS+E200; G: CIS+E100 vs. CIS+E200.

cisplatin-induced decline in TDM and %TM in both OF (Figures 1(c) and 1(d)) and EPM (Figures 2(c) and 2(d)) tests. SH in this dose applied with cisplatin significantly increased TDM in both tests (Figures 1(c) and 1(d) and Figures 2(c) and 2(d)) compared to the lower and higher doses ($p < 0.01$), while this effect was not significant for %TM with the extract in a higher dose. However, both the locomotor activities in both tests for the animals treated with the higher and lower doses of the extract remained significantly diminished compared to the control values ($p < 0.01$) except for %TM in EPM for the higher dose. SH, when applied with cisplatin in the dose of 100 mg/kg/d, was

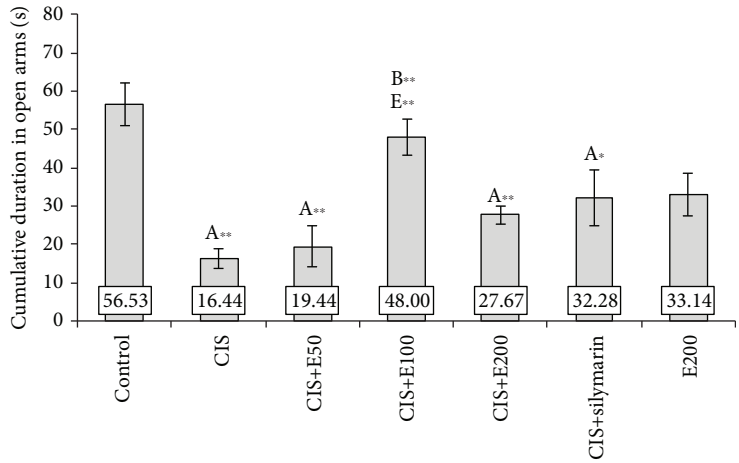

(a)

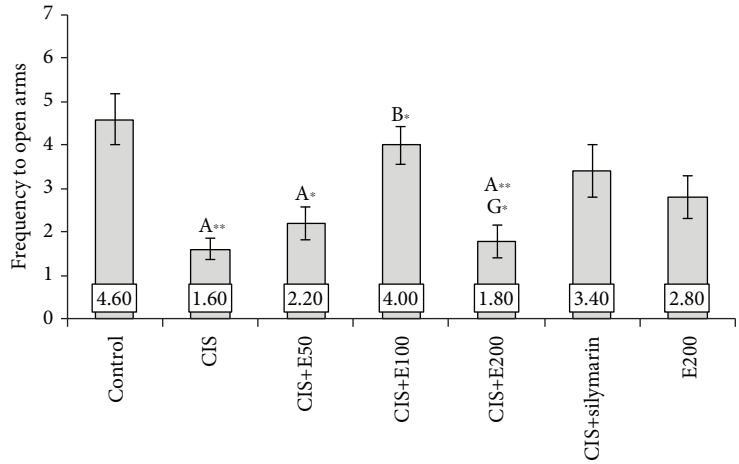

(b)

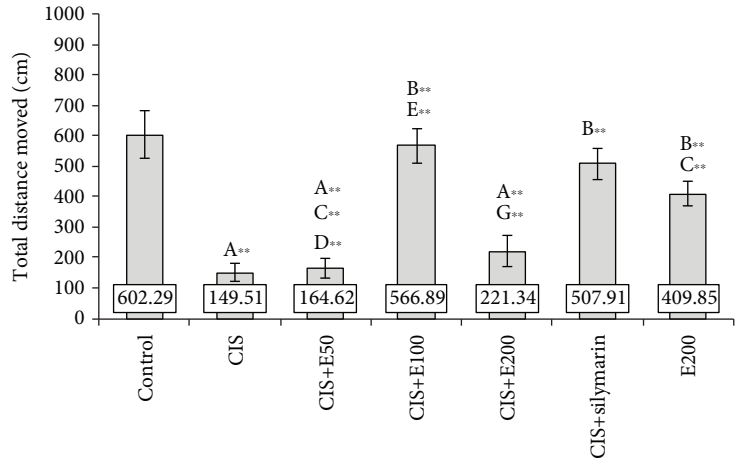

(c)

Figure 2: Continued.

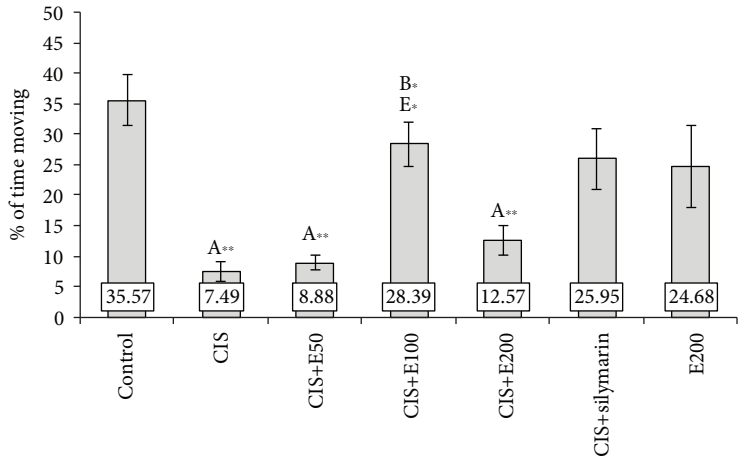

(d)

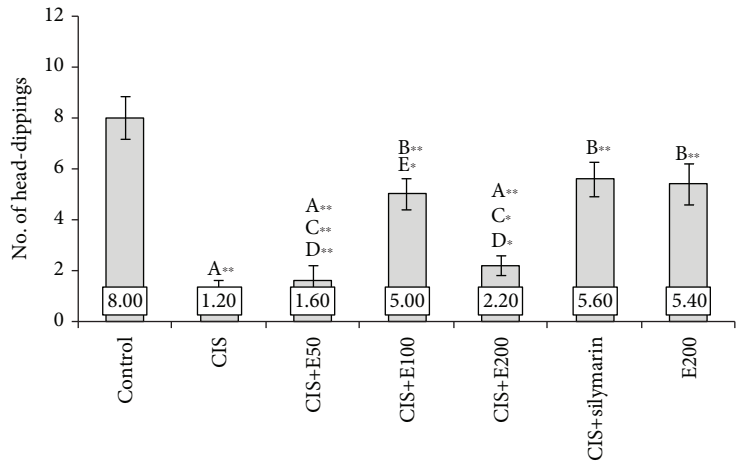

(e)

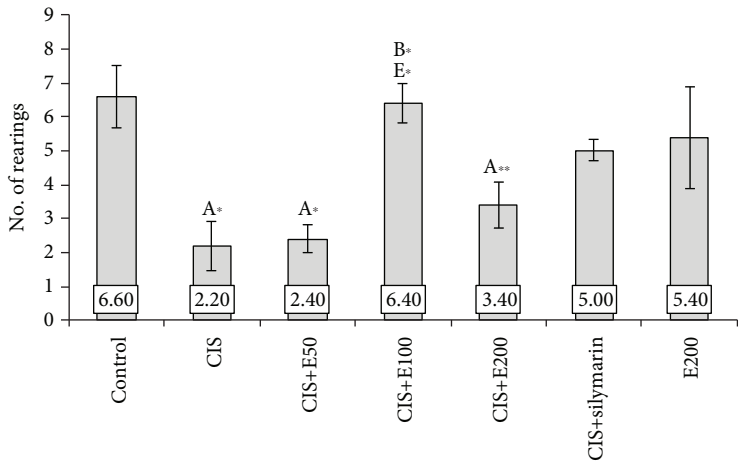

(f)

Figure 2: Continued.

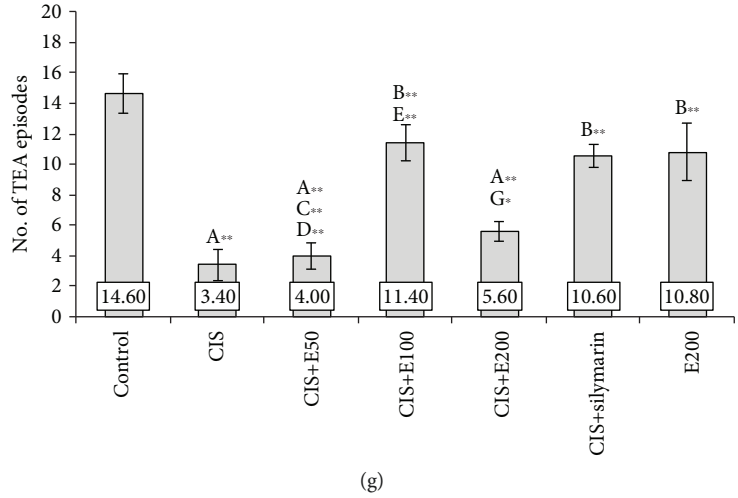

(g)

Figure 2: Parameters obtained in the elevated plus maze (EPM) test: (a) the cumulative duration in open arms (CDOA), (b) the frequency to open arms (FOA), (c) the total distance moved (TDM), (d) the percentage of time moving (%TM), (e) the number of head-dippings (HD), (f) the number of rearings, and (g) the number of TEA episodes. Values are the mean ± standard error of the mean (SEM); $n = 5$ per group. $*$ denotes a significant difference of $p < 0.05$; $**$ denotes a significant difference of $p < 0.01$. A: control vs. other groups; B: CIS vs. other groups; C: CIS+silymarin vs. other groups; D: E200 vs. other groups; E: CIS+E50 vs. CIS+E100; F: CIS+E50 vs. CIS+E200; G: CIS+E100 vs. CIS+E200.

sufficient to attenuate the cisplatin-induced decline in exploratory activity in both OF and EPM tests (Figure 1(e) and Figures 2(e)–2(g)). The lower dose of extract (50 mg/kg/d) failed to ameliorate this manifestation of anxiety-like behavior, which was manifested by significantly lower exploratory activity compared to the control values ($p < 0.01$), and even when compared to the effect of the middle dose of the extract ($p < 0.01$ for OF and TEA in EPM). Although the exploratory activity following the administration of the higher dose (200 mg/kg/d) along with cisplatin was not significantly lower compared to the middle dose (100 mg/kg/d), except for TEA, this anxiogenic feature of simultaneous administration of cisplatin and SH extract in the dose of 200 mg/kg/d remained significantly below the control values ($p < 0.01$), except for the number of rearings in EPM (Figure 2(f)).

When compared to SH, silymarin (a standardized plant extract with proven antioxidant effects *in vivo*) administration in a dose of 100 mg/kg/d showed similar protective effect on behavioral alterations induced by cisplatin in OF and EPM to the equivalent dose of SH (Figures 1 and 2) but still more pronounced than the effects of lower (50 mg/kg/d) and higher (200 mg/kg/d) doses of extract. As shown in Figure 2(a), silymarin did not prevent a decline in CDOA ($p < 0.01$) after cisplatin administration when compared to the control and did not produce a significant increase in any of the principle parameters for anxiety estimation in the applied tests. The protective effect following cisplatin application of silymarin was more pronounced by means of locomotor activity estimation, where it significantly increased cisplatin-induced decline in TDM (Figure 1(c) and Figure 2(c), $p < 0.01$), as well as exploratory activity in both tests (Figure 1(e) and Figures 2(e)–2(g), $p < 0.01$), except for the number of rearings in EPM.

3.2. Satureja hortensis L. Extract Prevents Oxidative Damage Induced by Cisplatin. All applied protocols resulted in significant alterations in oxidative stress markers: TBARS ($F = 5.400$, df = 6), SOD ($F = 6.103$), and CAT ($F = 4.396$). A single application of cisplatin (7.5 mg/kg b.w.) caused a significant ($p < 0.01$) increase in TBARS and decline in SOD and CAT activity ($p < 0.01$) in the hippocampus, when compared to the control group (Figures 3(a)–3(c), respectively). Except for the lowest estimated dose of *S. hortensis* extract (50 mg/kg b.w.), all tested concentrations of extract and silymarin provided a significant amelioration in the level of TBARS, in comparison with the cisplatin group. The application of SH at a dose of 100 mg/kg b.w. showed the most pronounced ($p < 0.01$) effect on the decrease of the TBARS level in hippocampal tissue in comparison with the cisplatin group. At the same time, the increase of SOD activity in the hippocampus, when compared to the cisplatin group, following administration of SH extracts was significant ($p < 0.05$) only with the dose of 100 mg/kg (Figure 3(b)). The activity of CAT in hippocampal tissue (Figure 3(c)) also significantly increased ($p < 0.05$) only in the extract-treated group at a dose of 100 mg/kg b.w., when compared to the cisplatin group. On the other hand, the GSH level in the hippocampus was decreased, although not significantly, by a single administration of cisplatin. However, the data presented in Figure 3(d) showed improvements in the GSH level in the groups treated with higher doses of SH (100 and 200 mg/kg) as well as with silymarin, but these effects were not significantly pronounced ($F = 3.034$). The level of GSH in the extract per se group was slightly increased ($p > 0.05$), compared to the control, and as such is statistically different from the cisplatin group ($p < 0.05$).

The application of silymarin (100 mg/kg b.w.) in combination with cisplatin showed almost equal effects in the

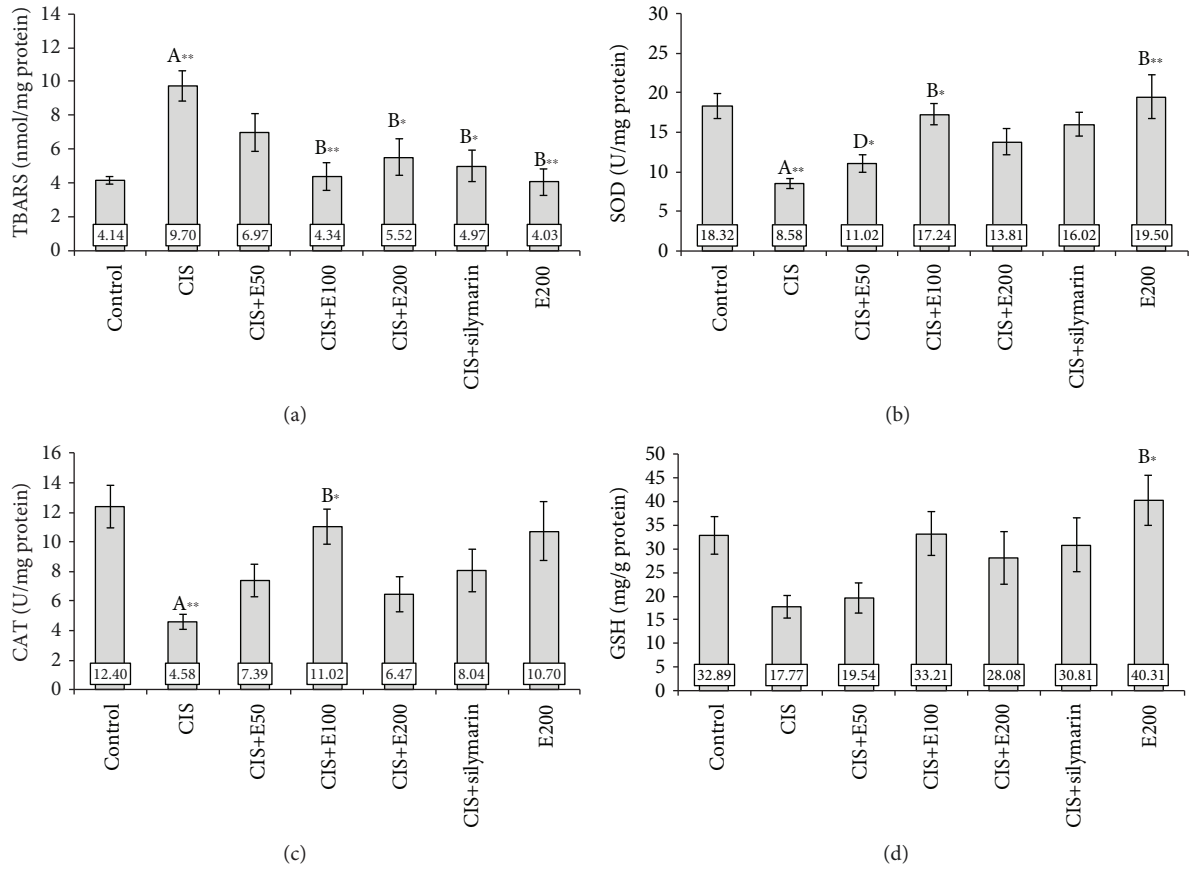

Figure 3: Oxidative stress markers in the rat hippocampus: (a) TBARS, (b) SOD, (c) CAT, and (d) GSH. Values are the mean ± standard error of the mean (SEM); $n = 5$ per group. ∗ denotes a significant difference of $p < 0.05$; ∗∗ denotes a significant difference of $p < 0.01$. A: control vs. other groups; B: CIS vs. other groups; C: CIS+silymarin vs. other groups; D: E200 vs. other groups; E: CIS+E50 vs. CIS+E100; F: CIS+E50 vs. CIS+E200; G: CIS+E100 vs. CIS+E200.

regulation of SOD and CAT activities in the hippocampus compared to *S. hortensis* extract at a dose of 100 mg/kg b.w. Application of extract at a dose of 200 mg/kg b.w. in combination with cisplatin was less effective in the regulation of all examined oxidative stress-related parameters compared to the extract dose of 100 mg/kg b.w. No significant changes were observed among the examined antioxidant hippocampal tissue parameters between the control group and the group treated with extract at a dose of 200 mg/kg b.w. without cisplatin application.

3.3. Diminishing of Cisplatin-Induced Proapoptotic Actions by Antioxidant Supplementation. The protocols applied in this study significantly altered the relative expression of genes involved in the regulation of cellular apoptosis, Bax ($F = 10.165$, df = 6), and Bcl-2 ($F = 58.950$) in hippocampal tissue. As shown in Figure 4, the application of cisplatin in the single dose induced a significant increase in Bax and decline in Bcl-2 relative gene expression compared to the control ($p < 0.01$), which resulted in significant augmentation of the Bax/Bcl-2 ratio ($F = 19.754$, $p < 0.01$). Although oral administration of SH did not significantly affect the hippocampal expression of those genes when applied alone, simultaneous oral intake of *S. hortensis* extract in a dose of 100 mg/kg reduced Bax and enhanced Bcl-2 hippocampal gene expression ($p < 0.01$), reversing the cisplatin-induced effects to control values (Figures 4(a) and 4(b)). On the other hand, administration of both lower and higher doses of *S. hortensis* extract (50 and 200 mg/kg) was not sufficient to significantly alter individual gene expression of Bax and Bcl-2 (Figure 4) but still significantly declined the Bax/Bcl-2 ratio in hippocampal tissue ($p < 0.01$). The effects of SH in a dose of 100 mg/kg/d on cisplatin-induced alterations of Bax and Bcl-2, as well as their ratio ($p < 0.01$), compared to the CIS group were very similar to the effects of simultaneous administration of silymarin in an equal dose. The relative gene expression of caspase-3, an apoptosis coordination enzyme, was also significantly affected by the applied protocols ($F = 53.467$) in the same manner as Bax. Thus, cisplatin administration significantly increased caspase-3 hippocampal expression (Figure 4(d)) compared to the control ($p < 0.01$). This manifestation of cisplatin proapoptotic action was lowered with all orally administered extracts (CIS+E100, CIS+E200, and CIS+silymarin) compared to the CIS group ($p < 0.01$), except for the lowest dose of *S. hortensis* extract (50 mg/kg/d).

As shown in Figure 5(a), simple regression analysis revealed a strong positive correlation between the index of lipid peroxidation expressed as TBARS and the Bax/Bcl-2 ratio ($R = 0.823$, $p = 1.26E\text{-}09$). The analysis also indicated

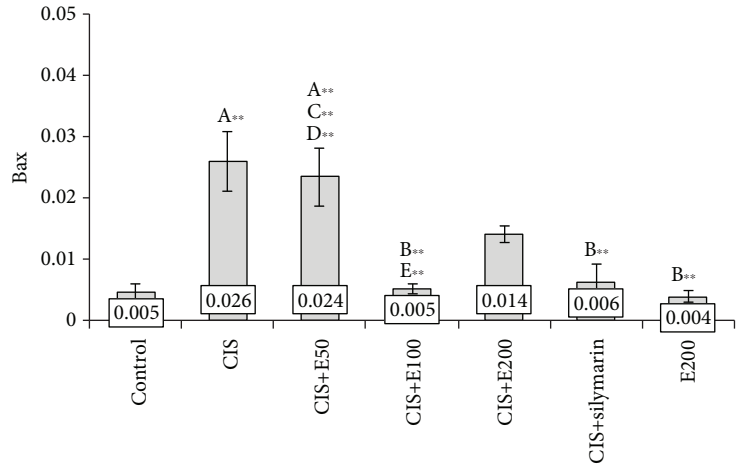

(a)

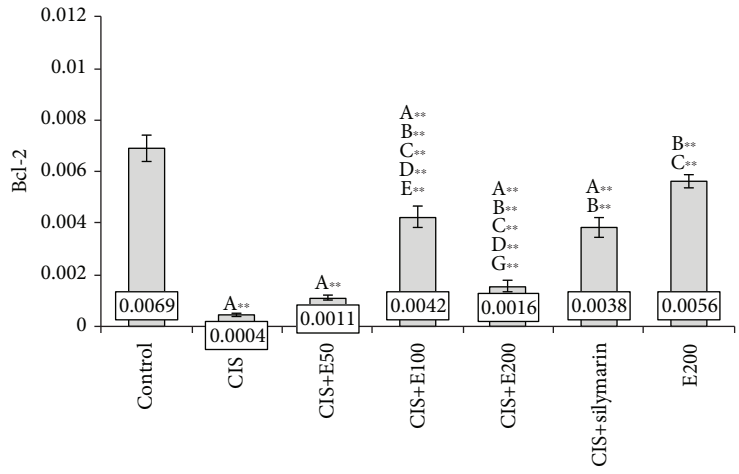

(b)

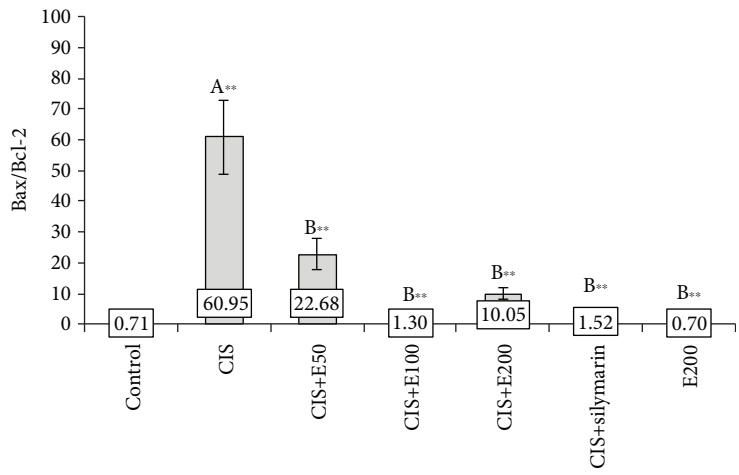

(c)

Figure 4: Continued.

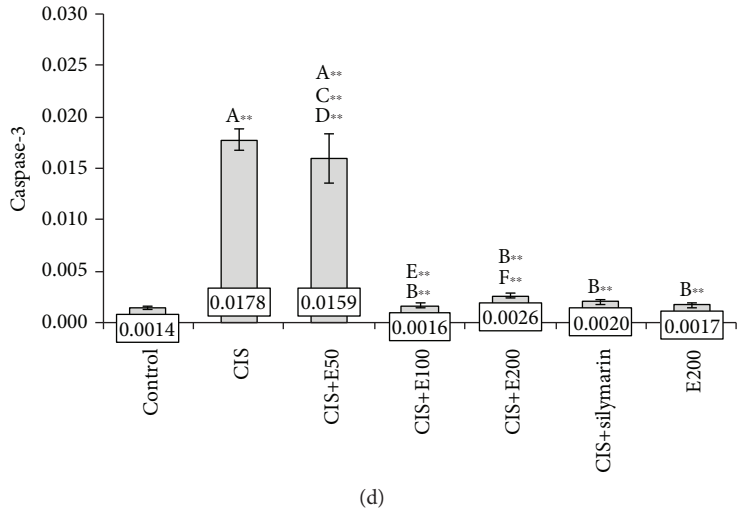

Figure 4: The relative expression of genes related to apoptosis in the rat hippocampus: (a) Bax, (b) Bcl-2, (c) Bax/Bcl-2 ratio, and (d) caspase-3. Values are the mean ± standard error of the mean (SEM); $n = 5$ per group. ∗ denotes a significant difference of $p < 0.05$; ∗∗ denotes a significant difference of $p < 0.01$. A: control vs. other groups; B: CIS vs. other groups; C: CIS+silymarin vs. other groups; D: E200 vs. other groups; E: CIS+E50 vs. CIS+E100; F: CIS+E50 vs. CIS+E200; G: CIS+E100 vs. CIS+E200.

strong but negative (Figure 5(b)) correlation between the hippocampal antioxidant capacity estimated by means of SOD activity and Bax/Bcl-2 ratio ($R = 0.688$, $p = 4.70E\text{-}06$). Finally, the analysis presented in Figure 5(c) confirms a strong, also negative, correlation between the Bax/Bcl-2 ratio and the principal indicator of the increased anxiety level obtained in the EPM test expressed as CDOA ($R = 0.601$, $p = 0.0001$).

4. Discussion

Although chemotherapy is one of the most employed approaches in the treatment of numerous malignancies, this therapeutic approach usually results in numerous adverse effects. Cisplatin, a widely used chemotherapeutic drug, has also been reported for serious clinical side effects, including severe manifestations of neurotoxicity, despite the fact that it poorly crosses the blood-brain barrier under physiological conditions [27], such as psychological, cognitive, and perceptual impairment [6, 28, 29]. The manifestations of neurotoxicity following cisplatin administration have also been confirmed in animal experimental models. Cisplatin-induced behavioral alterations include cognitive dysfunction [30] and depressive- and anxiety-like behaviors in rats [31, 32]. The results obtained in this study showed a clear anxiogenic effect of cisplatin (Figures 1 and 2). The anxiety-like behavior following cisplatin administration was manifested by means of the decline of the most convincing indicators in OF (CDCZ and FCZ) and EPM (CDOA and FOA) tests and confirmed by a decrease in locomotor and exploratory activities, in both tests, which is typical for anxiogenic features [33]. The anxiogenic effect of cisplatin applied in the single dose (7.5 mg/kg b.w.), as observed in this study, is in accordance with previously reported anxiety-like behavior following chronic cisplatin administration (5 mg/kg for five weeks and seven weeks) [5, 7].

Behavioral manifestations of cisplatin-induced neurotoxicity occur simultaneously with alterations in the hippocampus that involve inhibition in cell proliferation, differentiation, and neurogenesis with alterations in neurotransmitter content with morphological verification of neuronal damage [34–36]. Cisplatin also causes apoptosis [37], oxidative stress [38], and inflammation [39]. Our results show that the anxiogenic effect of cisplatin was accompanied by significant alterations in hippocampal tissue oxidative status (Figure 3). The increased lipid peroxidation following cisplatin administration observed in this study, as well as the decline in the antioxidant defense system, expressed by means of SOD and CAT activity in the hippocampus, is in line with reported alterations in oxidative status following chronic cisplatin treatment [7]. However, the lack of significant alteration in total hippocampal glutathione after a single dose of cisplatin, which is not in accordance with the reduction in GSH reported in that study, may be explained by different experimental protocols that included prolonged cisplatin treatment (seven weeks), sufficient to induce a significant decline in hippocampal glutathione. The postulated mechanisms of cisplatin neurotoxic effects in the rat hippocampus include the action via alteration in the expression of genes involved in antioxidative defense responses [7]. Changes in gene expression provoked by cisplatin implicate both downregulation of Nrf2, as a key regulator of protection against oxidative stress [40], and HO-1 (controlled by the Nrf2 gene level), as well as upregulation of NF-κB, which is responsible for cell damage in a various manner, including the increase of proinflammatory cytokines. Those mechanisms may lead to neuroinflammatory cascade in the hippocampus with the consequent behavioral deficits [41]. Inflammatory mediators have been reported to reduce hippocampal BDNF levels [42], which

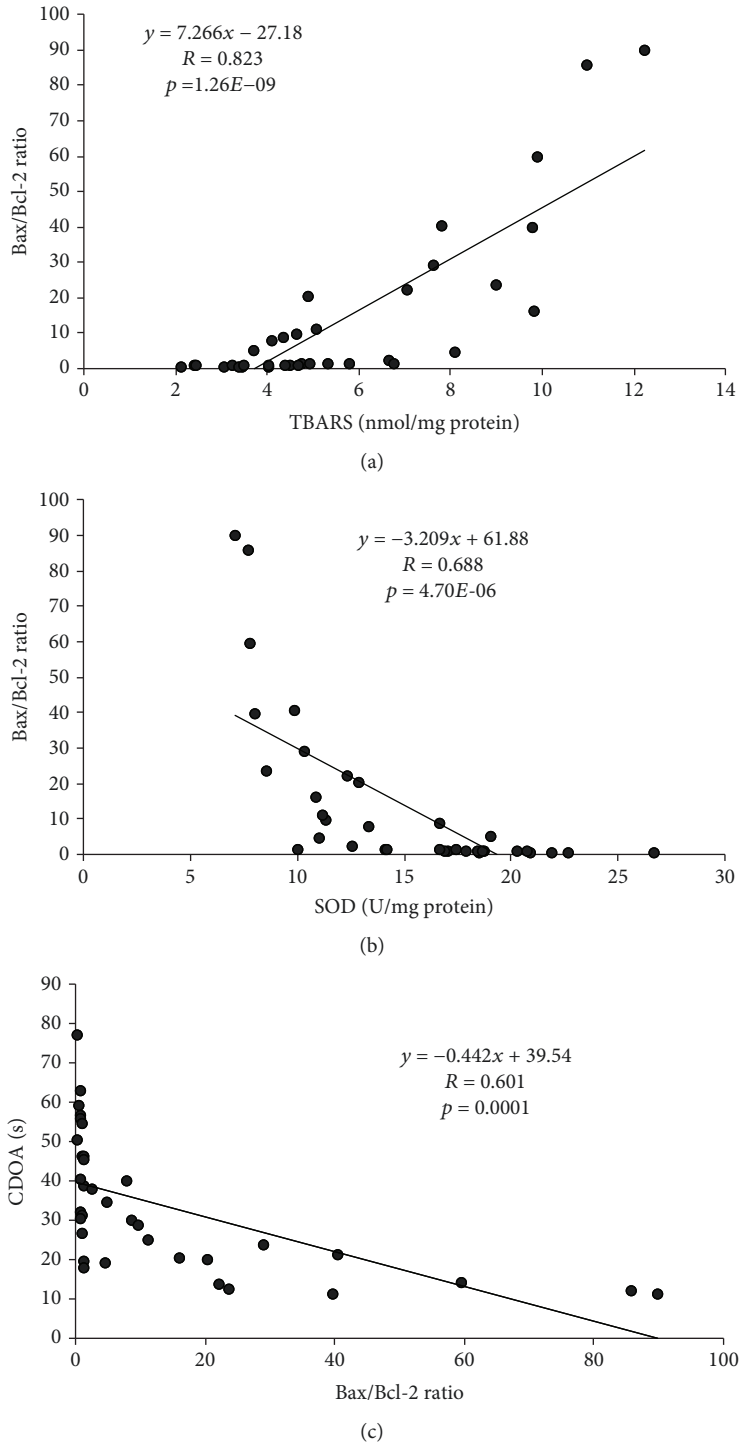

Figure 5: The relationship between (a) TBARS and Bax/Bcl-2 ratio, (b) SOD activity and Bax/Bcl-2 ratio, and (c) Bax/Bcl-2 ratio and CDOA in hippocampal tissue ($n = 35$).

may result in a decrease of hippocampal volume that, in turn, may be the principal cause of various mood disorders [43], including anxiety-like behavior.

Not surprisingly for the anticancer drug, cisplatin administration in this study exerted proapoptotic response (Figure 4). This action was manifested by both an increase in Bax and caspase-3 relative gene expression and a decline in Bcl-2 hippocampal expression. The significant alterations in apoptotic gene relative expression in the hippocampus were confirmed by a typical proapoptotic shift in the gene expression ratio, as the intracellular ratio of Bax and Bcl-2 stems from their antagonistic action in apoptosis control and describes the ability of a cell to respond to an apoptotic signal [44, 45]. A similar response to single cisplatin

application was reported by Manohar and coworkers [8]. That comprehensive study offered excellent insight in the individual proapoptotic gene expression pattern in a rat hippocampus, showing that the whole proapoptotic set of genes (Bid, Bik, and Bok) was elevated following cisplatin, while the antiapoptotic capacity of hippocampal neurons, expressed as Bcl2a1 relative gene expression, was simultaneously significantly deprived along with the marker of cell proliferation (Ki67). The proapoptotic outcome provoked by cisplatin, as observed in our study, accompanied by the previously described oxidative damage in the hippocampus, may be considered as potential biological mechanisms involved in emotional impairment manifested by anxiety-like behavior [5, 6].

Previously, we demonstrated that *S. hortensis* methanol extract used in this study was rich in phenolic compounds, particularly in rosmarinic acid (24.9 mg/g of dry extract) [17]. Several phenolic acids, such as chlorogenic, caffeic, syringic, *p*-coumaric, sinapic, and isoferulic acids, were identified in lower concentrations, as well as a certain amount of flavonoids (quercetin, apigenin, luteolin, and naringenin) and their derivatives [17]. Rosmarinic acid is mostly known for its antioxidant features [46], but it has shown many biological activities including cytotoxicity, antimicrobial, antiviral, antidiabetic, anti-inflammatory, antiallergic, and immunomodulatory activities [47–50]. In previous investigations, rosmarinic acid showed significant alleviation of oxidative stress and anti-inflammatory potential *in vivo* [47]. Especially important were antioxidant properties of rosmarinic acid during *in vivo* cisplatin treatment [48, 51]. Domitrović and coworkers proposed that protective effects of rosmarinic acid against CP-induced nephrotoxicity included reducing the levels of oxidative stress markers where rosmarinic acid decreased lipid peroxidation, 4-HNE, CYP2E1, and HO-1 immunoreactivity [48]. Also, this phenolic acid had an influence on inflammatory response in kidneys by lowering the expression of NF-κB p65 and TNF-α and reducing the parameters of apoptotic cell death (expression of p53 and p-p53) compared to the cisplatin treatment. A study of Lee and coworkers showed that rosmarinic acid was able to protect human dopaminergic neuronal cells against H_2O_2-induced oxidative stress by regulating the apoptotic process and suggested that this compound may be used in the prevention of neurodegenerative diseases [52]. Also, rosmarinic acid showed neuroprotective properties against H_2O_2-induced oxidative damage in astrocytes [53].

The restoration of equilibrium in the level of intrinsic antioxidant defense armory in tissue in cisplatin-treated rats after oral treatment with summer savory extract has been proposed as a dominant ameliorating mechanism [17]. The extract of *S. hortensis* in this study was able, not surprisingly, to reduce oxidative stress and apoptotic gene relative expression in the hippocampal tissue of experimental animals. Therefore, the neuroprotective effects of summer savory may be related to the presence of a high amount of rosmarinic acid in the extract [17]. Moreover, other phenolic compounds detected in *S. hortensis* showed significant *in vivo* antioxidant potential during the treatment with cisplatin. For example, quercetin [54] and naringenin [55] reduced cisplatin-induced nephrotoxicity while luteolin inhibited the accumulation of platinum, inflammation, and apoptosis in renal tissues during treatment with cisplatin [56].

Accompanying oxidative stress, mitochondrial damage and induced cell death may be involved in neurological disorders and neural dysfunction [57]. In our study, a single application of cisplatin increased the expression of proapoptotic Bax gene in the hippocampus, in response to the increased level of ROS. Additionally, cisplatin downregulated the antiapoptotic Bcl-2 gene, which is in line with previous studies [8]. Oral administration of *S. hortensis* extract (100 mg/kg/d), as well as silymarin, significantly changed the balance between Bcl-2 and Bax expression, indicating that the apoptosis in the hippocampus was inhibited by the application of the extract. Our results were in accordance with another research, which demonstrated that *S. hortensis* extract controlled apoptosis in H_2O_2-challenged Jurkat cells [18]. Considering the positive correlation observed between the Bax/Bcl-2 ratio and TBARS level, it could be concluded that the main denominator of the apoptotic pathway may be lipid peroxidation, which is the main factor in disturbance of cellular integrity.

The plants from genus *Satureja* (Lamiaceae) are known for their various pharmacological activities, including antioxidant, anti-inflammatory, immunostimulant, hepatoprotective, and anticancer properties [16, 58], but the studies regarding the behavioral effects of *Satureja* species have not been reported so far. In this study, for the first time, it was shown that the *Satureja* species may also have an influence on the reduction of cisplatin-induced neurotoxicity. The effects of *S. hortensis* extract on the regulation of oxidative stress and proapoptotic factors in the hippocampal tissue were comparable to silymarin. When applied in the same doses, both exhibited very similar effects on these parameters. Silymarin, as a standardized herbal preparation known for its antioxidant effects, was able to reduce the toxic effects caused by many xenobiotics, including drug-induced toxicity [59]. The protective effects of silymarin on cisplatin-induced ototoxicity [60], as well as liver, kidney, and testicular toxicities, have been reported so far [17].

In summary, anxiogenic action of cisplatin, accompanied with increased oxidative stress and proapoptotic manifestations in the hippocampus, can be attenuated by antioxidant supplementation with a simultaneous diminishing of oxidative damage and enhanced antiapoptotic capacity in rats, suggesting a potential beneficial role of antioxidant-rich natural products in the treatment of cisplatin-induced neurotoxicity patterns.

Data Availability

The data used to support the findings of this study are available from the corresponding author upon request.

Conflicts of Interest

The authors declare that there is no conflict of interest regarding the publication of this article.

Authors' Contributions

Authors Igor Kumburovic and Dragica Selakovic contributed equally to this study.

Acknowledgments

This work was supported by the Faculty of Medical Sciences, University of Kragujevac, Serbia (JP 06/18), and the Ministry of Education, Science and Technological Development of the Republic of Serbia (project No. III43004).

Supplementary Materials

Supplement 1: RT-PCR primers used in this study. *(Supplementary Materials)*

References

[1] W. Hassan, C. Barroso Silva, I. U. Mohammadzai, J. Teixeira da Rocha, and J. Landeira-Fernandez, "Association of oxidative stress to the genesis of anxiety: implications for possible therapeutic interventions," *Current Neuropharmacology*, vol. 12, no. 2, pp. 120–139, 2014.

[2] M. I. Turan, A. Cayir, N. Cetin, H. Suleyman, I. S. Turan, and H. Tan, "An investigation of the effect of thiamine pyrophosphate on cisplatin-induced oxidative stress and DNA damage in rat brain tissue compared with thiamine: thiamine and thiamine pyrophosphate effects on cisplatin neurotoxicity," *Human & Experimental Toxicology*, vol. 33, no. 1, pp. 14–21, 2014.

[3] D. Aydin, E. G. G. Peker, M. D. Karakurt et al., "Effects of Ginkgo biloba extract on brain oxidative condition after cisplatin exposure," *Clinical and Investigative Medicine*, vol. 39, no. 6, 2016.

[4] O. Kanat, H. Ertas, and B. Caner, "Platinum-induced neurotoxicity: a review of possible mechanisms," *World Journal of Clinical Oncology*, vol. 8, no. 4, pp. 329–335, 2017.

[5] M. Shabani, M. Nazeri, S. Parsania et al., "Walnut consumption protects rats against cisplatin-induced neurotoxicity," *NeuroToxicology*, vol. 33, no. 5, pp. 1314–1321, 2012.

[6] L. Troy, K. McFarland, S. Littman-Power et al., "Cisplatin-based therapy: a neurological and neuropsychological review," *Psychooncology*, vol. 9, no. 1, pp. 29–39, 2000.

[7] A. Jangra, M. Kwatra, T. Singh et al., "Edaravone alleviates cisplatin-induced neurobehavioral deficits via modulation of oxidative stress and inflammatory mediators in the rat hippocampus," *European Journal of Pharmacology*, vol. 791, pp. 51–61, 2016.

[8] S. Manohar, S. Jamesdaniel, and R. Salvi, "Cisplatin inhibits hippocampal cell proliferation and alters the expression of apoptotic genes," *Neurotoxicity Research*, vol. 25, no. 4, pp. 369–380, 2014.

[9] M. K. Parvez, "Natural or plant products for the treatment of neurological disorders: current knowledge," *Current Drug Metabolism*, vol. 19, no. 5, pp. 424–428, 2018.

[10] R. Hamidpour, S. Hamidpour, M. Hamidpour, M. Shahlari, and M. Sohraby, "Summer savory: from the selection of traditional applications to the novel effect in relief, prevention, and treatment of a number of serious illnesses such as diabetes, cardiovascular disease, Alzheimer's disease, and cancer," *Journal of Traditional and Complementary Medicine*, vol. 4, no. 3, pp. 140–144, 2014.

[11] P. N. Ravindran, G. S. Pillai, and M. Divakaran, "Other herbs and spices: mango ginger to wasabi," in *Handbook of Herbs and Spices*, K. V. Peter, Ed., pp. 557–582, Woodhead Publishing Series in Food Science, Technology and Nutrition, 2012.

[12] V. Hajhashemi, H. Sadraei, A. R. Ghannadi, and M. Mohseni, "Antispasmodic and anti-diarrhoeal effect of *Satureja hortensis* L. essential oil," *Journal of Ethnopharmacology*, vol. 71, no. 1-2, pp. 187–192, 2000.

[13] S. Mohtashami, V. Rowshan, L. Tabrizi, M. Babalar, and A. Ghani, "Summer savory (*Satureja hortensis* L.) essential oil constituent oscillation at different storage conditions," *Industrial Crops and Products*, vol. 111, pp. 226–231, 2018.

[14] P. Mašković, V. Veličković, M. Mitić et al., "Summer savory extracts prepared by novel extraction methods resulted in enhanced biological activity," *Industrial Crops and Products*, vol. 109, pp. 875–881, 2017.

[15] I. Fierascu, C. E. Dinu-Pirvu, R. C. Fierascu et al., "Phytochemical profile and biological activities of *Satureja hortensis* L.: a review of the last decade," *Molecules*, vol. 23, no. 10, p. 2458, 2018.

[16] B. Tepe and M. Cilkiz, "A pharmacological and phytochemical overview on *Satureja*," *Pharmaceutical Biology*, vol. 54, no. 3, pp. 375–412, 2015.

[17] T. Boroja, J. Katanić, G. Rosić et al., "Summer savory (*Satureja hortensis* L.) extract: phytochemical profile and modulation of cisplatin-induced liver, renal and testicular toxicity," *Food and Chemical Toxicology*, vol. 118, pp. 252–263, 2018.

[18] I. Chkhikvishvili, T. Sanikidze, N. Gogia et al., "Rosmarinic acid-rich extracts of summer savory (*Satureja hortensis*L.) protect Jurkat T cells against oxidative stress," *Oxidative Medicine and Cellular Longevity*, vol. 2013, Article ID 456253, 9 pages, 2013.

[19] H. Takeda, M. Tsuji, M. Inazu, T. Egashira, and T. Matsumiya, "Rosmarinic acid and caffeic acid produce antidepressive-like effect in the forced swimming test in mice," *European Journal of Pharmacology*, vol. 449, no. 3, pp. 261–267, 2002.

[20] J. Joksimovic, D. Selakovic, N. Jovicic et al., "Exercise attenuates anabolic steroids-induced anxiety via hippocampal NPY and MC4 receptor in rats," *Frontiers in Neuroscience*, vol. 13, p. 172, 2019.

[21] B. RF Jr. and S. IW, "A spectrophotometric method for measuring the breakdown of hydrogen peroxide by catalase," *Journal of Biological Chemistry*, vol. 195, no. 1, pp. 133–140, 1952.

[22] H. P. Misra and I. Fridovich, "The role of superoxide anion in the autoxidation of epinephrine and a simple assay for superoxide dismutase," *The Journal of Biological Chemistry*, vol. 247, pp. 3170–3175, 1972.

[23] G. L. Ellman, "Tissue sulfhydryl groups," *Archives of Biochemistry and Biophysics*, vol. 82, no. 1, pp. 70–77, 1959.

[24] H. Ohkawa, N. Ohishi, and K. Yagi, "Assay for lipid peroxides in animal tissues by thiobarbituric acid reaction," *Analytical Biochemistry*, vol. 95, no. 2, pp. 351–358, 1979.

[25] L. OH, R. NJ, F. AL, and R. RJ, "Protein measurement with Folin phenol reagent," *Journal of Biological Chemistry*, vol. 193, pp. 265–275, 1951.

[26] K. J. Livak and T. D. Schmittgen, "Analysis of relative gene expression data using real-time quantitative PCR and the $2^{-\Delta\Delta C}{}_{T}$ method," *Methods*, vol. 25, no. 4, pp. 402–408, 2001.

[27] S. Jacobs, C. L. McCully, R. F. Murphy, J. Bacher, F. M. Balis, and E. Fox, "Extracellular fluid concentrations of cisplatin, carboplatin, and oxaliplatin in brain, muscle, and blood measured using microdialysis in nonhuman primates," *Cancer Chemotherapy and Pharmacology*, vol. 65, no. 5, pp. 817–824, 2010.

[28] S. Kaasa, B. T. Olsnes, E. Thorud, and H. Høst, "Reduced short-term neuropsychological performance in patients with nonsmall-cell lung cancer treated with cisplatin and etoposide1," *Antibiotics and Chemotherapy*, vol. 41, pp. 226–231, 1988.

[29] C. C. P. Verstappen, J. J. Heimans, K. Hoekman, and T. J. Postma, "Neurotoxic complications of chemotherapy in patients with cancer: clinical signs and optimal management," *Drugs*, vol. 63, no. 15, pp. 1549–1563, 2003.

[30] N. Lomeli, K. Di, J. Czerniawski, J. F. Guzowski, and D. A. Bota, "Cisplatin-induced mitochondrial dysfunction is associated with impaired cognitive function in rats," *Free Radical Biology and Medicine*, vol. 102, pp. 274–286, 2017.

[31] N. F. Abdelkader, M. A. Saad, and R. M. Abdelsalam, "Neuroprotective effect of nebivolol against cisplatin-associated depressive-like behavior in rats," *Journal of Neurochemistry*, vol. 141, no. 3, pp. 449–460, 2017.

[32] M. Pantic and M. Minic, "The evaluation of the effects of N-acetylcysteine on cisplatin-induced alterations in exploratory activity in elevated plus maze test in rats," *Serbian Journal of Experimental and Clinical Research*, vol. 20, no. 1, pp. 65–72, 2017.

[33] A. Ennaceur, "Tests of unconditioned anxiety - pitfalls and disappointments," *Physiology & Behavior*, vol. 135, pp. 55–71, 2014.

[34] Y. Liu, N. Hamaue, T. Endo, M. Hirafuji, and M. Minami, "5-Hydroxytryptamine (5-HT) concentrations in the hippocampus, the hypothalamus and the medulla oblongata related to cisplatin-induced pica of rats," *Research Communications in Molecular Pathology and Pharmacology*, vol. 113–114, pp. 97–113, 2003.

[35] J. Dietrich, R. Han, Y. Yang, M. Mayer-Proschel, and M. Noble, "CNS progenitor cells and oligodendrocytesare targets of chemotherapeutic agents *in vitro* and *in vivo*," *Journal of Biology*, vol. 5, no. 7, p. 22, 2006.

[36] S. E. James, H. Burden, R. Burgess et al., "Anti-cancer drug induced neurotoxicity and identification of Rho pathway signaling modulators as potential neuroprotectants," *Neurotoxicology*, vol. 29, no. 4, pp. 605–612, 2008.

[37] D. Kong, L. Zhuo, C. Gao et al., "Erythropoietin protects against cisplatin-induced nephrotoxicity by attenuating endoplasmic reticulum stress-induced apoptosis," *Journal of Nephrology*, vol. 26, no. 1, pp. 219–227, 2013.

[38] Y. I. Chirino and J. Pedraza-Chaverri, "Role of oxidative and nitrosative stress in cisplatin-induced nephrotoxicity," *Experimental and Toxicologic Pathology*, vol. 61, no. 3, pp. 223–242, 2009.

[39] K. P. Kang, D. H. Kim, Y. J. Jung et al., "Alpha-lipoic acid attenuates cisplatin-induced acute kidney injury in mice by suppressing renal inflammation," *Nephrology Dialysis Transplantation*, vol. 24, no. 10, pp. 3012–3020, 2009.

[40] M. R. Vargas, D. A. Johnson, D. W. Sirkis, A. Messing, and J. A. Johnson, "Nrf2 activation in astrocytes protects against neurodegeneration in mouse models of familial amyotrophic lateral sclerosis," *Journal of Neuroscience*, vol. 28, no. 50, pp. 13574–13581, 2008.

[41] W. F. Wang, S. L. Wu, Y. M. Liou, A. L. Wang, C. R. Pawlak, and Y. J. Ho, "MPTP lesion causes neuroinflammation and deficits in object recognition in Wistar rats," *Behavioral Neuroscience*, vol. 123, no. 6, pp. 1261–1270, 2009.

[42] K. Sulakhiya, G. P. Keshavlal, B. B. Bezbaruah et al., "Lipopolysaccharide induced anxiety- and depressive-like behaviour in mice are prevented by chronic pre-treatment of esculetin," *Neuroscience Letters*, vol. 611, pp. 106–111, 2016.

[43] A. J. Eisch, "Adult neurogenesis: implications for psychiatry," *Progress in Brain Research*, vol. 138, pp. 315–342, 2002.

[44] Z. N. Oltval, C. L. Milliman, and S. J. Korsmeyer, "Bcl-2 heterodimerizes in vivo with a conserved homolog, Bax, that accelerates programed cell death," *Cell*, vol. 74, no. 4, pp. 609–619, 1993.

[45] E. Yang and S. J. Korsmeyer, "Molecular thanatopsis: a discourse on the BCL2 family and cell death," *Blood*, vol. 88, no. 2, pp. 386–401, 1996.

[46] A. G. Adomako-Bonsu, S. L. F. Chan, M. Pratten, and J. R. Fry, "Antioxidant activity of rosmarinic acid and its principal metabolites in chemical and cellular systems: importance of physico-chemical characteristics," *Toxicology in Vitro*, vol. 40, pp. 248–255, 2017.

[47] M. Alagawany, M. E. Abd el-Hack, M. R. Farag et al., "Rosmarinic acid: modes of action, medicinal values and health benefits," *Animal Health Research Reviews*, vol. 18, no. 2, pp. 167–176, 2017.

[48] R. Domitrović, I. Potočnjak, Ž. Crnčević-Orlić, and M. Škoda, "Nephroprotective activities of rosmarinic acid against cisplatin-induced kidney injury in mice," *Food and Chemical Toxicology*, vol. 66, pp. 321–328, 2014.

[49] R. Iswandana, B. T. Pham, W. T. van Haaften et al., "Organ- and species-specific biological activity of rosmarinic acid," *Toxicology in Vitro*, vol. 32, pp. 261–268, 2016.

[50] Y. L. Ngo, C. H. Lau, and L. S. Chua, "Review on rosmarinic acid extraction, fractionation and its anti-diabetic potential," *Food and Chemical Toxicology*, vol. 121, pp. 687–700, 2018.

[51] M. Tavafi and H. Ahmadvand, "Effect of rosmarinic acid on inhibition of gentamicin induced nephrotoxicity in rats," *Tissue and Cell*, vol. 43, no. 6, pp. 392–397, 2011.

[52] H. J. Lee, H. S. Cho, E. Park et al., "Rosmarinic acid protects human dopaminergic neuronal cells against hydrogen peroxide-induced apoptosis," *Toxicology*, vol. 250, no. 2-3, pp. 109–115, 2008.

[53] P. Costa, B. Sarmento, S. Gonçalves, and A. Romano, "Protective effects of Lavandula viridis L'Hér extracts and rosmarinic acid against H2O2-induced oxidative damage in A172 human astrocyte cell line," *Industrial Crops and Products*, vol. 50, pp. 361–365, 2013.

[54] P. D. Sanchez-Gonzalez, F. J. Lopez-Hernandez, F. Perez-Barriocanal, A. I. Morales, and J. M. Lopez-Novoa, "Quercetin reduces cisplatin nephrotoxicity in rats without compromising its anti-tumour activity," *Nephrology Dialysis Transplantation*, vol. 26, no. 11, pp. 3484–3495, 2011.

[55] O. A. Badary, S. Abdel-Maksoud, W. A. Ahmed, and G. H. Owieda, "Naringenin attenuates cisplatin nephrotoxicity in rats," *Life Sciences*, vol. 76, no. 18, pp. 2125–2135, 2005.

[56] R. Domitrović, O. Cvijanović, E. P. Pugel, G. B. Zagorac, H. Mahmutefendić, and M. Škoda, "Luteolin ameliorates

cisplatin-induced nephrotoxicity in mice through inhibition of platinum accumulation, inflammation and apoptosis in the kidney," *Toxicology*, vol. 310, pp. 115–123, 2013.

[57] M. P. Mattson, "Apoptosis in neurodegenerative disorders," *Nature Reviews Molecular Cell Biology*, vol. 1, no. 2, pp. 120–130, 2000.

[58] F. Jafari, F. Ghavidel, and M. M. Zarshenas, "A critical overview on the pharmacological and clinical aspects of popular Satureja species," *Journal of Acupuncture and Meridian Studies*, vol. 9, no. 3, pp. 118–127, 2016.

[59] J.-W. Wu, L.-C. Lin, and T.-H. Tsai, "Drug–drug interactions of silymarin on the perspective of pharmacokinetics," *Journal of Ethnopharmacology*, vol. 121, no. 2, pp. 185–193, 2009.

[60] S. I. Cho, J. E. Lee, and N. Y. Do, "Protective effect of silymarin against cisplatin-induced ototoxicity," *International Journal of Pediatric Otorhinolaryngology*, vol. 78, no. 3, pp. 474–478, 2014.

Hindawi
Oxidative Medicine and Cellular Longevity
Volume 2019, Article ID 1615758, 9 pages
https://doi.org/10.1155/2019/1615758

Research Article

Cytotoxic Effects of *Artemisia annua* L. and Pure Artemisinin on the D-17 Canine Osteosarcoma Cell Line

Gloria Isani,[1] **Martina Bertocchi**,[1] **Giulia Andreani**,[1] **Giovanna Farruggia**,[2] **Concettina Cappadone**,[2] **Roberta Salaroli**,[1] **Monica Forni**,[1] **and Chiara Bernardini**[1]

[1]*Department of Veterinary Medical Sciences, University of Bologna, Ozzano Emilia, 40064 Bologna, Italy*
[2]*Department of Pharmacy and Biotechnology, University of Bologna, 40127 Bologna, Italy*

Correspondence should be addressed to Martina Bertocchi; martina.bertocchi3@unibo.it

Received 8 March 2019; Revised 21 May 2019; Accepted 13 June 2019; Published 4 July 2019

Guest Editor: Patrícia Rijo

Artemisia annua has been used for centuries in Traditional Chinese Medicine. Although used as an antimalarial drug, its active compound artemisinin and the semisynthetic derivatives have also been investigated for their anticancer properties, with interesting and promising results. The aims of this research were to evaluate (i) the cytotoxicity and the antiproliferative effect of pure artemisinin and a hydroalcoholic extract obtained from *A. annua* on the D-17 canine osteosarcoma cell line and (ii) the intracellular iron concentration and its correlation with the cytotoxic effects. Both artemisinin and hydroalcoholic extract induced a cytotoxic effect in a dose-dependent manner. Pure artemisinin caused an increase of cells in the S phase, whereas the hydroalcoholic extract induced an evident increase in the G_2/M phase. A significant decrease of iron concentration was measured in D-17 cells treated with pure artemisinin and hydroalcoholic extract compared to untreated cells. In conclusion, although preliminary, the data obtained in this study are indicative of a more potent cytotoxic activity of the hydroalcoholic extract than pure artemisinin, indicating a possible synergistic effect of the phytocomplex and a mechanism of action involving iron and possibly ferroptosis. Considering the similarities between human and canine osteosarcomas, progress in deepening knowledge and improving therapeutic protocols will probably be relevant for both species, in a model of reciprocal translational medicine.

1. Introduction

Since ancient time, *Artemisia annua* L. has been used as a medicinal plant for the treatment of several diseases in Traditional Chinese Medicine [1]. To date, the reputation of *A. annua* is linked to its antimalarial activity. In 2015, Youyou Tu was awarded the Nobel Prize for isolating the active molecule artemisinin from *A. annua*. Currently, artemisinin, its derivatives, and Artemisinin Combination Therapy (ACT) belong to the established standard treatments of malaria worldwide [2]. Over 600 phytochemicals have been identified as constituents of *A. annua*, but its phytochemistry is dominated by sesquiterpenoids, flavonoids, and coumarins, together with enzymes (such as β-galactosidase and β-glucosidase) and steroids (e.g., β-sitosterol and stigmasterol) [1]. However, *A. annua* is distinguished from the other 200 species of the *Artemisia* genus by the exclusive presence of artemisinin, the active compound present in dried leaves (WHO monograph) [3]. Artemisinin is a sesquiterpene trioxane lactone, which contains an endoperoxide bridge essential for its biological activity. The low amount of artemisinin extracted from the plant, its low hydro- and liposolubility, and its limited bioavailability can represent a serious limitation for the standardization and commercialization of the drug. In the last 30 years, several semisynthetic artemisinin derivatives were developed with different strategies, including genetic engineering [1, 4, 5]. Although developed as antimalarials, artemisinin and its semisynthetic derivatives have also been investigated for many other therapeutic properties, such as antiviral, antimicrobial, and anti-inflammatory activities [6]. However, since the late 1990s, anticancer properties of artemisinins have been well known and there has been a rapid increase of *in vitro* and *in vivo* studies, case reports, and clinical trials on the

antitumor properties of artemisinins [7]. The endoperoxide moiety is strategic for the bioactivity of artemisinin-type drugs. Its cleavage leads to reactive oxygen species (ROS) formation and induces oxidative stress. Furthermore, in the presence of ferrous iron or reduced heme, artemisinin can convert itself into cytotoxic carbon-centered radical, a highly potent alkylating agent, to induce direct oxidative damage to cancer cells [2, 7]. Indeed, it has been reported that artemisinins induce apoptosis and ferroptosis, reduce cell proliferation through cell cycle arrest, and inhibit angiogenesis and tissue invasion of the tumor, as well as cancer metastasis [2, 6, 7].

Spontaneously occurring osteosarcoma (OSA) in dogs has clinical presentation, biological behaviour, response to treatment, and disease progression similar to human OSA [8–10]. OSA is the most common primary malignancy of bone both in dogs and humans. It is significantly more prevalent in dogs, with an incidence rate 27 times higher in dogs than in people. OSA commonly occurs in old dogs (median age 7 years), while in humans is more common in adolescence (10- to 14-year-old age group) [8, 11]. The site of OSA development in children and dogs is strikingly similar, with a predilection for the weight-bearing region of long bones. Approximately 75% of canine OSA occurs in the appendicular skeleton, with the most common sites in the distal radius and proximal humerus. In human OSA, long bones are affected in up to 90% of cases, with the distal femur, proximal tibia, and the proximal humerus being the most common locations [9, 11]. Furthermore, mutations of specific genes involved in the etiopathogenesis of OSA are found in both species, including mutations in the tumor suppressor genes p53, RB1, and PTEN and alterations of the oncogenes MYC and MET [8]. However, therapeutic failures are recurrent in both dogs and humans and are mainly due to the development of multiple resistance and metastatic spread, making the development of new therapies essential.

Therefore, to provide new scientific evidence to support anticancer activity of *A. annua* L., the first purpose of the present research is to evaluate the cytotoxicity and the effects on the cell cycle of pure artemisinin and a hydroalcoholic extract obtained from *A. annua* on a canine osteosarcoma cell line (D-17). Considering the suggested crucial role of iron on artemisinin activity, the second aim was addressed to determine the intracellular iron concentration and its possible correlation with the observed effects.

2. Materials and Methods

2.1. Chemicals and Reagents. All reagents were obtained from Sigma Aldrich (St. Louis, MO, USA), if not otherwise specified, and were ultrapure grade, including 98% pure artemisinin (CAS number: 63968-64-9). Minimum Essential Media (MEM), heat-inactivated fetal bovine serum (FBS), and Dulbecco's phosphate-buffered saline (DPBS) were purchased from Gibco-Life Technologies (Carlsbad CA, USA). A commercial hydroalcoholic extract obtained from *A. annua* and composed of 65% ethanol, 20% of aerial parts, and water was used. This extract contained 2 mg artemisinin/ml (corresponding to 7 mM) as declared by the producer. All plastic supports were purchased from Falcon, Becton-Dickinson (Franklin Lakes, NJ, USA).

2.2. Cell Culture and Treatment. The canine osteosarcoma cell line (D-17) was purchased from the "Istituto Zooprofilattico Sperimentale della Lombardia e dell'Emilia Romagna—Sez. Brescia." Cells were cultured in Minimum Essential Media (MEM) added with 2 mM L-glutamine and FBS (5%) in a 5% CO_2 atmosphere at 37°C. The first seeding after thawing was always performed in T-75 tissue culture flasks (4×10^6 cells/flask), and subsequent experiments were conducted in T-25 flasks (cell cycle analysis and iron quantification) and in 96-well assay plates (cytotoxicity). Artemisinin was dissolved in DMSO to obtain a 50 mM stock solution then diluted in culture medium to obtain the required concentrations. Hydroalcoholic extract of *A. annua* was directly diluted in culture medium to obtain the required concentrations. For each treatment, the same concentration of the specific vehicle was used as control, DMSO for artemisinin and a solution of 65% ethanol for hydroalcoholic extract. Cells grown in culture medium (MEM + 5% FBS with 2 mM L-glutamine) without treatments were considered "untreated cells."

2.3. Cytotoxicity. 1.5×10^4 cells/well were seeded in a 96-well plate and exposed for 24 h to increasing concentration of pure artemisinin (50, 100, 250, 500, 750, 1000, and 2000 μM) or increasing doses of *A. annua* hydroalcoholic extract corresponding to artemisinin concentrations of 14, 35, 70, 140, 280, 420, and 700 μM, on the base of the declared concentration of 2 mg artemisinin/ml in hydroalcoholic extract. For each treatment, the same concentration of the specific vehicle was used as control, DMSO for artemisinin and a solution of 65% ethanol for hydroalcoholic extract. Cytotoxicity was measured using tetrazolium salt (*In Vitro* Toxicology Assay Kit, MTT-based). The formazan absorbance was measured at a wavelength of 570 nm, using Infinite® F50/Robotic Absorbance microplate readers, TECAN (Life Science). The background absorbance of multiwall plates at 690 nm was also measured and subtracted from the 570 nm measurements. The concentrations of artemisinin required for 50% inhibition of cell viability (IC_{50}) were calculated by Prism GraphPad software, and the IC_{50} values were used for subsequent experiments.

2.4. Cell Cycle Analysis. For the analysis of cell cycle in flow cytometry, after 24 h of treatment, aliquots of 1×10^6 cells in duplicate for each treatment and for the specific vehicle used as control (IC_{50} standard artemisinin, IC_{50} *A. annua* hydroalcoholic extract, the same concentration of DMSO for artemisinin and a solution of 65% ethanol for hydroalcoholic extract) were washed from growth medium by centrifuging at 240 x g for ten minutes. Then, the resulting pellet was resuspended in 1 ml of a solution containing 0.1% sodium citrate, 0.1% Nonidet, 10 μg/ml of RNAse, and 50 μg/mL of propidium iodide (final concentration 1×10^6 cells/ml). After 30 min at 37°C in the dark, the isolated nuclei were analysed by using a Bryte HS flow cytometer (Bio-Rad) equipped with a Xe/Hg lamp and a filter set to obtain an excitation at

488 nm. PI fluorescence was collected on a linear scale at 600 nm, and the DNA distribution was analysed by the ModFit software (Verity, USA). For microscopical evaluation, cells (7000 cells/well) were seeded on an eight-well chamber slide (BD Falcon, Franklin Lakes, NJ). After 24 h of treatment, cells were stained with Hoechst 33342 15 μg/ml for 30 minutes in a 5% CO_2 incubator at 37°C. After 3 washes in DPBS, cells were analysed using an Eclipse E600 epifluorescence microscope equipped with a Nikon digital camera and the ACT-2U software for image capturing (Nikon, Tokyo, Japan). Images were analysed by counting a minimum of 400 nuclei in order to evaluate the percentage of apoptotic ones.

2.5. Iron Quantification. For the iron determination, a Spectra AA-20 atomic absorption spectrometer (Varian) equipped with a GTA-96 graphite tube atomizer and the sample dispenser was used. The optimization of the analytical method was obtained following Tüzen [12] with minor changes. The graphite tubes employed were coated GTA tubes (Agilent Technologies, Germany), the hollow cathode lamp current was 7 mA, and measurements were performed at 248.3 nm resonance lines using a spectral slit width of 0.2 nm. During spectrophotometer readings, the internal argon flow rate in the partition graphite tubes was maintained at 300 ml/min and was interrupted in the atomization phase. Ramp and hold times for drying, pyrolysis, atomization, and cleaning temperatures were optimized to obtain maximum absorbance without significant background absorption; therefore, background correction was not necessary.

The calibration curve was obtained by diluting 1 mg/ml standard stock solution of iron (BDH Chemicals, Poole, England) with Milli-Q water to obtain working standards containing 0, 20, 40, and 60 ng/ml of iron and by plotting the absorbance at 248.3 nm against iron concentrations. The equation of the curve was $y = 0.0109x$, and the calculated regression coefficient (r) was 0.993. The method was validated with standard reference material (BDH Chemicals, Poole, England), and the accuracy of the method, calculated as the percentage of the certified value, resulted to 105%.

For the quantification of intracellular iron, cells were grown in a T-75 flask (4×10^6 cells) until confluence. Then, cells were treated with IC_{50} standard artemisinin and IC_{50} *A. annua* hydroalcoholic extract, for 24 h. For each treatment, the same concentration of the specific vehicle was used as control, DMSO for artemisinin and a solution of 65% ethanol for hydroalcoholic extract. After that, aliquots of 1×10^6 cells for each treatment were harvested, counted, and centrifuged at 800 x g for 10 min. The pellet was washed twice with DPBS and then resuspended in a solution of 1 M HNO_3 at a final concentration of 1×10^6 cells/ml, digested at room temperature until completely dissolved, and finally used for iron quantification as reported by Sargenti et al. [13]. The detection limit (LOD), defined as the concentration corresponding to 3 times the standard deviation of 6 blanks, was 0.8 ng/ml. Iron concentration is reported as ng Fe/1×10^6 cells.

2.6. Statistical Analysis. Data for MTT and iron were analysed with a one-way analysis of variance (ANOVA) followed by *post hoc* Dunnett's multiple comparison test. Data of the cell cycle were analysed with two-way analysis of variance (ANOVA) followed by the Bonferroni multiple comparisons. Differences of at least $p < 0.05$ were considered significant. Statistical analysis was carried out using Prism GraphPad software.

3. Results

3.1. Effect of Artemisia annua Hydroalcoholic Extract and Artemisinin on Cell Viability. The effect of artemisinin and *A. annua* hydroalcoholic extract was evaluated on D-17 cells by the MTT assay. Both artemisinin and hydroalcoholic extract induced a decrease of cell viability at all concentrations and exerted cytotoxic effect in a dose-dependent manner (Figures 1(a) and 1(b)). After 24 h, both products provoked an increased number of detached cells with round shape and condensation of cytoplasmic constituents, more evident in the presence of hydroalcoholic extract (Figures 1(d) and 1(e)). Data obtained from MTT analyses were elaborated to assess the concentration of artemisinin required for 50% inhibition of cell viability (IC_{50}): the values corresponded to 548 μM for the standard and 65 μM for the hydroalcoholic extract (Figures 1(a) and 1(b)).

3.2. Effect of Artemisia annua Hydroalcoholic Extract and Artemisinin on the Cell Cycle. The effect of *A. annua* hydroalcoholic extract and artemisinin on the D-17 cell cycle was evaluated by flow cytometry, and data were analysed with ModFit software. Untreated cells presented a typical cytogram of a diploid cell population (Figures 2(a) A and 2(d)). As shown in Figures 2(a) C and E and 2(d), significant changes in the D-17 cell cycle were determined in the presence of both pure artemisinin and hydroalcoholic extract. A significant decrease ($p < 0.0001$) of cells in the G_0/G_1 phase was observed after both treatments. Pure artemisinin caused a significant increase ($p < 0.01$) of cells in the S phase, while hydroalcoholic extract induced a significant ($p < 0.0001$) increase of cells in the G_2/M phase. The pattern of the DNA distribution revealed only in the samples treated with the hydroalcoholic extract a significant increase of a sub-G1 population. DNA fragments of very variable measures indicated the presence of debris, typical of a necrotic death rather than a tight sub-G1 peak suggestive of apoptosis. These results were also supported by the microscopic examination of the cells stained with the vital nuclear stain Hoechst 33342, where almost no fragmented nuclei, a distinct morphological mark of apoptosis, were detected (Figures 2(a) E and 2(c)). The vehicles, DMSO and ethanol 65%, did not significantly affect the cell cycle (Figures 2(a) B and D and 2(d)).

3.3. Effect of Artemisia annua Hydroalcoholic Extract and Artemisinin on Intracellular Iron. Iron concentrations in D-17 cells were reported in Figure 3. Intracellular mean iron concentration in untreated D-17 cells was 70 ± 22.9 ng/1×10^6 cells. Cells exposed to pure artemisinin and *A. annua*

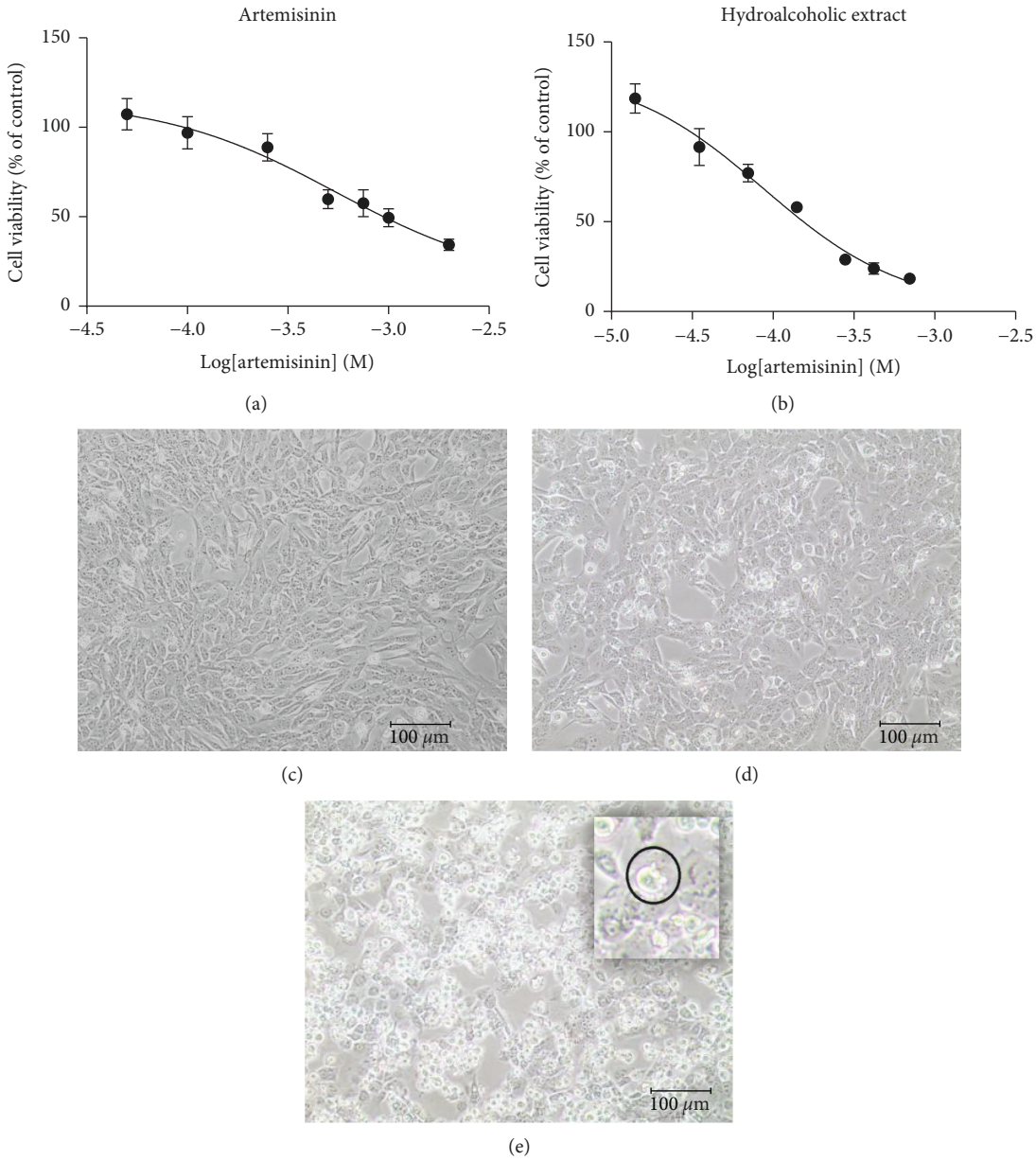

Figure 1: Effect of artemisinin and *A. annua* hydroalcoholic extract on D-17 cells. Dose-response curve: D-17 cell viability upon treatment with different concentrations of (a) pure artemisinin and (b) *A. annua* hydroalcoholic extract. For each treatment, the same concentration of the specific vehicle was used as the control, DMSO for artemisinin and a solution of 65% ethanol for hydroalcoholic extract. Representative images of D-17 cell morphology: (c) untreated cells and in the presence of (d) artemisinin and (e) hydroalcoholic extract, to note the extensive presence of cells with rounded morphology and condensation of cytoplasmic constituents. Dose-response curves are reported as the mean ± SD from two independent experiments ($n = 2$), each performed in sextuple.

hydroalcoholic extract had significantly lower concentrations of intracellular iron than the untreated cells ($p < 0.05$) (Figures 3(a) and 3(b)). The cells treated with the extract had a lower concentration of iron than those treated with pure artemisinin; this difference was not statistically significant. The intracellular iron concentration of cells exposed to the same concentration of the specific vehicle, DMSO for artemisinin and a solution of 65% ethanol for hydroalcoholic extract, was not statistically different from that of the untreated cells.

4. Discussion

Osteosarcoma (OSA) is the most common primary bone tumor in humans and in dogs and is characterized by locally aggressive and highly metastatic behaviour [8, 9]. The development of new drugs is necessary to improve the therapeutic outcome, in particular in the presence of multiple resistance and metastatic OSA. Therefore, the first aim of this study was to investigate the cytotoxic effect of artemisinin in comparison with a hydroalcoholic extract obtained from *A.*

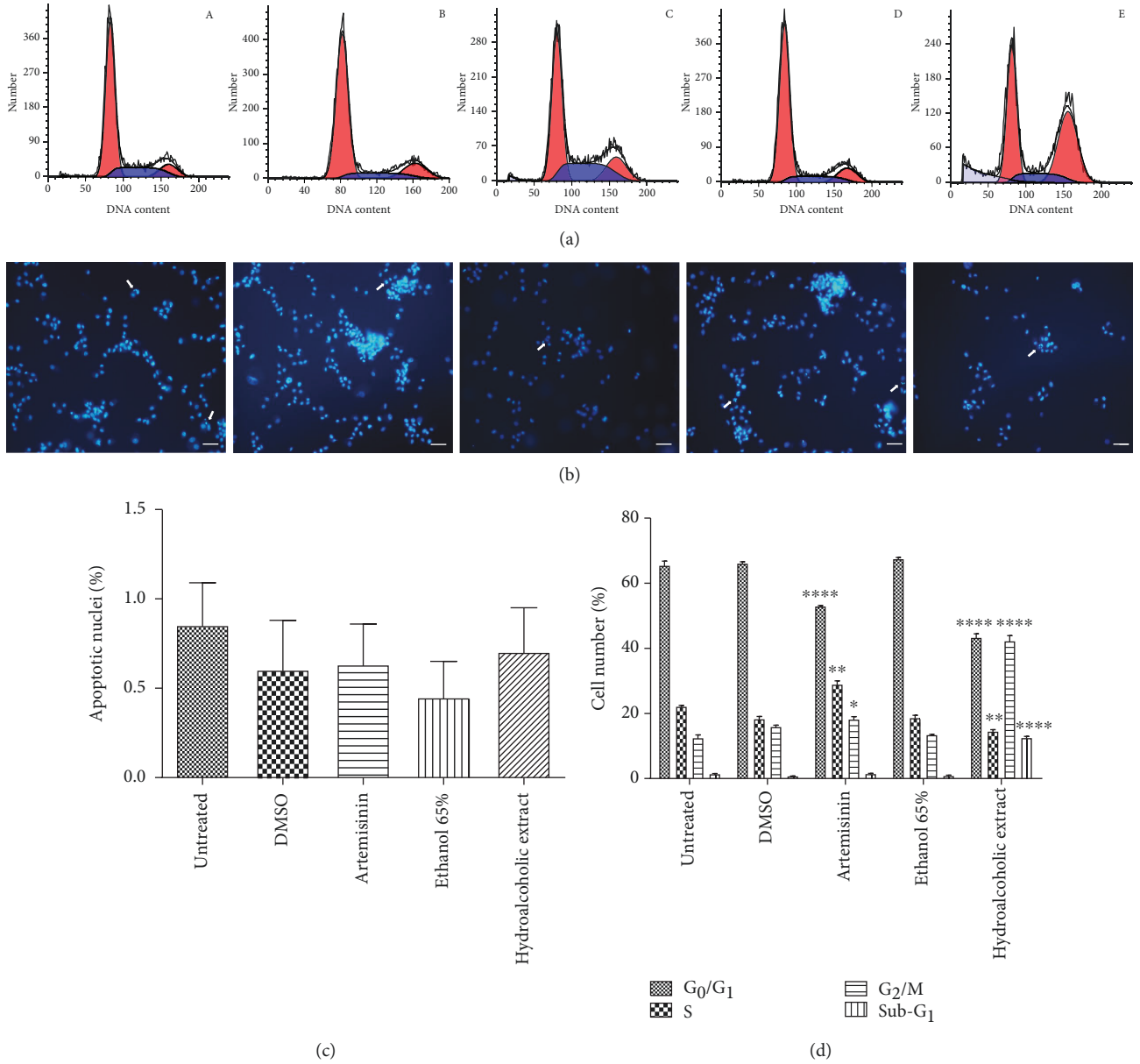

FIGURE 2: Representative image of cell cycle analysis (a) and nuclear staining with Hoechst 33342 (b) of D-17 cells after 24 hours of treatment: (A) untreated cells and in the presence of (B) DMSO, (C) 548 μM artemisinin, (D) a solution of 65% ethanol, and (E) hydroalcoholic extract corresponding to 65 μM artemisinin. (c) Percentage of apoptotic nuclei. (d) Cell cycle distribution. Data are reported as the mean ± SD ($n = 2$). Significant differences *vs.* untreated cells, comparing cell cycle phases (G_0/G_1, S, G_2/M, and Sub-G_1), are indicated by $^{*}p < 0.05$ and by $^{**}p < 0.01$ and $^{****}p < 0.0001$ (two-way ANOVA followed by the Bonferroni multiple comparisons). Arrows indicate apoptotic nuclei. Scale bar = 50 μm.

annua, on a canine osteosarcoma cell line (D-17). Our results demonstrated the cytotoxic effect of both artemisinin and hydroalcoholic extract in a dose-dependent manner. In particular, IC_{50} for artemisinin corresponded to 548 μM whilst for the hydroalcoholic extract the value was significantly lower (65 μM). For artemisinin, the obtained values are in the range of those reported in human tumor cell lines; in fact, Efferth et al. [14] reported a wide range of IC_{50} values of pure artemisinin for a panel of different human cell lines, from 57.1 μM for leukaemia cells to 1602 μM for HeLa cells. In 2014, Jirangkul et al. [15] reported IC_{50} values of pure artemisinin for two human osteosarcoma cell lines, MG63 and 148B, with IC_{50} of 167 μM and 178 μM, respectively. To our knowledge, only dihydroartemisinin (DHA) cytotoxicity was evaluated on canine OSA cell lines. In particular, Hosoya et al. [16] investigated the cytotoxic effect of DHA on four canine OSA cell lines, D-17, OSCA2, OSCA16, and OSCA50, reporting IC_{50} values of 8.7, 43.6, 16.8, and 14.8 μM, respectively.

In accordance with Efferth et al. [14], who reported in HeLa cells that *A. annua* extract is more cytotoxic than pure artemisinin, our results indicated an IC_{50} for the plant extract

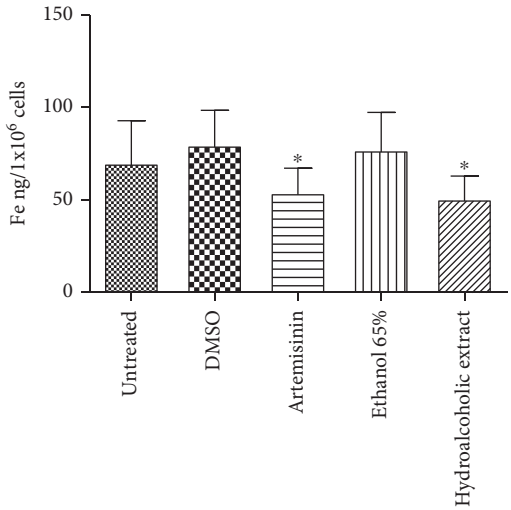

(a)

D-17	Fe ng/1x10^6 cells
Untreated	70.0 ± 22.9
DMSO	79.7 ± 18.7
Artemisinin	53.9 ± 13.2
Ethanol 65%	77.1 ± 20.3
Hydroalcoholic extract	50.5 ± 12.2

(b)

Figure 3: Iron intracellular concentration in D-17 cells measured by atomic absorption spectrometer. For each treatment, the same concentration of the specific vehicle was used as the control, DMSO for artemisinin and a solution of 65% ethanol for hydroalcoholic extract. Data are reported as the mean ± SD from three independent experiments ($n = 3$), each performed in quintuplicate. Significant differences *vs.* untreated cells are indicated by $*$ ($p < 0.05$ one-way ANOVA followed by post hoc Dunnett's multiple comparison test).

one order of magnitude lower than pure artemisinin. The same authors tested fourteen extracts of seven different *A. annua* preparations with different phytogeographical origins. They extracted plants in dichloromethane or methanol and evaluated the activity of the extracts on HeLa cells, obtaining IC_{50} values ranging from 54.1 to 275.5 μg/ml for dichloromethane extracts and from 276.3 to 1540.8 μg/ml for methanol extracts. A phytochemical investigation of the extracts by GLC-MS revealed the presence of artemisinin, arteanuine B, and scopoletin in all extracts, confirming *in vitro* the synergistic effect of the mixture of compounds that constitute the phytocomplex. Breuer and Efferth [17] in 2014 reported the successful use of *Herba A. annua Luparte®* as adjuvant therapy for veterinary sarcoma treatment. They found that this extract contained a high amount of scopoletin, while artemisinin represented just a minor component. Scopoletin could contribute to the anticancer activity of the phytoextract analysed in this study as suggested by other authors [18]. It has also been reported that an ethanolic extract from *Artemisia nilagirica* which does not contain artemisinin showed anticancer activity [19]. Therefore, it seems unlikely that the significantly higher cytotoxic effect of the hydroalcoholic extract is due to artemisinin only but more probably it is due to a synergistic effect of different molecules of the phytocomplex, which deserves more attention and careful characterization in future studies.

In the literature, heterogeneous results are reported on the action of artemisinin and its derivatives on the cell cycle arrest. It has been reported that artemisinin and its derivatives cause cell cycle arrest mainly in the G_0/G_1 phase through downregulation of cyclin E, cyclin D1, and cyclin-dependent kinases 2 and 4 in several tumor cell lines, including human breast cancer cells [20], gallbladder cancer cell lines [21], neuroblastoma [22], lung carcinoma cells (A549), and nonsmall lung cancer cells (H1299) [23]. In the D-17 canine osteosarcoma cell line, pure artemisinin slightly but significantly increased the number of cells in the S phase, and this has been observed also in EN2 tumor cells by Beekman et al. [24]. On the other hand, the hydroalcoholic extract caused a significant increase of D-17 cells at the G_2/M phase. Other authors found that artemisinin-derived drugs induced G_2/M cell cycle arrest. In particular, dihydroartemisinin induced G_2 arrest in the human osteosarcoma cell line [25], ovarian carcinoma cell line [26], and hepatocellular carcinoma cell line [27], while artesunate induced G_2 arrest in breast carcinoma cell lines [28], rat pituitary adenoma cell line [29], and kidney carcinoma cell lines [30]. However, the effects of a pure compound could be different from those induced from phytoextracts, whose complexity has to be considered [31]. *A. annua* extracts could contain several molecules, and their composition could be changed not only by the strategy of extraction but also by the time and the place where the plant is harvested [32, 33]. Kim et al. [34] evaluated the effect of an *A. annua* extract on human colon cancer cell line HCT116 and found that cell cycle arrest occurred at the G_1/S phase mediated by the Akt/mTOR pathway. Later on, they demonstrated that *A. annua* extract induced apoptosis through the regulation of specific proteins such as Bax, Bak, and cytochrome *c* in PDK1/Akt signaling pathways via a PTEN/p53-independent manner [35]. In this work, cell cycle analysis suggested that a modified cellular distribution in different phases of the cycle occurred in the treated cells and that the sub-G1 peak observed was due to cellular debris rather than fragmented DNA, which is typical of apoptosis. The differences in cell cycle phase arrest might be ascribed to the phytochemical complexity of the extract, in which the synergy of the different compounds could lead to alternative molecular

interactions hampering one pathway or another. More research is needed to unravel the complex mechanism underlying the effect of *A. annua* extract on the cell cycle.

Often tumor cells present an altered iron metabolism and higher iron intake than normal cells to deal with their enhanced metabolic demand, thus presenting an increased number of transferrin receptors [6, 36, 37]. Therefore, the determination of intracellular iron concentration is a prerequisite for any further analyses and can provide an important support to the involvement of this metal. In the present study, iron concentration determined in untreated D-17 cells falls within the range of those reported by other authors in different mammalian cells [38], though different preparation protocols, analytical methods, and measurement systems hampered in many cases a direct comparison of data. Following the incubation in the presence of pure artemisinin and *A. annua* extract, an alteration of iron metabolism in D-17 cells was determined, namely, a significant decrease of intracellular total iron. On the basis of previous papers, it is well known that, in the presence of ferrous ions, the leading event in the artemisinin-induced cytotoxic cascade is represented by the activation of the molecule by the cleavage of the endoperoxide bridge producing a carbon-centered radical able to induce intracellular oxidative damage [2, 7]. However, the link between the complex molecular machinery which regulates iron metabolism and the anticancer activity of artemisinin and *A. annua* extracts is far from being clarified. When analysing the effect of artemisinin on HeLa cancer cell proteome, Zhou et al. [39] identified as artemisinin targets 79 proteins involved mainly in membrane transport, protein trafficking, cell death and survival, and nucleic acid metabolism. The authors hypothesized that among these protein transferrin receptors, which are overexpressed in several tumor cells [36, 37], could be alkylated and subsequently inactivated by artemisinin, leading to a selective depletion of iron in cancer cells. The decrease of intracellular iron reported in the present research supports this hypothesis and shows additional evidence regarding the alteration of iron metabolism induced by artemisinin and *A. annua* extracts.

The ability of iron to gain and lose electrons makes this transition metal essential for life but also enables iron to participate in potentially deleterious reactions; therefore, the intracellular iron concentrations are finely regulated [40]. In particular, a controlled labile iron pool, e.g., a pool of loosely bound redox-active iron, is present within the cells and serves as a crossroad of intracellular iron metabolism [41]. In normal cells, this pool is maintained within a narrow range of concentrations, while in cancer cells, a reduction of ferritin iron storage can increase this labile iron pool and the risk of oxidative stress, which can ultimately determine the death of the cells [36]. The examination of D-17 cells did not show fragmented nuclei but revealed many dead cells with a clear rounded shape and a "ballooning" phenotype, in particular following the treatment with *A. annua* extract. This phenotype was recently reported as a hallmark of a novel mode of iron-dependent cell death, namely, ferroptosis [42]. Ferroptosis is a regulated cell death characterized by an increase of free intracellular iron followed by an iron-dependent accumulation of lipid hydroperoxides and a specific phenotype morphologically distinct from those associated with apoptosis and necrosis [43]. To date, different types of tumors have shown sensitivity to ferroptosis [44, 45]; however, the role of iron in this new type of cell death is far from being fully elucidated. In treated D-17 cells, it can be hypothesized that the low total intracellular iron, due to the alkylation of transferrin receptors, triggers the activation of ferritin degradation which can occur by either autophagic [46] or lysosomal degradation of the protein [47]. In turn, this event might contribute to increase the labile redox-active iron pool, determining a subsequent iron-driven lipid peroxidation and the activation of ferroptosis. Further analyses are needed to verify this challenging hypothesis.

5. Conclusions

Overall, the results reported in this research showed a more potent cytotoxic activity of the hydroalcoholic extract than pure artemisinin on the D-17 canine osteosarcoma cell line, indicating a possible synergistic effect of other bioactive molecules. These findings offer additional evidence on the biological activity of artemisinin and *A. annua* extract for their possible and safer therapeutic use. Moreover, they support the dog as a spontaneous animal model for the study of osteosarcoma. Despite the detection of intracellular total iron by a sensitive and specific technique that showed clear evidence of an alteration of iron metabolism, this paper is affected by limitations, namely, the lack of investigation about the expression of iron-related genes and ROS involvement in ferroptosis. Future researches should therefore be focused on these pivotal topics and on the role of the iron labile pool.

Data Availability

The data used to support the findings of this study are available from the corresponding author upon request.

Conflicts of Interest

The authors declare that there is no conflict of interest regarding the publication of this paper.

Acknowledgments

This study was supported by a grant from the University of Bologna (RFO) to GI, GA, and MF.

References

[1] G. D. Brown, "The biosynthesis of artemisinin (Qinghaosu) and the phytochemistry of *Artemisia annua* L. (Qinghao)," *Molecules*, vol. 15, no. 11, pp. 7603–7698, 2010.

[2] T. Efferth, "From ancient herb to modern drug: *Artemisia annua* and artemisinin for cancer therapy," *Seminars in Cancer Biology*, vol. 46, pp. 65–83, 2017.

[3] WHO, *Monograph on good agricultural and collection practices (GACP) for Artemisia annua L.*, WHO Press, World Health Organization, Geneva, Switzerland, 2006.

[4] Q. Sun, J. Wang, Y. Li et al., "Synthesis and evaluation of cytotoxic activities of artemisinin derivatives," *Chemical Biology & Drug Design*, vol. 90, no. 5, pp. 1019–1028, 2017.

[5] S. L. Badshah, A. Ullah, N. Ahmad, Z. M. Almarhoon, and Y. Mabkhot, "Increasing the Strength and Production of Artemisinin and Its Derivatives," *Molecules*, vol. 23, no. 1, p. 100, 2018.

[6] W. E. Ho, H. Y. Peh, T. K. Chan, and W. S. F. Wong, "Artemisinins: pharmacological actions beyond anti-malarial," *Pharmacology & Therapeutics*, vol. 142, no. 1, pp. 126–139, 2014.

[7] A. Bhaw-Luximon and D. Jhurry, "Artemisinin and its derivatives in cancer therapy: status of progress, mechanism of action, and future perspectives," *Cancer Chemotherapy and Pharmacology*, vol. 79, no. 3, pp. 451–466, 2017.

[8] H. L. Gardner, J. M. Fenger, and C. A. London, "Dogs as a model for cancer," *Annual Review of Animal Biosciences*, vol. 4, no. 1, pp. 199–222, 2016.

[9] J. M. Fenger, C. A. London, and W. C. Kisseberth, "Canine osteosarcoma: a naturally occurring disease to inform pediatric oncology," *ILAR Journal*, vol. 55, no. 1, pp. 69–85, 2014.

[10] S. S. Pinho, S. Carvalho, J. Cabral, C. A. Reis, and F. Gärtner, "Canine tumors: a spontaneous animal model of human carcinogenesis," *Translational Research*, vol. 159, no. 3, pp. 165–172, 2012.

[11] S. Simpson, M. D. Dunning, S. de Brot, L. Grau-Roma, N. P. Mongan, and C. S. Rutland, "Comparative review of human and canine osteosarcoma: morphology, epidemiology, prognosis, treatment and genetics," *Acta Veterinaria Scandinavica*, vol. 59, no. 1, pp. 71–71, 2017.

[12] M. Tüzen, "Determination of heavy metals in soil, mushroom and plant samples by atomic absorption spectrometry," *Microchemical Journal*, vol. 74, no. 3, pp. 289–297, 2003.

[13] A. Sargenti, G. Farruggia, E. Malucelli et al., "A novel fluorescent chemosensor allows the assessment of intracellular total magnesium in small samples," *Analyst*, vol. 139, no. 5, pp. 1201–1207, 2014.

[14] T. Efferth, F. Herrmann, A. Tahrani, and M. Wink, "Cytotoxic activity of secondary metabolites derived from *Artemisia annua* L. towards cancer cells in comparison to its designated active constituent artemisinin," *Phytomedicine*, vol. 18, no. 11, pp. 959–969, 2011.

[15] P. Jirangkul, P. Srisawat, T. Punyaratabandhu, T. Songpattanaslip, and M. Mungthin, "Cytotoxic effect of artemisinin and its derivatives on human osteosarcoma cell lines," *Journal of the Medical Association of Thailand*, vol. 97, pp. S215–S221, 2014.

[16] K. Hosoya, S. Murahari, A. Laio, C. A. London, C. G. Couto, and W. C. Kisseberth, "Biological activity of dihydroartemisinin in canine osteosarcoma cell lines," *American Journal of Veterinary Research*, vol. 69, no. 4, pp. 519–526, 2008.

[17] E. Breuer and T. Efferth, "Treatment of iron-loaded veterinary sarcoma by *Artemisia annua*," *Natural Products and Bioprospecting*, vol. 4, no. 2, pp. 113–118, 2014.

[18] X. Cai, J. Yang, J. Zhou et al., "Synthesis and biological evaluation of scopoletin derivatives," *Bioorganic & Medicinal Chemistry*, vol. 21, no. 1, pp. 84–92, 2013.

[19] N. Sahu, S. Meena, V. Shukla et al., "Extraction, fractionation and re-fractionation of *Artemisia nilagirica* for anticancer activity and HPLC-ESI-QTOF-MS/MS determination," *Journal of Ethnopharmacology*, vol. 213, pp. 72–80, 2018.

[20] A. S. Tin, S. N. Sundar, K. Q. Tran, A. H. Park, K. M. Poindexter, and G. L. Firestone, "Antiproliferative effects of artemisinin on human breast cancer cells requires the downregulated expression of the E2F1 transcription factor and loss of E2F1-target cell cycle genes," *Anti-Cancer Drugs*, vol. 23, no. 4, pp. 370–379, 2012.

[21] J. Jia, Y. Qin, L. Zhang et al., "Artemisinin inhibits gallbladder cancer cell lines through triggering cell cycle arrest and apoptosis," *Molecular Medicine Reports*, vol. 13, no. 5, pp. 4461–4468, 2016.

[22] S. Zhu, W. Liu, X. Ke et al., "Artemisinin reduces cell proliferation and induces apoptosis in neuroblastoma," *Oncology Reports*, vol. 32, no. 3, pp. 1094–1100, 2014.

[23] Y. Tong, Y. Liu, H. Zheng et al., "Artemisinin and Its derivatives can significantly inhibit lung tumorigenesis and tumor metastasis through Wnt/β-catenin signaling," *Oncotarget*, vol. 7, no. 21, pp. 31413–31428, 2016.

[24] A. C. Beekman, A. R. W. Barentsen, H. J. Woerdenbag et al., "Stereochemistry-dependent cytotoxicity of some artemisinin derivatives," *Journal of Natural Products*, vol. 60, no. 4, pp. 325–330, 1997.

[25] Y. Ji, Y. C. Zhang, L. B. Pei, L. L. Shi, J. L. Yan, and X. H. Ma, "Anti-tumor effects of dihydroartemisinin on human osteosarcoma," *Molecular and Cellular Biochemistry*, vol. 351, no. 1–2, pp. 99–108, 2011.

[26] Y. Jiao, C. M. Ge, Q. H. Meng, J. P. Cao, J. Tong, and S. J. Fan, "Dihydroartemisinin is an inhibitor of ovarian cancer cell growth," *Acta Pharmacologica Sinica*, vol. 28, no. 7, pp. 1045–1056, 2007.

[27] C. Z. Zhang, H. Zhang, J. Yun, G. G. Chen, and P. B. S. Lai, "Dihydroartemisinin exhibits antitumor activity toward hepatocellular carcinoma in vitro and in vivo," *Biochemical Pharmacology*, vol. 83, no. 9, pp. 1278–1289, 2012.

[28] K. Chen, L. M. Shou, F. Lin et al., "Artesunate induces G2/M cell cycle arrest through autophagy induction in breast cancer cells," *Anti-Cancer Drugs*, vol. 25, no. 6, pp. 652–662, 2014.

[29] Z. G. Mao, J. Zhou, H. Wang et al., "Artesunate inhibits cell proliferation and decreases growth hormone synthesis and secretion in GH3 cells," *Molecular Biology Reports*, vol. 39, no. 5, pp. 6227–6234, 2012.

[30] D. E. Jeong, H. J. Song, S. Lim et al., "Repurposing the antimalarial drug artesunate as a novel therapeutic agent for metastatic renal cell carcinoma due to its attenuation of tumor growth, metastasis, and angiogenesis," *Oncotarget*, vol. 6, no. 32, pp. 33046–33064, 2015.

[31] D. J. Rassias and P. J. Weathers, "Dried leaf *Artemisia annua* efficacy against non-small cell lung cancer," *Phytomedicine*, vol. 52, pp. 247–253, 2019.

[32] S. Iqbal, U. Younas, K. W. Chan, M. Zia-Ul-Haq, and M. Ismail, "Chemical composition of *Artemisia annua* L. leaves and antioxidant potential of extracts as a function of extraction solvents," *Molecules*, vol. 17, no. 5, pp. 6020–6032, 2012.

[33] T. Carbonara, R. Pascale, M. P. Argentieri et al., "Phytochemical analysis of a herbal tea from *Artemisia annua* L," *Journal of Pharmaceutical and Biomedical Analysis*, vol. 62, pp. 79–86, 2012.

[34] B. M. Kim, G. T. Kim, E. G. Lim et al., "Cell cycle arrest of extract from Artemisia annua Linné via Akt-mTOR signaling pathway in HCT116 colon cancer cells," *KSBB Journal*, vol. 30, no. 5, pp. 223–229, 2015.

[35] E. J. Kim, G. T. Kim, B. M. Kim, E. G. Lim, S. Y. Kim, and Y. M. Kim, "Apoptosis-induced effects of extract from *Artemisia annua* Linné by modulating PTEN/p53/PDK1/Akt/ signal pathways through PTEN/p53-independent manner in HCT116 colon cancer cells," *BMC Complementary and Alternative Medicine*, vol. 17, no. 1, p. 236, 2017.

[36] S. V. Torti and F. M. Torti, "Iron and cancer: more ore to be mined," *Nature Reviews. Cancer*, vol. 13, no. 5, pp. 342–355, 2013.

[37] A. Fanzani and M. Poli, "Iron, Oxidative Damage and Ferroptosis in Rhabdomyosarcoma," *International Journal of Molecular Sciences*, vol. 18, no. 8, p. 1718, 2017.

[38] G. Cerchiaro, T. M. Manieri, and F. R. Bertuchi, "Analytical methods for copper, zinc and iron quantification in mammalian cells," *Metallomics*, vol. 5, no. 10, pp. 1336–1345, 2013.

[39] Y. Zhou, W. Li, and Y. Xiao, "Profiling of multiple targets of artemisinin activated by hemin in cancer cell proteome," *ACS Chemical Biology*, vol. 11, no. 4, pp. 882–888, 2016.

[40] A. R. Bogdan, M. Miyazawa, K. Hashimoto, and Y. Tsuji, "Regulators of iron homeostasis: new players in metabolism, cell death, and disease," *Trends in Biochemical Sciences*, vol. 41, no. 3, pp. 274–286, 2016.

[41] O. Kakhlon and Z. I. Cabantchik, "The labile iron pool: characterization, measurement, and participation in cellular processes," *Free Radical Biology and Medicine*, vol. 33, no. 8, pp. 1037–1046, 2002.

[42] M. Dodson, R. Castro-Portuguez, and D. D. Zhang, "NRF2 plays a critical role in mitigating lipid peroxidation and ferroptosis," *Redox Biology*, p. 101107, 2019.

[43] S. J. Dixon, K. M. Lemberg, M. R. Lamprecht et al., "Ferroptosis: an iron-dependent form of nonapoptotic cell death," *Cell*, vol. 149, no. 5, pp. 1060–1072, 2012.

[44] B. Lu, X. B. Chen, M. D. Ying, Q. J. He, J. Cao, and B. Yang, "The role of ferroptosis in cancer development and treatment response," *Frontiers in Pharmacology*, vol. 8, p. 992, 2018.

[45] E. Ooko, M. E. M. Saeed, O. Kadioglu et al., "Artemisinin derivatives induce iron-dependent cell death (ferroptosis) in tumor cells," *Phytomedicine*, vol. 22, no. 11, pp. 1045–1054, 2015.

[46] G. O. Latunde-Dada, "Ferroptosis: role of lipid peroxidation, iron and ferritinophagy," *Biochimica et Biophysica Acta (BBA) - General Subjects*, vol. 1861, no. 8, pp. 1893–1900, 2017.

[47] G.-Q. Chen, F. A. Benthani, J. Wu, D. Liang, Z.-X. Bian, and X. Jiang, "Artemisinin compounds sensitize cancer cells to ferroptosis by regulating iron homeostasis," *Cell Death and Differentiation*, 2019.

Hindawi
Oxidative Medicine and Cellular Longevity
Volume 2019, Article ID 4750795, 14 pages
https://doi.org/10.1155/2019/4750795

Research Article

Biotransformation of Cranberry Proanthocyanidins to Probiotic Metabolites by *Lactobacillus rhamnosus* Enhances Their Anticancer Activity in HepG2 Cells *In Vitro*

H. P. Vasantha Rupasinghe,[1,2] **Indu Parmar**,[1] **and Sandhya V. Neir**[1]

[1]*Department of Plant, Food, and Environmental Sciences, Faculty of Agriculture, Dalhousie University, Truro, Nova Scotia, Canada*
[2]*Department of Pathology, Faculty of Medicine, Dalhousie University, Halifax, Nova Scotia, Canada*

Correspondence should be addressed to H. P. Vasantha Rupasinghe; vrupasinghe@dal.ca

Received 30 December 2018; Accepted 2 April 2019; Published 17 June 2019

Guest Editor: Milica Pesic

This study was designed to unravel the role of *Lactobacillus rhamnosus* in the bioconversion of cranberry proanthocyanidins and cytotoxicity of resulting metabolites to hepatocellular carcinoma HepG2 cells. Crude (CR) and flavonol+dihydrochalcone- (FL+DHC-), anthocyanin- (AN-), proanthocyanidin- (PR-), and phenolic acid+catechin- (PA+C-) rich fractions were subjected to fermentation with *L. rhamnosus* at 37°C for 12, 24, and 48 h under anaerobic conditions. The major metabolites produced by bioconversion of polyphenols were 4-hydroxyphenylacetic acid, 3-(4-hydroxyphenyl)propionic acid, hydrocinnamic acid, catechol, and pyrogallol. Furthermore, cytotoxicity of the biotransformed extracts was compared to their parent extracts using human hepatocellular carcinoma HepG2 cells. The results showed that PR-biotransformed extract completely inhibited HepG2 cell proliferation in a dose- and time-dependent manner with IC_{50} values of 47.8 and 20.1 μg/mL at 24 and 48 h, respectively. An insight into the molecular mechanisms involved revealed that the cytotoxic effects of PR at 24 h incubation were mitochondria-controlled and not by proapoptotic caspase-3/7 dependent. The present findings suggest that the application of a bioconversion process using probiotic bacteria can enhance the pharmacological activities of cranberry proanthocyanidins by generating additional biologically active metabolites.

1. Introduction

Primary liver cancer, also known as hepatocellular carcinoma (HCC), is the fifth common cancer and the third leading cause of cancer mortality in the world [1]. HCC is caused in a milieu of oxidative stress and inflammation, with its pathogenesis represented by the production of cytokines and chemokines, generation of free radicals, such as reactive oxygen and nitrogen species, viral infections, hepatitis, hepatic cirrhosis, and hepatocarcinogens. From the very few clinically relevant therapeutic options available of HCC, sorafenib (Nexavar™), a vascular endothelial growth factor receptor tyrosine-kinase inhibitor, is the only approved drug. However, clinical administration of sorafenib is challenged by the low survival rate and several adverse effects in patients including hematological toxicity [2]. Therefore, a need for alternative anticancer strategies holds importance for clinical and experimental oncology.

Plant polyphenols are known to possess strong antioxidant properties and have been shown to exhibit anti-inflammatory, antiproliferative, and proapoptotic properties, suggesting their role as chemopreventive agents [3]. However, the use of polymeric polyphenols such as proanthocyanidins is limited in chemoprevention because of their poor bioavailability in the human body. The bioavailability and physiological functions of proanthocyanidins are largely influenced by their molecular weight, structural complexity, digestibility, intestinal absorption, metabolism, and gut microbiota. Structural modification, nanoencapsulation, and biotransformation are some of the strategies to combat the issue of low bioavailability of polyphenols [4]. Biotransformation of polyphenol-rich foods can be

performed by incubating with microorganisms, especially probiotics which enable deglycosylation, ring fission, dehydroxylation, demethylation, lactonization, aromatic hydroxylation, reduction of carbon-carbon double bonds, or decarboxylation [5, 6], converting some polyphenols into more bioavailable and/or bioactive forms than their original forms [7].

Cranberry pomace is a by-product of the cranberry juice-processing industry, which is rich in numerous phenolic compounds with potential health benefits. Some of the major phenolics present in cranberry pomace include anthocyanins, proanthocyanidins, flavonols, phenolic acids, and flavan-3-ols [8]. Cranberry press cake-based flavonoid extract has been demonstrated to exhibit significant effects against various cancer cell lines including the prostate (LNCaP), melanoma (MDA-MB-435), malignant melanoma (SK-MEL-5), colon (HT-29), lung (DMS114), and brain (U87) [9]. Our recent investigation has shown that only small molecular weight phenolic acid-rich fractions were able to impart antiproliferation activity at low concentrations in human HCC cell line HepG2 as reflected from their IC_{50} values [8].

Lactobacillus species is one of the predominant members of the intestinal microflora, and some strains have been characterized as probiotics. Species of *Lactobacillus* possess β-glucosidase activity and participate in the hydrolysis of plant β-glycosides [10]. *Lactobacillus plantarum* has been shown to metabolize phenolic acids and esters of phenolic acids by the activities of tannase [11], feruloyl esterase [12], phenolic acid decarboxylase, and phenolic acid reductase [13]. These activities of Lactobacilli may contribute to the release of phenolic acids bound to insoluble cell wall material, particularly protocatechuic and *p*-hydroxybenzoic acids. However, little is known about flavonoid biotransformation by Lactobacilli and their resulting anticancer properties [6]. Herein, we investigated the capability of *L. rhamnosus* to biotransform five different polyphenol-rich fractions from cranberry pomace and explored their anticancer activity against HCC using HepG2 cells in comparison to sorafenib. In addition, their mechanistic approach to the cytotoxicity has also been presented through ATP depletion and caspase-3 activity.

2. Materials and Methods

2.1. Chemicals and Standards. The liquid chromatography standards used for the study were obtained as follows: quercetin-3-*O*-rhamnoside and quercetin-3-*O*-galactoside were from Indofine Chemical Co. (Hillsborough, NJ, USA); quercetin-3-*O*-rutinoside, (-)-epicatechin, (+)-catechin, epigallocatechin (EGC), epicatechin gallate (ECG), epigallocatechin gallate (EGCG), and procyanidin B1 and B2 were from ChromaDex (Santa Ana, CA, USA); and cyanidin-3-*O*-galactoside was obtained from Extrasynthese (Paris, France). High-performance liquid chromatography (HPLC) grade methanol, acetonitrile, and formic acid; quercetin-3-*O*-glucoside, quercetin, phloridzin, myricetin, and phenolic acids (caffeic acid, ferulic acid, gallic acid, protocatechuic acid, chlorogenic acid, *trans*-cinnamic acid, p-coumaric acid, isoferulic acid, *p*-hydroxybenzaldehyde, p-hydroxybenzoic acid, vanillic acid, and vanillin); syringic acid, gallic acid, homogentisic acid (2,5-dihydroxyphenylacetic acid), sinapic acid (3,5-dimethoxy-4-hydroxycinnamic acid), DMB propionic acid (3–20,50-dimethoxybenzoylpropionic acid), p-hydroxybenzaldehyde, p-hydroxybenzoic acid, vanillic acid, and vanillin; syringic acid (3,5-dimethoxy-4-hydroxybenzoic acid), homogentisic acid (2,5-dihydroxyphenylacetic acid), sinapic acid (3,5-dimethoxy-4-hydroxycinnamic acid), p-coumaric acid (trans-4-hydroxycinnamic acid), DMB propionic acid (3–20,50-dimethoxybenzoylpropionic acid), and dimethyl sulfoxide were obtained from Sigma-Aldrich (Mississauga, ON, Canada). The remaining chemicals were obtained from Fisher Scientific (Ottawa, ON, Canada).

2.2. Isolation of Bioactive Fractions from Cranberry Pomace. The cranberry pomace was collected from a commercial cranberry juice manufacturer (Cranberry Acres Farm, Aylesford, NS, Canada). Immediately after juice processing, the excess water was drained and within 3 h, the cranberry pomace was transported in plastic containers to the laboratory facility and stored in a freezer (-20°C). Five hundred grams of frozen cranberry pomace was ground with 2 L extraction solvent (70% acetone : 29.9% water : 0.1% acetic acid by $v:v:v$) using a Waring glass blender (Model CAC32, Fisher Scientific (Ottawa, ON, Canada) for 3 min. The slurry was then subjected to sonication for 30 min × 3 at 30°C with 10 min intervals in between every 15 cycles to avoid increase in temperature. The suspension was then passed through eight layers of cheesecloth followed by vacuum filtration using Fisherbrand P8 filters. The crude extract was then rendered solvent free using the rotary vacuum evaporation system (Rotavapor HR-200; Buchi, Flawil, Switzerland) at 37°C until completely dry. A representative sample was taken and named as crude (CR) extract. The concentrated extract was dissolved into 120 mL of 50% ethanol-water mixture.

Flash chromatography with a sorbent (Sorbent SP207-05 Sepabeads resin brominated styrenic adsorbent; particle size 250 mm, surface area 630 m^2/g; Sorbent Technologies, Atlanta, GA, USA) was used to fractionate the concentrated cranberry pomace extract as described above. A detailed diagram of the process is presented in Figure 1. The crude extract was loaded onto a chromatography column (3.86 × 45 cm, Sati International Scientific Inc., Dorval, QC, Canada) that contained 400 g of adsorbent and had been conditioned with deionized water and equilibrated in 50% ethanol-water mixture. After loading the extract, the column was immediately washed with water until the sugars were removed up to a Brix value of <0.1%, as measured by a digital hand-held refractometer. The phenolic compounds retained in the column were eluted using a step gradient of ethanol (1 L per elution). The phenolic acid, flavonol, flavan-3-ol, and anthocyanin-rich fractions were eluted with 20-100% ethanol with an increment of 5% ethanol per elution. Then, a step gradient of acetone (1 L per elution) was carried out to elute oligomeric and polymeric proanthocyanidin-rich fractions. These elutions were carried out using 20%, 30%, 50%, 60%, 70%, 80%, and 100% acetone, pooled together,

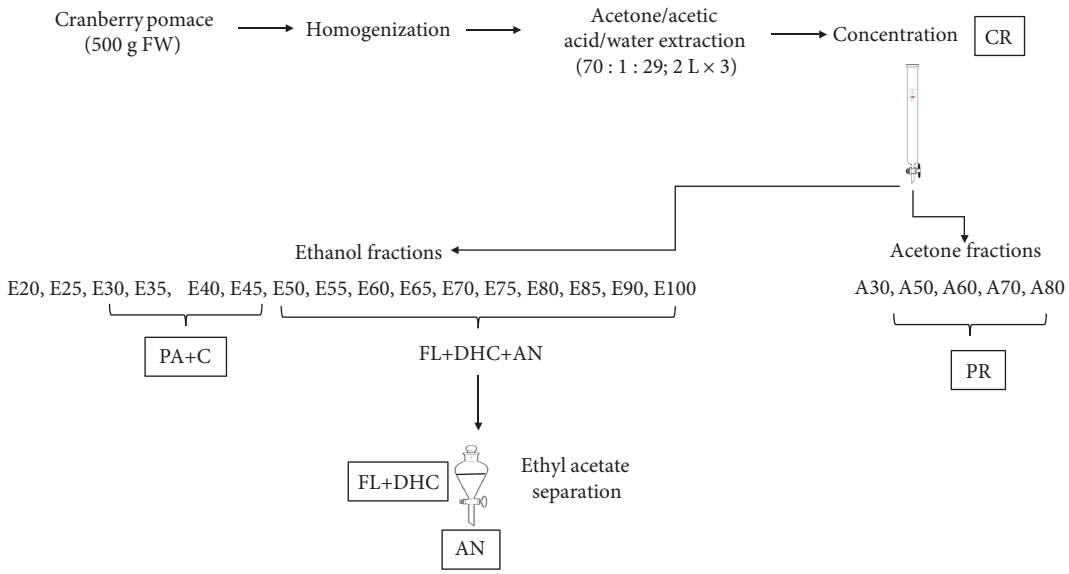

Figure 1: Process flow chart for extraction and fractionation of cranberry pomace (CP). PA: phenolic acids; DHC: hihydrochalcones; AN: anthocyanins; PR: proanthocyanidins; FL: flavonols.

and evaporated to a completely dry powder that was labeled as PR. The fractions rich in phenolic acids and catechins were combined and evaporated to produce PA+C extract. A liquid-liquid separation method using ethyl acetate and water was employed for the separation of anthocyanins (AN) from fractions rich in flavonols and dihydrochalcones (FL+DHC). Eluates were concentrated to completely dried extracts using a rotary evaporator at 40°C.

2.3. Bacterial Strain and Culture Conditions. A strain of *Lactobacillus rhamnosus* (ATCC 9595) was cultivated in De Man, Rogosa, and Sharpe broth (MRS; BD, Becton, Dickinson, and Co., Sparks, MD, USA) at 37°C for 24 h in anaerobic jars (Gas-Pack, AnaeroGen; Oxoid, Nepean, ON, Canada). Bacterial growth was carried out in triplicate wells of sterile 96-well microplates with a lid, containing 300 μL of MRS broth with or without different concentrations of extracts. Wells were inoculated (1%; about 10^7 colony-forming units/mL) with a fresh culture of the strain incubated in MRS broth at 37°C for 16 h. Appropriate controls were used by incubating noninoculated MRS broth, CP extracts (blank), and MRS broth inoculated with the strain (growth control). Incubations were carried out at 37°C for 48 h under shaking of 70 rpm. Growth was monitored by recording the OD_{600} variations after 6, 12, 24, and 48 h of incubation at 37°C using a BMG FLUOstar Optima microplate reader.

2.4. Microbiological Analysis and pH Measurement. A 10 mL fresh broth was inoculated overnight with an *L. rhamnosus* culture at a concentration level of McFarland 0.5 standard. Dried CP extracts were added to the culture media to give final concentrations of 1 mg/mL. The cultures were shaken well and incubated according to the above-mentioned conditions. Bacterial growth curves were determined by reading the sample OD_{625} at various time points (0-48 h). The pH value of each fermented sample (10 mL) was measured after 0, 24, and 48 h of fermentation using a pH meter (Table 1).

2.5. Biotransformation of CP Extracts. Cultures used to follow catabolism of CP extracts by *L. rhamnosus* were performed in MRS broth by scaling volumes up to 100 mL using 125 mL sterile Erlenmeyer flasks. Solutions of extracts (0.25, 0.5, and 1 mg/mL) were prepared in the bacterial medium and sterile filtered before use. During incubation (37°C) with a previously grown 24 h culture, samples were taken at desired intervals of 12, 24, and 48 h. Cell pellets were sonicated for 30 min to lyse cells and release any phenolics that had been adsorbed on or in the bacteria cells. Cell lysates were centrifuged at 4900 ×*g* for 10 min, and supernatants were separated, which were used to extract phenolic metabolites from media using ethyl acetate (EA) partition technique. Briefly, equal volumes of supernatant and EA were mixed in a separation funnel and allowed to stand for 24 h until complete phase separation. Then, the EA and aqueous layers were separately collected. The EA layer was evaporated using a rotary vacuum evaporator, re-dissolved in 80% methanol, filtered through 0.22 μm nylon filters, and kept at −20°C until further analysis.

2.6. Qualitative Analysis Corresponds to the Identification of Individual Phenolic Compounds in CP Fractions. Total phenolic content (TPC) was determined using the Folin-Ciocalteu method as described by Singleton and Rossi [14] and modified by Rupasinghe et al. [15]. The results are expressed in mg gallic acid equivalents (GAE)/L. Total anthocyanin contents (TAC) were determined using the pH differential method (AOAC method 2005.02) as previously described by Ratnasooriya et al. [16], and their concentration was expressed as mg cyanidin-3-*O*-glucoside equivalence (C3G) per 100 g FW using a molar extinction coefficient (ε) 28,000 and molecular weight (MW) 484.8 for C3G. Total

Table 1: Changes in pH of different cranberry pomace (CP) extracts during bioconversion with *L. rhamnosus*.

Time	Control	Type of extract				
		CR	FL+DHC	PA+C	AN	PR
0 h	5.84	5.84	5.86	5.84	5.85	5.85
24 h	3.81	3.85	3.83	3.63	3.78	3.59
48 h	3.32	3.40	3.33	3.22	3.41	3.40

CR: crude; FL+DHC: flavonol+dihydrochalcone; PA+C: phenolic acid +catechin; AN: anthocyanin; PR: proanthocyanidin. Control contains *L. rhamnosus* and media with no CP extracts added.

flavonoid content (TFC) was measured using the aluminum chloride method as described previously [17], and total proanthocyanidin content (TPr.C) was assessed using the dimethyl cinnamaldehyde method [18]. The results are expressed as mg quercetin equivalents (QE)/L for TFC and mg catechin equivalents (CE)/L for TPr.C.

2.7. Determination of Phenolic Compounds and Their Metabolites. Out of each extract, 10 mg was weighed out and dissolved in 10 mL methanol, followed by required dilution, filtration through a 0.22 μm nylon filter, and placing into amber vials. An ultrahigh performance liquid chromatography (UHPLC) (Model H-class system, Waters, Milford, MA, USA) equipped with an Acquity UHPLC BEH C_{18} column (2.1×100 mm, 1.7 μm) (Waters, Milford, MA, USA) was used for analysis. For the analysis of nonanthocyanin phenolics, gradient elution was carried out with 0.1% formic acid in water (solvent A) and 0.1% formic acid in acetonitrile (solvent B), with the flow rate of 0.2 mL/min and an injection volume of 2.0 μL. A linear gradient profile was used with the following proportions of solvent A applied at time t (min): (t, A%): (0, 94%), (2, 83.5%), (2.61, 83%), (2.17, 82.5%), (3.63, 82.5%), (4.08, 81.5%), (4.76, 80%), (6.75, 20%), (8.75, 94%), and (12, 94%). The analysis of anthocyanins was performed as described below; the mobile phases were 5% (v/v) formic acid in water (solvent A) and 5% (v/v) formic acid in methanol (solvent B). The linear gradients used were as follows: (t, A%): (0, 10%), (8, 30%), (17, 40%), (19, 40%), (20, 10%), and (22, 10%).

MS-MS analysis was performed with a Micromass Quattro micro API MS/MS system, which is controlled by a MassLynx V4.1 data analysis system (Micromass, Cary, NC, USA) as described by Bhullar and Rupasinghe [18]. Electrospray ionization in negative ion mode (ESI-) was used for the ionization of the flavonol and flavan-3-ol compounds. The mass spectrometry conditions included capillary voltage of 3000 V with nebulizing gas (N_2) at a temperature of 375°C. Electrospray ionization in positive mode (ESI+) was used for the analysis of anthocyanins. The mass spectroscopy conditions used were a capillary voltage of +3500 V with nebulizer gas at 375°C and a flow rate of 0.35 mL/min. The cone voltage (25-50 V) was optimized for each compound. Individual samples were identified using a multiple reaction monitoring mode and specific precursor-product ion with quantified calibration curves generated by external standards. For the analysis of phenolic metabolized produced by *L. rhamnosus*, ESI- mode (as described above) and single-ion monitoring (SIM) mode were used as follows: m/z 183 for benzoic acid, m/z 179 for caffeic acid, m/z 353 for chlorogenic acid, m/z 163 for p-coumaric acid, m/z 193 for ferulic acid and isoferulic acid, m/z 149 for hydrocinnamic acid, m/z 151 for 4-hydroxyphenylacetic acid, m/z 165 for 3-(4-hydroxyphenyl)propionic acid, m/z 117 for succinic acid, m/z 197 for syringic acid, and m/z 153 for protocatechuic acid.

2.8. Biological Activity Determination

2.8.1. Cell Lines and Culture Conditions. Human hepatocellular carcinoma (HepG2) cells was purchased from the American Type Culture Collection (ATCC HB-8065, Rockville, MD, USA) and cultured as recommended by the ATCC as described by Nair et al. [19]. HepG2 cells were grown in Eagle's modified minimum essential media (EMEM) supplemented with 10% FBS (FBS; ATCC, Rockville, MD, USA) and 1% penicillin-streptomycin (ATCC, Rockville, MD, USA). Cells were maintained at 37°C in an incubator under 5% CO_2/95% air atmosphere at above 85% relative humidity constantly. Cells were counted using a hemocytometer (Bright-Line Hemacytometer, Sigma-Aldrich, Mississauga, ON, Canada) and were plated according to the number of cells for each experiment in a 6-, 24-, or 96-well format for 24 h prior to the addition of test compounds. All the test samples were solubilized in sterile filtered DMSO (<0.5% in the culture medium) before addition to the culture media. Control cells were also run in parallel and subjected to the same changes in media with <0.5% DMSO.

2.8.2. Antiproliferation Activity before and after Bioconversion. HepG2 cells (5×10^3 cells/100 μL/well) were seeded in a sterile flat bottom 96-well plate (BD Biosciences, Mississauga, ON, Canada) and stabilized by incubation for 24 h at 37°C in a humidified incubator containing 5% CO_2 (VWR, Mississauga, ON, Canada) [19]. CP metabolites after 24 h bioconversion were used for their ability to inhibit human liver cancer cell proliferation and compared with their parent fractions (0 h). These samples were selected based on their polyphenol metabolite characterization as analyzed by UPLC/MS. From each extract (CR, AN, FL+DHC, and PA+C), 10 mg was weighed out and dissolved in DMSO to produce a stock solution of 5000 mg/L. PR 0 h, PR 24 h, 3-(4-hydroxyphenyl)propionic acid, 4-hydroxyphenylacetic acid, and sorafenib were dissolved in DMSO and diluted in media, and 100 μL of each treatment was added to each well, each treatment in three replications. Thereby, cells were exposed to various concentrations (10, 50, 100, 250, and 500 μg/mL) of each treatment. Controls consist of cells with media containing DMSO (<0.5%), and blank wells contained media with no cells. After 24 and 48 h of test compound incubation, 20 μL of the MTS reagent in combination with the electron-coupling agent, phenazine methosulfate, was added to the wells and cells were incubated in a humidified CO_2 incubator for 3 h. Absorbance at 490 nm (OD_{490}) was monitored with a plate reader (FLUOstar Optima, BMG Labtech, Durham, NC, USA) to obtain the number of viable cells relative to the control population. Percentage of viability in the test compound-treated cells

is expressed as a percentage compared to the control (<0.5% DMSO). Data are expressed as mean values ± SD and obtained from thee different experiments against each cell line ($n = 3$ per plate per time point).

2.8.3. ATP Luminescent Cell Viability Assay. The CellTiter-Glo® Luminescent Cell Viability Assay Kit (Promega, Madison, WI, USA) was used as a homogeneous method to determine the number of viable cells in culture was based on a quantification of ATP levels [19]. HepG2 cells (5×10^3 cells/100 μL/well) were seeded on opaque-walled 96-well black plates (BD Biosciences, San Jose, CA, USA) and allowed to attach for 24 h. Cells were then exposed to various concentrations (10, 20, 50, and 100 μM) of PR 0 h, PR 24 h, 3-(4-hydroxyphenyl)propionic acid, 4-hydroxyphenylacetic acid, and sorafenib or DMSO (control) in the EMEM medium for 24 h. CellTiter-Glo® Reagent (100 μL) was added to each well and mixed for 2 min on an orbital shaker to induce cell lysis. After 10 min of incubation at room temperature, luminescence was recorded using the above-described microplate reader.

2.8.4. Caspase 3/7 Activity Assay. HepG2 cells (5000 cells/100 μL/well) were seeded in white-walled 96-well plates and treated with 50 and 100 μM of PR 0 h, PR 24 h, 3-(4-hydroxyphenyl)propionic acid, 4-hydroxyphenylacetic acid, and sorafenib or DMSO (control). After 24 h of incubation in 37°C/5% CO_2 humidified incubator, 100 μL of Caspase-Glo® 3/7 reagent was added to each well of a white-walled 96-well plate containing 100 μL of blank, negative control cells, or treated cells in the culture medium. After mixing the contents of wells using a plate shaker for 30 s, plates were incubated at room temperature for 3 h. Luminescence was measured using the previously described microplate reader.

2.9. Experimental Design and Statistical Analysis. All analyses were conducted twice for three replicates per experiment. The data were analyzed using the Statistical Analysis System software (SAS Institute Inc., Cary, NC, USA). The general linear model (GLM) procedure was used to evaluate the main effect of treatment. Tukey's studentized test was used to compare the means among treatments at a p value of 0.05.

3. Results and Discussion

3.1. Isolation and Quantification of CP Fractions. The phenolic characterization of CP is presented in Figure 2. Based on some of the major phenolics present in CP, different fractions were pooled accordingly to obtain five major fractions: phenolic acid and catechin- (PA+C-), flavonol+ dihydrochalcone- (FL+DHC-), anthocyanin- (AN-), and proanthocyanidin- (PR-) rich fractions and crude (CR) fraction. Fractions E25-E45 exhibited the highest amounts of phenolic acids (sum of chlorogenic acid, ferulic acid, isoferulic acid, and caffeic acid) and flavan-3-ols (sum of EGC, catechin, epicatechin, EGCG, and ECG) and hence were pooled together to obtain PA+C. E50-E90 displayed the highest amount of flavonols (sum of quercetin aglycones and its various glycosides including galactoside, glucoside, rhamnoside, rutinoside, and arabinoside) and dihydrochalcones, anthocyanins (cyanidin-3-*O*-glucoside), and dihydrochalcones (phloridzin and phloretin). In order to separate anthocyanins, further liquid-liquid extraction was carried out using the ethyl acetate-water solvent system. The ethyl acetate fraction exhibited the highest amount of flavonols and dihydrochalcones (FL+DHC), while the water extract contained most of the anthocyanins (AN). All acetone fractions were pooled together to obtain PR. The CR showed the presence of almost all the analyzed phenolic compounds at moderate concentration levels. While the AN was rich in cyanidin-3-*O*-glucoside, it also had a small quantity of flavonols, especially quercetin galactoside. PR fraction was rich in proanthocyanidins, as determined by the DMAC analysis. The FL+DHC fraction exhibited the high amounts of quercetin glycosides, especially the galactosides and rhamnosides along with phloridzin as dihydrochalcone. In addition, the FL+DHC also contained some low molecular weight phenolic acids such as ferulic acid and isoferulic acid. The PA+C consisted of major phenolic acid and flavan-3-ols, including catechin and epicatechin, and minor amounts of EGC, EGCG, and ECG.

3.2. Bacterial Growth in the Presence of CP Fractions. The concentration of 1000 mg/L was used for all three extracts as the growth of *L. rhamnosus* was not inhibited significantly by any of the CP extracts at this concentration (Table 2). This could be due to the growth promotion of probiotic bacteria such as *Lactobacilli* by polyphenols. Whereas all the polyphenol-rich extracts were effective, the concentration level of 250 mg/L stimulated the greatest percentage increases (Table 2). At the end of 24 h using 1000 mg/L, the percentage growth of *L. rhamnosus* was not significantly different from those in the control, except in the AN extract. However, concentration levels above 1000 mg/L significantly affected the bacterial growth. In addition, it was found out that different extracts exhibited varying sensitivity towards *L. rhamnosus*. *L. rhamnosus* was capable of growing in the presence of different CP extracts, yet the growth was being affected in a dose-dependent fashion (Table 2). The results showed a progressive decrease in maximal OD_{625} from a concentration of 250 to 1500 mg/L. The decrease in the growth rate was most evident in the presence of AN extract, although the extracts did not completely inhibit the growth of *L. rhamnosus*. The CR did not exhibit any significant inhibition at the tested concentration levels. This was in line with a previous study where cranberry extracts produced no major inhibition at concentrations of 250-1000 mg/L against *L. plantarum* [20]. The same study also showed cranberry-specific proanthocyanidin A2 as a growth promoter of *L. plantarum*, which was found to be true for *L. rhamnosus* in the present study. Interestingly, the AN and PA+C were found to inhibit *L. rhamnosus* by 35% and 31%, respectively, at a concentration of 1500 mg/L. For PA+C, this could be due to the presence of galloylated flavanols having high hydrophobicity and thus high affinity for the phospholipid cell membrane [21].

3.3. Polyphenol Biotransformation by L. rhamnosus. As *L. rhamnosus* was found to tolerate the presence of all selected CP fractions at concentrations less than 1500 mg/L, our

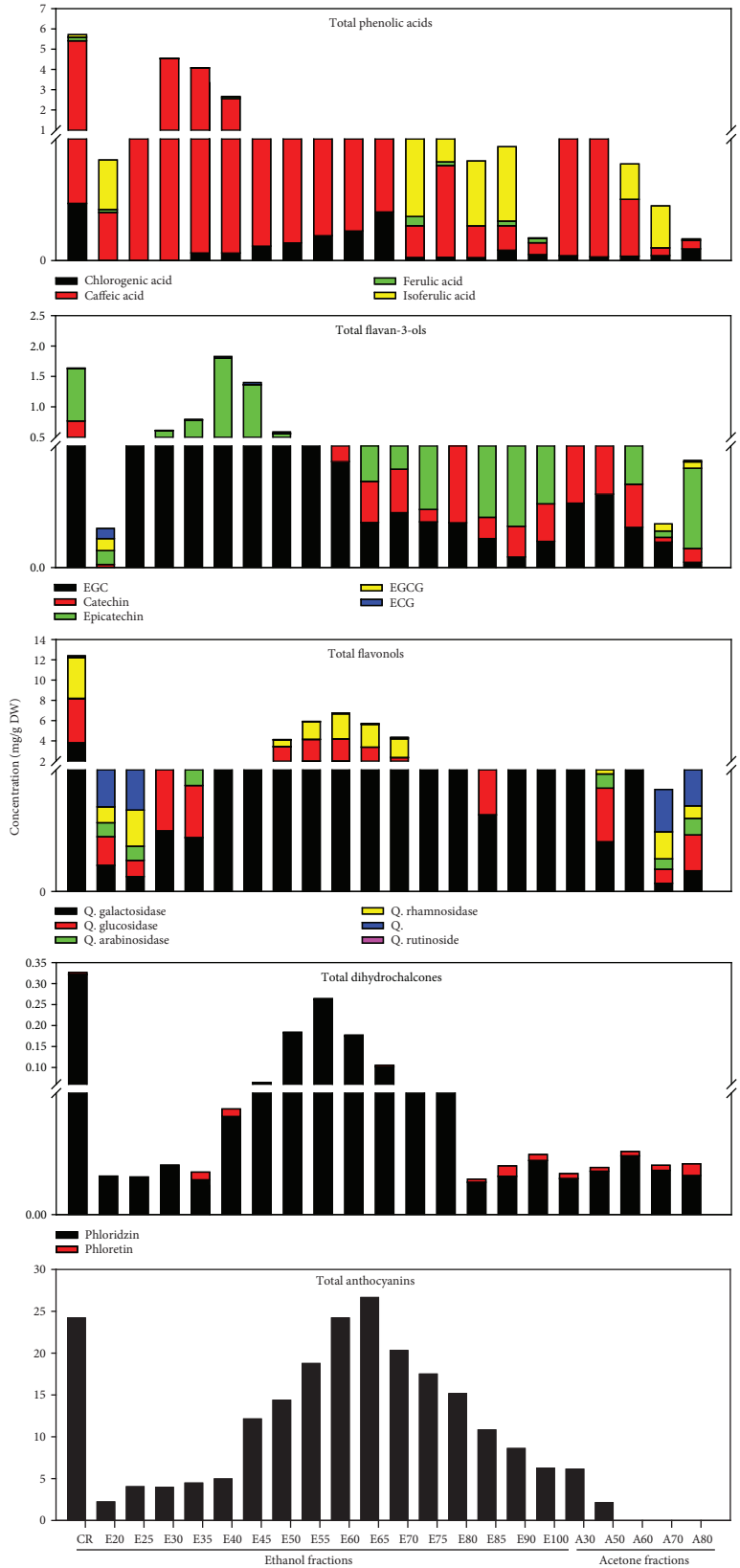

Figure 2: Characterization of different cranberry pomace fractions by UPLC-ESI-MS. Flavan-3-ols are represented by the sum of catechin, epicatechin, EGC, ECG, and EGCG. Phenolic acids are a sum of chlorogenic, ferulic, and caffeic acids. Flavonols are a sum of quercetin glucoside and galactoside; Dihydrochalcones represent the sum of phloridzin and phloretin. Anthocyanins represent cyanidin-3-*O*-glucoside, the most predominant anthocyanin.

Table 2: The percent growth of *L. rhamnosus* in the presence of various cranberry fractions with a comparison to the control.

CP extract	Concentration (mg/L)			
	250	500	1000	1500
CR	122.9 ± 2.0	110 ± 4.4	94.2 ± 5.2	77.1 ± 4.0
AN	106.6 ± 1.0	92.9 ± 1.4	74.3 ± 3.9	62.5 ± 5.7
PR	120.0 ± 2.5	107.5 ± 2.5	95.0 ± 4.5	86.3 ± 4.5
FL+DHC	125.2 ± 0.3	103.8 ± 3.8	91.3 ± 3.8	76.7 ± 3.8
PA+C	115.0 ± 7.5	100.8 ± 6.4	90.0 ± 2.5	68.8 ± 3.7

The growth of *L. rhamnosus* was measured by optical density at 625 nm. The control does not contain any fractions but the growth medium and *L. rhamnosus*. CR: crude; FL+DHC: flavonol+dihydrochalcone; PA+C: phenolic acid+catechin; AN: anthocyanin; PR: proanthocyanin.

strategy for this study was to stimulate metabolism of different polyphenol-rich CP fractions over a range of time points in order to investigate their biotransformation using *L. rhamnosus*. We used only one bacterial strain because probiotic bacteria and the polyphenol interactions for the production of biotransformed metabolites were the objectives of this study. This approach has been previously followed to study the biotransformation capability of grape seed [20] and wine polyphenols [22]. The incubations resulted in partial to complete depletion of parent compounds with the formation of new products. The results explicitly showed that the catabolic activity of *L. rhamnosus* modified the phenolic profiles of the tested CP extracts (Figures 3 and 4). A drop in concentration was observed in the selected polyphenol-rich media without bacteria, which could be due to their instability (oxidation and epimerization) during incubation in solutions with pH ~5.5.

Major phenolic compounds present in the CP, including flavonols (quercetin galactoside and quercetin rhamnoside), flavan-3-ols (catechins and epicatechins), anthocyanins, and proanthocyanidins, decreased in concentration after incubation with *L. rhamnosus*, while the concentrations of other phenolic acids and aromatic derivatives, including 4-hydroxyphenyl acetic acid, 3-(4-hydroxyphenyl)propionic acid, hydrocinnamic acid, catechol, and pyrogallol, increased. However, the stability of individual compounds also varied between different extracts and also with respect to time of incubation, as reflected from their percentage recovery. Interestingly, succinic acid present in CP fractions was used up by the bacteria in the first 12 h; however, its concentration was found to increase concerning incubation time post 12 h. There were exceptions to this phenomenon with PR fraction exhibiting a sharp increase in succinic acid concentration after 12 h, followed by a continuous decrease. Succinic acid is produced by *Lactobacilli* species when grown in MRS media [23]. Therefore, the data presented in Figure 4 has been corrected with respect to the control.

3.3.1. PR Fraction. The most noticeable increase in metabolite concentration was found in the PR fraction with 18-23-fold increase during 12-48 h incubation time, thereby clearly demonstrating extensive catabolism of their polymeric structure by the *L. rhamnosus*. An increase in catechin (0.78 mg/g), epicatechin (0.3 mg/g), benzoic acid (1.7 mg/g), 4-hydroxyphenylacetic acid (17.5 mg/g), and most importantly, 3-(4-hydroxyphenyl)propionic acid (19.5 mg/g) after 48 h incubation described the bioconversion process. Interestingly, the concentration of protocatechuic acid also increased by 8.5-fold after 48 h of incubation. Most likely, it could have been derived from 3,4-dihydroxyphenylpropionic acid by its decarboxylation and dehydroxylation to 3-hydroxybenzoic and 4-hydroxybenzoic acids catalyzed by the gut microorganisms [24]. Unlike the previous study with *L. plantarum* IFPL935 [20], the concentration of pyrogallol did not change during incubation of PR and PA+C fractions with *L. rhamnosus*. This can be because the CP used in the present study did not contain high amounts of galloylated flavanols as present in grape seed extract used by the previous study. As we know, a majority of the procyanidins in cranberry press cake come with a high degree of polymerization (DP) [25]. Although several of their biological activities have been shown [26], yet they are poorly absorbed relative to their corresponding monomers. Cranberry proanthocyanidins are microbially catabolized to generate low molecular weight derivatives that further undergo phase II metabolism inside the liver before reaching plasma and tissues [27]. Therefore, it is interesting to identify further biologically active components of metabolized proanthocyanidins in order to justify their *in vitro* biological activity.

3.3.2. PA+C Fraction. A decrease in the response was observed for caffeic, ferulic, isoferulic, and benzoic acids. Concurrently with the disappearance of these compounds, the formation of 4-hydroxyphenylacetic acid and catechol, together with a significant increase in the response of hydrocinnamic acid and 3-(4-hydroxyphenyl)propionic acid, was observed. None of these metabolites were found in the incubations of *L. rhamnosus* growth control. Metabolism of ferulic acid is known to result in coumaric acid, which is further decarboxylated to hydroxybenzoic acid, benzoic acid, phenol, and catechol [13, 28]. However, in our case, coumaric acid degraded after 12 h, but its concentration increased again after 24 h and stayed statistically insignificant after 48 h. The formation of hydroxyphenyl propionic acids from C–C double-bond reduction in *m*-coumaric and ferulic acids by other *Lactobacillus* strains including *L. plantarum* has been described previously [29]. Besides, the formation of 3-hydroxyphenylpropionic and benzoic acids from caffeic acid esters also has been established [30]. The formation of catechol from phenolic acids such as protocatechuic acid and caffeic acid can be explained by the decarboxylase action of *Lactobacillus* spp. [29]. Catechin and epicatechin suffered a progressive diminution during incubation and practically 77% and 44% loss of concentration at 48 h, respectively. According to previous studies, the catabolism of epicatechin using human intestinal bacteria, through a series of steps, produces valerolactones [20, 31], which were not analyzed in the present study. However, the appearance of high concentrations of 3-(4-hydroxyphenyl)-propionic acid and methyl 3,4,5-trihydroxybenzoate during the incubation of PA+C may suggest the catechin family catabolism through phenylpropionic acids and benzoic acids.

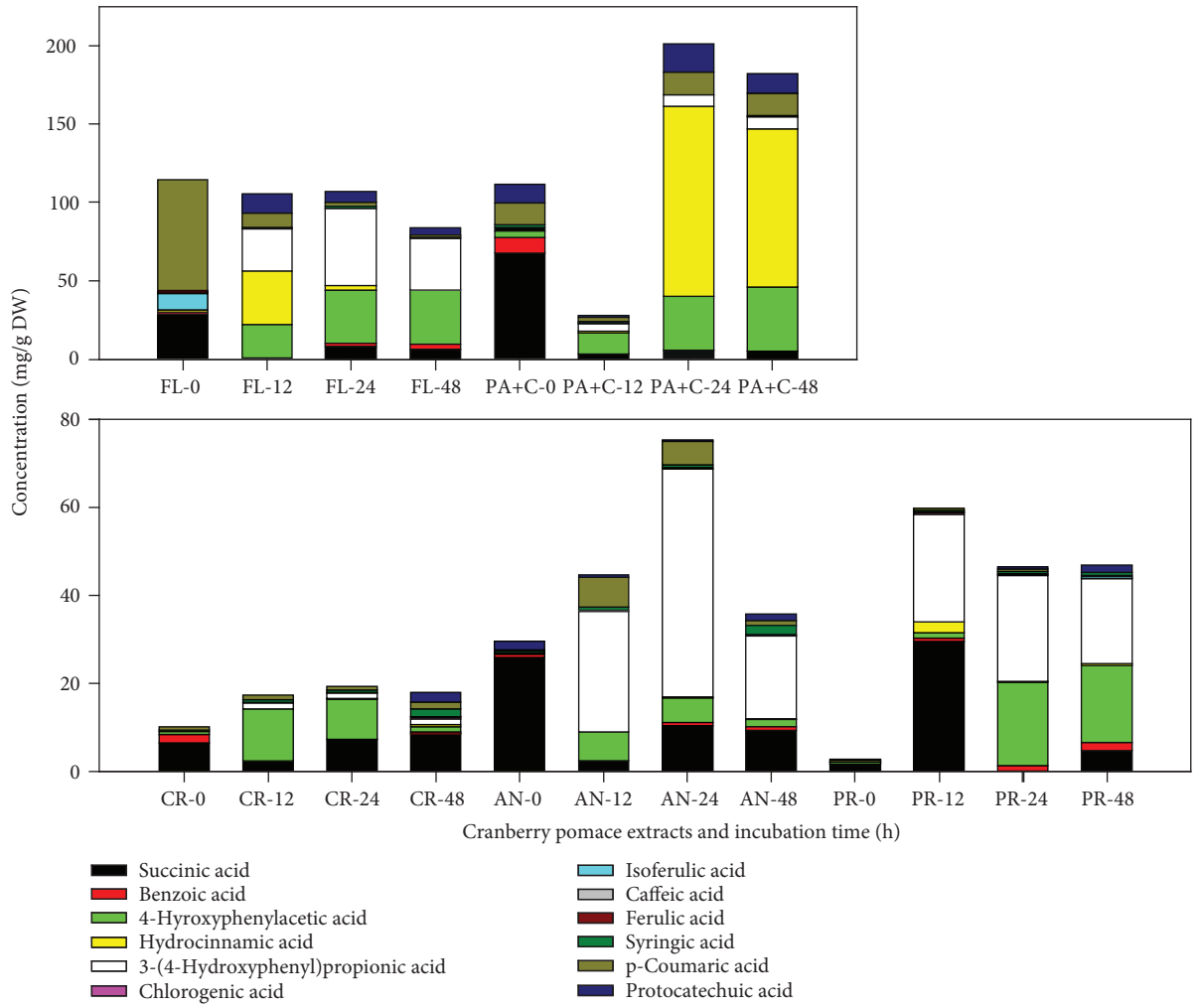

Figure 3: Changes in concentration of different phenolic acids as a result of bioconversion of cranberry proanthocyanidins using *L. rhamnosus* during the incubation. Data presented the mean values of $n = 3$ with respect to the medium control. CR: crude; AN: anthocyanin; PR: proanthocyanidin: FL: flavonol; PA+C: phenolic acid+catechin. 0, 12, 24, and 48 are the incubation time (hours).

In addition, the galloylated monomeric flavan-3-ols (ECG and EGCG), which were low in concentration at the beginning, were also degraded during the incubation.

3.3.3. CR Fraction. To expand the spectrum of phenolic substrates catabolized by *L. rhamnosus*, the present study also investigated its ability through a crude cranberry pomace extract. With respect to the data prior to incubation, the CR fraction showed an increase of total LCMS-based phenolic acids by 1.7-, 2.0-, and 1.8-fold after 12, 24, and 48 h, respectively. Some of the interesting features were the increase in concentrations of hydroxycinnamic acids, including ferulic, caffeic acids, and *p*-coumaric (the later to a lesser extent) after 48 h of incubation. This was in contrast to the previous study by Sánchez-Patán et al. [20] that showed a decrease in concentrations of these compounds, after incubation with *L. plantarum* IFPL935. The concentration of hydroxybenzoic acids, majorly protocatechuic acid, in this case, decreased within the first 24 h to almost half of its concentration, but again increased by more than 10-fold after 48 h. Also, a new compound, 3-(4-hydroxyphenyl)propionic acid, appeared within the first 12 h, together with a significant increase in the responses of 4-hydroxyphenylacetic acid and pyrogallol (present at very low concentration in the beginning), was observed. On the other hand, benzoic acid was found to degrade over time, while succinic acid showed an increase. The formation of hydroxyphenylpropionic acids by *Lactobacillus* species from the C-C double bond reduction of hydroxycinnamic acids has been explained [29]. Owing to anthocyanin metabolism, the concentration of syringic acid went high by 9-fold during the bioconversion.

3.3.4. AN Fraction. The AN fraction was generally less stable and presented large variations in the phenolic acid concentrations from 0 h to 48 h. Hydrolysis of anthocyanin glycosides by enzymes by cleavage of the 3-glycosidic linkage is proposed as the first step within 20 min to 2 h for subsequent bacterial degradation and the formation of a set of new metabolites that have not yet been identified [32, 33]. For that very reason, no aglycones were detected under any of the collection times assayed. The released aglycones formed transitorily could have been degraded into the corresponding

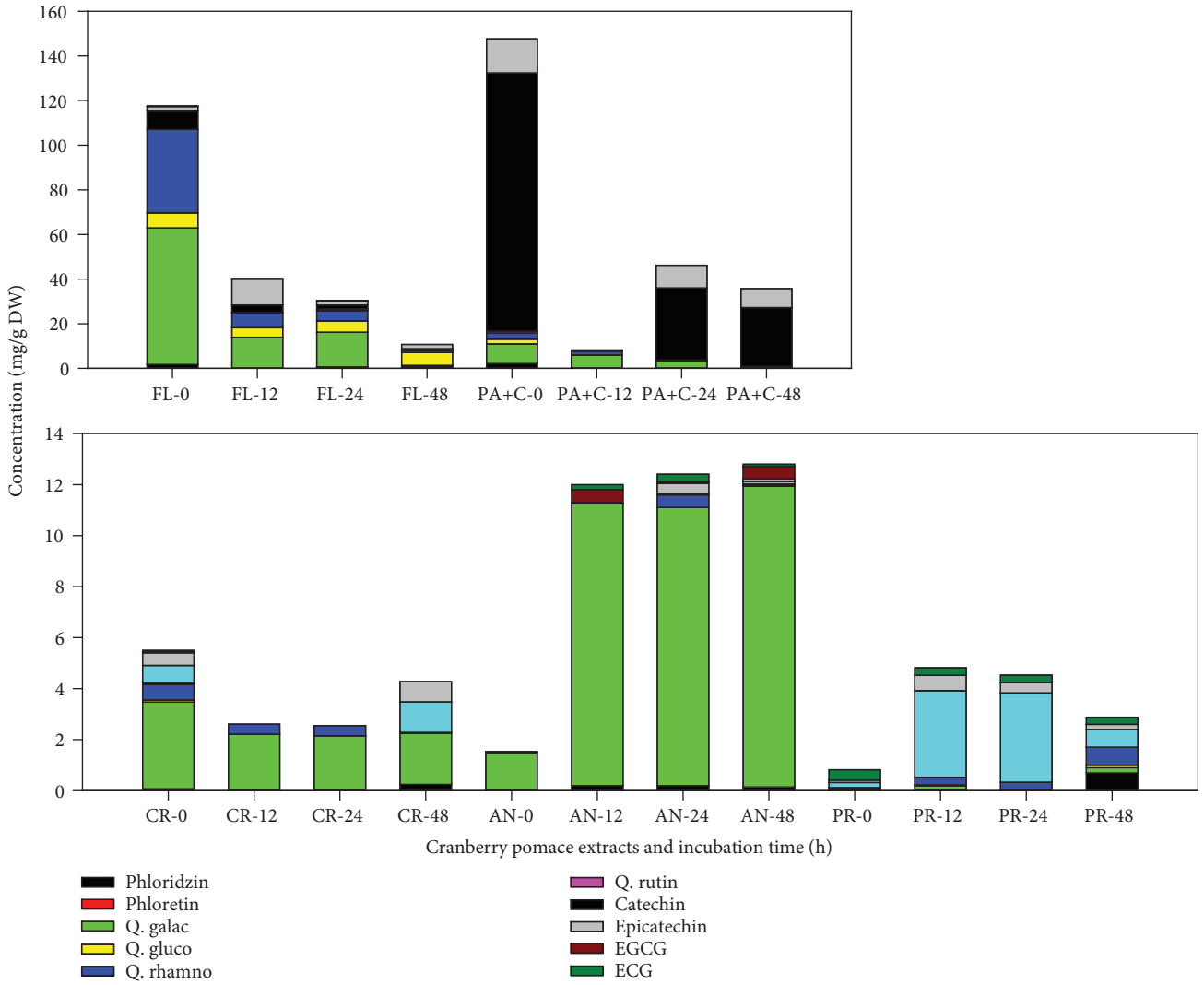

Figure 4: Effects of incubation with *L. rhamnosus* on the degradation of flavonoids present in cranberry pomace fractions. Data presented the mean values of $n = 3$ with respect to medium control. CR, crude; AN: anthocyanin; PR: proanthocyanidin: FL: flavonol; PA+C: phenolic acid +catechin. 0, 12, 24, and 48 are the incubation time (hours).

phenolic acids emanating from the B ring [32–34]. Concerning the AN fraction, as expected, mainly formation of gallic, syringic, and p-coumaric acids took place. The concentration of syringic acid increased continuously during incubation and went up by almost 10-fold after 48 h. As previously established, syringic acid is the major metabolite of anthocyanins, particularly malvidin glucosides [35]. Incubation of AN fraction with *L. rhamnosus* also yielded pyrogallol, indicating further metabolism such as decarboxylation of the metabolites such as gallic acid. During the first 24 h, p-coumaric acid increased by 23-fold, suggesting the bioconversion of anthocyanins using *L. rhamnosus*. In addition, small amounts of methyl gallate and protocatechuic acid were also produced during incubation. Protocatechuic acid has been identified as the major degradation product of cyanidin-3-*O*-glucoside, after incubation with human feces [34].

Interestingly, the concentration of 4-hydroxyphenylacetic acid spiked in the 12 h incubation by more than 21-fold, which was further reduced to 5.3-fold at the end of 48 h. This reduction could be due to further degradation of 4-hydroxyphenylacetic acid to simpler metabolites such as benzoic acid, which showed a slight increase in its concentration after 48 h. Similar information on the production of phenylacetic acids and hydrated acids has been described earlier by some authors [27, 36–38].

3.3.5. FL Fraction. Most of the quercetin glycosides are not absorbed in the small intestine and deglycosylated under the effect of bacterial β-glucosidases and α-rhamnosidase in the large intestine. Enzymes of intestinal bacteria not only deglycosylate quercitrin (quercetin-3-*O*-rhamnoside) but also further metabolize it with the break of quercetin heterocycle and formation of phenol acids such as 3,4-dihydroxyphenylacetic, hydroxyphenylacetic, and 3-methoxy-4-hydroxyphenylacetic acids [39]. Similar results were found in this study using *L. rhamnosus* incubation. The concentration of quercetin glycosides went down drastically, with the concurrent increase of metabolite concentrations

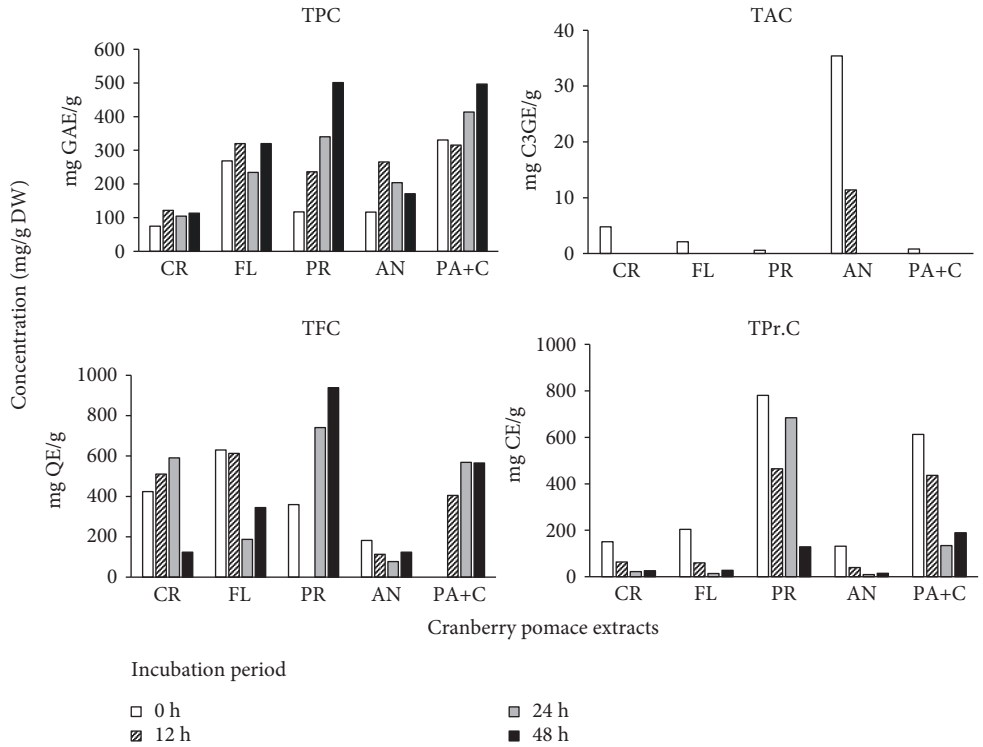

Figure 5: Total phenolic content (TPC), total anthocyanin content (TAC), total proanthocyanidin content (TPr.C), and total flavonoid content (TFC) of cranberry pomace fractions. Data presented the mean values of $n = 3$ with respect to the medium control. CR: crude; AN: anthocyanin; PR: proanthocyanidin: FL: flavonol; PA+C: phenolic acid+catechin.

including 4-hydroxyphenylacetic acid, hydrocinnamic acid, 3-(4-hydroxyphenyl)propionic acid, and protocatechuic acid, along with metabolic pathway end products like benzoic acid. The first 12 h incubation presented a 20-fold increase in protocatechuic concentration, which decreased by 3-fold after 48 h. On the other hand, the concentrations of 4-hydroxyphenylacetic acid and 3-(4-hydroxyphenyl)propionic acid showed a steep increase of 21-35 and 28-33 mg/g DW, respectively. Also, the benzoic acid concentration was found to increase by 1.6-fold, after 48 h incubation. Apart from the quercetin glycosides, the phenolic acid concentration of the FL fraction as well degraded during the bioconversion process.

3.4. Qualitative Measurements. The data for total phenolic content (TPC), total anthocyanin content (TAC), total proanthocyanidin content (TPr.C), and total flavonoid content (TFC) is represented in Figure 5. The bioconversion process significantly increased the TPC of all bioconverted fractions when compared to the fractions without biotransformation. While there were no similar studies on cranberry at the time of writing, these results were in line with a report that showed that fermentation of *C. lanceolata* increased the TPC in comparison to extracts without any fermentation [40]. The surge in the TPC for both PA+C and PR fractions was remarkable at 48 h as compared to 0 h. Fractions AN, PR, FL, and PA+C increased about 2-4 times in their TPC than the CR extract. A similar trend was observed for TFC, except for the AN fraction. On the contrary, the TAC and TPr.C degraded significantly during the bioconversion. Again, this is possibly due to the catabolism of these fractions into their respective metabolites. Interestingly, after initial degradation at 12 h, the TPr.C was noticed to increase in PR fraction at 24 h. This could be because of initial catabolism of proanthocyanidin polymers into monomeric flavan-3-ols that were read as catechin equivalents.

3.5. Biotransformed CP Polyphenol Fractions Cytotoxic to Cancer Cells at Lower Concentrations than Their Parent Fractions

3.5.1. Screening of CP Fractions and Their Metabolites on the Viability of HepG2 Cells. As a cell model of anticancer, we have used a widely investigated HCC HepG2 cells. This cell line can provide us an insight into the chemotherapeutic potential of the bioconverted metabolites for controlling malignant hepatocyte growth of liver cancer. The liver is an important organ which is the pivotal site for toxicity of xenobiotics, drugs, and oxidative stress [41]. Also, the liver is important for metabolic activation or inactivation of potentially antioxidative or other biologically active substances. We first sought to standardize the optimum concentration of CP fractions to inhibit the proliferation of the HCC cell line. The HepG2 cells were administered with increasing concentrations (1, 10, 50, 100, 250, and 500 μg/mL) of sorafenib or CP fractions before and after 24 h of bioconversion using *L. rhamnosus*, and cell viability was evaluated at 24 and 48 h after treatment. The obtained data resulted in a time- and concentration-dependent decrease in cell viability (Figure S1). In general, the CP metabolite

Table 3: The IC_{50} (mg/L) for cytotoxic effect in HepG2 cells of various cranberry fractions before and after bioconversion.

Assay	Source	Bioconversion	24 h	48 h
MTS	CR	Before	>500	>500
		After	340.9	319.6
	AN	Before	130.1	121.3
		After	241.7	266.7
	FL+DHC	Before	206.8	223.0
		After	115.8	102.6
	PA+C	Before	58.9	47.8
		After	41.2	36.4
	PR	Before	164.9	107.2
		After	47.8	20.1
	4-Hydroxyphenylacetic acid		183.5	136.9
	3-(4-Hydroxyphenyl)propionic acid		219.0	153.6

The cell viability was measured using the MTS assay after incubation of HepG2 cells with test extracts for either 24 or 48 h. CR: crude; FL+DHC: flavonol +dihydrochalcone; PA+C: phenolic acid+catechin; AN: anthocyanin; PR: proanthocyanin. Control contains *L. rhamnosus* and growth medium with no CP extracts added.

extracts after 24 h bioconversion were more effective in inhibiting HepG2 cell proliferation than their parent counterparts (0 h), except for anthocyanin-rich fraction. Among all the treatments given, PR 24 h showed the most potent antiproliferation activity, by displaying no viability at 100 μg/mL and displaying an IC_{50} value of 48 and 20 μg/mL (Table 3). This was followed by PA 24 h exhibiting 37% cell viability at 100 μg/mL which was not significantly different from the 28% viability demonstrated by the drug sorafenib. Therefore, it is evident that the *L. rhamnosus* bioconversion of cranberry pomace proanthocyanidins (PR 24 h) produces metabolites which are biologically more active than their intact forms. This high biological activity could be associated with their low molecular weight phenolic acid structures and monomeric flavan-3-ols, which can penetrate through the cell wall efficiently [8]. This is in agreement with a previous study that showed water-soluble phenolic extracts of cranberry and its products (mainly low molecular weight phenolic acids and their derivatives) effectively inhibited the proliferation of HT-29 and LS-513 colon cancer cell lines [42].

The other CP fractions including CR, AN, and FL showed significantly lower antiproliferation activity than the above-discussed PR and PA extracts. Therefore, these three fractions were excluded from a further study. The low biological activity of anthocyanin and flavonol-rich fractions can be attributed to their glycosylation, which could render the molecules more water-soluble but less reactive towards free radicals and metals, diminishing their antioxidant activity [5]. Additional experimentation was carried out using proanthocyanidins fraction before and after 24 h bioconversion and compared to two of its most prominent metabolites formed after 24 h, i.e., 3-(4-hydroxyphenyl)propionic acid and 4-hydroxyphenylacetic acid, along with sorafenib. The results obtained for the MTS assay revealed that at 100 μg/mL, the PR 24 h showed the highest antiproliferative activity compared to all the test compounds. The PR 24 h showed significantly higher ($p < 0.05$) activity than the prescribed drug sorafenib at the tested concentration. The two metabolites tested (3-(4-hydroxyphenyl)propionic acid and 4-hydroxyphenylacetic acid) did not show any significant activity at the concentrations between 10 and 100 μg/mL. Therefore, it can be speculated that the observed antiproliferative activity of PR 24 h could be due to the combined effects of several bioactive metabolites present in the fractions and this synergistic action can be better than any single compound. Further, a concentration of 50 and 100 μg/mL was selected for PR fractions for further studies.

Table 4: Total ATP content of HepG2 cells after 24 h when treated with cranberry extracts before and after bioconversion using *L. rhamnosus*.

Treatment	Bioconversion (24 h)	Total ATP content (mg/L)
PR	Before	105.6
PR	After	3.7
4-Hydroxyphenylacetic acid		431.3
3-(4-Hydroxyphenyl)propionic acid		>500
Sorafenib		0.01

PR: proanthocyanin.

3.5.2. PR 24 h Led to Metabolic Depletion of ATP in HepG2 Cells. Previous studies have shown that mitochondria play an essential role in the regulation of apoptosis in cells. After initial screening of CP fractions against HepG2 cell proliferation, we selected PR 24 h as the most potent candidate for further analyses based on its IC_{50} values. Two of its most abundant metabolites, i.e., 3-(4-hydroxyphenyl)propionic acid and 4-hydroxyphenylacetic acid and sorafenib, were compared for their total ATP-depleting activity. As shown in Table 4 and Figure S2, the cellular ATP activity decreased with the increasing concentration of PR 24 h and sorafenib and both displayed comparable effects at 100 μg/mL ($p \leq 0.05$) *in vitro*. However, at the lower concentrations of 10-20 μg/mL, the ATP activity displayed by sorafenib was

half than that exhibited by PR 24 h. Surprisingly, the data suggested that 3-(4-hydroxyphenyl)propionic acid and 4-hydroxyphenylacetic acid stimulated cellular proliferation at the lower concentrations with data points close to 100% cell viability. Given the cellular ATP depletion by PR 24 h, it could be speculated that this metabolic extract could activate Apaf-1 function and mitochondria-controlled apoptosis, as suggested by Ferrari et al. [43].

3.5.3. Induction of Caspase-3 by PR 24 h. Activation of caspase-3 is a key step in multiple apoptotic cell death pathways. Caspases contribute to apoptosis by cleavage of various cellular substrates and modulate both cellular integrity and cell cycle through chromatin condensation, loss of cell adhesion, cell shrinkage, membrane blebbing, DNA fragmentation, and formation of apoptotic bodies that are engulfed by phagocytes. Therefore, we examined the effect of PR 0 h, PR 24 h, and the two selected metabolites for stimulating caspase-3 activation. Enzymatic activity of caspase-3 changed after 24 h of incubation with the anticancer candidates using all treatments, except the control (Figure S3). The assay also revealed that with compounds' treatment the proportion of caspase enzyme-activated cells increased time-dependently, indicating the activation of these enzymes in the cells. In line with a previous study, sorafenib triggered the expression of caspase-3 enzyme among all the assayed compounds [44], which was significantly higher than all the assayed extracts/compounds. The CP fraction PR 24 h displayed the highest caspase-3 release at both 50 μg/mL and 100 μg/mL in comparison to PR 0 h and the two selected pure compounds. The activity of the caspase was threefold higher at 50 μg/mL but decreased to less than two times at a concentration of 100 μg/mL. Nevertheless, it can be suggested that cell death was not much influenced by the activation of effected caspases 3 and 7. However, further studies are required to identify other target pathways responsible for the cytotoxic activity of the CP fraction PR 24 h. Moreover, it is also interesting to investigate the ability of probiotic metabolites of cranberry proanthocyanins in the prevention of carcinogen-induced HCC in response to recently reported reduction of chemical-induced DNA damage by some common microbial metabolites of proanthocyanidins [45].

4. Conclusion

Despite the fast-growing research on fruit polyphenols and their potential health benefits, poor bioavailability of polymeric proanthocyanidins endorses the development of biotransformation approaches. While there have been reports on the improvement in biological activities of polyphenols upon their probiotic biotransformation, to our knowledge, this is the first study that investigated the bioconversion of cranberry proanthocyanidins and the effect of their metabolites on HCC cells *in vitro*. Biotransformation of proanthocyanidins into low molecular weight phenolic metabolites displayed cytotoxic activity against HepG2 cells at physiologically relevant concentrations. Further analyses revealed the involvement of mitochondrial ATP depletion and partial caspase 3/7 activation that attributed to their potential anticancer activity.

Data Availability

All the data are included in the manuscript and under supplementary data.

Conflicts of Interest

The authors have no conflicts of interest to declare.

Acknowledgments

This work was supported by the Discovery Grant of the Natural Sciences and Engineering Research Council (NSERC) of Canada (HPVR).

Supplementary Materials

Figure S1: percentage viability of HEPG2 cells as affected by the different concentrations of cranberry pomace polyphenols before and after bioconversion (24 h). Cell viability was analyzed by the MTS assay. Data ($mean \pm SE$, $n = 5$) are expressed as percentages of the MTS level detected in untreated control cells. Figure S2: ATP activity of HEPG2 cells as affected by the different concentrations of cranberry pomace polyphenols, pure compounds, and a drug after 24 h. Figure S3: caspase-3/7 activity of HEPG2 cells as affected by the different concentrations of cranberry pomace polyphenols, pure compounds, and a drug after 24 h. 4-HPAA: 4-hydroxyphenylacetic acid; 3-4HPPA: 3-4-hydroxyphenylpropionic acid. *(Supplementary Materials)*

References

[1] F. Bray, J. Ferlay, I. Soerjomataram, R. L. Siegel, L. A. Torre, and A. Jemal, "Global cancer statistics 2018: GLOBOCAN estimates of incidence and mortality worldwide for 36 cancers in 185 countries," *CA: A Cancer Journal for Clinicians*, vol. 68, no. 6, pp. 394–424, 2018.

[2] K. S. Bhullar, N. O. Lagarón, E. M. McGowan et al., "Kinase-targeted cancer therapies: progress, challenges and future directions," *Molecular Cancer*, vol. 17, no. 1, pp. 48–67, 2018.

[3] D. Stagos, G. D. Amoutzias, A. Matakos, A. Spyrou, A. M. Tsatsakis, and D. Kouretas, "Chemoprevention of liver cancer by plant polyphenols," *Food and Chemical Toxicology*, vol. 50, no. 6, pp. 2155–2170, 2012.

[4] S. Thilakarathna and H. P. V. Rupasinghe, "Flavonoid bioavailability and attempts for bioavailability enhancement," *Nutrients*, vol. 5, no. 9, pp. 3367–3387, 2013.

[5] C. Rice-Evans, N. Miller, and G. Paganga, "Antioxidant properties of phenolic compounds," *Trends in Plant Science*, vol. 2, no. 4, pp. 152–159, 1997.

[6] A. M. Aura, "Microbial metabolism of dietary phenolic compounds in the colon," *Phytochemistry Reviews*, vol. 7, no. 3, pp. 407–429, 2008.

[7] W. W. Thilakarathna, M. G. Langille, and H. P. V. Rupasinghe, "Polyphenol-based prebiotics and synbiotics: potential for cancer chemoprevention," *Current Opinion in Food Science*, vol. 20, pp. 51–57, 2018.

[8] H. P. V. Rupasinghe, S. V. Neir, and I. Parmar, "Polyphenol characterization, anti-oxidant, anti-proliferation and anti-tyrosinase activity of cranberry pomace," *Functional Foods in Health and Disease*, vol. 6, no. 11, pp. 754–768, 2016.

[9] P. J. Ferguson, E. Kurowska, D. J. Freeman, A. F. Chambers, and D. J. Koropatnick, "A flavonoid fraction from cranberry extract inhibits proliferation of human tumor cell lines," *Journal of Nutrition*, vol. 134, no. 6, pp. 1529–1535, 2004.

[10] J. A. Marazza, M. S. Garro, and G. Savoy de Giori, "Aglycone production by *Lactobacillus rhamnosus* CRL981 during soymilk fermentation," *Food Microbiology*, vol. 26, no. 3, pp. 333–339, 2009.

[11] J. A. Curiel, H. Rodríguez, I. Acebrón, J. M. Mancheño, B. de Las Rivas, and R. Muñoz, "Production and physicochemical properties of recombinant *Lactobacillus plantarum* tannase," *Journal of Agricultural and Food Chemistry*, vol. 57, no. 14, pp. 6224–6230, 2009.

[12] X. Wang, X. Geng, Y. Egashira, and H. Sanada, "Purification and characterization of a feruloyl esterase from the intestinal bacterium *Lactobacillus acidophilus*," *Applied and Environmental Microbiology*, vol. 70, no. 4, pp. 2367–2372, 2004.

[13] H. Rodríguez, J. M. Landete, B. Rivas, and R. Muñoz, "Metabolism of food phenolic acids by *Lactobacillus plantarum* CECT 748T," *Food Chemistry*, vol. 107, no. 4, pp. 1393–1398, 2008.

[14] V. L. Singleton and J. A. Rossi, "Colorimetry of total phenolics with phosphomolybdic-phosphotungstic acid reagents," *American Journal of Enology and Viticulture*, vol. 16, pp. 144–158, 1965.

[15] H. P. V. Rupasinghe, G. M. Huber, C. Embree, and P. L. Forsline, "Red-fleshed apple as a source for functional beverages," *Canadian Journal of Plant Science*, vol. 90, no. 1, pp. 95–100, 2010.

[16] C. C. Ratnasooriya, H. P. V. Rupasinghe, and A. R. Jamieson, "Juice quality and polyphenol concentration of fresh fruits and pomace of selected Nova Scotia-grown grape cultivars," *Canadian Journal of Plant Science*, vol. 90, no. 2, pp. 193–205, 2010.

[17] H. P. V. Rupasinghe, L. J. Yu, K. S. Bhullar, and B. Bors, "Short Communication: Haskap (*Lonicera caerulea*): A new berry crop with high antioxidant capacity," *Canadian Journal of Plant Science*, vol. 92, no. 7, pp. 1311–1317, 2012.

[18] K. S. Bhullar and H. P. V. Rupasinghe, "Antioxidant and cytoprotective properties of partridgeberry polyphenols," *Food Chemistry*, vol. 168, pp. 595–605, 2015.

[19] S. V. G. Nair, Ziaullah, and H. P. V. Rupasinghe, "Fatty acid esters of phloridzin induce apoptosis of human liver cancer cells through altered gene expression," *PLoS One*, vol. 9, no. 9, article e107149, 2014.

[20] F. Sánchez-Patán, R. Tabasco, M. Monagas et al., "Capability of *Lactobacillus plantarum* IFPL935 to catabolize flavan-3-ol compounds and complex phenolic extracts," *Journal of Agricultural and Food Chemistry*, vol. 60, no. 29, pp. 7142–7151, 2012.

[21] Y. Uekusa, M. Kamihira-Ishijima, O. Sugimoto et al., "Interaction of epicatechin gallate with phospholipid membranes as revealed by solid-state NMR spectroscopy," *Biochimica et Biophysica Acta (BBA) - Biomembranes*, vol. 1808, no. 6, pp. 1654–1660, 2011.

[22] E. Barroso, F. Sánchez-Patán, P. J. Martin-Alvarez et al., "*Lactobacillus plantarum* IFPL935 favors the initial metabolism of red wine polyphenols when added to a colonic microbiota," *Journal of Agricultural and Food Chemistry*, vol. 61, no. 42, pp. 10163–10172, 2013.

[23] C. Kaneuchi, M. Seki, and K. Komagata, "Production of succinic acid from citric acid and related acids by *Lactobacillus* Strains," *Applied and Environmental Microbiology*, vol. 54, no. 12, pp. 3053–3056, 1988.

[24] R. R. Scheline, *Handbook of Mammalian Metabolism of Plant Compounds*, CRC Press, Boca Raton, FL, USA, 1991.

[25] J. D. Reed, C. G. Krueger, and M. M. Vestling, "MALDI-TOF mass spectrometry of oligomeric food polyphenols," *Phytochemistry*, vol. 66, no. 18, pp. 2248–2263, 2005.

[26] A. E. Hagerman, K. M. Riedl, G. A. Jones et al., "High molecular weight plant polyphenolics (tannins) as biological antioxidants," *Journal of Agricultural and Food Chemistry*, vol. 46, no. 5, pp. 1887–1892, 1998.

[27] S. Déprez, C. Brezillon, S. Rabot et al., "Polymeric proanthocyanidins are catabolized by human colonic microflora into low-molecular-weight phenolic acids," *Journal of Nutrition*, vol. 130, no. 11, pp. 2733–2738, 2000.

[28] I. Parmar and H.P.V. Rupasinghe, "Proanthocyanidins in cranberry and grape seeds: metabolism, bioavailability and biological activity," in *Nutraceuticals and Functional Foods: Natural Remedy*, S. K. Brar, S. Kaur, and G. S. Dhillon, Eds., pp. 119–145, Nova Science Publishers, 2014.

[29] H. Rodríguez, J. A. Curiel, J. M. Landete et al., "Food phenolics and lactic acid bacteria," *International Journal of Food Microbiology*, vol. 132, no. 2-3, pp. 79––90, 2009.

[30] M. P. Gonthier, C. Rémésy, A. Scalbert et al., "Microbial metabolism of caffeic acid and its esters chlorogenic and caftaric acids by human faecal microbiota *in vitro*," *Biomedicine and Pharmacotherapy*, vol. 60, no. 9, pp. 536–540, 2006.

[31] S. Sang, M. J. Lee, I. Yang, B. Buckley, and C. S. Yang, "Human urinary metabolite profile of tea polyphenols analyzed by liquid chromatography/electrospray ionization tandem mass spectrometry with data-dependent acquisition," *Rapid Communications in Mass Spectrometry*, vol. 22, no. 10, pp. 1567–1578, 2008.

[32] A.-M. Aura, P. Martin-Lopez, K. A. O'Leary et al., "In vitro metabolism of anthocyanins by human gut microflora," *European Journal of Nutrition*, vol. 44, no. 3, pp. 133–142, 2005.

[33] K. Keppler and H. U. Humpf, "Metabolism of anthocyanins and their phenolic degradation products by the intestinal microflora," *Bioorganic & Medicinal Chemistry*, vol. 13, no. 17, pp. 5195–5205, 2005.

[34] J. Fleschhut, F. Kratzer, G. Rechkemmer, and S. E. Kulling, "Stability and bio-transformation of various dietary anthocyanins *in vitro*," *European Journal of Nutrition*, vol. 45, no. 1, pp. 7–18, 2006.

[35] M. Hidalgo, M. J. Oruna-Concha, S. Kolida et al., "Metabolism of anthocyanins by human gut microflora and their influence on gut bacterial growth," *Journal of Agricultural and Food Chemistry*, vol. 60, no. 15, pp. 3882–3890, 2012.

[36] J. Winter, L. H. Moore, Dowell VR Jr, and V. D. Bokkenheuser, "C-ring cleavage of flavonoids by human intestinal bacteria," *Applied and Environmental Microbiology*, vol. 55, no. 5, pp. 1203–1208, 1989.

[37] M.-P. Gonthier, V. Cheynier, J. L. Donovan et al., "Microbial aromatic acid metabolites formed in the gut account for a major fraction of the polyphenols excreted in urine of rats fed red wine polyphenols," *Journal of Nutrition*, vol. 133, no. 2, pp. 461–467, 2003.

[38] G. van't Slot and H.-U. Humpf, "Degradation and metabolism of catechin, epigallocatechin-3-gallate (EGCG), and related compounds by the intestinal microbiota in the pig cecum model," *Journal of Agricultural and Food Chemistry*, vol. 57, no. 17, pp. 8041–8048, 2009.

[39] A. R. Rechner, M. A. Smith, G. Kuhnle et al., "Colonic metabolism of dietary polyphenols: influence of structure on microbial fermentation products," *Free Radical Biology and Medicine*, vol. 36, no. 2, pp. 212–225, 2004.

[40] X. He, Y. Zou, W. B. Yoon, S. J. Park, D. S. Park, and J. Ahn, "Effects of probiotic fermentation on the enhancement of biological and pharmacological activities of *Codonopsis lanceolata* extracted by high pressure treatment," *Journal of Bioscience and Bioengineering*, vol. 112, no. 2, pp. 188–193, 2011.

[41] H. Jaeschke, G. J. Gores, A. I. Cederbaum, J. A. Hinson, D. Pessayre, and J. J. Lemasters, "Mechanisms of hepatotoxicity," *Toxicological Sciences*, vol. 65, no. 2, pp. 166–176, 2002.

[42] K. D. Vu, H. Carlettini, J. Bouvet et al., "Effect of different cranberry extracts and juices during cranberry juice processing on the antiproliferative activity against two colon cancer cell lines," *Food Chemistry*, vol. 132, no. 2, pp. 959–967, 2012.

[43] D. Ferrari, A. Stepczynska, M. Los, S. Wesselborg, and K. Schulze-Osthoff, "Differential regulation and ATP requirement for caspase-8 and caspase-3 activation during CD95- and anticancer drug-induced apoptosis," *Journal of Experimental Medicine*, vol. 188, no. 5, pp. 979–984, 1998.

[44] R. Sonntag, N. Gassler, J.-M. Bangen, C. Trautwein, and C. Liedtke, "Pro-apoptotic Sorafenib signaling in murine hepatocytes depends on malignancy and is associated with PUMA expression in vitro and in vivo," *Cell Death and Disease*, vol. 5, no. 1, article e1030, 2014.

[45] W. P. D. W. Thilakarathna and H. P. V. Rupasinghe, "Microbial metabolites of proanthocyanidins reduce chemical carcinogen-induced DNA damage in human lung epithelial and fetal hepatic cells *in vitro*," *Food and Chemical Toxicology.*, vol. 125, pp. 479–493, 2019.

Hindawi
Oxidative Medicine and Cellular Longevity
Volume 2019, Article ID 5719483, 14 pages
https://doi.org/10.1155/2019/5719483

Research Article

Ethanolic Extract of *Senna velutina* Roots: Chemical Composition, *In Vitro* and *In Vivo* Antitumor Effects, and B16F10-Nex2 Melanoma Cell Death Mechanisms

David Tsuyoshi Hiramatsu Castro,[1] Jaqueline Ferreira Campos,[1] Marcio José Damião,[1] Heron Fernandes Vieira Torquato,[2] Edgar Julian Paredes-Gamero,[2,3] Carlos Alexandre Carollo,[4] Elaine Guadelupe Rodrigues,[5] Kely de Picoli Souza,[1] and Edson Lucas dos Santos[1]

[1]*Research Group on Biotechnology and Bioprospecting Applied to Metabolism (GEBBAM), Federal University of Grande Dourados, Dourados, CEP: 79804-970 MS, Brazil*
[2]*Department of Biochemistry, Federal University of São Paulo, São Paulo, CEP: 04044-020, SP, Brazil*
[3]*Faculty of Pharmaceutical Sciences, Food and Nutrition, Federal University of Mato Grosso do Sul, Campo Grande, CEP: 79070-900, MS, Brazil*
[4]*Laboratory of Natural Products and Mass Spectrometry, Federal University of Mato Grosso do Sul, Campo Grande, CEP: 79070-900 MS, Brazil*
[5]*Department of Microbiology, Immunology, and Parasitology, Paulista School of Medicine, Federal University of São Paulo (EPM-UNIFESP), São Paulo, CEP: 04023-062 SP, Brazil*

Correspondence should be addressed to Edson Lucas dos Santos; edsonsantosphd@gmail.com

Received 7 December 2018; Revised 18 April 2019; Accepted 24 April 2019; Published 12 June 2019

Guest Editor: Patrícia Rijo

Cutaneous melanoma is among the most aggressive types of cancer, and its rate of occurrence increases every year. Current pharmacological treatments for melanoma are not completely effective, requiring the identification of new drugs. As an alternative, plant-derived natural compounds are described as promising sources of new anticancer drugs. In this context, the objectives of this study were to identify the chemical composition of the ethanolic extract of *Senna velutina* roots (ESVR), to assess its *in vitro* and *in vivo* antitumor effects on melanoma cells, and to characterize its mechanisms of action. For these purposes, the chemical constituents were identified by liquid chromatography coupled to high-resolution mass spectrometry. The *in vitro* activity of the extract was assessed in the B16F10-Nex2 melanoma cell line using the 3-(4,5-dimethylthiazol-2-yl)-2,5-diphenyltetrazolium bromide (MTT) assay and based on the apoptotic cell count; DNA fragmentation; necrostatin-1 inhibition; intracellular calcium, pan-caspase, and caspase-3 activation; reactive oxygen species (ROS) levels; and cell cycle arrest. The *in vivo* activity of the extract was assessed in models of tumor volume progression and pulmonary nodule formation in C57Bl/6 mice. The chemical composition results showed that ESVR contains flavonoid derivatives of the catechin, anthraquinone, and piceatannol groups. The extract reduced B16F10-Nex2 cell viability and promoted apoptotic cell death as well as caspase-3 activation, with increased intracellular calcium and ROS levels as well as cell cycle arrest at the sub-G_0/G_1 phase. *In vivo*, the tumor volume progression and pulmonary metastasis of ESVR-treated mice decreased over 50%. Combined, these results show that ESVR had *in vitro* and *in vivo* antitumor effects, predominantly by apoptosis, thus demonstrating its potential as a therapeutic agent in the treatment of melanoma and other types of cancer.

1. Introduction

Cancer is among the leading causes of death worldwide [1]. In particular, cutaneous melanoma is a potentially lethal form of skin cancer and occurs when melanocytes, cells responsible for producing the melanin pigment, undergo changes mediated by endogenous and/or exogenous events, thereby becoming malignant [2, 3]. The main factors responsible for the onset of melanoma are intrinsic and extrinsic. Intrinsic factors primarily include genetic susceptibility and family history, whereas the main extrinsic factor is excessive exposure to ultraviolet radiation [4, 5].

In recent decades, the incidence of cutaneous melanoma has increased, and according to the World Health Organization, approximately 132,000 cases of melanoma are diagnosed every year worldwide [6]. Its incidence varies among different populations, and the highest rates are reported in countries such as Australia and New Zealand [7]. When melanoma is detected early, surgical removal increases the treatment efficacy in approximately 99% of cases [8]. Chemotherapy, immunotherapy, and molecular therapy are among the main treatments for melanoma [9, 10]. Although patient survival rates are increasing, therapies and their combinations are still limited because they cause toxicity [11]. In addition, advanced-stage melanoma is resistant to drug therapy [12].

As an alternative to current therapies, phytochemical molecules have gained prominence as promising agents for the development of new drugs in the treatment of neoplasia [13]. Some studies have demonstrated that these substances show low toxicity in normal cells and act as melanoma treatment adjuvants, enhancing the anticancer effects of chemotherapeutic agents [14, 15].

In the scientific literature, the anticancer properties of more than 3000 plant species have been described [16]. Furthermore, in the last 70 years, 175 anticancer molecules were approved by the Food and Drug Administration (FDA), and 85 of them are derived from natural products or their derivatives [17].

These molecules, known as secondary metabolites, are complex compounds with diverse structures responsible for various biological activities [18]. These characteristics, together with the high degree of biodiversity in Brazil, may provide a promising source of new drugs. The genus *Senna* (Fabaceae) is found in the Brazilian Cerrado and has more than 250 species whose antimicrobial [19], antidiabetic [20], antioxidant [21], anti-inflammatory [22], and anticancer [23–25] properties have been described.

The species *Senna velutina*, a shrub of the genus *Senna*, commonly known as São João, vermelhinho, or Fedegoso-do-Cerrado, is found in the Central-West, Southeast, and Northeast regions of Brazil [26, 27]. Although the species is used by the population for medicinal purposes, only one article has described the antileukemic activity of the leaves of this plant [24]. However, no scientific study has described the chemical constituents and anticancer properties of the roots of this plant. In this context, the objective of this study was to characterize the chemical composition, assess the *in vitro* and *in vivo* antitumor effects, and identify the mechanisms through which the ethanolic extract of *S. velutina* roots (ESVR) promotes B16F10-Nex2 melanoma cell death.

2. Materials and Methods

*2.1. Plant Material and Extract Preparation. S. velutina*roots were collected in the Cerrado region (Brazilian biome), in the state of Mato Grosso do Sul (S 22° 05′ 545″ and W 055° 20′ 746″), in the Central-West region of Brazil and identified by a botanist. A dried sample of the species was deposited in the Herbarium of the Federal University of Grande Dourados-UFGD, Dourados, Mato Grosso do Sul (MS), Brazil, with registration number 4665. Root collection was authorized by the Sistema de Autorização e Informação em Biodiversidade (Biodiversity Information and Authorization System; SISBIO, permit number 54470-1). Subsequently, the plant roots were rinsed, dried in an air circulation oven for 15 days at 36°C, and pulverized; 200 g was then macerated in 95% ethanol (7 : 1) at room temperature for 7 days. Then, the extract was filtered and the residue was subjected to the same procedure twice. After 21 days, the filtrate was concentrated in a rotary vacuum evaporator (Gehaka, São Paulo, SP, Brazil) and subsequently freeze-dried (model Savant MicroModulyo, Thermo Fisher Scientific, Massachusetts, EUA). The dry extract yield was 23%, calculated using the following formula: $\text{extraction yield}\,(\%) = (\text{weight of the freeze} - \text{dried extract} \times 100)/(\text{weight of the original sample})$. The ESVR was stored at -20°C for subsequent experiments.

2.2. Phytochemical Analysis. ESVR was analyzed in an ultrafast liquid chromatograph (UFLC, Shimadzu) coupled to a diode array detector (DAD, Shimadzu) and electrospray ionization time-of-flight mass spectrometer (ESI-QTOF-micrOTOF QII, Bruker Daltonics; operating in the positive and negative ionization modes, 120-1200 Da). A C-18 column was used (Kinetex, 2.6 μm, 150 × 2.2 mm, Phenomenex), protected by a guard precolumn of the same material. The mobile phase was water (solvent A) and acetonitrile (solvent B), both with 0.1% formic acid, in a gradient of 0-2 min 3% B, 2-25 min 3-25% B, and 25-40 min 25-80% B, followed by the washing and reconditioning of the columns (8 min). The flow rate was 0.3 mL/min, and 1 μL of the extract (1 mg/mL) was injected. The other micrOTOF QII parameters were as follows: temperature, 200°C; N_2 gas flow rate, 9 L/min; nebulizer, 4.0 bar; capillary voltage, 3500 V (negative), +4500 V (positive); and internal calibration with sodium trifluoroacetate (TFA-Na) injected at the end of the chromatographic analysis. The catechin and piceatannol authentic standards were purchased from Sigma-Aldrich with ≥95% purity. The metabolites present in ESVR were identified based on the interpretation of mass and UV absorption spectra and based on comparison with the literature. When available, the compounds were confirmed by comparison with authentic standards.

2.3. Cell Lines and Cell Cultures. Human peripheral blood mononuclear cells (PBMCs) were collected after donor consent. Mononuclear cells were separated by centrifugation using Ficoll Histopaque-1077 (1.077 g/cm^3) (Sigma-Aldrich, Germany) according to the manufacturer's instructions at 400 × g for 30 min. The use of human blood was approved by the Ethics Committee of the Federal University of Grande Dourados (UFGD) under protocol 123/12. The murine melanoma subline (B16F10-Nex2) was isolated at the Oncology Experimental

Unit (Federal University of São Paulo, UNIFESP) from the B16F10 cell line and cultured in RPMI 1640 medium (Gibco/Invitrogen, Minneapolis, MN) supplemented with 4-(2-hydroxyethyl)piperazine-1-ethanesulfonic acid (HEPES, 10 nM) and sodium bicarbonate (24 nM). Human lung fibroblasts (MRC-5) and human melanoma cell lines (SK-Mel-28 and SK-Mel-103) were cultured in high-glucose Dulbecco's Modified Eagle's Medium (DMEM). All cell lines were supplemented with 10% fetal bovine serum (FBS, purchased from Gibco/Invitrogen) and 40 mg/mL gentamicin (Hipolabor Farmacêutica, Sabará, MG, Brazil). They were kept in flasks at 37°C in 5% CO_2.

2.4. MTT Cell Viability Assay. The cell viability was assessed using the 3-(4,5-diphenyltetrazolium-2-yl)-2,5-diphenyltrazolium bromide (MTT) colorimetric assay. Adherent cells were plated at a density of 5×10^3 cells/well, and PBMCs were plated at 10^5 cells/well in 96-well microtiter plates. After 24 and 48 h, solutions with different ESVR concentrations (25-125 μg/mL), diluted in medium with 0.1% DMSO, were added, and medium with only 0.1% DMSO was used as a control. At the end of both periods, 100 μL MTT (0.5 mg/mL) was added to each well. The cell culture was incubated for another 4 h, and 100 μL of DMSO was then added to solubilize the formazan crystals. The absorbance was determined at 570 nm using a SpectraMax 250 reader (Molecular Devices). Cell viability inhibition was calculated using the following formula:

$$\text{Cell viability } (\%) = [\text{Abs}_{\text{treated cells}}/\text{Abs}_{\text{control}}] \times 100. \quad (1)$$

2.5. Effect of ESVR on B16F10-Nex2 Cells. B16F10-Nex2 cells (5×10^3 cells/well) were subjected to solutions with different ESVR concentrations (25-125 μg/mL) diluted in RPMI 1640 solution with 0.1% DMSO for 24 h. RPMI 1640 solution with 0.1% DMSO was used as a control. Subsequently, cell images were acquired under a Nikon TE2000E (Nikon Instruments Inc.) microscope (10x objective).

2.6. Cell Death Profile. The cell death profile was determined using the method described by Paredes-Gamero et al. in 2012 [28] with a few modifications. B16F10-Nex2 cells were plated in 48-well plates (10^4 cells/well) and cultured in RPMI 1640 with 10% FBS for 24 h as well as with the half-maximal inhibitory concentration (IC_{50}) of ESVR (52 μg/mL). After this period, the cells were washed with phosphate-buffered saline (PBS), detached, and resuspended in buffer solution (0.01 M HEPES, pH = 7.4, 0.14 M NaCl, and 2.5 mM $CaCl_2$). The suspension was labeled with annexin V-fluorescein isothiocyanate (FITC) and propidium iodide (Becton Dickinson, USA) according to the manufacturer's instructions. The cells were incubated with the IC_{50} concentration of ESVR diluted in the medium to assess whether the extract showed fluorescence under the study parameters. The cells were incubated for 15 min at room temperature, and subsequently, 10,000 events per sample were collected and analyzed in the Accuri™ C6 flow cytometer (Becton Dickinson, USA) using the software FlowJo v10.2 LCC (Oregon, USA).

2.7. Apoptotic B16F10-Nex2 Cell Nuclei Count. To count the apoptotic cell nuclei, 6×10^4 B16F10-Nex2 cells/well were plated on coverslips in 24-well plates. Subsequently, the cells were treated with 52 μg/mL ESVR diluted in RPMI 1640 solution with 0.1% DMSO for 24 h. As a control, RPMI 1640 solution with 0.1% DMSO was used. After this period, the supernatant was discarded, and the cells were washed with PBS twice and fixed with 2% paraformaldehyde for 20 min at room temperature. Then, the cells were washed with PBS and permeabilized with 0.01% saponin for 20 min.

To detect apoptotic nuclei, coverslips were placed on slides and labeled with 4′-6′-diamidino-2-phenylindole (DAPI) dihydrochloride. Cells were counted under a LEICA DMI 6000B confocal microscope (Leica Microsystems, Germany).

2.8. DNA Fragmentation. B16F10-Nex2 cells were plated at 1×10^6 cells/well. After 24 h, the cells were treated with 52 μg/mL ESVR diluted in RPMI 1640 solution with 0.1% DMSO. RPMI 1640 solution with 0.1% DMSO was used as a control for 12 and 24 h. Subsequently, the DNA was extracted with phenol/chloroform, followed by incubation with RNAse (20 μg/mL). The DNA integrity was visualized in a 2.5% agarose gel stained with ethidium bromide (0.5 μg/mL).

2.9. Caspase-3 Activity. Caspase-3 activation was assessed by flow cytometry according to the method described by Moraes et al. in 2013 [29] with minor modifications. B16F10-Nex2 cells (6×10^4 cells/well) were treated with ESVR (52 μg/mL) and diluted in RPMI 1640 solution with 0.1% DMSO for 24 h. RPMI 1640 solution with 0.1% DMSO was used as a control. After the treatment, the cells were fixed with 2% paraformaldehyde for 30 min and then permeabilized with 0.01% saponin in PBS for 20 min at room temperature. Subsequently, the cells were incubated for 1 h with cleaved caspase-3 (Asp175) antibody (Alexa Fluor® 488 conjugate) at room temperature and protected from light. After the incubation period, the fluorescence was acquired in 10,000 events in the Accuri C6 flow cytometer (Becton Dickinson, San Jose, CA) and analyzed using the software FlowJo v8.7 (Ashland, USA).

2.10. Determination of the Reactive Oxygen Species (ROS) Levels. ROS levels were determined by flow cytometry using the 2′,7′-dichlorodihydrofluorescein diacetate (H_2DCFDA) dye (Molecular Probe-Life Technologies, Carlsbad, CA). For this purpose, B16F10-Nex2 cells (6×10^4 cells/well) were treated for 24 h with ESVR (52 μg/mL) diluted in RPMI 1640 solution with 0.1% DMSO, and RPMI 1640 solution with 0.1% DMSO was used as a control. Subsequently, the cells were trypsinized and incubated with 10 μM H_2DCFDA for 30 min at room temperature and protected from light. After the incubation period, the fluorescence, related to the ROS levels, was acquired in 15,000 events in the Accuri C6 flow cytometer (Becton Dickinson, San Jose, CA) and analyzed using the software FlowJo v8.7. (Ashland, US).

2.11. Pan-Caspase, Intracellular Calcium, and Necrostatin-1 Inhibition. To assess the involvement of caspases, intracellular calcium, and RIPK1 in ESVR-promoted cell death, B16F10-Nex2 cells (5×10^3 cells/well) were pretreated for

1 h with carbobenzoxy-valyl-alanyl-aspartyl-(O-methyl)-fluoromethylketone (Z-VAD-FMK; irreversible, cell-permeant pan-caspase inhibitor), 1,2-bis(2-aminophenoxy)ethane-N,N,N′, N′-tetraacetic acid tetra(acetoxymethyl ester) (BAPTA-AM; cell-permeant calcium chelator), or necrostatin-1 (NEC-1) inhibitor. Then, the cells were treated with ESVR (52 μg/mL) diluted in RPMI 1640 solution with 0.1% DMSO for 24 h. RPMI 1640 solution with 0.1% DMSO was used as a control. After this period, the cell viability was determined using the MTT assay, which was previously described in Section 2.4.

2.12. Cell Cycle Phases. The distribution of cell cycle phases was assessed using the method described by Paredes-Gamero et al. in 2012 [28]. For this purpose, B16F10-Nex2 cells (6×10^4 cells/well) were treated with ESVR (1/2 IC_{50} = 26 μg/mL and IC_{50} = 52 μg/mL) diluted in RPMI 1640 solution with 0.1% DMSO for 24 h. RPMI 1640 solution with 0.1% DMSO was used as a control. Subsequently, the cells were fixed and permeabilized as described above and incubated with RNAse (4 mg/mL) (Sigma-Aldrich, Germany) for 1 h at 37°C. For DNA labeling, the cells were incubated with SYTOX Green (5 μg/mL) (Molecular Probes Inc., Oregon). The percentage of cells at each cell cycle phase (sub-G_0/G_1, S, and G_2/M) was determined in 40,000 events in an Accuri C6 flow cytometer (Becton Dickinson, San Jose, CA). The results were analyzed using the software FlowJo v.8.7.

2.13. Animals. Male C57Bl/6 mice 4-6 weeks of age were obtained from the Centro de Desenvolvimento de Modelos Experimentais para Medicina e Biologia (Center for the Development of Experimental Models for Medicine and Biology-Federal University of São Paulo (CEDEME-UNIFESP), São Paulo, Brazil). In all experiments, the "Principles of Laboratory Animal Care" guidelines were followed (National Institute of Health (NIH) publication Number 85-23, revised in 1985), and animal experimentation was performed using protocols approved by the Animal Ethics Committee of the Federal University of São Paulo (UNIFESP) under number 1234/11.

2.14. In Vivo Antitumor Assay. Previously cultured B16F10-Nex2 melanoma cells (5×10^4 cells/animals) were subcutaneously implanted in the lumbosacral region of C57Bl/6 mice (seven animals per group). From the second day of implantation, the mice were intraperitoneally injected with ESVR (520 μg/mL) every other day for 30 days. The dose chosen was 10 times higher than the IC_{50} observed in the *in vitro* assays. The mice from the control group were intraperitoneally injected with the vehicle RPMI 1640 with 0.1% DMSO. The tumor volume was monitored after the 16th day of treatment, and the tumor diameter was measured three times a week. The tumor volume was determined using the following formula:

$$\text{Tumor volume } \left(\text{mm}^3\right) = \text{larger diameter} \times \text{smaller diameter}^2 \times 0.52. \quad (2)$$

2.15. In Vivo Pulmonary Metastasis Evaluation. The experiment was conducted according to Pereira et al. in 2016 [30] with minor modifications. Thus, 5×10^5 B16F10-Nex2 melanoma cells were injected through the caudal vein into C57Bl/6 mice (five animals per group). From the second day of implantation, the mice were intraperitoneally injected with ESVR (520 μg/mL) every other day for 14 days. The mice from the control group were intraperitoneally injected with vehicle RPMI 1640 with 0.1% DMSO. On the 15th day, the mice were anesthetized and euthanized. The lungs were removed, and the lung nodules were counted using a stereoscope (Nikon SMZ745T), with the images recorded using a Ds-Fi2 camera.

2.16. Statistical Analysis. All data are expressed as the mean ± standard error of the mean (SEM). The half-maximal inhibitory concentrations (IC_{50}) with confidence limits of 95% were determined by nonlinear regression using the software GraphPad Prism 6 software (San Diego, CA, USA). Significant differences between groups were determined using the unpaired Student's *t*-test (in apoptotic B16F10-Nex2 cell count, caspase-3 activity, determination of ROS levels, cell cycle phase, *in vivo* antitumor assay, and *in vivo* pulmonary metastasis evaluation) for comparison between two groups and analysis of variance (ANOVA) followed by Dunnett's test for comparison of two or more groups (in pan-caspase, intracellular calcium, and necrostatin-1 inhibition) using the GraphPad Prism 5 software (San Diego, CA, USA). The results were considered significant when $p < 0.05$.

3. Results

3.1. Phytochemical Composition of ESVR. Compounds relative to the twenty one chromatographic peaks were detected in the ethanolic extract of *S. velutina* roots, including sugar derivatives, gallocatechin, epigallocatechin, catechin, epicatechin, butiniflavan-(epi)gallocatechin, butiniflavan-(epi)catechin, piceatannol, cassiaflavan-(epi)gallocatechin, cassiaflavan-(epi) catechin, and dimeric tetrahydroanthracene derivatives (Figure 1 and Table 1).

3.2. Cell Viability Assay. Figure 2 shows that B16F10-Nex2 cells were sensitive to ESVR in a concentration-dependent manner after 24 h (IC_{50} of 52 μg/mL) and 48 h (IC_{50} of 59 μg/mL) of treatment. In both treatment periods, the ESVR decreased the number of viable cells. On the other hand, ESVR cytotoxicity was lower in the PBMC and MRC-5 cell lines than in B16F10-Nex2 cells; it was observed that even after 48 h of incubation with the highest dose tested (125 μg/mL), the extract was cytotoxic to only 20-30% of the cells. Additionally, the effect of ESVR against human melanoma cell lines SK-Mel-28 (IC_{50} of 420.21 μg/mL in 24 h and 330.48 μg/mL in 48 h) and SK-Mel-103 (IC_{50} of 245.23 μg/L in 24 h and 94.09 μg/mL in 48 h) was evaluated (reported in supplementary Figure 1). However, in both SK-Mel cell lines the results were lower than those observed against B16F10-Nex2 cells. B16F10-Nex2 cells were chosen for the next analyses, since they were more sensitive to the action of ESVR.

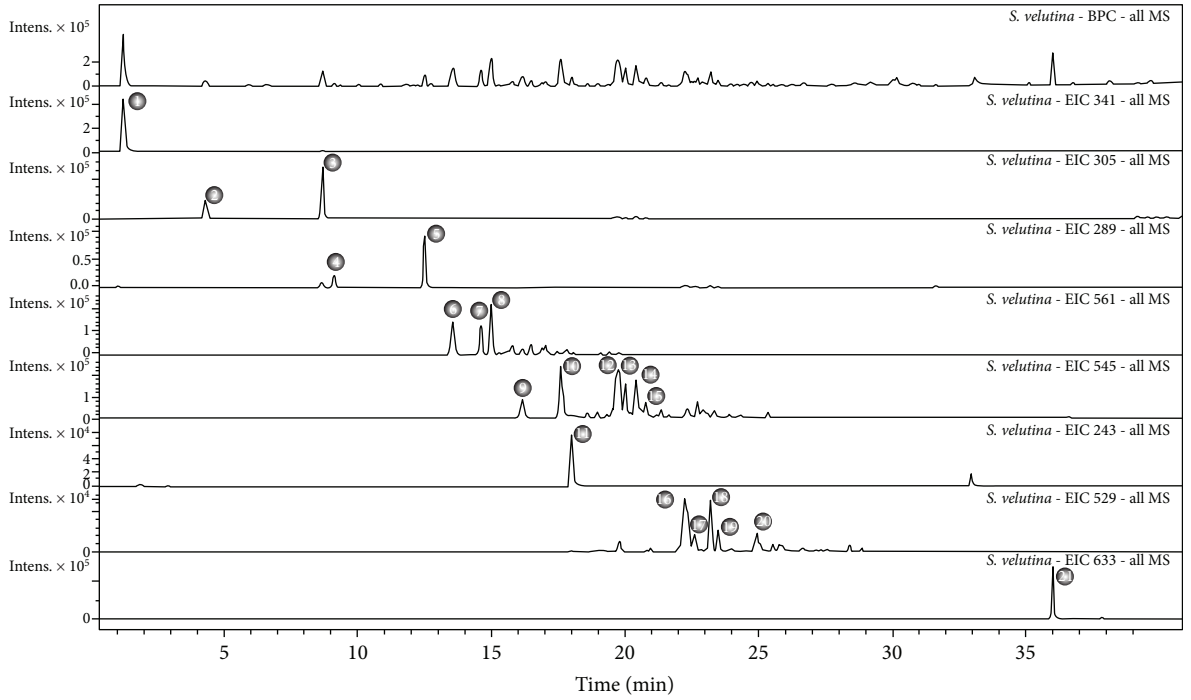

Figure 1: Characterization of the compounds identified in ESVR by UFLC-MS. Chromatograms with the base peaks and peaks identified in the extract.

Table 1: ESVR chemical profile as analyzed by UFLC-MS (negative mode).

Peak	Retention time	UV	Molecular formula	(M-H)	PPM error	MS/MS	Compound
1	1.1	—	$C_{12}H_{20}O_{11}$	341.1086	0.6	341: 179	Sugar derivative
2	4.2	270	$C_{15}H_{14}O_7$	305.0657	3.2	305: 261, 221, 219, 179, 167, 165	Gallocatechin
3	8.6	270	$C_{15}H_{14}O_8$	305.0660	2.3	305: 261, 221, 219, 179, 167, 165	Epigallocatechin
4	9.1	280	$C_{15}H_{14}O_9$	289.0709	3.0	289: 245, 205, 203	Catechin
5	12.5	280	$C_{15}H_{14}O_{10}$	289.0714	1.3	289: 245, 205, 203	Epicatechin
6, 7, 8	12.5/13.5/14.6	278	$C_{30}H_{26}O_{11}$	561.1402/561.1402	1.1	561: 407, 305, 177, 165	Butiniflavan-(epi)gallocatechin
9, 10	16.1/17.6	280	$C_{30}H_{26}O_{10}$	545.1453/545.1445	0.7	545: 391, 289, 245	Butiniflavan-(epi)catechin
11	18	289/321	$C_{14}H_{12}O_4$	243.0662	0.3	243: 201, 159	Piceatannol
12, 13, 14, 15	19.6/20/20.4/20.7	280	$C_{30}H_{26}O_{10}$	545.1441	2.3	545: 305, 239, 165	Cassiaflavan-(epi)gallocatechin
16, 17, 18, 19, 20	22.2/22.7/23.2/23.5/24.9	280	$C_{30}H_{26}O_9$	529.1488	3.0	529: 289, 245, 239, 203	Cassiaflavan-(epi)catechin
21	36.1	279/320/406	$C_{34}H_{34}O_{12}$	633.1992	2.2	633: 615, 597, 579, 557, 555, 539, 317, 299, 298, 259	Dimeric tetrahydroanthracene derivative

3.3. Effects of ESVR on B16F10-Nex2 Cells. Figure 3 shows the effects of different ESVR concentrations on B16F10-Nex2 cell viability and morphology after 24 h of treatment. At images of the 25 to 60 μg/mL of the extract concentration, a reduction in the cell number was observed without changing the morphology of unaffected cells that remain attached to the extracellular matrix present at the well. On the other hand, cells treated with doses equal or higher than 70 μg/mL of the extract showed a marked reduction in the cell number and strongly modified morphology of the remaining cells with loose attachment to the extracellular matrix.

3.4. Cell Death Profile. Cells were incubated with ESVR diluted in culture media at IC_{50} without annexin V-FITC or

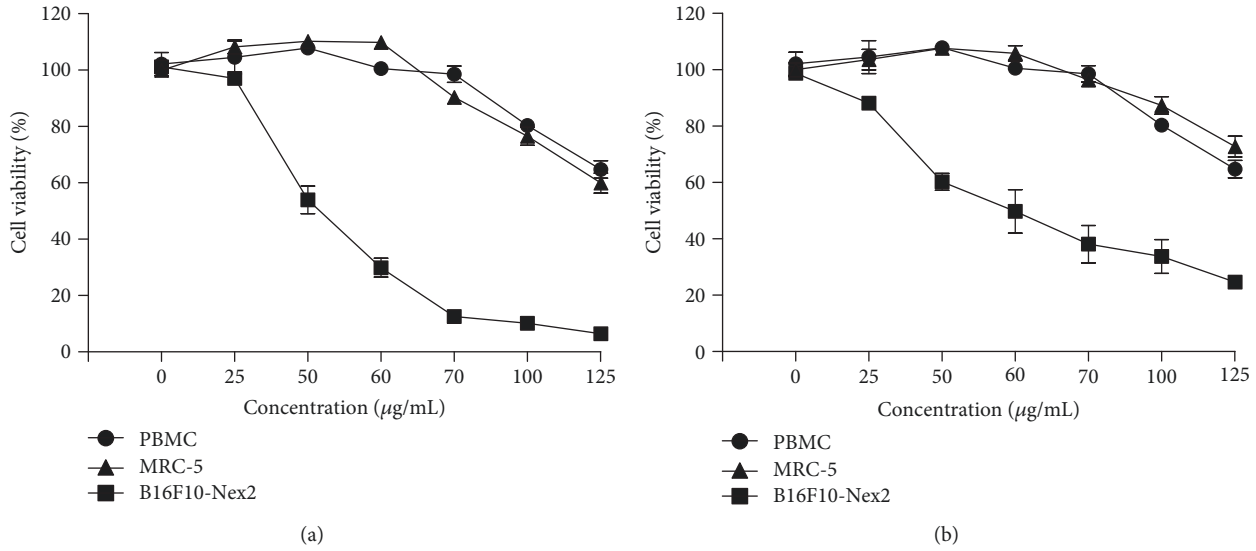

Figure 2: The cytotoxic effect of ESVR on PBMC, MRC-5, and B16F10-Nex2 cells treated with different ESVR concentrations for (a) 24 and (b) 48 h. The data are expressed as the means ± SEM in three independent experiments in triplicate.

propidium iodide. However, the fluorescence of the extract was similar to that of the markers, thereby precluding the correct interpretation of these tests (data not shown).

3.5. Apoptotic B16F10-Nex2 Cell Count. Nuclear morphological changes are characteristic of apoptotic cell death and can be determined by microscopy using specific fluorescence markers. In these analyses, the number of apoptotic B16F10-Nex2 cells treated with ESVR (52 μg/mL) counted under confocal microscopy shows that the extract promoted nuclear damage in 32.4% of cells, whereas only 5.2% of untreated cells were damaged (Figure 4). Only nuclei that showed extreme chromatin condensation, DNA fragmentation, and high fluorescence intensity were considered apoptotic nuclei.

3.6. DNA Fragmentation. Compounds that activate cell death pathways such as apoptosis are able to induce DNA degradation. The DNA fragmentation data shown in Figure 5 demonstrate that ESVR-treated B16F10-Nex2 cells show time-dependent DNA fragmentation, which is observed after 12 h and is intensified after 24 h and 48 h of treatment. After these incubation periods, the control cells showed no sign of DNA fragmentation.

3.7. Caspase-3 Activity. Caspase-3 is an effector caspase that plays a central role in the execution phase of apoptosis. Caspase-3 activation was assessed to identify the possible cell death pathways activated by ESVR in melanoma cells. In this assay, Figure 6(a) shows right-shifted fluorescence values, thus confirming caspase-3 activation and indicating apoptosis-induced cell death. The increase in cleaved caspase-3 in ESVR-treated B16F10-Nex2 cells was twice as high as that in control cells (Figure 6(b)).

3.8. Determination of the Reactive Oxygen Species (ROS) Levels. ROS were evaluated in this study to verify whether they were involved in ESVR-induced cell death. The levels of ROS increased in ESVR-treated cells, as shown by the right-shifted fluorescence values (Figure 7(a)). The mean values obtained in the fluorescence intensity were 24.271 ± 4.309 for treated cells with ESVR and 2.787 ± 408 for the control cells (Figure 7(b)). The ROS levels increased 8.7-fold in B16F10-Nex2 cells treated with the extract after 24 h of incubation compared with control cells without treatment.

3.9. Pan-Caspase, Intracellular Calcium, and Necrostatin-1 Inhibition. Aiming to identify cell death modalities induced by ESVR in B16F10-Nex2 cells, different markers of apoptosis and necrosis were analyzed. Figure 8 shows that neither control B16F10-Nex2 cells nor the B16F10-Nex2 cells treated with only the inhibitors showed changes in cell viability. Conversely, cells treated with ESVR (52 μg/mL) for 24 h showed 52.0 ± 3.3% viable cells. This result was partially reversed in the presence of the inhibitors Z-VAD-FMS (77.9 ± 1.4%), BAPTA-AM (73.7 ± 3.1%), and NEC-1 (66.7 ± 1.2%).

3.10. Cell Cycle Phases. Cell cycle control in tumor cells is considered an important therapeutic target for the treatment of cancer. Thus, demonstrating the effects of the extract on the progression of the cell cycle will contribute to a better understanding of its mechanisms of action. Figure 9(a) shows histograms of the cell cycle distribution of control B16F10-Nex2 cells and B16F10-Nex2 cells treated with 1/2 IC_{50} = 26 μg/mL and IC_{50} = 52 μg/mL ESVR for 24 h. The control cells and cells treated with 26 μg/mL of ESVR showed no differences in cell cycle distribution (Figure 9(b)). The comparison between cells treated with 52 μg/mL of ESVR and control cells shows that ESVR promoted cell cycle arrest at the G_0/G_1 phase (54.3 ± 3.8% versus 42.3 ± 2.6%, $^*p < 0.05$) and decreased the percentage of S phase cells (22.5 ± 2.2% versus 36.6 ± 4.2%, $^*p < 0.05$) without changing the number of cells in the G_2/M phase (19.9 ± 0.8% versus 20.9 ± 2.4%) (Figure 9(b)).

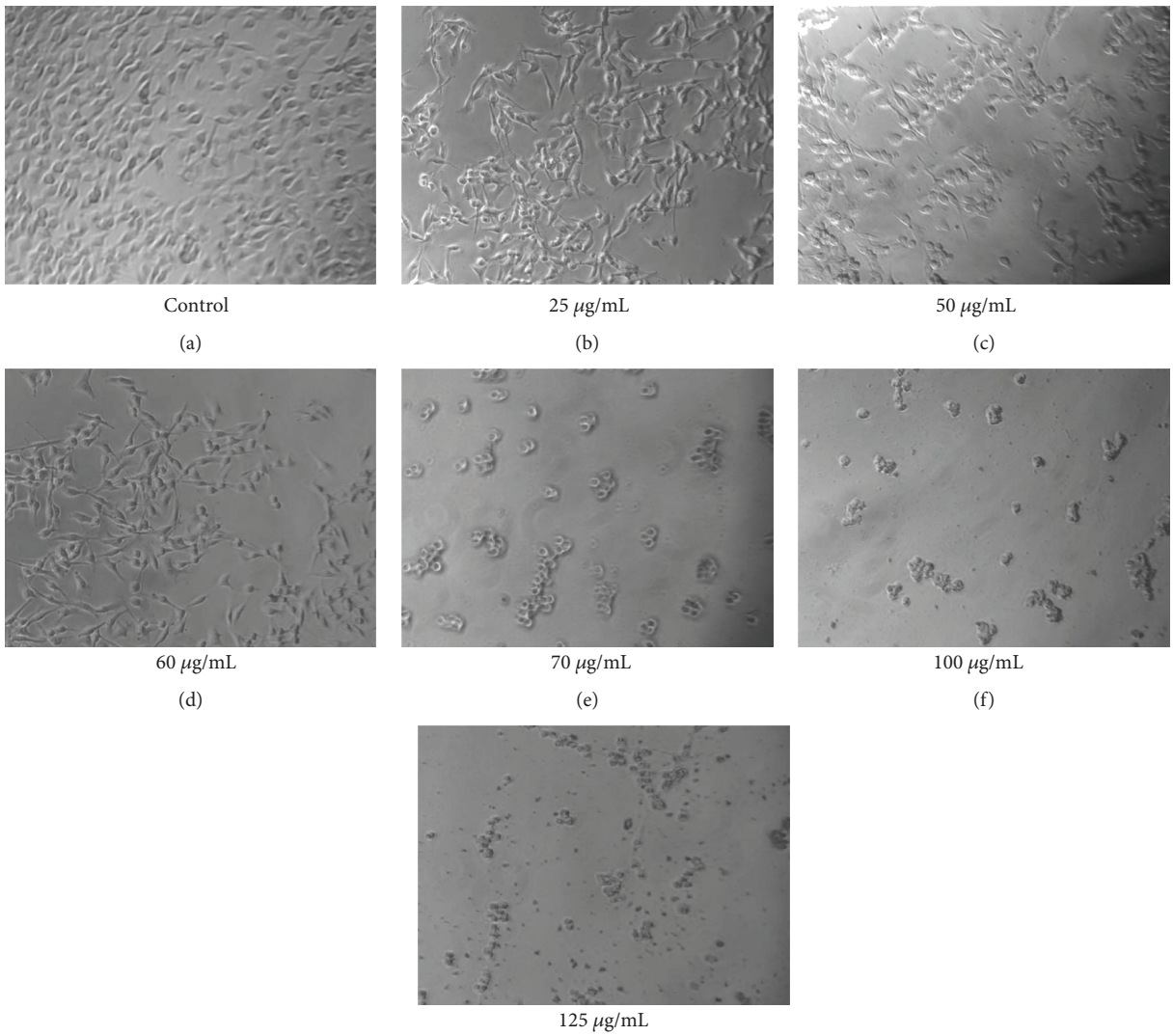

Figure 3: Reduced viability of B16F10-Nex2 cells treated with different ESVR concentrations for 24 h. Images are representative of those seen from at least three such fields of view per sample and three independent replicates.

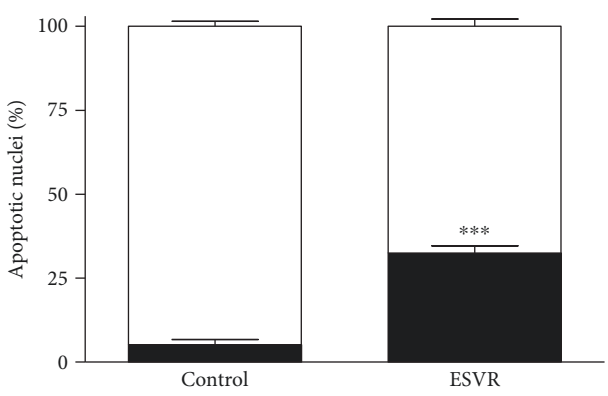

Figure 4: Count of apoptotic nuclei in B16F10-Nex2 cells treated for 24 h with 52 μg/mL of ESVR. The data are expressed as the means ± SEM of four independent experiments in duplicate. $^{***}p < 0.001$ compared with control cells.

3.11. In Vivo Effect of ESVR on the Tumor Volume. After observing that ESVR had a cytotoxic effect on B16F10-Nex2 cells *in vitro*, we next evaluated the effect of the extract *in vivo* during tumor progression. ESVR treatment of B16F10-Nex2-inoculated mice significantly delayed subcutaneous tumor development in all animals analyzed (Figure 10(a)). Figure 10(b) shows that the mean tumor volume of mice 30 days after the treatment was 57.5% smaller than the tumor volume of the control mice.

3.12. In Vivo Effect of ESVR on Pulmonary Metastasis. Next, we analyzed the effect of ESVR on metastatic B16F10-Nex2 cells developing in the lungs after endovenous inoculation at the caudal vein. It was observed that ESVR-treated animals showed 119 ± 25 pulmonary melanotic nodules 14 days after cell inoculation, while the control group showed 286 ± 6 pulmonary nodules, a 54% reduction (Figure 11).

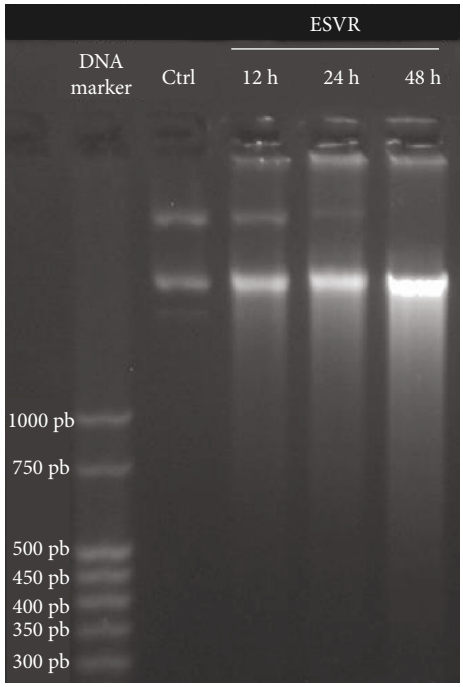

Figure 5: DNA fragmentation in B16F10-Nex2 cells analyzed by agarose gel electrophoresis after 12 h, 24 h, and 48 h of treatment with 52 µg/mL of ESVR. Ctrl = B16F10-Nex2 cells after 48 h without treatment with ESVR.

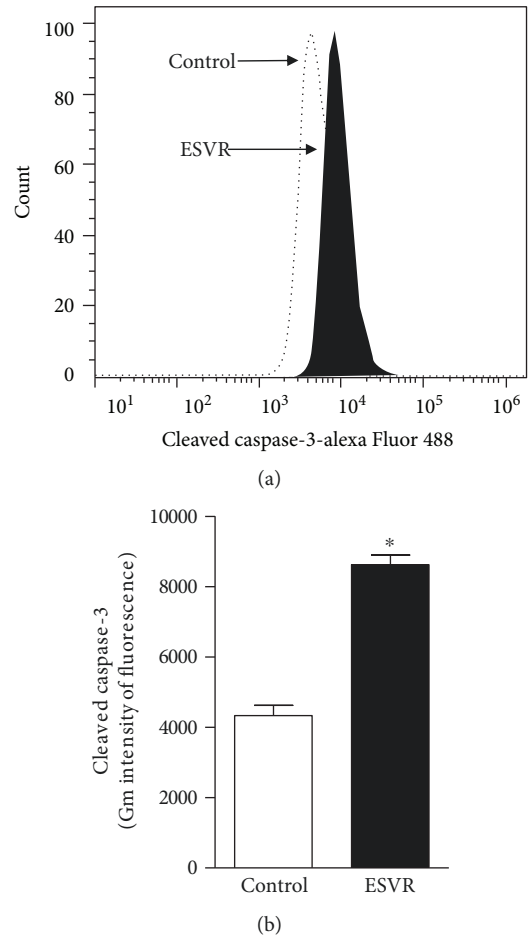

Figure 6: Caspase-3 activation by ESVR after 24 h represented in a histogram (a) and bar graph (b). The data are expressed as the means ± SEM of three independent experiments in duplicate. $^{*}p < 0.05$ compared with control cells.

4. Discussion

The search for new anticancer drugs with greater selectivity and lower adverse effects is an ongoing process. Natural compounds are among the alternatives that stand out as promising sources of new molecules with pharmacological potential. Accordingly, several anticancer drugs of natural origin are available on the market [31]. In this context, scientific studies have shown that Brazilian biodiversity due to its various biomes provides various natural compounds with anticancer potential both *in vitro* [32, 33] and *in vivo* [30, 34]. In the present study, we assessed the anticancer effects of the ethanolic extract of the roots of *S. velutina*, a plant species native to Brazil whose phytochemical composition and potential pharmacological applications have been poorly studied.

Phytochemical analysis of ESVR identified its main compounds as flavonoid derivatives of the catechin and piceatannol (active metabolite of resveratrol) groups as well as dimeric tetrahydroanthracene derivatives. These phenolic compounds derived from plant secondary metabolism exhibit great structural diversity and are responsible for innumerable biological activities, including anticancer properties [35, 36].

The assessment of the effect of ESVR on B16F10-Nex2 melanoma cell viability revealed a dose-dependent death profile. This effect was confirmed by microscopy, as shown by the activity of the extract at different concentrations. In addition, ESVR showed higher selectivity against B16F10-Nex2 cells than against human leukocytes (PBMC) or human fibroblasts (MRC5). This result is highly relevant because systemic collateral effects from chemotherapeutic agent activity are a consequence of reduced selectivity against tumor cells.

The ability of the extract to promote the death of melanoma cells may be related to the isolated or synergistic effects of its chemical constituents, since the main constituents and chemical classes identified in the ESVR are well described in the literature for their antitumor activities. Catechins are described by the ability to reduce the viability of breast carcinoma cells [37] and to promote the cytotoxic effect in B16F10 murine melanoma cells [38]. Anthraquinone compounds have been reported as promising therapeutic agents for the treatment of malignant melanoma for presenting high cytotoxicity against different malignant melanoma cells and low toxicity to melanocytes and other primary cell [39]. Piceatannol, defined as a promising therapeutic agent for the treatment of various cancers, inhibited growth and induced apoptosis in human melanoma cell lines [40].

Different studies report that catechins [41, 42], anthraquinones [39], and piceatannol [43, 44] induce apoptosis in tumor cells. Corroborating this is the analysis of the mechanism whereby ESVR-promoted B16F10-Nex2 cell death showed an increased number of apoptotic nuclei, which are

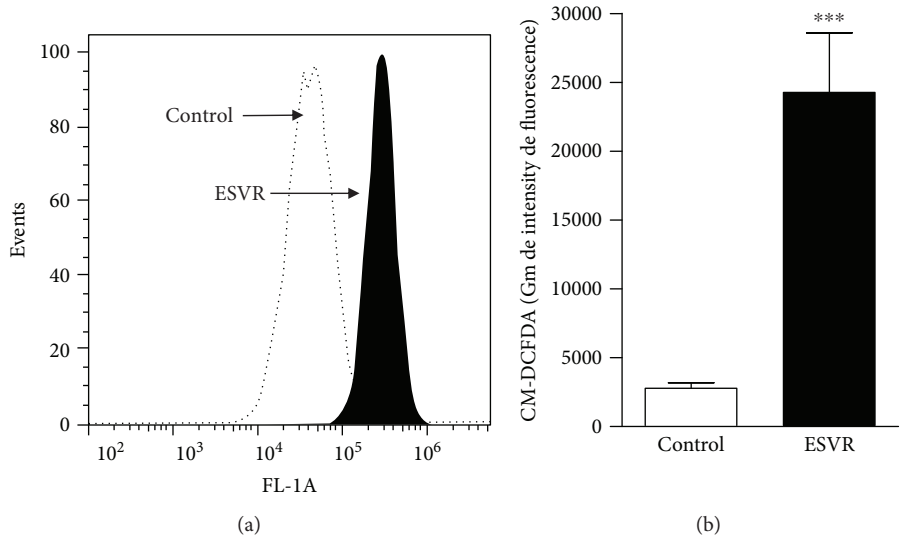

Figure 7: Determination of the levels of ROS in B16F10-Nex2 cells treated for 24 h with 52 μg/mL of ESVR, represented in a histogram (a) and bar graph (b). The data are expressed as the means ± SEM of three independent experiments in duplicate. $^{***}p < 0.001$ compared with control cells.

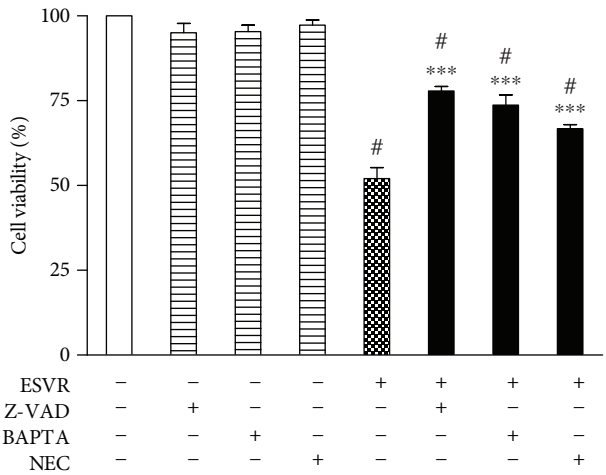

Figure 8: Effect of pan-caspase (Z-VAD-FMK), intracellular calcium channels (BAPTA-AM), and necrostatin-1 (NEC) inhibitors on B16F10-Nex2 cells treated or untreated for 24 h with ESVR at a concentration of 52 μg/mL. The data are expressed as the means ± SEM of three independent experiments in duplicate. $^{\#}p < 0.05$ compared with negative control cells and $^{***}p < 0.001$ compared with ESVR-treated cells.

characterized by chromatin condensation and DNA fragmentation, characteristic stages of death by apoptosis [45]. Apoptosis is considered a cell death process essential to homeostasis, mainly activated by extrinsic and intrinsic pathways [46]. In the extrinsic pathway, apoptotic receptors promote extracellular signaling. Conversely, in the intrinsic pathway, activation occurs in response to intracellular damage mediated by the mitochondria [47], a process characterized by the release of proapoptotic proteins into the cytosol, thereby promoting caspase activation and nuclear apoptosis.

Caspases are essential apoptotic cell death mediators [48]. Among these proteases, caspase-3 is one of the main effectors of programmed cell death because it is directly involved in nuclear apoptosis and cell death [49]. In this study, ESVR-treated B16F10-Nex2 cells showed doubled activated caspase-3 levels. In addition, the pan-caspase inhibitor Z-VAD-FMK reduced the percentage of cell death, thus demonstrating the involvement of caspases in the mechanism of cell death promoted by the extract.

Assessment of the activity of inhibitors showed that calcium and the necroptosis pathway are among the mechanisms involved in ESVR-induced cell death. High cytoplasmic Ca^{2+} levels are responsible for mitochondrial membrane permeabilization with cytochrome c release, thereby enhancing the signs of apoptosis [50–52].

Necroptosis is a form of cell death that shows characteristics of necrosis, but unlike necrosis, it may be regulated by receptor-interacting proteins 1 (RIP1) and 3 (RIP3) [53]. Furthermore, recent studies show that oxidative stress may promote necroptosis activation [54, 55]. Although necroptosis is not the main mechanism of death characterized by the action of ESVR, this finding is interesting, one which can be an alternative form of cell death to populations of cells exhibiting resistance to death by apoptosis.

Conversely, cancer cells also have a persistent prooxidative state and high ROS levels [56]. This different metabolism promotes an adaptive response that plays a key role in cancer cell proliferation, cell death signaling disruption, metastasis, and resistance to antitumor drugs [57, 58]. Nevertheless, cancer cells become vulnerable to prooxidant agents that further increase ROS levels, thus promoting cell death [56].

Some flavonoids, the main compounds of ESVR, are described in the literature as prooxidant agents in cancer cells [41, 59] because they can directly increase ROS production, resulting in superoxide radical formation [60], a mechanism

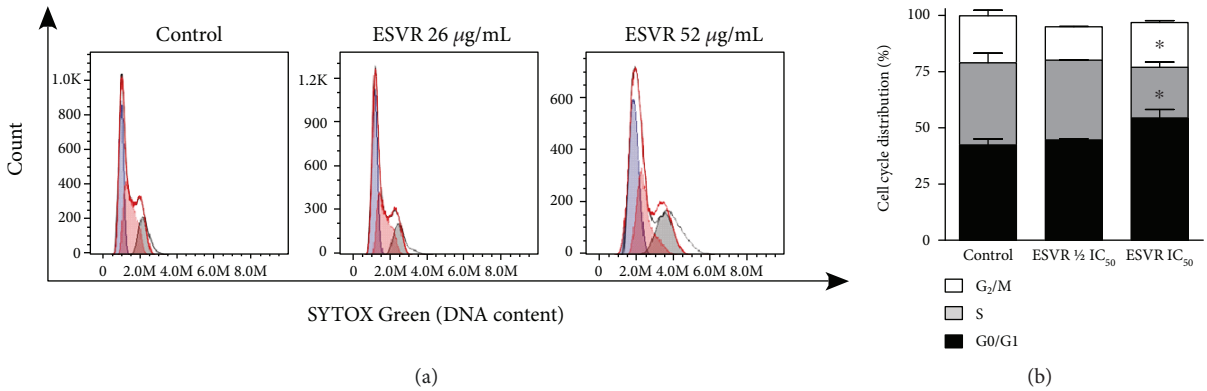

Figure 9: Histograms (a) and a bar graph (b) representative of the cell cycle distribution of control (untreated) B16F10-Nex2 cells and B16F10-Nex2 cells treated for 24 h with 1/2 IC_{50} = 26 μg/mL and IC_{50} = 52 μg/mL ESVR. The data are expressed as the means ± SEM of four independent experiments. $^{*}p < 0.05$ compared with control cells.

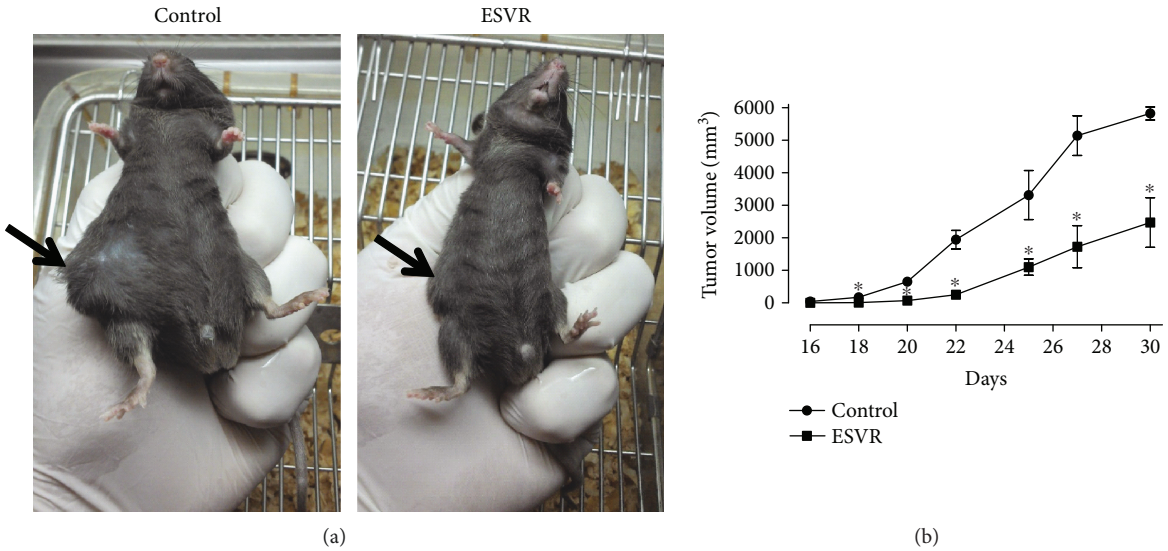

Figure 10: The effect of ESVR on the tumor volume of B16F10-Nex2 cells induced in C57Bl-6 mice. Representative images of 30-day tumors (arrows) in (a) control animals treated with RPMI 1640 medium and animals treated with ESVR. (b) A representative plot of tumor volume progression during 30 days of treatment. The data are expressed as the means ± SEM ($n = 7$). $^{*}p < 0.05$ compared with the control group.

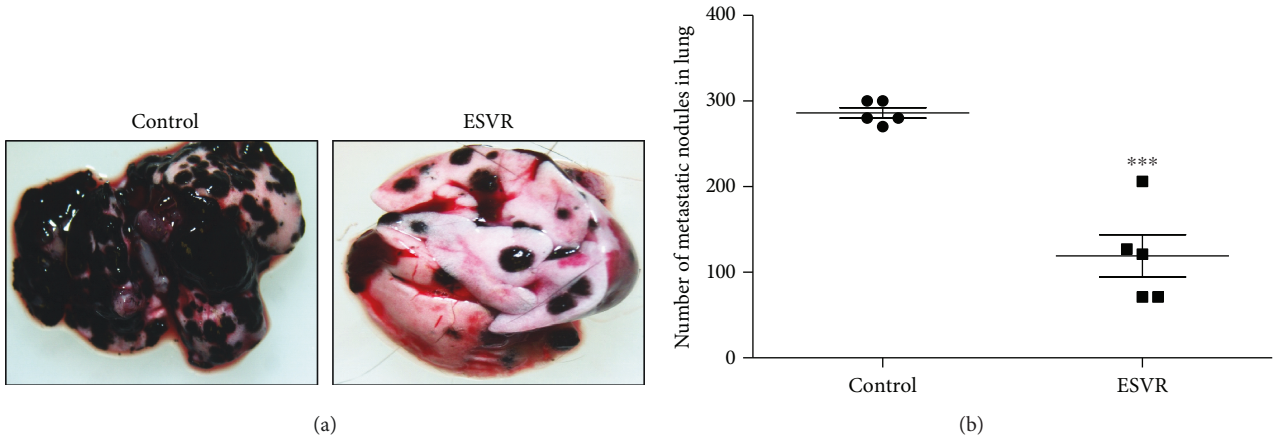

Figure 11: The effect of ESVR on the pulmonary metastasis of B16F10-Nex2 cells induced in C57Bl/6 mice. Representative lung images of (a) control animals treated with RPMI 1640 and animals treated with ESVR. (b) A graph representing the number of pulmonary metastasis in all animals after 14 days of endogenous cell inoculation. The data are expressed as the means ± SEM ($n = 5$). $^{***}p < 0.001$ compared with the control group.

whereby ESVR may have contributed to B16F10-Nex2 cell death because the intracellular ROS levels were high. Furthermore, anthracene derivatives, another group of compounds identified in ESVR, are described for inducing apoptosis by increasing ROS production [54].

Another activity promoted by the extract was cell cycle arrest at the sub-G_0/G_1 phase, accompanied by a decrease in the percentage of S phase cells. Some flavonoids, such as catechins, can cause cell cycle arrest at the G_0/G_1 phase of the cell cycle [55, 61]. Piceatannol decreases cyclin-dependent kinase 1 (CDK1), which is responsible for cell cycle progression from the G_1 phase to the S phase [62]. Thus, considering the importance of the cyclin-dependent kinases involved in cell cycle regulation and the uncontrolled cell proliferation in tumor cells, compounds capable of inhibiting the cell cycle progression of these cells may be important alternatives for tumor volume control [63, 64].

In this study, after confirmed *in vitro* antitumor action in B16F10-Nex2 murine melanoma cells, we demonstrated that ESVR produces antitumor activity on tumor volume progression and pulmonary nodule formation *in vivo*. Our data from *in vivo* antitumor assessment showed that primary tumor progression in ESVR-treated mice decreased by more than 50% compared with control mice. Cutaneous melanoma is one of the most aggressive forms of cancer, and no fully effective pharmacological therapy for advanced-stage metastatic melanoma is currently available [65, 66]. In these cases, metastases are responsible for the poor prognosis [67], affecting several organs, such as the bones, liver, and lungs [68]. The progression of pulmonary metastasis in ESVR-treated mice was markedly reduced, as observed in the formation of pulmonary nodules. This result may be related to the ability of the extract to reduce the migration and invasion of melanoma cells into the lungs. These effects may be related to the chemical constituents of ESVR, since epigallocatechin (one of the identified catechins), anthraquinones, and resveratrol (precursor molecule of piacetannol) are compounds reported to inhibit tumor growth [69–71] and progression of pulmonary metastasis [70] in animal models for melanoma. In addition, phenolic compounds are well described because they hamper metastasis by decreasing metalloprotease-9 expression in murine melanoma cells [72, 73]. Moreover, other studies showed that epigallocatechin can inhibit genes that synthesize proteins related to extracellular matrix degradation and cellular mobility, thereby reducing the process of melanoma metastasis [74].

In conclusion, this study demonstrated that ESVR contains flavonoid derivatives of catechins, anthraquinones, and piceatannol among its chemical constituents and promotes B16F10-Nex2 melanoma cell death via apoptosis induced by caspase-3 activation, the elevation of intracellular calcium and ROS levels, and cell cycle arrest at the G_0/G_1 phase. Furthermore, the extract showed *in vivo* antitumor activity in models of primary tumor volume progression and pulmonary nodule formation. These promising results open the door for further studies, both with the crude extract and with fractions isolated from *Senna velutina* roots, exploring its potential use in the treatment of melanoma and other cancers.

Data Availability

The experimental data used to support the findings of this study are included within the article.

Conflicts of Interest

The authors declare that there are no conflicts of interest.

Acknowledgments

This work was supported by grants from Fundação de Apoio ao Desenvolvimento do Ensino, Ciência e Tecnologia do Estado de Mato Grosso do Sul (FUNDECT); Coordenação de Aperfeiçoamento de Pessoal de Nível Superior (CAPES); and Conselho Nacional de Desenvolvimento Científico e Tecnológico (CNPq).

Supplementary Materials

Figure S1: the cytotoxic effect of ESVR on human melanoma cell lines SK-Mel-28 and SK-Mel-103 treated with different concentrations for (A) 24 h and (B) 48 h. The data are expressed as the means ± SEM in three independent experiments in triplicate. *(Supplementary Materials)*

References

[1] GBD 2015 Mortality and Causes of Death Collaborators, "Global, regional, and national life expectancy, all-cause mortality, and cause-specific mortality for 249 causes of death, 1980-2015: a systematic analysis for the global burden of disease study 2015," *The Lancet*, vol. 388, no. 10053, pp. 1459–1544, 2016.

[2] M. Eggermont, A. Spatz, and C. Robert, "Cutaneous melanoma," *The Lancet*, vol. 383, no. 9919, pp. 816–827, 2014.

[3] B. C. Bastian, "The molecular pathology of melanoma: an integrated taxonomy of melanocytic neoplasia," *Annual Review of Pathology: Mechanisms of Disease*, vol. 9, no. 1, pp. 239–271, 2014.

[4] D. C. Whiteman, C. A. Whiteman, and A. C. Green, "Childhood sun exposure as a risk factor for melanoma: a systematic review of epidemiologic studies," *Cancer Causes and Control*, vol. 12, no. 1, pp. 69–82, 2001.

[5] S. Gandini, F. Sera, M. S. Cattaruzza et al., "Meta-analysis of risk factors for cutaneous melanoma: III. Family history, actinic damage and phenotypic factors," *European Journal of Cancer*, vol. 41, no. 14, pp. 2040–2059, 2005.

[6] World Health Organization, "Skin cancers: how common is skin cancer," 2018, http://www.who.int/uv/faq/skincancer/en/index1.html.

[7] F. Erdmann, J. Lortet-Tieulent, and J. Schuz, "International trends in the incidence of malignant melanoma 1953–2008—are recent generations at higher or lower risk?," *Internacional Journal of Cancer*, vol. 132, no. 2, pp. 385–400, 2013.

[8] H. Tsao, M. B. Atkins, and A. J. Sober, "Management of cutaneous melanoma," *The New England Journal of Medicine*, vol. 351, no. 10, pp. 998–1012, 2004.

[9] M. Patel, E. Smyth, P. B. Chapman et al., "Therapeutic implications of the emerging molecular biology of uveal melanoma," *Clinical Cancer Research*, vol. 17, no. 8, pp. 2087–2100, 2011.

[10] A. M. Eggermont and C. Robert, "New drugs in melanoma: it's a whole new world," *European Journal of Cancer*, vol. 47, no. 14, pp. 2150–2157, 2011.

[11] T. Kim, R. N. Amaria, C. Spencer, A. Reuben, Z. A. Cooper, and J. A. Wargo, "Combining targeted therapy and immune checkpoint inhibitors in the treatment of metastatic melanoma," *Cancer Biology & Medicine*, vol. 11, no. 4, pp. 237–246, 2014.

[12] B. S. Kalal, D. Upadhya, and V. R. Pai, "Chemotherapy resistance mechanisms in advanced skin Cancer," *Oncology Reviews*, vol. 11, no. 1, p. 326, 2017.

[13] L. R. Strickland, H. C. Pal, C. A. Elmets, and F. Afaq, "Targeting drivers of melanoma with synthetic small molecules and phytochemicals," *Cancer Letters*, vol. 359, no. 1, pp. 20–35, 2015.

[14] S. J. Chatterjee and S. Pandey, "Chemo-resistant melanoma sensitized by tamoxifen to low dose curcumin treatment through induction of apoptosis and autophagy," *Cancer Biology & Therapy*, vol. 11, no. 2, pp. 216–228, 2011.

[15] A. Ghorbani and A. Hosseini, "Cancer therapy with phytochemicals: evidence from clinical studies," *Avicenna Journal of Phytomedicine*, vol. 5, no. 2, pp. 84–97, 2015.

[16] E. Solowey, M. Lichtenstein, S. Sallon, H. Paavilainen, and H. Lorberboum-Galski, "Evaluating medicinal plants for anticancer activity," *The Scientific World Journal*, vol. 2014, Article ID 721402, 12 pages, 2014.

[17] D. J. Newman and G. M. Cragg, "Natural products as sources of new drugs from 1981 to 2014," *Journal of Natural Products*, vol. 79, no. 3, pp. 629–661, 2016.

[18] J. Clardy and C. Walsh, "Lessons from natural molecules," *Nature*, vol. 432, no. 7019, pp. 829–837, 2004.

[19] S. L. Jothy, A. Torey, I. Darah et al., "*Cassia spectabilis* (DC) Irwin et Barn: A Promising Traditional Herb in Health Improvement," *Molecules*, vol. 17, no. 9, pp. 10292–10305, 2012.

[20] G. K. Varghese, L. V. Bose, and S. Habtemariam, "Antidiabetic components of *Cassia alata* leaves: identification through α-glucosidase inhibition studies," *Pharmaceutical Biology*, vol. 51, no. 3, pp. 345–349, 2013.

[21] M. P. Mokgotho, S. S. Gololo, P. Masoko et al., "Isolation and chemical structural characterisation of a compound with antioxidant activity from the roots of *Senna italica*," *Evidence-based Complementary and Alternative Medicine*, vol. 2013, Article ID 519174, 6 pages, 2013.

[22] A. D. C. Susunaga-Notario, S. Pérez-Gutiérrez, M. Á. Zavala-Sánchez et al., "Bioassay-Guided Chemical Study of the Anti-Inflammatory Effect of *Senna villosa* (Miller) H.S. Irwin & Barneby (Leguminosae) in TPA-Induced Ear Edema," *Molecules*, vol. 19, no. 7, pp. 10261–10278, 2014.

[23] G. Aviello, I. Rowland, C. I. Gill et al., "Anti-proliferative effect of rhein, an anthraquinone isolated from *Cassia* species, on Caco-2 human adenocarcinoma cells," *Journal of Cellular and Molecular Medicine*, vol. 14, no. 7, pp. 2006–2014, 2010.

[24] J. F. Campos, D. T. H. de Castro, M. J. Damião et al., "The chemical profile of *Senna velutina* leaves and their antioxidant and cytotoxic effects," *Oxidative Medicine and Cellular Longevity*, vol. 2016, Article ID 8405957, 12 pages, 2016.

[25] R. M. Pereira, G. Á. Ferreira-Silva, M. Pivatto et al., "Alkaloids derived from flowers of *Senna spectabilis*, (−)-cassine and (−)-spectaline, have antiproliferative activity on HepG2 cells for inducing cell cycle arrest in G_1/S transition through ERK inactivation and downregulation of cyclin D1 expression," *Toxicology In Vitro*, vol. 31, pp. 86–92, 2016.

[26] P. T. O. Saiki, B. Silva, and C. Lomônaco, "Expression of reproductive and vegetative characters of *Senna velutina* (Vogel) H. S. Irwin & Barneby (Leguminosae, Caesalpinioideae) in two distinct "cerrado" environments," *Brazilian Journal of Botany*, vol. 31, no. 2, pp. 363–369, 2008.

[27] S. M. Loverde-Oliveira, M. N. Freitas, P. K. B. Araújo, and I. B. C. Costa, "Fragmento de cerrado urbano da Universidade Federal de Mato Grosso, campus de Rondonópolis, Mato Grosso," *Biodiversidade*, vol. 9, no. 1, 2010.

[28] E. J. Paredes-Gamero, M. N. Martins, F. A. Cappabianco, J. S. Ide, and A. Miranda, "Characterization of dual effects induced by antimicrobial peptides: regulated cell death or membrane disruption," *Biochimica et Biophysica Acta (BBA) - General Subjects*, vol. 1820, no. 7, pp. 1062–1072, 2012.

[29] V. W. Moraes, A. C. Caires, E. J. Paredes-Gamero, and T. Rodrigues, "Organopalladium compound 7b targets mitochondrial thiols and induces caspase-dependent apoptosis in human myeloid leukemia cells," *Cell Death & Disease*, vol. 4, article e658, no. 6, 2013.

[30] F. V. Pereira, A. C. Melo, F. M. de Melo et al., "TLR4-mediated immunomodulatory properties of the bacterial metalloprotease arazyme in preclinical tumor models," *Oncoimmunology*, vol. 5, no. 7, article e1178420, 2016.

[31] B. Shen, "A new golden age of natural products drug discovery," *Cell*, vol. 163, no. 6, pp. 1297–1300, 2015.

[32] J. F. Campos, P. P. T. Espindola, H. F. V. Torquato et al., "Leaf and root extracts from *Campomanesia adamantium* (Myrtaceae) promote apoptotic death of leukemic cells via activation of intracellular calcium and caspase-3," *Frontiers in Pharmacology*, vol. 8, no. 8, article 466, 2017.

[33] T. Bonamigo, J. F. Campos, A. S. Oliveira et al., "Antioxidant and cytotoxic activity of propolis of *Plebeia droryana* and *Apis mellifera* (Hymenoptera, Apidae) from the Brazilian Cerrado biome," *PLoS One*, vol. 12, no. 9, p. e0183983, 2017.

[34] G. B. Longato, L. Y. Rizzo, I. M. Sousa et al., "*In vitro* and *in vivo* anticancer activity of extracts, fractions, and eupomatenoid-5 obtained from *Piper regnellii* leaves," *Planta Medica*, vol. 77, no. 13, pp. 1482–1488, 2011.

[35] W. Y. Huang, Y. Z. Cai, and Y. Zhang, "Natural phenolic compounds from medicinal herbs and dietary plants: potential use for cancer prevention," *Nutrition and Cancer*, vol. 62, no. 1, pp. 1–20, 2010.

[36] S. Gorlach, J. Fichna, and U. Lewandowska, "Polyphenols as mitochondria-targeted anticancer drugs," *Cancer Letters*, vol. 366, no. 2, pp. 141–149, 2015.

[37] L. Schroder, P. Marahrens, J. G. Koch et al., "Effects of green tea, matcha tea and their components epigallocatechin gallate and quercetin on MCF-7 and MDA-MB-231 breast carcinoma cells," *Oncology Reports*, vol. 41, no. 1, pp. 387–396, 2018.

[38] C. C. Chen, D. S. Hsieh, K. J. Huang et al., "Improving anticancer efficacy of (-)-epigallocatechin-3-gallate gold nanoparticles in murine B16F10 melanoma cells," *Drug Design Development and Therapy*, vol. 8, pp. 459–474, 2014.

[39] M. Genov, B. Kreiseder, M. Nagl, E. Drucker, and e. al, "Tetrahydroanthraquinone derivative (±)-4-deoxyaustrocortilutein induces cell cycle arrest and apoptosis in melanoma cells via upregulation of p21 and p53 and downregulation of NF-kappaB," *Journal of Cancer*, vol. 7, no. 5, pp. 555–568, 2016.

[40] M. Du, Z. Zhang, and T. Gao, "Piceatannol induced apoptosis through up-regulation of microRNA-181a in melanoma cells," *Biological Research*, vol. 50, no. 1, p. 36, 2017.

[41] S. Li, L. Wu, J. Feng et al., "*In vitro* and *in vivo* study of epigallocatechin-3-gallate-induced apoptosis in aerobic glycolytic hepatocellular carcinoma cells involving inhibition of phosphofructokinase activity," *Scientific Reports*, vol. 6, no. 1, article 28479, 2016.

[42] K. Phuriwat, P. Pattamaphron, R. Lysiane, P. Dumrongsak, and S. Piyarat, "Epistructured catechins, EGCG and EC facilitate apoptosis induction through targeting de novo lipogenesis pathway in HepG2 cells," *Cancer Cell International*, vol. 18, no. 1, 2018.

[43] G. A. Potter, L. H. Patterson, E. Wanogho et al., "The cancer preventative agent resveratrol is converted to the anticancer agent piceatannol by the cytochrome P450 enzyme CYP1B1," *British Journal of Cancer*, vol. 86, no. 5, pp. 774–778, 2002.

[44] Y. H. Kim, C. Park, J. O. Lee et al., "Induction of apoptosis by piceatannol in human leukemic U937 cells through down-regulation of Bcl-2 and activation of caspases," *Oncology Reports*, vol. 19, no. 4, pp. 961–967, 2008.

[45] S. Nagata, "Apoptotic DNA fragmentation," *Experimental Cell Research*, vol. 256, no. 1, pp. 12–18, 2000.

[46] G. Xu and Y. Shi, "Apoptosis signaling pathways and lymphocyte homeostasis," *Cell Research*, vol. 17, no. 9, pp. 759–771, 2007.

[47] T. Vanden Berghe, W. J. Kaiser, M. J. Bertrand, and P. Vandenabeele, "Molecular crosstalk between apoptosis, necroptosis, and survival signaling," *Molecular & Cellular Oncology*, vol. 2, no. 4, article e975093, 2015.

[48] D. R. McIlwain, T. Berger, and T. W. Mak, "Caspase functions in cell death and disease," *Cold Spring Harbor Perspectives in Biology*, vol. 5, no. 4, article a008656, 2013.

[49] A. G. Porter and R. U. Janicke, "Emerging roles of caspase-3 in apoptosis," *Cell Death & Differentiation*, vol. 6, no. 2, pp. 99–104, 1999.

[50] R. Rizzuto, P. Pinton, W. Carrington et al., "Close contacts with the endo-plasmic reticulum as determinants of mitochondrial Ca^{2+} responses," *Science*, vol. 280, no. 5370, pp. 1763–1766, 1998.

[51] Y. Yan, C. L. Wei, W. R. Zhang, H. P. Cheng, and J. Liu, "Cross-talk between calcium and reactive oxygen species signaling," *Acta Pharmacologica Sinica*, vol. 27, no. 7, pp. 821–826, 2006.

[52] C. Giorgi, A. Romagnoli, P. Pinton, and R. Rizzuto, "Ca^{2+} signaling, mitochondria and cell death," *Current Molecular Medicine*, vol. 8, no. 2, pp. 119–130, 2008.

[53] M. D'Arcy, "Cell death: A review of the major forms of apoptosis, necrosis and autophagy," *Cell Biology International*, 2019.

[54] S. Q. Xie, Z. Q. Zhang, G. Q. Hu, M. Xu, and B. S. Ji, "HL-37, a novel anthracene derivative, induces ca(2+)-mediated apoptosis in human breast cancer cells," *Toxicology*, vol. 254, no. 1-2, pp. 68–74, 2008.

[55] G. J. Du, Z. Zhang, and X. D. Wen, "Epigallocatechin gallate (EGCG) is the most effective cancer chemopreventive polyphenol in green tea," *Nutrients*, vol. 4, no. 11, pp. 1679–1691, 2012.

[56] L. Gibellini, M. Pinti, M. Nasi et al., "Interfering with ROS metabolism in cancer cells: the potential role of quercetin," *Cancers*, vol. 2, no. 2, pp. 1288–1311, 2010.

[57] D. Trachootham, J. Alexandre, and P. Huang, "Targeting cancer cells by ROS-mediated mechanisms: a radical therapeutic approach?," *Nature Review Drug Discovery*, vol. 8, no. 7, pp. 579–591, 2009.

[58] L. Zhu, L. Ren, Y. Chen, J. Fang, Z. Ge, and X. Li, "Redox status of high-mobility group box 1 performs a dual role in angiogenesis of colorectal carcinoma," *Journal of Cellular and Molecular Medicine*, vol. 19, no. 9, pp. 2128–2135, 2015.

[59] C. Martin-Cordero, A. J. Leon-Gonzalez, J. M. Calderon-Montano, E. BurgosMoron, and M. Lopez-Lazaro, "Pro-oxidant natural products as anticancer agents," *Current Drug Targets*, vol. 13, no. 8, pp. 1006–1028, 2012.

[60] W. F. Hodnick, E. B. Milosavljevic, J. H. Nelson, and R. S. Pardini, "Electrochemistry of flavonoids: Relationships between redox potentials, inhibition of mitochondrial respiration, and production of oxygen radicals by flavonoids," *Biochemical Pharmacology*, vol. 37, no. 13, pp. 2607–2611, 1988.

[61] I. Cordero-Herrera, M. A. Martín, L. Bravo, L. Goya, and S. Ramos, "Epicatechin gallate induces cell death via p53 activation and stimulation of p38 and JNK in human colon cancer SW480 cells," *Nutrition and Cancer*, vol. 65, no. 5, pp. 718–728, 2013.

[62] Y. M. Lee, D. Y. Lim, H. J. Cho et al., "Piceatannol, a natural stilbene from grapes, induces G1 cell cycle arrest in androgen-insensitive DU145 human prostate cancer cells via the inhibition of CDK activity," *Cancer Letters*, vol. 285, no. 2, pp. 166–173, 2009.

[63] W. Nam, J. Tak, J. K. Ryu et al., "Effects of artemisinin and Its derivatives on growth inhibition and apoptosis of oral cancer cells," *Head & Neck*, vol. 29, no. 4, pp. 335–340, 2007.

[64] S. Diaz-Moralli, M. Tarrado-Castellarnau, A. Miranda, and M. Cascante, "Targeting cell cycle regulation in cancer therapy," *Pharmacology & Therapeutics*, vol. 138, no. 2, pp. 255–271, 2013.

[65] Y. Kotobuki, L. Yang, S. Serada et al., "Periostin accelerates human malignant melanoma progression by modifying the melanoma microenvironment," *Pigment Cell Melanoma Research*, vol. 27, no. 4, pp. 630–639, 2014.

[66] F. Zhao, X. He, J. Sun et al., "Cancer stem cell vaccine expressing ESAT-6-gpi and IL-21 inhibits melanoma growth and metastases," *American Journal of Translational Research*, vol. 7, no. 10, pp. 1870–1882, 2015.

[67] E. Maverakis, L. A. Cornelius, G. M. Bowen et al., "Metastatic melanoma—a review of current and future treatment options," *Acta Dermato-Venereologica*, vol. 95, no. 5, pp. 516–524, 2015.

[68] F. Tas, "Metastatic behavior in melanoma: timing, pattern, survival, and influencing factors," *Journal of Oncology*, vol. 2012, Article ID 647684, 9 pages, 2012.

[69] J. Zhang, Z. Lei, Z. Huang et al., "Epigallocatechin-3-gallate(EGCG) suppresses melanoma cell growth and metastasis by targeting TRAF6 activity," *Oncotarget*, vol. 7, no. 48, pp. 79557–79571, 2016.

[70] J. Xie, J. P. Yun, Y. N. Yang et al., "A novel ECG analog 4-(*S*)-(2,4,6-trimethylthiobenzyl)-epigallocatechin gallate selectively induces apoptosis of B16-F10 melanoma via activation of autophagy and ROS," *Scientific Reports*, vol. 7, no. 1, article 42194, 2017.

[71] H. J. Ku, O. S. Kwon, B. S. Kang, D. S. Lee, H. S. Lee, and J. W. Park, "IDH2 knockdown sensitizes tumor cells to emodin cytotoxicity in vitro and in vivo," *Free Radical Research*, vol. 50, no. 10, pp. 1089–1097, 2016.

[72] H. G. Farina, M. Pomies, D. F. Alonso, and D. E. Gomez, "Antitumor and antiangiogenic activity of soy isoflavone genistein in mouse models of melanoma and breast cancer," *Oncology Reports*, vol. 16, no. 4, pp. 885–891, 2006.

[73] S. J. Pradhan, R. Mishra, P. Sharma, and G. C. Kundu, "Quercetin and sulforaphane in combination suppress the progression of melanoma through the down-regulation of matrix metalloproteinase-9," *Experimental and Therapeutic Medicine*, vol. 1, no. 6, pp. 915–920, 2010.

[74] M. W. Roomi, T. Kalinovsky, A. Niedzwiecki, and M. Rath, "Modulation of MMP-2 and -9 secretion by cytokines, inducers and inhibitors in human melanoma A-2058 cells," *Oncology Reports*, vol. 37, no. 6, pp. 3681–3687, 2017.

Hindawi
Oxidative Medicine and Cellular Longevity
Volume 2019, Article ID 5083158, 14 pages
https://doi.org/10.1155/2019/5083158

Research Article

Betulinic Acid Induces ROS-Dependent Apoptosis and S-Phase Arrest by Inhibiting the NF-κB Pathway in Human Multiple Myeloma

Min Shen,[1] **Yiqiang Hu**,[2] **Yan Yang**,[1] **Lanlan Wang**,[3] **Xin Yang**,[1] **Bo Wang**,[4] **and Mei Huang**[1]

[1]*Department of Hematology, Tongji Hospital, Tongji Medical College, Huazhong University of Science and Technology, Wuhan 430030, China*
[2]*Department of Orthopaedics, Union Hospital, Tongji Medical College, Huazhong University of Science and Technology, Wuhan 430022, China*
[3]*Department of Hematology, Wuhan First Hospital, Huazhong University of Science and Technology, Wuhan 430022, China*
[4]*Department of Rehabilitation, Union Hospital, Tongji Medical College, Huazhong University of Science and Technology, Wuhan 430022, China*

Correspondence should be addressed to Mei Huang; cherrywjw@163.com

Received 4 February 2019; Revised 8 April 2019; Accepted 24 April 2019; Published 9 June 2019

Guest Editor: Ana S. Fernandes

Betulinic acid (BA), as a prospective natural compound, shows outstanding antitumor bioactivities against many solid malignancies. However, its mechanism against multiple myeloma (MM) remains elusive. Herein, for the first time, we studied the antitumor activity of BA against MM both *in vivo* and *in vitro*. We showed that BA mediated cytotoxicity in MM cells through apoptosis, S-phase arrest, mitochondrial membrane potential (MMP) collapse, and overwhelming reactive oxygen species (ROS) accumulation. Moreover, when the ROS scavenger N-acetyl cysteine (NAC) effectively abated elevated ROS, the BA-induced apoptosis was partially reversed. Our results revealed that BA-mediated ROS overproduction played a pivotal role in anticancer activity. Molecularly, we found that BA resulted in marked inhibition of the aberrantly activated NF-κB pathway in MM. As demonstrated by using the NF-κB pathway-specific activator TNF-α and the inhibitor BAY 11-7082, BA-mediated inhibition of the NF-κB pathway directly promoted the overproduction of ROS and, ultimately, cell death. Furthermore, BA also exerted enormous tumor-inhibitory effects via repressing proliferation and inhibiting the NF-κB pathway in our xenograft model. Overall, by blocking the NF-κB pathway that breaks redox homeostasis, BA, as a potent NF-κB inhibitor, is a promising therapeutic alternative for MM.

1. Introduction

Multiple myeloma (MM), an incurable plasma cell cancer, is the second most prevalent hematological malignancy [1]. Many patients do not respond to current therapies and ultimately succumb to the disease, primarily because of drug resistance, apoptosis evasion, and an ability to grow independent of the bone marrow microenvironment, especially for patients in high-risk biological states [2, 3]. Thus, there is an urgent need to find effective drugs for treating MM.

Betulinic acid (BA), a lupane-structured pentacyclic triterpenoid, is a plant-derived product ubiquitously distributed throughout the plant kingdom [4]. Previous studies have demonstrated its multiple bioactivities, such as antitumor, anti-inflammatory, anti-HIV, and hepatoprotective activities [5, 6]. Among these properties, the antitumor activities have attracted considerable attention worldwide. Indeed, without causing obvious toxicity toward normal cells [7], growing evidence indicates that BA exhibits significant cytotoxicity against many malignancies [4, 8–10]. However, with regard

to MM, its underlying mechanisms and relevant molecular targets have not yet been thoroughly elucidated.

Reactive oxygen species (ROS), which are byproducts of normal mitochondrial metabolism and homeostasis, include oxygen free radicals and nonradical oxidants such as O_2^-, OH^-, H_2O_2, and NO [11, 12]. ROS generally play a dual role in living systems [13]. Specifically, ROS play a beneficial role at low or moderate levels, whereas a burst of ROS can destroy cellular homeostasis, as manifested by disruption of the mitochondrial membrane potential (MMP), release of cytochrome c (cyt c), activation of the caspase cascade, and ultimate induction of apoptosis [11, 14]. BA-induced cell death via excessive ROS has actually been reported in other tumors [15, 16], and we hypothesized that BA may act in a similar way against MM.

The nuclear factor-kappa B (NF-κB) pathway, a key link between inflammation and cancer, plays important roles in inflammation, cell proliferation, and apoptosis [17–20]. Aberrant and stable activation of NF-κB signaling has been reported in a wide range of malignancies, particularly MM [18, 21, 22]. Although the BA-mediated transcriptional activities of NF-κB vary in cancers [10, 23], the dysregulation of the NF-κB pathway is closely related to ROS levels and cellular redox balance [24–26]; however, this phenomenon has not yet been tested in MM, and its potential mechanism remains a mystery.

Accordingly, we aimed to evaluate the efficacy of BA against MM both *in vitro* and *in vivo*, to investigate the underlying mechanisms, and to illuminate the complex regulatory interactions between ROS and the NF-κB pathway.

2. Material and Methods

2.1. Reagents and Antibodies. BA (purity ≥ 98%, Sigma-Aldrich, St. Louis, MO, USA) was dissolved in DMSO (Sigma-Aldrich) as a 40 mM stock solution and stored at −20°C. BAY 11-7082 and N-acetyl cysteine (NAC) were purchased from Beyotime (Shanghai, China). TNF-α was acquired from PeproTech (Rocky Hill, NJ, USA). Primary antibodies specific for Bax, Bcl-2, cleaved caspase-3, NF-κB p65, NF-κB p65 (phosphoS536), IκBα, IκBα (phosphoS32), cleaved PARP1, cyt c, CDK2, and cyclin A2 were purchased from Abcam (Cambridge, MA, USA). Primary antibodies specific for cleaved caspase-8, cleaved caspase-9, phospho-IKKα/β (Ser176/180), GAPDH, $p21^{Waf1/Cip1}$, and $p27^{Kip}$ were purchased from Cell Signaling Technology (Danvers, MA, USA). Secondary rabbit anti-mouse and goat anti-rabbit antibodies were purchased from Santa Cruz Biotechnology (Dallas, Texas, USA).

2.2. Cell Culture and Treatments. Human multiple myeloma U266 and RPMI 8226 cell lines were obtained from the China Center for Type Culture Collection (CCTCC). U266 and RPMI 8226 cells were routinely cultured in RPMI 1640 medium (HyClone, Logan, UT, USA) with 10% fetal bovine serum (FBS, Thermo Fisher Scientific, Waltham, MA, USA) and 1% penicillin/streptomycin (Beyotime, China). The cells were maintained in a humidified incubator at 37°C with 5% CO_2 and subcultured at approximately 80-90% confluence. The cells were treated with various concentrations of BA (10, 20, and 40 μM), and DMSO (0.1%) was used as a vehicle/control.

2.3. Hoechst 33342 Staining. Apoptotic cells were detected by Hoechst 33342 (Invitrogen, Carlsbad, CA, USA) staining. BA-treated cells were collected and fixed with 1 ml of 4% paraformaldehyde for approximately 20 min. After fixation, the cells were washed three times with PBS and incubated with 1 ml of Hoechst 33342 dye for 20 min in the dark. Morphological changes in nuclear chromatin were observed under a fluorescence microscope (Olympus, Japan).

2.4. CCK-8 and EdU Proliferation Assay. Cell viability was estimated using the CCK-8 kit (Dojindo, Kumamoto, Japan). MM cells were seeded in 100 μl of medium in 96-well plates at a density of 1×10^4 cells per well, and 10 μl of CCK-8 solution was added after 6, 12, 24, and 48 h of incubation. The absorbance at 450 nm was measured 4 h later. Each experiment was performed independently in triplicate. Cell proliferation was detected using the Click-iT™ EdU-555 kit (Life Technologies, Grand Island, NY, USA) according to the manufacturer's instructions. After staining, fluorescence images were obtained using a fluorescence microscope (Olympus, Japan).

2.5. Annexin V/Propidium Iodide (PI) Double Staining. Apoptosis was detected by annexin V/PI (BD Biosciences, San Jose, CA, USA) double staining. The cells were harvested and washed twice with PBS at 4°C, resuspended in 200 μl of binding buffer, and labeled with 5 μl of annexin V and 5 μl of PI in the dark for 15 min. The total apoptosis ratio was calculated as the sum of early and late apoptosis, as detected by flow cytometry (BD LSR II, USA).

2.6. Cell Cycle Analysis. The cell cycle was analyzed using a cell cycle kit (BD Biosciences) according to the manufacturer's protocol. Briefly, the cells were collected and fixed overnight in 70% ethanol at −20°C. After centrifugation at 600 ×g for 5 min, the cells were rehydrated in 3 ml of PBS for 15 min and then resuspended and incubated in 1 ml of DNA staining solution at 37°C for 30 min in the dark. The cell cycle distribution was detected by flow cytometry.

2.7. Measurement of MMP ($\Delta\psi M$). A JC-1 assay kit (Beyotime) was used to explore MMP transition. The cells were harvested, loaded with a 10 μM concentration of the JC-1 probe, and then incubated at 37°C with 5% CO_2 for 20 min in the dark. After incubation, the cells were washed twice with cold staining buffer and resuspended. The MMP transition was measured by flow cytometry, and fluorescence graphs were acquired using a fluorescence microscope (Olympus, Japan).

2.8. Evaluation of ROS. Intracellular ROS generation was measured using a ROS detection kit (Invitrogen). The cells were stained with a 2,7-dichlorofluorescin diacetate (DCFH-DA) probe (10 μM) at 37°C for approximately 30 min and washed with serum-free medium. The median fluorescence intensity of ROS was measured by flow cytometry.

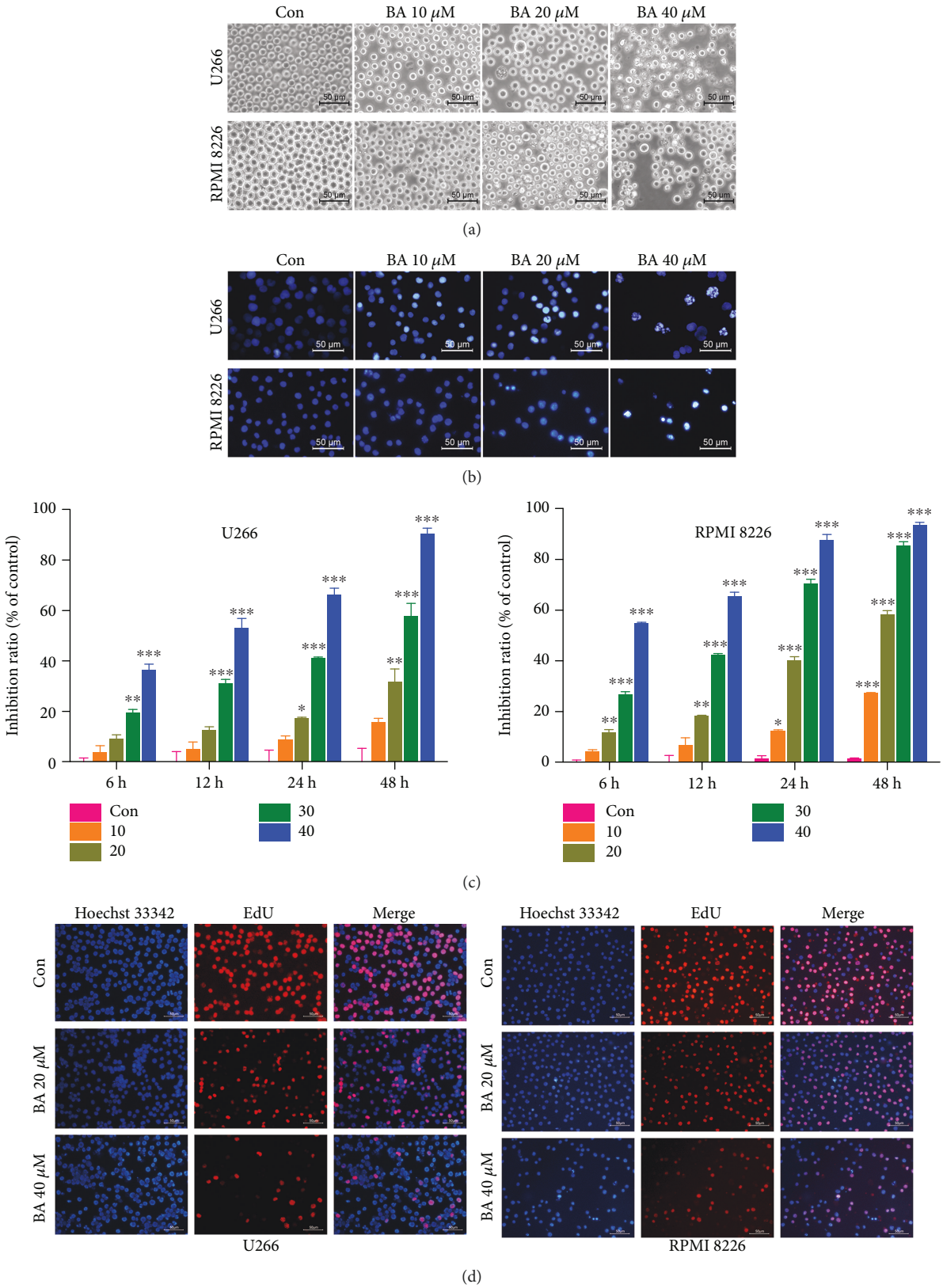

Figure 1: Continued.

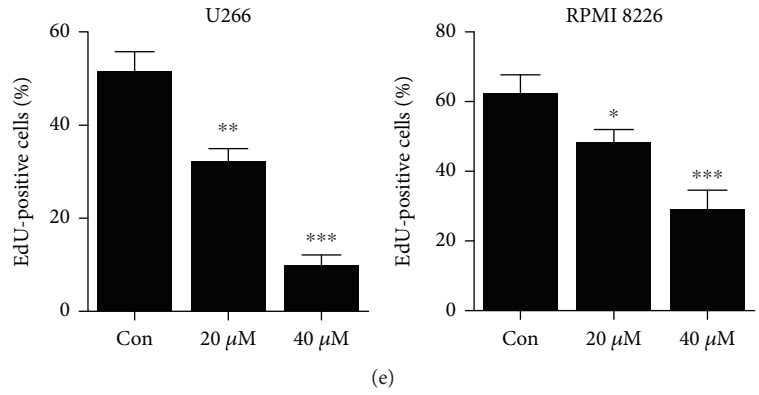

Figure 1: BA changed the morphology and inhibited the proliferation of MM cells. U266 and RPMI 8266 cells were exposed to different concentrations of BA (10, 20, 30, and 40 μM) or 0.1% DMSO (control group) for 12 h. (a) BA induced obvious morphological changes, with shrunken and broken dead cells visible under phase-contrast microscopy. (b) Apoptotic cells with nuclear pyknosis and asymmetric chromatin condensation were brightly stained with Hoechst 33342. (c) CCK-8 was used to evaluate inhibitory effects after treatment with different concentrations of BA for various hours (6, 12, 24, and 48 h). The results are presented as the mean ± SD of three independent experiments. $^{*}P < 0.05$; $^{**}P < 0.01$; and $^{***}P < 0.001$. (d) EdU staining was used to detect cell proliferation. EdU-positive cells (red fluorescence) were significantly decreased in a concentration-dependent manner after BA treatment for 12 h. (e) Quantitative analysis of EdU-positive cells. $^{*}P < 0.05$; $^{**}P < 0.01$; and $^{***}P < 0.001$.

All steps were strictly executed according to the manufacturer's instructions.

2.9. Malondialdehyde (MDA) Assay and Superoxide Dismutase (SOD) Assay. Lipid peroxidation was evaluated by a MDA assay kit (Nanjing Jiancheng Bioengineering Institute, China) based on the thiobarbituric acid (TBA) method. The absorbance was measured at 532 nm. Intracellular antioxidant SOD activity was assessed using a commercially available kit (Nanjing Jiancheng Bioengineering Institute) based on the autooxidation of hydroxylamine. The absorbance was measured at 550 nm. All the procedures were carried out following the manufacturer's instructions.

2.10. Real-Time PCR. After 12 hours of treatment with 40 μM BA, total RNA was extracted from U266 cells using the TRIzol reagent (Invitrogen) according to the manufacturer's protocol. The isolated RNA was subsequently reverse-transcribed into complementary DNA with reverse transcriptase (Toyobo, Japan). The PCR reaction mixture was prepared using an SYBR Green master mix (Toyobo) with primers as follows: GAPDH: forward 5′-AATCCCATCAC CATCTTCCAG-3′ and reverse 5′-GAGCCCCAGCCTTC TCCAT-3′; SOD2: forward 5′-AACCTCACATCAACGC GCA-3′ and reverse 5′-TCTCCTCGGTGACGTTCAGG-3′; FHC: forward 5′-CATCAACCGCCAGATCAACC-3′ and reverse 5′-CACATCATCGCGGTCAAAGT-3′; GCLM: forward 5′-ACCTCTGATCTAGACAAAACA CAGT-3′ and reverse 5′-ACACAGCAGGAGGCAAGAT TA-3′; and GSTM: forward 5′-AACCAGTTTATGGACA GCCG-3′ and reverse 5′-AGGCAGCTGGGCTCAAATA C-3′. The real-time quantitative PCR was performed using an ABI 7900HT Sequence Detection System (Applied Biosystems, Foster City, CA). Relative quantification of target mRNA expression was calculated using the $2^{(-\Delta\Delta CT)}$ method and further normalized to GAPDH mRNA.

2.11. Western Blot Analysis. RIPA lysis buffer (Sigma) containing a proteinase inhibitor cocktail (Servicebio, Wuhan, China) and phenylmethanesulfonyl fluoride (Servicebio) was used to extract total proteins. The protein concentration was measured using a BCA assay (Invitrogen). Proteins (30 μg) were separated by 12% SDS-PAGE and electrotransferred onto polyvinylidene fluoride (PVDF) membranes (Millipore, USA). The membranes were blocked with 5% nonfat milk for 1 h, followed by overnight incubation with specific primary antibodies at 4°C. The membranes were washed three times for 10 min each, incubated with a secondary antibody for 1 h at room temperature, and washed again. Finally, the bands were visualized using an ECL kit (Thermo Scientific, Rockford, IL, USA).

2.12. Immunofluorescence Staining. Cells were attached to glass slides using cytospin, fixed with 4% paraformaldehyde, and permeabilized with 0.3% Triton X-100. After being blocked with 5% BSA for 15 min at room temperature, the cells were incubated overnight at 4°C with primary antibody, washed 3 times with PBS, and stained with an Alexa Fluor 488-conjugated secondary antibody for 1 h. Nuclei were stained with Hoechst 33342. Images were captured using a fluorescence microscope. The standard semiquantitative evaluation of NF-κB p65 was performed using ImageJ software (NIH, Bethesda, MD).

2.13. Nude Mouse Xenograft Model. Experiments involving animals were approved by the Experimental Animal Ethical Committee of Huazhong University of Science and Technology and were conducted in strict accordance with the National Institutes of Health Guide for the Care and Use of Laboratory Animals. Five-week-old BALB/c nude mice (16-20 g) were purchased from Beijing HFK Bioscience. U266 cells (1×10^7) were suspended in 100 μl of PBS and subcutaneously inoculated into the axilla of the right forelimbs of the mice. Nine days later, the majority of tumors grew to

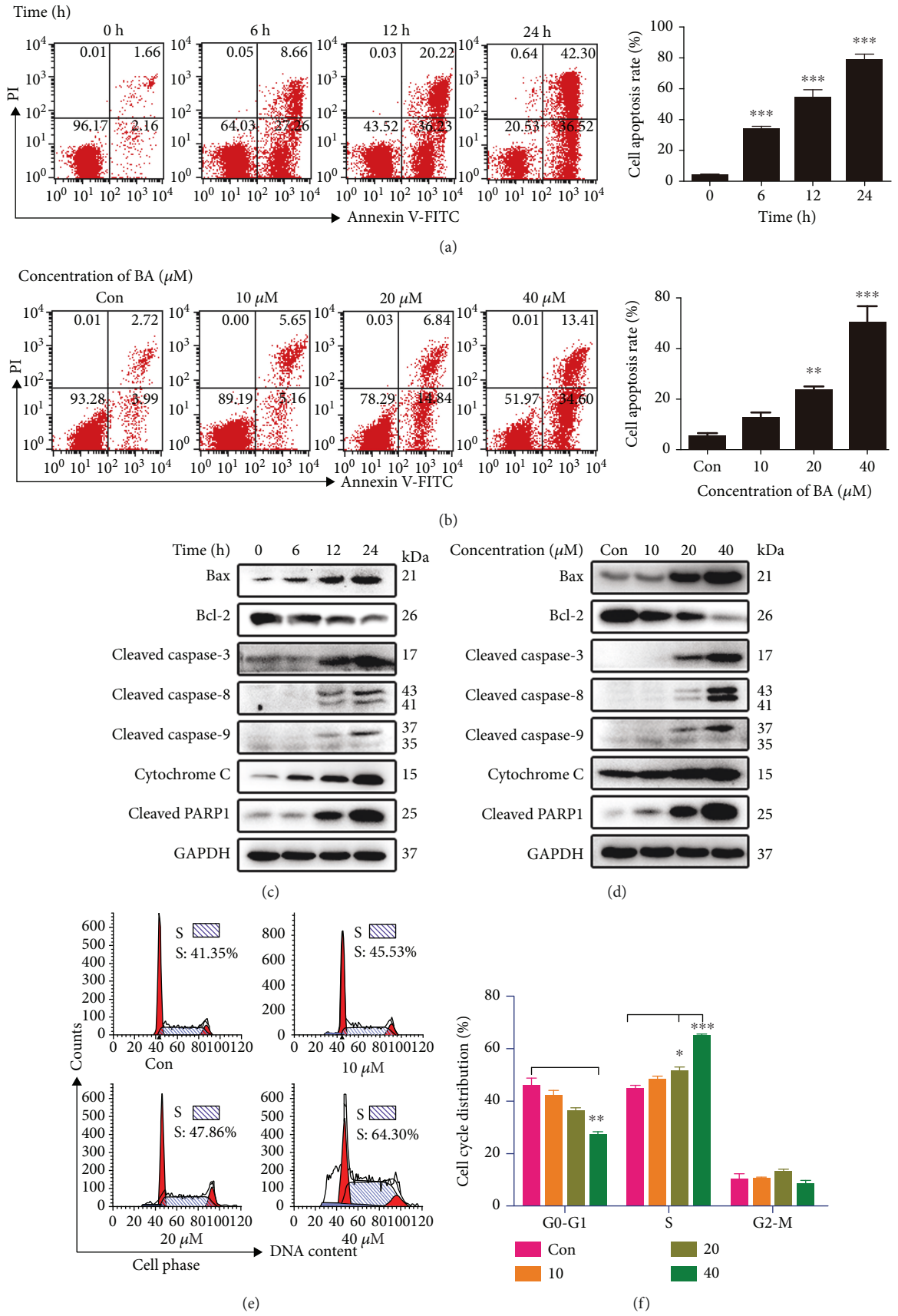

Figure 2: Continued.

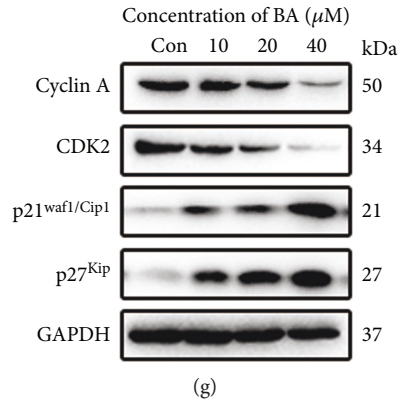

Figure 2: BA promoted apoptosis and S-phase arrest in U266 cells. (a) BA (40 μM) was applied to U266 cells for different periods of time, and representative graphs and statistical analysis of annexin V/PI double staining are displayed; $^{***}P < 0.001$. (b) U266 cells were cultured with the indicated concentrations of BA for 12 h, and representative flow cytometry graphs and statistical analysis of apoptosis are shown. $^{**}P < 0.01$; $^{***}P < 0.001$. (c, d) The expression levels of the mitochondrial apoptosis proteins Bax, Bcl-2, cleaved caspase-3, caspase-8, and caspase-9, cytochrome C, and cleaved PARP1 were evaluated by Western blotting after treatment with 40 μM BA for the indicated times or after exposure to the indicated concentrations for 12 h. (e, f) The indicated concentrations of BA were applied to U266 cells for 12 h. Representative graphs and quantitative cell cycle analysis after flow cytometry. $^{*}P < 0.05$; $^{**}P < 0.01$; and $^{***}P < 0.001$. (g) Expression levels of the S-phase-related proteins cyclin A, CDK2, $p21^{Waf1/Cip1}$, and $p27^{Kip}$ were detected by Western blotting.

approximately 100 mm^3, and the tumor-bearing mice were randomly assigned into two groups (five mice per group). The control and experimental groups were intraperitoneally administered a solvent (100 μl of PBS with 0.1% DMSO) or BA (20 mg/kg), respectively, at 3-day intervals. Using a caliper, the tumor volume was calculated as the length $(mm) \times$ width $(mm)^2/2$. At the end of the experiment, the mice were sacrificed, and the tumors were isolated for further study.

2.14. Immunohistochemistry (IHC). Subcutaneous xenograft tumors were prepared for IHC analysis. IHC was performed in a Leica Bond Max automated system (Leica Biosystems, Nussloch, Germany) using the Leica-Refine detection kit (Leica Biosystems, DS9800). Briefly, after deparaffinization, rehydration, and antigen retrieval, the sections were incubated with an anti-Ki-67 antibody (1 : 200, Abcam) and an anti-NF-κB p65 antibody (1 : 100, Abcam) for 30 min at room temperature. After washing, the sections were incubated with a horseradish peroxidase-conjugated secondary antibody, visualized with diaminobenzidine, and counterstained with hematoxylin. The stained slides were observed under a microscope (Olympus, Japan).

2.15. Statistical Analysis. Data obtained from at least three separate experiments are presented as the means ± SD. Differences between three or more groups were assessed using one-way ANOVA, followed by Tukey's multiple comparison test. Two-tailed Student's t-test was used in the analysis of two-group parameters. All statistical analyses were performed using GraphPad Prism 6.0. $P < 0.05$ was defined as statistically significant.

3. Results

3.1. BA Promotes Morphological Changes in MM Cells. Incubation of MM cells with different concentrations of BA for 12 h elicited marked morphological changes that included shrunken and broken dead cells and cell debris under phase-contrast microscopy (Figure 1(a)). Apoptotic cells with wrinkled membranes, condensed nuclei, and fragmented chromatin were brightly stained and clearly visible after Hoechst 33342 staining (Figure 1(b)), especially in the high-dose group. These morphological observations indicated the concentration-dependent antitumor effects of BA on MM cells.

3.2. BA Inhibits MM Cell Viability and Proliferation. To objectively investigate the antitumor activities of BA against MM cells, we first employed the CCK-8 assay to evaluate cytotoxic effects. As shown in Figure 1(c), cell viability was inhibited in a concentration-dependent manner in both cell lines. Additionally, the EdU assay visually suggested the inhibitory effects of BA (Figure 1(d)). After treatment with different concentrations of BA for 12 h, the frequency of red-fluorescent MM cells (proliferative cells) was significantly decreased (Figure 1(e)). Thus, we confirmed that BA has a potent inhibitory effect on MM cells *in vitro*.

3.3. BA Activates the Mitochondrial Apoptosis Pathway in U266 Cells. We next measured cell apoptosis, which is a crucial process causing cell death. BA at 40 μM increased the number of apoptotic cells in a time-dependent manner (Figure 2(a)). Similarly, increasing concentrations of BA resulted in higher proportions of apoptotic cells (Figure 2(b)). These results indicate that BA promotes apoptosis in a time- and concentration-dependent manner. To further investigate the potential proapoptotic molecules involved, mitochondrial apoptosis proteins were detected using Western blot. As shown in Figures 2(c) and 2(d), levels of the antiapoptotic effector Bcl-2 were decreased, whereas levels of the proapoptotic effector Bax increased in a time- and concentration-dependent manner. Moreover, we further

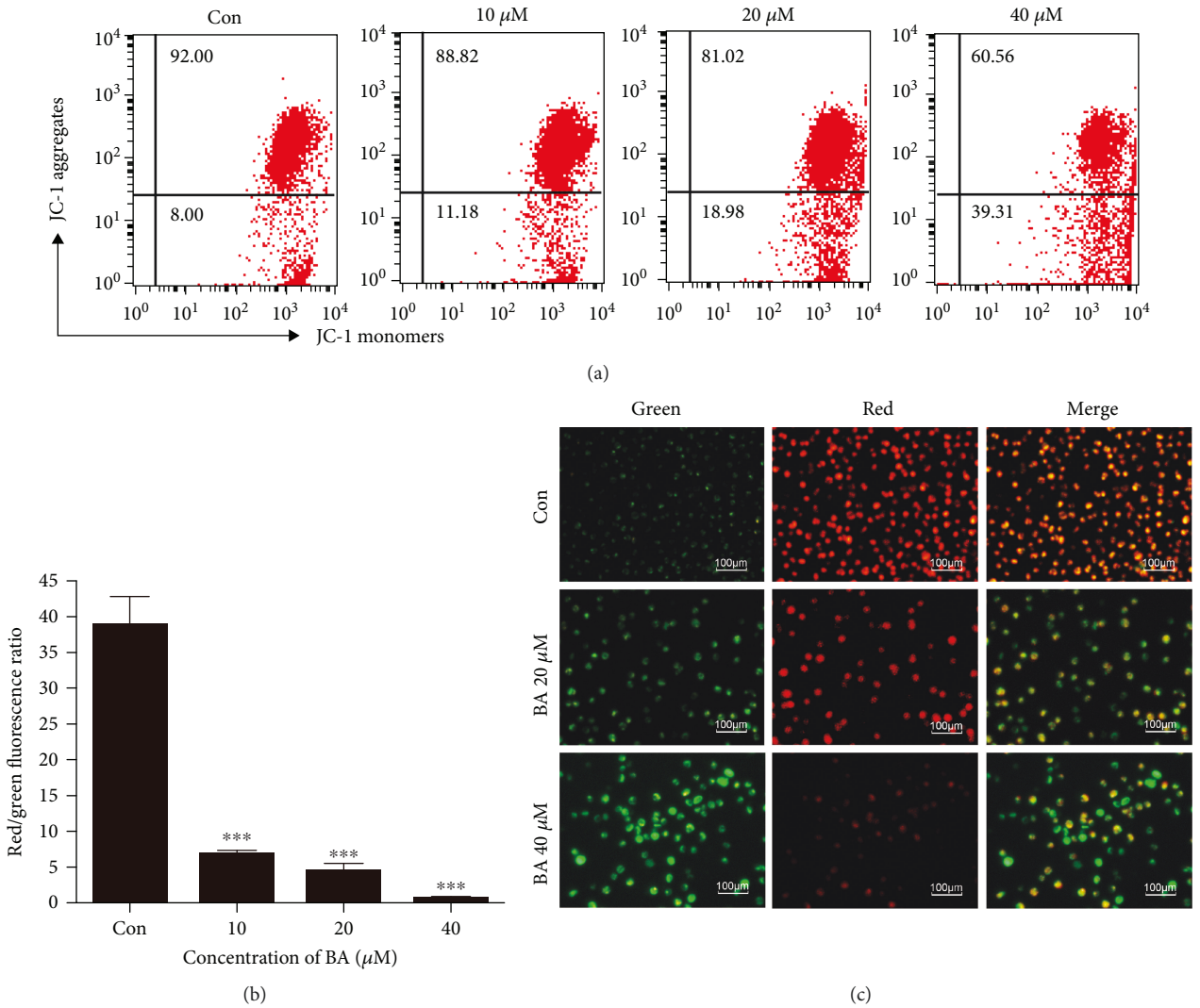

Figure 3: BA induced MMP loss in U266 cells. (a) Representative flow cytometry graphs of MMP after treatment with the indicated concentrations of BA for 12 h. (b) Quantitative analysis of the red-to-green fluorescence ratio; $^{***}P < 0.001$. (c) Representative fluorescence graphs of MMP transition in U266 cells after JC-1 staining.

confirmed that BA mediated the release of cyt c and activated cleaved caspase-3, caspase-8, and caspase-9 and cleaved PARP1 (Figures 2(c) and 2(d)), indicating that the mitochondrial apoptosis pathway was invoked in the process of the BA-mediated cell death.

3.4. BA Mediates S-Phase Arrest in U266 Cells. As another potent antitumor indicator, the cell cycle phase was examined in treated cells. Our representative flow cytometry plots (Figure 2(e)) and statistical analysis (Figure 2(f)) of U266 cells showed that BA exerted its antiproliferative effect by increasing the percentage of S-phase cells. However, no significant increase was observed at a low concentration level (Figure 2(f)), suggesting that other mechanisms of inducing cell death were functional at low concentrations. The proteins cyclin A, CDK2, $p21^{Waf1/Cip1}$, and $p27^{Kip}$ are important molecules for S-phase arrest [27], and as shown in Figure 2(g), BA concentration dependently decreased cyclin A and CDK2 but increased $p21^{Waf1/Cip1}$ and $p27^{Kip}$. These results further demonstrated the BA-induced S-phase arrest.

3.5. BA Causes MMP Collapse in U266 Cells. MMP is an important parameter of mitochondrial function, and MMP transition is generally perceived as an early sign of apoptosis. Flow cytometry plots (Figure 3(a)) and statistical analysis (Figure 3(b)) showed that BA induced a concentration-dependent decrease in red/green fluorescence ratios in U226 cells, as indicated by a shift from red JC-1 aggregates to green JC-1 monomers. In Figure 3(c), the control group mainly exhibited a higher incidence of red fluorescence, while the BA-treated group showed an obvious transition to green fluorescence, which indicated damaged mitochondria.

3.6. BA Induces ROS-Mediated U266 Cell Death. Mitochondria are important sources of intracellular ROS, and accumulation of ROS is closely related to cellular proliferation and apoptosis [12, 14]. After 12 h of treatment with BA (0, 10,

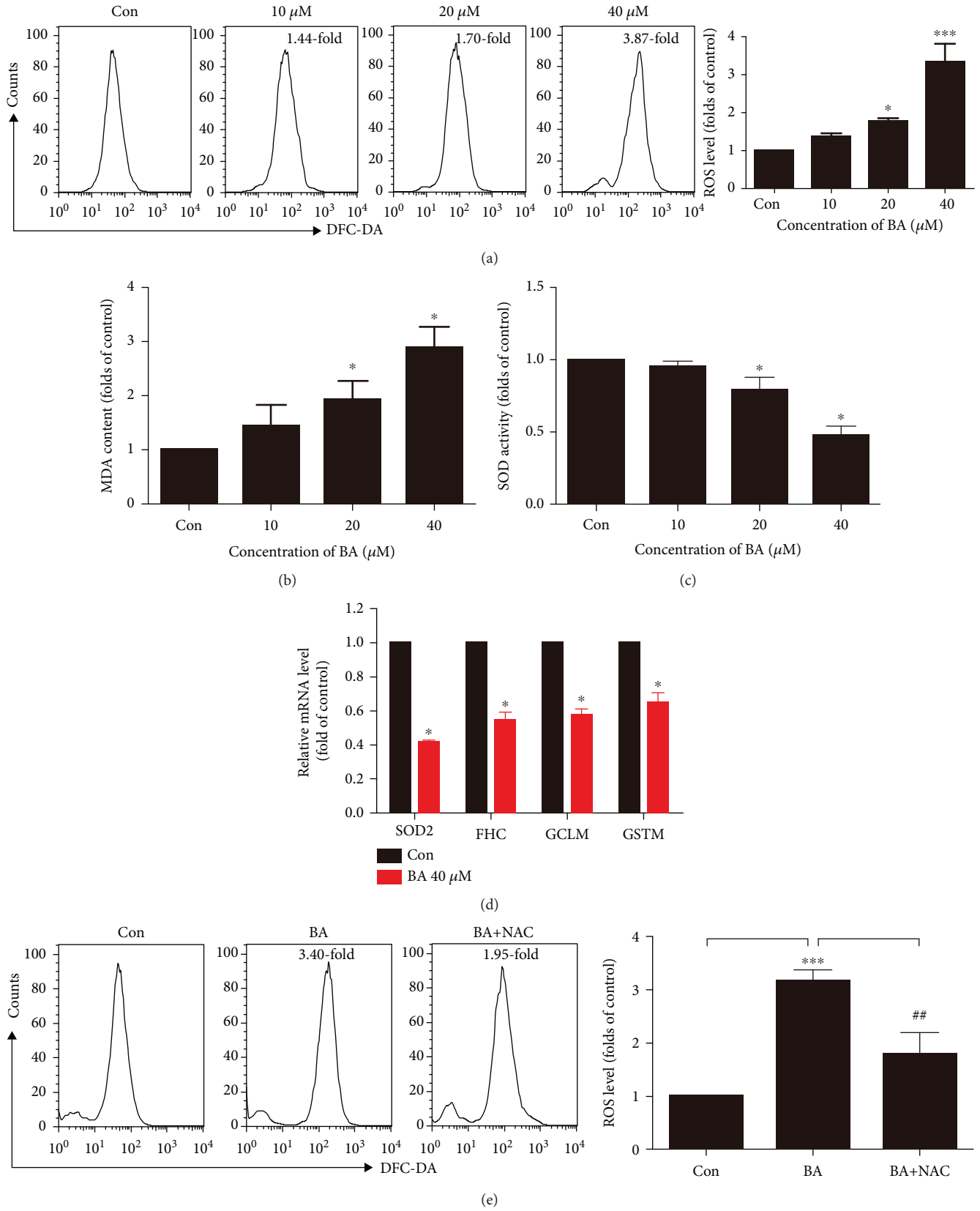

Figure 4: Continued.

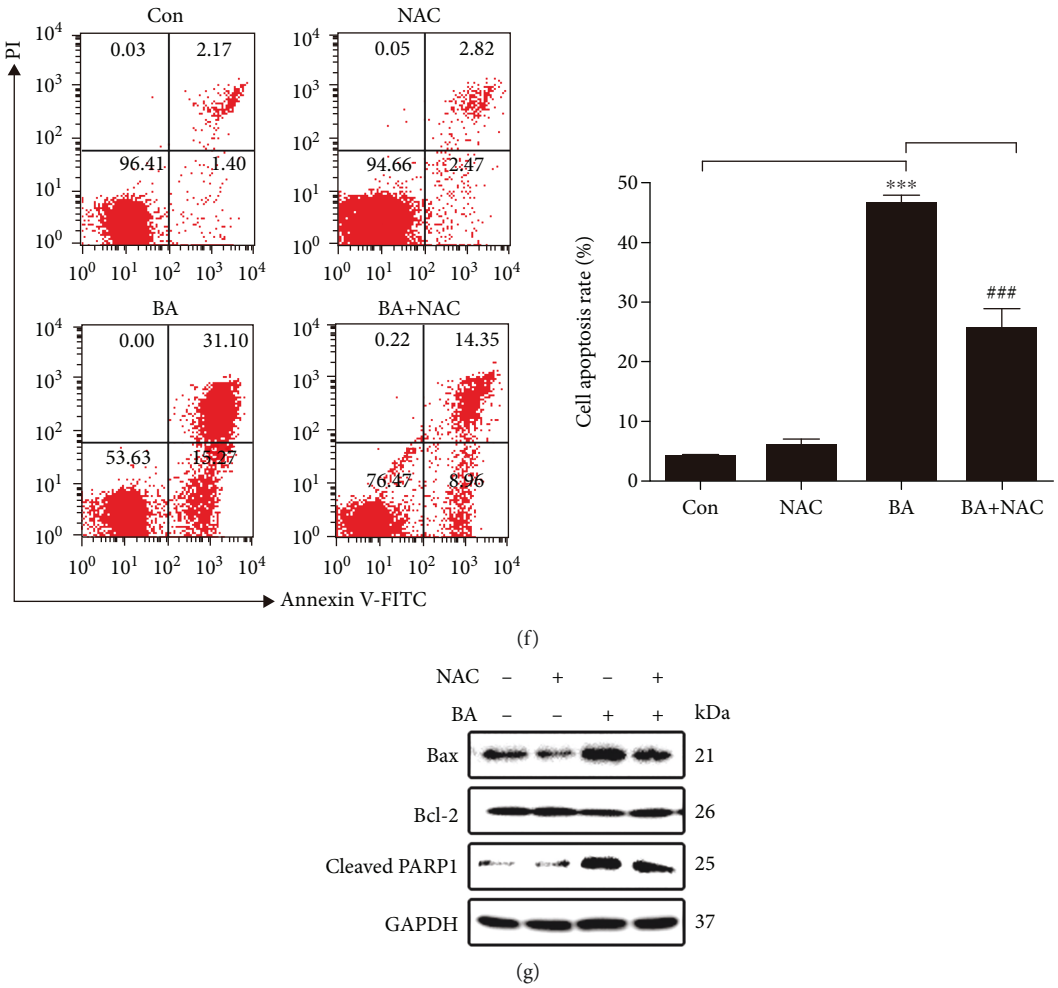

Figure 4: BA induced ROS accumulation in U266 cells in a concentration-dependent manner. (a) Representative plots of flow cytometric analysis using a DCFH-DA probe after 12 h of treatment and the quantitative analysis of the intracellular ROS level. $^{*}P < 0.05$ and $^{***}P < 0.001$. (b) Intracellular MDA content in different concentrations of BA; $^{*}P < 0.05$. (c) SOD activity in different concentrations of BA; $^{*}P < 0.05$. (d) Expression of SOD2, FHC, GCLM, and GSTM by real-time PCR after 40 μM BA for 12 h; $^{*}P < 0.05$. (e) Representative cytometric graphs and quantitative analysis of the ROS generation level with or without 10 mM NAC for 12 h. $^{***}P < 0.001$*vs.* the control group; $^{\#\#}P < 0.01$*vs.* the BA-treated group. (f) U266 cells were treated with 40 μM BA with or without 10 mM NAC, the apoptosis rate was detected by flow cytometry, and quantitative analysis was shown. $^{***}P < 0.001$*vs.* the control group; $^{\#\#\#}P < 0.001$*vs.* the BA-treated group. (g) Expression levels of apoptosis-related proteins were evaluated by Western blotting after treatment with or without 10 mM NAC.

20, and 40 μM), U266 cells exhibited concentration-dependent increases in intracellular ROS (Figure 4(a)). To further confirm the oxidative function of BA, oxidation product MDA and reductive substance SOD were measured. As shown in Figures 4(b) and 4(c), there is a concentration-dependent increase in MDA contents and reduction in SOD activities, especially for the high concentration group. There are many genes participating in the regulation of ROS. Moreover, our real-time PCR results showed that the expression of genes SOD2, FHC, GCLM, and GSTM was all decreased following treatment with BA (40 μM) (Figure 4(d)), which indicate the underlying regulatory targets of ROS. When we investigated the role of ROS in BA-induced cell death, we firstly observed that BA-induced (40 μM) ROS was significantly decreased by 10 mM NAC (Figure 4(e)). Subsequently, we detected apoptosis in the presence or absence of 10 mM NAC (Figure 4(f)). As expected, when ROS levels were reduced with the ROS scavenger NAC, apoptosis was effectively attenuated. In addition, the expression levels of Bax and cleaved PARP1 were decreased, while Bcl-2 levels were increased upon exposure to NAC (Figure 4(g)). Overall, our results suggest that BA exerted its apoptosis-promoting effect in U266 cells by enhancing intracellular ROS generation.

3.7. BA Blocks the NF-κB Pathway to Promote ROS Accumulation in U266 Cells. We then determined whether BA has an effect on the NF-κB pathway. According to the Western blot results, BA significantly reduced the levels of NF-κB p65 and p-NF-κB p65 in a time- and concentration-dependent manner (Figures 5(a) and 5(b)). Moreover, the immunofluorescence staining indicated lower expression and less nuclear binding levels of NF-κB p65 (Figure 5(c)). The activated IKK complex is responsible for IκB

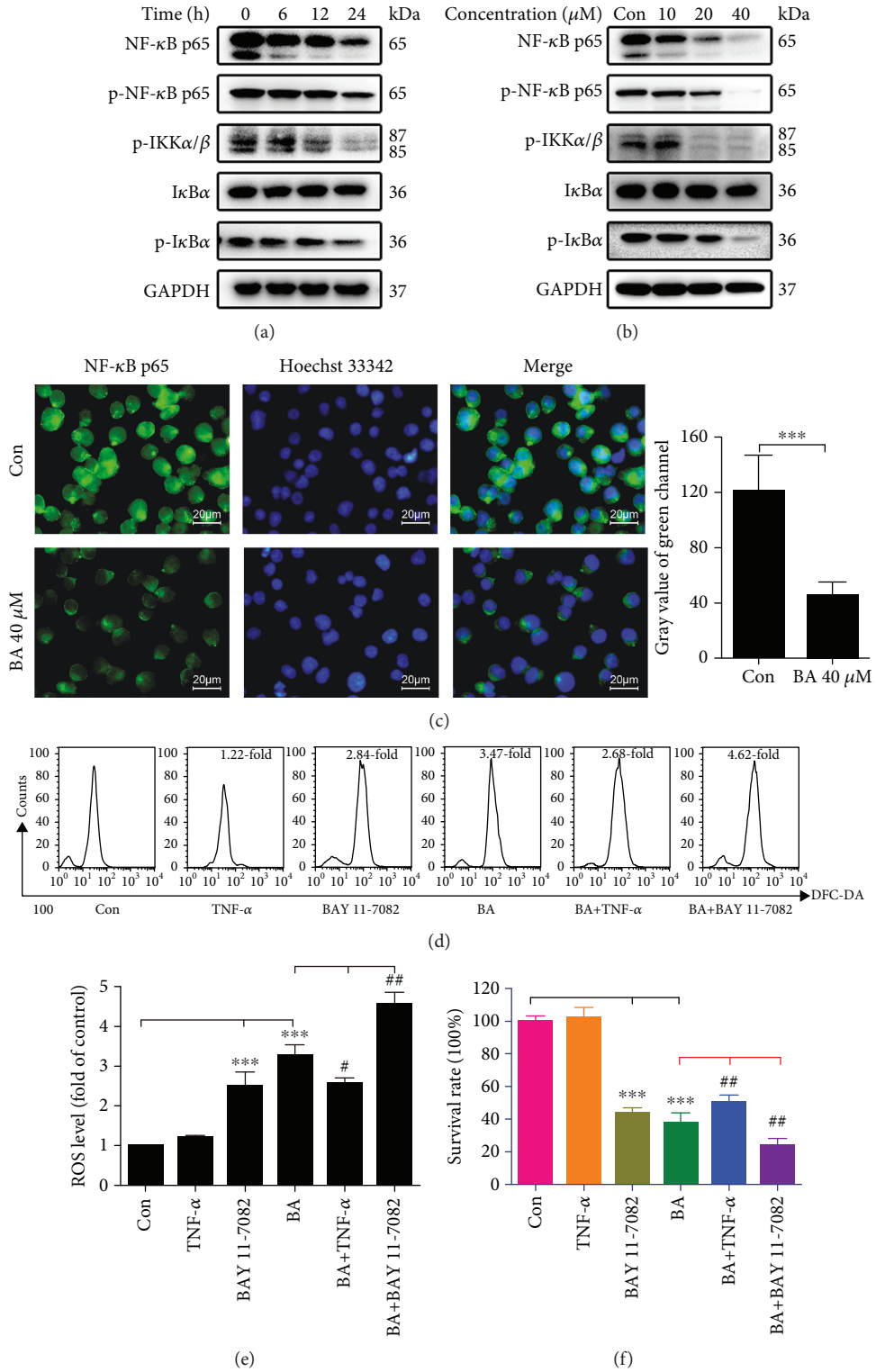

Figure 5: BA induced inhibition of the NF-κB pathway, resulting in accumulation of ROS in U266 cells. (a, b) The expression levels of NF-κB p65, p-NF-κB p65, p-IKKα/β, IκBα, and p-IκBα in U266 cells were evaluated by Western blotting after exposure to 40 μM BA for the indicated times or after exposure to the indicated concentrations for 12 h. (c) U266 cells incubated with 40 μM BA or 0.1% DMSO for 12 h were analyzed for NF-κB p65 expression and distribution by immunofluorescence; $^{***}P < 0.001$. (d) Representative flow cytometry plots using DCFH-DA after treatment with 40 μM BA for 12 h in the presence or absence of 10 ng/ml TNF-α and 5 μM BAY 11-7082. (e) Quantitative analysis of ROS levels with or without TNF-α and BAY 11-7082 in BA-treated U266 cells. $^{***}P < 0.001$*vs.* the control group; $^{\#}P < 0.05$*vs.* the BA-treated group; and $^{\#\#}P < 0.01$*vs.* the BA-treated group. (f) Quantitative analysis of survival rates by a CCK-8 assay via comparison between groups in the presence or absence of TNF-α and BAY 11-7082 and exposure to BA. $^{***}P < 0.001$*vs.* the control group; $^{\#\#}P < 0.01$*vs.* the BA-treated group.

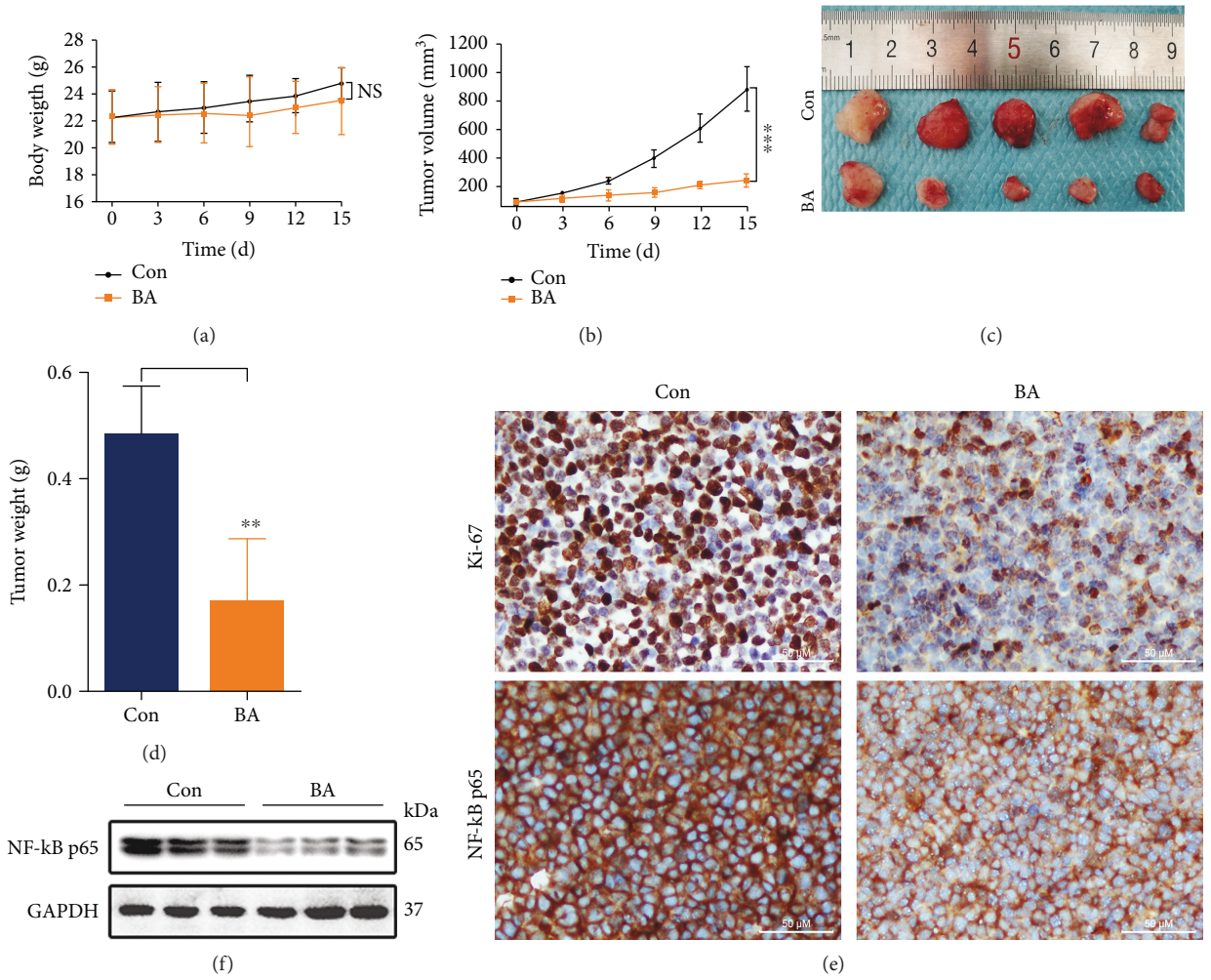

Figure 6: BA inhibited MM xenograft tumor growth *in vivo*. Tumor-bearing mice were randomly assigned to the control and BA-treated groups. The body weights (a) and tumor volumes (b) were measured every third day. NS indicates no significant difference *vs.* the control group; $^{***}P < 0.001$. (c) Photographs of isolated tumors. (d) The weights of stripped tumors; $^{**}P < 0.01$. (e) Tumor tissues were stained with Ki-67 and NF-κB p65 via immunohistochemistry. (f) The level of NF-κB p65 in xenograft tumors was assessed by Western blotting.

phosphorylation and degradation, thus contributing to the release and translocation of free NF-κB dimers. The p-IKKα/β and p-IκBα were all time- and concentration-dependently decreased after BA treatment (Figures 5(a) and 5(b)). The above results demonstrate that BA strongly inhibits the NF-κB pathway.

Additionally, it has been reported that NF-κB suppresses ROS levels in cancer cells [25]. To explore the regulatory relationship between these two factors, we chose the pathway-specific activator TNF-α and the inhibitor BAY 11-7082 to stimulate and suppress the NF-κB pathway, respectively, and then assessed intracellular ROS levels and cell viability. Our results showed that the pathway-specific activator partially reversed the elevated ROS levels (Figures 5(d) and 5(e)) and cytotoxicity induced by BA (Figure 5(f)), whereas the pathway inhibitor acted in the opposite fashion. These findings indicate that blocking this pathway has the potential to elicit strong antitumor responses, partly through breaking cellular redox homeostasis.

3.8. BA Inhibits the Growth of MM Xenograft Tumors In Vivo. We further performed *in vivo* studies in nude mice. Indeed, chemotherapy is often accompanied by dramatic side effects, such as substantial body weight loss. Interestingly, no significant difference in body weight loss existed between the two groups (Figure 6(a)). As is statistically and visually displayed in Figures 6(b) and 6(c), the xenograft volumes in the BA-treated group were significantly reduced (inhibition ratio of approximately 72.1%). Moreover, the tumor weights (Figure 6(d)) of the experimental group (0.17 ± 0.05 g) were much lower than those of the control group (0.48 ± 0.04 g). Assessment of cellular proliferation by Ki-67 immunohistochemistry is a consistent and powerful prognosticator in MM [28]. Our IHC graphs showed that proliferating cells with brown-stained Ki-67$^+$ nuclei were more frequently observed in the control group (Figure 6(e)). Consistent with our *in vitro* experiments, BA inhibited the expression of NF-κB p65 *in vivo*, as indicated by IHC and Western blot results (Figures 6(e) and 6(f)).

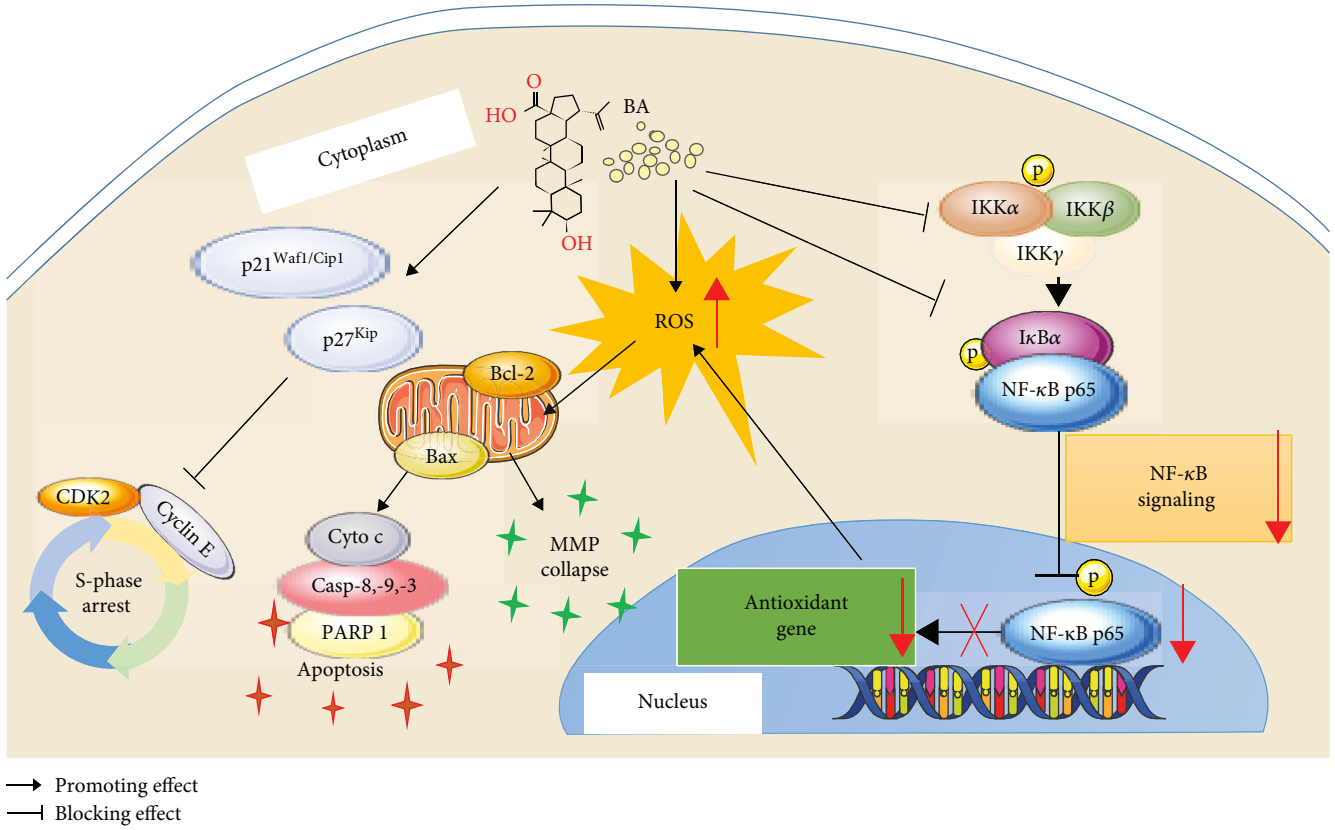

Figure 7: Illustration of the potential mechanisms occurring in BA-treated MM cells.

4. Discussion

Studies explosively report the treatments currently in use for MM. These therapies include high-dose chemotherapy, autologous stem cell transplant, cell immunotherapy, and novel agents [2]. However, few studies have explored traditional Chinese medicines, such as BA. Herein, we focus on the anticancer activities of BA against MM *in vitro* and *in vivo*. We demonstrate that BA induces apoptosis, S-phase arrest, MMP collapse, and ROS overproduction. Subsequently, we investigate the effects of BA on NF-κB signaling and finally reveal the role of the NF-κB system on ROS. To our knowledge, our study is the first to report that BA inhibits MM cells by suppressing NF-κB transcriptional activity, which in return disrupts redox homeostasis.

The mitochondrial pathway is believed to be one of the most crucial mechanisms of BA-mediated cell death in various cancers [9, 29, 30]. Molecularly, Bcl-2 families, regulating the balance of proapoptotic (Bax) and antiapoptotic (Bcl-2) proteins, determine whether a cell survives or undergoes apoptosis [31]. As systematically summarized, the mitochondrial apoptosis pathway is activated by a litany of stimuli that trigger the release of cyt c, facilitate the formation of the apoptosome, and activate apical caspases (caspase-8 and caspase-9) and then downstream caspase-3, which results in cell death [12, 32]. Additionally, we revealed that BA effectively activated apoptosis in a process dependent on the upregulation of Bax, the downregulation of Bcl-2, and the activation of cleaved caspase-3, caspase-8, and caspase-9, cyt c, and cleaved PARP1. All of these evidences indicate that the mitochondrial apoptosis pathway plays a crucial role in BA-mediated U266 cell death.

Loss of cell checkpoint controls is one of the hallmarks of tumorigenesis. Treatments targeting the cell cycle are emerging as a most promising cancer therapy, and intense efforts are now underway [27]. Goswami et al. showed that BA induced G_0/G_1 arrest in SiHa cells [15]. However, it was reported that BA blocked breast cancer at the G_2/M checkpoint [33], whereas its derivatives mainly targeted the S-phase in human hepatocellular carcinoma and leukemia [34]. Such cell-selective and tumor-specific characteristics indicate that a certain checkpoint block may occur in BA-treated U266 cells. Our findings confirmed that BA-treated MM stalled at the S-phase. Molecularly, the cell cycle, which involves a series of tightly integrated events, is regulated by cyclin/CDK complexes, which are again modulated by a host of CDK inhibitors [27]. We confirmed that S-phase arrest was mainly driven by a synergistic mechanism involving inhibition of the cyclin A2/CDK2 complex as well as stimulation of $p21^{Waf1/Cip1}$ and $p27^{Kip}$.

In comparison to their normal counterparts, cancer cells inherently obtain a moderately elevated ROS level, which contributes to cancer initiation, malignancy, and resistance to chemotherapy [14]. Nevertheless, the elevated ROS usually plays a deleterious role [13]. BA clearly

induces overwhelming oxidative stress, which initiates cell death in many cancers [15, 16, 30]. Similar results were observed in our study, that is, BA concentration-dependently induced depolarization of MMP, accumulation of ROS, and activation of the mitochondrial pathway. These findings suggest that ROS mediate a unique way of eliminating MM cells, as further confirmed by our results that cell death was partially attenuated by ROS scavengers (Figure 4).

The NF-κB system, which regulates the tumor microenvironment and modulates inflammation, tumorigenesis, and therapy resistance [10, 17, 20], has long been proven to be implicated in MM [35]. However, the BA-mediated transcriptional activities of NF-κB have caused massive controversies, namely, BA blocks NF-κB activity to inhibit cervical cancer [36], prostate cancer [26], and breast cancer [19]. Whereas, in human endometrial adenocarcinoma [37] and prostate cancer of LNCaP cells [23], BA activates the NF-κB pathway to sensitize cells to death. Thus, we sought to determine the transcriptional levels of the NF-κB pathway in BA-treated U266 cells. In accordance with the majority of findings, our results showed that BA may act as a potent NF-κB pathway inhibitor, not an activator.

The NF-κB pathway also closely interacts with ROS. Researchers have reported that upregulated NF-κB activities promote expression of downstream antioxidant genes, such as the ROS-related genes ferritin heavy chain (FHC) and SOD2 [24], thereby protecting cells from the insults of oxidative damage. Moreover, our results found that upregulated NF-κB activity partially reversed the excess ROS and attenuated cytotoxicity induced by BA, whereas BA and the pathway-specific inhibitor BAY 11-7082 exerted synergistic cytotoxic effects by further elevating ROS. Therefore, we conclude that the inhibition of the NF-κB pathway enhances downstream oxidant effectors and promotes ROS production in BA-treated MM cells.

5. Conclusion

In our novel findings, we intensively elaborated on the inhibitory effects of BA on MM cells both *in vitro* and *in vivo*. The potential mechanisms mainly include mitochondrial apoptosis induction, cell cycle blockade, MMP disruption, intracellular ROS accumulation, and NF-κB signaling inhibition (Figure 7). And we especially elucidated the complex regulatory roles between ROS and the NF-κB pathway in MM. Overall, BA provides valuable insight for clinical applications in treating MM, though further studies are warranted to reveal its broader mechanisms and to ensure its drug safety.

Data Availability

The data used to support the findings of this study are available from the corresponding author upon request.

Conflicts of Interest

All authors declare no conflicts of interest.

Authors' Contributions

Mei Huang, Yan Yang, and Min Shen conceived and designed the experiments. Min Shen, Yiqiang Hu, and Xin Yang performed the experiments. Bo Wang and Yiqiang Hu analyzed the data and prepared the figures. Lanlan Wang and Mei Huang supervised the research. Min Shen wrote the original manuscript. Mei Huang, Yiqiang Hu, and Yan Yang revised the manuscript. All authors were involved in discussing and editing the final version of the manuscript. Min Shen and Yiqiang Hu contributed equally to this work.

Acknowledgments

This project was supported by a grant from the National Natural Science Foundation of China (No. 81270599).

References

[1] P. Roy, U. Sarkar, and S. Basak, "The NF-κB activating pathways in multiple myeloma," *Biomedicines*, vol. 6, no. 2, p. 59, 2018.

[2] J. L. Harousseau and M. Attal, "How I treat first relapse of myeloma," *Blood*, vol. 130, no. 8, pp. 963–973, 2017.

[3] C. Pawlyn and G. J. Morgan, "Evolutionary biology of high-risk multiple myeloma," *Nature Reviews Cancer*, vol. 17, no. 9, pp. 543–556, 2017.

[4] D. M. Zhang, H. G. Xu, L. Wang et al., "Betulinic acid and its derivatives as potential antitumor agents," *Medicinal Research Reviews*, vol. 35, no. 6, pp. 1127–1155, 2015.

[5] A. Saneja, D. Arora, R. Kumar, R. D. Dubey, A. K. Panda, and P. N. Gupta, "Therapeutic applications of betulinic acid nanoformulations," *Annals of the New York Academy of Sciences*, vol. 1421, no. 1, pp. 5–18, 2018.

[6] S. Xiao, Z. Tian, Y. Wang, L. Si, L. Zhang, and D. Zhou, "Recent progress in the antiviral activity and mechanism study of pentacyclic triterpenoids and their derivatives," *Medicinal Research Reviews*, vol. 38, no. 3, pp. 951–976, 2018.

[7] V. Zuco, R. Supino, S. C. Righetti et al., "Selective cytotoxicity of betulinic acid on tumor cell lines, but not on normal cells," *Cancer Letters*, vol. 175, no. 1, pp. 17–25, 2002.

[8] H. Gali-Muhtasib, R. Hmadi, M. Kareh, R. Tohme, and N. Darwiche, "Cell death mechanisms of plant-derived anticancer drugs: beyond apoptosis," *Apoptosis*, vol. 20, no. 12, pp. 1531–1562, 2015.

[9] L. Potze, F. B. Mullauer, S. Colak, J. H. Kessler, and J. P. Medema, "Betulinic acid-induced mitochondria-dependent cell death is counterbalanced by an autophagic salvage response," *Cell Death & Disease*, vol. 5, no. 4, article e1169, 2014.

[10] Y. Takada and B. B. Aggarwal, "Betulinic acid suppresses carcinogen-induced NF-κB activation through inhibition of IκBα kinase and p65 phosphorylation: abrogation of cyclooxygenase-2 and matrix metalloprotease-9," *The Journal of Immunology*, vol. 171, no. 6, pp. 3278–3286, 2003.

[11] D. B. Zorov, M. Juhaszova, and S. J. Sollott, "Mitochondrial reactive oxygen species (ROS) and ROS-induced ROS release," *Physiological Reviews*, vol. 94, no. 3, pp. 909–950, 2014.

[12] K. Sinha, J. Das, P. B. Pal, and P. C. Sil, "Oxidative stress: the mitochondria-dependent and mitochondria-independent

pathways of apoptosis," *Archives of Toxicology*, vol. 87, no. 7, pp. 1157–1180, 2013.

[13] M. Buelna-Chontal and C. Zazueta, "Redox activation of Nrf2 & NF-κB: a double end sword?," *Cellular Signalling*, vol. 25, no. 12, pp. 2548–2557, 2013.

[14] S. Galadari, A. Rahman, S. Pallichankandy, and F. Thayyullathil, "Reactive oxygen species and cancer paradox: to promote or to suppress?," *Free Radical Biology and Medicine*, vol. 104, pp. 144–164, 2017.

[15] P. Goswami, S. Paul, R. Banerjee, R. Kundu, and A. Mukherjee, "Betulinic acid induces DNA damage and apoptosis in SiHa cells," *Mutation Research*, vol. 828, pp. 1–9, 2018.

[16] H. Shen, L. Liu, Y. Yang, W. Xun, K. Wei, and G. Zeng, "Betulinic acid inhibits cell proliferation in human oral squamous cell carcinoma via modulating ROS-regulated p53 signaling," *Oncology Research*, vol. 25, no. 7, pp. 1141–1152, 2017.

[17] G. M. Matthews, R. de Matos Simoes, E. Dhimolea et al., "NF-κB dysregulation in multiple myeloma," *Seminars in Cancer Biology*, vol. 39, pp. 68–76, 2016.

[18] J. A. DiDonato, F. Mercurio, and M. Karin, "NF-κB and the link between inflammation and cancer," *Immunological Reviews*, vol. 246, no. 1, pp. 379–400, 2012.

[19] R. Luo, D. Fang, P. Chu, H. Wu, Z. Zhang, and Z. Tang, "Multiple molecular targets in breast cancer therapy by betulinic acid," *Biomedicine & Pharmacotherapy*, vol. 84, pp. 1321–1330, 2016.

[20] V. Baud and M. Karin, "NF-κB, inflammation, immunity and cancer: coming of age," *Nature Reviews: Immunology*, vol. 18, no. 5, pp. 309–324, 2009.

[21] P. Roy, U. Sarkar, and S. Basak, "The NF-κB a good target for cancer therapy? Hopes and pitfalls," *Nature Reviews Drug Discovery*, vol. 8, no. 1, pp. 33–40, 2018.

[22] L. M. Staudt, "Oncogenic activation of NF-κB," *Cold Spring Harbor Perspectives in Biology*, vol. 2, no. 6, pp. a000109–a000109, 2010.

[23] R. Parrondo, A. Pozas, T. Reiner, P. Rai, and C. Perez-Stable, "NF-κB activation enhances cell death by antimitotic drugs in human prostate cancer cells," *Molecular Cancer*, vol. 9, no. 1, p. 182, 2010.

[24] M. J. Morgan and Z. G. Liu, "Crosstalk of reactive oxygen species and NF-κB signaling," *Cell Research*, vol. 21, no. 1, pp. 103–115, 2011.

[25] S. J. Stein and A. S. Baldwin, "NF-κB suppresses ROS levels in BCR–ABL$^+$ cells to prevent activation of JNK and cell death," *Oncogene*, vol. 30, no. 45, pp. 4557–4566, 2011.

[26] E. Shankar, A. Zhang, D. Franco, and S. Gupta, "Betulinic acid-mediated apoptosis in human prostate cancer cells involves p53 and nuclear factor-kappa B (NF-κB) pathways," *Molecules*, vol. 22, no. 2, p. 264, 2017.

[27] M. Ingham and G. K. Schwartz, "Cell-cycle therapeutics come of age," *Journal of Clinical Oncology*, vol. 35, no. 25, pp. 2949–2959, 2017.

[28] S. Ely, P. Forsberg, I. Ouansafi et al., "Cellular proliferation by multiplex immunohistochemistry identifies high-risk multiple myeloma in newly diagnosed, treatment-naive patients," *Clinical Lymphoma, Myeloma & Leukemia*, vol. 17, no. 12, pp. 825–833, 2017.

[29] C. Yang, Y. Li, L. Fu, T. Jiang, and F. Meng, "Betulinic acid induces apoptosis and inhibits metastasis of human renal carcinoma cells in vitro and in vivo," *Journal of Cellular Biochemistry*, vol. 119, no. 10, pp. 8611–8622, 2018.

[30] X. Wang, X. Lu, R. Zhu et al., "Betulinic acid induces apoptosis in differentiated PC12 cells via ROS-mediated mitochondrial pathway," *Neurochemical Research*, vol. 42, no. 4, pp. 1130–1140, 2017.

[31] S. Das, J. Das, A. Samadder, N. Boujedaini, and A. R. Khuda-Bukhsh, "Apigenin-induced apoptosis in A375 and A549 cells through selective action and dysfunction of mitochondria," *Experimental Biology and Medicine*, vol. 237, no. 12, pp. 1433–1448, 2012.

[32] C. C. Wu and S. B. Bratton, "Regulation of the intrinsic apoptosis pathway by reactive oxygen species," *Antioxidants and Redox Signaling*, vol. 19, no. 6, pp. 546–558, 2013.

[33] Y. Cai, Y. Zheng, J. Gu et al., "Betulinic acid chemosensitizes breast cancer by triggering ER stress-mediated apoptosis by directly targeting GRP78," *Cell Death & Disease*, vol. 9, no. 6, p. 636, 2018.

[34] R. C. Santos, J. A. R. Salvador, R. Cortés, G. Pachón, S. Marín, and M. Cascante, "New betulinic acid derivatives induce potent and selective antiproliferative activity through cell cycle arrest at the S phase and caspase dependent apoptosis in human cancer cells," *Biochimie*, vol. 93, no. 6, pp. 1065–1075, 2011.

[35] T. D. Gilmore, "Multiple myeloma: lusting for NF-κB," *Cancer Cell*, vol. 12, no. 2, pp. 95–97, 2007.

[36] B. L. Tan, M. E. Norhaizan, and L. C. Chan, "ROS-mediated mitochondrial pathway is required for *Manilkara zapota* (L.) P. Royen leaf methanol extract inducing apoptosis in the modulation of caspase activation and EGFR/NF-κB activities of HeLa human cervical cancer cells," *Evidence-Based Complementary and Alternative Medicine*, vol. 2018, Article ID 6578648, 19 pages, 2018.

[37] E. Karna and J. A. Palka, "Mechanism of betulinic acid inhibition of collagen biosynthesis in human endometrial adenocarcinoma cells," *Neoplasma*, vol. 56, no. 4, pp. 361–366, 2009.